

Treffitz and Collocation Methods

Zi-Cai Li, Tzon-Tzer Lu, Hsin-Yun Hu
National Sun Yat-sen University, Taiwan
National Center for Theoretical Sciences, Taiwan

and

Alexander H.-D. Cheng
University of Mississippi

To our friends,

Wen-Jang Huang and Mong-Na Lo Huang.

Contents

Preface	xiii
Acknowledgements	xvi
0 Preliminary	1
0.1 Algorithms of CM, TM and CTM	1
0.1.1 Algorithms of CM	1
0.1.2 Viewpoint of Boundary Approximation Methods	4
0.1.3 Viewpoint of Least Squares Methods	8
0.1.4 Complete Systems of Solutions	10
0.2 Coupling Techniques	13
0.2.1 Six Combinations	13
0.2.2 The Original TM	16
0.2.3 The Direct TM	16
0.2.4 Trefftz-Herrera Approaches for Coupling Problems	18
0.3 Boundary Element Methods	20
0.3.1 Green Theorem	21
0.3.2 Discrete Approximation	22
0.3.3 Natural BEM	23
0.4 Other Kinds of Boundary Methods	24
0.5 Comparisons	27

Part I	Collocation Trefftz Method	31
1	Basic Algorithms and Theory	37
1.1	Notations and Preliminaries	38
1.2	Approximation Problems	40
1.3	Error Estimates	42
1.4	Debye–Huckel Equation	46
1.5	Stability Analysis	51
1.6	Two Models of Singularity Problems	56
2	Motz’s and Cracked Beam Problems	61
2.1	Introduction	61
2.2	Basic Algorithms of Collocation TM	63
2.3	Error Bounds and Integration Approximation	69
2.4	The Cracked Beam Problem	74
2.5	Discussions and Comparisons	77
2.6	Concluding Remarks	82
3	Coupling Techniques	95
3.1	Introduction	95
3.2	Description of Generalized GTMs	98
3.3	Penalty TMs	100
3.4	Simplified Hybrid TMs	104
3.5	Penalty plus Hybrid TMs	106
3.6	Lagrange Multiplier TM	111
3.7	Effective Condition Number	116
3.8	Numerical Experiments	120
4	Biharmonic Equations with Crack Singularities	133
4.1	Introduction	133

4.2	The Green Formulas of $\Delta^2 u$	134
4.2.1	On Rectangular Domains	134
4.2.2	Corner Effects on Polygons	136
4.2.3	Boundary Conditions for Biharmonic Equations on Polygons	140
4.3	The Collocation Trefftz Methods	142
4.3.1	Three Crack Models	142
4.3.2	Description of the Method	145
4.3.3	The Collocation Trefftz Method with Natural Corners	146
4.3.4	Formulas of Partial Derivatives	147
4.4	Error Bounds	148
4.5	Numerical Experiments	150
4.6	Concluding Remarks	151
Part II Collocation Methods		159
5	Collocation Methods	163
5.1	Introduction	163
5.2	Description of Collocation Methods	164
5.3	Error Analysis	168
5.4	The Robin Boundary Conditions	174
5.5	Inverse Inequalities	178
5.6	Numerical Experiments	182
5.6.1	Radial Basis Functions for Different Boundary Conditions	182
5.6.2	Piecewise Admissible Functions	184
5.7	Final Remarks	185
6	Combinations of Collocation and Finite Element Methods	189
6.1	Introduction	189
6.2	Combinations of FEMs	190
6.3	Linear Algebraic Equations of Combination of FEM and CM	193

6.4	Uniformly V_h^0 - Elliptic Inequality	199
6.5	Uniformly V_h^0 - Elliptic Inequality Involving Integration Approximation . .	204
6.6	Final Remarks	210
7	Radial Basis Collocation Methods	211
7.1	Introduction	211
7.2	Radial Basis Functions	212
7.3	Description of Radial Basis Collocation Methods	214
7.3.1	Radial Basis Collocation Method (RBCM) for Different Boundary Conditions	214
7.3.2	Combination of FEM and RBCM	221
7.4	Inverse Estimates for Radial Basis Functions	226
7.5	Numerical Experiments	229
7.5.1	Radial Basis Collocation Methods with Different Boundary Con- ditions	229
7.5.2	Adding Method of Singular Functions	231
7.5.3	Subtracting Method of Singular Functions	231
7.6	Comparisons and Conclusions	233
Part III	Advanced Topics	239
8	Hybrid and Other TMs Using Piecewise Particular Solutions	245
8.1	Introduction	245
8.2	The Hybrid Techniques	248
8.3	Error Analysis for the Hybrid Trefftz Method	251
8.3.1	Basic Error Analysis	252
8.3.2	Integration Approximation for the Hybrid Trefftz Method	257
8.4	The Penalty plus Hybrid Techniques	262
8.5	Lagrange Multiplier Techniques	269
8.6	Numerical Experiments	271

9 Interior Boundary Conditions in the Schwarz Alternating Method	283
9.1 Introduction	283
9.2 Different Boundary Conditions on Γ_1	285
9.3 Different Boundary Conditions on Γ_1 and Γ_2	290
9.4 Special Cases of the Mixed SAMs	292
10 Combinations with High Order FEMs	297
10.1 Introduction	297
10.2 Combinations of TM and Lagrange FEMs	298
10.3 Global Superconvergence	303
10.4 Adini's Elements	308
10.5 Numerical Experiments	311
10.6 Concluding Remarks	316
11 Eigenvalue Problems	321
11.1 Introduction	321
11.2 New Numerical Algorithms for Eigenvalue Problems	323
11.2.1 The Trefftz Methods for (11.1.6)	323
11.2.2 Heuristic Ideas of Degeneracy of (11.1.6)	325
11.2.3 New Iteration Algorithms for Seeking Eigenvalues and Eigenfunctions	326
11.2.4 Solution of Nonlinear Equations	327
11.3 Error Bounds of Eigenvalues	329
11.4 Error Bounds of Eigenfunctions	333
11.5 Computational Models and Numerical Experiments	336
11.5.1 A Sample of Eigenvalue Problems and Particular Solutions	336
11.5.2 Description of the Detailed Algorithms for TM	341
11.5.3 Investigation of Behavior for the Function $f(k)$ as $k^2 \rightarrow \lambda_1$	343
11.5.4 Computation for the Minimal Eigenvalue and Corresponding Eigenfunction	344

11.6 Eigenvalues for the Cracked Beam	346
11.7 Summaries and Discussions	350
12 The Helmholtz Equation	361
12.1 Introduction	361
12.2 The Trefftz Method	364
12.3 Error Analysis	365
12.3.1 Preliminary Lemmas	365
12.3.2 Error Bounds	368
12.3.3 Exponential Rates of Convergence	370
12.3.4 Estimates on Bounds of Constant $K_{m,n}$	372
12.4 Summaries and Discussions	375
13 Particular Solutions of Laplace's Equations	377
13.1 Introduction	377
13.2 The Harmonic Functions	378
13.2.1 General Cases	381
13.2.2 Formulas for special Θ	384
13.3 Harmonic Solutions Involving Neumann Conditions	386
13.3.1 The case of the N-D type	386
13.3.2 The case of the D-N type	388
13.3.3 The case of the N-N type	389
13.4 Extensions and Analysis on Singularity	391
13.4.1 Particular Solutions for Poisson's Equations	391
13.4.2 Extensions to Not Smooth Functions of g_D and g_N	392
13.4.3 Regularity and Singularity of the Solutions of $\Theta = \frac{\pi}{2}, \frac{3\pi}{2}, \pi, 2\pi$	394
13.5 New Models of Singularities for Laplace's Equation	399
13.5.1 Two Models	399
13.5.2 The Trefftz Methods	402

13.5.3 Numerical Experiments	403
13.6 Concluding remarks	406
A Historic Review of Boundary Methods	417
A.1 Potential Theory	418
A.1.1 Euler	419
A.1.2 Lagrange	420
A.1.3 Laplace	421
A.1.4 Fourier	421
A.1.5 Poisson	422
A.1.6 Hamilton	423
A.2 Existence and Uniqueness	423
A.2.1 Dirichlet	425
A.2.2 Neumann	426
A.2.3 Kellogg	426
A.3 Reduction in Dimensions and Green's Formula	427
A.3.1 Gauss	428
A.3.2 Green	429
A.3.3 Ostrogradski	430
A.3.4 Stokes	430
A.4 Integral Equations	431
A.4.1 Cauchy	433
A.4.2 Hadamard	434
A.4.3 Fredholm	435
A.5 Extended Green's Formula	436
A.5.1 Helmholtz	439
A.5.2 Betti	440
A.5.3 Kelvin	440
A.5.4 Rayleigh	441

A.5.5	Volterra	442
A.5.6	Somigliana	442
A.5.7	Kolosov	443
A.6	Pre-Electronic Computer Era	443
A.6.1	Ritz	447
A.6.2	von Kármán	448
A.6.3	Trefftz	448
A.6.4	Muskhelishvili	449
A.7	Electronic Computer Era	449
A.7.1	Kupradze	455
A.7.2	Jaswon	455
A.8	Boundary Integral Equation and Boundary Element Method	456
A.8.1	Rizzo	459
A.8.2	Cruse	459
A.8.3	Brebbia	459
	Reference	461
	Glossary of Symbols	483
	Index	487

Preface

This book covers a class of numerical methods that are generally referred to as *Collocation Methods*. Different from the finite element and the finite difference methods, the discretization and approximation of the collocation method is based on a set of unstructured points in space. This *meshless* feature is attractive because it eliminates the bookkeeping requirements of the *element* based methods. Particularly, if the basis functions used satisfy the governing equation, the collocation is conducted only on the boundary. The boundary collocation methods are also known as Trefftz methods. The main advantages of these methods include the flexible representation of the irregular and deforming geometry, ease of data input and preprocessing, high accuracy of the numerical solution, and the efficient computation.

This book contains a preliminary, an appendix, and 13 chapters in which several types of collocation methods are discussed. These include the radial basis function method, the Trefftz method, the Schwarz alternating method, and the coupled collocation and finite element method. Governing equations investigated include Laplace, Poisson, Helmholtz, and bi-harmonic equations. Regular boundary value problems, boundary value problems with singularity, and eigenvalue problems are also examined. Rigorous mathematical proofs are contained in these chapters, and numerical experiments are also provided to support the algorithms and to verify the theory. A tutorial on the applications of these methods is provided in the preliminary, and a historic review of boundary methods in the Appendix.

This book is an extension of the leading author's earlier books [287, 291] on combined methods based on the theoretical analysis of finite element method (FEM). However, this book has several distinct features, which are addressed as follows:

1. In this book, the boundary collocation method, which is a form of Trefftz method (TM) [462], is presented, and referred to as the collocation Trefftz method (CTM). The boundary approximation method (BAM) as discussed in [316], which involves numerical integration, is also classified as a CTM. New analysis of exponential convergence and excellent numerical results are demonstrated. The CTM is shown to be the most accurate numerical method not only for the global solutions, but also for the leading coefficient of the singularity expansion, which is important for problems like fracture mechanics.
2. This book also covers the original TM, the hybrid TM, the direct TM and the indirect TM. There was a special journal issue published in 1995 celebrating 70 years of Trefftz method [246, 261]. Although a number of papers on TMs were collected, only a few involved analysis. The analysis of TMs lags behind that of the FEM and the boundary element method (BEM). For the TM, there is a significant gap between the excellent computation and the theoretical analysis to support the results. This book presents a systematic analysis for the CTM, the hybrid TM, the

- indirect TM, and the direct TM to bridge the gap.
3. This book also demonstrates the advantages of the CTM over other TMs. The CTM is the simplest algorithm because the collocation equations can be assembled in a straightforward way. For solving Motz's problem, the CTM provides the most accurate solutions not only in the global H^1 sense, but also in its leading singular term. More importantly, the condition number of the stiffness matrix from the CTM is significantly smaller than that from the other TMs. It should be mentioned that the application of CTM is limited to those PDEs whose particular solutions or local particular solutions can be found explicitly.
 4. More topics are explored in this book, such as the biharmonic equation, the Helmholtz equation, and eigenvalue problems by means of particular solutions of elliptic equations. The combinations of the collocation Trefftz method with high order FEM are also discussed, as compared to the linear and bilinear FEMs reported earlier [287, 291]. Different interior boundary conditions in the Schwarz alternating methods are explored, while only the Dirichlet condition was treated in the earlier work [291].
 5. Particular solutions are essential to the Trefftz methods. We provide the particular solutions for the Laplace equation on a polygon, particularly those involving mild singularity.
 6. The collocation method (CM) on the entire domain, in contrast to boundary collocation, is studied. The CM can be interpreted as the least squares method with numerical integration. The analysis can be conducted by means of the FEM approach, and optimal weights for different collocation equations resulting from the PDE and different boundary conditions can be found theoretically.
 7. The radial basis functions (RBF) are a new approximation tool for smooth functions. In this book the RBF has been developed to solve the elliptic equation with singularities.
 8. To enhance the education value, a historical review of the boundary methods is provided as an appendix.

This book is organized as follows. Chapter 0 is a preliminary that reviews the fundamentals of the collocation and the Trefftz methods from several view points. The remainder of the book is divided into three parts, Part I: The Collocation Trefftz Method; Part II: The Collocation Methods; and Part III: Advanced Topics. Part I is mainly concerned with the algorithms, the error estimates, and stability analysis of both the Trefftz method and the collocation Trefftz method. Several popular examples of PDEs with singularities, including Poisson's equation (Motz's and cracked beam problems), and the biharmonic equations with crack singularities are examined. Part II is to give a unified framework of combinations of collocation methods with other numerical methods. Part III is to introduce advanced topics for the collocation Trefftz method.

To appeal to both applied mathematicians and engineers, we have carefully selected only the necessary analyses and significant numerical experiments. The mathematics retained is necessary to provide a deeper insight into the numerical algorithms proposed. For easy reading of the book, each chapter can be treated as an independent unit; hence, readers can directly refer to the chapters that interest them. We hope that through this

book we can bring the engineering and applied mathematics community a step closer to recognizing the power of the collocation and Trefftz methods.

Zi-Cai Li

Tzon-Tzer Lu

Hsin-Yun Hu

Alexander H.-D. Cheng

June 2006

Acknowledgements

We are obliged to Professors C. S. Huang, H. T. Huang, I. Herrera, G. G. Georgiou, C. Xenohontos, J. Huang, T. Lü, S. Wang, L. Ling, and Dr. R. C. D. Chen for their collaboration or valuable suggestions on the research works related to this book, and to the graduate students, Y. L. Chen, H. S. Tsai, C. H. Hung, S. Y. Tsai, W. L. Jhou, S. L. Huang, S. J. Jian and J. R. Wang for reading the manuscript and giving their comments and suggestions. We also are indebted to S. Y. Wang, W. L. Jhou and S. L. Huang for typing the manuscript.

We are grateful to Professor C. A. Brebbia and the editorial staff at the WIT press for their encouraging and assistance in publishing this book. We also wish to thank Professors C. C. Chang, J. C. Yao, N. C. Wong and C. K. Law at National Sun Yat-sen University, Taiwan, for their support during the writing process.

This book and the related works were supported in part by the National Science Council of Taiwan, and National Center for Theoretical Sciences, Mathematics Division, Taiwan.

Chapter 0

Preliminary

In this chapter, we survey the algorithms of the collocation method (CM), the Trefftz method (TM) and the collocation Trefftz method (CTM), and summarize the coupling techniques for the exterior and interior boundary conditions, which include the very original TM, the hybrid TM, the indirect TM and the direct TM. Also the boundary element methods and other kinds of boundary methods are briefly described. In the last section, discussions and comparisons of the CTM with other numerical methods are made.

0.1 Algorithms of CM, TM and CTM

We choose the solution of a boundary value problem to be a continuously differentiable function, and then enforce it to exactly satisfy the partial differential equation and the boundary conditions at a set of points. This leads to CM, or in engineering literature, it is called the residual method [379, 380]. By an equivalence between the Galerkin-FEM and the CM, e.g., see Swartz and Wendroff [449], the linear algebraic equations can be easily constructed for the CM, which leads to an approximate solution of the boundary value problem.

0.1.1 Algorithms of CM

Consider the second order elliptic boundary problem

$$\begin{cases} \mathcal{L}u = f, & \text{in } S, \\ Bu = g, & \text{on } \partial S, \end{cases} \quad (0.1.1)$$

where

$$\mathcal{L} = -\frac{\partial}{\partial x} p \frac{\partial}{\partial x} - \frac{\partial}{\partial y} p \frac{\partial}{\partial y} + c,$$

and the operators, $B = 1$, $p\frac{\partial}{\partial\nu}$, or $p\frac{\partial}{\partial\nu} + \alpha$, represent the Dirichlet, the Neumann and the Robin boundary conditions respectively, where ν is the unit outward normal of ∂S . In this book, the constant c may be chosen as $c = 0$, $c > 0$ and $c < 0$. Choose the smooth basis functions $\{\Psi_i\}$, which are complete, linearly independent, and at least twice differentiable. The orthogonal polynomials and the Fourier functions, as well as piecewise cubic splines are often chosen as the admissible functions. Then we can express the solution by

$$u = \sum_{i=1}^{\infty} \bar{a}_i \Psi_i, \quad (0.1.2)$$

where \bar{a}_i are the true expansion coefficients. If only finite terms are chosen in (0.1.2), we obtain the approximate solution

$$v = \sum_{i=1}^N a_i \Psi_i, \quad (0.1.3)$$

where the coefficients a_i are an approximation of \bar{a}_i . Hence Eq. (0.1.1) leads to

$$\begin{cases} \sum_{i=1}^N a_i \mathcal{L}\Psi_i = f, \\ \sum_{i=1}^N a_i B\Psi_i = g. \end{cases}$$

Since there are N unknowns, we may choose $M(\geq N)$ collocation points to enforce (0.1.3) such that

$$\begin{aligned} \sum_{i=1}^N a_i \mathcal{L}\Psi_i(Q_j) &= f(Q_j), \quad j = 1, 2, \dots, M_1, \quad Q_j \in S, \\ \sum_{i=1}^N a_i B\Psi_i(Q_j) &= g(Q_j), \quad j = M_1 + 1, \dots, M, \quad Q_j \in \partial S. \end{aligned} \quad (0.1.4)$$

Since the differential equation and the boundary conditions play different roles in the boundary value problem, different weights should be imposed on (0.1.4),

$$\begin{aligned} \sum_{i=1}^N a_i \mathcal{L}\Psi_i(Q_j) &= f(Q_j), \quad j = 1, 2, \dots, M_1, \quad Q_j \in S, \\ \sum_{i=1}^N w_B a_i B\Psi_i(Q_j) &= w_B g(Q_j), \quad j = M_1 + 1, \dots, M, \quad Q_j \in \partial S, \end{aligned} \quad (0.1.5)$$

where the weight functions $w_B > 0$ may be different for different boundary conditions, $w_B = w_D, w_N, w_R$, respectively. Hence we obtain the discrete equations

$$\mathbf{Ax} = \mathbf{b}, \quad (0.1.6)$$

where $\mathbf{x} = (a_1, \dots, a_N)^T$ is the unknown vector, \mathbf{b} is a known vector, and the stiffness matrix is $\mathbf{A} = \mathbf{A}_{M \times N} = (a_{i,j})$. The matrix entries are given by

$$a_{j,i} = \mathcal{L}\Psi_i(Q_j), \quad j \leq M_1, \quad a_{j,i} = w_B B\Psi_i(Q_j), \quad j > M_1.$$

When $M > N$, Eq. (0.1.6) is an over-determined system, which can be solved by the least squares method, to provide the approximate coefficients a_i .

When $f = 0$ and the basis functions Ψ_i are particular solutions of $\mathcal{L}\Psi_i = 0$, the boundary equations are reduced to (i.e., $M_1 = 0$ in (0.1.5))

$$\sum_{i=1}^N w_B a_i B\Psi_i(Q_j) = w_B g(Q_j), \quad Q_j \in \partial S, \quad j = 1, 2, \dots, M.$$

This is called the CTM in this book, which is also referred as the indirect Trefftz method in Kita and Kamiya [261], or the boundary solution procedure in Zienkiewicz, Kelley and Bettess [508], and the TM in Zielinski and Zienkiewicz [507], Zielinski and Herrera [506] and Lefebvre [281].

We may represent (0.1.1) in the residual form

$$\begin{aligned} \iint_S R_E v \, ds &= \iint_S (\mathcal{L}u - f) v \, ds = 0, \\ \int_{\partial S} w_B R_B v \, dl &= \int_{\partial S} w_B (Bu - g) v \, dl = 0, \end{aligned} \quad (0.1.7)$$

where R_E and R_B are the residuals of the PDE and their boundary conditions. Let the test function v be the Dirac's delta function,

$$v = \delta(P - Q_i) = \begin{cases} \infty, & P = Q_i, \\ 0, & P \neq Q_i. \end{cases}$$

Since

$$\iint_S \delta(P - Q_i) f \, ds = f(Q_i),$$

Eq. (0.1.7) leads to (0.1.5) the CM.

In the early time, the CM was used for solving ODE, see Ascher, et al. [7], Russell and Shampine [416], Lucas and Reddien [333], Russell [414, 415], Parter and Sun [376], Dunn and Wheeler [140], Diaz [130] and Wheeler [486]. Later the CM is applied for solving PDE as well, see Bialecki and Cai [41], Prenter and Russell [389], Sun [448] and Quarteroni and Zampieri [393]. Besides, the residual method was studied by Percell and Wheeler [379] and Oliveira [368]. Recently, there have been a number of reports on the CM, see Bialecki [40], Bialecki and Fernandes [44], Bialecki and Dryja [42], Bialecki, Fairweather and Kargeorghis [43], Brunner, Pedas and Vainikko [68], Cao, Herdman and Xu [77], Chen, Micchelli and Xu [94], Laubin and Baiwir [277], Layton [278], Li, Fairweather and

Bialecki [283], Ma and Sun [334], Parter [374, 375], and Parter and Sun [376] and Russell and Sun [417]. Moreover, textbooks involving the CM have appeared, such as Ascher, Mattheij and Russell [7] for ODE, Quarteroni and Valli [392] for PDE, and Canuto et al. [75] for spectral methods.

The method using the orthogonal polynomials is also called the spectral method in Bernardi and Maday [37]. The spectral method as the Galerkin-FEM involving integration approximation may lead to the CM if some special nodes are chosen, such as the Gauss-Lobatto nodes (i.e., the roots of the polynomials)¹. References of spectral methods include Kreiss and Olinger [265], Gottlieb and Orszag [178], Boyd [52] and Canuto and Quarteroni [76].

0.1.2 Viewpoint of Boundary Approximation Methods

Consider the non-homogeneous elliptic equation with the Robin boundary condition,

$$\begin{aligned}\mathcal{L}u &= f, \text{ in } S, \\ p\frac{\partial u}{\partial \nu} + \alpha u &= g, \text{ on } \partial S,\end{aligned}$$

where $\alpha \geq 0$ and ν is the outward normal of ∂S . Suppose that a particular solution Ψ_0 can be found to satisfy

$$\mathcal{L}\Psi_0 = f.$$

By the transformation $w = u - \Psi_0$, we obtain the homogeneous elliptic equation with the revised Robin condition

$$\begin{aligned}\mathcal{L}w &= 0, \text{ in } S, \\ p\frac{\partial w}{\partial \nu} + \alpha w &= \bar{g}, \text{ on } \partial S,\end{aligned}$$

where $\bar{g} = g - (p\frac{\partial \Psi_0}{\partial \nu} + \alpha \Psi_0)$. Assuming that particular solutions can be found below, without the loss of generality, we may only consider the homogeneous equation,

$$\begin{aligned}\mathcal{L}u &= 0, \text{ in } S, \\ p\frac{\partial u}{\partial \nu} + \alpha u &= g, \text{ on } \partial S.\end{aligned}\tag{0.1.8}$$

Suppose that a complete set of particular solutions Ψ_i of (0.1.8) can be found explicitly,

$$\mathcal{L}\Psi_i = 0, \quad i = 1, 2, \dots$$

¹Note that since the Galerkin-FEM leads to the CM, which is different from (0.1.4), the error analysis is also different from this book.

Therefore the solution of (0.1.8) can be approximated by

$$u_L = \sum_{i=1}^L a_i \Psi_i, \quad (0.1.9)$$

where the coefficients a_i are to be determined. Let V_L denote the finite dimensional collection of u_L in (0.1.9). The weak solution of (0.1.8) can be expressed by

$$a(u, v) = f(v),$$

where

$$\begin{aligned} a(u, v) &= \iint_S (p \nabla u \cdot \nabla v + cuv) ds, \\ f(v) &= \oint_{\partial S} g v dl. \end{aligned}$$

The notation $\nabla = \vec{i} \frac{\partial}{\partial x} + \vec{j} \frac{\partial}{\partial y}$, and \vec{i} and \vec{j} are the unit vectors along the x and the y directions, respectively.

Since the admissible functions u_L in (0.1.9) already satisfy the equation $Lu = 0$, for v satisfying $\mathcal{L}v = 0$ we obtain from the Green theorem

$$\begin{aligned} a(u, v) &= \iint_S (p \nabla u \cdot \nabla v + cuv) ds + \int_{\partial S} \alpha uv dl \\ &= \oint_{\partial S} \left(p \frac{\partial u}{\partial \nu} + \alpha u \right) v dl = \oint_{\partial S} g v dl. \end{aligned}$$

This gives

$$\oint_{\partial S} \left(p \frac{\partial u_L}{\partial \nu} + \alpha u_L \right) v dl = \oint_{\partial S} g v dl, \quad \forall v \in V_L. \quad (0.1.10)$$

Since only the boundary condition is involved in (0.1.10), it is called the boundary approximation method (BAM) in Li [285, 287, 291].

Below we provide a variational approach. Since the admissible functions have satisfied the equation $Lu = 0$ already, then the coefficients a_i in (0.1.9) are chosen to satisfy the boundary conditions as best as possible. The solution of (0.1.10) can also be obtained as: To find $u_L \in V_L$ such that

$$I_R(u_L) = \min_{v \in V_L} I_R(v),$$

where

$$I_R(v) = \oint_{\partial S} \left(p \frac{\partial v}{\partial \nu} + \alpha v - g \right)^2 dl.$$

When the Dirichlet condition also occurs, we shall utilize the boundary penalty technique. Consider the elliptic boundary value problem

$$\begin{cases} \mathcal{L}u = 0, & \text{in } S, \\ u = g_1, & \text{on } \Gamma_D, \\ p \frac{\partial u}{\partial \nu} + \alpha u = g_3, & \text{on } \Gamma_M \cup \Gamma_N, \end{cases} \quad (0.1.11)$$

where $\alpha > 0$ on Γ_M , $\alpha = 0$ on Γ_N and $\Gamma_D \neq \emptyset$ for uniqueness of the solution. Define the energy

$$I_B(v) = \int_{\Gamma_D} (v - g_1)^2 dl + w^2 \int_{\Gamma_M \cup \Gamma_N} \left(p \frac{\partial v}{\partial \nu} + \alpha v - g_3 \right)^2 dl, \quad (0.1.12)$$

where w is a positive weight to balance two different boundary conditions. Since the solution derivatives are usually larger than the solutions themselves, we choose $w < 1$. Of course, a better choice of w should depend upon error analysis (see Chapter 1). The BAM for (0.1.12) is designed as: To seek $u_L \in V_L$ such that

$$I_B(u_L) = \min_{v \in V_L} I_B(v). \quad (0.1.13)$$

Eq (0.1.13) leads to

$$\mathbf{Ax} = \mathbf{b}, \quad (0.1.14)$$

where \mathbf{A} is symmetric and positive definite, but not sparse, and \mathbf{x} is the unknown vector consisting of components a_i . Eq. (0.1.14) is called the algebraic normal equations.

A remarkable advantage of BAM is high accuracy, due to its exponential convergence rates. The BAM is much simpler and more efficient than the original Ritz-Galerkin method (RGM), because the approximate process is reduced to that on ∂S only. The relation between RGM and BAM is analogous to that between FEM and BEM. However, the BAM is limited to elliptic equations with constant coefficients where particular solutions can be found. Also, the solution can be unstable if the discretized system is large. A remedy is that the solution domain may be divided into several or many subdomains with or without overlaps, and different particular solutions or different numerical methods can be used in different subdomains, see Herrera [201, 203].

In practical computation, the BAM (0.1.13) always involves the integration approximation of (0.1.12). Choose the simplest middle-point rule of integration, for example,

$$\int_a^b f(x) dx \approx \int_a^{\tilde{b}} f(x) dx = (b - a) f\left(\frac{a + b}{2}\right).$$

We partition ∂S into subintervals with the following partition nodes:

$$\begin{aligned} \Gamma_D : s_0 < s_1 < \dots < s_{M_2}, \\ \Gamma_M \cup \Gamma_N : s_{M_2} < s_{M_2+1} < \dots < s_M. \end{aligned}$$

Hence the integrals in (0.1.12) become

$$\begin{aligned} I_B(v) &\approx \tilde{I}_B(v) = \int_{\Gamma_D} (v - g_1)^2 d\ell + w^2 \int_{\Gamma_M \cup \Gamma_N} \left(p \frac{\partial v}{\partial \nu} + \alpha v - g_3 \right)^2 d\ell \\ &= \sum_{i=1}^{M_2} \left(f_{i-\frac{1}{2}} \right)^2 \delta s_i + w^2 \sum_{i=M_2+1}^M \left(f_{i-\frac{1}{2}}^* \right)^2 \delta s_i, \end{aligned} \quad (0.1.15)$$

where $\delta s_i = s_i - s_{i-1}$, $f = v - g_1$, $f^* = p \frac{\partial v}{\partial \nu} + \alpha v - g_3$, and $f_{i-\frac{1}{2}} = f(s_{i-\frac{1}{2}})$ with $s_{i-\frac{1}{2}} = \frac{s_i + s_{i-1}}{2}$. The BAM involving integration approximation is designed as: To seek $\tilde{u}_L \in V_L$ such that

$$\tilde{I}_B(\tilde{u}_L) = \min_{v \in V_L} \tilde{I}_B(v).$$

On the other hand, for (0.1.11) we may enforce functions (0.1.3) directly to satisfy the collocation equations at the midpoints of $[s_{i-1}, s_i]$

$$\begin{cases} f_{i-\frac{1}{2}} = 0, & i = 1, 2, \dots, M_2, \\ f_{i-\frac{1}{2}}^* = 0, & i = M_2 + 1, M_2 + 2, \dots, M. \end{cases} \quad (0.1.16)$$

Suppose that $M > N$, the number of equations is larger than that of unknown coefficients a_i . In the sense of the weighted least squares method, we should add some weights to the equations in (0.1.16) to balance the effects of different boundary conditions and different subsections. We multiply (0.1.16) by $\sqrt{\delta s_i}$ and $w\sqrt{\delta s_i}$ on Γ_D and $\Gamma_M \cup \Gamma_N$, respectively, to lead to

$$\begin{cases} \sqrt{\delta s_i} f_{i-\frac{1}{2}} = 0, & i = 1, 2, \dots, M_2, \\ w\sqrt{\delta s_i} f_{i-\frac{1}{2}}^* = 0, & i = M_2 + 1, M_2 + 2, \dots, M. \end{cases} \quad (0.1.17)$$

This is just the discrete CTM of (0.1.11), which is just the indirect TM in Kamiya and Kita [246, 261]. Summing the squares of all left sides in (0.1.17) yields exactly the energy approximation $\tilde{I}_B(v)$ in (0.1.15). For this reason, we call the BAM involving integration approximation as the CTM in this book.

In fact, we rewrite (0.1.17) as the over-determined system

$$\mathbf{F}\mathbf{x} - \mathbf{d} = 0, \quad (0.1.18)$$

where $\mathbf{F} \in R^{M \times N}$, $M > N$, $\mathbf{x} \in R^N$ and $\mathbf{d} \in R^M$. Then, from the above arguments we obtain for $v \in V_L$

$$\begin{aligned} \tilde{I}_B(v) &= (\mathbf{F}\mathbf{x} - \mathbf{d})^T (\mathbf{F}\mathbf{x} - \mathbf{d}) \\ &= \mathbf{x}^T \mathbf{F}^T \mathbf{F} \mathbf{x} - (\mathbf{d}^T \mathbf{F} \mathbf{x} + \mathbf{x}^T \mathbf{F}^T \mathbf{d}) + \mathbf{d}^T \mathbf{d}. \end{aligned}$$

Minimizing of $\tilde{I}_B(v)$ yields the normal equations

$$0 = \frac{\partial}{\partial \mathbf{x}} \tilde{I}_B(v) = \mathbf{F}^T \mathbf{F} \mathbf{x} - \mathbf{F}^T \mathbf{d},$$

i.e.,

$$\mathbf{A}\mathbf{x} = \mathbf{F}^T \mathbf{F}\mathbf{x} = \mathbf{F}^T \mathbf{d}. \quad (0.1.19)$$

Denote $\mathbf{b} = \mathbf{F}^T \mathbf{d}$, then the normal equation (0.1.19) is just (0.1.14).

There are two methods to seek the coefficients a_i : (a) To solve (0.1.18), and (b) to solve (0.1.19). Although the solution method (b) is simpler, the condition number is quadratically larger, given by

$$\text{Cond.}(\mathbf{A}) = \frac{\lambda_{max}(\mathbf{A})}{\lambda_{min}(\mathbf{A})} = \frac{\sigma_{max}^2(\mathbf{F})}{\sigma_{min}^2(\mathbf{F})} = \{\text{Cond.}(\mathbf{F})\}^2,$$

where σ_{max} and σ_{min} are the maximal and minimal singular values of \mathbf{F} , respectively. For method (a), we may employ the least squares method using the QR method or the singular value decomposition method in Golub and Loan [176], with the small condition number $\text{Cond.}(\mathbf{F}) = \frac{\sigma_{max}(\mathbf{F})}{\sigma_{min}(\mathbf{F})}$. Hence, method (a) solving the over-determined system (0.1.18) is strongly recommended.

The references on BAM are given in Delves [124], Delves and Hall [126], Delves and Freeman [125], Li [285, 287, 291], Li, Mathon and Sermer [316], Li and Mathon [314, 315], and Zielinski and Zienkiewicz [507].

In summary, the BAM is classified as TM in this book, and the BAM involving integration approximation is just the CTM. They are also called the indirect TM in Kita and Kamiya [261]. The theoretical analysis for the TM (i.e., BAM) was given in the Doctoral dissertation [285] of the first author in 1986, and that for the CTM in Chapter 2 in this book, also see Lu, Hu and Li [329].

0.1.3 Viewpoint of Least Squares Methods

Consider the three boundary conditions,

$$\begin{aligned} \mathcal{L}u &= f \quad \text{in } S, \\ u &= g_1 \quad \text{on } \Gamma_D, \\ p \frac{\partial u}{\partial \nu} &= g_2 \quad \text{on } \Gamma_N, \\ p \frac{\partial u}{\partial \nu} + \alpha u &= g_3 \quad \text{on } \Gamma_M. \end{aligned} \quad (0.1.20)$$

For solving (0.1.20), we may choose the objective functional as

$$\begin{aligned} I(v) &= \iint_S (\mathcal{L}v - f)^2 ds + w_1^2 \int_{\Gamma_D} (v - g_1)^2 d\ell + w_2^2 \int_{\Gamma_N} \left(p \frac{\partial v}{\partial \nu} - g_2 \right)^2 d\ell \\ &\quad + w_3^2 \int_{\Gamma_M} \left(p \frac{\partial v}{\partial \nu} + \alpha v - g_3 \right)^2 d\ell, \end{aligned} \quad (0.1.21)$$

where w_i are positive weight constants. The least squares method (LSM) is described as: To seek the solution $u \in V_H$ such that

$$I(u) = \min_{\forall v \in V_H} I(v),$$

where $V_H (\subset H^2(S))$ is the finite dimensional collection of admissible functions without satisfying any boundary conditions, and $H^2(S)$ is the Sobolev space. The least squares method can also be viewed as the squares residual method.

The advantages of LSM are that the associated matrix \mathbf{A} is always symmetric and positive definite (or semi-definite), and that rather complicated constraints of the solutions can be easily incorporated with the numerical method. However, the disadvantage of LSM is that the condition number will increase significantly, compared with FEM. Moreover, both essential and natural boundary conditions must be expressed in the energy explicitly.

One way to overcome the large condition number is to divide the domain into subregions. Given the continuity of solutions and flux along the interior boundary $\Gamma_0 = S^+ \cap S^-$ of two subdomains S^+ and S^- , the problem can be solved as follows. Let

$$u = \begin{cases} v^+ & \text{in } S^+, \\ v^- & \text{in } S^-. \end{cases}$$

Then the objective functional is modified as

$$\widehat{I}(v) = \iint_{S^+} (\mathcal{L}v - f)^2 ds + \iint_{S^-} (\mathcal{L}v - f)^2 ds + D(v),$$

where

$$\begin{aligned} D(v) &= w_4^2 \int_{\Gamma_0} (v^+ - v^-)^2 dl + w_5^2 \int_{\Gamma_0} \left(p \frac{\partial v^+}{\partial \nu} - p \frac{\partial v^-}{\partial \nu} \right)^2 dl \\ &+ w_1^2 \int_{\Gamma_D} (v - g_1)^2 dl + w_2^2 \int_{\Gamma_N} \left(p \frac{\partial v}{\partial \nu} - g_2 \right)^2 dl \\ &+ w_3^2 \int_{\Gamma_M} \left(p \frac{\partial v}{\partial \nu} + \alpha v - g_3 \right)^2 dl, \end{aligned}$$

and $w_i > 0$ are the weight constants. Hence, the LSM, the CM and the CTM can handle the interior boundary condition as well.

LSM may deal with complicated problems easily, as Navier-Stokes and even hyperbolic equations, see Aziz, Kellogg and Stephen [12], Bramble and Schatz [56, 57, 58], Bramble and Nitsche [55], Zhou and Feng [502], Aziz, Kellogg and Stephen [12], Bohmer and Locker [51], Huffel and Vandewalle [229], Bjorck [48] and Bochev and Gunzburger [49]. Note that these algorithms require high smoothness of admissible functions. Besides, reduction from PDEs to first-order systems of equations makes LSM reactive, see Carey

and Shen [79]. More reports of the least squares methods are given by Kim, Lee and Shin [258], Liu [325], Jiang [235] and Aziz and Liu [13]

In application, since the integrals in (0.1.21) can not be evaluated exactly, the numerical integration should be used. Then the integration nodes of quadrature rules should be chosen as the collocation nodes, and the LSM leads to exactly the CM. This linkage of the CM to the LSM is a key for error analysis in this book, which is different from most of the existing literature of the CM cited in Section 0.1.1. In the traditional CM, the special rules with special nodes such as the Gauss-Lobatto nodes are chosen so that the domain is limited to rectangles, and the Galerkin-FEM involving the integration approximation leads to the CM. The error bounds are obtained by the Strang lemma, where the true errors include both the interpolation errors and the integration errors. In this book, the integration errors play a role only to satisfy the uniformly V_h - elliptic inequality, so that the simplest central rule may retain high convergence rates, such as exponential convergence rates of the CTM, even for polygonal domains or other bounded domains.

0.1.4 Complete Systems of Solutions

The algorithm for the CTM requires the explicit knowledge of the particular solutions. For the standard PDEs with the constant coefficients on the regular domains, such as the rectangular and sectorial domains, the particular solutions can be found by the techniques of separation of variables. A number of particular solutions are provided in the PDE textbooks. In some cases, a special analysis as in Li [286] is also necessary in order to derive the particular solutions needed. In this subsection, we collect the particular solutions of a few typical equations in 2D, which are often used in application. The problems on the unbounded domains and in 3D can be similarly solved by following the approaches in this book.

First, consider the disc

$$S = \{(r, \theta) \mid 0 \leq r < R, \quad 0 \leq \theta \leq 2\pi\}, \quad (0.1.22)$$

and the unbounded domain outside a disc

$$S_\infty = \{(r, \theta) \mid R < r < \infty, \quad 0 \leq \theta \leq 2\pi\}. \quad (0.1.23)$$

We list the following particular solutions for a few PDEs, see also Tikhonov and Samarskii [458], Herrera [201] and Zielinski [505],

I. For the Laplace equation, $\Delta u = 0$, the particular solutions for (0.1.22) and (0.1.23) are

$$\begin{aligned} &1, \quad r^n \cos n\theta, \quad r^n \sin n\theta, \quad n = 1, 2, \dots, \quad (r, \theta) \in S, \\ &\ln \frac{1}{r}, \quad r^{-n} \cos n\theta, \quad r^{-n} \sin n\theta, \quad n = 1, 2, \dots, \quad (r, \theta) \in S_\infty, \end{aligned}$$

respectively.

II. For the equation, $-\Delta u + k^2 u = 0$ with real $k > 0$, the particular solutions for (0.1.22) and (0.1.23) are

$$\begin{aligned} I_0(kr), \quad I_n(kr) \cos n\theta, \quad I_n(kr) \sin n\theta, \quad n = 1, 2, \dots, \quad (r, \theta) \in S, \\ K_0(kr), \quad K_n(kr) \cos n\theta, \quad K_n(kr) \sin n\theta, \quad n = 1, 2, \dots, \quad (r, \theta) \in S_\infty, \end{aligned}$$

respectively, where $I_\mu(r)$ and $K_\mu(r)$ are the Bessel and Hankel functions for a purely imaginary argument respectively, defined by

$$\begin{aligned} I_\mu(r) &= \sum_{k=0}^{\infty} \frac{1}{\Gamma(k+1)\Gamma(k+\mu+1)} \left(\frac{r}{2}\right)^{2k+\mu}, \\ K_\mu(r) &= \frac{1}{2} \int_{-\infty}^{\infty} \exp(-r \cosh \eta - \mu\eta) d\eta. \end{aligned}$$

When $k = 1$, $-\Delta u + u = 0$ is the Debye-Huckel equation.

III. For the Helmholtz equation, $\Delta u + k^2 u = 0$ with real $k > 0$. Suppose that k^2 is not an eigenvalue of Laplace's operator, then the particular solutions for (0.1.22) and (0.1.23) are

$$\begin{aligned} J_0(kr), \quad J_n(kr) \cos n\theta, \quad J_n(kr) \sin n\theta, \quad n = 1, 2, \dots, \quad (r, \theta) \in S, \\ H_0^{(1)}(kr), \quad H_n^{(1)}(kr) \cos n\theta, \quad H_n^{(1)}(kr) \sin n\theta, \quad n = 1, 2, \dots, \quad (r, \theta) \in S_\infty, \end{aligned}$$

respectively, where $J_\mu(r)$ and $H_\mu^{(1)}(r)$ are the Bessel and Hankel functions of the first kind respectively, defined by

$$\begin{aligned} J_\mu(r) &= \sum_{k=1}^{\infty} \frac{(-1)^k}{\Gamma(k+1)\Gamma(k+\mu+1)} \left(\frac{r}{2}\right)^{2k+\mu}, \\ H_\mu^{(1)}(r) &= \frac{i}{\sin \nu\pi} \{\exp(-\mu\pi i)J_\mu(r) - J_{-\mu}(r)\}. \end{aligned}$$

For the unbounded domain problem on S_∞ , the Sommerfeld radiation condition is satisfied.

IV. For the biharmonic equation, $\Delta^2 u = 0$, the particular solutions for (0.1.22) are

$$\begin{aligned} 1, \quad r^n \cos n\theta, \quad r^n \sin n\theta, \quad n = 1, 2, \dots, \\ r^2, \quad r^{n+2} \cos n\theta, \quad r^{n+2} \sin n\theta, \quad n = 1, 2, \dots, \quad (r, \theta) \in S. \end{aligned}$$

In application, we should consider the particular solutions on a sector with different boundary conditions. In Chapter 13, detailed results are provided for the Laplace

equation. Here we only give the particular solutions on

$$S^* = \{(r, \theta) \mid 0 \leq r < R, \ 0 \leq \theta \leq \Theta\}, \Theta \leq 2\pi, \quad (0.1.24)$$

and the unbounded domain outside a sector

$$S_\infty^* = \{(r, \theta) \mid R < r < \infty, \ 0 \leq \theta \leq \Theta\}, \Theta \leq 2\pi. \quad (0.1.25)$$

Let $\Theta = \pi$, then the S^* is a semi-disc. Suppose that the mixed type of the Dirichlet and Neumann conditions are provided as

$$\frac{\partial u}{\partial \nu} = 0 \quad \text{at} \quad \theta = 0; \quad u = 0 \quad \text{at} \quad \theta = \pi, \quad (0.1.26)$$

which result in Motz's problem and the interior crack problems. We also list their particular solutions without proof.

V. For the Laplace equation, $\Delta u = 0$, the particular solutions for (0.1.24) and (0.1.25) are

$$r^{n+\frac{1}{2}} \cos(n + \frac{1}{2})\theta, \quad n = 0, 1, \dots, \quad (r, \theta) \in S^*, \quad (0.1.27)$$

$$r^{-(n+\frac{1}{2})} \cos(n + \frac{1}{2})\theta, \quad n = 0, 1, \dots, \quad (r, \theta) \in S_\infty^*,$$

respectively.

VI. For the equation, $-\Delta u + k^2 u = 0$ with real $k > 0$, the particular solutions for (0.1.24) and (0.1.25) are

$$I_{n+\frac{1}{2}}(kr) \cos(n + \frac{1}{2})\theta, \quad n = 0, 1, \dots, \quad (r, \theta) \in S^*,$$

$$K_{n+\frac{1}{2}}(kr) \cos(n + \frac{1}{2})\theta, \quad n = 0, 1, \dots, \quad (r, \theta) \in S_\infty^*,$$

respectively.

VII. For the Helmholtz equation, $\Delta u + k^2 u = 0$ with real $k > 0$, the particular solutions for (0.1.24) and (0.1.25) are

$$J_{n+\frac{1}{2}}(kr) \cos(n + \frac{1}{2})\theta, \quad n = 0, 1, \dots, \quad (r, \theta) \in S^*,$$

$$H_{n+\frac{1}{2}}^{(1)}(kr) \cos(n + \frac{1}{2})\theta, \quad n = 0, 1, \dots, \quad (r, \theta) \in S_\infty^*,$$

respectively.

VIII. For the biharmonic equation, $\Delta^2 u = 0$, with the symmetric and clamped boundary conditions are given on the boundary of S^* as

$$\frac{\partial u}{\partial \nu} = \frac{\partial^3 u}{\partial \nu^3} = 0 \text{ at } \theta = 0; \quad u = \frac{\partial u}{\partial \nu} = 0 \text{ at } \theta = \Theta.$$

Then the particular solutions are given by

$$\begin{aligned} & r^{n+1} [\cos(n-1)\theta - \cos(n+1)\theta], \\ & r^{n+\frac{1}{2}} \left[\cos(n-\frac{3}{2})\theta - \frac{n-\frac{3}{2}}{n+\frac{1}{2}} \cos(n+\frac{1}{2})\theta \right], \quad n = 1, 2, \dots, \quad (r, \theta) \in S^*. \end{aligned} \quad (0.1.28)$$

The TM using (0.1.28) is reported in Chapter 4.

There are some systematic methods for deriving the complete systems of particular solutions. Of course, the separation of variables is most popular. Maybe, the most extensive one stems from the function theoretic approach, which was pioneered by Bergman [33] and Vekua [469], and then further developed by Colton, Gilbert, Kracht-Kreyzig, Lanckau and others. A good survey of these methods is given in [30]. The other approach of T-complete systems proposed by Herrera and his colleagues (see [199, 200]) has been applied for a variety of problems. For instant, the T-complete systems for Stokes problems and biharmonic equations were given in [207] and [179], respectively, and a remarkably simple T-complete system developed for plane waves of the Helmholtz equation (or called the reduced wave equation) was also reported in [419]. Other developments of T-complete systems include Jirousek and Wroblewski [242] and Jirousek and Zielinski [243].

0.2 Coupling Techniques

For matching different particular solutions in the TM, or matching the TM with other methods, an effective coupling strategy is essential, in order to yield optimal convergence rates and good stability of the numerical solutions. To minimize the error, we use an additional integral equation along the common boundary, and apply a penalty plus hybrid technique. Such techniques have been applied in the standard FEM in Arnold [5], Baker [21], Barrett and Elliott [26], Nitsche [363], Fairweather [150] and Gatica, Harbrecht and Schneider [163].

0.2.1 Six Combinations

Below, we list six efficient coupling techniques for combinations of the TM and FEM. Details are given in [297, 299, 291]. Consider a general elliptic equation

$$-\frac{\partial}{\partial x} \left(p \frac{\partial u}{\partial x} \right) - \frac{\partial}{\partial y} \left(p \frac{\partial u}{\partial y} \right) + cu = f, \quad (x, y) \in S, \quad (0.2.1)$$

with the boundary conditions

$$u = g_1 \text{ on } \Gamma_D, \quad (0.2.2)$$

$$\frac{\partial u}{\partial \nu} + qu = g_2 \text{ on } \Gamma_M, \quad (0.2.3)$$

where the domain S is a bounded polygon with the exterior boundary $\Gamma = \Gamma_D \cup \Gamma_M$ and $\text{Meas}(\Gamma_D) > 0$. The functions p, c, f, q, g_1 and g_2 are sufficiently smooth, and

$$c = c(x, y) \geq 0, \quad q = q(x, y) \geq 0, \quad p = p(x, y) \geq p_0 > 0,$$

where p_0 is a constant.

The solution of the problem (0.2.1) – (0.2.3) can be equivalently expressed by minimizing a quadratic functional $I(v)$ ²:

$$I(u) = \min_{v \in H_*^1(S)} I(v), \quad (0.2.4)$$

where the quadratic functional is

$$I(v) = \frac{1}{2} \iint_S [p(\nabla v \cdot \nabla v) + cv^2] ds + \frac{1}{2} \int_{\Gamma_M} qv^2 dl - \iint_S fv ds - \int_{\Gamma_M} g_2 v dl,$$

and $H_*^1(S)$ is a set of the space defined as

$$H_*^1(S) = \{v \mid v, v_x, v_y \in L^2(S), \text{ and } v|_{\Gamma_D} = g_1\}.$$

Let S be divided by Γ_0 , the piecewise straight line, into S_1 and S_2 . The TM is used in S_2 , and the $k(\geq 1)$ -order Lagrange finite element method is used in S_1 , where the true solution is supposed to be smooth enough such that $u \in H^{k+1}(S_1)$. Therefore, the admissible functions can be written as follows:

$$v = \begin{cases} v^- = V_1^k & \text{in } S_1, \\ v^+ = \sum_{i=1}^N a_i \Psi_i & \text{in } S_2, \end{cases} \quad (0.2.5)$$

where V_1^k are piecewise k -order Lagrange interpolation polynomials on the quasiuniform triangulation of S_1 with the maximal boundary length h , $\{\Psi_i\}$ are analytic, complete and linearly independent basis functions on S_2 , and a_i are unknown coefficients to be sought. Note that the admissible functions v^+ in (0.2.5) may not satisfy the elliptic equation (0.2.1) exactly.

²In some cases, e.g., $P_c = 0$, $\alpha = 1$ and $\beta = 0$ for the simplified hybrid combined method, the minimum (0.2.4) does not hold. However, the first variation of $I_n^{(1,0)}(v)$ provides the desired equation of the solution.

Define a space

$$H = \{v \mid v \in L^2(S), v \in H^1(S_1), v \in H^1(S_2) \text{ and } v|_{\Gamma_D \cap \partial S_1} = g_1\}.$$

Let $V_h^* \subset H$ be a finite-dimensional collection of the functions (0.2.5). For simplicity, we assume that the functions $v \in V_h^*$ will strictly satisfy the Dirichlet boundary condition (0.2.2) on $\Gamma_D \cap \partial S_1$ where the FEM is used (otherwise, see Strang and Fix [446]). In this subsection, the combination using the penalty plus hybrid techniques is designed as: To seek an approximate solution $u_h \in V_h^*$ such that³

$$I_h^{(\alpha, \beta)}(u_h) = \min_{v \in V_h^*} I_h^{(\alpha, \beta)}(v), \quad (0.2.6)$$

where

$$\begin{aligned} I_h^{(\alpha, \beta)}(v) = & \frac{1}{2} \iint_{S_1} (p(\nabla v \cdot \nabla v) + cv^2) ds + \frac{1}{2} \iint_{S_2} (p(\nabla v \cdot \nabla v) + cv^2) ds \quad (0.2.7) \\ & + \frac{1}{2} \int_{\Gamma_M} qv^2 dl + \frac{P_c}{2h^{*\sigma}} \int_{\Gamma_D \cap S_2} (v^+ - g_1)^2 dl \\ & - \int_{\Gamma_D \cap S_2} p \frac{\partial v^+}{\partial n} (v^+ - g_1) dl + \frac{P_c}{2h^{*\sigma}} \int_{\Gamma_0} (v^+ - v^-)^2 dl \\ & - \int_{\Gamma_0} p \left(\alpha \frac{\partial v^+}{\partial n} + \beta \frac{\partial v^-}{\partial n} \right) (v^+ - v^-) dl - \iint_S f v ds - \int_{\Gamma_M} g_2 v dl, \end{aligned}$$

where α and β are two real parameters, $P_c > 0$, $\sigma > 0$, and h^* is the maximal boundary length of finite elements on Γ_0 . The right hand side of (0.2.7) shows the general approach of using additional integral for interface coupling, which contains the following six possible combinations, based on different α and β values:

1. **Combination I:** $P_c > 0$, and $\alpha = 0$, $\beta = 1$.
2. **Combination II:** $P_c > 0$, and $\alpha = 1$, $\beta = 0$.
3. **Symmetric Combination:** $P_c > 0$, and $\alpha = \beta = \frac{1}{2}$.
4. **The Simplified Hybrid Combined Method:** $P_c = 0$, $\alpha = 1$ and $\beta = 0$.
5. **The Penalty Combination in Li [290]:** $P_c > 0$, and $\alpha = \beta = 0$.
6. **The Nonconforming Combination in Li [284]:** as $P_c \rightarrow \infty$, or $\sigma \rightarrow \infty$.

The important analysis in [291] and the references cited wherein to prove that the optimal convergence rates of

$$\|\varepsilon\|_h = \{ \|\varepsilon\|_{1, S_1}^2 + \|\varepsilon\|_{1, S_2}^2 \}^{\frac{1}{2}} = O(h^k)$$

can be achieved for coupling the k -order FEM with the TM. Also a stability analysis indicates that the condition number of the stiffness matrix is

$$Cond. = O(h^{-2} + P_c h^{-(2+\sigma)}), \quad \sigma \in (0, 1].$$

³For the simplified hybrid combined method, Eq. (0.2.6) should be replaced by seeking the critical point, $\frac{\partial I_h^{(1,0)}(v)}{\partial v} = 0$.

0.2.2 The Original TM

Consider the Laplace equation with the Dirichlet boundary condition $u = g$ on Γ , and the TM is used on the whole domain with no interior boundary Γ_0 . The simplified hybrid method is given from (0.2.6) as: To seek an approximate solution $u_L \in V_L$ such that

$$I_{Simp}(u_L) = \min_{v \in V_L} I_{Simp}(v), \quad (0.2.8)$$

where

$$I_{Simp}(v) = \frac{1}{2} \iint_S (\nabla v \cdot \nabla v) ds - \int_{\Gamma} \frac{\partial v}{\partial n} (v - g) d\ell.$$

Suppose that the admissible functions are also harmonic,

$$v_L = \sum_{i=1}^L a_i \Psi_i, \quad \nabla^2 \Psi_i = 0, \quad \text{in } S,$$

where a_i are real coefficients, and V_L is the finite dimensional collection of v_L . Eq. (0.2.8) is just the original TM in Trefftz [461], see Section A.6, and more discussions are given in Section 3.4. The error analysis of such a method is reported in Li and Liang [308], Li and Bui [296, 298], Li [293] and Li and Huang [303]. The indirect TM is reported in Kita, Ikeda and Kamiya [260] and Chang et al. [86]. The TM with FEM and boundary element method (BEM) is discussed in Qin [391].

0.2.3 The Direct TM

In order to accommodate

$$u^+ = u^-, \quad \text{on } \Gamma_0, \quad (0.2.9)$$

in the nonconforming combination, the direct constraints of the admissible functions as the collocation equations,

$$v^+(Q_i) = v^-(Q_i), \quad \forall Q_i \in \Gamma_0 \quad (0.2.10)$$

can be employed, without using the additional integral on Γ_0 . In (0.2.10), Q_i denote the element nodes on Γ_0 . Define by $\bar{V}_h \subset H$ a finite dimensional collection of the admissible functions (0.2.5) that satisfy the constraint conditions (0.2.10) and the Dirichlet boundary condition (0.2.2). We obtain the nonconforming combination from (0.2.7) as $P_c = \alpha = \beta = 0$

$$\frac{\partial}{\partial v} I_h^{(0,0)}(u_h) = 0, \quad v \in \bar{V}_h.$$

Now we turn to the continuity requirement (0.2.9), by introducing an additional integral $\int_{\Gamma_0} \lambda(v^+ - v^-) d\ell$, where λ is a continuous function of Lagrange multipliers. We

describe the Lagrange multiplier coupling as: To seek $(u_h, \lambda) \in \bar{V}_h \times R$ such that

$$B(u_h, v; \lambda, \mu) = f(v), \quad (v, \mu) \in \bar{V}_h \times R, \quad (0.2.11)$$

where

$$\begin{aligned} B(u, v; \lambda, \mu) &= \iint_{S_1} (p \nabla u \cdot \nabla v + cuv) ds \\ &+ \iint_{S_2} (p \nabla u \cdot \nabla v + cuv) ds + D(u, v; \lambda, \mu), \end{aligned} \quad (0.2.12)$$

where $(v, \mu) \in \bar{V}_h \times R$ denotes that $v \in \bar{V}_h$ and $\mu \in R$, and the boundary integrals are

$$\begin{aligned} D(u, v; \lambda, \mu) &= \int_{\Gamma_N} q u v d\ell - \int_{\Gamma_D \cap S_2} \lambda v d\ell - \int_{\Gamma_D \cap S_2} \mu u d\ell \\ &- \int_{\Gamma_0} \lambda (v^+ - v^-) d\ell - \int_{\Gamma_0} \mu (u^+ - u^-) d\ell, \end{aligned}$$

and the Lagrange multiplier λ has the true solution, $\lambda = p \frac{\partial u}{\partial n} \Big|_{\Gamma_0}$. In (0.2.12), the λ is treated as an extra variable.

Consider the Laplace equation with the Dirichlet condition $u = g$ on Γ , the TM is used in the entire domain without interior boundary. We have from (0.2.11)

$$\iint_S \nabla u \cdot \nabla v ds - \int_{\Gamma} \mu (u - g) d\ell - \int_{\Gamma} \lambda v d\ell = 0, \quad (0.2.13)$$

where $p = 1$, $\lambda = \frac{\partial u}{\partial n}$ is treated as unknown, and $\lambda, \mu \in H^{-\frac{1}{2}}(\Gamma)$. $H^{-\frac{1}{2}}(\Gamma)$ is the negative norm in the Sobolev space. In fact, we may define a function

$$F(v) = \frac{1}{2} \iint_S \nabla v \cdot \nabla v ds - \int_{\Gamma} \mu (v - g) d\ell.$$

The variational equation, $\frac{\partial F(v)}{\partial v} = 0$, leads to (0.2.13). This is called the Lagrange multiplier method in [291], which is just the direct TM in Jin and Cheung [237] and Kamiya and Kita [246]. The direct TM is explored in Li [292, 291], and in Section 3.6.

The Lagrange multiplier method was first introduced by Babuska [14] to treat the constraint Dirichlet boundary condition as a natural boundary condition, and to relax the limitation on the admissible functions used. Since then the techniques of Lagrange multipliers have drawn much attention. Such techniques have been adopted to mixed and hybrid methods, see Brezzi and Fortin [65] and Raviart and Thomas [395].

The boundary condition using Lagrange multipliers is also extended to that involving flux in Bramble [54]. More analysis and applications are given in Fix [153], Pitkaranta [383, 384], Lee [280], Barbosa and Hughes [25], and particularly for domain decomposition methods in Liang and Liang [319], Liang and He [318], and Mandel and Tezaur [340].

0.2.4 Trefftz-Herrera Approaches for Coupling Problems

By the Green formulas, the Trefftz method (TM) can be extended to general elliptic equations, the framework of which was given by the algebraic approaches in Herrera [201] in 1984. Since the algebraic notations and operations are simple and easily understood (see Section A.5 in Appendix), the Trefftz method (or called the Trefftz-Herrera approaches in this book) has been applied to many engineering problems, in particular, the coupling problems where there exist the jumps of both the solutions and their derivatives along the interior boundary Γ_0 (see Section A.7). A great progress has been made by Herrera and his colleagues, and numerous papers have been published. Here we only mention a few important works, Herrera [200, 201, 202, 203], Herrera and Diaz [205, 206] and Herrera and Solano [208], and a complete list of references for the Trefftz-Herrera approaches can be found in [200, 203].

Consider the self-adjoint second order elliptic equations,

$$-\nabla \cdot (p^\pm \nabla u^\pm) + c^\pm u^\pm = f^\pm \text{ in } S^\pm, \quad (0.2.14)$$

$$u = g \text{ on } \Gamma, \quad (0.2.15)$$

where $\Gamma = \partial S$, $S = S^+ \cup S^- \cup \Gamma_0$, and Γ_0 is the interior boundary with the jumps

$$[u]_{\Gamma_0} = \delta, \quad [pu_\nu]_{\Gamma_0} = \delta_\nu. \quad (0.2.16)$$

In (0.2.16), the notations are

$$[u]_{\Gamma_0} = u^+ \Big|_{\Gamma_0} - u^- \Big|_{\Gamma_0}, \quad [pu_\nu]_{\Gamma_0} = p^+ u_\nu^+ \Big|_{\Gamma_0} - p^- u_\nu^- \Big|_{\Gamma_0},$$

and δ and δ_ν are the known jump functions. In (0.2.14) – (0.2.16), the coefficient functions satisfy $p^\pm > p_0 > 0$ and $c^\pm \geq 0$. We assume that the functions $p^\pm, c^\pm, f^\pm, \delta$ and δ_ν are smooth enough so that the solutions within S^+ and S^- are also smooth⁴. When $\delta \neq 0$ or $\delta_\nu \neq 0$, Eqs. (0.2.14) – (0.2.16) are also called the coupling problems in some engineering literature.

Denote the subsets

$$H_*^\#(S) = \{v = v^\pm \in H^1(S^\pm), v \Big|_\Gamma = g, \text{ and } [v] \Big|_{\Gamma_0} = \delta\},$$

$$H_0^\#(S) = \{v = v^\pm \in H^1(S^\pm), v \Big|_\Gamma = 0, \text{ and } [v] \Big|_{\Gamma_0} = 0\}.$$

The solution u of (0.2.14) – (0.2.16) can be expressed in a weak form: To seek $u \in H_*^\#(S)$ such that

$$A(u, v) = f(v), \quad \forall v \in H_0^\#(S), \quad (0.2.17)$$

⁴Such a smoothness of the solutions does not include the case of crossing Γ_0 .

where

$$\begin{aligned} A(u, v) &= \iint_{S^+} (p^+ \nabla u^+ \cdot \nabla v^+ + c^+ u^+ v^+) + \iint_{S^-} (p^- \nabla u^- \cdot \nabla v^- + c^- u^- v^-), \\ f(v) &= \iint_{S^+} f^+ v^+ + \iint_{S^-} f^- v^- + \frac{1}{2} \int_{\Gamma_0} \delta_\nu (v^+ + v^-). \end{aligned}$$

First let us choose the FEM. Denote the finite dimensional collections $V_h^*(\subset H_*^\#(S))$ and $V_h^0(\subset H_0^\#(S))$ for the piecewise k -order polynomials. The FEM can be expressed by: To seek $u_h \in V_h^*$ such that

$$A(u_h, v) = f(v), \quad \forall v \in V_h^0. \quad (0.2.18)$$

Since to formulate the admissible functions v satisfying $[v]_{\Gamma_0} = \delta$ and $v|_{\Gamma} = g$ is rather complicated, we resort to the coupling techniques. Take the penalty coupling for example. The admissible functions do not necessarily satisfy $[v]_{\Gamma_0} = \delta$ and $v|_{\Gamma} = g$. Denote $H_*(s) = \{v^\pm \in H^1(S^\pm)\}$, and the finite dimensional collection $V_h(\subset H_*(S))$ of piecewise k -order polynomials. The penalty method can be expressed by: To seek $u_h^P \in V_h$ such that

$$A_h(u_h^P, v) = f(v), \quad \forall v \in V_h, \quad (0.2.19)$$

where

$$\begin{aligned} A_h(u, v) &= A(u, v) \\ &+ \frac{P_c}{h^{2\sigma}} \widehat{\int}_{\Gamma_0} (u^+ - u^- - \delta)(v^+ - v^-) + \frac{P_c}{h^{2\sigma}} \widehat{\int}_{\Gamma} (u - g)v, \end{aligned} \quad (0.2.20)$$

$A(u, v)$ and $f(v)$ are given in (0.2.17), and $\widehat{\int}_{\Gamma_0}$ is the approximation of \int_{Γ_0} by some rules. In (0.2.20), the parameters $\sigma (> 0)$ may be suitably chosen to be independent of h , where h is the the maximal boundary of triangular elements Δ_{ij} or rectangular elements \square_{ij} . Suppose that the solutions u^\pm within S^\pm are smooth enough, and that the Δ_{ij} or the \square_{ij} are quasiuniform, the optimal convergence $O(h^k)$ and the superconvergence $O(h^{k+p})$, $p = 1, 2$ in H^1 norm can be achieved. When there exists a singularity of solutions on ∂S^\pm , the combinations of the TM and the FEMs can be employed, to reach the same optimal convergence and the same superconvergence, see Chapter 10.

Suppose that $f^\pm \equiv 0$, we may use the CTM in Section 0.1.2. Let Φ_i^\pm satisfy the elliptic equations exactly

$$\nabla(p^\pm \nabla \Phi_i^\pm) + c^\pm u^\pm = 0 \text{ in } S^\pm.$$

Then the solution can be approximated by the linear combination of Φ_i^\pm ,

$$u_n = u_n^\pm = \sum_{i=0}^{n^\pm} a_i^\pm \Phi_i^\pm \text{ in } S^\pm, \quad (0.2.21)$$

where n^\pm are positive integers, and the coefficients a_i^\pm can be sought by fitting the exterior and interior boundary conditions as best as possible. Denote the energy

$$I(v) = \widehat{\int}_{\Gamma_0} (v^+ - v^- - \delta)^2 + w^2 \widehat{\int}_{\Gamma_0} (p^+ v_\nu^+ - p^- v_\nu^- - \delta_\nu)^2 + \widehat{\int}_{\Gamma} (v - g)^2,$$

where $w > 0$ is a suitable weight. The solution \hat{u}_n can be obtained by

$$I(\hat{u}_n) = \min_{v \in V_n} I(v), \quad (0.2.22)$$

where V_n is the finite dimensional collection of (0.2.21). Suppose that the simplest central rule is applied to get $\widehat{\int}_{\Gamma_0}$. Then Eq.(0.2.22) can be reduced to the least squares problem of the following collocation equations,

$$\begin{aligned} [u_n] \Big|_{Q_i} &= \delta \Big|_{Q_i}, \quad w[p(u_n)_\nu] \Big|_{Q_i} = w\delta_\nu \Big|_{Q_i}, \quad Q_i \in \Gamma_0, \\ u_n \Big|_{P_i} &= g \Big|_{P_i}, \quad P_i \in \Gamma, \end{aligned}$$

where Q_i and P_i are the middle nodes of small intervals of Γ_0 and Γ respectively. Obviously, This CTM is simpler and more efficient than the FEM in (0.2.18). Its error and stability analysis is demonstrated in this book, and the exponential convergence rates can be achieved, see Chapters 1 and 2. When the piecewise k -order polynomials are replaced by (0.2.21), Eq. (0.2.19) may lead to the penalty TM. Other kinds of TMs can be further developed.

The Trefftz-Herrera domain decomposition is described in Herrera and Diaz [206] for the general second order elliptic equation

$$-\nabla \cdot (p^\pm \nabla u^\pm) + \nabla \cdot (\mathbf{b}^\pm u^\pm) + c^\pm u^\pm = f^\pm, \quad \text{in } S^\pm, \quad (0.2.23)$$

with interior jump conditions, where \mathbf{b}^\pm is a vector. The non-self-adjoint term $\nabla \cdot (\mathbf{b}^\pm u^\pm)$ results from the convection flow. When the norm $\|\mathbf{b}^\pm\|$ is large, the solution of (0.2.23) may represent the convection-dominant flow with a boundary layer singularity. Moreover, for the general $2m$ order elliptic equations, the Green formulas are given in Oden and Reddy [365], p.165, in which the interior jump conditions can be obtained, and the algorithms of CTM may be easily formulated. Based on the regularity of solutions in Chapter 5 in [365], the error bounds of the solutions by the CTM for the general elliptic equations involving the solution jumps on Γ_0 may be further developed; details will be reported later.

0.3 Boundary Element Methods

In this section, we provide a concise introduction of the boundary element method (BEM) for smooth solutions. The systematic and comprehensive introduction of BEM can be found in Brebbia [60], Brebbia and Dominguez [64] and Atkinson [10].

0.3.1 Green Theorem

Let ∂S be piecewise smooth, and functions $u, v \in C^2(S)$. Then the Green formula is given by

$$\iint_S (vTu - uTv) ds = \oint_{\partial S} \left(v p \frac{\partial u}{\partial \nu} - u p \frac{\partial v}{\partial \nu} \right) d\ell,$$

where

$$Tu = \left(\frac{\partial}{\partial x} p \frac{\partial u}{\partial x} + \frac{\partial}{\partial y} p \frac{\partial u}{\partial y} \right).$$

For simplicity, let us consider Poisson's equation.

$$-\Delta u = f \text{ in } S, \quad u = g_1 \text{ on } \Gamma_D, \quad \frac{\partial u}{\partial \nu} = g_2 \text{ on } \Gamma_N, \quad (0.3.1)$$

where $\Delta = \frac{\partial^2}{\partial x^2} + \frac{\partial^2}{\partial y^2}$. Choose the fundamental solution of Laplace's equation

$$w = \frac{1}{2\pi} \ln \frac{1}{r}, \quad r = \sqrt{(x - x_0)^2 + (y - y_0)^2}, \quad M_0 = (x_0, y_0) \in S.$$

We provide two important lemmas without proof.

Lemma 0.3.1 *Let $\frac{\partial u}{\partial \nu} \in C(\partial S)$, then the solution*

$$u(M_0) = \frac{1}{2\pi} \left\{ \int_{\partial S} \left[\left(\ln \frac{1}{r} \right) \frac{\partial u}{\partial \nu} - u \frac{\partial}{\partial \nu} \left(\ln \frac{1}{r} \right) \right] d\ell + \iint_S \left(\ln \frac{1}{r} \right) f ds \right\}, \quad \forall M_0 \in S. \quad (0.3.2)$$

It can be seen from (0.3.2) that, if both u and $\frac{\partial u}{\partial \nu}$ on ∂S are known, the interior solutions may be obtained immediately. However, if only one of u and $\frac{\partial u}{\partial \nu}$ at each point of ∂S is known from the boundary conditions in (0.3.1), then the other boundary values can be obtained as below.

Lemma 0.3.2 *Let $\frac{\partial u}{\partial \nu} \in C(\partial S)$, then*

$$u(M_0) = \frac{1}{\pi} \left\{ \int_{\partial S} \left[\ln \left(\frac{1}{r} \right) \frac{\partial u}{\partial \nu} - u \frac{\partial}{\partial \nu} \left(\ln \frac{1}{r} \right) \right] d\ell + \iint_S \left(\ln \frac{1}{r} \right) f ds \right\}, \quad \forall M_0 \in \partial S. \quad (0.3.3)$$

From the boundary conditions in (0.3.1), we have

$$\begin{aligned} \int_{\partial S} u \frac{\partial}{\partial \nu} \ln \left(\frac{1}{r} \right) d\ell &= \int_{\Gamma_D} g_1 \frac{\partial}{\partial \nu} \ln \left(\frac{1}{r} \right) d\ell + \int_{\Gamma_N} u \frac{\partial}{\partial \nu} \ln \left(\frac{1}{r} \right) d\ell, \\ \int_{\partial S} \ln \left(\frac{1}{r} \right) \frac{\partial u}{\partial \nu} d\ell &= \int_{\Gamma_D} \ln \left(\frac{1}{r} \right) \frac{\partial u}{\partial \nu} d\ell + \int_{\Gamma_N} g_2 \ln \left(\frac{1}{r} \right) d\ell. \end{aligned}$$

Hence we obtain from Lemma 0.3.2

$$\begin{aligned} u(M_0) &= \frac{1}{\pi} \left\{ \int_{\Gamma_D} \frac{\partial u}{\partial \nu} \ln \left(\frac{1}{r} \right) d\ell - \int_{\Gamma_N} u \frac{\partial}{\partial \nu} \ln \left(\frac{1}{r} \right) d\ell - \int_{\Gamma_D} g_1 \frac{\partial}{\partial \nu} \ln \left(\frac{1}{r} \right) d\ell \right. \\ &\quad \left. + \int_{\Gamma_N} g_2 \ln \left(\frac{1}{r} \right) d\ell + \iint_S \ln \left(\frac{1}{r} \right) f ds \right\}, \quad \forall M_0 \in \partial S. \end{aligned} \quad (0.3.4)$$

0.3.2 Discrete Approximation

Below, let us describe the simplest BEM discretization form of (0.3.3) by following the FEM approaches. Let ∂S be divided into quasiuniform subintervals (s_i, s_{i+1}) with the arc length h_{i+1} , where $s_{i+1} = s_i + h_{i+1}$ and $s_0 = s_N$. Also choose piecewise constant and linear functions as the admissible functions of $u_\nu = \frac{\partial u}{\partial \nu}$ and u respectively,

$$\frac{\partial u}{\partial \nu} = \sum_{i=1}^N (u_\nu)_i \Psi_i(s), \quad u = \sum_{i=1}^N u_i \Phi_i(s),$$

where $\Psi_i(s)$ and $\Phi_i(s)$ are the basis functions given by

$$\Psi_i(s) = \begin{cases} 1, & s_i - \frac{h_i}{2} < s < s_i + \frac{h_{i+1}}{2}, \\ 0, & \text{otherwise,} \end{cases}$$

and

$$\Phi_i(s) = \begin{cases} \frac{1}{h_i}(s - s_{i-1}), & s_{i-1} \leq s \leq s_i, \\ 1 - \frac{1}{h_{i+1}}(s - s_i), & s_i \leq s \leq s_{i+1}, \\ 0, & \text{otherwise.} \end{cases}$$

Substitute these two series into (0.3.4), and use the integration approximation in (0.3.4), then there come up N equations and N unknowns including either u_i or $(\frac{\partial u}{\partial \nu})_i$, leading to a linear algebraic system,

$$\mathbf{A}_B \mathbf{x}_B = \mathbf{b}, \quad (0.3.5)$$

where \mathbf{A}_B is an $N \times N$ matrix, which is neither symmetric nor sparse. Once the solution of (0.3.5) is obtained, we may seek the solution in S from Lemma 0.3.1

$$u(M_0) = \frac{1}{2\pi} \left[\sum_{i=1}^N (u_\nu)_i \int_{\partial S} \Psi_i(t) \ln \left(\frac{1}{r} \right) dl - \sum_{i=1}^N u_i \int_{\partial S} \Phi_i(t) \frac{\partial}{\partial \nu} \ln \left(\frac{1}{r} \right) dl + \iint_S \ln \left(\frac{1}{r} \right) f ds \right].$$

Note that in the BEM, both u_i and $(u_\nu)_i$ are treated as unknowns. We may employ other FEM approaches to obtain the BEM solutions. Both BEM and TM are of one-dimensional solver, one dimension lower than that in FEM, so the unknown number in BEM is substantially smaller than that in FEM. This is a remarkable advantage. However, when $f \neq 0$, the approximation integration of $\iint_S \ln \left(\frac{1}{r} \right) f ds$ may consume much more CPU time than the solution procedure of (0.3.5). Hence, BEM is strongly recommended for $f \equiv 0$. This can be done by a transformation $v = u - \bar{u}$, where \bar{u} is a special solution of $\mathcal{L}\bar{u} = f$. Note that the BEM is even more beneficial for 3D elliptic problems.

0.3.3 Natural BEM

Consider the pure Neumann-Laplace problem

$$\Delta u = 0 \quad \text{in } S, \quad \frac{\partial u}{\partial \nu} = g \quad \text{on } \partial S.$$

The consistent condition

$$\int_{\partial S} \frac{\partial u}{\partial \nu} dl = \oint_{\partial S} g dl = 0$$

guarantees existence of the solutions. There are multiple solutions, and each differs by a constant. From (0.3.3), we have

$$u(Y) = \frac{1}{\pi} \left\{ \int_{\partial S} \frac{\partial u(X)}{\partial \nu_X} \ln \frac{1}{|X-Y|} dl(X) - \int_{\partial S} u(X) \frac{\partial}{\partial \nu_X} \ln \frac{1}{|X-Y|} dl(X) \right\},$$

to lead to

$$\frac{\partial u(Y)}{\partial \nu_Y} = \frac{1}{\pi} \left\{ \int_{\partial S} \frac{\partial u(X)}{\partial \nu_X} \frac{\partial}{\partial \nu_Y} \ln \frac{1}{|X-Y|} dl(X) - \int_{\partial S} u(X) \frac{\partial}{\partial \nu_X} \frac{\partial}{\partial \nu_Y} \ln \frac{1}{|X-Y|} dl(X) \right\}.$$

By applying the Neumann boundary condition $\frac{\partial u}{\partial \nu_X} = g$ on Γ , we obtain

$$g = \frac{1}{\pi} \left\{ \int_{\partial S} g \frac{\partial}{\partial \nu_Y} \ln \frac{1}{|X-Y|} dl(Y) - \int_{\partial S} u(X) \frac{\partial}{\partial \nu_Y} \frac{\partial}{\partial \nu_X} \ln \frac{1}{|X-Y|} dl(Y) \right\}.$$

Hence, the solutions on ∂S can be sought by the natural BEM: Find $u \in H^{\frac{1}{2}}(\Gamma)/P_0$ such that

$$D(u, v) = \int_{\partial S} g v dl,$$

where P_0 is the space of an arbitrary constant, and

$$D(u, v) = \frac{1}{\pi} \left\{ \int_{\partial S} \int_{\partial S} \left(g \frac{\partial}{\partial \nu_Y} \ln \frac{1}{|X - Y|} \right) v \, d\ell(Y) \, d\ell(X) - \int_{\partial S} \int_{\partial S} \left(\frac{\partial}{\partial \nu_Y} \frac{\partial}{\partial \nu_X} \ln \frac{1}{|X - Y|} \right) u v \, d\ell(Y) \, d\ell(X) \right\}.$$

The discretization schemes of the natural BEM can be found in Yi [498].

The key difference between the BEM and the CM is that the fundamental functions and the particular solutions are chosen in the related boundary equations for the BEM and the CM, respectively. References on BEM are given in Brebbia [60], Wendland [485], Chen and Zhou [92] and Brebbia and Dominguez [64]. More study can be found in Cruse [116], Bayliss, Gunzburger and Turkel [29], Han and Wu [194], Hsiao [214, 215], and Feng and Yu [152].

0.4 Other Kinds of Boundary Methods

Other kinds of boundary methods are found in the integral solutions of the PDE. Take the Poisson integral on a unit disk for example. A harmonic function satisfies

$$u(r, \theta) = \int_0^{2\pi} K(r, \theta, \xi) u(1, \xi) d\xi, \quad r \leq 1, \quad (0.4.1)$$

where the Poisson kernel is

$$K(r, \theta, \xi) = \frac{1 - r^2}{2\pi} \frac{1}{1 - 2r \cos(\theta - \xi) + r^2}.$$

When the Dirichlet condition for the Laplace equation is given, the solution within the unit disc can be obtained from (0.4.1). Next, consider a sector $S^* = \{(r, \theta) \mid 0 \leq \theta \leq \Theta, 0 \leq r \leq 1\}$, with the Dirichlet, the Neumann, or their mixed boundary conditions on two edges $\theta = 0$ and $\theta = \Theta$ where $\Theta \leq \pi$. The general Poisson integrals are derived by Volkov [472, 473] as

$$u(r, \theta) = \int_0^\Theta K^*(r, \theta, \xi) u(1, \xi) d\xi, \quad (r, \theta) \in S^*, \quad (0.4.2)$$

with the explicit kernels $K^*(r, \theta, \xi)$. Then the block method is developed to seek the Laplace's solutions on polygons, by dividing the solution domain into several sectors with overlaps, and by employing the Schwarz alternating method (SAM).

In fact, the solution on the unit disk can be expressed by the particular solutions,

$$u(r, \theta) = \frac{\bar{a}_0}{2} + \sum_{i=0}^{\infty} (\bar{a}_i r^i \cos i\theta + \bar{b}_i r^i \sin i\theta), \quad (0.4.3)$$

where the true coefficients are

$$\bar{a}_i = \frac{1}{\pi} \int_{-\pi}^{\pi} u(1, \theta) \cos i\theta d\theta, \quad \bar{b}_i = \frac{1}{\pi} \int_{-\pi}^{\pi} u(1, \theta) \sin i\theta d\theta. \quad (0.4.4)$$

Substituting (0.4.4) into (0.4.3) leads to the Poisson's integral (0.4.1).

Next, consider the particular solutions (0.1.27) on the unit semi-disk, to give the solution

$$u(r, \theta) = \sum_{i=0}^{\infty} \bar{a}_i r^{i+\frac{1}{2}} \cos(i + \frac{1}{2})\theta, \quad 0 \leq r \leq 1, \quad (0.4.5)$$

where the true coefficients are

$$\bar{a}_i = \frac{2}{\pi} \int_0^{\pi} u(1, \theta) \cos(i + \frac{1}{2})\theta d\theta. \quad (0.4.6)$$

Substituting (0.4.6) into (0.4.5) gives the following kernel for the harmonic functions satisfying the boundary conditions (0.1.26)

$$K^*(r, \theta, \xi) = \frac{\sqrt{r}(1-r)}{\pi} \left\{ \frac{\cos(\frac{\theta+\xi}{2})}{1-2r \cos(\theta+\xi) + r^2} + \frac{\cos(\frac{\theta-\xi}{2})}{1-2r \cos(\theta-\xi) + r^2} \right\}, \quad r \leq 1.$$

The above analysis displays that the series solution consisting of particular solutions is linked to the Poisson's kernel. The errors of the TM are mainly from the truncation of the finite series, but the errors of the block method as well as the BEM are from the approximation of the solution by low order polynomials.

The block method is developed for singularity problems, such as Motz's problem in Volkov and Kornoukhov [474], and Dosiyevev [133]. Note that from Li et al. [311, 312], for solving Poisson's equation, the CTM is much simpler than the Poisson integral (0.4.2).

It is well known that the potential of a double layer of density μ over a closed surface Γ defined by

$$u(P) = -\frac{1}{2\pi} \int_{\Gamma} \mu(Q) \frac{\partial}{\partial \nu_Q} \ln \|P - Q\| dS_Q, \quad P \notin \Gamma \quad (0.4.7)$$

is harmonic, where $\|\cdot\|$ is the Euclidean norm. For Laplace's equation with the Dirichlet condition,

$$\Delta u = 0 \quad \text{in } S, \quad u = g \quad \text{on } \Gamma, \quad (0.4.8)$$

where S is a bounded domain and Γ is its exterior boundary. The density function $\mu(P)$ on Γ can be found by

$$-\frac{1}{2}\mu(P) = -\frac{1}{2\pi} \int_{\Gamma} \mu(Q) \frac{\partial}{\partial \nu_Q} \ln \|P - Q\| dS_Q = g(P), \quad P \in \Gamma. \quad (0.4.9)$$

For the exterior problem of the Laplace equation,

$$\Delta u = 0 \quad \text{in } S_{\infty}, \quad u = g \quad \text{on } \Gamma, \quad (0.4.10)$$

where S_{∞} is a unbounded domain, and Γ is its interior boundary. The density function $\mu(P)$ on Γ can be found by

$$\frac{1}{2}\mu(P) = -\frac{1}{2\pi} \int_{\Gamma} \mu(Q) \frac{\partial}{\partial \nu_Q} \ln \|P - Q\| dS_Q = g(P), \quad P \in \Gamma. \quad (0.4.11)$$

There exist only the sign differences between (0.4.9) and (0.4.11). The existence of the solutions for (0.4.9) and (0.4.11) was proven in Courant and Hilbert [110], p. 301. both (0.4.9) and (0.4.11) are the Fredholm equation of the second kind. Note that Eqs. (0.4.7) and (0.4.9), (or (0.4.11)) are analogous to Lemmas 0.3.1 and 0.3.2, respectively. Once function $\mu(P)$ is obtained from (0.4.9) or (0.4.11), the solution in S or S_{∞} is given by (0.4.7).

The potential of a single layer of density σ over a closed surface Γ defined by

$$u(P) = -\frac{1}{2\pi} \int_{\Gamma} \sigma(Q) \ln \|P - Q\| dS_Q, \quad P \in \Gamma, \quad (0.4.12)$$

is also harmonic. Based on (0.4.12), similar boundary integral equations can be found in textbooks for the Laplace equation with the Neumann boundary condition. However, we may directly apply (0.4.12) for the Laplace equation with the Dirichlet boundary condition. Since $u(P)$ in (0.4.12) is continuous, the solution of both (0.4.8) and (0.4.10) is then expressed by

$$g(P) = -\frac{1}{2\pi} \int_{\Gamma} \sigma(Q) \ln \|P - Q\| dS_Q, \quad P \in \Gamma. \quad (0.4.13)$$

Note that Eq. (0.4.13) is the Fredholm equation of the first kind. Since there exist some difficulties. Eq. (0.4.13) is considered unsolvable (see Section A.7). To overcome such a difficulty in solving (0.4.13), several numerical methods are proposed, such as the Galerkin method in Stephan and Wendland [443] and Sloan and Spence [435], the collocation method in Costabel et al. [108], Elschner and Graham [144] and Yan [496], and the quadrature method in Sidi and Israrli [433], Saranen [420] and Saranen and Sloan [421]. Other numerical reports are given in Carstensen and Praetorius [80] and Huang and Shaw [228]. Recently, a new quadrature method, called the mechanical quadrature method (MQM), is developed by Huang [221] and Huang and Lü [222]. The MQM has the $O(h^3)$ order of convergence rates, and the excellent stability with $\text{Cond.} = O(h^{-1})$, where h is the maximal meshspacing of the quadrature nodes, and Cond. is the traditional condition number. Furthermore, the high order $O(h^5)$ can also be achieved for both smooth and

singular solutions by the MQM using the extrapolation and the splitting extrapolation techniques, see [221, 222].

In (0.4.13), since the resource points Q are located on Γ , to cause a logarithmic singularity. If we choose Q outside of S , Eq. (0.4.13) can easily be solved by the Galerkin, the collocation and the quadrature methods. Such a method was first proposed by Kupradze [269]. We may interpret this method as the TM using fundamental solutions, which is also called the fundamental solutions method (FSM). Choose the admissible functions

$$u_N = \sum_{i=1}^N c_i \ln |\overline{PQ}_i|, \quad P \in S \cup \Gamma, \quad (0.4.14)$$

where c_i are coefficients, and the resource points Q_i are located uniformly on an outside circle (see Bogomolny [50]),

$$Q_i = \{(x_i, y_i) \mid x_i = R \cos(i\Delta\theta), y_i = R \sin(i\Delta\theta)\}, \quad (0.4.15)$$

where $\Delta\theta = \frac{2\pi}{N}$ and $R > \max_S r$. For the Dirichlet boundary condition in (0.4.8), the collocation equations are obtained as

$$w_j \sum_{i=1}^N c_i \ln |\overline{P_j Q}_i| = w_j g(P_j), \quad P_j \in \Gamma, \quad (0.4.16)$$

where $w_j (> 0)$ are suitable weights. If P_i are chosen as the quadrature nodes, and if w_j are the quadrature weights, Eq. (0.4.16) is just the quadrature method of (0.4.13). On the other hand, Eq. (0.4.16) can be regarded as the TM using fundamental solutions, instead of particular solutions.

For the FSM, the polynomial convergence rates are proved for smooth solutions in Bogomolny [50], and the exponential convergence rates are provided in Katsurda and Okamoto [251]. However, the ill-conditioning of FSM is severe, to have the exponential growth rates of Cond., which are proven for Dirichlet problems on disk domains in Christiansen [102]. In fact, the exponential rates of Cond. can be proved for other kinds of boundary conditions, and on non-disk domains. Since the coefficients c_i in (0.4.14) obtained from the FSM are large and highly oscillating, the subtraction cancellation of instability occurs in the final harmonic solutions (0.4.14). Details of stability by the FSM will appear elsewhere. More discussions on the boundary methods are given in Appendix.

0.5 Comparisons

To close this introduction, let us make a brief comparisons of different numerical methods. First, the FEM gains the most popularity owing to its high flexibility, in particular for arbitrary geometric shape of S , variable coefficients, and different elliptic equations. Since the triangular partition and piecewise low order polynomials (e.g., Lagrange or Hermite

elements) are very flexible, the FEM may fit into very wide scale of elliptic problems. Therefore, FEM has been well developed in both practical numerical algorithms and rigorous theoretical analysis. However, the FEM has a few deficiencies. First, the mesh generation cannot be fully automatized, despite the help of auto mesh generator. Second, the evaluation of the stiffness matrix is CPU time consuming. Third, its accuracy is limited by the low order polynomial approximation and interpolation.

For certain type of simple elliptic equations, other numerical methods, e.q., BEM, TM, etc. may be more efficient. The BEM and the TM are confined to certain linear and constant coefficient elliptic equations, where the fundamental functions and the particular solutions can be found in textbooks or by analytical work. The high efficiency of TM is not surprising, because the particular solutions are best to approximate the true solutions. Moreover, the high accuracy with the exponential convergence rates can be achieved by both TM and CTM. However, such particular solutions may not be found for rather arbitrary S .

The BEM and the TM are simpler and more efficient than FEM, FDM and FVM. The TM is also simpler than the BEM, because the expansion solutions from the TM are more explicit in use. In particular, their leading coefficient displays explicitly the singularity of the solutions, and gives the fracture intensity factor. The advantages of the TM are also given in Jirousek and Wróblewski [241, 242].

Let us compare the CTM with the direct TM as referred in [237]. In the CM and the CTM, there is no Lagrangian multiplier λ needed, and the error analysis is rather easy, see this book. On the other hand, in the direct TM, the stiffness matrix is symmetric but indefinite, and the difficult Ladyzhenskaya-Babuska-Brezzi (LBB) condition must be verified for the error analysis. Moreover, the TM using collocation equation is also simpler than the original TM, i.e., the simplified hybrid method. Overall, the CTM is the simplest and most accurate and the most stable method, and detailed discussions and numerical results are reported in Chapters 2 and 3.

However, *there is no perfect method, and merits and drawbacks are twins*. The high efficiency of the TM relies on the following:

1. The explicit particular solutions must exist, and have high convergence rates.
2. The solution domain should be divided into several subdomains with or without overlaps, in order to reduce instability and to retain the high accuracy. The Trefftz-Herrera method and the Trefftz-Herrera domain decomposition are developed by Herrera [201, 203]. The shape of the domain and its partition may greatly affect the efficiency of the TM. The stability analysis on the domain shapes is explored in Li and Mathon [315], and its computational aspects in Kita, Kamiya and Ikeda [259].
3. The suitable coupling techniques are also imperative to enforcement of the exterior and interior boundary conditions, see Qin [391]. In the TM, we may choose the central or the Gaussian rules to formulate directly the collocation equations, see Chapter 2. In Chapter 9, different interior boundary conditions are explored for the Schwarz alternating methods of the CM.

4. For rather complicated PDE, with no explicit particular solutions on the entire domain, we may still apply the TM locally, by combining it with the FEM, FDM and FVM. The examples are given in Chapter 10.

The TM has been developing for many engineering problems since the important work by Zienkiewicz, Kelley and Bettess [508] and Jirousek and Leon [240] in 1977. Before 1995, TM was investigated by Shaw, Huang and Zhao [428], Cheung, Jin and Zienkiewicz [100], Ruge [413] and Zielinski and Herrera [506]. After 1995, it was studied by Dong, Lo et al. [132], Sladek, Sladek and van Keer [434], Domingues, Portela and de Castro [131], Portela and Charafi [387], Reutskiy [400], Abou-Dina [1], de Freitas and Leitao [123], Herrera [204], Jin and Cheung [237], Kita et al. [262], Leitao [282], Zielinski [505], Jirousek and Wroblewski [241, 242] and Herrera and Solano [208]. Moreover, an equivalence of the Trefftz method and the boundary method using the fundamental solutions is explored in Chen et al. [91]. Only a few reports of the TM involve analysis, see Christiansen and Hansen [103] and Herrera and Díaz [205]. Hence, the analysis of the TM is behind that of the BEM. There exists a gap between the excellent numerical results (see Piltner [381] and Zheng and Yao [501]) and the theoretical analysis. In 1995, there was a special issue on the TM in *Advances in Engineering Software*, edited by Kamiya and Kita [246, 261], which draw significant attention. Inspired by the special issue, we have carried out new studies on the BAM (i.e., the TM), and summarized the recent new results of the CM and the CTM. It is our hope that the existing gap of the TM between theory and computation is narrowed by the present effort.

*The boundaries which divide Life from Death
are at best shadowy and vague.
Who shall say where the one ends,
and where the other begins?
—— The Premature Burial (1844) ——*

*Edger Allan Poe
(1809-1849)*

Part I

Collocation Trefftz Method

The Trefftz method (TM) was first proposed in 1926 [461]. The method can be classified a boundary-type solution procedure. The main idea of the TM is to use particular solutions as the admissible functions, which satisfy the partial differential equation exactly. The numerical efforts is required only to approximate the boundary conditions only.

There exists an extensive list of literatures on the TM in engineering journals. In 1995, there was a special issue on the TM, edited by Kamiya and Kita [246], concerning the fundamentals, applications and analysis schemes (cf. [261, 237, 504]). Other applications include Jin, Cheung and Zienkiewicz [238], Herrera [201], Jirousek and Guex [239], Zieliński [503], Zieliński and Zienkiewicz [507], Zienkiewicz, Kelly and Bettess [508], Piltner and Taylor [382], Kolodziej [263], Herrera and Diaz [205], and Leitão [282]. The TM has also been applied to the interface problems and the unbounded domain problems in [314, 315].

Here, let us summarize the terminologies used in the literature and in this book. The boundary approximation method (BAM) was studied in Li et al. in [285, 287, 316, 314, 315, 291]. Its numerical implementation leads to the collocation Trefftz method (CTM) called in this book. In Kita and Kamiya [261] the Trefftz method (TM) is classified into a direct and an indirect method. The direct method is referred to as the method of fundamental solutions (MFS) [99, 237], which has a close relation with the discretized form of the boundary element method (BEM). Because the theory of BEM has been well developed, this book focuses on the analysis of the indirect TM, i.e., the CTM.

The theory of the indirect TM without integration approximation was first established in the Doctoral dissertation of the first author in 1986 as the BAM, see Li [285] and also Li [287], whose materials were published in Li, Mathon and Sermer [316] and Li and Mathon [314, 315]. Only recently it was realized that the BAM and the indirect TM not only share the same theoretical basis, but also are identical in algorithm. Since the TM has been used in the engineering community for a long time, in this book we choose the term TM for communication with more engineering researchers.

The singularity problems have drawn much attention in the last several decades, and reported in numerous papers. Most of them dealt with the second order PDEs including the point singularity [357, 291, 453] and singular boundary layers [353, 411]. There exist a few books and papers for the fourth order PDEs, such as the biharmonic equations with crack singularities, see Grisvard [186], Lefebvre [281], Schiff et al. [423], Whitman [488], Russo [418], and Karageorghis [250]. Textbooks and papers on biharmonic equations by the finite element method (FEM), the finite difference method (FDM), and the BEM include Chien [101], Oden and Carey [78], Birkhoff and Lynch [47], Arad et al. [4] and Brebbia and Dominguez [64]. In Part I, we pursue the more accurate crack solutions by using series expansion around the singularity with of very high convergence rates. At the same time, we employ highly accurate numerical methods, such as CTMs, for obtaining their solutions. There are three key issues in the approaches: (1) Find the particular solutions of PDEs, even locally in some special regions, see Herrera [201], Zieliński [504], Li [291], etc. (2) Splitting the domain S into subdomains and find piecewise particular solutions. This technique provides better stability and accuracy; some interesting examples can be found in Li [291]. (3) The coupling techniques on the exterior and interior

boundary conditions are important in the CTM. In Li [291], a number of efficient coupling techniques are introduced for matching the particular solutions for the TM and the matching of other methods, such as the FEM, FDM, FVM, etc.

Part I consists of four chapters:

Chapter 1: Basic Algorithms and Theory.

Chapter 2: Motz's and Cracked Beam Problems.

Chapter 3: Coupling Techniques.

Chapter 4: Biharmonic Equations with Crack Singularities.

A brief description of Part I is given as follows.

Chapter 1 gives the theoretical foundation of the TM. The error analysis is made on the entire domain by the Sobolev norm, and the exponential convergence rates can be achieved. However, the condition number of the stiffness matrix is also exponentially increasing when the number of particular solutions increases. When the solution domain is divided into several subdomains, and when suitable piecewise particular solutions are chosen, the condition number will decline significantly. Because of the high accuracy of the method, only a few terms of particular solutions are needed for practical application, so the instability of the TM is not severe. Hence, the TM can be used with a good balance between accuracy and instability.

Chapter 2 uses the CTM to seek the approximate solutions of benchmark singularity problems. The Gaussian rules with high order (in contrast to the central rule) are used to approximate the integrals in variational approaches. Such algorithms will provide exact solution, which is much more accurate than any published literatures [291, 316].

Chapter 3 is a continuation of the study of Li [291], to explore the generalized boundary approximation methods (GBAMs) for partial differential equation with singularities. GBAMs use the local particular solutions of PDEs, but adopt other coupling strategies to deal with the boundary conditions, which are different from the classic BAM in Li [291]. Three new GBAMs are discussed, and a new analysis is explored. Since suitable coupling techniques for interior and exterior boundary conditions are essential to a wide range of success of the method, this chapter enriches the BAM with variant formulations which are beneficial to wide applications. The CTM is most recommended due to its high accuracy and less computational cost, although all TMs are efficient. The effective condition number is also discussed. New computation formulas for the effective condition numbers are derived to provide a reasonable bound of the relative errors of the TM. The new formulas are easy to apply in practical application. Numerical experiments are conducted for the TMs with the effective condition number formulas.

Chapter 4 extends the CTM to biharmonic equations with singularity. First, we derive the Green formulas for biharmonic equations on bounded domains with non-smooth boundary, and the corner terms are studied. Next, three models are provided, in which a brief analysis of error bounds is performed. Two of those models are shown to be superior,

and can be used as benchmarks of biharmonic problems; numerical experiments have also been carried out in this chapter.

Due to the historical development, different names have been assigned to the same (or basically the same) method. Before starting Part I, the equivalence of terminologies used in Parts I and III is summarized below for easy reference.

Boundary Method

- Trefftz Method (TM)
 - Traditional Trefftz Method: Similar to Ritz method, minimize an energy functional, but uses homogeneous particular solutions as trial functions.
 - Boundary Approximation Method (BAM): When particular solutions satisfying the governed equation are chosen, the approximate solutions are obtained by satisfying the interior and exterior boundary conditions as best as possible in the least squares sense, as described in Li [287, 291].
 - Collocation Trefftz Method (CTM), also called
 - ◊ Indirect Trefftz Method (Indirect TM),
 - ◊ BAM with quadrature rule.
 - General Trefftz Method (GTM): Use penalty and other methods to satisfy the boundary conditions. There are four different TMs discussed in this book:
 - (1) Penalty TM,
 - (2) Hybrid TM,
 - (3) Penalty Plus Hybrid TM,
 - (4) Lagrangian Multiplier TM, also called as
 - ◊ Direct Trefftz Method (Direct TM).
- Boundary Element Method (BEM), based on
 - Direct Method: Green's formula.
 - ◊ Similar to direct TM, but uses fundamental solution as particular solution.
 - Indirect Method: Fredholm integral equations.
 - Method of Functional Equations: Kupradze's method.
 - Method of Fundamental Solution (MFS).
 - ◊ Similar to CTM (Indirect TM), but uses fundamental solution as particular solution.

Chapter 1

Basic Algorithms and Theory

For solving homogeneous elliptic equations, the Trefftz method (TM) uses particular solutions to approximate the boundary conditions as accurately as possible, usually in a least squares sense. In the interior of a given region, the approximate solution satisfies the differential equation exactly. The TM can cope easily with complicated boundaries and boundary conditions, as well as with singularities and infinite domains.

Approximation by particular solutions using harmonic polynomials was first applied by Kantorovich and Krylov [249] to solve Laplace's equation. Fox, Henrici and Moler [156] used particular solutions to find eigenvalues of the Laplace operator. Bergman's (Bergman [33], Bergman and John [34, 35]) and Vekua's (Vekua [469]) integral representations of solutions yielded particular solution expansions for a large class of elliptic equations. The error analysis for the Bergman-Vekua method was worked out by Eisenstat [142].

From a computational point of view, the TM is easy to use, and benefiting from the reduced complexity of boundary approximation. In addition, it is often possible to control the errors of the approximate solutions by the computable errors on the boundary, even for elliptic problems which do not possess the maximum principle (see Mathon and Sermer [345]).

However, difficulties may arise in the situations where a large number of particular solutions is needed to achieve a satisfactory approximation, which can lead to ill-conditioning of the associated least squares matrices. For the problems with material interfaces, singularities and unbounded domains, it may not be possible to find a single, uniform expansion as particular solutions which is valid in the entire domain. It is therefore necessary to divide the domain into several subdomains and to use different expansions in each of them. A solution is then obtained by approximating both the exterior boundary conditions and the interior continuity conditions across the various interfaces. We note that for a good subdivision, only a few terms are needed in each subdomain to achieve a highly accurate approximation, and to mitigate the numerical instability. Moreover, the numerical stability is greatly improved and the least squares matrices have many zero entries.

We will study the TM for solving homogeneous self-adjoint elliptic equations that

combine several expansions of particular solutions from different parts of the region. In this chapter, we first give an error analysis and stability analysis of the TM, which provide the basic theory of the TM in this book. Two benchmark models of singularity problems, Motz's and the cracked beam problems, are given, whose solutions have a close form expansion. The coefficients of the solutions of Motz's problem can be obtained by the conformal transformation method of Rosser and Papamichael [412]. By Mathematica, 100 highly accurate coefficients are provided in [309] for testing numerical methods. The contents in this chapter are adopted from Li [287, 289, 291], Li and Lu [309], Li, Mathon and Sermer [316] and Li and Mathon [314, 315].

1.1 Notations and Preliminaries

Let S be a bounded polygon in the plane R^2 with a piecewise smooth boundary ∂S . We will consider the problem

$$\Delta u = \frac{\partial^2 u}{\partial x^2} + \frac{\partial^2 u}{\partial y^2} = 0 \quad \text{in } S, \quad (1.1.1)$$

$$u = f \quad \text{on } \Gamma_D, \quad u_\nu = g \quad \text{on } \Gamma_N, \quad (1.1.2)$$

where f and g are sufficiently smooth functions, Γ_D and Γ_N are non-overlapped compact subsets of ∂S , $\Gamma_D \neq \phi$, $\Gamma_D \cup \Gamma_N = \partial S$, and u_ν is the normal derivative.

Let Γ_0 be an interface which divides S into two subdomains, S^+ and S^- , and let u^+ and u^- be defined on S^+ and S^- respectively. If u^+ and u^- satisfy (1.1.1) and (1.1.2) on the corresponding subdomains and boundaries, and

$$u^+ = u^-, \quad u_\nu^+ = u_\nu^- \quad \text{on } \Gamma_0, \quad (1.1.3)$$

then $u^+ = u$ in S^+ and $u^- = u$ in S^- .

For an integer $k \geq 0$, $H^k(S)$ denote the Sobolev spaces of order k of real-valued functions with the Sobolev norms $\|\cdot\|_{k,S}$ and seminorms $|\cdot|_{k,S}$:

$$\|v\|_{k,S} = \left\{ \sum_{|\alpha| \leq k} \iint_S |D^\alpha v|^2 ds \right\}^{\frac{1}{2}}, \quad |v|_{k,S} = \left\{ \sum_{|\alpha|=k} \iint_S |D^\alpha v|^2 ds \right\}^{\frac{1}{2}}.$$

If S is divided by an interface Γ_0 into S^+ and S^- , we will use a new space H :

$$H = H(S) = \{v \in L_2(S) | v \in H^1(S^+), v \in H^1(S^-), \text{ and } \Delta v = 0 \text{ in } S^+ \text{ and } S^-\},$$

where $L_2(S)$ is the usual space of square integrable functions in S with the inner product $(u, v) = \iint_S uv ds$ and the norm $\|u\|_0 = (u, u)^{\frac{1}{2}}$. The space H is equipped with the

norm and seminorm:

$$\|v\|_1 = \left\{ \|v\|_{1,S^+}^2 + \|v\|_{1,S^-}^2 \right\}^{\frac{1}{2}}, \quad |v|_1 = \left\{ |v|_{1,S^+}^2 + |v|_{1,S^-}^2 \right\}^{\frac{1}{2}}.$$

If γ is a curve, then $|\cdot|_{k,\gamma}$ denotes the norms in the Sobolev spaces $H^k(\gamma)$ of functions defined on γ .

For $v \in H$, $f \in L_2(\Gamma_D)$ and $g \in L_2(\Gamma_N)$ given by (1.1.2), we define a functional

$$\begin{aligned} I(v) &= \int_{\Gamma_D} (v - f)^2 dl + w^2 \int_{\Gamma_N} (v_\nu - g)^2 dl + \int_{\Gamma_0} (v^+ - v^-)^2 dl + \\ &\quad + w^2 \int_{\Gamma_0} (v_\nu^+ - v_\nu^-)^2 dl, \end{aligned}$$

where w is some positive weight. On $H \times H$, we will consider a bilinear form $[\cdot, \cdot]$ given by

$$\begin{aligned} [u, v] &= \int_{\Gamma_D} uv dl + w^2 \int_{\Gamma_N} u_\nu v_\nu dl + \int_{\Gamma_0} (u^+ - u^-)(v^+ - v^-) dl \\ &\quad + w^2 \int_{\Gamma_0} (u_\nu^+ - u_\nu^-)(v_\nu^+ - v_\nu^-) dl. \end{aligned}$$

Clearly, $[\cdot, \cdot]$ is an inner product which induces the norm on Γ_0

$$|v|_B^2 = [v, v]. \quad (1.1.4)$$

We need the following lemma.

Lemma 1.1.1 *If $v \in H$, then there exists a positive constant C independent of v such that*

$$\|v\|_1 \leq C \{ |v|_1 + |v|_{0,\Gamma_D} + |v^+ - v^-|_{0,\Gamma_0} \}.$$

Proof. For a curve $\gamma \in \partial S$ and $v \in H^1(S)$, we have (Sobolev [438], p. 68)

$$\|v\|_{1,S} \leq C \{ |v|_{1,S} + |v|_{0,\gamma} \}. \quad (1.1.5)$$

Applying this inequality to S^+ and S^- , we obtain

$$\begin{aligned} \|v\|_1 &\leq C \{ |v|_1 + |v|_{0,\Gamma_D \cap S^-} + |v^+|_{0,\Gamma_0} \} \\ &\leq C \{ |v|_1 + |v|_{0,\Gamma_D} + |v^-|_{0,\Gamma_0} + |v^+ - v^-|_{0,\Gamma_0} \}, \end{aligned} \quad (1.1.6)$$

where we assume, without loss of generality, that $\Gamma_D \cap S^- \neq \emptyset$. Using the Sobolev imbedding theorem (Sobolev [438], p. 84) and (1.1.5), we obtain

$$\begin{aligned} |v^-|_{0,\Gamma_0} &\leq C \|v\|_{1,S^-} \leq C \{ |v|_{1,S^-} + |v|_{0,\Gamma_D \cap S^-} \} \\ &\leq C \{ |v|_1 + |v|_{0,\Gamma_D} \}. \end{aligned} \quad (1.1.7)$$

The desired result follows from (1.1.6) and (1.1.7). ■

1.2 Approximation Problems

Let $\{\psi_i^+\}$ and $\{\psi_i^-\}$ ($i = 1, 2, \dots$) be complete sets of particular solutions of (1.1.1) on S^+ and S^- respectively. Consider finite-dimensional subspaces $S_{m,n} \subseteq H$ defined by

$$S_{m,n} = \left\{ v \mid v = v^+ = \sum_{i=1}^m c_i \psi_i^+ \text{ on } S^+, \text{ and } v = v^- = \sum_{i=1}^n d_i \psi_i^- \text{ on } S^- \right\},$$

where c_i and d_i are real coefficients.

A function $u_{m,n} \in S_{m,n}$ will be called a TM approximation to the solution u of (1.1.1) – (1.1.3) if it minimizes I over $S_{m,n}$, i.e.,

$$I(u_{m,n}) \leq I(v), \quad \forall v \in S_{m,n}. \quad (1.2.1)$$

The space $S_{m,n}$ is assumed to satisfy the following two properties:

Inverse Property: For any $v \in S_{m,n}$, we have

$$|v_\nu|_{0,\Gamma_D} \leq k_{m,n} \|v\|_1, \quad |v_\nu^+|_{0,\Gamma_0} \leq k_{m,n} \|v\|_1, \quad (1.2.2)$$

where $k_{m,n}$ is unbounded as $m, n \rightarrow \infty$.

Approximability Property: For any $u \in H$, there exists a function $v \in S_{m,n}$ such that

$$\|u^+ - v^+\|_{l,\partial S^+} \leq \alpha_{n,k,l}^+ |u^+|_{k,\partial S^+}, \quad 0 \leq l \leq k, \quad (1.2.3)$$

and

$$\|u^- - v^-\|_{l,\partial S^-} \leq \alpha_{m,t,l}^- |u^-|_{t,\partial S^-}, \quad 0 \leq l \leq t, \quad (1.2.4)$$

where $\alpha_{n,k,l}^+, \alpha_{m,t,l}^- \rightarrow 0$ as $m, n \rightarrow \infty$. The bounds of the constants, $\alpha_{n,k,l}^+$ and $\alpha_{m,t,l}^-$, can be obtained from Cheney [95] and Eisenstat [142]. In (1.2.3) and (1.2.4), the Sobolev norms on the boundary ∂S are defined by

$$\|v\|_{l,\partial S} = \left\{ \sum_{|\alpha| \leq l} \int_{\partial S} \left(\frac{\partial^\alpha v}{\partial s^\alpha} \right)^2 d\ell \right\}^{\frac{1}{2}}, \quad |v|_{l,\partial S} = \left\{ \sum_{|\alpha|=l} \int_{\partial S} \left(\frac{\partial^\alpha v}{\partial s^\alpha} \right)^2 d\ell \right\}^{\frac{1}{2}}.$$

We require the following estimates.

Lemma 1.2.1 *If $v \in S_{m,n}$ and the inverse property (1.2.2) holds, then*

$$\|v\|_1 \leq C(k_{m,n} + w^{-1})|v|_B, \quad (1.2.5)$$

where C is a positive constant independent of m and n .

Proof. By using Green's theorem and that $\Delta v = 0$ in S^+ and S^- , we have

$$0 = \iint_{S^+} v \Delta v ds + \iint_{S^-} v \Delta v ds = -|v|_1^2 + \int_{\partial S^+} v v_\nu dl + \int_{\partial S^-} v v_\nu dl.$$

Hence, from Hölder's inequality it follows that

$$\begin{aligned} |v|_1^2 &= \int_{\Gamma_D} v v_\nu dl + \int_{\Gamma_N} v v_\nu dl + \int_{\Gamma_0} [(v^+ - v^-)v_\nu^+ + v^-(v_\nu^+ - v_\nu^-)] dl \\ &\leq |v|_{0,\Gamma_D} |v_\nu|_{0,\Gamma_D} + |v|_{0,\Gamma_N} |v_\nu|_{0,\Gamma_N} \\ &\quad + |v^+ - v^-|_{0,\Gamma_0} |v_\nu^+|_{0,\Gamma_0} + |v^-|_{0,\Gamma_0} |v_\nu^+ - v_\nu^-|_{0,\Gamma_0}. \end{aligned} \quad (1.2.6)$$

By applying the Sobolev imbedding theorem and the inverse property, we obtain $|v|_1^2 \leq Cq\|v\|_1$, where

$$q = k_{m,n}(|v|_{0,\Gamma_D} + |v^+ - v^-|_{0,\Gamma_0}) + |v_\nu|_{0,\Gamma_N} + |v_\nu^+ - v_\nu^-|_{0,\Gamma_0}.$$

From the imbedding theorem, Lemma 1.1.1 and that $k_{m,n} \geq 1$ we have

$$\begin{aligned} \|v\|_1^2 &\leq C \{ |v|_1^2 + |v|_{0,\Gamma_D}^2 + |v^+ - v^-|_{0,\Gamma_0} (|v^+|_{0,\Gamma_0} + |v^-|_{0,\Gamma_0}) \} \\ &\leq C \{ |v|_1^2 + (|v|_{0,\Gamma_D} + |v^+ - v^-|_{0,\Gamma_0}) \|v\|_1 \} \\ &\leq Cq\|v\|_1. \end{aligned}$$

Dividing both sides by $\|v\|_1$ and noting that $q \leq (k_{m,n} + w^{-1})|v|_B$, we obtain the desired result. ■

Concerning the existence, uniqueness and stability of $u_{m,n}$ defined by (1.2.1), we have the following lemma.

Lemma 1.2.2 *Suppose that u is the solution of (1.1.1) and (1.1.2). Then for any $w > 0$, there exists a unique function $u_{m,n} \in S_{m,n}$ which satisfies*

$$[u_{m,n}, v] = \int_{\Gamma_D} f v dl + w^2 \int_{\Gamma_N} g v_\nu dl, \quad \forall v \in S_{m,n}, \quad (1.2.7)$$

$$[u - u_{m,n}, v] = 0, \quad \forall v \in S_{m,n}, \quad (1.2.8)$$

and

$$\|u_{m,n}\|_1 \leq C(k_{m,n} + w^{-1}) \{ |f|_{0,\Gamma_D} + w|g|_{0,\Gamma_N} \}. \quad (1.2.9)$$

Also, $u_{m,n}$ minimizes $I(v)$ over $S_{m,n}$ if and only if it satisfies (1.2.7).

Proof. Since $f = u$ on Γ_D , $g = u_\nu$ on Γ_N , and u and u_ν are continuous across Γ_0 , the right-hand side expression in (1.2.7) equals $[u, v]$, and so (1.2.8) easily follows from (1.2.7). In (1.2.7), let $v = u_{m,n}$ and apply the Schwarz inequality to obtain

$$|u_{m,n}|_B^2 = [u_{m,n}, u_{m,n}] = [u, u_{m,n}] \leq |u|_B |u_{m,n}|_B.$$

Consequently,

$$|u_{m,n}|_B \leq |u|_B = \{ |f|_{0,\Gamma_D}^2 + w^2 |g|_{0,\Gamma_N}^2 \}^{\frac{1}{2}},$$

and therefore there exists a unique solution of (1.2.7) by the Riesz representation theory, since $S_{m,n}$ is finite-dimensional. By applying the last inequality to (1.2.5), we obtain (1.2.9) which expresses stability of the TM solutions with respect to perturbations of the boundary data f and g .

To prove the last part of the lemma, assume that $\eta \in S_{m,n}$. Then, we have

$$I(u_{m,n} + \eta) = I(u_{m,n}) + 2[u_{m,n} - u, \eta] + |\eta|_B^2.$$

If $u_{m,n}$ satisfies (1.2.8), then

$$I(u_{m,n} + \eta) = I(u_{m,n}) + |\eta|_B^2 \geq I(u_{m,n}),$$

and hence it minimizes $I(v)$ over $S_{m,n}$. On the other hand, if $u_{m,n}$ minimizes I , then for any $v \in S_{m,n}$ and scalar α :

$$\frac{\partial I(u_{m,n} + \alpha v)}{\partial \alpha} = 2[u_{m,n} - u, v] + 2\alpha |v|_B^2.$$

Letting $\alpha = 0$ shows that $u_{m,n}$ satisfies (1.2.8). ■

1.3 Error Estimates

In this section, error estimates are derived for $u - u_{m,n}$ in the space H . Since for any $v \in H$, $\|v\|_0 \leq \|v\|_1$, this will automatically imply convergence of the approximation in the L_2 -norm.

Theorem 1.3.1 *Let $u \in H^1(S)$ be the solution of (1.1.1) and (1.1.2), and let $u_{m,n} \in S_{m,n}$ be the TM approximation satisfying (1.2.7). If the inverse property holds, then for any $w > 0$, there exists a positive constant C independent of m , n and u such that*

$$\|u - u_{m,n}\|_1 \leq \inf_{v \in S_{m,n}} \{ \|u - v\|_1 + C(k_{m,n} + w^{-1})|u - v|_B \}, \quad (1.3.1)$$

where $k_{m,n}$ is defined in (1.2.2).

Proof. For $v \in S_{m,n}$, let $\eta = v - u_{m,n}$. Then since $\eta \in S_{m,n}$, Lemma 1.2.1 implies that

$$\begin{aligned} \|u - u_{m,n}\|_1 &\leq \|u - v\|_1 + \|\eta\|_1 \\ &\leq \|u - v\|_1 + C(k_{m,n} + w^{-1})|\eta|_B. \end{aligned} \quad (1.3.2)$$

Applying the orthogonality property (1.2.8), we obtain

$$|\eta|_B^2 = [\eta, \eta] = [v - u, \eta] \leq |u - v|_B |\eta|_B.$$

Hence, $|\eta|_B \leq |u - v|_B$ and (1.3.1) follows directly from (1.3.2). ■

Next we estimate bounds of the error in H , in terms of errors on the boundary and the interface.

Theorem 1.3.2 *Let u and $u_{m,n}$ be the same as in Theorem 1.3.1 and let $v \in S_{m,n}$ be an approximation to u . If the inverse property holds and $w = 1/k_{m,n}$, then there exists a positive constant C independent of m , n , u and v such that*

$$\begin{aligned} \|u - u_{m,n}\|_1 &\leq C \left\{ (|r|_{0,\Gamma_D} |r_\nu|_{0,\Gamma_D})^{\frac{1}{2}} + (|r|_{0,\Gamma_N} |r_\nu|_{0,\Gamma_N})^{\frac{1}{2}} \right. \\ &\quad + k_{m,n} (|r|_{0,\Gamma_D} + |r^+|_{0,\Gamma_0} + |r^-|_{0,\Gamma_0}) \\ &\quad \left. + |r_\nu|_{0,\Gamma_N} + |r_\nu^+|_{0,\Gamma_0} + |r_\nu^-|_{0,\Gamma_0} \right\}, \end{aligned} \quad (1.3.3)$$

where $r = u - v$.

Proof. From (1.3.1) we obtain the following bounds:

$$\|u - u_{m,n}\|_1 \leq \|r\|_1 + Ck_{m,n}|r|_B. \quad (1.3.4)$$

To estimate $\|r\|_1$, we have from Lemma 1.1.1 and the triangle inequality

$$\|r\|_1 \leq C \{ |r|_1 + |r|_{0,\Gamma_D} + |r^+|_{0,\Gamma_0} + |r^-|_{0,\Gamma_0} \}.$$

Since $\Delta r = 0$ on S^+ and S^- , the inequality (1.2.6) is also valid for r and so

$$\begin{aligned} |r|_1^2 &\leq |r|_{0,\Gamma_D} |r_\nu|_{0,\Gamma_D} + |r|_{0,\Gamma_N} |r_\nu|_{0,\Gamma_N} \\ &\quad + (|r^+|_{0,\Gamma_0} + |r^-|_{0,\Gamma_0})(|r_\nu^+|_{0,\Gamma_0} + |r_\nu^-|_{0,\Gamma_0}). \end{aligned}$$

Using the Minkowski inequality and the inequality $\sqrt{ab} \leq \frac{a+b}{2}$, we obtain

$$\begin{aligned} \|r\|_1 &\leq C \left\{ (|r|_{0,\Gamma_D} |r_\nu|_{0,\Gamma_D})^{\frac{1}{2}} + (|r|_{0,\Gamma_N} |r_\nu|_{0,\Gamma_N})^{\frac{1}{2}} \right. \\ &\quad \left. + |r|_{0,\Gamma_D} + |r^+|_{0,\Gamma_0} + |r^-|_{0,\Gamma_0} + |r_\nu^+|_{0,\Gamma_0} + |r_\nu^-|_{0,\Gamma_0} \right\}, \end{aligned} \quad (1.3.5)$$

$$\begin{aligned} |r|_B &\leq |r|_{0,\Gamma_D} + |r^+|_{0,\Gamma_0} + |r^-|_{0,\Gamma_0} \\ &\quad + w \{ |r_\nu|_{0,\Gamma_N} + |r_\nu^+|_{0,\Gamma_0} + |r_\nu^-|_{0,\Gamma_0} \}. \end{aligned} \quad (1.3.6)$$

Substitution of (1.3.5) and (1.3.6) into (1.3.4) and the fact that $k_{m,n} \geq 1$ lead to the desired result (1.3.3). ■

Assuming that Eqs. (1.2.2) – (1.2.4) are valid in $S_{m,n}$, we obtain the following theorem.

Theorem 1.3.3 *Let u and $u_{m,n}$ be the same as in Theorem 1.3.1. If both the inverse and approximability properties hold and $w = k_{m,n}^{-1}$, then there exists a positive constant C independent of m , n and u such that*

$$\begin{aligned} \|u - u_{m,n}\|_1 \leq C \left\{ \left(k_{m,n} \alpha_{n,k,0}^+ + \alpha_{n,k,1}^+ \right) |u^+|_{k,\partial S^+} \right. \\ \left. + \left(k_{m,n} \alpha_{m,t,0}^- + \alpha_{m,t,1}^- \right) |u^-|_{t,\partial S^-} \right\}, \end{aligned} \quad (1.3.7)$$

where $k, t > 1$.

Proof. Note that both square roots on the right-hand side of (1.3.3) are bounded from above by

$$\begin{aligned} & \left\{ (|r^+|_{0,\partial S^+} + |r^-|_{0,\partial S^-}) (|r_\nu^+|_{0,\partial S^+} + |r_\nu^-|_{0,\partial S^-}) \right\}^{\frac{1}{2}} \\ & \leq C \left\{ k_{m,n} (|r^+|_{0,\partial S^+} + |r^-|_{0,\partial S^-}) + |r_\nu^+|_{0,\partial S^+} + |r_\nu^-|_{0,\partial S^-} \right\}, \end{aligned}$$

where again we use the inequality $\sqrt{ab} \leq \frac{a+b}{2}$. Consequently, from (1.3.3) it follows that

$$\begin{aligned} \|u - u_{m,n}\|_1 \leq C \left\{ k_{m,n} (|r^+|_{0,\partial S^+} + |r^-|_{0,\partial S^-}) \right. \\ \left. + |r_\nu^+|_{0,\partial S^+} + |r_\nu^-|_{0,\partial S^-} \right\}. \end{aligned} \quad (1.3.8)$$

Finally, the equation (1.3.7) is obtained from (1.2.3), (1.2.4) and (1.3.8). ■

Note that the approximation $u_{m,n}$ may have a different number of terms in S^+ from that in S^- , depending on the smoothness of u on ∂S^+ and ∂S^- . Hence, k and t in (1.2.3) and (1.2.4) may have different values.

Let us now investigate two special cases in which the error estimates (1.3.3) and (1.3.7) apply.

First, assume that the admissible functions $v \in S_{m,n}$ satisfy also the continuity conditions (1.1.3) on Γ_0 . Then we can modify (1.3.3) as follows.

Corollary 1.3.1 *Suppose that in addition to the conditions of Theorem 1.3.2, the functions in $S_{m,n}$ satisfy (1.1.3). Then there exists a positive constant C such that*

$$\begin{aligned} \|u - u_{m,n}\|_1 \leq C \left\{ (|r|_{0,\Gamma_D} |r_\nu|_{0,\Gamma_D})^{\frac{1}{2}} + (|r|_{0,\Gamma_N} |r_\nu|_{0,\Gamma_N})^{\frac{1}{2}} \right. \\ \left. + k_{m,n} |r|_{0,\Gamma_D} + |r_\nu|_{0,\Gamma_N} \right\}. \end{aligned}$$

Second, assume that the admissible functions $v \in S_{m,n}$ also satisfy the boundary conditions (1.1.2) on ∂S . Then we can write (1.3.7) as follows.

Corollary 1.3.2 *Suppose that u is a solution of (1.1.1) and (1.1.2). Let $u_{m,n}$ be the TM approximation satisfying (1.2.7) in $S_{m,n}$ and (1.1.2) on ∂S . If the inverse property is satisfied, $w = k_{m,n}^{-1}$, and for any $v \in S_{m,n}$ and $0 \leq l \leq k$,*

$$\|u - v^+\|_{l,\Gamma_0} \leq \beta_{n,k,l}^+ |u|_{k,\Gamma_0}, \quad (1.3.9)$$

and

$$\|u - v^-\|_{l,\Gamma_0} \leq \beta_{m,k,l}^- |u|_{k,\Gamma_0}. \quad (1.3.10)$$

Then there exists a positive constant C such that for $k \geq 1$,

$$\|u - u_{m,n}\|_1 \leq C \left\{ k_{m,n} (\beta_{n,k,0}^+ + \beta_{m,k,0}^-) + \beta_{n,k,1}^+ + \beta_{m,k,1}^- \right\} |u|_{k,\Gamma_0}.$$

Note that the bounds (1.3.9) and (1.3.10) can be conveniently applied to problems with singularities on the boundary $\partial S = \Gamma_D \cup \Gamma_N$, because the differentiability of u is required only on the interior boundary Γ_0 .

We will close this section with an estimate of the factor $k_{m,n}$ in (1.2.2) as a function of m and n . Consider the special case when Γ_0 is a circular arc.

A harmonic function can be written as

$$v = \sum_{i=1}^n \rho^{\mu_i} (a_i \cos \mu_i \theta + b_i \sin \mu_i \theta), \quad (\rho, \theta) \in S_0, \quad (1.3.11)$$

where S_0 is a simply connected region, a_i and b_i are coefficients, and the powers μ_i (not necessarily integers) are arranged in ascending order.

Let Γ_0 be a circular arc ($\rho = R_0$, $0 \leq \theta \leq \Theta \leq 2\pi$), and denote by S_0 the corresponding sector ($0 \leq \rho \leq R_0$, $0 \leq \theta \leq \Theta$). Suppose that the trigonometric functions $\cos \mu_i \theta$ and $\sin \mu_i \theta$ form an orthogonal system on $[0, \Theta]$. For a function v of the form (1.3.11), the orthogonality and Sobolev's imbedding theorem imply that

$$\begin{aligned} R_0^2 |v_\nu|_{0,\Gamma_0}^2 &= \Theta \sum_{i=1}^n \mu_i^2 R_0^{2\mu_i+1} \frac{(a_i^2 + b_i^2)}{2} \leq \mu_n^2 \Theta \sum_{i=1}^n R_0^{2\mu_i+1} \frac{(a_i^2 + b_i^2)}{2} \\ &= \mu_n^2 |v|_{0,\Gamma_0}^2 \leq C \mu_n^2 \|v\|_{1,S_0}^2. \end{aligned}$$

Consequently, we have

$$|v_\nu|_{0,\Gamma_0} \leq C \mu_n \|v\|_{1,S_0}.$$

Hence, if S^+ is a sector with circular boundary Γ_0 and the admissible functions v^+ are of the form (1.3.11), then

$$k_{m,n} = C \mu_n. \quad (1.3.12)$$

We will use (1.3.12) for the weight selections in the numerical experiments in computation.

1.4 Debye–Huckel Equation

Consider an elliptic boundary value problem on a domain divided into several subdomains by artificial or material interfaces. If the admissible functions consist of particular solutions of the underlying elliptic equation on the subdomains, a boundary approximation solution can be obtained by satisfying the exterior boundary conditions and the continuity conditions on the interior interface as much as possible in a least squares sense. Since the boundary approximation is performed only on the interior and exterior boundaries, we call this method the *the Trefftz method* (TM).

The advantages of the TM are again summarized as follows:

1. It is easy to solve the problems with corners and interface singularities as well as with unbounded domains, with which the standard finite element and finite difference methods have difficulties to cope.
2. The solution procedure is simple, because only the interior and exterior boundary conditions are taken into account in the solution process.
3. A very accurate solution can be obtained by using relatively few expansion terms of particular solutions (approximation in one lower dimension), thus great saving on CPU time and storage space.
4. It is possible to estimate errors of the approximate solutions, even though the exact solution of the physical problem is unknown. In this section, a useful relation for the error behavior will be established:

$$\|\varepsilon\|_1 = O(M^\alpha |\varepsilon|_B), \quad (1.4.1)$$

where $\alpha = 1$ or $\frac{1}{2}$, and M is the total number of unknown coefficients in the piecewise expansions used. The formula (1.4.1) is significant in practical calculation because we can evaluate error $\|\varepsilon\|_1$ in the domain in terms of the errors on the boundary, $|\varepsilon|_B$, which is naturally obtained from the TM. Once the errors of solutions are known, we can easily control the calculation procedure.

However, the following two difficulties arise in using the TM.

1. Piecewise particular solutions of elliptic equations have to be known. For the most important elliptic equations in application, we may find useful particular solutions in textbooks of partial differential equations, e.g., Tikhonov and Samarskii [458]. Nevertheless quite often, it is necessary to find asymptotic expansions near singular points and infinity, in order to obtain accurate solutions for all numerical methods.
2. Stability of numerical solutions is also important. In fact, stability will rely substantially on both the choice of piecewise particular solutions and the partition of the solution domain. Our intention here is to use stability analysis to guide us in choosing partitions so that better solutions can be obtained via the TM.

It is worth pointing out that the TM may fall into the class of general weighted least squares methods for elliptic systems of Aziz, Kellogg and Stephen [12], which are applied both within small elements (viewed here as subdomains) and on their boundaries (viewed as interfaces). Since only particular solutions are chosen to be admissible functions, the

number of unknown coefficients decreases drastically. A good TM approximation can be obtained even if several subdomains are used. It would also be interesting to develop an adaptive least squares methods in which the number of trial functions (as in this part) and the number of subdomains (as in [12]) are both changing, as done in the h - p version of FEM.

In this and the next sections, we will present an analysis of errors and in particular stability for the Debye–Huckel equation

$$-\Delta u + u = 0. \quad (1.4.2)$$

It should be noted that the infinite elements of Han [193] and Thatcher [455, 456] cannot be applied to (1.4.2).

Kellogg’s singular functions for interface problems (Kellogg [254, 255, 256]) are not complete when the intersection angles of interfaces are $\Theta = \pi/n$, $n = 2, 3, \dots$. The additional analytic functions found in Li [286] together with Kellogg’s function form a complete set for interface problems. Of course, a complete system of particular solutions is essential not only to theoretical research, but also to numerical methods, such as the TM and the combined methods discussed in this book.

Moreover, we will establish an error norm relation (1.4.1), analyze the stability of the TM approximations and investigate different shapes of subdomains divided by circular arcs and straight lines.

Let the bounded domain S be divided by Γ_0 into two non-overlapped subdomains S^+ and S^- , i.e., $S = S^+ \cup S^-$ and $\Gamma_0 = S^+ \cap S^-$. In the rest of this chapter, we will consider the piecewise equations

$$-\Delta u + u = 0 \quad \text{in } S^+ \quad \text{and } S^-, \quad (1.4.3)$$

with the interior and exterior boundary conditions

$$u^+ = u^-, \quad \frac{\partial u^+}{\partial \nu} = \frac{\partial u^-}{\partial \nu} \quad \text{on } \Gamma_0, \quad (1.4.4)$$

$$u = f \quad \text{on } \Gamma_D, \quad u_\nu = g \quad \text{on } \Gamma_N. \quad (1.4.5)$$

For (1.4.3) – (1.4.5), the TM is exactly the same as (1.2.7).

For the space $S_{m,n}$, we assume that the inverse property (1.2.2), and the approximability property (1.2.3) and (1.2.4) still hold. Approximability properties may be found in Cheney [95] for some spaces, or in Eisenstat [142] for the Bergman-Vekua space. For the equation $-\Delta u + u = 0$, the approximability properties of $S_{m,n}$ can be obtained only when the given subdomains are embedded into sectors, which are within the solution domains. In other cases, further study of the approximating spaces needs to be done (refer to the density study in Aziz, Dorr and Kellogg [11] and Browder [66]).

To provide more precise estimates, we assume that $S_{m,n}$ also satisfies the following inverse property.

Second inverse property: For any $v \in S_{m,n}$,

$$|v|_{0,\Gamma_N} \leq q_{m,n} \|v\|_1, \quad |v|_{0,\Gamma_0} \leq q_{m,n} \|v\|_1, \quad (1.4.6)$$

where $q_{m,n}$ is constant.

Obviously, the constant $q_{m,n}$ is bounded because of the Sobolev imbedding theorem (Sobolev [438]); but in some cases, there may exist better estimates:

$$q_{m,n} = o(1) \text{ as } m, n \longrightarrow \infty,$$

for the errors $v = u - u_{m,n}$.

Under these assumptions, we will provide error estimates and establish the relation (1.4.1). First, we give two lemmas.

Lemma 1.4.1 *Let $v \in S_{m,n}$ and suppose that the inverse property (1.2.2) and the second inverse property hold. Then when $w > 0$, there exist the norm bounds*

$$\|v\|_1 \leq (k_{m,n} + q_{m,n}/w) |v|_B.$$

Proof. By using Green's theorem and the fact

$$-\Delta v + v = 0 \quad \text{in } S^+ \text{ and } S^-,$$

we obtain

$$\begin{aligned} 0 &= \iint_{S^+} (\Delta v^+ - v^+) v^+ ds + \iint_{S^-} (\Delta v^- - v^-) v^- ds \\ &= - \iint_{S^+} [(v_x^+)^2 + (v_y^+)^2 + (v^+)^2] ds - \iint_{S^-} [(v_x^-)^2 + (v_y^-)^2 + (v^-)^2] ds \\ &\quad + \int_{\partial S^+} (v_\nu^+) v^+ ds + \int_{\partial S^-} (v_\nu^-) v^- ds. \end{aligned}$$

Then we have for $v = v^\pm$ in S^\pm

$$\begin{aligned} \|v\|_1^2 &= \left| \int_{\partial S^+} (v_\nu^+) v^+ d\ell + \int_{\partial S^-} (v_\nu^-) v^- d\ell \right| \\ &\leq \left| \int_{\Gamma_D} (v_\nu) v d\ell \right| + \left| \int_{\Gamma_N} (v_\nu) v d\ell \right| \\ &\quad + \left| \int_{\Gamma_0} [(v^+ - v^-)(v_\nu^+) + v^-(v_\nu^+ - v_\nu^-)] d\ell \right| \\ &\leq |v|_{0,\Gamma_D} |v_\nu|_{0,\Gamma_D} + |v|_{0,\Gamma_N} |v_\nu|_{0,\Gamma_N} \\ &\quad + |v^+ - v^-|_{0,\Gamma_0} |v_\nu^+|_{0,\Gamma_0} + |v^-|_{0,\Gamma_0} |v_\nu^+ - v_\nu^-|_{0,\Gamma_0} \end{aligned}$$

Therefore, from the inverse property (1.2.2) and the second inverse property (1.4.6), we can obtain

$$\begin{aligned} \|v\|_1^2 \leq & \{k_{m,n}|v|_{0,\Gamma_D} + q_{m,n}|v_\nu|_{0,\Gamma_N} + k_{m,n}|v^+ - v^-|_{0,\Gamma_0} \\ & + q_{m,n}|v_\nu^+ - v_\nu^-|_{0,\Gamma_0}\} \|v\|_1. \end{aligned}$$

The desired result is obtained by dividing both sides by $\|v\|_1$ and by noting the definition $|v|_B$ in (1.1.4). ■

We can prove the following lemma by using the same arguments as in Lemma 1.2.2.

Lemma 1.4.2 *Let u be the solution of (1.4.3) – (1.4.5). Then for any $w > 0$, there exists a unique function, $u_{m,n} \in S_{m,n}$, such that*

$$[u_{m,n}, v] = \int_{\Gamma_D} f v \, dl + w^2 \int_{\Gamma_N} g v_\nu \, dl, \quad \forall v \in S_{m,n}, \quad (1.4.7)$$

$$[u - u_{m,n}, v] = 0, \quad \forall v \in S_{m,n}, \quad (1.4.8)$$

and

$$\|u_{m,n}\|_1 \leq (k_{m,n} + q_{m,n}/w) \{|f|_{0,\Gamma_D} + w|g|_{0,\Gamma_N}\}.$$

Also, $u_{m,n}$ minimizes $I(v)$ over $S_{m,n}$ if and only if (1.4.7) holds.

Now, we have an error estimate theorem.

Theorem 1.4.1 *Let $u \in H^1(S)$ be the solution of (1.4.3) – (1.4.5), and let $u_{m,n} \in S_{m,n}$ be the TM approximation satisfying (1.4.7). If the inverse property (1.2.2) and the second inverse property hold, then for any $w > 0$ there exists a constant C independent of m , n and u such that*

$$\|u - u_{m,n}\|_1 \leq \inf_{v \in S_{m,n}} \{\|u - v\|_1 + (k_{m,n} + q_{m,n}/w)|u - v|_B\}, \quad (1.4.9)$$

where $k_{m,n}$ is defined in (1.2.2), and $q_{m,n}$ in (1.4.6).

Proof. Let $v \in S_{m,n}$ and $\eta = v - u_{m,n}$. We have from Lemma 1.4.1

$$\begin{aligned} \|u - u_{m,n}\|_1 & \leq \|u - v\|_1 + \|\eta\|_1 \\ & \leq \|u - v\|_1 + (k_{m,n} + q_{m,n}/w)|\eta|_B. \end{aligned} \quad (1.4.10)$$

Applying the orthogonality property (1.4.8), we obtain

$$|\eta|_B^2 = [\eta, \eta] = [v - u, \eta] \leq |u - v|_B |\eta|_B.$$

Hence $|\eta|_B \leq |u - v|_B$, and the desired inequality (1.4.9) follows from (1.4.10). ■

Obviously, Theorem 1.3.1 is a special case of Theorem 1.4.1 because the constant $q_{m,n} \leq C$.

Similar error bounds as Theorems 1.3.2 and 1.3.3, and Corollaries 1.3.1 and 1.3.2 can be easily derived. However, here we only investigate the relation between $\|u - u_{m,n}\|_1$ and $|u - u_{m,n}|_B$.

Let u be the solution of (1.4.3) – (1.4.5), then the error norms satisfy

$$\begin{aligned} I(u_{m,n}) &= |\varepsilon|_B^2 = |u - u_{m,n}|_B^2 = \int_{\Gamma_D} (u_{m,n} - f)^2 d\ell \\ &\quad + w^2 \int_{\Gamma_N} \left(\frac{\partial u_{m,n}}{\partial \nu} - g \right)^2 d\ell + \int_{\Gamma_0} (u_{m,n}^+ - u_{m,n}^-)^2 d\ell \\ &\quad + w^2 \int_{\Gamma_0} \left(\frac{\partial u_{m,n}^+}{\partial \nu} - \frac{\partial u_{m,n}^-}{\partial \nu} \right)^2 d\ell. \end{aligned} \quad (1.4.11)$$

We note that the explicit, true solution u disappears in $|\varepsilon|_B$ (see (1.4.11)) and the values of $|\varepsilon|_B$ are easily computed in the least squares procedure employed in the TM. We are then interested in evaluating $\|\varepsilon\|_1$ in terms of $|\varepsilon|_B$. Such a relation of these two norms is given in the following theorem:

Theorem 1.4.2 *Let $u \in H^1(S)$ be the solution of (1.4.3) – (1.4.5) and $u_{m,n} \in S_{m,n}$ be the TM approximation (1.4.7). If the inverse property (1.2.2) and the second inverse property hold for the difference $u - u_{m,n}$, then for any $w > 0$ there exists a constant C independent of m , n and u such that*

$$\|u - u_{m,n}\|_1 \leq (k_{m,n} + q_{m,n}/w) |u - u_{m,n}|_B. \quad (1.4.12)$$

Proof. Letting $v = u_{m,n} \in S_{m,n}$, we have from (1.4.4)

$$\begin{aligned} \|u - v\|_1^2 &\leq \left| \int_{\partial S^+} (u_\nu^+ - v_\nu^+) (u^+ - v^+) d\ell + \int_{\partial S^-} (u_\nu^- - v_\nu^-) (u^- - v^-) d\ell \right| \\ &\leq \left| \int_{\Gamma_D} (u_\nu - v_\nu) (f - v) d\ell \right| + \left| \int_{\Gamma_N} (g - v_\nu) (u - v) d\ell \right| \\ &\quad + \left| \int_{\Gamma_0} [(v^+ - v^-) (u_\nu^+ - v_\nu^+) + (u^- - v^-) (v_\nu^+ - v_\nu^-)] d\ell \right| \\ &\leq |u_\nu - v_\nu|_{0,\Gamma_D} |f - v|_{0,\Gamma_D} + |g - v_\nu|_{0,\Gamma_N} |u - v|_{0,\Gamma_N} \\ &\quad + |v^+ - v^-|_{0,\Gamma_0} |u_\nu^+ - v_\nu^+|_{0,\Gamma_0} + |u^- - v^-|_{0,\Gamma_0} |v_\nu^+ - v_\nu^-|_{0,\Gamma_0} \\ &\leq \{k_{m,n} |f - v|_{0,\Gamma_D} + q_{m,n} |g - v_\nu|_{0,\Gamma_N} \\ &\quad + k_{m,n} |v^+ - v^-|_{0,\Gamma_0} + q_{m,n} |v_\nu^+ - v_\nu^-|_{0,\Gamma_0}\} \|u - v\|_1. \end{aligned}$$

Dividing both sides by $\|u - v\|_1$ and using (1.4.11), we obtain

$$\|u - v\|_1 \leq (k_{m,n} + q_{m,n}/w) |u - v|_B.$$

The inequality (1.4.12) follows from the substitution $v = u_{m,n}$. ■

Based on Theorem 1.4.2, we can easily obtain the following two corollaries as the desired result (1.4.1). By noting $q_{m,n} \leq C$ Theorem 1.4.2 leads to the following corollary.

Corollary 1.4.1 *Let the weight $w = 1/M$, where $M = \text{Max}(m, n)$ and $m = O(n)$, and all the conditions in Theorem 1.4.2 hold. Also, suppose that the constant $k_{m,n}$ in the inverse property satisfies*

$$k_{m,n} \leq CM,$$

where C is a bounded constant independent of m , n and u . Then

$$\|u - u_{m,n}\|_1 = O(M|u - u_{m,n}|_B).$$

Corollary 1.4.2 *Let the weight $w = \frac{1}{M}$, where $M = \text{Max}(m, n)$ and $m = O(n)$, and all the conditions in Theorem 1.4.2 hold. Also, suppose that for $u - u_{m,n}$ the constants $k_{m,n}$ and $q_{m,n}$ in the inverse property and the second inverse property satisfy*

$$k_{m,n} \leq C\sqrt{M}, \quad q_{m,n} \leq C/\sqrt{M}.$$

Then,

$$\|u - u_{m,n}\|_1 = O(M^{\frac{1}{2}}|u - u_{m,n}|_B).$$

1.5 Stability Analysis

In this section, we present stability analysis for TM based on domain decomposition, and discuss the choice of geometric shapes for the subdomains used.

In order to discuss stability of the solution $u_{m,n}$, we need to estimate the values of condition numbers using the least squares method (see Golub and Loan [176])

$$\text{Cond.} = \left(\frac{\lambda_{\text{Max}}(\mathbf{B})}{\lambda_{\text{Min}}(\mathbf{B})} \right)^{\frac{1}{2}}.$$

Here the associated coefficient matrix \mathbf{B} is defined by

$$\mathbf{x}^T \mathbf{B} \mathbf{x} = |v|_B^2, \quad v \in S_{m,n},$$

where the vector \mathbf{x} is composed of the unknown coefficients.

Let \underline{S}^\pm and \overline{S}^\pm be the bounded domains such that

$$\underline{S}^+ \subseteq S^+ \subseteq \overline{S}^+, \quad \underline{S}^- \subseteq S^- \subseteq \overline{S}^-. \quad (1.5.1)$$

We define two matrices as follows:

$$\mathbf{F}_{S^+} = (f_{i,j}^+), \quad \mathbf{F}_{S^-} = (f_{i,j}^-),$$

where the matrix elements $f_{i,j}^\pm$ are

$$f_{i,j}^+ = (\psi_i^+, \psi_j^+)_{S^+} + \left(\frac{\partial \psi_i^+}{\partial x}, \frac{\partial \psi_j^+}{\partial x} \right)_{S^+} + \left(\frac{\partial \psi_i^+}{\partial y}, \frac{\partial \psi_j^+}{\partial y} \right)_{S^+}$$

and

$$f_{i,j}^- = (\psi_i^-, \psi_j^-)_{S^-} + \left(\frac{\partial \psi_i^-}{\partial x}, \frac{\partial \psi_j^-}{\partial x} \right)_{S^-} + \left(\frac{\partial \psi_i^-}{\partial y}, \frac{\partial \psi_j^-}{\partial y} \right)_{S^-}.$$

Then we have

$$(\mathbf{x}^+)^T \mathbf{F}_{S^+} \mathbf{x}^+ = \|v^+\|_{1,S^+}^2, \quad (\mathbf{x}^-)^T \mathbf{F}_{S^-} \mathbf{x}^- = \|v^-\|_{1,S^-}^2,$$

where the notations are

$$v^+ = \sum_{i=1}^m c_i \psi_i^+, \quad v^- = \sum_{i=1}^n d_i \psi_i^-,$$

$$\mathbf{x}^+ = (c_1, c_2, \dots, c_m)^T, \quad \mathbf{x}^- = (d_1, d_2, \dots, d_n)^T.$$

We now prove a main theorem.

Theorem 1.5.1 *Suppose that for any $v \in S_{m,n}$, the following bounds are satisfied:*

$$|v_\nu|_{0,\Gamma_N} \quad \text{and} \quad |v_\nu^\pm|_{0,\Gamma_0} \leq k_{m,n} \|v\|_1, \quad (1.5.2)$$

$$|v|_{0,\Gamma_D} \quad \text{and} \quad |v^\pm|_{0,\Gamma_0} \leq q_{m,n} \|v\|_1, \quad (1.5.3)$$

with the positive constants, $k_{m,n}$ and $q_{m,n}$. Then for any $w > 0$, there exists a bounded constant C independent of m, n and u such that

$$\text{Cond.} \leq w [k_{m,n} + q_{m,n}/w]^2 \times \left\{ \frac{\text{Max}[\lambda_{\text{Max}}(\mathbf{F}_{S^+}), \lambda_{\text{Max}}(\mathbf{F}_{S^-})]}{\text{Min}[\lambda_{\text{Min}}(\mathbf{F}_{S^+}), \lambda_{\text{Min}}(\mathbf{F}_{S^-})]} \right\}^{\frac{1}{2}}.$$

Proof. We have from Lemma 1.4.1:

$$|v|_B^2 \geq \frac{\|v\|_1^2}{(k_{m,n} + q_{m,n}/w)^2} \geq \frac{\|v^+\|_{1,S^+}^2 + \|v^-\|_{1,S^-}^2}{(k_{m,n} + q_{m,n}/w)^2}.$$

Then,

$$\lambda_{\text{Min}}(\mathbf{B}) = \min \frac{|v|_B^2}{\mathbf{x}^T \mathbf{x}} \geq \frac{1}{(k_{m,n} + q_{m,n}/w)^2} \min \frac{\|v^+\|_{1,S^+}^2 + \|v^-\|_{1,S^-}^2}{\mathbf{x}^T \mathbf{x}}.$$

Let the matrix \mathbf{T} be denoted by

$$\mathbf{T} = \begin{bmatrix} \mathbf{F}_{S^+} & \mathbf{0} \\ \mathbf{0} & \mathbf{F}_{S^-} \end{bmatrix},$$

then we obtain a relation for the smallest eigenvalues of the matrices \mathbf{T} , $\mathbf{F}_{\underline{S}^+}$ and $\mathbf{F}_{\underline{S}^-}$:

$$\lambda_{Min}(\mathbf{T}) = \min \frac{\|v^+\|_{1,\underline{S}^+}^2 + \|v^-\|_{1,\underline{S}^-}^2}{\mathbf{x}^T \mathbf{x}} = \min[\lambda_{Min}(\mathbf{F}_{\underline{S}^+}), \lambda_{Min}(\mathbf{F}_{\underline{S}^-})].$$

Obviously,

$$\lambda_{Min}(\mathbf{B}) \geq \frac{1}{(k_{m,n} + q_{m,n}/w)^2} \min[\lambda_{Min}(\mathbf{F}_{\underline{S}^+}), \lambda_{Min}(\mathbf{F}_{\underline{S}^-})]. \quad (1.5.4)$$

Similarly, from the assumption (1.5.2), (1.5.3) and the Sobolev imbedding theorem we can see that

$$\|v\|_B^2 \leq (q_{m,n} + w k_{m,n})^2 \|v\|_1^2 \leq (q_{m,n} + w k_{m,n})^2 [\|v^+\|_{1,\overline{S}^+}^2 + \|v^-\|_{1,\overline{S}^-}^2].$$

Therefore,

$$\lambda_{Max}(\mathbf{B}) \leq (q_{m,n} + w k_{m,n})^2 \max[\lambda_{Max}(\mathbf{F}_{\overline{S}^+}), \lambda_{Max}(\mathbf{F}_{\overline{S}^-})]. \quad (1.5.5)$$

It follows by computing (1.5.4) and (1.5.5) that

$$\frac{\lambda_{Max}(\mathbf{B})}{\lambda_{Min}(\mathbf{B})} \leq w^2 [k_{m,n} + q_{m,n}/w]^4 \times \frac{\max[\lambda_{Max}(\mathbf{F}_{\overline{S}^+}), \lambda_{Max}(\mathbf{F}_{\overline{S}^-})]}{\min[\lambda_{Min}(\mathbf{F}_{\underline{S}^+}), \lambda_{Min}(\mathbf{F}_{\underline{S}^-})]}.$$

Now Eq. (1.5.4) is obtained by Cond. = $\sqrt{\frac{\lambda_{max}(\mathbf{B})}{\lambda_{min}(\mathbf{B})}}$ for solving the over-determined system, see Chapter 2. ■

Below, we will apply Theorem 1.5.1 to the problem using the division displayed in Figure 1.1 and the admissible functions:

$$v^+ = \sum_{i=1}^m c_i \frac{I_{\mu_i^+}(r)}{I_{\mu_i^+}(R_0^+)} \sin \mu_i^+ \theta, \quad (r, \theta) \in S^+ \quad (1.5.6)$$

and

$$v^- = \sum_{i=1}^n d_i \frac{I_{\mu_i^-}(\rho)}{I_{\mu_i^-}(R_0^-)} \sin \mu_i^- \phi, \quad (\rho, \phi) \in S^-, \quad (1.5.7)$$

where c_i and d_i are unknown coefficients, $\mu_i^\pm = i\pi/\Theta^\pm$, Θ^\pm are the intersection angles; (r, θ) and (ρ, ϕ) are the polar coordinates with the origins at A and A^* , respectively, and the radii R_0^\pm are defined by the following formulae (1.5.9) below. In (1.5.6) and

(1.5.7), the Bessel functions $I_\mu(r)$ for a purely imaginary argument can be expressed by (Abramowitz and Stegun [2])

$$I_\mu(r) = \frac{\left(\frac{r}{2}\right)^\mu}{\Gamma\left(\frac{1}{2}\right)\Gamma\left(\mu + \frac{1}{2}\right)} \int_{-1}^1 e^{\pm rt} (1-t^2)^{\mu-\frac{1}{2}} dt. \quad (1.5.8)$$

Let the sectors \bar{S}^\pm and \underline{S}^\pm satisfy (1.5.1) such that

$$\begin{aligned} \bar{S}^- &= \{0 < \rho < R_0^- \text{ and } 0 < \phi < \Theta^-\}, \\ \underline{S}^- &= \{0 < \rho < r_0^- \text{ and } 0 < \phi < \Theta^-\}, \\ \bar{S}^+ &= \{0 < r < R_0^+ \text{ and } 0 < \theta < \Theta^+\}, \\ \underline{S}^+ &= \{0 < r < r_0^+ \text{ and } 0 < \theta < \Theta^+\}. \end{aligned} \quad (1.5.9)$$

Then we have the following corollary.

Corollary 1.5.1 *Let v^\pm be admissible functions given by (1.5.6) and (1.5.7) on the division in Figure 1.1. If $m = O(n)$ and the conditions in Theorem 1.5.1 are satisfied, then there exists a bounded constant C independent of m, n and u such that*

$$\text{Cond.} \leq Cw [k_{m,n} + q_{m,n}/w]^2 \max \left\{ \left[\frac{R_0^+}{r_0^+} \right]^{\mu_m^+}, \left[\frac{R_0^-}{r_0^-} \right]^{\mu_n^-} \right\}, \quad (1.5.10)$$

where the radii, R_0^\pm and r_0^\pm , are defined in (1.5.9).

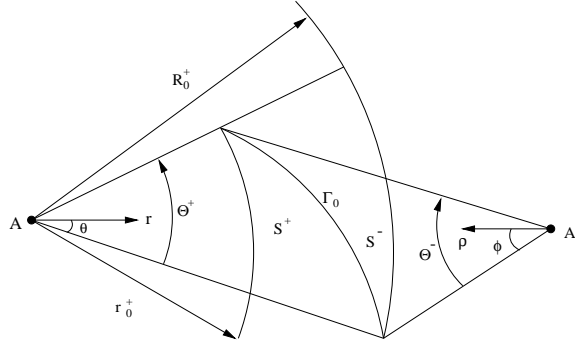


Figure 1.1: A division with $S = S^+ \cup S^-$.

Proof. Using the orthogonality of $\sin \mu_i^+ \theta$, we can see that

$$\|v^+\|_{1, \bar{S}^+}^2 = \frac{\Theta^+}{2} \sum_{i=0}^m c_i^2 \int_0^{R_0^+} r G_i^+(r) dr$$

and

$$\|v^+\|_{1, \underline{S}^+}^2 = \frac{\Theta^+}{2} \sum_{i=0}^m c_i^2 \int_0^{r_0^+} r G_i^+(r) dr,$$

where

$$G_i^+(r) = \frac{\left[[I'_{\mu_i^+}(r)]^2 + \frac{(\mu_i^+)^2}{r^2} I_{\mu_i^+}^2(r) + I_{\mu_i^+}^2(r) \right]}{I_{\mu_i^+}^2(R_0^+)}.$$

On the other hand, there exist the bounds in terms of the definition $I_\mu(r)$ in (1.5.8):

$$\beta_\mu r^\mu e^{-Max\ r} \leq I_\mu(r) \leq \beta_\mu r^\mu e^{Max\ r},$$

where the constants are

$$\beta_\mu = \frac{\left(\frac{1}{2}\right)^\mu}{\Gamma\left(\frac{1}{2}\right)\Gamma\left(\mu + \frac{1}{2}\right)} \int_{-1}^1 (1-t^2)^{\mu-\frac{1}{2}} dt,$$

with $\beta_{\mu+1} \leq \beta_\mu$. Moreover, by noting the formula (see Gradshteyn and Ryzhik [181]):

$$I'_\mu(r) = \frac{\mu}{r} I_\mu(r) + I_{\mu+1}(r),$$

we can obtain the following bounds:

$$\int_0^{R_0^+} r G_i^+(r) dr \leq C \mu_i^+ e^{4R_0^+}, \quad \int_0^{r_0^+} r G_i^+(r) dr \geq \delta_0 \mu_i^+ e^{-4R_0^+} \left[\frac{r_0^+}{R_0^+} \right]^{2\mu_i^+},$$

with constants $0 < \delta_0 < C < \infty$. This yields

$$\lambda_{Max}(\mathbf{F}_{\bar{S}^+}) \leq C \mu_m^+, \quad \lambda_{Min}(\mathbf{F}_{\underline{S}^+}) \geq \delta_0 \min \left[1, \mu_m^+ \left(\frac{r_0^+}{R_0^+} \right)^{2\mu_m^+} \right].$$

Similarly, we obtain

$$\lambda_{Max}(\mathbf{F}_{\bar{S}^-}) \leq C \mu_n^-, \quad \lambda_{Min}(\mathbf{F}_{\underline{S}^-}) \geq \delta_0 \min \left[1, \mu_n^- \left(\frac{r_0^-}{R_0^-} \right)^{2\mu_n^-} \right].$$

At least, one of the following two inequalities:

$$r_0^+ < R_0^+ \quad \text{and} \quad r_0^- < R_0^-$$

must hold. Therefore,

$$\begin{aligned} & \min[\lambda_{Min}(\mathbf{F}_{\underline{S}^+}), \lambda_{Min}(\mathbf{F}_{\underline{S}^-})] \\ &= \min \left(1, \mu_m^+ \left[\frac{r_0^+}{R_0^+} \right]^{2\mu_m^+}, \mu_n^- \left[\frac{r_0^-}{R_0^-} \right]^{2\mu_n^-} \right) \\ &= \min \left(\mu_m^+ \left[\frac{r_0^+}{R_0^+} \right]^{2\mu_m^+}, \mu_n^- \left[\frac{r_0^-}{R_0^-} \right]^{2\mu_n^-} \right), \end{aligned}$$

for some large numbers μ_m^+ and μ_n^- . Consequently, Theorem 1.5.1 yields

$$\begin{aligned} \text{Cond.} &\leq C w (k_{min} + q_{m,n}/w)^2 \\ &\times \left[\frac{\max[\mu_m^+, \mu_n^-]}{\min[\mu_m^+ (r_0^+/R_0^+)^{2\mu_m^+}, \mu_n^- (r_0^-/R_0^-)^{2\mu_n^-}]} \right]^{\frac{1}{2}}. \end{aligned}$$

The desired inequality (1.5.10) is obtained from the fact

$$\mu_m^+ = O(\mu_n^-),$$

which results from $\mu_i^\pm = i\pi/\Theta^\pm$ and the assumption $m = O(n)$. ■

As a result of Corollary 1.5.1, the following formula holds for $w = 1/M$:

$$\text{Cond.} = O \left\{ M \times \max \left[\left(\frac{R_0^+}{r_0^+} \right)^{\mu_m^+}, \left(\frac{R_0^-}{r_0^-} \right)^{\mu_n^-} \right] \right\} \quad (1.5.11)$$

provided that the bounds $k_{m,n} \leq CM$ are satisfied. To end this section, let us consider the geometric shapes of solution domains while using the TM. For the solution domain as a rhomboid (Figure 1.2), the values of Cond. in the case of B with a straight line Γ_0 are smaller than those in the case of A with a circular arc Γ_0 , based on (1.5.10) or (1.5.11). Also the divisions in Figure 1.3 will yield a good stability of numerical solutions by TMs.

1.6 Two Models of Singularity Problems

In this section, two benchmarks of singularity models, Motz's and the cracked beam problems, are described, which will be used for the testing models in this book quite often.

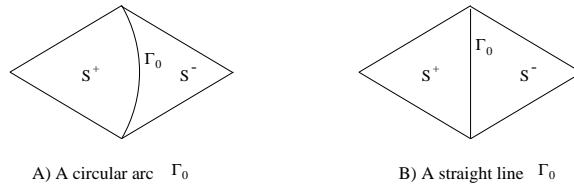


Figure 1.2: Division of a rhomboid.

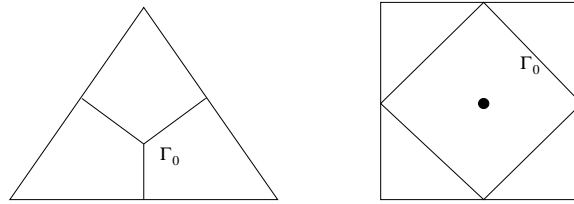


Figure 1.3: Good divisions for the TM.

Motz's problem is to seek a Laplacian solution satisfying the mixed Dirichlet-Neumann conditions in a rectangular domain (Figure 1.4).

$$\begin{aligned} \Delta u &= 0, \quad \text{in } S, \\ u|_{x=1} &= 500, \quad u|_{y=0 \cap -1 < x < 0} = 0, \\ \frac{\partial u}{\partial y} \Big|_{y=1} &= \frac{\partial u}{\partial y} \Big|_{y=0 \cap 0 < x < 1} = 0, \quad \frac{\partial u}{\partial x} \Big|_{x=-1} = 0. \end{aligned}$$

First, we approximate u in the entire domain S by the particular solutions

$$v = \sum_{l=0}^L D_l r^{l+\frac{1}{2}} \cos\left(l + \frac{1}{2}\right)\theta. \tag{1.6.1}$$

When we exchange the boundary conditions on $x = 1$ and $y = 1$, to obtain the cracked beam problem:

$$\begin{aligned} \Delta u &= 0, \quad \text{in } S, \\ u|_{y=1} &= 500, \quad u|_{y=0 \cap -1 < x < 0} = 0, \\ \frac{\partial u}{\partial y} \Big|_{y=0 \cap 0 < x < 1} &= 0, \quad \frac{\partial u}{\partial x} \Big|_{x=1 \cup x=-1} = 0. \end{aligned}$$

The solution of the cracked beam problem can also be expressed by (1.6.1).

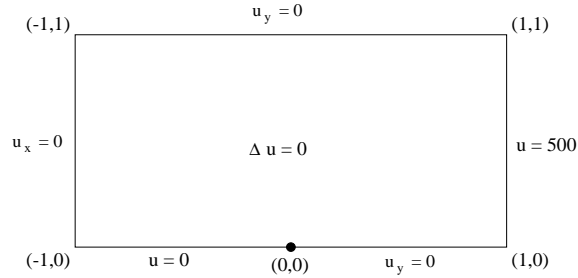


Figure 1.4: Motz's problem.

For Motz's problem, we may use the conformal transformation method of Whiteman and Papamichael [489] and Papamichael and Whiteman [371], to seek the most accurate leading coefficients. However, for the cracked beam problems, the conformal transformation method needs to be further developed to provide the leading coefficients. Let us consider Motz's problem only. Based on the recursive algorithms in Rosser and Papamichael [412], the coefficients $D_0 \sim D_{99}$ listed in [309] are obtained by Mathematica using 200 working digits. Note that all decimal digits appearing in the table are *significant* in the sense that all digits are *correct* except the last digit may have, at most, an error of half a unit, based on comparisons with the more accurate coefficients in Li and Lu [309], and based on an a priori error analysis and a priori choices of the truncation errors and the rounding errors in Chen [87]. It can be seen that D_0 has 199 significant decimal digits, and D_{99} has 89 significant decimal digits. These very highly accurate coefficients may serve as benchmark test case for other numerical methods. In Table 1.1, we only list the first 9 leading and the last coefficients, other coefficients can be found in [309].

Table 1.1: $D_0 \sim D_8$ and D_{99} by Mathematica with 200 significant digits

$D_0=$	401.16 24537 45234 42044 31378 39458 16089 26992 51065 85986 65518 26306 01725 23161 30188 12431 27889 69253 90702 08219 26757 21171 78423 66904 13922 92491 56495 49727 47287 98159 24672 04842 37467 00355 56529 56501 76619 38359 05333 0860
$D_1=$	87.655 92019 50879 16964 78412 14332 05792 19968 44301 15411 01582 38050 35569 85547 67842 90603 69409 43880 43016 93304 17719 21652 06083 99484 40485 94952 44529 68912 67064 71570 69140 78423 75795 92554 85635 80734 53435 91630 11852 08
$D_2=$	17.237 91507 94468 09287 38603 58611 43932 06015 00491 63038 74772 78674 59834 22120 18474 43616 27807 31446 12280 00046 29555 36315 96292 25440 07092 23528 53274 70564 40943 54679 73778 04531 96200 20166 14305 08786 11111 98441 59095 37
$D_3=$	-8.0712 15259 69813 44498 22306 15251 29971 94144 54273 59398 24436 83760 06764 82600 16376 33733 18346 29163 33865 18773 25777 60587 83964 46374 68559 29572 32794 09470 67810 29377 47609 09836 75415 68561 19944 39783 01779 68808 95188
$D_4=$	1.4402 72717 02285 69808 63415 89244 41287 23699 83453 19793 30190 31626 48913 31831 84851 76302 67871 05417 05480 23555 29559 17338 72577 19118 96338 30719 54082 71558 32124 71588 40392 80725 21601 69072 17049 72356 25549 19505 5531
$D_5=$	3.3105 48859 20736 05753 93559 72221 56905 96747 27346 63730 83825 29610 61756 46118 24629 28510 51061 24382 45987 03178 04161 18396 45225 37995 00782 84716 63047 59369 76786 73451 39895 45292 88479 96980 29984 51788 67061 80176 33E-1
$D_6=$	2.7543 73445 09180 80009 14976 83962 01013 04427 13749 71426 46007 17422 65881 83285 66869 02739 77040 57942 52992 72481 40629 51683 23320 43572 29384 52772 87439 00550 23187 87016 54338 16956 63921 33124 74714 76044 82893 75542 4E-1
$D_7=$	-8.6932 99452 55366 88642 22470 54185 98242 97321 27665 95962 30933 52182 04384 27527 01393 61784 62277 67670 46103 85606 44352 16249 99756 06597 52174 36026 58152 65385 89680 58566 21968 24118 22305 58055 95203 16400 38966 01793E-2
$D_8=$	3.3604 87842 65369 51127 65265 99094 30556 06044 85880 03691 87524 04059 78069 01849 30487 04642 15038 00943 32743 06824 22486 72764 07464 79267 10282 77822 80962 16858 85759 46930 62015 95128 26614 58013 41445 28901 83614 3684E-2
$D_{99}=$	-3.6353 68995 39164 25337 11549 72592 79574 05411 97162 61432 70522 61447 69433 85786 86661 79230 96462 4633E-31

Chapter 2

Motz's and Cracked Beam Problems

In this chapter we develop the TM in Chapter 1 involving integration approximation, to lead to the collocation Trefftz method (called the collocation TM, or the CTM). We choose the high order Gaussian rules and the central rule, link the collocation method and the least squares method (LSM), and demonstrate exponential convergence rates of the obtained solutions. For Motz's problem and the cracked beam problem, the collocation TM is used to seek their approximate solutions $u_N = \sum_{i=0}^N D_i r^{i+\frac{1}{2}} \cos(i+\frac{1}{2})\theta$, where D_i are the expansion coefficients. Compared with the solutions in the previous literature, the present Motz's solutions are more accurate and the leading coefficient D_0 using the Gaussian rule with six nodes can achieve 17 significant (decimal) digits. Similarly for the cracked beam problem, the collocation TM also provides the highly accurate solutions, with D_0 accurate up to 17 significant digits by the Gaussian rule. This chapter proves that when the rules of quadrature involved have the relative errors less than three quarters, the solution from the collocation TM may converge exponentially. Such an analysis provides the theoretical support that the collocation TM is the most accurate method for Motz's and the cracked beam problems.

2.1 Introduction

Motz's problem was first discussed by Motz [357] in 1947 for the relaxation method. Since then, many researchers have selected Motz's problem as a prototype of singularity problems for verifying efficiency of numerical methods (see [291]).

Motz's problem solves the Laplace equation on the rectangle $S = \{(x, y) \mid -1 < x < 1, 0 < y < 1\}$

$$\Delta u = \frac{\partial^2 u}{\partial x^2} + \frac{\partial^2 u}{\partial y^2} = 0 \quad \text{in } S, \quad (2.1.1)$$

with the mixed Neumann-Dirichlet boundary conditions, see Figure 2.1,

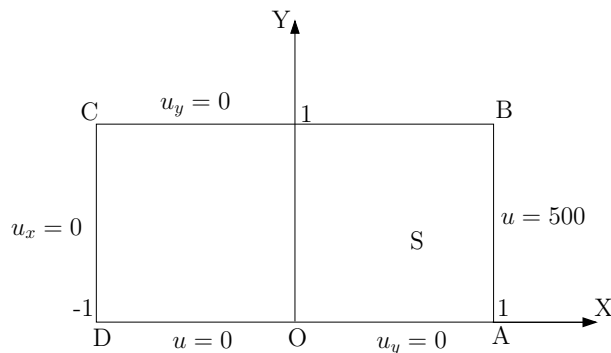


Figure 2.1: The Motz's problem.

$$u|_{x<0 \cap y=0} = 0, \quad u|_{x=1} = 500, \quad (2.1.2)$$

$$\frac{\partial u}{\partial y} \Big|_{y=1} = \frac{\partial u}{\partial y} \Big|_{x>0 \cap y=0} = \frac{\partial u}{\partial x} \Big|_{x=-1} = 0. \quad (2.1.3)$$

Note that there exists a singularity at the origin $(0,0)$ due to the intersection of the Neumann-Dirichlet boundary conditions. In fact, the singular solutions of (2.1.1) – (2.1.3) are found as

$$u(r, \theta) = \sum_{i=0}^{\infty} d_i r^{i+\frac{1}{2}} \cos\left(i + \frac{1}{2}\right)\theta, \quad (2.1.4)$$

where d_i are the true expansion coefficients, and (r, θ) are the polar coordinates with the origin at $(0,0)$. Since its convergence radius, $r = 2$, is analyzed in Rosser and Papamichael [412], the series expansions (2.1.4) are well suited to the entire solution domain S . Hence, the admissible functions with finite terms,

$$u_N(r, \theta) = \sum_{i=0}^N D_i r^{i+\frac{1}{2}} \cos\left(i + \frac{1}{2}\right)\theta, \quad (2.1.5)$$

where D_i are the unknown coefficients, are most efficient as numerical Motz's solutions. The exponential convergence rates $O(e^{-cN})$ can be obtained for (2.1.5) with some positive constant c . When functions (2.1.5) are chosen, Eq. (2.1.1), $u|_{x<0 \cap y=0} = 0$ and $\frac{\partial u}{\partial y} \Big|_{x>0 \cap y=0} = 0$ are satisfied. Then the coefficients D_i are sought by satisfying the rest of boundary conditions in (2.1.2) and (2.1.3). This is called the boundary approximation method (BAM) in [291, 316] or the collocation TM in this chapter. Under the computation in double precision and $N = 34$, the maximal absolute error at $x = 1$ (e.g., on

\overline{AB}) of the Motz's solution in [316] reaches up to 5.47×10^{-9} . Also the leading coefficient D_0 in [316] has 12 significant digits by the central rule. The solutions in [316] have been recognized to be the very accurate solutions for Motz's problem, see [169, 168, 332]. In this chapter, to pursue the better leading coefficient D_0 , we choose the Gaussian rules of high orders. Surprisingly, the obtained D_0 may have 17 significant digits by Fortran programs in double precision. Based on the new results in this chapter, we may address that the collocation TM (i.e., the BAM) is the highly accurate method for Motz's problem, not only in the global solutions but also in the leading coefficient D_0 . As for Motz's problem, the conformal transformation method of Rosser and Papamichael [412] can also yield the most accurate leading coefficient D_0 .

The same approaches are applied to the cracked beam problem, which is the other frequently used benchmark model for testing new numerical methods [154, 169, 168, 369, 446]. Its highly accurate solutions are also provided with the leading D_0 having 17 significant digits. The advantage of the cracked beam problem over Motz's problem is that half of the expansion coefficients are zero.

This chapter is organized as follows. In Section 2.2, basic algorithms of the collocation TM are provided for Motz's problem, and the highly accurate solutions are obtained in double precision. In Section 2.3, a new analysis is made for the quadrature involved. In Section 2.4, the cracked beam problem is discussed, and its highly accurate solutions and the leading coefficient D_0 with 17 significant digits are also reported. In Section 2.5, some discussions and comparisons are made, and in the last section, concluding remarks are addressed.

2.2 Basic Algorithms of Collocation TM

Since the expansions (2.1.5) satisfy the Laplace equation and boundary conditions at $y = 0$, the coefficients D_i should be chosen to satisfy the rest of the boundary conditions,

$$u|_{x=1} = u|_{\overline{AB}} = 500, \quad (2.2.1)$$

$$\frac{\partial u}{\partial y}\Big|_{y=1} = \frac{\partial u}{\partial \nu}\Big|_{\overline{BC}} = 0, \quad \frac{\partial u}{\partial \nu}\Big|_{\overline{CD}} = -\frac{\partial u}{\partial x}\Big|_{x=-1} = 0, \quad (2.2.2)$$

as best as possible, where $u_\nu = \frac{\partial u}{\partial \nu}$ is the outward normal derivative to ∂S , and \overline{AB} , \overline{BC} and \overline{CD} are shown in Figure 2.1. Hence, the least squares method (LSM) may be designed as follows. Denote

$$[u, v] = \int_{\overline{AB}} uv \, d\ell + w^2 \int_{\overline{BC} \cup \overline{CD}} u_\nu v_\nu \, d\ell,$$

where w is a positive weight constant, and a good choice of the weight,

$$w = \frac{1}{N+1}, \quad (2.2.3)$$

can be found in Chapter 1. Denote by V_N the collection of finite dimensional functions (2.1.5). Then, we may seek $u_N \in V_N$ such that

$$[u_N, v] = 500 \int_{\overline{AB}} v \, dl, \quad \forall v \in V_N. \quad (2.2.4)$$

Denote the energy

$$I(v) = \int_{\overline{AB}} (v - 500)^2 \, dl + w^2 \int_{\overline{BC \cup CD}} v_v^2 \, dl. \quad (2.2.5)$$

The solution of (2.2.4) can also be expressed by: To seek $u_N \in V_N$ such that

$$I(u_N) = \min_{v \in V_N} I(v). \quad (2.2.6)$$

Both (2.2.4) and (2.2.6) lead to the same linear algebraic system

$$\mathbf{A}\mathbf{x} = \mathbf{b}, \quad (2.2.7)$$

where $\mathbf{x} \in R^{N+1}$ is the unknown vector consisting of coefficients D_i , $i = 0, \dots, N$, $\mathbf{b} \in R^{N+1}$ is the known vector resulting from the non-homogeneous Dirichlet condition (2.2.1), and the matrix, $\mathbf{A} \in R^{(N+1) \times (N+1)}$, is symmetric positive definite, but not sparse. By the Gaussian elimination without pivoting [176], the coefficients D_i (i.e., \mathbf{x}) can be obtained. Once the coefficients D_i are known, the errors on $\overline{AB \cup BC \cup CD}$

$$\begin{aligned} \|u - u_N\|_B &= \left[\int_{\overline{AB}} (500 - u_N)^2 \, dl + w^2 \int_{\overline{BC \cup CD}} (u_N)_v^2 \, dl \right]^{\frac{1}{2}} \\ &= \sqrt{I(u_N)} \end{aligned}$$

are computable, where the notation

$$\|v\|_B = |v|_B = \sqrt{[v, v]}. \quad (2.2.8)$$

Suppose that certain rules of integration are adopted to the integrals in (2.2.5). Let \overline{AB} be divided into small segments $\overline{Z_i Z_{i+1}}$, i.e., $\overline{AB} = \bigcup_i \overline{Z_i Z_{i+1}}$. Then the integral is approximated by some rules,

$$\int_{\overline{AB}} v^2 \, dl \approx \widetilde{\int}_{\overline{AB}} v^2 \, dl = \sum_i \widetilde{\int}_{\overline{Z_i Z_{i+1}}} v^2 \, dl. \quad (2.2.9)$$

For example, the central and the trapezoidal rules are given by

$$\begin{aligned} \widetilde{\int}_{\overline{Z_i Z_{i+1}}} v^2 \, dl &= v_{i+\frac{1}{2}}^2 h_i, \quad \text{and} \\ \widetilde{\int}_{\overline{Z_i Z_{i+1}}} v^2 \, dl &= \frac{1}{2}(v_i^2 + v_{i+1}^2)h_i, \end{aligned} \quad (2.2.10)$$

respectively, where $h_i = \overline{Z_i Z_{i+1}}$, $v_i = v(Z_i)$, $v_{i+\frac{1}{2}} = v(Z_{i+\frac{1}{2}})$ and $Z_{i+\frac{1}{2}} = \frac{Z_i + Z_{i+1}}{2}$. Other kinds of the Newton-Cotes and the Gaussian rules can also be employed and will

be discussed later. Hence, for the numerical quadrature, we may seek $\tilde{u}_N \in V_N$ such that

$$\tilde{I}(\tilde{u}_N) = \min_{v \in V_N} \tilde{I}(v), \quad (2.2.11)$$

where

$$\tilde{I}(v) = \int_{\widetilde{AB}} (v - 500)^2 dl + w^2 \int_{\widetilde{BC \cup CD}} v^2 dl. \quad (2.2.12)$$

The minimization of $\tilde{I}(v)$ also leads to a linear system like (2.2.7). This is a direct implementation of the LSM involving numerical integration, called the normal method (NM).

Now, we turn to the collocation TM, which can be regarded as a certain kind of the LSM involving specific quadratures. For simplicity in exposition, let us first consider the central rule (2.2.10). Divide the boundaries \overline{AB} , \overline{BC} and \overline{CD} into uniform sub-intervals (see Figure 2.1). Then

$$h = \frac{\overline{AB}}{M} = \frac{\overline{CD}}{M} = \frac{\overline{CB}}{2M}.$$

Eqs. (2.2.1) and (2.2.2) can be transformed to the boundary collocation equations,

$$u_N(P_i) = 500, \quad i = 1, 2, \dots, M, \quad (2.2.13)$$

$$\frac{\partial u_N}{\partial x}(P_i^*) = -\frac{\partial u_N}{\partial \nu}(P_i^*) = 0, \quad i = 1, 2, \dots, M, \quad (2.2.14)$$

$$\frac{\partial u_N}{\partial y}(Q_i^\pm) = \frac{\partial u_N}{\partial \nu}(Q_i^\pm) = 0, \quad i = 1, 2, \dots, M. \quad (2.2.15)$$

Let $x_i^\pm = \pm(i - \frac{1}{2})h$ and $y_i = (i - \frac{1}{2})h$. The nodes $P_i = (1, y_i) \in \overline{AB}$, $P_i^* = (-1, y_i) \in \overline{CD}$ and $Q_i^\pm = (x_i^\pm, 1) \in \overline{BC}$, and their polar coordinates are computed by

$$P_i = (r_i, \theta_i), \quad r_i = \sqrt{1 + y_i^2}, \quad \theta_i = \cos^{-1}\left(\frac{1}{\sqrt{1 + y_i^2}}\right),$$

$$P_i^* = (r_i, \theta_i^*), \quad \theta_i^* = \pi - \theta_i,$$

where $0 < \theta_i < \frac{\pi}{2}$. Besides,

$$Q_i^\pm = (\bar{r}_i, \theta_i^\pm), \quad \bar{r}_i = \sqrt{1 + x_i^2}, \quad \theta_i^\pm = \sin^{-1}\left(\frac{1}{\sqrt{1 + x_i^2}}\right),$$

where $0 < \theta_i^+ < \frac{\pi}{2}$ and $\theta_i^- = \pi - \theta_i^+$.

In (2.2.13) – (2.2.15), there are $m = 4M$ equations, but $N + 1$ unknown coefficients. Usually, we select $m > N + 1$. We invoke the standard LSM in [176] to solve the overdetermined system of (2.2.13) – (2.2.15). Denote (2.2.13) – (2.2.15) by

$$\mathbf{F}_i \mathbf{x} = \mathbf{b}_i, \quad i = 1, 2, 3, \quad (2.2.16)$$

respectively, where \mathbf{F}_i and \mathbf{b}_i are the known matrices and vectors, respectively. Since Eqs. (2.2.16) result from different boundary conditions, different weights should be assigned.

When the weights \sqrt{h} and $w\sqrt{h}$ are applied to the first and the other two equations in (2.2.16) respectively, the global target function becomes

$$T(\mathbf{x}) = h\|\mathbf{F}_1\mathbf{x} - \mathbf{b}_1\|^2 + w^2h\sum_{i=2}^3\|\mathbf{F}_i\mathbf{x} - \mathbf{b}_i\|^2, \quad (2.2.17)$$

where $\|\cdot\|$ is the Euclidean norm, and w is a suitable weight constant given in (2.2.3). We can easily verify the following lemma by direct manipulation.

Lemma 2.2.1 *Let the central rule (2.2.10) be used in (2.2.12), and (2.2.16) be the collocation equations (2.2.13) – (2.2.15). Then we have*

$$\tilde{I}(\tilde{u}_N) = T(\mathbf{x}),$$

where $\tilde{I}(\tilde{u}_N)$ and $T(\mathbf{x})$ are defined in (2.2.12) and (2.2.17), respectively.

Note that the admissible functions and their derivatives are given by

$$\begin{aligned} u_N &= u_N(r, \theta) = \sum_{l=0}^N D_l r^{l+\frac{1}{2}} \cos(l + \frac{1}{2})\theta, \\ \frac{\partial u_N}{\partial x} &= \sum_{l=0}^N D_l (l + \frac{1}{2}) r^{l-\frac{1}{2}} \cos(l - \frac{1}{2})\theta, \\ \frac{\partial u_N}{\partial y} &= \sum_{l=0}^N D_l (l + \frac{1}{2}) r^{l-\frac{1}{2}} \sin(\frac{1}{2} - l)\theta. \end{aligned}$$

Then, Lemma 2.2.1 enables us to obtain the solutions D_l by solving the following overdetermined system of the equations

$$\sqrt{h} \sum_{l=0}^N D_l r_i^{l+\frac{1}{2}} \cos(l + \frac{1}{2})\theta_i = 500\sqrt{h}, \quad 1 \leq i \leq M, \quad (2.2.18)$$

$$w\sqrt{h} \sum_{l=0}^N D_l (l + \frac{1}{2}) (r_i)^{l-\frac{1}{2}} \cos(l - \frac{1}{2})\theta_i^* = 0, \quad 1 \leq i \leq M, \quad (2.2.19)$$

$$w\sqrt{h} \sum_{l=0}^N D_l (l + \frac{1}{2}) (\bar{r}_i)^{l-\frac{1}{2}} \sin(\frac{1}{2} - l)\theta_i^\pm = 0, \quad 1 \leq i \leq M \quad (2.2.20)$$

where $m = 4M > N + 1$. Denote the overdetermined system of (2.2.18) – (2.2.20) by

$$\mathbf{F}\mathbf{x} = \mathbf{b}^*, \quad (2.2.21)$$

where the associated matrix $\mathbf{F} \in R^{m \times (N+1)}$, $\mathbf{b}^* \in R^m$ and $\mathbf{x} \in R^{N+1}$. In fact, the entries of $\mathbf{F} = (F_{i,l})$ are given by

$$F_{i,l} = \begin{cases} \sqrt{hr_i^{l+\frac{1}{2}}} \cos(l + \frac{1}{2})\theta_i, & 1 \leq i \leq M, 0 \leq l \leq N, \\ w\sqrt{h}(l + \frac{1}{2})r_{i-M}^{l-\frac{1}{2}} \cos(l - \frac{1}{2})\theta_{i-M}^*, & M < i \leq 2M, 0 \leq l \leq N, \\ w\sqrt{h}(l + \frac{1}{2})\bar{r}_{i-2M}^{l-\frac{1}{2}} \sin(\frac{1}{2} - l)\theta_{i-2M}^+, & 2M < i \leq 3M, 0 \leq l \leq N, \\ w\sqrt{h}(l + \frac{1}{2})\bar{r}_{i-3M}^{l-\frac{1}{2}} \sin(\frac{1}{2} - l)\theta_{i-3M}^-, & 3M < i \leq 4M, 0 \leq l \leq N. \end{cases} \quad (2.2.22)$$

In general, we can rewrite the overdetermined system of (2.2.18) – (2.2.20) as

$$\alpha_i(u_N(P_i) - 500) = 0, \quad P_i \in \overline{AB}, \quad (2.2.23)$$

$$w\beta_i \frac{\partial u_N}{\partial x}(P_i^*) = 0, \quad P_i^* \in \overline{CD}, \quad (2.2.24)$$

$$w\gamma_i \frac{\partial u_N}{\partial y}(Q_i) = 0, \quad Q_i \in \overline{BC}, \quad (2.2.25)$$

where P_i and P_i^* and Q_i are the nodes of integration rules, and α_i , β_i and γ_i are positive weights. Eqs. (2.2.23) – (2.2.25) may be obtained from other quadratures. Take the Gaussian rules for example. Denote $h_k = \overline{Z_k Z_{k+1}}$. By using an affine transformation, the interval $[Z_k, Z_{k+1}]$ can be converted to $[-1, 1]$. Hence by this transformation, $x \in \overline{Z_k Z_{k+1}}$ is mapped to $t \in [-1, 1]$, $f(x)$ to $\hat{f}(t)$, and the integral on $\overline{Z_k Z_{k+1}}$ is changed to

$$\int_{\overline{Z_k Z_{k+1}}} f(x)dx = \frac{h_k}{2} \int_{-1}^1 \hat{f}(t)dt.$$

The Gaussian rules with r nodes are given by

$$\int_{-1}^1 f(t)dt \approx \int_{-1}^1 \widetilde{f}(t)dt = \int_{-1}^1 \hat{f}(t)dt = \sum_{i=1}^{\ell} \omega_i f(t_i), \quad (2.2.26)$$

where the locations of nodes $t_i \in [-1, 1]$ and positive weights ω_i are provided in textbooks (e.g., [9]). For (2.2.23), a point P_i located at the j -th node of $\overline{Z_k Z_{k+1}} \in \overline{AB}$ has the weights $\alpha_i = \sqrt{\frac{\omega_j h_k}{2}}$. The weights β_i and γ_i can be obtained similarly. When $\ell = 1$, the Gaussian rule is just the central rule with $t_1 = 0$ and $\omega_1 = 2$. For the Gaussian rules, we have the following proposition, similar to Lemma 2.2.1.

Proposition 2.2.1 *Let the Gaussian rules (2.2.26) be used in (2.2.12), and $m \geq N + 1$. Then the coefficients D_ℓ from the corresponding collocation equations (2.2.23) – (2.2.25) are just the solutions from (2.2.11).*

Let us consider the computer complexity of this method. In (2.2.22) we may employ the recursive formulas to save CPU time:

$$\cos\left(l + \frac{1}{2}\right)\theta = 2\cos\theta\cos\left(l - \frac{1}{2}\right)\theta - \cos\left(l - \frac{3}{2}\right)\theta,$$

$$r_i^{l+\frac{1}{2}} = r_i \cdot r_i^{l-\frac{1}{2}}.$$

To solve the least squares solution of (2.2.21) with full rank \mathbf{F} , we may use the QR method by the Householder orthogonalization with the flops ([176], p. 248),

$$T_L = 2mn^2 - \frac{2n^3}{3}, \quad n = N + 1.$$

On the other hand, the normal equations from (2.2.21) are

$$\mathbf{A}\mathbf{x} = \mathbf{F}^T\mathbf{F}\mathbf{x} = \mathbf{F}^T\mathbf{b}^* = \mathbf{b}, \quad (2.2.27)$$

where \mathbf{A} is symmetric positive definite. Then the flops for $\mathbf{F}^T\mathbf{F}$ and the Gaussian elimination of symmetric matrices are $m(n^2 + n)$ and $\frac{1}{3}n^3$ respectively. So the main flops needed is

$$T_N = mn^2 + \frac{1}{3}n^3.$$

In our case, $n = N + 1$ and $m = 4N$. Evidently, when $m \gg n$, we have $T_L \leq 2T_N$, and when $m \geq n$,

$$T_L - T_N = (m - n)n^2 \geq 0.$$

Then we conclude the following:

Corollary 2.2.1 *The flops needed to solve a least squares problem (2.2.21) by the Householder QR method are larger than, but at most double of, those by the normal method (2.2.27).*

Besides the QR method, the singular value decomposition (SVD) can also be used to solve the overdetermined system (2.2.21). A comparison between the QR method and the SVD is given in [128]. In general, the latter uses more flops than the former. So the SVD is not recommended here.

Since the condition number of matrix \mathbf{A} is nearly square of that of matrix \mathbf{F} (see [176]), using the normal equations incurs a serious loss of solution accuracy for Motz's problem. Some numerical experiments of the NM were reported in Lefebvre [281], where only four and five significant digits of Motz's solutions were obtained from the computation in double precision. Hence to obtain the numerical solutions of Motz's problem, we always choose the QR method to solve (2.2.21). Such a numerical approach is called the BAM in [291, 316] and the collocation TM in this chapter¹. Note that stability analysis of the collocation TM has been explored in [291, 315].

¹Strictly speaking, the description of BAM in [291, 316] does not involve numerical quadrature; the computed results in [291, 316] are, indeed, obtained by the algorithms described in this chapter using the central rule. The BAM involving numerical integration leads to the collocation TM. We join the BAM into the Trefftz family recently for easy communication with others.

To close this section, we provide numerical experiments for Motz's problem. First, for the central rule, errors of the solutions and condition numbers are listed in Tables 2.1 and 2.2, where $\varepsilon = u - u_N$, M denotes the number of collocation nodes along \overline{AB} , and the total number of all collocation nodes used is $4M$. In these tables, $\Delta D_i = d_i - D_i$, $\|\varepsilon\|_{\infty, \overline{AB}} = \max_{\overline{AB}} |\varepsilon|$, and the condition number is defined by

$$\text{Cond.} = \left\{ \frac{\lambda_{\max}(\mathbf{F}^T \mathbf{F})}{\lambda_{\min}(\mathbf{F}^T \mathbf{F})} \right\}^{\frac{1}{2}} = \left\{ \frac{\lambda_{\max}(\mathbf{A})}{\lambda_{\min}(\mathbf{A})} \right\}^{\frac{1}{2}}, \quad (2.2.28)$$

where $\lambda_{\max}(\mathbf{A})$ and $\lambda_{\min}(\mathbf{A})$ are the maximal and the minimal eigenvalues of \mathbf{A} respectively. It can be seen from Table 2.2 that M should be chosen as $M \geq \frac{N}{2}$ for $N = 34$. Tables 2.1 – 2.17 are all computed by means of Fortran programs in double precision.

Moreover, for the Gaussian rule with six nodes and those with 1,2,4,6,8 and 10 nodes, the results are listed in Tables 2.3 and 2.4 respectively, and the best leading coefficients in Table 2.5 by the Gaussian rule with six nodes as $N = 34$ and $M = 30$. Note that the central rule is the simplest Gaussian rule with $r = 1$. When using the Gaussian rule, there seems no significant effect to reduce the errors $\|\varepsilon\|_B$ and $\|\varepsilon\|_{\infty, \overline{AB}}$ (e.g., from $\|\varepsilon\|_B = 0.839(-8)$ down to $0.428(-8)$, see Table 2.4). From Table 2.4, however, the Gaussian rules of high order do improve evidently the accuracy of leading coefficients. For $N = 34$, $M = 30$, and the Gaussian rule of six nodes, the highly accurate solutions are listed in Table 2.5 with the best leading coefficient

$$D_0 = 401.162453745234416. \quad (2.2.29)$$

Compared this D_0 in (2.2.29) with more accurate values in Table 1.1 using Mathematica, the relative error is less than the rounding error of double precision²! Note that D_0 in (2.2.29) has 17 significant digits; while the D_0 in [291, 316] has only 12 significant digits. This is an improvement over [291, 316]. Besides, we also list D_i with significant digits (Sig. digits) in Table 2.5, which are obtained from D_i with all digits by rounding. The errors of significant digits occur only at the last digit at most with a half unit, compared with the more accurate coefficients in [309]. Although $D_{28} - D_{34}$ are incorrect, they are indispensable to reach the global optimal solutions. Hence, the solutions from this chapter are optimal in the global errors, and the highly accurate leading coefficients are its natural consequences.

2.3 Error Bounds and Integration Approximation

Define the norm

$$\|v\|_1 = \|v\|_{1,S} = \left[\iint_S (v^2 + v_x^2 + v_y^2) ds \right]^{\frac{1}{2}}.$$

²This seems impossible! In fact, there exist some guard digits in computer for arithmetic of floating point numbers by noting that there are 18 digits in computer outputs of double precision, and some cancellation of rounding errors in statistics may also happen in the computation. In fact, the effective condition number is much smaller. For Motz's problem, the effective condition number is about 30, see Section 3.7. Hence, this occasionally excellent results may happen at random.

We obtain a lemma based on the theories developed in Chapter 1.

Lemma 2.3.1 *Let $u \in H^1(S)$ be the solution of Motz's problem. If the following inverse property holds:*

$$\|v_\nu\|_{0,\overline{AB}} \leq K_N \|v\|_1, \quad v \in V_N, \quad (2.3.1)$$

where $\|v_\nu\|_{0,\overline{AB}} = \{\int_{\overline{AB}} v_\nu^2 d\ell\}^{\frac{1}{2}}$. Then for any $w > 0$, there exists a constant C independent of N and u such that

$$\|u - u_N\|_1 \leq C(K_N + \frac{1}{w}) \|u - u_N\|_B.$$

The constant C in this chapter is used as a generic, bounded constant; their values may be different in different contexts.

Below, new analysis is devoted to the collocation TM involving numerical approximation of integration. Denote

$$\begin{aligned} [u, v]_{\tilde{B}} &= \int_{\overline{AB}} u v d\ell + w^2 \int_{\overline{BC \cup CD}} u_\nu v_\nu d\ell, \\ \|v\|_{\tilde{B}} = |v|_{\tilde{B}} &= \sqrt{[v, v]_{\tilde{B}}} = \left\{ \int_{\overline{AB}} v^2 d\ell + w^2 \int_{\overline{BC \cup CD}} v_\nu^2 d\ell \right\}^{\frac{1}{2}}. \end{aligned} \quad (2.3.2)$$

The solutions \tilde{u}_N of (2.2.11) will satisfy

$$\|u - \tilde{u}_N\|_{\tilde{B}} = \min_{v \in V_N} \|u - v\|_{\tilde{B}} = \min_{v \in V_N} \sqrt{\tilde{I}(v)}.$$

For the integration rules involved, we denote

$$\|v\|_{\tilde{B}}^2 = \|\hat{v}\|_B^2,$$

where \hat{v}^2 are piecewise interpolation polynomials of v^2 with order k along $\Gamma = \partial S$. Note that the true solution u satisfies (2.2.13) – (2.2.15) exactly. Then for (2.3.2), we have³

$$[u, v]_{\tilde{B}} = 0. \quad (2.3.3)$$

We can prove the following lemma, similarly based on Chapter 1.

Lemma 2.3.2 *The solutions \tilde{u}_N obtained by the collocation TMs with integral approximation satisfy*

$$[u - \tilde{u}_N, v]_{\tilde{B}} = 0, \quad \forall v \in V_N, \quad (2.3.4)$$

and

$$\|v - \tilde{u}_N\|_{\tilde{B}} \leq \|u - v\|_{\tilde{B}}, \quad \forall v \in V_N. \quad (2.3.5)$$

³Eq.(2.3.3) holds for the collocation method; this is different from the FEM, the finite volume method (FVM), etc., where the true solution does not satisfy the algorithms involving integration approximations of numerical solutions. Hence, the same conclusions involving integration approximation made for the collocation method in this book may not be applied to other numerical methods such as FEM.

Next, let us examine the errors from integration rules. Suppose that the rules are chosen to have the following relative errors for v and $u - v$, where $v \in V_N$,

$$\left| \frac{(\int_{AB} - \tilde{\int}_{AB})v^2 d\ell}{\int_{AB} v^2 d\ell} \right| \leq b < \frac{3}{4}, \quad (2.3.6)$$

$$\left| \frac{(\int_{BC} - \tilde{\int}_{BC})v^2 d\ell}{\int_{BC} v^2 d\ell} \right| \leq b < \frac{3}{4}, \quad (2.3.7)$$

$$\left| \frac{(\int_{CD} - \tilde{\int}_{CD})v^2 d\ell}{\int_{CD} v^2 d\ell} \right| \leq b < \frac{3}{4}, \quad (2.3.8)$$

where b is a constant. Then we have the following proposition.

Proposition 2.3.1 *For those rules of quadrature satisfying (2.3.6) – (2.3.8), the following bound holds:*

$$\left| \frac{\|v\|_B - \|v\|_{\tilde{B}}}{\|v\|_B} \right| \leq a < \frac{1}{2}, \quad v \in V_N, \quad (2.3.9)$$

where $a = 1 - \sqrt{1 - b}$ is a constant.

Proof We have from the assumptions,

$$\frac{\left| \|v\|_B^2 - \|v\|_{\tilde{B}}^2 \right|}{\|v\|_B^2} \leq \frac{\left| (\int_{AB} - \tilde{\int}_{AB})v^2 d\ell + (\int_{BC \cup CD} - \tilde{\int}_{BC \cup CD})v^2 d\ell \right|}{\int_{AB} v^2 d\ell + \int_{BC \cup CD} v^2 d\ell} \leq b. \quad (2.3.10)$$

We obtain

$$1 - b \leq \frac{\|v\|_{\tilde{B}}^2}{\|v\|_B^2} \leq 1 + b.$$

The above equation gives

$$\sqrt{1 - b} \leq \frac{\|v\|_{\tilde{B}}}{\|v\|_B} \leq \sqrt{1 + b}. \quad (2.3.11)$$

Next, we have from (2.3.10) and (2.3.11),

$$\begin{aligned} \frac{\left| \|v\|_B - \|v\|_{\tilde{B}} \right|}{\|v\|_B} &\leq \frac{b}{\|v\|_B + \|v\|_{\tilde{B}}} \|v\|_B \\ &\leq \frac{b}{1 + \frac{\|v\|_{\tilde{B}}}{\|v\|_B}} \leq \frac{b}{1 + \sqrt{1 - b}} = 1 - \sqrt{1 - b} = a < \frac{1}{2}. \quad \blacksquare \end{aligned}$$

Take the central rule in (2.2.9) and (2.2.10) for example. We have from [9]

$$\left(\int_{AB} - \tilde{\int}_{AB} \right) f d\ell = \frac{h^2}{24} f''(\xi), \quad (2.3.12)$$

where $f = v^2$ or $f = (u - v)^2$, and $\xi \in \overline{AB}$. Since $f'' = 2\{(v')^2 + vv''\}$ for $f = v^2$, the requirements of quadrature errors in Proposition 2.3.1 imply that

$$\frac{1}{4} \int_{AB} v^2 dl \leq \int_{AB}^{\sim} v^2 dl \leq \frac{7}{4} \int_{AB} v^2 dl,$$

or equivalently

$$\frac{h^2}{12} |((v')^2 + vv'')(\xi)| \leq \frac{3}{4} \int_{AB} v^2 dl.$$

Next, we give a new lemma.

Lemma 2.3.3 *Suppose that the rules of integrations in (2.2.12) are chosen to satisfy the bound (2.3.9). Then, the norms $\|\cdot\|_B$ and $\|\cdot\|_{\tilde{B}}$ defined in (2.2.8) and (2.3.2) are equivalent to each other:*

$$C_1 \|v\|_B \leq \|v\|_{\tilde{B}} \leq C_2 \|v\|_B, \quad v \in V_N, \quad (2.3.13)$$

where C_1 and C_2 are two positive constants independent of v and N .

Proof We have from (2.3.9)

$$\|v\|_B - \|v\|_{\tilde{B}} \leq a \|v\|_B,$$

and then

$$\|v\|_B \leq \frac{1}{1-a} \|v\|_{\tilde{B}}. \quad (2.3.14)$$

Also from (2.3.9)

$$\|v\|_{\tilde{B}} - \|v\|_B \leq a \|v\|_B,$$

and then

$$\|v\|_{\tilde{B}} \leq (1+a) \|v\|_B. \quad (2.3.15)$$

Hence, the desired result (2.3.13) follows from (2.3.14) and (2.3.15). ■

Accordingly, we have a new important theorem.

Theorem 2.3.1 *Let the condition (2.3.1) hold, and the rules of integrations involved in (2.2.12) satisfy (2.3.9) for v and $u - v$, $\forall v \in V_N$. Then,*

$$\|u - \tilde{u}_N\|_1 \leq \inf_{v \in V_N} \{\|u - v\|_1 + C(K_N + 1/w)\|u - v\|_B\}, \quad (2.3.16)$$

where C is a bounded constant independent of u, v and N . Moreover,

$$\|u - \tilde{u}_N\|_1 \leq \|R_N\|_1 + C(K_N + 1/w)\|R_N\|_B, \quad (2.3.17)$$

where

$$R_N = \sum_{i=N+1}^{\infty} d_i r^{i+\frac{1}{2}} \cos(i + \frac{1}{2})\theta, \quad (2.3.18)$$

and d_i are the true expansion coefficients.

Proof From Lemma 1.2.1 in Chapter 1, we have

$$\|v\|_1 \leq C(K_N + 1/w)\|v\|_B, \quad \forall v \in V_N. \quad (2.3.19)$$

Let $\eta = v - \tilde{u}_N$, then $\eta \in V_N$ if $v \in V_N$. In view of (2.3.19) and the norm equivalence (2.3.13),

$$\begin{aligned} \|u - \tilde{u}_N\|_1 &\leq \|u - v\|_1 + \|\eta\|_1 \\ &\leq \|u - v\|_1 + C(K_N + 1/w)\|\eta\|_B \\ &\leq \|u - v\|_1 + \frac{C}{C_1}(K_N + 1/w)\|\eta\|_{\tilde{B}}. \end{aligned} \quad (2.3.20)$$

From the orthogonal property (2.3.4) we obtain

$$\|\eta\|_{\tilde{B}}^2 = [\eta, \eta]_{\tilde{B}} = [v - u, \eta]_{\tilde{B}} \leq \|u - v\|_{\tilde{B}}\|\eta\|_{\tilde{B}}.$$

The above bound and the norm equivalence for $u - v$ leads to

$$\|\eta\|_{\tilde{B}} \leq \|u - v\|_{\tilde{B}} \leq C\|u - v\|_B. \quad (2.3.21)$$

Combining (2.3.20) and (2.3.21) gives the first desired result (2.3.16).

Next, the solution (2.1.4) with the true coefficients d_i can be split into

$$u = \bar{u}_N + R_N,$$

where

$$\bar{u}_N = \sum_{i=0}^N d_i r^{i+\frac{1}{2}} \cos(i + \frac{1}{2})\theta,$$

and the remainder R_N is given by (2.3.18). Then let $v = \bar{u}_N$ in (2.3.16) we obtain

$$\begin{aligned} \|u - \tilde{u}_N\|_1 &\leq \|u - \bar{u}_N\|_1 + C(K_N + 1/w)\|u - \bar{u}_N\|_B \\ &\leq \|R_N\|_1 + C(K_N + 1/w)\|R_N\|_B. \end{aligned}$$

This is the second bound (2.3.17) as desired. ■

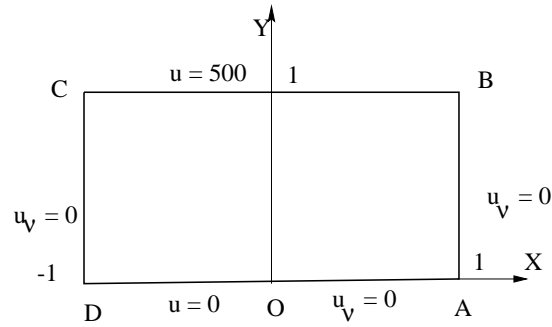


Figure 2.2: The cracked beam problem.

Even for a rough quadrature like the simplest central rule, the relative errors of its approximate integrals has no difficulty to be less than three quarters. So the conditions (2.3.6) – (2.3.9) can be satisfied easily. Hence, the solutions \hat{u}_N may still have the exponential convergence rates. More explanation will be given in Section 2.5. This is a significant difference from the traditional role of integration in the finite element analysis. Besides, from Theorem 2.3.1, there is not much difference between lower-order and higher-order quadratures. However, for the accuracy of the leading coefficient D_0 , the high order rules, such as the Gaussian quadratures with six and eight nodes, may raise its accuracy, based on Tables 2.3 and 2.4. Note that the new analysis of quadratures in this section provides an excellent theoretical foundation for the high accuracy of the collocation TM.

2.4 The Cracked Beam Problem

As a variant of Motz's problem, the cracked beam problem is discussed in the rest of this chapter. Its highly accurate solution can be sought similarly by the collocation TM. Not only its highly accurate solutions are obtained in this chapter, but also the highly accurate leading coefficient with 17 significant digits can be achieved by the Gaussian rule. Half of its expansion coefficients are zero, which is supported by a posteriori analysis. Hence, as a singularity model, the cracked beam problem given in this section seems to be superior to Motz's problem in Sections 2.2 and 2.3.

When the boundary conditions on \overline{AB} and on \overline{BC} in Figure 2.1 are exchanged as

$$u|_{\overline{BC}} = 500, \quad u|_{\overline{OD}} = 0, \quad u_\nu|_{\overline{OA}} = 0, \quad u_\nu|_{\overline{ABUCD}} = 0, \quad (2.4.1)$$

this Laplace boundary value problem gives the cracked beam problem, see Figure 2.2. Its original model in [154, 168, 169, 369, 446] was defined on the domain $\hat{S} = \{(x, y) \mid -\frac{1}{2} \leq$

$x \leq \frac{1}{2}, 0 \leq y \leq \frac{1}{2}$ in Figure 2.3. These two models, in S and \hat{S} , are of the same nature. In fact, their solutions can be scaled from one to the other, which will be explained in Section 2.5. Since functions (2.1.4) are also the solutions of the cracked beam problem, we choose

$$u_N(r, \theta) = \sum_{i=0}^N \hat{D}_i r^{(i+\frac{1}{2})} \cos(i + \frac{1}{2})\theta, \quad (2.4.2)$$

where the notation \hat{D}_i with a hat on the head is used to distinguish itself from the D_i of Motz's problem in Section 2.2.

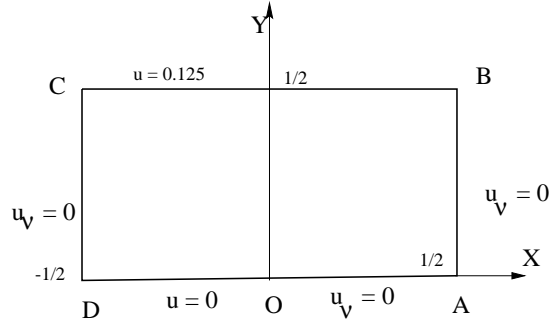


Figure 2.3: The traditional cracked beam problem in \hat{S} .

We also use V_N as the finite collection of functions (2.4.2). Since u_N satisfies the Laplace equation in S and the boundary conditions on $\overline{OD} \cup \overline{OA}$ already, the coefficients \hat{D}_i should be chosen to satisfy the rest of the boundary conditions as best as possible. Define the error norm on $\overline{AB} \cup \overline{BC} \cup \overline{CD}$:

$$\|u - v\|_B = \left\{ \int_{\overline{BC}} (v - 500)^2 + w^2 \int_{\overline{AB} \cup \overline{CD}} v_\nu^2 \right\}^{\frac{1}{2}}, \quad w = \frac{1}{N+1}.$$

The solution u_N can be obtained by

$$\|u - u_N\|_{\hat{B}} = \inf_{v \in V_N} \|u - v\|_{\hat{B}},$$

where

$$\|v\|_{\hat{B}} = \left\{ \widetilde{\int}_{\overline{BC}} v^2 + w^2 \widetilde{\int}_{\overline{AB} \cup \overline{CD}} v_\nu^2 \right\}^{\frac{1}{2}}. \quad (2.4.3)$$

We first employ the central rule with a uniform distributed points P_i on $\overline{AB} \cup \overline{BC} \cup \overline{CD}$. We may require $\sqrt{h}v = \sqrt{h}500$ at $P_i \in \overline{BC}$ and $\sqrt{h}wu_\nu = 0$ at $P_i \in \overline{AB} \cup \overline{CD}$. Let the number $4M$ of all collocation nodes P_i be larger than $N+1$, then we obtain an over-determined system of linear algebraic equations $\mathbf{F}\mathbf{x} = \mathbf{b}$, where \mathbf{F} is a matrix of

$4M \times (N + 1)$, and \mathbf{x} is the unknown vector consisting of \hat{D}_i . We employ the CTM in Section 2.2 to solve it. The errors, condition numbers and the leading coefficients are given in Tables 2.7 and 2.8. It is interesting from Table 2.8 to note that $\hat{D}_{4\ell+2} \approx \hat{D}_{4\ell+3} \approx 0^4$. Hence, we may simply seek a solution of the following simplified forms:

$$u_N^* = \sum_{\ell=0}^L \sum_{k=0}^1 \hat{D}_{4\ell+k} r^{4\ell+k+\frac{1}{2}} \cos(4\ell + k + \frac{1}{2})\theta, \quad (2.4.4)$$

where $N = 4L+2$. Denote by V_N^* the finite collection of functions in (2.4.4). Hence another collocation TM can be formulated as in Section 2.2: to seek the solution $u_N^* \in V_N^*$ such that

$$\|u - u_N^*\|_{\tilde{B}} = \inf_{v \in V_N^*} \|u - v\|_{\tilde{B}},$$

where $\|v\|_{\tilde{B}}$ is defined in (2.4.3). Its results are given in Tables 2.9 and 2.10. From Tables 2.7 and 2.9, we have observed the asymptotes:

$$\|u - u_N\|_B = O(0.553^N), \quad \|u - u_N\|_{\infty, \overline{BC}} = O(0.564^N), \quad (2.4.5)$$

$$\text{Cond.} = O(1.42^N),$$

$$\|u - u_N^*\|_B = O(0.558^N), \quad \|u - u_N^*\|_{\infty, \overline{BC}} = O(0.558^N), \quad (2.4.6)$$

$$\text{Cond.} = O(1.39^N).$$

Note that the convergence rates and the condition numbers in (2.4.6) are close to those in (2.4.5), but only half coefficients of u_N in (2.4.2) are needed. Hence, for the computational purpose, the solutions (2.4.4) with Tables 2.9 and 2.10 may be better. From this point of view, the cracked beam using (2.4.4) may serve as a better testing model of singularity problems than Motz's problem.

Compared with the more accurate solutions from the collocation TM [453] using Mathematica with more working digits, the leading coefficients \hat{D}_0 and \hat{D}_1 in Table 2.10 have 15 significant digits.

The analysis in Section 2.3 can be similarly applied to the collocation TM for the cracked beam problem. To confirm the admissible functions as (2.4.4), we only prove the following proposition.

Proposition 2.4.1 *Let the errors $\varepsilon_N = u - u_N^*$, $N = 4L + 1$ and*

$$\|(\varepsilon_N)_\nu\|_{0, \overline{BC}} \leq K_N \|\varepsilon_N\|_{1, S},$$

where the constant $K_N (\geq 1)$ may be unbounded as $N \rightarrow \infty$. Suppose

$$(K_N + \frac{1}{w}) \|\varepsilon_N\|_B \rightarrow 0, \quad \text{as } N \rightarrow \infty. \quad (2.4.7)$$

⁴This fact has been double checked under the Mathematica system using high working digits and more expansion terms. In fact, u_{400} has been obtained in Tang [453], which clearly shows that $\hat{D}_{4\ell+2} \approx \hat{D}_{4\ell+3} \approx 0$.

Then the solution of the cracked beam problem can be expressed by

$$u = \sum_{\ell=0}^{\infty} \sum_{k=0}^1 \hat{D}_{4\ell+k} r^{4\ell+k+\frac{1}{2}} \cos(4\ell+k+\frac{1}{2})\theta.$$

Proof From the bounds similar to Lemma 2.3.1, we have

$$\|\varepsilon_N\|_{1,S} = \|u - u_N^*\|_{1,S} \leq C(K_N + \frac{1}{w})\|\varepsilon_N\|_B, \quad (2.4.8)$$

where C is a bounded constant independent of N . From (2.4.7) and (2.4.8), $\{\varepsilon_N\}$ is a bounded sequence. Based on the Kandrasov or Rellich theorem [105], any bounded sequence in the space $H^1(S)$ contains a subsequence that converges in $H^0(S)$. Then there must exist a subsequence $\{\varepsilon_N^+\}$ in $H^0(S)$ such that $\lim_{N \rightarrow \infty} \varepsilon_N^+ = \bar{\varepsilon}$. Since $\{\varepsilon_N^+\}$ are bounded in $H^1(S)$, the convergent limit $\bar{\varepsilon} \in H^1(S)$. This implies that

$$\lim_{N \rightarrow \infty} u_N^+ = \lim_{N \rightarrow \infty} (u - \varepsilon_N) = u - \bar{\varepsilon} = \bar{u} \in H^1(S).$$

Moreover, since $K_N \geq 1$ and $w = \frac{1}{N+1}$, we conclude that $\|\bar{u} - 500\|_{0,\overline{BC}} = 0$ and $\|\bar{u}_\nu\|_{0,\overline{AB \cup CD}} = 0$. Hence, \bar{u} must be the unique solution of the cracked beam problem. Obviously, the entire sequence u_N^* also converges to $\bar{u}(=u)$ based on $\|u - u_N^*\|_B \rightarrow 0$ as $N \rightarrow \infty$ from (2.4.7) and (2.4.8). ■

When $w = \frac{1}{N+1}$, the empirical exponential convergent rates in (2.4.6) guarantee (2.4.7). The analysis of Proposition 2.4.1 is made based on the a posteriori numerical results, so we call it a posteriori analysis. Proposition 2.4.1 implies that $\hat{D}_{4\ell+2} = \hat{D}_{4\ell+3} = 0, \forall \ell \geq 0$. We also note that condition (2.4.7) is stronger than that $\|\varepsilon_N\|_B \rightarrow 0$ as $N \rightarrow \infty$.

Next, we pursue better accuracy of the leading coefficient \hat{D}_0 by using the Gaussian rules. Denote by M the collocation number along \overline{AB} , and then $4M$ is the total number of collocation nodes. First, we choose the Gaussian rule of eight nodes, and set the positions of collocation nodes as required, then its solutions and condition numbers by the collocation TM are listed in Table 2.11. Moreover, for the Gaussian rules with 1,2,4,6,8 and 12 nodes, their solution errors and condition numbers are listed in Table 2.12. The errors $\|u - u_N^*\|_B$ decrease nearly a half, from 0.614(-10) with $r = 1$ down to 0.319(-10) with $r = 8$. For $N = 43$ and $M = 24$, the leading coefficients $\hat{D}_{4\ell+k}, k = 0, 1$ obtained by the Gaussian rule of eight nodes are reported in Table 2.13. Compared with the more accurate results in [453], the relative error of

$$\hat{D}_0 = 540.565122713627488338,$$

from Table 2.13 has 17 significant digits, and \hat{D}_1 has 16 significant digits.

2.5 Discussions and Comparisons

Let us consider the cracked beam problem on a scaled domain, $\hat{S} = \{(\xi, \eta) \mid -a < \xi < a, 0 < \eta < a\}$, where the parameter satisfies $0 < a \leq 1$. The scaled cracked beam

problem is described by the Laplace equation $\Delta w = 0$ on \hat{S} satisfying the following boundary conditions:

$$w(\xi, a) = b, \quad -a < \xi < a, \quad (2.5.1)$$

$$w(\xi, 0) = 0, \quad -a < \xi < 0, \quad \frac{\partial w}{\partial \nu}(\xi, 0) = 0, \quad 0 < \xi < a, \quad (2.5.2)$$

$$\frac{\partial w}{\partial \nu}(\pm a, \eta) = 0, \quad 0 < \eta < a, \quad (2.5.3)$$

where b is a constant, and ν is the outward normal to $\partial\hat{S}$. Here, another Cartesian coordinate system (ξ, η) is chosen. For Figure 2.2, $a = 1$ and $b = 500$, and for Figure 2.3 from the traditional model [154, 169, 168, 369, 446], $a = \frac{1}{2}$ and $b = 0.125$. The Laplace solution satisfying (2.5.1) – (2.5.3) can also be expressed by

$$w(\xi, \eta) = \sum_{i=0}^{\infty} \alpha_i \rho^{i+\frac{1}{2}} \cos(i + \frac{1}{2})\theta,$$

where α_i are the coefficients, (ρ, θ) are the polar coordinates at the origin O , and $\rho = \sqrt{\xi^2 + \eta^2}$. There exist the relations for the coefficients of \hat{D}_i in Table 2.13 and α_i :

$$\alpha_i = \frac{b}{500} a^{-(i+\frac{1}{2})} \hat{D}_i. \quad (2.5.4)$$

Now, let us prove (2.5.4). Under the affine transformation $T : (x, y) \rightarrow (\xi, \eta)$, where $\xi = ax$ and $\eta = ay$, domain S is converted to \hat{S} , and the boundary conditions (2.4.1) are transformed to

$$\begin{aligned} u(\xi, a) &= b, \quad -a < \xi < a, \\ u(\xi, 0) &= 0, \quad -a < \xi < 0, \quad \frac{\partial u}{\partial \nu}(\xi, 0) = 0, \quad 0 < \xi < a, \\ \frac{\partial u}{\partial \nu}(\pm a, \eta) &= 0, \quad 0 < \eta < a. \end{aligned} \quad (2.5.5)$$

Compared (2.5.5) with $u|_{BC} = 500$ in (2.4.1), we find the relations between w and u ,

$$w = \frac{b}{500} u.$$

This gives

$$\sum_{i=0}^{\infty} \alpha_i \rho^{i+\frac{1}{2}} \cos(i + \frac{1}{2})\theta = \frac{b}{500} \sum_{i=0}^{\infty} \hat{D}_i r^{i+\frac{1}{2}} \cos(i + \frac{1}{2})\theta. \quad (2.5.6)$$

Since $r = \sqrt{x^2 + y^2}$, we have $r = \frac{\rho}{a}$. Eq. (2.5.6) is reduced to

$$\sum_{i=0}^{\infty} \left\{ \alpha_i - \frac{b}{500} a^{-(i+\frac{1}{2})} \hat{D}_i \right\} \rho^{i+\frac{1}{2}} \cos(i + \frac{1}{2})\theta = 0.$$

Since functions $\{\rho^{i+\frac{1}{2}} \cos(i + \frac{1}{2})\theta\}$ are linearly independent, we obtain

$$\alpha_i - \frac{b}{500} a^{-(i+\frac{1}{2})} \hat{D}_i = 0,$$

which is the desired (2.5.4).

By means of (2.5.4), the coefficients α_i can be obtained for $a = \frac{1}{2}$ and $b = 0.125$, which are listed in Table 2.15. Our leading coefficients

$$\alpha_0 = .19111863197187209, \quad \alpha_1 = -.1181160719665095, \quad (2.5.7)$$

from Table 2.15 have 17 and 16 significant digits, respectively, compared with the more accurate values:

$$\begin{aligned} \alpha_0 &= .19111863197187208906830, \\ \alpha_1 &= -.11811607196650946846348. \end{aligned} \quad (2.5.8)$$

Eqs. (2.5.8) possessing 23 significant digits are cited from [453] by the same collocation TM but using higher working digits under Mathematica. Besides, the significant digits of other coefficients are also provided in Table 2.15, compared with more accurate α_i in [453].

We have also completed the direct computation for the traditional cracked beam problem in Figure 2.3. The errors, condition numbers and the leading coefficients are listed in Tables 2.14 – 2.17. Interestingly, in Table 2.16, the same α_0 and α_1 as (2.5.7) are obtained. Let us compare two approaches: (1) From Table 2.13 by (2.5.4), (2) Direct computation from the problem defined in Figure 2.3. The global errors from Table 2.12 are ten times smaller than those from direct computation (see Table 2.17). On the other hand, the leading coefficients α_4 and α_5 from direct computation are slightly better than those in Table 2.15. We note that the condition number from the direct computation is huge, and the ratio of condition numbers between these two approaches is

$$\frac{\text{Cond.} \Big|_{\text{Direct}}}{\text{Cond.} \Big|_{\text{From Table 2.12}}} = \frac{0.186(10)}{0.447(6)} = 416.$$

Hence, the approach from Table 2.13 seems to be superior.

In Georgiou, Boudouvis and Poulikkas [168], the integrated singular basis method (ISBM) and the integral method are used to seek the solutions of the traditional cracked beam problem, and their leading coefficients are listed in Table 2.6 with the number of significant digits. Evidently, the leading coefficients in Tables 2.15 and 2.16 have more significant digits than those in Table 2.6.

In this chapter, the same S is chosen for both Motz's and the cracked beam problems, in order to unify the theoretical frame work and to make comparisons. Let us look at the coefficients in Tables 2.5 and 2.13. The coefficients D_i decrease monotonically in magnitude as $i \rightarrow \infty$, but \hat{D}_ℓ do not. However, each of $\hat{D}_{4\ell}$ and $\hat{D}_{4\ell+1}$ does decrease

monotonically. We have carefully checked the coefficients from Tables 2.5, 2.13 and [309, 453], to find the following empirical asymptotes

$$\begin{aligned} D_i &\leq C_0 \times 2.04^{-i}, \\ \hat{D}_{4\ell} &\leq C_1 \times 2.05^{-4\ell}, \\ \hat{D}_{4\ell+1} &\leq C_2 \times 2.01^{-4\ell-1}, \end{aligned}$$

where C_0 , C_1 and C_2 are positive constants. Hence, we may assume the true coefficients d_i in (2.1.4) also satisfy the same asymptotes

$$d_i \leq C(2 + \epsilon)^{-i}, \quad (2.5.9)$$

where ϵ is a small positive constant. Rewrite (2.1.4) as the sum of

$$\bar{u}_N = \sum_{i=0}^N d_i r^{i+\frac{1}{2}} \cos\left(i + \frac{1}{2}\right)\theta,$$

and the remainder

$$R_N = \sum_{i=N+1}^{\infty} d_i r^{i+\frac{1}{2}} \cos\left(i + \frac{1}{2}\right)\theta.$$

Below, we show the following exponential convergence:

$$\|u - \bar{u}_N\|_{1,S} = \|R_N\|_{1,S} \leq C_3 \left(\frac{\sqrt{2}}{2}\right)^N, \quad (2.5.10)$$

where C_3 is a constant independent of N .

Denote a half-disk domain $S_R = \{(r, \theta) \mid 0 \leq r \leq R, \ 0 \leq \theta \leq \pi\}$. Then $S \subset S_{\sqrt{2}}$. We have

$$\begin{aligned} \|R_N\|_{1,S}^2 &\leq \|R_N\|_{1,S_{\sqrt{2}}}^2 \\ &= \int_0^\pi \int_0^{\sqrt{2}} \left\{ \left(\frac{\partial R_N}{\partial r}\right)^2 + \frac{1}{r^2} \left(\frac{\partial R_N}{\partial \theta}\right)^2 + R_N^2 \right\} r \, dr d\theta, \end{aligned}$$

where

$$\begin{aligned} \frac{\partial R_N}{\partial r} &= \sum_{i=N+1}^{\infty} d_i \left(i + \frac{1}{2}\right) r^{i-\frac{1}{2}} \cos\left(i + \frac{1}{2}\right)\theta, \\ \frac{1}{r} \frac{\partial R_N}{\partial \theta} &= - \sum_{i=N+1}^{\infty} d_i \left(i + \frac{1}{2}\right) r^{i-\frac{1}{2}} \sin\left(i + \frac{1}{2}\right)\theta. \end{aligned}$$

By using the orthogonality of trigonometric functions, we obtain

$$\begin{aligned}
I_1 &= \int_0^\pi \int_0^R \left(\frac{\partial R_N}{\partial r}\right)^2 r \, dr d\theta = \frac{\pi}{4} R \sum_{i=N+1}^{\infty} \left(i + \frac{1}{2}\right) R^{2i} d_i^2, \\
I_2 &= \int_0^\pi \int_0^R \frac{1}{r^2} \left(\frac{\partial R_N}{\partial \theta}\right)^2 r \, dr d\theta = \frac{\pi}{4} R \sum_{i=N+1}^{\infty} \left(i + \frac{1}{2}\right) R^{2i} d_i^2, \\
I_3 &= \int_0^\pi \int_0^R R_N^2 r \, dr d\theta = \frac{\pi}{4} \sum_{i=N+1}^{\infty} \frac{1}{i + \frac{3}{2}} R^{2i+3} d_i^2 \\
&\leq \frac{\pi R^3}{4} \sum_{i=N+1}^{\infty} \left(i + \frac{1}{2}\right) R^{2i} d_i^2.
\end{aligned}$$

Then, we have

$$\|R_N\|_{1,S}^2 \leq (I_1 + I_2 + I_3) \Big|_{R=\sqrt{2}} \leq \sqrt{2}\pi \sum_{i=N+1}^{\infty} \left(i + \frac{1}{2}\right) \sqrt{2}^{2i} d_i^2.$$

Under (2.5.9), we have

$$\|R_N\|_{1,S}^2 \leq C \sum_{i=N+1}^{\infty} \left(i + \frac{1}{2}\right) \left(\frac{\sqrt{2}}{2+\epsilon}\right)^{2i}. \quad (2.5.11)$$

From calculus, for $d = \frac{\sqrt{2}}{2+\epsilon} < 1$,

$$\sum_{i=N+1}^{\infty} \left(i + \frac{1}{2}\right) d^{2i} \leq C_1 N d^{2N} \leq C_3 \left(\frac{\sqrt{2}}{2}\right)^{2N}, \quad (2.5.12)$$

where C_3 is a constant independent of N . Combining (2.5.11) and (2.5.12) gives the desired result (2.5.10).

Under (2.5.9), the exponential convergence rates in the infinite norm $\|\cdot\|_{1,\infty}$ and $\|\cdot\|_B$ can be proven similarly:

$$\|u - \bar{u}_N\|_{1,\infty} = \|R_N\|_{1,\infty} \leq C_4 \left(\frac{\sqrt{2}}{2}\right)^N, \quad (2.5.13)$$

$$\|u - \bar{u}_N\|_B = \|R_N\|_B \leq C_5 \left(\frac{\sqrt{2}}{2}\right)^N, \quad (2.5.14)$$

where C_4 and C_5 are also positive constants. Then from (2.3.5), (2.3.13) and (2.5.14) we have

$$\|u - \tilde{u}_N\|_B \leq C \|u - \bar{u}_N\|_B \leq C \|R_N\|_B \leq C C_5 \left(\frac{\sqrt{2}}{2}\right)^N,$$

and from Theorem 2.3.1

$$\|u - \tilde{u}_N\|_1 \leq C\left(\frac{\sqrt{2}}{2}\right)^N.$$

For the cracked beam in Figure 2.2, the same exponential convergence rates hold as (2.5.10), (2.5.13) and (2.5.14). The numerical rates $O(0.56^N)$ in (2.4.5) and (2.4.6) are coincident with the a posteriori estimates $O(0.707^N)$. For the traditional scaled cracked beam in Figure 2.3, the coefficients in Table 2.15 have

$$\alpha_i \leq C\left(\frac{2}{2+\epsilon}\right)^i.$$

By noting that $\rho \leq \sqrt{2}$, the same exponential convergence rates as (2.5.10), (2.5.13) and (2.5.14) can also be obtained.

For the Laplace equations on sectors of disks, half-disks and disks, the exponential convergence rates of the expansion solutions are proven theoretically in Volkov [473], p. 41. The proof for the exponential rates on the rectangular domains in S and \hat{S} is given in this section by the a posteriori analysis, where the assumption (2.5.9) is purely based on numerical observation of the obtained results. The rigorous proof of exponential convergence rates on the rectangular S without (2.5.9) needs to be further explored.

2.6 Concluding Remarks

1. Computational algorithms of the collocation TM are provided in Section 2.2. The overdetermined system (2.2.21) is recommended in computation since its algorithm is simple, which is, indeed, just the collocation method at the boundary nodes, based on Proposition 2.2.1. The remarkable advantage of (2.2.21) is that the condition numbers of the stiffness matrix can be dramatically reduced, compared to (2.2.27) of the normal equation.

2. Different quadratures, such as the central and Gaussian rules, are investigated for the TM. Theorem 2.3.1 reveals that different integration rules do not make much differences in the global errors over the entire domain S . However, the rules used may affect significantly the accuracy of the leading coefficient, based on numerical experiments in this chapter.

3. The quadrature is used to link the collocation method and the LSM. However from our error analysis, the accuracy of a quadrature may be very rough, in the sense that its relative errors are less than three quarters! This feature is significantly different from the traditional integral approximation in error analysis, e.g., the FEM analysis, where the integration errors should be chosen to balance the optimal errors of the solutions. Based on the analysis in Section 2.3, the solutions of Motz's and the cracked beam problems solved by the collocation TM have the exponential convergence rates. Note that Theorem 2.3.1 and Proposition 2.3.1 are new, which provide an excellent theoretical foundation for

high accuracy of the collocation TM (e.g., the BAM). This is also a justification for the collocation TM to become the most accurate method for Motz's and the cracked beam problems. The collocation methods both in S and on ∂S , on the other hand, are explored in Chapter 5.

4. The numerical results in Section 2.2 are better than those in [291, 316]. The Gaussian rule with six nodes are used to raise the accuracy of the leading coefficient to

$$D_0 = 401.162453745234416 \quad (2.6.1)$$

by the collocation TM. Compared with the more accurate value of D_0 in [291, 309], this D_0 has exactly 17 significant digits, which error happens to coincide with the rounding errors of double precision. Note that coefficient D_0 in [316] has only 12 significant digits. This new discovery will change the evaluation of the BAM (i.e., the collocation TM) given in [291]. Based on the numerical results in [316] using the central rule, it is pointed out in [291], p.133, that "*BAM may produce the best global solutions*", but "*the conformal transformation method is the highly accurate method for leading coefficients*". Now we may address that for Motz's problem, the collocation TM (i.e., the BAM) by the Gaussian rule of high order is a highly accurate method, not only for the global solutions but also for the leading coefficient D_0 .

5. The new numerical results by the collocation TM in Section 2.4 provide a highly accurate solution for the cracked beam problem. The Gaussian rules of high order are used to raise the accuracy of the leading coefficient to

$$\hat{D}_0 = 540.56512271362749, \quad (2.6.2)$$

which also has 17 significant digits. For the traditional cracked beam problems in Figure 2.3, coefficients

$$\alpha_0 = .19111863197187209, \quad \alpha_1 = -.1181160719665095 \quad (2.6.3)$$

from Table 2.15 have 17 and 16 significant digits respectively. Thus the collocation TM using the Gaussian rule of high order is also a highly accurate method for the cracked beam problem, not only for the global solutions but also for the leading coefficient \hat{D}_0 .

6. Although the condition number of the collocation TM is large, the effective condition number is, indeed, small. For Motz's problem, the effective condition number about 30 in Table 3.7 in the next chapter explains well the highly accurate solution and the D_0 with 17 significant digits. More study on stability is given in [305] for Motz's and the cracked beam problems by the collocation TM.

7. Motz's and the cracked beam problems are linked and compared by considering the same domain S . The traditional cracked model in [154, 168, 169, 369, 446] is formulated as a special case of the scaled cracked beam problem in this chapter, whose solutions can be obtained straightforwardly by (2.5.4). Besides, numerical experiments by the approaches of Table 2.13 using (2.5.4) and by direct computation of the problem defined in Figure 2.3 have been reported. The former seems to be superior due to its smaller condition numbers. Motz's and the cracked beam problems are the Laplace solutions on S with

two different boundary conditions along the edges. Hence, different boundary conditions on ∂S may have different impacts on the singular behavior of the Laplace solutions in S . These computational results will be reported in Chapter 13.

8. There was a special issue on the Trefftz methods, i.e., *Advances in Engineering Software*, Volume 24, 1995. Overviews of the method can be found in Kita and Kamiya [261], Zielinski [504] and Jin and Cheung [237]. In [261, 237], the Trefftz methods are classified into the indirect and direct methods. The collocation TM in this chapter is the indirect Trefftz method. We use the same terminology, the Trefftz collocation method, as in Leitao [282]. The direct Trefftz method is analogous to the method of fundamental solutions, in which the fundamental functions are replaced by the singular function in the trial space. We report in this chapter the new computational results and the new analysis of the indirect Trefftz method. These results have narrowed the gap existing before between excellent computation and the theoretical support of this method.

N	M	$\ \varepsilon\ _B$	$\ \varepsilon\ _{\infty, \overline{AB}}$	Cond.	$ \frac{\Delta D_0}{D_0} $	$ \frac{\Delta D_1}{D_1} $	$ \frac{\Delta D_2}{D_2} $	$ \frac{\Delta D_3}{D_3} $
10	8	0.250(-1)	0.149(-1)	94.3	0.189(-5)	0.491(-5)	0.601(-5)	0.928(-3)
18	12	0.133(-3)	0.811(-4)	0.193(4)	0.158(-7)	0.113(-6)	0.290(-6)	0.502(-6)
26	16	0.973(-6)	0.734(-6)	0.366(5)	0.216(-9)	0.155(-8)	0.380(-8)	0.202(-8)
34	24	0.839(-8)	0.459(-8)	0.666(6)	0.169(-11)	0.121(-10)	0.296(-10)	0.152(-10)

Table 2.1: The error norms and condition numbers from the collocation TM for Motz's problem by the central rule.

M	$\ \varepsilon\ _B$	$\ \varepsilon\ _{\infty, \overline{AB}}$	Cond.	$ \frac{\Delta D_0}{D_0} $	$ \frac{\Delta D_1}{D_1} $	$ \frac{\Delta D_2}{D_2} $	$ \frac{\Delta D_3}{D_3} $
9	0.135(-8)	0.496(-6)	0.267(8)	0.377(-9)	0.266(-8)	0.641(-8)	0.342(-8)
12	0.587(-8)	0.713(-7)	0.992(6)	0.337(-10)	0.239(-9)	0.578(-9)	0.305(-9)
16	0.772(-8)	0.189(-7)	0.679(6)	0.729(-11)	0.520(-10)	0.127(-9)	0.655(-10)
24	0.839(-8)	0.459(-8)	0.669(6)	0.169(-11)	0.121(-11)	0.296(-10)	0.152(-10)
32	0.849(-8)	0.462(-8)	0.669(6)	0.769(-11)	0.550(-11)	0.134(-10)	0.695(-11)

Table 2.2: The error norms and condition numbers from the collocation TM for Motz's problem by the central rule as $N = 34$.

M	$\ \varepsilon\ _B$	$\ \varepsilon\ _{\infty, \overline{AB}}$	Cond.	$ \frac{\Delta D_0}{D_0} $	$ \frac{\Delta D_1}{D_1} $	$ \frac{\Delta D_2}{D_2} $	$ \frac{\Delta D_3}{D_3} $
12	0.359(-8)	0.721(-8)	0.675(6)	0.531(-13)	0.646(-12)	0.405(-11)	0.868(-11)
18	0.494(-8)	0.629(-8)	0.679(6)	0.468(-14)	0.211(-14)	0.620(-13)	0.352(-14)
24	0.491(-8)	0.530(-8)	0.679(6)	0.567(-15)	0.324(-15)	0.103(-14)	0.337(-13)
30	0.493(-8)	0.520(-8)	0.676(6)	0*	0.162(-15)	0.124(-14)	0.317(-13)
36	0.494(-8)	0.520(-8)	0.679(6)	0.850(-15)	0.324(-15)	0.103(-14)	0.308(-13)

* in this table and in Tables 2.4, 2.12 and 2.14 denotes errors less than computer rounding errors in double precision.

Table 2.3: The error norms and condition numbers from the collocation TM for Motz's problem as $N = 34$ by the Gaussian rule with 6 nodes.

r	M	$\ \varepsilon\ _B$	$\ \varepsilon\ _{\infty, \overline{AB}}$	Cond.	$ \frac{\Delta D_0}{D_0} $	$ \frac{\Delta D_1}{D_1} $	$ \frac{\Delta D_2}{D_2} $	$ \frac{\Delta D_3}{D_3} $
1	24	0.839(-8)	0.459(-8)	0.669(6)	0.169(-11)	0.121(-11)	0.296(-10)	0.152(-10)
2	24	0.854(-8)	0.369(-8)	0.672(6)	0.708(-13)	0.512(-12)	0.133(-11)	0.106(-11)
4	24	0.610(-8)	0.540(-8)	0.679(6)	0.425(-15)	0.535(-14)	0.641(-13)	0.755(-13)
6	30	0.493(-8)	0.520(-8)	0.676(6)	0*	0.162(-15)	0.124(-14)	0.317(-13)
8	24	0.428(-8)	0.519(-8)	0.679(6)	0.142(-15)	0.648(-15)	0.618(-15)	0.315(-13)
10	20	0.639(-8)	0.521(-8)	0.679(6)	0.142(-15)	0*	0.412(-15)	0.308(-13)

Table 2.4: The error norms and condition numbers from the collocation TM for Motz's problem by different Gaussian rules with r nodes as $N = 34$.

i	All digits	Sig. digits	No. of Sig. digits
0	401.162453745234416	401.16245374523442	17
1	87.6559201950879299	87.6559201950879	15
2	17.2379150794467897	17.2379150794468	15
3	-8.0712152596987790	-8.07121525970	12
4	1.44027271702238968	1.44027271702	12
5	0.331054885920006037	0.33105488592	12
6	0.275437344507860671	0.27543734451	11
7	-0.869329945041107943(-1)	-0.869329945(-1)	9
8	0.336048784027428854(-1)	0.336048784(-1)	9
9	0.153843744594011413(-1)	0.153843745(-1)	9
10	0.730230164737157971(-2)	0.7302302(-2)	7
11	-0.318411361654662899(-2)	-0.3184114(-2)	7
12	0.122064586154974736(-2)	0.1220646(-2)	7
13	0.530965295822850803(-3)	0.530965(-3)	6
14	0.271512022889081647(-3)	0.271512(-3)	6
15	-0.120045043773287966(-3)	-0.12005(-3)	5
16	0.505389241414919585(-4)	0.5054(-4)	4
17	0.231662561135488172(-4)	0.2317(-4)	4
18	0.115348467265589439(-4)	0.11535(-4)	5
19	-0.529323807785491411(-5)	-0.529(-5)	3
20	0.228975882995988624(-5)	0.229(-5)	3
21	0.106239406374917051(-5)	0.106(-5)	3
22	0.530725263258556923(-6)	0.531(-6)	3
23	-0.245074785537844696(-6)	-0.25(-6)	2
24	0.108644983229739802(-6)	0.11(-6)	2
25	0.510347415146524412(-7)	0.5(-7)	1
26	0.254050384217598898(-7)	0.3(-7)	1
27	-0.110464929421918792(-7)	-0.1(-7)	1
28	0.493426255784041972(-8)	/	0
29	0.232829745036186828(-8)	/	0
30	0.115208023942516515(-8)	/	0
31	-0.345561696019388690(-9)	/	0
32	0.153086899837533823(-9)	/	0
33	0.722770554189099639(-10)	/	0
34	0.352933005315648864(-10)	/	0

Table 2.5: The leading coefficients D_i from the collocation TM for Motz's problem by the Gaussian rule with 6 nodes as $N = 34$ and $M = 30$.

i	ISBFM	No. of Sig.	Integrated method	No. of Sig.
0	.191118631972	12	.191118631972	12
1	-.1181160720	10	-.118116071967	12
4	-.1254698598(-1)	10	-.1254698598(-1)	10
5	-.1903340371(-1)	10	-.1903340371(-1)	10
8	-.6541248(-3)	7	-.654125(-3)	6
9	-.75959348(-2)	8	-.7595935(-2)	7
12	-.505411(-3)	6	-.5054(-3)	4
13	-.4477115(-2)	7	-.44771(-2)	5
16	-.190964(-3)	5	-.19(-3)	2
17	-.300990(-2)	6	-.301(-2)	3
20	-.1179(-3)	4	NA	/
21	-.22019(-2)	5	NA	/
24	-.72(-4)	2	NA	/

In the table "NA" denotes "Not Available".

Table 2.6: The leading coefficients α_i cited from Georgiou et al. [168] for the traditional cracked beam problem in Figure 2.3.

$N + 1$	$\ u - u_N\ _B$	$\ u - u_N\ _{\infty, \overline{BC}}$	Cond.
12	0.174(-1)	0.192(-1)	118
20	0.103(-3)	0.143(-3)	0.242(4)
28	0.780(-6)	0.126(-5)	0.457(5)
36	0.697(-8)	0.123(-7)	0.828(6)
44	0.655(-10)	0.128(-9)	0.148(8)

Table 2.7: The errors and condition numbers from the collocation TM by the central rule for the cracked beam problem with u_N , where $w = 1/(N + 1)$.

i	\hat{D}_i	i	\hat{D}_i
0	540.565122713627	22	.741136835680306(-12)
1	-167.041350909274	23	.417873188876248(-11)
2	.198198742457744(-13)	24	-.121996855522588(-7)
3	-.219185365289299(-13)	25	-.143269204396301(-6)
4	-2.21801471698044	26	.853944744811233(-12)
5	-1.68233110389621	27	.392784692715081(-11)
6	-.214659464703740(-14)	28	-.519522874909708(-9)
7	.975152635890286(-14)	29	-.716697851376144(-8)
8	-.722712676630922(-2)	30	.562441620804752(-12)
9	-.419620077504757(-1)	31	.210052519224617(-11)
10	.158368581564262(-13)	32	-.226112209663434(-10)
11	.977095083882188(-13)	33	-.361688092767140(-9)
12	-.349003797729518(-3)	34	.209940550959741(-12)
13	-.154580008052455(-2)	35	.631754175553925(-12)
14	.893242771123692(-13)	36	-.907100573484872(-12)
15	.733457764014275(-12)	37	-.166314437291397(-10)
16	-.824172461669611(-5)	38	.411725887639002(-13)
17	-.649512698211018(-4)	39	.988154926645705(-13)
18	.356068309179608(-12)	40	-.230535024761913(-13)
19	.244904048630545(-11)	41	-.493264784148099(-12)
20	-.317915391408544(-6)	42	.328644957534978(-14)
21	-.296970610620140(-5)	43	.621165127407370(-14)

Table 2.8: The coefficients from the collocation TM by the central rule for the cracked beam problem with u_N as $N = 43$.

$N + 1$	$\ u - u_N^*\ _B$	$\ u - u_N^*\ _{\infty, \overline{BC}}$	Cond.
12	0.181(-1)	0.143(-1)	14.7
20	0.108(-3)	0.860(-4)	179
28	0.835(-6)	0.673(-6)	0.241(4)
36	0.731(-8)	0.593(-8)	0.340(5)
44	0.689(-10)	0.563(-10)	0.492(6)

Table 2.9: The errors and condition numbers from the collocation TM by the central rule for the cracked beam problem with u_N^* , where $w = 1/(N + 1)$.

i	\hat{D}_i	i	\hat{D}_i
0	540.565122713627	21	-.296970704226108(-5)
1	-167.041350909274	24	-.122002935723549(-7)
4	-2.21801471698038	25	-.143270030434461(-6)
5	-1.68233110389617	28	-.519982420026741(-9)
8	-.722712676632975(-2)	29	-.716735060983968(-8)
9	-.419620077505017(-1)	32	-.228004937465962(-10)
12	-.349003797758166(-3)	33	-.361766490834198(-9)
13	-.154580008066482(-2)	36	-.946724588701563(-12)
16	-.824172478281220(-5)	37	-.166363445310374(-10)
17	-.649512703568597(-4)	40	-.263335130630466(-13)
20	-.317915829660462(-6)	41	-.492957376797978(-12)

Table 2.10: The coefficients from the collocation TM by the central rule for the cracked beam problem with u_N^* as $N = 43$.

M	$\ u - u_N^*\ _B$	$\ u - u_N^*\ _{\infty, \overline{BC}}$	Cond.	$ \frac{\Delta \hat{D}_0}{\hat{D}_0} $	$ \frac{\Delta \hat{D}_1}{\hat{D}_1} $	$ \frac{\Delta \hat{D}_4}{\hat{D}_4} $	$ \frac{\Delta \hat{D}_5}{\hat{D}_5} $
16	0.317(-10)	0.579(-10)	0.447(6)	0.421(-15)	0.340(-15)	0.340(-14)	0.647(-14)
24	0.319(-10)	0.527(-10)	0.447(6)	0*	0.510(-15)	0.701(-14)	0.103(-13)
32	0.319(-10)	0.526(-10)	0.447(6)	0.841(-15)	0.340(-15)	0.541(-14)	0.594(-14)
40	0.319(-10)	0.526(-10)	0.447(6)	0.631(-15)	0*	0.801(-15)	0.792(-14)

Table 2.11: The error norms and condition numbers from the collocation TM for the cracked beam problem as $N = 43$ by the Gaussian rule with 8 nodes.

r	M	$\ u - u_N^*\ _B$	$\ u - u_N^*\ _{\infty, \overline{BC}}$	Cond.	$ \frac{\Delta \hat{D}_0}{\hat{D}_0} $	$ \frac{\Delta \hat{D}_1}{\hat{D}_1} $	$ \frac{\Delta \hat{D}_4}{\hat{D}_4} $	$ \frac{\Delta \hat{D}_5}{\hat{D}_5} $
1	24	0.614(-10)	0.102(-9)	0.434(6)	0.294(-14)	0.715(-14)	0.177(-12)	0.175(-12)
2	24	0.623(-10)	0.602(-10)	0.446(6)	0.210(-15)	0.187(-14)	0.617(-13)	0.523(-13)
4	24	0.448(-10)	0.519(-10)	0.446(6)	0.210(-15)	0.119(-14)	0.921(-14)	0.462(-14)
6	24	0.367(-10)	0.576(-10)	0.447(6)	0.210(-15)	0*	0.661(-14)	0.726(-14)
8	24	0.319(-10)	0.527(-10)	0.447(6)	0*	0.510(-15)	0.701(-14)	0.103(-13)
12	24	0.261(-10)	0.524(-10)	0.447(6)	0.210(-15)	0.340(-15)	0.741(-14)	0.488(-14)

Table 2.12: The error norms and condition numbers from the collocation TM for the cracked beam problem by different Gaussian rules with r nodes as $N = 43$.

i	\hat{D}_i	i	$\hat{D}_i(i)$
0	540.565122713627488338	21	-.296970804065775927138(-5)
1	-167.041350909274314063	24	-.122000024043979050718(-7)
4	-2.21801471698042096392	25	-.143271318148128170607(-6)
5	-1.68233110389623896630	28	-.519737845303284863567(-9)
8	-.722712676629304936332(-2)	29	-.716825117065194526952(-8)
9	-.419620077504989710815(-1)	32	-.226916180319381751640(-10)
12	-.349003797752273547863(-3)	33	-.362109309069568822496(-9)
13	-.154580008073283248042(-2)	36	-.922553631817261539388(-12)
16	-.824172472675852766202(-5)	37	-.167027744142682193722(-10)
17	-.649512707503007010942(-4)	40	-.242365241977693826580(-13)
20	-.317915648270962735950(-6)	41	-.498065701032834816745(-12)

Table 2.13: The leading coefficients from the collocation TM for the cracked beam problem by the Gaussian rule with 8 nodes as $N = 43$ and $M = 24$.

r	$\ w - w_N^*\ _B$	$\ w - w_N^*\ _{\infty, \overline{BC}}$	Cond.	$ \frac{\Delta \hat{D}_0}{\hat{D}_0} $	$ \frac{\Delta \hat{D}_1}{\hat{D}_1} $	$ \frac{\Delta \hat{D}_4}{\hat{D}_4} $	$ \frac{\Delta \hat{D}_5}{\hat{D}_5} $
1	0.180(-13)	0.159(-13)	0.191(10)	0.203(-14)	0.493(-14)	0.142(-12)	0.140(-12)
2	0.160(-13)	0.141(-13)	0.191(10)	0*	0.141(-14)	0.684(-13)	0.483(-13)
4	0.116(-13)	0.141(-13)	0.187(10)	0.102(-14)	0.940(-15)	0.124(-13)	0.140(-13)
6	0.955(-14)	0.144(-13)	0.186(10)	0*	0.117(-15)	0.111(-14)	0.729(-15)
8	0.833(-14)	0.143(-13)	0.185(10)	0.290(-15)	0.235(-15)	0.166(-14)	0.365(-14)
12	0.680(-14)	0.143(-13)	0.185(10)	0.145(-15)	0.117(-15)	0.138(-15)	0.419(-14)

Table 2.14: The error norms and condition numbers from the collocation TM directly for the traditional cracked beam problem in Figure 2.3 by different Gaussian rules with r nodes as $N = 43$ and $M = 24$.

i	All digits	Sig. digits	No. of Sig. digits
0	.191118631971872093844	.19111863197187209	17
1	-.118116071966509542102	-.1181160719665095	16
4	-.125469859771873346044(-1)	-.12546985977187(-1)	14
5	-.190334037082572939126(-1)	-.19033403708257(-1)	14
8	-.654124844152399417298(-3)	-.65412484415(-3)	11
9	-.759593477954055400214(-2)	-.759593477954(-2)	12
12	-.505411485799405575323(-3)	-.5054114858(-3)	10
13	-.447711526684630486267(-2)	-.447711527(-2)	9
16	-.190964676787037826271(-3)	-.19096468(-3)	8
17	-.300990359104527302470(-2)	-.3009904(-2)	7
20	-.117860105316055165819(-3)	-.117860(-3)	6
21	-.220190546979016346305(-2)	-.220191(-2)	6
24	-.723660418005184549999(-4)	-.7237(-4)	4
25	-.169966822206286320533(-2)	-.1700(-2)	4
28	-.493263780013297154056(-4)	-.49(-4)	2
29	-.136062389932649135602(-2)	-.136(-2)	3
32	-.344572276541308970127(-4)	-.3(-4)	1
33	-.109972615269026243248(-2)	-.1(-2)	1
36	-.224143667286699527393(-4)	/	0
37	-.811621347953916006009(-3)	/	0
40	-.942161102160732748267(-5)	/	0
41	-.387232200462756144532(-3)	/	0

Table 2.15: The leading coefficients α_i from Table 2.13 by (2.5.4) for $a = \frac{1}{2}$ and $b = 0.125$ in the scaled cracked beam problem.

i	All digits	Sig. digits	No. of Sig. digits
0	.191118631971872093844	.19111863197187209	17
1	-.118116071966509458835	-.1181160719665095	16
4	-.125469859771874230753(-1)	-.125469859771874(-1)	15
5	-.190334037082570510513(-1)	-.190334037082571(-1)	15
8	-.654124844153439167181(-3)	-.65412484415(-3)	11
9	-.759593477953802304059(-2)	-.759593477954(-2)	12
12	-.505411485758066030688(-3)	-.5054114858(-3)	10
13	-.447711526664487571153(-2)	-.447711527(-2)	9
16	-.190964673066832069321(-3)	-.1909647(-3)	7
17	-.300990357223324123126(-2)	-.3009904(-2)	7
20	-.117859936451135464920(-3)	-.11786(-3)	5
21	-.220190469161906385645(-2)	-.22019(-2)	5
24	-.723620522995536540750(-4)	-.724(-4)	3
25	-.169965180428740376094(-2)	-.1700(-2)	4
28	-.492760129615704093459(-4)	-.49(-4)	2
29	-.136043628609274110108(-2)	-.136(-2)	3
32	-.341170517533278386583(-4)	-.3(-4)	1
33	-.109855994151387601453(-2)	-.1(-2)	1
36	-.212639663103781256836(-4)	/	0
37	-.807933182726571115506(-3)	/	0
40	-.789995944027442427633(-5)	/	0
41	-.382605289154327110005(-3)	/	0

Table 2.16: The leading coefficients α_i from the collocation TM directly from the traditional cracked beam problem in Figure 2.3 by the Gaussian rule with six nodes as $N = 43$ and $M = 24$.

r	From Table 2.12 by (2.5.6)			Direct computation		
	$\frac{b}{500} \cdot \ u - u_N^*\ _B$	$\frac{b}{500} \cdot \ u - u_N^*\ _{\infty, BC}$	Cond.	$\ w - w_N^*\ _B$	$\ w - w_N^*\ _{\infty, BC}$	Cond.
1	0.154(-14)	0.255(-14)	0.434(6)	0.180(-13)	0.159(-13)	0.191(10)
2	0.156(-14)	0.151(-14)	0.446(6)	0.160(-13)	0.141(-13)	0.191(10)
4	0.112(-14)	0.130(-14)	0.446(6)	0.116(-13)	0.141(-13)	0.187(10)
6	0.918(-15)	0.144(-14)	0.447(6)	0.955(-14)	0.144(-13)	0.186(10)
8	0.798(-15)	0.132(-14)	0.447(6)	0.833(-14)	0.143(-13)	0.185(10)
12	0.653(-15)	0.131(-14)	0.447(6)	0.680(-14)	0.143(-13)	0.185(10)

Table 2.17: Comparisons of the error norms and condition numbers from from Table 2.12 by (2.5.6) and directly from the traditional cracked beam problem in Figure 2.3 as $N = 43$ and $M = 24$.

Chapter 3

Coupling Techniques

We begin with Laplace's equation with singularities by the boundary approximation method (BAM), i.e., the collocation Trefftz method (CTM). Different coupling techniques to match the boundary conditions are explored. This chapter also examines the generalized Trefftz methods (GTMs) for partial differential equations (PDEs) with singularities. GTMs use the local particular solutions of PDEs, but adopt the coupling strategies to deal with the boundary conditions, which are different from the classic BAM in Chapter 1 and the CTM in Chapter 2. Three new kinds of GTMs are discussed: (1) the hybrid TM, (2) the penalty plus hybrid TM, (3) the multiplier TM. An a priori error analysis of GTMs is provided, to choose the optimal parameters used, and to derive the optimal exponential order of convergence rates. To study the stability, the condition number is replaced by the effective condition number to provide a better upper bound of relative errors for the TM solutions resulting from rounding errors. New computational formulas are derived for the effective condition number and its simplified forms. Numerical experiments are carried out for Motz's problem, to verify the error analysis. Comparisons are made to show that the CTM is the best among all TMs in accuracy, stability and simplicity of the algorithm, although all TMs are efficient. On the other hand, the boundary element method (BEM) uses the fundamental solutions satisfying the PDEs. Both the GTMs and the BEM deal with only the boundary conditions. However, the GTMs are easier for handling the solutions with singularity and other complicated boundary conditions. Since proper coupling techniques for interior and exterior boundary conditions are imperative, the study of this chapter may enrich not only the Trefftz method (TM) with variant formulations, but also a wide range of other numerical methods.

3.1 Introduction

We consider Motz's problem that solves the Laplace equation on the rectangle $S = \{(x, y) \mid -1 < x < 1, 0 < y < 1\}$

$$\Delta u = \frac{\partial^2 u}{\partial x^2} + \frac{\partial^2 u}{\partial y^2} = 0 \quad \text{in } S, \quad (3.1.1)$$

with the mixed Neumann-Dirichlet boundary conditions, see Figure 3.1,

$$u|_{\overline{OD}} = 0, \quad u|_{\overline{AB}} = 500, \quad (3.1.2)$$

$$\frac{\partial u}{\partial y}\Big|_{\overline{OA}} = \frac{\partial u}{\partial y}\Big|_{\overline{BC}} = \frac{\partial u}{\partial x}\Big|_{\overline{CD}} = 0. \quad (3.1.3)$$

In fact, the singular solutions of (3.1.1) – (3.1.3) are found as

$$u(r, \theta) = \sum_{i=0}^{\infty} d_i r^{i+\frac{1}{2}} \cos\left(i + \frac{1}{2}\right)\theta, \quad (3.1.4)$$

where d_i are the true expansion coefficients, and (r, θ) are the polar coordinates with the origin at $(0, 0)$ (see Figure 3.1). Hence the admissible functions of finite terms,

$$u_N(r, \theta) = \sum_{i=0}^N D_i r^{i+\frac{1}{2}} \cos\left(i + \frac{1}{2}\right)\theta \quad (3.1.5)$$

with the unknown coefficients D_i , are most efficient in matching Motz's solutions numerically, to yield the exponential convergence rates $O(e^{-cN})$, where c is a positive constant. When functions (3.1.5) are chosen, Eq. (3.1.1) and $u|_{\overline{OD}} = 0$ and $\frac{\partial u}{\partial y}\Big|_{\overline{OA}} = 0$ are satisfied automatically. Then the coefficients D_i are sought by the collocation equations of the rest of boundary conditions in (3.1.2) and (3.1.3), which is called the Trefftz method (TM) in this book.

The highly accurate solution, obtained in double precision with the 35 leading coefficients, $\tilde{D}_0 - \tilde{D}_{34}$, was provided in [316]. It should be noted that an error at the power of \tilde{D}_{31} was discovered by Lucas and Oh [332]. This highly accurate solution can be regarded as a true solution for testing other numerical methods. In Chapter 2, the more accurate leading coefficients are achieved by the Gaussian rule. In Georgiou, et al. [169], the same

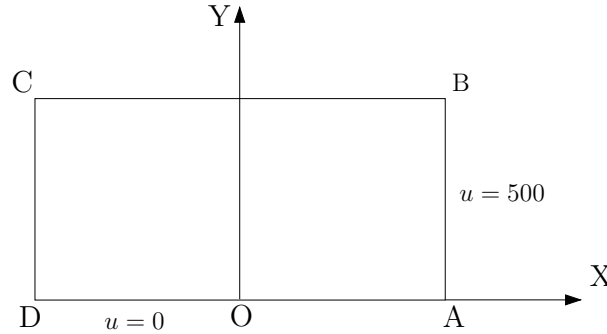


Figure 3.1: Motz's problem.

singular functions as in [316] are chosen, but the boundary conditions are matched by Lagrange multiplier method. Here questions arise: Are there other matching techniques to deal with the boundary conditions, when the same particular solutions have been chosen? If yes, what are the error bounds of the approximate solutions by the new methods? And how about their computational performance? To answer these questions is one of the objectives of this chapter.

In Li [291], a solution domain S is split into two subdomains S_1 and S_2 , and the particular solutions are used in just one subdomain S_2 , and other numerical methods are used in S_1 , such as the finite element method (FEM), the finite difference method (FDM), finite volume method (FVM), etc. The comprehensive coupling strategies are investigated wherein. In this chapter we employ these coupling techniques for matching different particular solutions in S_1 and S_2 along their interfaces $\Gamma_0 = \partial S_1 \cap \partial S_2$, which have not been discussed before. Four new TMs are explored in this chapter: (1) The penalty TM, (2) the hybrid TM, (3) the penalty plus hybrid TM, and (4) the Lagrange multiplier TM in [169]. Brief analysis is conducted to derive error bounds and to find optimal parameters used. Note that the conclusions drawn in this chapter are rather different from those in [291]. For instance, it is concluded in the present work that the penalty combination is quite efficient for matching the TM using the particular solutions and the FEM using piecewise polynomials of low order; the penalty TM, on the other hand, should not be chosen due to inferior accuracy of the solutions obtained. Moreover, since a worse instability occurs in the hybrid TM and the penalty plus hybrid TM, the leading coefficients $\tilde{D}_0 - \tilde{D}_3$ are less accurate than those by the collocation Trefftz method (CTM) discussed in Chapter 2. In this chapter, if the straightforward collocation Trefftz method by the central rule or the Gaussian rule is used, the CTM is called. If the particular solutions of PDEs are chosen, and if the approximate solutions are obtained by satisfying only the boundary conditions, the GTMs are called.

In numerical computations for the PDE solutions, accuracy and stability of numerical solutions are two critical issues, which are related to each other.

The FEM provides good numerical stability, but low accuracy. Whenever feasible, we should first try one of the high accuracy methods presented in this book. If the present methods do not apply, then methods, such as the FEM, or a coupling of the FEM with TMs should be used.

This chapter is organized as follows. In the next section, the GTMs are described. In Sections 3.3 – 3.5, the penalty TM, hybrid TM, and penalty plus hybrid TM are explored for Motz's problem, with a concise error analysis. In Section 3.6, a brief analysis is made for the Lagrange multiplier TM. In Section 3.7, formulas are derived for the effective condition numbers. In the last section, numerical experiments are carried out, and comparisons and conclusions are made. The materials of this chapter are adapted from Li et al. [300, 312].

3.2 Description of Generalized GTMs

Consider Poisson's equation

$$\Delta u = \frac{\partial^2 u}{\partial x^2} + \frac{\partial^2 u}{\partial y^2} = f \quad \text{in } S, \quad (3.2.1)$$

with the mixed type of boundary conditions

$$u = g_1 \quad \text{on } \Gamma_D, \quad (3.2.2)$$

$$\frac{\partial u}{\partial n} + qu = g_2 \quad \text{on } \Gamma_N, \quad (3.2.3)$$

where the domain S is bounded, simply connected polygon with the exterior boundary Γ , $\Gamma = \Gamma_D \cup \Gamma_N$, $\text{Meas}(\Gamma_D) > 0$, the functions q , g_1 and g_2 are sufficiently smooth, and $q = q(x, y) \geq 0$.

The solution of the problem (3.2.1) – (3.2.3) can be equivalently expressed by minimizing an energy $I(v)$:

$$I(u) = \min_{v \in H_*^1(S)} I(v),$$

where the energy is given by

$$I(v) = \frac{1}{2} \iint_S |\nabla v|^2 ds + \frac{1}{2} \int_{\Gamma_N} qv^2 d\ell - \int_{\Gamma_N} g_2 v d\ell,$$

and $H_*^1(S)$ is the Sobolev space¹ defined by

$$H_*^1(S) = \{v \mid v, v_x, v_y \in L^2(S), \text{ and } v|_{\Gamma_D} = g_1\}.$$

Let S be divided by Γ_0 into S_1 and S_2 , see Figure 3.2.

The Ritz-Galerkin method is used in both S_1 and S_2 , with the admissible functions as

$$v = \begin{cases} v^- = \Phi_0 + \sum_{i=1}^M a_i \Phi_i & \text{in } S_1, \\ v^+ = \Psi_0 + \sum_{i=1}^N b_i \Psi_i & \text{in } S_2, \end{cases} \quad (3.2.4)$$

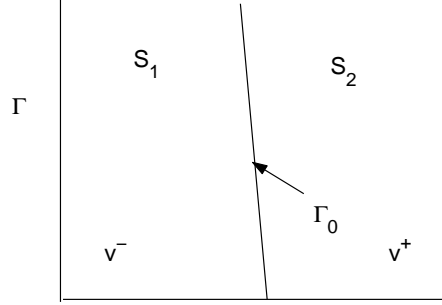
where

$$\begin{aligned} \Delta \Phi_0 &= f, \text{ in } S_1, \quad \Delta \Psi_0 = f, \text{ in } S_2, \\ \Delta \Phi_i &= 0, \text{ in } S_1, \text{ for } i \geq 1, \quad \Delta \Psi_i = 0, \text{ in } S_2, \text{ for } i \geq 1. \end{aligned}$$

¹More precisely, the Sobolev space is only for the linear space

$$H_0^1(S) = \{v \mid v, v_x, v_y \in L^2(S), \text{ and } v|_{\Gamma} = 0\},$$

since the linear combinations must be in the same space. On the other hand, $H_*^1(S)$ is the space to $H_0^1(S)$ by a translation.

Figure 3.2: Partition of S .

The functions $\{\Phi_i\}$ and $\{\Psi_i\}$ are analytic, complete and linearly independent basis functions in S_1 and S_2 respectively, and a_i and b_i are unknown coefficients to be determined.

Define a space

$$H = \{v \mid v \in L^2(S), v \in H^1(S_1), v \in H^1(S_2)\}.$$

Let $V_N^* \subset H$ be a finite-dimensional collection of (3.2.4). The TMs using the generalized coupling techniques are designed to seek an approximate solution $u_N \in V_N^*$ such that

$$I_h(u_N) = \min_{v \in V_N^*} I_h(v), \quad (3.2.5)$$

where the energy

$$\begin{aligned} I_h(v) &= \frac{1}{2} \iint_{S_1} |\nabla v|^2 ds + \frac{1}{2} \iint_{S_2} |\nabla v|^2 ds \\ &+ \frac{1}{2} \int_{\Gamma_N} qv^2 dl + w^2 \int_{\Gamma_D} (v - g_1)^2 dl \\ &- \alpha^* \int_{\Gamma_D} \frac{\partial v}{\partial n} (v - g_1) dl + w^2 \int_{\Gamma_0} (v^+ - v^-)^2 dl \\ &- \int_{\Gamma_0} \left(\alpha \frac{\partial v^+}{\partial n} + \beta \frac{\partial v^-}{\partial n} \right) (v^+ - v^-) dl - \int_{\Gamma_N} g_2 v dl - \iint_S f v, \end{aligned} \quad (3.2.6)$$

where $w(\geq 0)$ is a weight, n is the outward normal of ∂S_2 and ∂S , and α , α^* and β are parameters. Since the solutions v^+ and v^- satisfy the Laplace equation already, we have from the Green formula

$$\iint_{S_1} |\nabla v^-|^2 ds + \iint_{S_2} |\nabla v^+|^2 ds = - \int_{\partial S_1} v^- \frac{\partial v^-}{\partial n} dl + \int_{\partial S_2} v^+ \frac{\partial v^+}{\partial n} dl.$$

Hence, the energy (3.2.6) is reduced to

$$\begin{aligned}
I_h(v) &= -\frac{1}{2} \int_{\partial S_1} v^- \frac{\partial v^-}{\partial n} dl + \frac{1}{2} \int_{\partial S_2} v^+ \frac{\partial v^+}{\partial n} dl \\
&+ \frac{1}{2} \int_{\Gamma_N} qv^2 dl + w^2 \int_{\Gamma_D} (v - g_1)^2 dl \\
&- \alpha^* \int_{\Gamma_D} \frac{\partial v}{\partial n} (v - g_1) dl + w^2 \int_{\Gamma_0} (v^+ - v^-)^2 dl \\
&- \int_{\Gamma_0} \left(\alpha \frac{\partial v^+}{\partial n} + \beta \frac{\partial v^-}{\partial n} \right) (v^+ - v^-) dl - \int_{\Gamma_N} g_2 v dl - \iint_S f v. \tag{3.2.7}
\end{aligned}$$

Note that in (3.2.7), the integrals are involved only in the interior and exterior boundaries. In fact, the combinations as in (3.2.7) are general approaches using additional integrals, which contain the following three variants of TMs:

1. **The Penalty TM:** $w > 0$, $\alpha = \beta = 0$ and $\alpha^* = 0$.
2. **The Simplified Hybrid TM:** $w = 0$, $\alpha = 1$, $\beta = 0$ and $\alpha^* = 1$.
3. **The Penalty plus Hybrid TM:** $w > 0$, $\alpha = \beta = \frac{1}{2}$ and $\alpha^* = 1$.

In addition, the Lagrange multipliers method is given by [169, 291] as

$$B(\lambda, \mu; u, v) = \int_{\Gamma_N} g_2 v dl + \int_{\Gamma_D} \mu g_1 dl,$$

where

$$\begin{aligned}
B(\lambda, \mu; u, v) &= \iint_{S_1} \nabla u \cdot \nabla v ds + \iint_{S_2} \nabla u \cdot \nabla v ds + D(\lambda, \mu; u, v) \\
&= - \int_{\partial S_1} \left(v^- \frac{\partial u}{\partial n} \right) dl + \int_{\partial S_2} \left(v^+ \frac{\partial u}{\partial n} \right) dl + D(\lambda, \mu; u, v),
\end{aligned}$$

and the boundary integrals are given by

$$\begin{aligned}
D(\lambda, \mu; u, v) &= \int_{\Gamma_N} q u v dl - \int_{\Gamma_D} \lambda v dl - \int_{\Gamma_D} \mu u dl \\
&- \int_{\Gamma_0} \lambda (v^+ - v^-) dl - \int_{\Gamma_0} \mu (u^+ - u^-) dl.
\end{aligned}$$

Note that the λ is treated as an extra variable.

3.3 Penalty TMs

We will study the case of $S = S_1$ and $S_2 = \Gamma_0 = \emptyset$, i.e., no division of S , and provide a brief analysis of the GTMs for the Motz's problem in the rest of this chapter. The analysis of the case the $\Gamma_0 \neq \emptyset$ for (3.2.4) can be similarly developed, see Chapter 8.

The admissible functions (3.1.4) satisfy Laplace equation (3.1.1) and two boundary conditions $u|_{\overline{OD}} = 0$ and $\frac{\partial u}{\partial y}|_{\overline{OA}} = 0$ already, see Figure 3.1. We should choose the approximate coefficients D_i in (3.1.5) to satisfy the rest of the boundary conditions of (3.1.2) – (3.1.3) as best as possible. Therefore, the optimal solution u_N can be sought by the penalty TMs, which is given from (3.2.7) by noting $S = S_2$, $S_1 = \Gamma_0 = \emptyset$, $\alpha^* = 0$, $f = q = g_2 = 0$ and $g_1 = 500$. We seek \tilde{u}_N^P from

$$I_h(\tilde{u}_N^P) = \min_{v \in V_N} I_h(v),$$

where

$$I_h(v) = \frac{1}{2} \int_{\overline{AB \cup BC \cup CD}} v \frac{\partial v}{\partial n} dl + w^2 \int_{\overline{AB}} (v - 500)^2 dl,$$

in which V_N is a finite dimensional collection of the admissible functions in (3.1.5) and $w > 0$ is a weight parameter.

The solutions of the minimal energy is given by

$$I_h(\tilde{u}_N^P) = \min_{v \in V_N} T_1(v), \quad (3.3.1)$$

where

$$I_h(v) = \int_{\Gamma_N^*} v \frac{\partial v}{\partial n} dl + w^2 \int_{\overline{AB}} (v - 500)^2 dl,$$

and $\Gamma_N^* = \overline{AB} \cup \overline{BC} \cup \overline{CD}$.

In this section, we use the equivalence notations $a \asymp b$ or $a \asymp O(b)$ of a and $b(> 0)$, to indicate that there exist two constants $C_1(> 0)$ and $C_2(> 0)$ such that

$$C_1 b \leq |a| \leq C_2 b, \quad b > 0.$$

From the theory of the Sobolev space, we cite the following lemma from Sobolev [438].

Lemma 3.3.1 *For $Meas(\Gamma_D) \neq 0$, there exists an equivalence relation:*

$$|v|_{1,S}^2 + \|v\|_{0,\Gamma_D}^2 \asymp \|v\|_{1,S}^2.$$

Define a new norm

$$\|v\|_H = \left\{ \int_{\Gamma_N^*} v \frac{\partial v}{\partial n} dl + w^2 \int_{\overline{AB}} v^2 dl \right\}^{\frac{1}{2}}, \quad w \geq 1. \quad (3.3.2)$$

Since $\int_{\Gamma_N^*} v \frac{\partial v}{\partial n} dl = |v|_{1,S}^2$, $\forall v \in V_N$, we have the following lemma.

Lemma 3.3.2 *Let $Meas(\Gamma_D) \neq 0$ and $w = 1$,*

$$\|v\|_H \asymp \|v\|_{1,S}, \quad \forall v \in V_N.$$

Lemma 3.3.3 *Let $\text{Meas}(\Gamma_D) \neq 0$ and $w \geq 1$, there exist the bounds for $\forall v \in V_N$,*

$$C_1 \|v\|_{1,S} \leq \|v\|_H \leq C_2 w \|v\|_{1,S}, \quad (3.3.3)$$

where C_1 and C_2 are two constants independent of v .

Proof. Since for $w \geq 1$, we have from Lemma 3.3.1,

$$\|v\|_H^2 \geq |v|_{1,S}^2 + \|v\|_{0,\Gamma_D}^2 \geq C_0 \|v\|_{1,S}^2,$$

and from Lemma 3.3.2

$$\|v\|_H^2 = w^2 \left\{ \frac{1}{w^2} |v|_{1,S}^2 + \|v\|_{0,\Gamma_D}^2 \right\} \leq w^2 \{ |v|_{1,S}^2 + \|v\|_{0,\Gamma_D}^2 \} \leq C w^2 \|v\|_{1,S}^2.$$

The desired results (3.3.3) follow. ■

Next let us give an a priori error analysis.

Theorem 3.3.1 *The solution \tilde{u}_N^P from (3.3.1), the penalty TM, has the error bound,*

$$\|u - \tilde{u}_N^P\|_H \leq C \left(\inf_{v \in V_N} \|u - v\|_H + \frac{1}{w} \left\| \frac{\partial u}{\partial n} \right\|_{0,\overline{AB}} \right).$$

Proof. We may rewrite the penalty TM in (3.3.1) as

$$B_1(\tilde{u}_N^P, v) = f_1(v), \quad \forall v \in V_N, \quad (3.3.4)$$

where

$$B_1(u, v) = \int_{\Gamma_N^*} \frac{\partial u}{\partial n} v dl + w^2 \int_{\overline{AB}} u v dl,$$

$$f_1(v) = 500 w^2 \int_{\overline{AB}} v dl.$$

Since the true solution u of Motz's problem satisfies

$$B_1(u, v) = \int_{\overline{AB}} \frac{\partial u}{\partial n} v dl + f_1(v),$$

we obtain from (3.3.4)

$$B_1(u - \tilde{u}_N^P, v) = \int_{\overline{AB}} \frac{\partial u}{\partial n} v dl. \quad (3.3.5)$$

Let $\delta = \tilde{u}_N^P - v$, $v \in V_N$ and then $\delta \in V_N$. From Lemma 3.3.3, (3.3.2) and (3.3.5), and the bound $|B(u, v)| \leq C \|u\|_H \|v\|_H$, we have

$$\begin{aligned} \|\delta\|_H^2 &= B_1(\tilde{u}_N^P - v, \delta) = B_1(u - v, \delta) - \int_{\overline{AB}} \frac{\partial u}{\partial n} \delta dl \\ &\leq C \|u - v\|_H \|\delta\|_H + \left\| \frac{\partial u}{\partial n} \right\|_{0,\overline{AB}} \|\delta\|_{0,\overline{AB}} \\ &\leq C \left(\|u - v\|_H + \frac{1}{w} \left\| \frac{\partial u}{\partial n} \right\|_{0,\overline{AB}} \right) \|\delta\|_H. \end{aligned} \quad (3.3.6)$$

Dividing two sides of (3.3.6) by $\|\delta\|_H$ gives

$$\|\delta\|_H \leq C(\|u - v\|_H + \frac{1}{w} \|\frac{\partial u}{\partial n}\|_{0,\overline{AB}}).$$

Then we have

$$\begin{aligned} \|u - \tilde{u}_N^P\|_H &\leq \|u - v\|_H + \|v - \tilde{u}_N^P\|_H \\ &\leq C(\|u - v\|_H + \frac{1}{w} \|\frac{\partial u}{\partial n}\|_{0,\overline{AB}}). \quad \blacksquare \end{aligned}$$

Choose

$$v = u_N = \sum_{i=0}^N d_i r^{i+\frac{1}{2}} \cos(i + \frac{1}{2})\theta,$$

where d_i are the true coefficients. Let $u = u_N + r_N$, where the remainder

$$r_N = \sum_{i=N+1}^{\infty} d_i r^{i+\frac{1}{2}} \cos(i + \frac{1}{2})\theta.$$

We have the following lemma.

Lemma 3.3.4 *There exists the bound for the remainder,*

$$\|r_N\|_H \leq \|r_N\|_{0,\Gamma_N^*}^{\frac{1}{2}} \|\frac{\partial r_N}{\partial n}\|_{0,\Gamma_N^*}^{\frac{1}{2}} + w \|r_N\|_{0,\overline{AB}}. \quad (3.3.7)$$

Proof. We have

$$\begin{aligned} \|r_N\|_H^2 &= \|r_N \frac{\partial r_N}{\partial n}\|_{0,\Gamma_N^*} + w^2 \|r_N\|_{0,\overline{AB}}^2 \\ &\leq \|r_N\|_{0,\Gamma_N^*} \|\frac{\partial r_N}{\partial n}\|_{0,\Gamma_N^*} + w^2 \|r_N\|_{0,\overline{AB}}^2. \end{aligned}$$

The desired results (3.3.7) are obtained from $\sqrt{a^2 + b^2} \leq |a| + |b|$. \blacksquare

Corollary 3.3.1 *Suppose that for $0 < a < 1$,*

$$\begin{aligned} \|r_N\|_{0,\overline{AB}} &\leq C a^N, \quad \|r_N\|_{0,\Gamma_N^*} \leq C a^N, \\ \|\frac{\partial r_N}{\partial n}\|_{0,\Gamma_N^*} &\leq C N a^N. \end{aligned}$$

Then, when the optimal parameter $w = a^{-\frac{N}{2}}$, the error of the numerical solution \tilde{u}_N^P by the penalty TM has the bound²:

$$\|u - \tilde{u}_N^P\|_H \leq C \sqrt{N} a^{\frac{N}{2}}. \quad (3.3.8)$$

²When $\sqrt{N} a^{\frac{N}{2}} \leq C$, Eq. (3.3.8) may be modified by $\|u - \tilde{u}_N^P\|_H \leq C a^{\frac{N}{2}}$.

Proof. Let $v = u_N$. Then from $u = u_N + r_N$, Theorem 3.3.1 and Lemma 3.3.4, we have

$$\begin{aligned} \|u - \tilde{u}_N^P\|_H &\leq C(\inf_{v \in V_N} \|u - v\|_H + \frac{1}{w} \|\frac{\partial u}{\partial n}\|_{0, \overline{AB}}) \leq C(\|r_N\|_H + \frac{1}{w} \|\frac{\partial u}{\partial n}\|_{0, \overline{AB}}) \\ &\leq C\{\|r_N\|_{0, \Gamma_N^*}^{\frac{1}{2}} \|\frac{\partial r_N}{\partial n}\|_{0, \Gamma_N^*}^{\frac{1}{2}} + w\|r_N\|_{0, \overline{AB}} + \frac{1}{w} \|\frac{\partial u}{\partial n}\|_{0, \overline{AB}}\} \\ &\leq C(\sqrt{N}a^N + wa^N + \frac{1}{w}). \end{aligned}$$

The optimal parameter $w = O(a^{-\frac{N}{2}})$ and the desired result (3.3.8) is obtained. ■

It is worthy noting that the extreme large parameter $w = O(a^{-\frac{N}{2}})$ damages stability and lowers the convergence rates down to $O(\sqrt{N}a^{\frac{N}{2}})$, although which are still exponential. Below, we will pursue better TMs, to lead to optimal convergence rates and better stability.

3.4 Simplified Hybrid TMs

In this section, we consider the hybrid TM for Motz's problem in Figure 3.1. Denote

$$H_0^1(S) = \{v \mid v, v_x, v_y \in L^2(S), v|_{\overline{OD}} = 0, \frac{\partial v}{\partial n}|_{\overline{OA}} = 0\}. \quad (3.4.1)$$

We seek $u \in H_0^1(S)$ such that

$$\iint_S \nabla u \cdot \nabla v ds - \int_{\overline{AB}} \frac{\partial u}{\partial n} v dl + \int_{\overline{AB}} \frac{\partial v}{\partial n} (u - 500) dl = 0, \quad \forall v \in H_0^1(S). \quad (3.4.2)$$

From the Green Theorem, Eq. (3.4.2) is reduced to

$$\int_{\overline{BC} \cup \overline{CD}} \frac{\partial u}{\partial n} v dl + \int_{\overline{AB}} \frac{\partial v}{\partial n} (u - 500) dl = 0. \quad (3.4.3)$$

Let V_N be the space of functions v in (3.1.5). Then the hybrid TM is designed to seek $\tilde{u}_N^H \in V_N$ such that

$$\int_{\overline{BC} \cup \overline{CD}} \frac{\partial \tilde{u}_N^H}{\partial n} v dl + \int_{\overline{AB}} \frac{\partial v}{\partial n} (\tilde{u}_N^H - 500) dl = 0, \quad \forall v \in V_N. \quad (3.4.4)$$

A relation between (3.4.4) and (3.2.7) is explored in Li [291]. We may also rewrite the above equation as: to seek $\tilde{u}_N^H \in V_N$ such that

$$B_2(\tilde{u}_N^H, v) = f_2(v), \quad \forall v \in V_N, \quad (3.4.5)$$

where

$$B_2(u, v) = \int_{\overline{BC} \cup \overline{CD}} \frac{\partial u}{\partial n} v dl + \int_{\overline{AB}} u \frac{\partial v}{\partial n} dl,$$

and

$$f_2(v) = 500 \int_{AB} \frac{\partial v}{\partial n} dl.$$

We have the following theorem.

Theorem 3.4.1 *For the solutions by the hybrid TM, there exists the error bound,*

$$|u - \tilde{u}_N^H|_{1,S} \leq 2 \inf_{v \in V_N} |u - v|_{1,S}. \quad (3.4.6)$$

Proof. First we note from (3.4.2)

$$B_2(v, v) = \int_{\Gamma_N^*} \frac{\partial v}{\partial n} v dl = \iint_S |\nabla v|^2 ds = |v|_{1,S}^2.$$

Also it follows from (3.4.3) and (3.4.4)

$$B_2(u - \tilde{u}_N^H, v) = 0, \quad \forall v \in V_N, \quad (3.4.7)$$

where u is the true solution of Motz's problem. Let $\delta = \tilde{u}_N^H - v$ for $v \in V_N$, then $\delta \in V_N$. We have from (3.4.7)

$$\begin{aligned} |\delta|_{1,S}^2 &= B_2(\tilde{u}_N^H - v, \delta) = B_2(u - v, \delta) \\ &\leq \{B_2(u - v, u - v)B_2(\delta, \delta)\}^{\frac{1}{2}} = |u - v|_{1,S} |\delta|_{1,S}. \end{aligned}$$

This leads to $|\delta|_{1,S} \leq |u - v|_{1,S}$. Therefore, for $v \in V_N$, we obtain

$$|u - \tilde{u}_N^H|_{1,S} \leq |u - v|_{1,S} + |\delta|_{1,S} \leq 2|u - v|_{1,S}.$$

The desired result (3.4.6) is obtained. ■

By following the analysis in Section 3.3, we have the following corollary.

Corollary 3.4.1 *Let the conditions in Corollary 3.3.1 hold. Then there exists the bound*

$$\|u - \tilde{u}_N^H\|_{1,S} \leq C\sqrt{N}a^N. \quad (3.4.8)$$

Compared to the error bounds $O(\sqrt{N}a^{\frac{N}{2}})$ by the penalty TM in Section 3.3, the convergence rate in (3.4.8) by the hybrid TM is higher.

Let us consider the integration approximation in (3.4.4). The hybrid TM involving integral approximation is designed to seek $\hat{u}_N^H \in V_N$ such that

$$\tilde{\int}_{BC \cup CD} \frac{\partial \hat{u}_N^H}{\partial n} v dl + \tilde{\int}_{AB} \frac{\partial v}{\partial n} (\hat{u}_N^H - 500) dl = 0, \quad \forall v \in V_N, \quad (3.4.9)$$

where $\tilde{\int}$ is an approximation of \int by some rules. We have the following theorem.

Theorem 3.4.2 *For the solutions by the hybrid TM, there exists the error bound,*

$$|u - \hat{u}_N^H|_{1,S} \leq C \inf_{v \in V_N} |u - v|_{1,S} \quad (3.4.10)$$

$$+ C \sup_{v \in V_N} \frac{1}{\|v\|_{1,S}} \left\{ \left| \left(\int_{\overline{BC \cup CD}} - \int_{\widetilde{BC \cup CD}} \right) \frac{\partial u}{\partial n} v \, d\ell \right| + \left| \left(\int_{\overline{AB}} - \int_{\widetilde{AB}} \right) \frac{\partial v}{\partial n} u \, d\ell \right| \right\}.$$

The proof of Theorem 3.4.2 can be completed by following the analysis in Chapter 8. Note that the additional errors from the integration approximation in (3.4.10) are analogous to those in FEM, but not to the CTM in Section 2.3, where the integration errors are fairly small to guarantee the uniformly V_N elliptic inequality. Since the integration rules are formulated based on k -order polynomials, such as the Gaussian and Newton-Cotes rules in [9], only the polynomial convergence rates can be obtain from (3.4.10).

3.5 Penalty plus Hybrid TMs

The numerical solutions \tilde{u}_N^{HP} may be sought by minimizing the following energy:

$$T_3^*(\tilde{u}_N^{HP}) = \min_{v \in V_N} T_3^*(v), \quad (3.5.1)$$

where

$$T_3^*(v) = \frac{1}{2} \int_{\Gamma_N^*} \frac{\partial v}{\partial n} v \, d\ell - \alpha \int_{\overline{AB}} \frac{\partial v}{\partial n} (v - 500) d\ell + w^2 \int_{\overline{AB}} (v - 500)^2 d\ell, \quad (3.5.2)$$

in which $0 \leq \alpha \leq 1$ and $w \geq 0$. Eqs. (3.5.1) and (3.5.2) are obtained from (3.2.5) and (3.2.7) by choosing $S = S_2$, $S_1 = \Gamma_0 = \emptyset$, $f = q = g_2 = 0$ and $g_1 = 500$.

Below, let us consider how to choose two parameters α and w . First, w^2 should be chosen to balance the first and the second terms on the right-hand side in (3.5.2). For the simple case of $S = S_R$ as in Lemma 3.5.2 below, it is better to choose $w^2 = O(N+1)$, i.e., $w^2 = P_c(N+1)$, where P_c is a constant independent of N . Also we shall find the optimal choice $\alpha = 1$, by means of a priori error estimates given in Theorem 3.5.1.

For simplicity, choose a semi-disk $S_R = \{(r, \theta) \mid r \leq R, 0 \leq \theta \leq \pi\}$, and a semi-circle $l_R = \{(r, \theta) \mid r = R, 0 \leq \theta \leq \pi\}$. We have the following lemma from the orthogonality of $\cos(i + \frac{1}{2})\theta$ on l_R .

Lemma 3.5.1 *There exist the equalities for $v = \sum_{i=0}^N D_i r^{i+\frac{1}{2}} \cos(i + \frac{1}{2})\theta$ with arbitrary D_i ,*

$$\begin{aligned} \int_{l_R} v^2 dl &= \frac{\pi}{2} \sum_{i=0}^N D_i^2 R^{2i+2}, \\ \int_{l_R} v \frac{\partial v}{\partial n} dl &= \frac{\pi}{2} \sum_{i=0}^N D_i^2 (i + \frac{1}{2}) R^{2i+1}, \\ \int_{l_R} (\frac{\partial v}{\partial n})^2 dl &= \frac{\pi}{2} \sum_{i=0}^N D_i^2 (i + \frac{1}{2})^2 R^{2i}, \\ \iint_{S_R} v^2 ds &= \frac{\pi}{2} \sum_{i=0}^N \frac{D_i^2}{2i+3} R^{2i+3}. \end{aligned}$$

Now we prove a lemma.

Lemma 3.5.2 *For $S = S_R$ and there exists the bound for $v \in V_N$*

$$\int_{l_R} v \frac{\partial v}{\partial n} dl \leq \frac{N+1}{R} \int_{l_R} v^2 dl.$$

Proof. From Lemma 3.5.1, we have

$$\begin{aligned} \int_{l_R} v \frac{\partial v}{\partial n} dl &= \frac{\pi}{2} \sum_{i=0}^N D_i^2 (i + \frac{1}{2}) R^{2i+1} \\ &\leq \frac{(N+1)\pi}{R} \sum_{i=0}^N D_i^2 R^{2i+2} = \frac{(N+1)}{R} \int_{l_R} v^2 dl. \quad \blacksquare \end{aligned}$$

Based on Lemmas 3.5.1 and 3.5.2 we may choose the parameter $w^2 = P_c(N+1)$, where P_c is a positive constant but independent of N as shown in Lemma 3.5.3 below. The equation (3.5.1) may be rewritten as: To seek $\tilde{u}_N^{PH} \in V_N$ such that

$$B_3(\tilde{u}_N^{PH}, v) = f_3(v), \quad \forall v \in V_N, \quad (3.5.3)$$

where

$$\begin{aligned} B_3(u, v) &= \int_{\Gamma_N^*} \frac{\partial u}{\partial n} v dl - \alpha \int_{AB} (\frac{\partial u}{\partial n} v + \frac{\partial v}{\partial n} u) dl + P_c(N+1) \int_{AB} uv dl \\ &= \int_{BC \cup CD} \frac{\partial u}{\partial n} v dl + (1-\alpha) \int_{AB} \frac{\partial u}{\partial n} v dl \\ &\quad - \alpha \int_{AB} \frac{\partial v}{\partial n} u dl + P_c(N+1) \int_{AB} uv dl, \end{aligned}$$

and

$$f_3(v) = 500P_c(N+1) \int_{AB} v \, d\ell - 500\alpha \int_{AB} \frac{\partial v}{\partial n} d\ell.$$

Define a norm

$$\|v\|_h = \{ |v|_{1,S}^2 + P_c(N+1) \|v\|_{0,AB}^2 \}^{\frac{1}{2}}. \quad (3.5.4)$$

We have the following lemma.

Lemma 3.5.3 *Suppose that there exists a constant C independent of N such that*

$$\left\| \frac{\partial v}{\partial n} \right\|_{0,AB} \leq C(N+1) \|v\|_{0,AB}, \quad \forall v \in V_N. \quad (3.5.5)$$

Then, when $0 < \alpha \leq 1$ and P_c is chosen to be large enough but independent of N , there exists the uniformly V_N - elliptic inequality,

$$B_3(v, v) \geq \frac{1}{2} \|v\|_h^2, \quad \forall v \in V_N, \quad (3.5.6)$$

and

$$B_3(u, v) \leq C \|u\|_h \|v\|_h,$$

where C is a constant independent of N .

Proof. We have

$$B_3(v, v) = \iint_S |\nabla v|^2 ds - 2\alpha \int_{AB} \frac{\partial v}{\partial n} v \, d\ell + P_c(N+1) \int_{AB} v^2 d\ell.$$

From (3.5.5),

$$\int_{AB} \frac{\partial v}{\partial n} v d\ell \leq \left\| \frac{\partial v}{\partial n} \right\|_{0,AB} \|v\|_{0,AB} \leq C(N+1) \|v\|_{0,AB}^2,$$

where C is a constant independent of N . Then we obtain

$$B_3(v, v) \geq \iint_S |\nabla v|^2 ds + (P_c - 2C\alpha)(N+1) \|v\|_{0,AB}^2.$$

When P_c is chosen large enough to satisfy $P_c - 2C\alpha \geq \frac{P_c}{2}$, i.e., $P_c \geq 4C\alpha$. We then have

$$B_3(v, v) \geq \iint_S |\nabla v|^2 ds + \frac{P_c}{2}(N+1) \|v\|_{0,AB}^2 \geq \frac{1}{2} \|v\|_h^2.$$

This is (3.5.6).

Next, we have similarly,

$$\begin{aligned} B_3(u, v) &= \iint_S \nabla u \cdot \nabla v ds - \alpha \int_{AB} \left(\frac{\partial u}{\partial n} v + \frac{\partial v}{\partial n} u \right) dl + P_c(N+1) \int_{AB} uv dl \\ &\leq \left| \iint_S \nabla u \cdot \nabla v ds \right| + \alpha \left(\left| \int_{AB} \frac{\partial u}{\partial n} v dl \right| + \left| \int_{AB} \frac{\partial v}{\partial n} u dl \right| \right) + P_c(N+1) \left| \int_{AB} uv dl \right|. \end{aligned}$$

Moreover,

$$\left| \int_{AB} \frac{\partial u}{\partial n} v dl \right| \leq \left\| \frac{\partial u}{\partial n} \right\|_{-\frac{1}{2}, \overline{AB}} \|v\|_{\frac{1}{2}, \overline{AB}}, \quad (3.5.7)$$

where the norms

$$\begin{aligned} \|v\|_{\frac{1}{2}, \Gamma} &= \left\{ \|v\|_{0, \Gamma}^2 + \int_{\Gamma} \int_{\Gamma} \frac{(v(P) - v(Q))^2}{\|P - Q\|^2} dl(P) dl(Q) \right\}^{\frac{1}{2}}, \\ \|u\|_{-\frac{1}{2}, \Gamma} &= \frac{\sup_v \left| \int_{\Gamma_0} uv dl \right|}{\|v\|_{\frac{1}{2}, \Gamma}}. \end{aligned}$$

Since the Laplacian solutions have the following bounds,

$$\left\| \frac{\partial u}{\partial n} \right\|_{-\frac{1}{2}, \overline{AB}} \leq \left\| \frac{\partial u}{\partial n} \right\|_{-\frac{1}{2}, \partial S} \leq C \|u\|_{1, S} \leq C_1 |u|_{1, S} \leq C_1 \|u\|_h, \quad (3.5.8)$$

and

$$\|v\|_{\frac{1}{2}, \overline{AB}} \leq C \|v\|_{1, S} \leq C_1 \|v\|_h, \quad (3.5.9)$$

where C_1 and C are also constants independent of N . Combining (3.5.7) – (3.5.9) gives

$$\left| \int_{AB} \frac{\partial u}{\partial n} v dl \right| \leq C \|u\|_h \|v\|_h.$$

Similarly,

$$\left| \int_{AB} \frac{\partial v}{\partial n} u dl \right| \leq C \|u\|_h \|v\|_h.$$

Therefore we obtain from the Schwarz inequality

$$\begin{aligned} B_3(u, v) &\leq \left| \iint_S \nabla u \cdot \nabla v ds \right| + C\alpha \|u\|_h \|v\|_h + P_c(N+1) \left| \int_{AB} uv dl \right| \\ &\leq (1 + C\alpha) \|u\|_h \|v\|_h \leq C \|u\|_h \|v\|_h. \quad \blacksquare \end{aligned}$$

Theorem 3.5.1 *Let the condition (3.5.5) hold. Then there exists the error bound for \tilde{u}_N^{PH}*

$$\|u - \tilde{u}_N^{PH}\|_h \leq C \left\{ \inf_{v \in \mathcal{V}_N} \|u - v\|_h + \frac{|1 - \alpha|}{\sqrt{P_c(N+1)}} \left\| \frac{\partial u}{\partial n} \right\|_{0, \overline{AB}} \right\}. \quad (3.5.10)$$

Proof. For the true solution of Motz's problems satisfying (3.1.1) and (3.1.3), we have from (3.5.3)

$$B_3(u, v) = (1 - \alpha) \int_{AB} \frac{\partial u}{\partial n} v \, dl + f_3(v),$$

and then from (3.5.4)

$$\begin{aligned} B_3(u - \tilde{u}_N^{PH}, v) &= (1 - \alpha) \int_{AB} \frac{\partial u}{\partial n} v \, dl \\ &\leq |1 - \alpha| \left\| \frac{\partial u}{\partial n} \right\|_{0, \overline{AB}} \|v\|_{0, \overline{AB}} \leq C \frac{|1 - \alpha|}{\sqrt{P_c(N + 1)}} \left\| \frac{\partial u}{\partial n} \right\|_{0, \overline{AB}} \|v\|_h. \end{aligned}$$

For $\delta = v - \tilde{u}_N^{PH}$ with $v \in V_N$ and $\delta \in V_N$, we have from Lemma 3.5.3

$$\begin{aligned} \frac{1}{2} \|\delta\|_h^2 &\leq B_3(v - \tilde{u}_N^{PH}, \delta) \\ &= B_3(v - u, \delta) - (1 - \alpha) \left(\int_{AB} \frac{\partial u}{\partial n} \delta \, dl \right) \\ &\leq C \{ \|u - v\|_h \|\delta\|_h + \frac{|1 - \alpha|}{\sqrt{P_c(N + 1)}} \left\| \frac{\partial u}{\partial n} \right\|_{0, \overline{AB}} \|\delta\|_h \}. \end{aligned}$$

Therefore, we have

$$\|\delta\|_h \leq C \{ \|u - v\|_h + \frac{|1 - \alpha|}{\sqrt{P_c(N + 1)}} \left\| \frac{\partial u}{\partial n} \right\|_{0, \overline{AB}} \},$$

and

$$\begin{aligned} \|u - \tilde{u}_N^{PH}\|_h &\leq \|u - v\|_h + \|\delta\|_h \\ &\leq C \{ \|u - v\|_h + \frac{|1 - \alpha|}{\sqrt{P_c(N + 1)}} \left\| \frac{\partial u}{\partial n} \right\|_{0, \overline{AB}} \}. \end{aligned}$$

The desired result (3.5.10) is obtained. ■

Based on Theorem 3.5.1, we should choose $\alpha = 1$, to raise the accuracy of the solutions. In this case, the penalty plus hybrid TM (3.5.3) is reduced to

$$B_3(\tilde{u}_N^{PH}, v) = f_3(v), \quad (3.5.11)$$

where

$$B_3(u, v) = \int_{BC \cup CD} \frac{\partial u}{\partial n} v \, dl - \int_{AB} \frac{\partial v}{\partial n} u \, dl + P_c(N + 1) \int_{AB} uv \, dl,$$

and

$$f_3(v) = 500P_c(N + 1) \int_{AB} v \, dl - 500 \int_{AB} \frac{\partial v}{\partial n} dl,$$

where P_c is large enough but independent of N . For Motz's problem, $P_c = 1$ is a good choice by trial computation.

Theorem 3.5.2 *Let (3.5.5) and the conditions of Corollary 3.1 hold, $\alpha = 1$ and $w^2 = P_c(N + 1)$, where P_c is chosen large enough but independent of N . Then there exists the error bound for \tilde{u}_N^{PH}*

$$\|u - \tilde{u}_N^{PH}\|_h \leq C \inf_{v \in V_N} \|u - v\|_h = C_1 \sqrt{N} a^N,$$

where C_1 is also a constant independent of N .

Remark 3.5.1 *From the analysis in Sections 3.3 – 3.5, the penalty TM is less efficient. Such a conclusion is different from [291], where the penalty combination is quit efficient. Note that when $\alpha < 1$ is chosen in (3.5.4), the same reduced convergence rate as that of the penalty TM in Section 3.3 is obtained, based on Theorem 3.5.1. Both the hybrid TM and the penalty plus hybrid TM with $\alpha = 1$ are efficient for singularity problems.*

3.6 Lagrange Multiplier TM

For Motz's problem, we may regard the Dirichlet condition $u|_{AB} = 500$ as a constraint, to minimize the energy, $\frac{1}{2} \iint_S |\nabla v|^2 ds$. Then define a functional

$$I(v) = \frac{1}{2} \iint_S |\nabla v|^2 ds - \int_{AB} \lambda(v - 500) dl, \quad (3.6.1)$$

with the Lagrange multiplier λ . The critical point of (3.6.1) is given by: To seek $(u, \lambda) \in H_0^1(S) \times H^{-\frac{1}{2}}(\overline{AB})$ such that

$$\begin{aligned} \iint_S \nabla u \cdot \nabla v ds - \int_{AB} \lambda v dl - \int_{AB} \mu(u - 500) dl &= 0, \\ \forall (v, \mu) \in H_0^1(S) \times H^{-\frac{1}{2}}(\overline{AB}), \end{aligned} \quad (3.6.2)$$

where $H_0^1(S)$ is defined in (3.4.1).

Let λ_L be the L -order polynomials on \overline{AB} , which can be expressed as the Chebyshev polynomials,

$$\lambda_L = \sum_{i=0}^L \tilde{A}_i T_i(1 - 2y), \quad 0 \leq y \leq 1, \quad (3.6.3)$$

where \tilde{A}_i are the coefficients to be sought, and the Chybeshev polynomials are defined by

$$T_i(x) = \cos(i \arccos(x)), \quad -1 \leq x \leq 1. \quad (3.6.4)$$

Denote by $V_N \times T_L$ the collection of finite dimensions of (3.1.5) and (3.6.3). The discrete Lagrange multiplier method (i.e., the direct TM) is given by: To seek $(\tilde{u}_N, \lambda_h) \in V_N \times T_L$

such that

$$\begin{aligned} A(\tilde{u}_N, v) + b(\tilde{u}_N, v; \lambda_L, \mu) &= 0, \quad \forall (v, \mu) \in V_N \times T_L, \\ A(u, v) &= \int \int_S \nabla u \cdot \nabla v ds, \\ b(u, v; \lambda, \mu) &= - \int_{AB} \lambda v d\ell - \int_{AB} \mu(u - 500) d\ell. \end{aligned}$$

Below we give a brief justification for Laplace's equation only. In contrast, the analysis of the multiplier methods in Babuska [14] and Li [291] is made for the equation, $-\Delta u + u = 0$.

We obtain a theorem from [291].

Theorem 3.6.1 *Suppose the following three assumptions hold.*

(A1) *For $A(u, v)$, there exist two positive constants C_0 and C independent of N such that,*

$$\begin{aligned} C_0 \|v\|_{1,S}^2 &\leq A(v, v), \quad \forall v \in V_N, \\ |A(u, v)| &\leq C \|u\|_{1,S} \|v\|_{1,S}, \quad \forall v \in V_N. \end{aligned} \tag{3.6.5}$$

(A2) *For $\int_{AB} \mu v d\ell$, there exists the Ladyzhenskaya-Babuska-Brezzi (LBB) condition: $\forall \mu_L \in T_L, \exists v_N \in V_N, v_N \neq 0$ such that*

$$\left| \int_{AB} \mu_h v_N d\ell \right| \geq \beta \|v_N\|_{1,S} \|\mu_L\|_{-\frac{1}{2}, \overline{AB}}, \tag{3.6.6}$$

where $\beta > 0$ is a constant independent of N and L .

(A3) *Also the following bound holds*

$$\left| \int_{AB} \lambda v d\ell \right| \leq C \|\lambda\|_{-\frac{1}{2}, \overline{AB}} \|v\|_{1,S}, \quad \forall v \in V_N.$$

Then there exist the error bounds,

$$\begin{aligned} \|u - \tilde{u}_N^L\|_{1,S} &\leq C \left\{ \inf_{v \in V_N} \|u - v\|_{1,S} + \inf_{\eta \in T_L} \|\lambda - \eta\|_{-\frac{1}{2}, \overline{AB}} \right\}, \\ \|\lambda - \lambda_L\|_{-\frac{1}{2}, \overline{AB}} &\leq C \left\{ \inf_{v \in V_N} \|u - v\|_{1,S} + \inf_{\eta \in T_L} \|\lambda - \eta\|_{-\frac{1}{2}, \overline{AB}} \right\}, \end{aligned}$$

where C is a constant independent of N and L .

Here we only check the condition (3.6.5) and the LBB condition. We have

$$A(v, v) = |v|_{1,S}^2. \tag{3.6.7}$$

Since $v|_{\overline{OD}} = 0$, we obtain from the Poincare-Friedrichs inequality in Ciarlet [105],

$$|v|_{1,S} \geq C_0 \|v\|_{1,S}, \quad \forall v \in H_0^1(S). \tag{3.6.8}$$

Combining (3.6.7) and (3.6.8) gives (3.6.5).

Next, we verify the LBB condition. First we consider an auxiliary problem of Motz's problem, see Figure 3.1,

$$\begin{aligned} \Delta w &= 0, \quad \text{in } S, \\ \frac{\partial w}{\partial n} \Big|_{\overline{AB}} &= \mu_L, \\ w \Big|_{\overline{OD}} &= 0, \quad \frac{\partial w}{\partial n} \Big|_{\overline{OA \cup BC \cup CD}} = 0, \end{aligned} \quad (3.6.9)$$

where $\mu \in T_L$ and $w \in H_0^1(S)$. From (3.6.9) and (3.6.8), we have

$$\int_{\overline{AB}} \mu_L w \, d\ell = \int_{\overline{AB}} w \frac{\partial w}{\partial n} d\ell = \iint_S |\nabla w|^2 ds = |w|_{1,S}^2 \geq C_0 \|w\|_{1,S}^2. \quad (3.6.10)$$

Also since $\Delta w = 0$ in S , there exists the bound,

$$\|\mu_L\|_{-\frac{1}{2}, \overline{AB}} = \left\| \frac{\partial w}{\partial n} \right\|_{-\frac{1}{2}, \overline{AB}} \leq C \|w\|_{1,S}. \quad (3.6.11)$$

Therefore, we obtain from (3.6.10) and (3.6.11)

$$\int_{\overline{AB}} \mu_L w \, d\ell \geq C_0 \|w\|_{1,S}^2 \geq \beta \|w\|_{1,S} \|\mu_L\|_{-\frac{1}{2}, \overline{AB}}, \quad (3.6.12)$$

where β is a constant independent of w and h .

Next, let $w = w_N + r_N$, where $w_N \in V_N$, and r_N is the remainder. Then, we have from (3.6.12)

$$\begin{aligned} \int_{\overline{AB}} \mu_L w_N d\ell &= \int_{\overline{AB}} \mu_L w \, d\ell - \int_{\overline{AB}} \mu_L r_N d\ell \\ &\geq \beta \|w\|_{1,S} \|\mu_L\|_{-\frac{1}{2}, \overline{AB}} - C_1 \|r_N\|_{1,S} \|\mu_L\|_{-\frac{1}{2}, \overline{AB}} \\ &\geq \beta \|w_N\|_{1,S} \|\mu_L\|_{-\frac{1}{2}, \overline{AB}} - (C_1 + \beta) \|r_N\|_{1,S} \|\mu_L\|_{-\frac{1}{2}, \overline{AB}}, \end{aligned} \quad (3.6.13)$$

where we have used the bound

$$\int_{\overline{AB}} \mu_L r_N d\ell \leq \|\mu_L\|_{-\frac{1}{2}, \overline{AB}} \|r_N\|_{\frac{1}{2}, \overline{AB}} \leq C_1 \|\mu_L\|_{-\frac{1}{2}, \overline{AB}} \|r_N\|_{1,S}. \quad (3.6.14)$$

Since $w_N \in V_N$ converges exponentially to $w \in H_0^1(S)$, there exists an integer $N_0 > 0$ such that for $N \geq N_0$

$$\frac{\|r_N\|_{1,S}}{\|w_N\|_{1,S}} \leq \frac{\beta}{2(C_1 + \beta)}, \quad (3.6.15)$$

where C_1 is the positive constant in (3.6.14). Then we obtain from (3.6.13) and (3.6.15)

$$\int_{\overline{AB}} \mu_L w_N d\ell \geq \frac{\beta}{2} \|w_N\|_{1,S} \|\mu_L\|_{-\frac{1}{2}, \overline{AB}}.$$

This is the LBB condition (3.6.6) by letting $v_N = w_N$.

Let $\bar{\lambda}_L$ be the L -order polynomial interpolant of λ . Then we have

$$\begin{aligned} \inf_{\eta \in T_L} \|\lambda - \eta\|_{-\frac{1}{2}, \overline{AB}} &\leq \|\lambda - \bar{\lambda}_L\|_{-\frac{1}{2}, \overline{AB}} \\ &\leq C \|\lambda - \bar{\lambda}_L\|_{0, \overline{AB}} \leq C b^{L+1}, \end{aligned}$$

where $0 < b < 1$. We obtain the following corollary.

Corollary 3.6.1 *Let the conditions of Theorem 3.6.1 and Corollary 3.3.1 hold. Then there exist the bounds*

$$\begin{aligned} \|u - \tilde{u}_N\|_{1,S} &\leq C \{\sqrt{N} a^N + b^{L+1}\}, \\ \|\lambda - \lambda_L\|_{1,S} &\leq C \{\sqrt{N} a^N + b^{L+1}\}. \end{aligned}$$

Corollary 3.6.1 implies an optimal matching between N and L , obtained as:

$$b^{L+1} = O(\sqrt{N} a^N),$$

which leads approximately to

$$L \approx N \left| \frac{\ln a}{\ln b} \right|.$$

Remark 3.6.1 *In Kita and Kamiya [261], the CTM was classified as an indirect TM. Here we briefly give a description of the direct TM [99, 237], which is much closer to that of BEM.*

Rewrite Motz's problem in Section 3.1 as

$$\begin{aligned} \Delta u &= 0 \quad \text{in } S, \\ u &= \bar{u} \quad \text{on } \Gamma_D, \quad \frac{\partial u}{\partial n} = 0 \quad \text{on } \Gamma_N, \end{aligned}$$

where $\Gamma_D = \overline{AB} \cup \overline{OD}$, $\Gamma_N = \overline{BC} \cup \overline{CD} \cup \overline{OA}$, and

$$\bar{u} = \begin{cases} 500 & \text{on } \overline{AB}, \\ 0 & \text{on } \overline{OD}. \end{cases}$$

Applying the penalty plus hybrid TMs with a special case $w = 0$, we obtain

$$\iint_S \nabla u \cdot \nabla v ds - \int_{\Gamma_D} \frac{\partial v}{\partial n} (u - \bar{u}) dl - \int_{\Gamma_D} \frac{\partial u}{\partial n} v dl = 0.$$

Since

$$\iint_S \nabla u \cdot \nabla v ds = \int_{\Gamma_D \cup \Gamma_N} u \frac{\partial v}{\partial n} dl,$$

we have

$$\int_{\Gamma_N} u \frac{\partial v}{\partial n} dl - \int_{\Gamma_D} \frac{\partial u}{\partial n} v dl = - \int_{\Gamma_D} \bar{u} \frac{\partial v}{\partial n} dl. \quad (3.6.16)$$

Denote $q = \frac{\partial u}{\partial n}$, then (3.6.16) becomes

$$\int_{\Gamma_N} u \frac{\partial v}{\partial n} dl - \int_{\Gamma_D} qv dl = -500 \int_{AB} \frac{\partial v}{\partial n} dl. \quad (3.6.17)$$

In (3.6.17) u on Γ_N and q on Γ_D are unknowns, we may follow the approaches in the TM, to seek the nodal approximation.

Denote the values

$$\begin{aligned} q_i &= q(Q_i), \quad Q_i \in \Gamma_D, \\ u_i &= u(Q_i), \quad Q_i \in \Gamma_N, \end{aligned}$$

where h and H are the maximal meshspaces of Q_i on Γ_N and Γ_D , respectively. Let V_h and V_H be the finite dimensional collections of interpolant polynomials of order N and M , based on the nodal values q_i and u_i , respectively. Hence, the direct TM can be written as: To seek $(q_h, u_H) \in (V_h, V_H)$ such that

$$\int_{\Gamma_N} u_H \frac{\partial v}{\partial n} dl - \int_{\Gamma_D} q_h v dl = -500 \int_{AB} \frac{\partial v}{\partial n} dl, \quad \forall v \in V_L, \quad (3.6.18)$$

where V_L is spanned by

$$\phi_i = r^{i+\frac{1}{2}} \cos(i + \frac{1}{2})\theta, \quad i = 0, 1, 2, \dots, L. \quad (3.6.19)$$

Let us recall the BEM, and cite two formulas in Section 0.3.1 for $f \equiv 0$,

$$u(P_0) = \frac{1}{\pi} \int_{\partial S} [\ln(\frac{1}{r}) \frac{\partial u}{\partial n} - u \frac{\partial}{\partial n} (\ln \frac{1}{r})] dl, \quad \forall P_0 \in \partial S, \quad (3.6.20)$$

$$u(P_0) = \frac{1}{2\pi} \int_{\partial S} [\ln(\frac{1}{r}) \frac{\partial u}{\partial n} - u \frac{\partial}{\partial n} (\ln \frac{1}{r})] dl, \quad \forall P_0 \in S, \quad (3.6.21)$$

where $P_0 = (x_0, y_0)$ and $r = \sqrt{(x - x_0)^2 + (y - y_0)^2}$. Denote $w^* = \frac{1}{2\pi} \ln(\frac{1}{r})$, Eqs (3.6.20) – (3.6.21) for Motz's problem lead to

$$\begin{aligned} \int_{\Gamma_N} u \frac{\partial w^*}{\partial n} dl - \int_{\Gamma_D} qw^* dl + 2u(P_0) &= -500 \int_{AB} \frac{\partial w^*}{\partial n} dl, \quad \forall P_0 \in \partial S. \\ u(P_0) &= \int_{\Gamma_D} qw^* dl - 500 \int_{AB} \frac{\partial w^*}{\partial n} dl - \int_{\Gamma_N} u \frac{\partial w^*}{\partial n} dl, \quad \forall P_0 \in S. \end{aligned} \quad (3.6.22)$$

The BEM for (3.6.22) is given by: To seek $(q_h, u_H) \in (V_h, V_H)$ such that

$$\int_{\Gamma_N} u_H \frac{\partial v}{\partial n} dl - \int_{\Gamma_D} q_h v dl + 2u(P_0) = -500 \int_{AB} \frac{\partial v}{\partial n} dl, \quad \forall v \in V_H, \quad (3.6.23)$$

where $u(P_0) = \bar{u}$ when $P_0 \in \Gamma_D$, and $u(P_0) = u_H$ when $P_0 \in \Gamma_N$. An advantage of (3.6.18) and (3.6.23) is to avoid the singular function $w^* = \frac{1}{2\pi} \ln(\frac{1}{r})$ in the integrals.

We can see a great similarity of formulation between (3.6.18) and (3.6.23). Once the solutions q_h on Γ_D and u_H on Γ_N have been obtained from (3.6.18) or (3.6.23), the entire solution in S can be evaluated directly from (3.6.22).

The Motz's solution is given in (3.1.4) with the dominant leading coefficient $d_0 = 401.16245$. Then we have

$$\begin{aligned} \frac{\partial u}{\partial n} \Big|_{\overline{OD}} &= - \frac{1}{r} \frac{\partial u}{\partial \theta} \Big|_{\theta=\pi} = \sum_{i=0}^{\infty} d_i \left(i + \frac{1}{2}\right) r^{i-\frac{1}{2}} \sin\left(i + \frac{1}{2}\right)\theta \Big|_{\theta=\pi} \\ &= \sum_{i=0}^{\infty} (-1)^i d_i \left(i + \frac{1}{2}\right) r^{i-\frac{1}{2}}. \end{aligned}$$

When r is near the origin,

$$\frac{\partial u}{\partial n} \Big|_{\overline{OD}} \approx \frac{1}{2} \frac{d_0}{\sqrt{r}}, \quad \text{as } r \rightarrow 0,$$

similarly,

$$u \Big|_{\overline{OA}} \approx d_0 \sqrt{r}, \quad \text{as } r \rightarrow 0. \quad (3.6.24)$$

Eq (3.6.24) implies that the true value q_i near the origin is infinite so that q_i as unknowns in such a direct TM (or in BEM) is inappropriate. Even if we do so, a refinement of division Q_i near the origin must be done carefully, or the leading singular solutions of (3.6.19) should be added into, see Chapter 7. More techniques of BEM by passing the boundary singularity may be found on some textbooks of BEM. In contrast, the unknown $\lambda (= \frac{\partial u}{\partial n})$ on \overline{AB} in the Lagrange multiplier TM (3.6.2) is smooth enough due to far from the origin, the singularity point.

3.7 Effective Condition Number

In this section, we turn to the study stability by redefining the condition number. The traditional definition of condition number was given in Wilkinson [493], and then used in many books and papers, see Atkinson [9], Golub and Loan [176], and Quarteroni and Valli [392]. For solving the linear algebraic equation $\mathbf{Ax} = \mathbf{b}$ resulting from elliptic equations, the traditional condition number is defined as $\text{Cond.} = \frac{\sigma_1}{\sigma_n}$, where σ_1 and σ_n are the maximal and the minimal singular values of matrix \mathbf{A} respectively. The condition number is used to provide the bounds of the relative errors from the perturbation of both \mathbf{A} and \mathbf{b} . However, in real applications, we only deal with a certain vector \mathbf{b} , and the real relative errors may be smaller, or even much smaller than the worst Cond. Such a case was first studied in Chan and Foulser [83] and subsequently applied to a boundary value problem in Christiansen and Hansen [103], who called it the effective condition number. In this section, we will explore the computational formulas to evaluate the effective condition number, denoted by $\text{Cond.}_{\text{eff}}$. Moreover, we propose a new simplified

effective condition number Cond_E , which is easy to compute, because we only need the eigenvector of the minimal eigenvalue for \mathbf{A} or $\mathbf{A}^T\mathbf{A}$, as additional information.

For smooth solutions of elliptic boundary value problems, the simplified effective condition number Cond_E may be small. For the singular layer solutions, when the finite difference method (FDM) with the local refinements of grids near the singular layers are used, the Cond_E may be large, but it is significantly smaller than the huge $\text{Cond}_.$, defined in Strang and Fix [446]. The rather small Cond_E will benefit the solutions of both smooth and singularity problems. The results are reported in Li et al. [301, 306]. The new Cond_E can be applied to the spectral and Trefftz methods, where the solutions obtained are very accurate, while the traditional $\text{Cond}_.$ is very large. Small effective condition number explains well the high accuracy of these solutions, and strengthens the spectral and Trefftz methods reported in Li et al. [305].

First, let us derive the computational formulas for the effective condition number. Consider the over-determined system

$$\mathbf{F}\mathbf{x} = \mathbf{b}, \quad (3.7.1)$$

where matrix $\mathbf{F} \in R^{m \times n}$ and $m \geq n$. Suppose the rank of \mathbf{F} is n . When there exists a perturbation of \mathbf{F} and \mathbf{b} , we have

$$\mathbf{F}(\mathbf{x} + \Delta\mathbf{x}) = \mathbf{b} + \Delta\mathbf{b}, \quad (3.7.2)$$

$$(\mathbf{F} + \Delta\mathbf{F})(\mathbf{x} + \Delta\mathbf{x}) = \mathbf{b} + \Delta\mathbf{b}. \quad (3.7.3)$$

Let matrix \mathbf{F} be decomposed by the singular value decomposition

$$\mathbf{F} = \mathbf{U}\mathbf{\Sigma}\mathbf{V}^T, \quad (3.7.4)$$

where matrices $\mathbf{U} \in R^{m \times m}$ and $\mathbf{V} \in R^{n \times n}$ are orthogonal, and the matrix $\mathbf{\Sigma} \in R^{n \times m}$ is diagonal matrix with the positive singular values σ_i as

$$\sigma_1 \geq \sigma_2 \geq \dots \geq \sigma_n > 0.$$

The traditional condition number is defined by Golub and Loan [176], p. 223,

$$\text{Cond}_. = \frac{\sigma_1}{\sigma_n}. \quad (3.7.5)$$

First consider (3.7.2). Denote $\mathbf{U} = (\mathbf{u}_1, \dots, \mathbf{u}_m)$, we have the expansions

$$\mathbf{b} = \sum_{i=1}^m \beta_i \mathbf{u}_i, \quad \Delta\mathbf{b} = \sum_{i=1}^m \alpha_i \mathbf{u}_i,$$

where

$$\beta_i = \mathbf{u}_i^T \mathbf{b}, \quad \alpha_i = \mathbf{u}_i^T \Delta\mathbf{b}.$$

Denote the pseudoinverse matrix $\Sigma^+ \in R^{n \times m}$ of Σ to be diagonal with the entries $\frac{1}{\sigma_i}$. Hence the pseudoinverse matrix of \mathbf{F} is given by

$$\mathbf{F}^+ = \mathbf{V}\Sigma^+\mathbf{U}^T,$$

and the least squares solution is expressed by

$$\mathbf{x} = \mathbf{F}^+\mathbf{b} = \mathbf{V}\Sigma^+\mathbf{U}^T\mathbf{b}. \quad (3.7.6)$$

Also from (3.7.1) and (3.7.2)

$$\Delta\mathbf{x} = \mathbf{F}^+\Delta\mathbf{b} = \mathbf{V}\Sigma^+\mathbf{U}^T\Delta\mathbf{b}.$$

Hence, since \mathbf{U} is orthogonal, we obtain

$$\|\mathbf{x}\| = \|\Sigma^+\mathbf{U}^T\mathbf{b}\| = \sqrt{\sum_{i=1}^n \frac{\beta_i^2}{\sigma_i^2}}, \quad (3.7.7)$$

and³

$$\begin{aligned} \|\Delta\mathbf{x}\| &= \|\Sigma^+\mathbf{U}^T\Delta\mathbf{b}\| = \sqrt{\sum_{i=1}^n \frac{\alpha_i^2}{\sigma_i^2}} \\ &\leq \frac{1}{\sigma_n} \sqrt{\sum_{i=1}^n \alpha_i^2} \leq \frac{\|\Delta\mathbf{b}\|}{\sigma_n}. \end{aligned} \quad (3.7.8)$$

Hence we obtain

$$\frac{\|\Delta\mathbf{x}\|}{\|\mathbf{x}\|} \leq \frac{\|\Delta\mathbf{b}\|}{\sigma_n} \times \frac{1}{\sqrt{\sum_{i=1}^n \frac{\beta_i^2}{\sigma_i^2}}} \leq \text{Cond.eff} \times \frac{\|\Delta\mathbf{b}\|}{\|\mathbf{b}\|}, \quad (3.7.9)$$

where

$$\text{Cond.eff} = \frac{\|\mathbf{b}\|}{\sigma_n \|\mathbf{x}\|} = \frac{\|\mathbf{b}\|}{\sigma_n \sqrt{(\frac{\beta_1}{\sigma_1})^2 + \dots + (\frac{\beta_n}{\sigma_n})^2}}. \quad (3.7.10)$$

Note that when vector \mathbf{b} (i.e., \mathbf{x}) is just parallel to the eigenvector \mathbf{u}_1 , i.e.,

$$\beta_2 = \dots = \beta_n = 0, \quad (3.7.11)$$

we have $\|\mathbf{b}\| = |\beta_1|$. Hence, the effective condition number leads to the traditional condition number in (3.7.5). However, the cases in (3.7.11) may not happen for the real vector \mathbf{b} . Hence, the effective condition number may provide a better estimation on the upper

³In practical computation, the worst cases as in (3.7.8) may or may not happen. Then sometimes, $\|\Delta\mathbf{x}\| < \frac{1}{\sigma_n} \|\Delta\mathbf{b}\|$ may give a better numerical stability than Cond.eff defined in (3.7.10) below.

bound of relative errors of \mathbf{x} . Besides, the formula, $\text{Cond_eff} = \frac{\|\mathbf{b}\|}{\sigma_n \|\mathbf{x}\|}$ in (3.7.10), can also be found in Christiansen and Saranen [104] and Banoczi et al. [24].

From (3.7.6),

$$\mathbf{F}\mathbf{x} = \sum_{i=1}^n \beta_i \mathbf{u}_i, \quad \|\mathbf{F}\mathbf{x}\| = \sqrt{\sum_{i=1}^n \beta_i^2}.$$

When $m = n$, we have $\|\mathbf{F}\mathbf{x}\| = \|\mathbf{b}\|$. Since

$$\begin{aligned} \sum_{i=1}^n \frac{\beta_i^2}{\sigma_i^2} &= \sum_{i=1}^{n-1} \frac{\beta_i^2}{\sigma_i^2} + \frac{\beta_n^2}{\sigma_n^2} \\ &\geq \frac{1}{\sigma_1^2} \sum_{i=1}^{n-1} \beta_i^2 + \frac{\beta_n^2}{\sigma_n^2} = \frac{\|\mathbf{F}\mathbf{x}\|^2 - \beta_n^2}{\sigma_1^2} + \frac{\beta_n^2}{\sigma_n^2}, \end{aligned}$$

the simplified effective condition number is obtained from (3.7.10)

$$\text{Cond_E} = \frac{\|\mathbf{b}\|}{\sqrt{\frac{\|\mathbf{F}\mathbf{x}\|^2 - \beta_n^2}{\sigma_1^2} + \beta_n^2}}. \quad (3.7.12)$$

Moreover, when $\beta_n \neq 0$, we have the simplest effective condition number from an upper bound of (3.7.10)

$$\text{Cond_EE} = \frac{\|\mathbf{b}\|}{|\beta_n|}. \quad (3.7.13)$$

Hence we give the definitions of effective condition number.

Definition 3.7.1 Let $\mathbf{F} \in R^{m \times n}$, $m \geq n$ and $\text{rank}(\mathbf{F}) = \text{rank}(\mathbf{F} + \Delta\mathbf{F}) = n$, the relative errors of the solution \mathbf{x} can be bounded by the effective condition number, Cond_eff defined in (3.7.10), and the simplified effective condition number Cond_E defined in (3.7.12). Moreover, when $\beta_n \neq 0$, and the simplest effective condition number is also defined in (3.7.13).

Below we consider the perturbation in (3.7.3), and cite a theorem from Lu et al. [330].

Theorem 3.7.1 Let $\text{rank}(\mathbf{F}) = \text{rank}(\mathbf{F} + \Delta\mathbf{F}) = n$, and $\|\mathbf{F}^+ \|\|\Delta\mathbf{F}\| = \delta \ll 1$. There exist the bounds of the relative errors of \mathbf{x} ,

$$\frac{\|\Delta\mathbf{x}\|}{\|\mathbf{x}\|} \leq \text{Cond_eff} \times \frac{1}{1 - \delta} \left\{ \sqrt{2}\delta + \frac{\|\Delta\mathbf{b}\|}{\|\mathbf{b}\|} \right\}. \quad (3.7.14)$$

When $\Delta\mathbf{F} \equiv 0$, then $\delta = 0$, and Theorem 3.7.1 leads to (3.7.9).

Based on Theorem 3.7.1, Definition 3.7.1 is also valid for (3.7.3). From (3.7.4), we have

$$\mathbf{F}^T \mathbf{F} = (\mathbf{U} \mathbf{\Sigma} \mathbf{V}^T)^T (\mathbf{U} \mathbf{\Sigma} \mathbf{V}^T) = \mathbf{V} \mathbf{\Sigma}^T \mathbf{\Sigma} \mathbf{V}^T = \mathbf{V} \mathbf{D} \mathbf{V}^T,$$

where $\mathbf{D} = \mathbf{\Sigma}^T \mathbf{\Sigma}$ is a diagonal matrix consisting of σ_i^2 . Also from (3.7.4), we have

$$\mathbf{U} \mathbf{\Sigma} = \mathbf{F} \mathbf{V},$$

to give (see Atkinson [9], p. 478)

$$\mathbf{u}_i = \frac{1}{\sigma_i} \mathbf{F} \mathbf{v}_i, \quad i = 1, 2, \dots, n. \quad (3.7.15)$$

Hence we may first use the power method and the inverse power method (or DEVESF of IMSL subroutines) for matrix $\mathbf{F}^T \mathbf{F}$ to obtain the two eigenpairs $(\sigma_1^2, \mathbf{v}_1)$ and $(\sigma_n^2, \mathbf{v}_n)$, respectively, and then to obtain vectors \mathbf{u}_1 and \mathbf{u}_n from (3.7.15). Hence our definition Cond.E in (3.7.12) is easily applied in practical application, since $\|\mathbf{b}\|$, $\|\mathbf{F}\mathbf{x}\|$ and β_n can be easily computed.

3.8 Numerical Experiments

In this section, we carry out the numerical experiments for Motz's problem. The particular solutions (3.1.5) are chosen, and the hybrid TM (3.4.5), the penalty plus hybrid TM (3.5.11), and the CTM are used, where $P_c = 1$ is selected by trial computation.

For the penalty plus hybrid TM (3.5.11), we obtain the linear algebraic equations,

$$\mathbf{A}_3 \mathbf{x} = \mathbf{b}, \quad (3.8.1)$$

where the unknown \mathbf{x} consists of the leading coefficients \tilde{D}_i , and matrix \mathbf{A}_3 is symmetric, and positive definite if P_c is chosen to be suitably large, based on Lemma 3.5.3. The condition number is defined by

$$\text{Cond.} = \text{Cond}(\mathbf{A}_3) = \frac{\lambda_{\max}(\mathbf{A}_3)}{\lambda_{\min}(\mathbf{A}_3)}, \quad (3.8.2)$$

where $\lambda_{\max}(\mathbf{A}_3)$ and $\lambda_{\min}(\mathbf{A}_3)$ are the maximal and minimal eigenvalues of \mathbf{A}_3 .

For the hybrid TM, the algebraic equations from (3.4.5) is given by

$$\mathbf{A}_2 \mathbf{x} = \mathbf{b}, \quad (3.8.3)$$

where \mathbf{A}_2 is positive definite but non-symmetric. Then the condition number is given by

$$\text{Cond.} = \text{Cond}(\mathbf{A}_2) = \frac{\sqrt{\max_i \lambda_i(\mathbf{A}_2^T \mathbf{A}_2)}}{\sqrt{\min_i \lambda_i(\mathbf{A}_2^T \mathbf{A}_2)}}. \quad (3.8.4)$$

As for the CTM, the algorithms are described in the previous chapter. The division number of \overline{AB} is denoted by M , and $h = \frac{1}{M}$. From the boundary conditions, (3.1.2) and

(3.1.3), we establish the linear algebraic equations

$$\mathbf{F}\mathbf{x} = \mathbf{b}, \quad (3.8.5)$$

where \mathbf{x} consists of $N + 1$ coefficients $\tilde{D}_i (= D_i)$, and \mathbf{F} is the $4M \times (N + 1)$ matrix. Since we choose $4M \gg (N + 1)$, the least squares method is used to obtain the solution \mathbf{x} , e.g., \tilde{D}_i . Also the condition number is

$$\text{Cond.} = \left\{ \frac{\lambda_{\max}(\mathbf{F}^T \mathbf{F})}{\lambda_{\min}(\mathbf{F}^T \mathbf{F})} \right\}^{\frac{1}{2}}. \quad (3.8.6)$$

For the direct TM, the algebraic equations from (3.6.2) is given by

$$\mathbf{A}_3 \mathbf{y} = \mathbf{b}_3, \quad (3.8.7)$$

where \mathbf{y} is the unknown vector consisting of \tilde{D}_i and \tilde{A}_i in (3.6.3), \mathbf{b}_3 is a known vector, and \mathbf{A}_3 is non-singular but symmetric. Then the condition number is given by

$$\text{Cond.} = \text{Cond}(\mathbf{A}_3) = \frac{\max_i |\lambda_i(\mathbf{A}_3)|}{\min_i |\lambda_i(\mathbf{A}_3)|}, \quad (3.8.8)$$

Note that the condition number (3.8.6) with the square root by the collocation TM is much smaller than that by the other three TMs.

Denote the error $\varepsilon = u - \tilde{u}$ in the Sobolev norms:

$$|\varepsilon|_{0,S} = \left\{ \iint_S (u - \tilde{u})^2 ds \right\}^{\frac{1}{2}}, \quad (3.8.9)$$

$$|\varepsilon|_{1,S} = \left\{ \iint_S (|\nabla(u - \tilde{u})|^2 ds) \right\}^{\frac{1}{2}} = \left\{ \int_{\Gamma_N^*} (u - \tilde{u}) \frac{\partial(u - \tilde{u})}{\partial n} d\ell \right\}^{\frac{1}{2}}, \quad (3.8.10)$$

where $\Gamma^* = \overline{AB} \cup \overline{BC} \cup \overline{CD}$, and \tilde{u} is the approximate solutions by the CTM, the hybrid TM, or the penalty plus hybrid TM, and u is the solutions with more accurate coefficients d_i given in Li and Lu [309]. On ∂S , denote the maximal boundary errors,

$$|\varepsilon|_{\infty, \overline{AB}} = \max_{\overline{AB}} |\varepsilon|, \quad (3.8.11)$$

$$\left| \frac{\partial \varepsilon}{\partial n} \right|_{\infty, \overline{BC}} = \max_{\overline{BC}} \left| \frac{\partial \varepsilon}{\partial n} \right|, \quad (3.8.12)$$

$$\left| \frac{\partial \varepsilon}{\partial n} \right|_{\infty, \overline{CD}} = \max_{\overline{CD}} \left| \frac{\partial \varepsilon}{\partial n} \right|. \quad (3.8.13)$$

The more accurate coefficients D_i can be obtained by the CTM using Mathematica with unlimited significant digits, or by the conformal transformation method using Mathematica. The conformal transformation method was proposed by Whiteman and Papamichael [489], and the series solution in Rosser and Papamichael [412] provided the

most accurate coefficients of $D_0 - D_{19}$ under double precision. The coefficients $D_0 - D_{199}$ are obtained by the conformal transformation method using Mathematica with 200 working digits, and listed in [309], where D_0 and D_{99} have 199 and 89 significant decimal digits, respectively.

The solutions for Motz's problem are obtained from four TMs: (1) the hybrid TM, (2) the penalty plus hybrid TM, (3) the collocation TM (CTM), (4) the direct TM (i.e., the Lagrange multiplier TM). For the collocation TM, we choose Gaussian rule with high order. For the integral $\int_{-1}^1 f(x)dx$, the errors by the Gaussian rule with n nodes are found in Atkinson [9]

$$E_n^*(f) = \frac{2^{2n+1}(n!)^4}{(n+1)[(2n)!]^3} f^{(2n)}(\eta), \quad (3.8.14)$$

where $\eta \in (-1, 1)$. When $N = 34$, the Gaussian rule of six nodes is used, i.e., $n = 6$. Then we have

$$E_n^*(f) \approx 2 \times 10^{-11} f^{(12)}(\eta). \quad (3.8.15)$$

The error norms and condition numbers are listed in Table 3.1 for the first three TMs. From Table 3.1, we can see the exponential rates for the hybrid TM,

$$\begin{aligned} |u - \tilde{u}|_{\infty, \overline{AB}} &\rightarrow 3.5 \times 0.55^N, \\ |\epsilon|_{0,S} &\rightarrow 4.9 \times 0.57^N, \\ |\epsilon|_{1,S} &\rightarrow 3.5 \times 0.59^N, \\ \text{Cond.} &\rightarrow 0.7 \times 1.99^N. \end{aligned} \quad (3.8.16)$$

For the penalty plus hybrid TM,

$$\begin{aligned} |u - \tilde{u}|_{\infty, \overline{AB}} &\rightarrow 6.7 \times 0.54^N, \\ |\epsilon|_{0,S} &\rightarrow 5.8 \times 0.56^N, \\ |\epsilon|_{1,S} &\rightarrow 5.1 \times 0.61^N, \\ \text{Cond.} &\rightarrow 1.1 \times 1.99^N, \end{aligned} \quad (3.8.17)$$

and for the CTM,

$$\begin{aligned} |u - \tilde{u}|_{\infty, \overline{AB}} &\rightarrow 2.8 \times 0.55^N, \\ |\epsilon|_{0,S} &\rightarrow 5.0 \times 0.57^N, \\ |\epsilon|_{1,S} &\rightarrow 19.5 \times 0.58^N, \\ \text{Cond.} &\rightarrow 5.7 \times 1.41^N. \end{aligned} \quad (3.8.18)$$

Let us draw a few conclusions from (3.8.16) – (3.8.18) and Table 3.1.

(a) Global errors. For the error norms, the three TMs give almost the same magnitude, although the CTM yields slightly better accuracy. For $N = 34$, the error norms of the hybrid TM, the penalty plus hybrid TM and the CTM are given by

$$\begin{aligned} |\epsilon|_{0,S} &= 0.286(-7), & |\epsilon|_{1,S} &= 0.210(-6), & |u - \tilde{u}|_{\infty, \overline{AB}} &= 0.196(-7), \\ |\epsilon|_{0,S} &= 0.177(-7), & |\epsilon|_{1,S} &= 0.302(-6), & |u - \tilde{u}|_{\infty, \overline{AB}} &= 0.141(-7), \\ |\epsilon|_{0,S} &= 0.248(-7), & |\epsilon|_{1,S} &= 0.175(-6), & |u - \tilde{u}|_{\infty, \overline{AB}} &= 0.596(-8), \end{aligned}$$

respectively. Hence the CTM is still the best for the global errors in H^1 norms.

(b) Leading coefficients. We are interested in the accuracy of the leading coefficients. For the three TMs, the leading coefficients \tilde{D}_i with $i \leq 34$ are listed in Tables 3.2, 3.3, and 2.5 in the previous chapter. For the direct TM, the approximate solutions are obtained from (3.6.2), and the errors, condition numbers and the leading coefficients are listed in Tables 3.8 and 3.5, where $\Delta D_i = d_i - D_i$. Note that the computed results from the direct TM are better than those in [169]. To provide a clear view of comparisons, the number of significant digits of D_i from all TMs are provided in Table 3.6. From Table 3.6 we can see that the leading coefficients $\tilde{D}_0 - \tilde{D}_2$ by the CTM are more accurate than those in [316]; the \tilde{D}_0 by the CTM at $N = 34$ has 17 significant digits.

(c) Stability. For $N = 34$, Cond. of the collocation TM, hybrid TM, penalty plus hybrid TM, and the direct TM are

$$\text{Cond.} = 0.679(6), \quad 0.118(11), \quad 0.159(11), \quad 0.207(16), \quad (3.8.19)$$

respectively. Hence, the Cond. of the CTM is significantly smaller than that of the other TMs.

(d) Effective condition number. It is a puzzle that the Cond. is large, but the solutions and D_0 are extremely accurate. Such a puzzle can be clarified by the effective condition number given in Section 3.6. Let us evaluate the Cond_eff for the solution given in Table 2.5 in Chapter 2. The singular values σ_i of \mathbf{F} and the coefficients β_i are listed in Table 3.7. Since the computed values of Cond_E and Cond_EE are the same in three significant digits, we only provide the Cond_EE in Tables 3.1 and 3.8. Based on Table 3.7, we obtain the effective condition numbers, the traditional condition number, and their ratios,

$$\begin{aligned} \text{Cond_eff} &= 30.2, & \text{Cond_EE} &= 65.7, & \text{Cond.} &= 0.679(6), & (3.8.20) \\ \frac{\text{Cond.}}{\text{Cond_eff}} &= 0.225(5), & \frac{\text{Cond.}}{\text{Cond_EE}} &= 0.103(5). \end{aligned}$$

The fact that the effective condition number is about 30 may explain very well the high accuracy of \tilde{D}_0 with 17 significant digits. In general, the leading coefficient D_0 obtained should have 16 significant digits, and occasionally due to the cancellation of rounding errors, D_0 has 17 significant digits, as shown in Chapter 2. A recent study in Li et al. [305] on the effective condition number shows that for Motz's problem by the collocation

TM, there exist the bounds,

$$\text{Cond_eff} \leq CN, \quad \text{Cond.} \leq CN^{\frac{3}{2}}(\sqrt{2})^N,$$

where C is a constant independent of N .

For the solution in Table 3.5 by the direct TM, the singular values and the expansion coefficients from the direct TM are listed in Table 3.8, which show

$$\begin{aligned} \text{Cond_eff} &= 0.766(5), \quad \text{Cond_EE} = 0.794(6), \quad \text{Cond.} = 0.207(16), \quad (3.8.21) \\ \frac{\text{Cond.}}{\text{Cond_eff}} &= 0.270(10), \quad \frac{\text{Cond.}}{\text{Cond_EE}} = 0.260(9). \end{aligned}$$

For the optimal solutions at $N = 34$, the Cond_eff of the hybrid TM, penalty plus hybrid TM, the direct TM and the CTM are given by

$$\text{Cond_eff} = 0.107(6), \quad 0.174(6), \quad 0.766(5), \quad 30.2, \quad (3.8.22)$$

respectively. The effective condition number of the collocation TM is also significantly smaller than that of the other TMs. Interestingly, Cond_eff of the direct TM is not the largest, although its Cond. is, indeed, huge. A new stability analysis of the penalty plus hybrid and the direct TMs is made in [307], based on effective condition number.

(e) Complexity of the algorithms. Let us compare the number of nodes used in the Gaussian rule of six nodes. For the best leading coefficients in Tables 3.2, 3.3, 3.5 and Table 2.5 in Chapter 2,

$$N_p = 7680, 1920, 7680 \text{ and } 30$$

by the original TM, the penalty plus hybrid TM, the direct TM and the CTM, respectively. Note that $N_p = 30$ by the collocation TM is significant smaller than that by the other TMs. Hence, the collocation TM needs the less CPU time. The small number N_p is sufficient by the collocation TM, based on the analysis in Section 2.3 of Chapter 2, and the large N_p needed by the other TMs based on the analysis in Theorem 3.4.2. The algorithms of the CTM are simple; the algorithms of the Lagrange multiplier TM are the most complicated, because extra Lagrange multipliers as unknowns are needed, also see [169, 291].

In summary, in this chapter we explore three new efficient TMs: (1) the hybrid TM, (2) the penalty plus hybrid TM, (3) the direct TM, beyond the CTM in the Chapter 2. The drawback of the those three TMs is the worse stability; details are reported in [305, 307]. Based on the theoretical analysis in Sections 3.2 – 3.6 and the numerical experiments in this section, we can conclude that the hybrid TM, the penalty plus hybrid TM, and the Lagrange multiplier TM in [169] are all efficient, but the CTM is the best. They all form a family of GTMs, accompanied by the CTM described in Chapters 1 and 2. The TM and GTMs are highly efficient for singularity problems, to compete with the BEM, see Brebbia [60], Brebbia and Dominguez [64] and Lefeber [281]. Details of comparisons for the TMs are made in Li, et al. [312].

(a) the Hybrid TM

N	$ \frac{\partial \epsilon}{\partial n} _{\infty, \overline{BC}}$	$ \frac{\partial \epsilon}{\partial n} _{\infty, \overline{CD}}$	$ \epsilon _{\infty, \overline{AB}}$	$ \epsilon _{0,S}$	$ \epsilon _{1,S}$	Cond.	Cond_eff	Cond_EE
10	.400	.551	.397(-1)	.176(-1)	.759 (-1)	.753(3)	26.1	54.9
18	.524(-2)	.675(-2)	.258(-3)	.280(-3)	.844 (-3)	.184(6)	41.7	88.2
26	.719(-4)	.850(-4)	.222(-5)	.759(-5)	.125 (-4)	.464(8)	0.668(4)	0.141(5)
34	.883(-7)	.110(-6)	.196(-7)	.286(-7)	.210 (-6)	.118(11)	0.107(6)	0.226(6)

(b) the Penalty plus Hybrid TM

N	$ \frac{\partial \epsilon}{\partial n} _{\infty, \overline{BC}}$	$ \frac{\partial \epsilon}{\partial n} _{\infty, \overline{CD}}$	$ \epsilon _{\infty, \overline{AB}}$	$ \epsilon _{0,S}$	$ \epsilon _{1,S}$	Cond.	Cond_eff	Cond_EE
10	.461	.512	.143(-1)	.175(-1)	.361 (-1)	.104(4)	55.9	113
18	.605(-2)	.604(-2)	.120(-3)	.281 (-3)	.680 (-3)	.251(6)	739	0.148(4)
26	.815(-4)	.749(-4)	.123(-5)	.760 (-5)	.139 (-4)	.628(8)	0.122(5)	0.225(5)
34	.101(-5)	.944(-6)	.141(-7)	.177 (-7)*	.302 (-6)	.159(11)	0.174(6)	0.350(6)

(c) the collocation TM

N	$ \frac{\partial \epsilon}{\partial n} _{\infty, \overline{BC}}$	$ \frac{\partial \epsilon}{\partial n} _{\infty, \overline{CD}}$	$ \epsilon _{\infty, \overline{AB}}$	$ \epsilon _{0,S}$	$ \epsilon _{1,S}$	Cond.	Cond_eff	Cond_EE
10	.327	.296	.795(-2)	.216 (-1)	.936 (-1)	.955(2)	9.49	20.1
18	.328(-2)	.313(-2)	.658(-4)	.288 (-3)	.901 (-3)	.194(4)	16.4	35.6
26	.354(-4)	.366(-4)	.606(-6)	.761 (-5)	.114 (-4)	.374(5)	23.3	50.6
34	.387(-7)*	.445(-7)*	.596(-8)*	.248 (-7)	.175 (-6)*	.679(6) ‡	30.2‡	65.7‡

Table 3.1: The error norms and condition number for the three TMs, where $\epsilon = u - \tilde{u}$, the notation “*” denote the best results among three TMs, and “‡” the significantly better results.

i	\tilde{D}_i	i	\tilde{D}_i
0	401.162453745234473	18	0.115344586856346693(-4)
1	87.6559201950887967	19	-0.529383971600533853(-5)
2	17.2379150794466867	20	0.228968761170685612(-5)
3	-8.07121525969837172	21	0.106205437418978731(-5)
4	1.44027271702274806	22	0.530320399159913592(-6)
5	0.331054885921165332	23	-0.245482974272211971(-6)
6	0.275437344505324755	24	0.108586534173810375(-6)
7	-0.869329945145347338(-1)	25	0.508331075194888274(-7)
8	0.336048784037753304(-1)	26	0.251983941425914834(-7)
9	0.153843744469560912(-1)	27	-0.111713658279571516(-7)
10	0.730230161573248299(-2)	28	0.491399829190115203(-8)
11	-0.318411372759456763(-2)	29	0.227273234326509358(-8)
12	0.122064585795459064(-2)	30	0.110225587000263238(-8)
13	0.530965198451518235(-3)	31	-0.359491309519960114(-9)
14	0.271511850528096896(-3)	32	0.150623016997166540(-9)
15	-0.120045446953650001(-3)	33	0.665868344071349056(-10)
16	0.505388900096920195(-4)	34	0.307774180131843268(-10)
17	0.231659833363871765(-4)		

Table 3.2: The computed coefficients by the hybrid TM (i.e., the original TM) for Motz's problem at $N = 34$ by the Gaussian rule of six nodes with $M = 7680$ along \overline{AB} , where Cond. = 0.159(11) and Cond.eff = 0.226(6).

i	\tilde{D}_i	i	\tilde{D}_i
0	401.162453745235780	18	0.115349881701277696(-4)
1	87.6559201950809808	19	-0.529376122315752069(-5)
2	17.2379150794570393	20	0.229002261909030397(-5)
3	-8.07121525969756881	21	0.106257700723052036(-5)
4	1.44027271701435344	22	0.530877129212484370(-6)
5	0.331054885918999064	23	-0.245424903141403556(-6)
6	0.275437344510011672	24	0.108802035839763755(-6)
7	-0.869329945079974908(-1)	25	0.511393128467733109(-7)
8	0.336048784089699043(-1)	26	0.254875722596865296(-7)
9	0.153843744676367914(-1)	27	-0.111517612609778815(-7)
10	0.730230165812159951(-2)	28	0.497789230128346209(-8)
11	-0.318411371069231850(-2)	29	0.235669761775463569(-8)
12	0.122064593191541443(-2)	30	0.117383353377804351(-8)
13	0.530965354174686320(-3)	31	-0.357052180887959222(-9)
14	0.271512086017575616(-3)	32	0.157652196649668681(-9)
15	-0.120045395993149926(-3)	33	0.752044900590329238(-10)
16	0.505391338611362311(-4)	34	0.374844370146114913(-10)
17	0.231664115217506241(-4)		

Table 3.3: The computed coefficients by penalty plus hybrid TM for Motz’s problem at $N = 34$ by the Gaussian rule of six nodes with $M = 1920$ along \overline{AB} , where Cond.= 0.174(11) and Cond_eff = 0.350(6).

N	L	$ \varepsilon _{\infty, \overline{AB}}$	$ \lambda - \lambda_L _{\infty, \overline{AB}}$	$ \lambda - \lambda_L _{0, \overline{AB}}$	$ \frac{\partial \varepsilon}{\partial n} _{\infty, \overline{BC}}$	$ \frac{\partial \varepsilon}{\partial n} _{\infty, \overline{CD}}$
10	4	0.166(-1)	0.292	0.135	0.413	0.535
18	5	0.163(-3)	0.103	0.160(-1)	0.789(-2)	0.582(-2)
26	7	0.158(-5)	0.944(-2)	0.112(-2)	0.121(-3)	0.536(-4)
34	9	0.600(-8)	0.168(-3)	0.158(-4)	0.322(-5)	0.211(-5)
40	10	0.200(-7)	0.975(-4)	0.131(-4)	0.591(-5)	0.488(-5)

N	L	$ \varepsilon _{0, S}$	$ \varepsilon _{1, S}$	$ \frac{\Delta D_0}{D_0} $	Cond.	Cond_eff	Cond.EE
10	4	0.706(-2)	0.175	0.266(-6)	0.650(6)	0.375(3)	0.647(4)
18	5	0.292(-4)	0.493(-2)	0.356(-10)	0.850(9)	0.201(4)	0.235(5)
26	7	0.197(-6)	0.184(-3)	0.467(-12)	0.128(13)	0.121(8)	0.126(6)
34	9	0.463(-8)	0.785(-5)	0.471(-12)	0.207(16)	0.766(5)	0.794(6)
40	10	0.497(-8)	0.693(-6)	0.471(-12)	0.759(17)	0.442(5)	0.428(6)

Table 3.4: The error norms, condition number and errors of leading coefficients from the direct TM for Motz’s problem by the Gaussian rule of six nodes rule as $M = 240$, where $|\lambda|_{\infty, \overline{AB}} = 357$.

i	\tilde{D}_i	i	\tilde{D}_i	i	\tilde{A}_i
0	401.162453745234473	18	0.115357376458830408(-4)	0	340.470847534819598
1	87.6559201950883988	19	-0.529403268205044528(-5)	1	18.1576584805583181
2	17.2379150794469602	20	0.228968049742712711(-5)	2	0.490581518606606148
3	-8.07121525969850850	21	0.106253353627942843(-5)	3	-2.19556646178029169
4	1.44027271702260307	22	0.531674010537534927(-6)	4	-0.152479090907213927
5	0.331054885920439745	23	-0.245588935639265154(-6)	5	0.638314780462041764(-1)
6	0.275437344511575033	24	0.108599572158342144(-6)	6	0.143070661282430310(-1)
7	-0.869329945182076569(-1)	25	0.511072049985628876(-7)	7	0.298153855980607253(-3)
8	0.336048784013096499(-1)	26	0.258961666286623336(-7)	8	-0.609121543712076350(-3)
9	0.153843744655217714(-1)	27	-0.111973290170299084(-7)	9	-0.118299765484016262(-3)
10	0.730230171201515840(-2)	28	0.492162098344059451(-8)		
11	-0.318411377642627540(-2)	29	0.234519394304798108(-8)		
12	0.122064583787855107(-2)	30	0.127222786035216330(-8)		
13	0.530965339810580820(-3)	31	-0.361778166440610682(-9)		
14	0.271512403959266711(-3)	32	0.151771358294162104(-9)		
15	-0.120045603702773163(-3)	33	0.737166229537951134(-10)		
16	0.505388574434537121(-4)	34	0.463940700433669773(-10)		
17	0.231663774629916405(-4)				

Table 3.5: The computed coefficients by the direct TM for Motz's problem at $N = 34$ and $L = 9$ by the Gaussian rule of six nodes with $M = 7680$ along AB , where $\text{Cond.} = 0.207(16)$ and $\text{Cond.eff} = 0.765(5)$.

i	Original TM	P-H TM	Direct TM	[169]	Collocation TM
0	16	15	16	13	17
1	13	13	14	12	15
2	14	12	14	12	15
3	13	13	13	11	12
4	13	11	13	11	12
5	12	11	12	10	12
6	11	11	10	10	11
7	9	9	9	9	9
8	9	9	9	9	9
9	9	9	8	9	9
10	8	8	7	8	7
11	7	7	7	8	7
12	7	7	6	8	7
13	6	6	6	7	6
14	6	6	6	7	6
15	5	5	6	6	5
16	5	5	5	5	4
17	5	5	4	5	4
18	4	5	4	5	5

Table 3.6: The number of significant decimal digits of leading coefficients for the three BAMs at $N = 34$, as well as those in Georgiou et al. [169] at $N = 74$, and $N_\lambda = 33$, where N_λ is the number of the Lagrange multiplier used.

i	σ_i	β_i	i	σ_i	β_i
0	.158(5)	.420(2)	18	.156(1)	-.375(2)
1	.121(5)	.610(2)	19	.126(1)	-.602(1)
2	.846(4)	.133(2)	20	.113(1)	-.101(3)
3	.595(4)	.274(1)	21	.974	.130(2)
4	.558(3)	.584(2)	22	.827	-.117(3)
5	.386(3)	.246(2)	23	.720	.144(3)
6	.269(3)	.278(1)	24	.677	-.747(2)
7	.195(3)	-.177(2)	25	.560	.295(2)
8	.513(2)	-.591(2)	26	.463	.243(2)
9	.345(2)	-.544(1)	27	.368	-.180(2)
10	.249(2)	.146(2)	28	.305	-.136(2)
11	.189(2)	-.320(2)	29	.249	.134(2)
12	.931(1)	-.554(2)	30	.188	-.120(2)
13	.619(1)	.231(2)	31	.141	-.898(1)
14	.470(1)	-.421(2)	32	.102	-.908(1)
15	.381(1)	-.416(2)	33	.556(-1)	.815(1)
16	.267(1)	-.306(2)	34	.233(-1)	-.440(1)
17	.202(1)	.777(2)			

Table 3.7: The singular values σ_i and the coefficients β_i for the solution in Table 2.5 with the matrix resulting from the collation TM for Motz's problem at $N = 34$ by the Gaussian rule of six nodes with $M = 30$ along \overline{AB} , where the Cond. = 0.679(6) and Cond_eff=30.2.

i	σ_i	β_i	i	σ_i	β_i
0	.267(11)	.463(-4)	23	.645(2)	.156(1)
1	.134(11)	-.130(-3)	24	.464(2)	-.349(1)
2	.668(10)	-.169(-3)	25	.378(2)	.782(1)
3	.335(10)	.724(-4)	26	.308(2)	-.806(1)
4	.326(8)	.171(-2)	27	.250(2)	-.258(1)
5	.174(8)	.454(-2)	28	.200(2)	-.804(1)
6	.933(7)	.566(-2)	29	.158(2)	-.200(2)
7	.502(7)	-.221(-2)	30	.120(2)	-.255(2)
8	.272(6)	.215(-1)	31	.857(1)	-.158(2)
9	.158(6)	.550(-1)	32	.553(1)	-.266(2)
10	.920(5)	-.659(-1)	33	.314(1)	-.139(3)
11	.540(5)	.244(-1)	34	.141(1)	.243(3)
12	.874(4)	-.154	35	.913	.446(3)
13	.556(4)	.372	36	.166	.597(1)
14	.357(4)	.428	37	.933(-1)	.593(1)
15	.231(4)	-.152	38	.619(-1)	.486
16	.774(3)	.638	39	.455(-1)	.207(1)
17	.539(3)	.151(1)	40	.334(-1)	-.583
18	.379(3)	.168(1)	41	.212(-1)	-.950
19	.269(3)	.587	42	.125(-1)	-.768(-1)
20	.144(3)	.184(1)	43	.235(-2)	.124
21	.109(3)	.416(1)	44	.129(-4)	.666(-3)
22	.832(2)	.441(1)	/	/	/

Table 3.8: The singular values σ_i and the expansion coefficients β_i for the matrix resulting from Table 3.5 by the direct TM for Motz's problem at $N = 34$ by the Gaussian rule of six nodes with $M = 30$ along \overline{AB} , where the Cond. = 0.207(16) and Cond_eff=0.766(5).

Chapter 4

Biharmonic Equations with Crack Singularities

In this chapter, we give an extension of the collocation Trefftz method (CTM or collocation TM) in Chapter 2 for the biharmonic equations with crack singularities. First, this chapter derives the Green formulas for biharmonic equations on bounded domains with a non-smooth boundary, and corner terms are developed. The Green formulas are important to provide all the exterior and interior boundary conditions, which will be used in the collocation TM. Second, this chapter proposes three crack models (called Models I, II and III), and the collocation TM provides their most accurate solutions. In fact, Models I and II resemble Motz's problem in Chapter 2, and Model III with all the clamped boundary conditions originated from Schiff et al. [423]. Moreover, a brief analysis of error bounds for the collocation TM is made. Since the accuracy of the solutions obtained in this chapter is very high, they can be used as the typical models in testing numerical methods. The computed results show that as the singularity models, Models I and II are superior to Model III, because more accurate solutions can be obtained by the collocation TM.

4.1 Introduction

When an interior crack occurs within a thin elastic plate, determination of a stress intensity factor at the crack front is significant in fracture mechanics. Such a mechanical problem can be described as the biharmonic equations with the crack singularity, and the stress intensity factor is given by $K = \sqrt{2\pi}d_1$, where d_1 is the leading coefficient of singular particular solutions.

The singular problems have drawn much attention in the last several decades, and reported in many papers. Most of them deal with the second order partial differential equations (PDEs); there exist a few books and papers for the fourth order PDEs. Examples of textbooks and papers for biharmonic equations by the FEM, FDM and the boundary element method include Chien [101], Oden and Carey [78], Birkhoff and Lynch [47], Arad et al. [4] and Brebbia and Dominguez [64]. In this chapter, we pursue better crack models with series expansion solutions of very high convergent rates. Three crack

models are investigated: Models I and II are mimic Motz's problem in Chapter 2, and Model III results from Schiff et al. [423]. The TM and collocation TM introduced in Chapter 2 were studied in Li et al. [316, 314, 315, 291], as the boundary approximation method. It is noted that Li et al. [316, 291] using the central rule provides the highly accurate solutions for Motz's problem in double precision, with the 35 leading expansion coefficients on the entire solution domain, although a typo-error of one coefficient was pointed out by Lucas and Oh in [332]. In Chapter 2, by means of central and Gaussian rules, more accurate leading coefficient has been also obtained from the collocation TM. More detailed discussions about the model of Schiff et al. are provided by Hsu [213]. In this chapter, the collocation TM is developed to compute very accurate solutions for the crack models of biharmonic equations.

This chapter is organized as follows. In the next section, we derive the Green formulas for rectangular and polygonal domains, and provide different types of boundary conditions. In Section 4.3, three crack models are developed, and the collocation TM is described. In Section 4.4, a brief analysis for the collocation TM is made, and the collocation TM is applied to the interior boundary. In Section 4.5, numerical experiments are carried out to provide very accurate solutions for three models, and in the last section concluding remarks are made.

4.2 The Green Formulas of $\Delta^2 u$

4.2.1 On Rectangular Domains

First, consider the rectangular domain $S = \{(x, y) \mid 0 < x < a, 0 < y < b\}$. We will derive the following Green formulas for $\Delta^2 u$,

$$\begin{aligned} \iint_S \Lambda_\mu(u, v) &= \iint_S v \Delta^2 u - \int_{\partial S} m(u) v_n \\ &\quad - \int_{\partial S} p(u) v + 2(1 - \mu)([u_{xy}v]_3^4 - [u_{xy}v]_1^2), \end{aligned} \quad (4.2.1)$$

where $\Delta u = \frac{\partial^2 u}{\partial x^2} + \frac{\partial^2 u}{\partial y^2}$, $[v]_1^2 = v_2 - v_1$, and 1,2,3,4 are four corners of S , see Figure 4.1. The notations are

$$\begin{aligned} \Lambda_\mu(u, v) &= \Delta u \Delta v + (1 - \mu)(2u_{xy}v_{xy} - u_{xx}v_{yy} - u_{yy}v_{xx}) \\ &= u_{xx}v_{xx} + u_{yy}v_{yy} + \mu(u_{xx}v_{yy} + u_{yy}v_{xx}) + 2(1 - \mu)u_{xy}v_{xy}, \\ m(u) &= -u_{nn} - \mu u_{ss}, \quad p(u) = u_{nnn} + (2 - \mu)u_{ssn}, \end{aligned}$$

where $0 \leq \mu < 1$ and n and s are normal and tangent directions along the boundary ∂S of S , respectively, and $u_{xy} = \frac{\partial^2 u}{\partial x \partial y}$, $u_{xx} = \frac{\partial^2 u}{\partial x^2}$, $u_{nn} = \frac{\partial^2 u}{\partial n^2}$, $u_{ss} = \frac{\partial^2 u}{\partial s^2}$, etc. In (4.2.1), we assume that all integrands wherein are continuous.

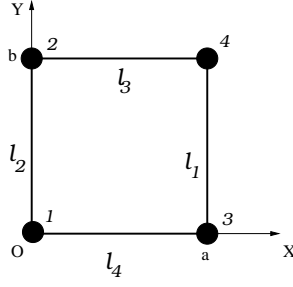


Figure 4.1: A rectangle.

Let us prove (4.2.1). In Figure 4.1, let ℓ_i with $i = 1, 2, 3, 4$ denote four edges of S , we obtain from integration by parts,

$$\begin{aligned} \iint_S u_{xx} v_{xx} &= \left(\int_{\ell_1} - \int_{\ell_2} \right) v_x u_{xx} - \iint_S v_x u_{xxx} \\ &= \left(\int_{\ell_1} - \int_{\ell_2} \right) v_x u_{xx} - \left(\int_{\ell_1} - \int_{\ell_2} \right) v u_{xxx} + \iint_S v u_{xxxx}, \end{aligned} \quad (4.2.2)$$

and

$$\iint_S u_{yy} v_{yy} = \left(\int_{\ell_3} - \int_{\ell_4} \right) v_y u_{yy} - \left(\int_{\ell_3} - \int_{\ell_4} \right) v u_{yyy} + \iint_S v u_{yyyy}. \quad (4.2.3)$$

Similarly, we have

$$\iint_S u_{yy} v_{xx} = \left(\int_{\ell_1} - \int_{\ell_2} \right) v_x u_{yy} - \left(\int_{\ell_1} - \int_{\ell_2} \right) v u_{xyy} + \iint_S v u_{xxyy}, \quad (4.2.4)$$

and

$$\iint_S u_{xx} v_{yy} = \left(\int_{\ell_3} - \int_{\ell_4} \right) v_y u_{xx} - \left(\int_{\ell_3} - \int_{\ell_4} \right) v u_{xxy} + \iint_S v u_{xxyy}. \quad (4.2.5)$$

Also, from integration by parts again we have

$$\begin{aligned} \iint_S u_{xy} v_{xy} &= \left(\int_{\ell_1} - \int_{\ell_2} \right) v_y u_{xy} - \iint_S v_y u_{xxy} \\ &= \left(\int_{\ell_1} - \int_{\ell_2} \right) v_y u_{xy} - \left(\int_{\ell_3} - \int_{\ell_4} \right) v u_{xxy} + \iint_S v u_{xxyy}, \end{aligned} \quad (4.2.6)$$

where

$$\left(\int_{\ell_1} - \int_{\ell_2} \right) v_y u_{xy} = [u_{xy} v]_3^4 - [u_{xy} v]_1^2 - \left(\int_{\ell_1} - \int_{\ell_2} \right) v u_{xxy}. \quad (4.2.7)$$

After some manipulations, we obtain from (4.2.2) – (4.2.7)

$$\begin{aligned}
\iint_S \Lambda_\mu(u, v) &= \iint_S \{u_{xx}v_{xx} + u_{yy}v_{yy} + \mu(u_{xx}v_{yy} + u_{yy}v_{xx}) + 2(1 - \mu)u_{xy}v_{xy}\} \\
&= \iint_S v\Delta^2 u + \left(\int_{\ell_1} - \int_{\ell_2}\right)(u_{xx} + \mu u_{yy})v_x \\
&\quad + \left(\int_{\ell_3} - \int_{\ell_4}\right)(u_{yy} + \mu u_{xx})v_y - \left(\int_{\ell_1} - \int_{\ell_2}\right)(u_{xxx} + (2 - \mu)u_{xyy})v \\
&\quad - \left(\int_{\ell_3} - \int_{\ell_4}\right)(u_{yyy} + (2 - \mu)u_{xxy})v + 2(1 - \mu)([u_{xy}v]_3^4 - [u_{xy}v]_1^2) \\
&= \iint_S v\Delta^2 u - \int_{\partial S} m(u)v_n - \int_{\partial S} p(u)v + 2(1 - \mu)([u_{xy}v]_3^4 - [u_{xy}v]_1^2). \blacksquare
\end{aligned}$$

4.2.2 Corner Effects on Polygons

For the rectangular domains in Figure 4.1, there do exist the corner terms

$$2(1 - \mu)([u_{xy}v]_3^4 - [u_{xy}v]_1^2) \quad (4.2.8)$$

in the Green formulas, which are different from those in Courant and Hilbert [109], p. 252 and Carey and Oden [78], p. 250. In fact, the formulas in [109] are valid only for the smooth boundary ∂S . There are many papers on Green formulas, see Herrera [202], Gourgeon and Herrera [179], and Russo [418], but only a few reports (e.g., Chien [101]) mention corner effects for biharmonic equations. Below, we will drive the Green formulas by different approaches from Section 4.2.1 and Chien [101].

Consider a polygon S in Figure 4.2, where the boundary $\partial S = \bigcup_{i=1}^m \Gamma_i$ and Γ_i are straight line segments. The corners are denoted by P_1, P_2, \dots, P_m . We have from calculus,

$$\iint_S \Delta u \Delta v = \iint_S (\Delta^2 u)v + \int_{\partial S} (\Delta u)v_n - \int_{\partial S} \frac{\partial(\Delta u)}{\partial n} v, \quad (4.2.9)$$

and

$$\begin{aligned}
\iint_S (u_{xx}v_{yy} + u_{yy}v_{xx}) &= \int_{\partial S} (u_{xx}v_y y_n + u_{yy}v_x x_n) - \iint_S (u_{xxy}v_y + u_{xyy}v_x) \\
&= \int_{\partial S} (u_{xx}v_y y_n + u_{yy}v_x x_n) - \int_{\partial S} u_{xy}(v_y x_n + v_x y_n) + 2 \iint_S u_{xy}v_{xy},
\end{aligned}$$

where x_n, y_n and x_s, y_s are the directional cosine of the outward normal and the tangent vectors, respectively. Since $x_n = y_s$ and $y_n = -x_s$, we obtain

$$\begin{aligned}
&\iint_S (2u_{xy}v_{xy} - u_{xx}v_{yy} - u_{yy}v_{xx}) \\
&= - \int_{\partial S} (u_{xx}v_y y_n + u_{yy}v_x x_n) + \int_{\partial S} u_{xy}(v_y y_s - v_x x_s).
\end{aligned} \quad (4.2.10)$$

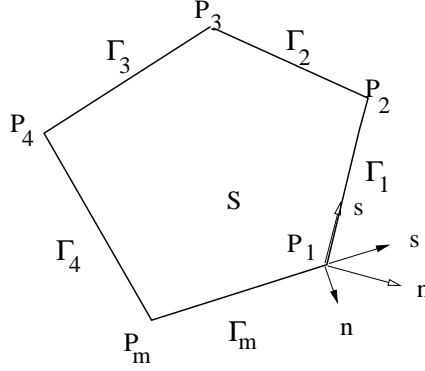


Figure 4.2: A polygon with corners.

Since x_s, x_n, y_s and y_n on the straight segments Γ_i are constant, we have the following derivative relations

$$\begin{aligned}
 v_y &= v_n y_n + v_s y_s, & v_x &= v_n x_n + v_s x_s, \\
 u_n &= u_x x_n + u_y y_n, & u_s &= u_x x_s + u_y y_s, \\
 u_{ss} &= u_{xx} x_s^2 + 2u_{xy} x_s y_s + u_{yy} y_s^2, \\
 u_{ns} &= u_{xx} x_n x_s + u_{xy} (x_n y_s + x_s y_n) + u_{yy} y_n y_s.
 \end{aligned} \tag{4.2.11}$$

Eq. (4.2.10) is then reduced to

$$\begin{aligned}
 & \iint_S (2u_{xy} v_{xy} - u_{xx} v_{yy} - u_{yy} v_{xx}) \\
 &= - \int_{\partial S} (u_{xx} x_s^2 + 2u_{xy} x_s y_s + u_{yy} y_s^2) v_n \\
 &+ \int_{\partial S} \{u_{xx} x_n x_s + u_{xy} (x_n y_s + x_s y_n) + u_{yy} y_n y_s\} \frac{\partial v}{\partial s} \\
 &= - \int_{\partial S} u_{ss} v_n + \int_{\partial S} u_{ns} \frac{\partial v}{\partial s}.
 \end{aligned} \tag{4.2.12}$$

Next, we have from integration by parts,

$$\int_{\partial S} u_{ns} \frac{\partial v}{\partial s} = \sum_{i=1}^m \int_{\Gamma_i} u_{ns} \frac{\partial v}{\partial s} = - \sum_{i=1}^m \delta[u_{ns}]_i v_i - \sum_{i=1}^m \int_{\Gamma_i} \left(\frac{\partial}{\partial s} u_{ns} \right) v, \tag{4.2.13}$$

where $v_i = v(P_i)$ and $\delta[u_{ns}]_i$ denote the jumps of u_{ns} at corner P_i counter-clockwise,

$$\delta[u_{ns}]_i = u_{ns}(P_i) \Big|_{\Gamma_i} - u_{ns}(P_i) \Big|_{\Gamma_{i-1}},$$

and $\Gamma_m = \Gamma_0$. From (4.2.9), (4.2.12) and (4.2.13), we obtain the Green formulas,

$$\begin{aligned}
\iint_S \Lambda_\mu(u, v) &= \iint_S \Delta u \Delta v + (1 - \mu) \int_{\partial S} (2u_{xy}v_{xy} - u_{xx}v_{yy} - u_{yy}v_{xx}) \\
&= \iint_S (\Delta^2 u)v + \int_{\partial S} (\Delta u)v_n - \int_{\partial S} \frac{\partial(\Delta u)}{\partial n} v \\
&+ (1 - \mu) \left\{ - \int_{\partial S} u_{ss}v_n - \int_{\partial S} \left(\frac{\partial}{\partial s} u_{ns} \right) v - \sum_{i=1}^m \delta[u_{ns}]_i v_i \right\} \\
&= \iint_S v \Delta u^2 - \int_{\partial S} (m(v)v_n + p(v)v) - (1 - \mu) \sum_{i=1}^m \delta[u_{ns}]_i v_i, \tag{4.2.14}
\end{aligned}$$

where the general forms of $m(v)$ and $p(v)$ are denoted by (see [109])

$$\begin{aligned}
m(u) &= -\Delta u + (1 - \mu)u_{ss} = -(u_{nn} + \mu u_{ss}), \tag{4.2.15} \\
p(u) &= \frac{\partial}{\partial n} \Delta u + (1 - \mu)u_{nss} = u_{nnn} + (2 - \mu)u_{nss}.
\end{aligned}$$

There also exist the corner terms in the Green formulas (4.2.14),

$$- (1 - \mu) \sum_{i=1}^m \delta[u_{ns}]_i v_i. \tag{4.2.16}$$

When the corner angles at P_i in Figure 4.2 are just $\frac{\pi}{2}$, and when the second order derivatives are also continuous:

$$u_{ns}(P_i) \Big|_{\Gamma_i} = -u_{ns}(P_i) \Big|_{\Gamma_{i-1}},$$

the corner conditions (4.2.16) are reduced to

$$- (1 - \mu) \delta[u_{ns}]_i v_i = 2(1 - \mu) u_{ns}(P_i) \Big|_{\Gamma_{i-1}}. \tag{4.2.17}$$

Note that Eq. (4.2.17) coincides well with (4.2.8). Obviously, for the smooth boundary ∂S , the corner terms disappear, and the Green formulas in [109] are obtained. This shows that the Green formulas in Courant and Hilbert [109] are the special cases of (4.2.14).

Remark 4.2.1 *Let us consider the piecewise curved boundary Γ_i . Denote by $\alpha = \alpha(s)$ the angle between the tangent direction of Γ_i and the x axis, then*

$$\begin{aligned}
x_s &= \cos \alpha, \quad y_n = -\cos \alpha, \quad x_n = y_s = \sin \alpha, \\
u_n &= u_x x_n + u_y y_n = (\sin \alpha)u_x - (\cos \alpha)u_y, \\
u_s &= u_x x_s + u_y y_s = (\cos \alpha)u_x + (\sin \alpha)u_y. \tag{4.2.18}
\end{aligned}$$

There exist the derivatives of α with respect to s : $\frac{\partial \alpha}{\partial s} = \frac{1}{\rho}$, where ρ denotes the curvature radius of Γ_i , ρ is positive if the curvature center is within S , or negative otherwise. We

have from (4.2.18) by calculus,

$$\begin{aligned} u_{ss} &= u_{xx}x_s^2 + 2u_{xy}x_sy_s + u_{yy}y_s^2 - \frac{u_n}{\rho}, \\ u_{ns} &= u_{xx}x_nx_s + u_{xy}(x_ny_s + x_sy_n) + u_{yy}y_ny_s + \frac{u_s}{\rho}. \end{aligned} \quad (4.2.19)$$

Note that there are two additional terms, $-\frac{u_n}{\rho}$ and $\frac{u_s}{\rho}$ in (4.2.19), compared with those in (4.2.11).

Similarly, Eq. (4.2.10) is reduced to

$$\begin{aligned} & \iint_S (2u_{xy}v_{xy} - u_{xx}v_{yy} - u_{yy}v_{xx}) \\ &= - \int_{\partial S} (u_{xx}x_s^2 + 2u_{xy}x_sy_s + u_{yy}y_s^2)v_n \\ &+ \int_{\partial S} \{u_{xx}x_nx_s + u_{xy}(x_ny_s + x_sy_n) + u_{yy}y_ny_s\} \frac{\partial v}{\partial s} \\ &= - \int_{\partial S} (u_{ss} + \frac{u_n}{\rho})v_n + \int_{\partial S} (u_{ns} - \frac{u_s}{\rho}) \frac{\partial v}{\partial s} \\ &= - \int_{\partial S} (u_{ss} + \frac{u_n}{\rho})v_n - \sum_{i=1}^n \delta[u_{ns} - \frac{u_s}{\rho}]_i v_i - \int_{\partial S} \frac{\partial}{\partial s} (u_{ns} - \frac{u_s}{\rho})v. \end{aligned} \quad (4.2.20)$$

From (4.2.9) and (4.2.20), we obtain the Green formulas,

$$\begin{aligned} \iint_S \Lambda_\mu(u, v) &= \iint_S \Delta u \Delta v + (1 - \mu) \int_{\partial S} (2u_{xy}v_{xy} - u_{xx}v_{yy} - u_{yy}v_{xx}) \\ &= \iint_S v \Delta u^2 - \int_{\partial S} \{m^*(v)v_n + p^*(v)v\} \\ &- (1 - \mu) \sum_{i=1}^m \delta[u_{ns} - \frac{u_s}{\rho}]_i v_i, \end{aligned} \quad (4.2.21)$$

where

$$\begin{aligned} m^*(u) &= -\Delta u + (1 - \mu)(u_{ss} + \frac{u_n}{\rho}) = m(u) + (1 - \mu)\frac{u_n}{\rho}, \\ p^*(u) &= \frac{\partial}{\partial n} \Delta u + (1 - \mu)(u_{nss} - \frac{\partial}{\partial s}(\frac{u_s}{\rho})) \\ &= p(u) - (1 - \mu)\frac{\partial}{\partial s}(\frac{u_s}{\rho}), \end{aligned}$$

and $m(u)$ and $p(u)$ are defined in (4.2.15). When natural boundary conditions are subjected to Γ_{i-1} and Γ_i , we obtain the boundary equations

$$m^*(u) = 0, \quad p^*(u) = 0 \quad \text{on } \Gamma_{i-1} \cup \Gamma_i, \quad (4.2.22)$$

and the corner conditions

$$\delta[u_{ns} - \frac{u_s}{\rho}]_i = 0 \text{ at } P_i. \quad (4.2.23)$$

Eqs. (4.2.21), (4.2.22) and (4.2.23) are given in Chien [101], p. 245, p. 238 and p. 59, respectively. Where Γ_i are straight lines, $\rho = \infty$, Eq. (4.2.21) leads to (4.2.14), and the corner terms $-(1 - \mu) \sum_{i=1}^m \delta[u_{ns} - \frac{u_s}{\rho}]_i v_i$ in (4.2.21) to (4.2.16).

4.2.3 Boundary Conditions for Biharmonic Equations on Polygons

Consider a polygon S , and the exterior boundary conditions on ∂S can be easily derived from the Green formulas. Let the solution $u \in H^2(S)$, where $H^2(S)$ is the Sobolev space defined in [438]. In $H^2(S)$, the biharmonic solution and its derivatives are continuous on the entire S , i.e., $u \in C^1(S)$. Then the generalized solution of the biharmonic equation, $\Delta^2 u + f = 0$ in S , can be expressed in a weak form: To seek $u \in H^2(S)$ such that

$$\iint_S \Lambda_\mu(u, v) + \iint_S f v = 0, \quad v \in H_0^2(S),$$

where $H_0^2(S)$ is a subspace of $H^2(S)$ satisfying suitable homogeneous boundary conditions for v . Based on the Green formulas in Section 4.2.1,

$$\begin{aligned} 0 &= \iint_S (\Delta^2 u + f)v - \int_{\partial S} (m(u)v_n + p(u)v) \\ &\quad + 2(1 - \mu)([u_{xy}v]_3^4 - [u_{xy}v]_1^2), \end{aligned}$$

we obtain three equations from an arbitrary function v ,

$$\iint_S (\Delta^2 u + f)v = 0, \quad (4.2.24)$$

$$\int_{\partial S} (m(u)v_n + p(u)v) = 0, \quad (4.2.25)$$

$$2(1 - \mu)([u_{xy}v]_3^4 - [u_{xy}v]_1^2) = 0. \quad (4.2.26)$$

Since v in S is arbitrary, we obtain the biharmonic equation, $\Delta^2 u + f = 0$ in S from (4.2.24), where f also represents the exterior surface force. Next, let us consider different exterior boundary conditions. For the clamped condition: $u = g_1$ and $u_n = g_2$ on ∂S , in view of $v = 0$ and $v_n = 0$ on ∂S , we can see that the boundary integrals satisfy (4.2.25) automatically. Next, for the simply supported condition $u = g_1$, since v_n on ∂S is arbitrary, then the additional condition, the boundary bending moment $m(u) = 0$ on ∂S , is obtained from (4.2.25). For the special case: $u = \text{constant}$, we have $u_{ss} = 0$, which gives $m(u) = -u_{nn} - \mu u_{ss} = -u_{nn} = 0$. Hence we obtain a concise form of the simply supported conditions: $u = \text{constant}$ and $u_{nn} = 0$ on ∂S .

For symmetric conditions, $u_n = 0$ on ∂S , we have the additional condition: $p(u) = u_{nnn} + (2 - \mu)u_{nss} = 0$ from (4.2.25). Since $u_{nss} = 0$ on ∂S , $p(u) = 0$ is also simplified to

$u_{nnn} = 0$ on ∂S . So we obtain the symmetric conditions: $u_n = u_{nnn} = 0$ on ∂S . For the simple natural boundary condition, e.g., no constraints are given on ∂S , then $m(u) = 0$ and $p(u) = 0$ from (4.2.25). Suppose that the natural boundary conditions are given by the exterior boundary force $p(u) = g_3$ and the bending moment $m(u) = g_4$ on Γ_N , where Γ_N is part of ∂S , and the clamped boundary condition is subjected on $\partial S \setminus \Gamma_N$. The unique solution of biharmonic equations is then expressed as: To seek $u \in H^2(S)$ such that

$$\iint_S \Lambda_\mu(u, v) + \iint_S f v + \int_{\Gamma_N} (g_3 v + g_4 v_n) = 0, \quad v \in H_0^2(S).$$

We may consider the mixed types of different boundary conditions, where different conditions are given on different edges of ∂S . In this case, the corner terms must be considered for the natural corners, where two adjacent edges are *all* subjected to the natural conditions. Since v is arbitrary, we obtain the corner condition $u_{xy} = 0$ from (4.2.26), which is important for the collocation TM, see Section 4.3.3, because all boundary conditions including the corner conditions must be satisfied as best as possible. Moreover, the corner condition $u_{xy} v = 0$ is satisfied automatically, if one adjacent edge of the corner is subjected to one of the following cases: (1) the clamped condition, (2) the symmetric condition, or (3) the simply supported condition with $u_n = \text{constant}$. It is easy to see that either $v = 0$ or $u_{ns} = u_{xy} = 0$ on one edge yields $u_{xy} v = 0$ automatically at the corner.

We may discuss the uniqueness of the solutions by considering the homogeneous biharmonic equation $\Delta^2 u = 0$. A solution u can be also described as the minimal energy:

$$E(u) = \min_{v \in H_0^2(S)} E(v),$$

where

$$\begin{aligned} E(v) &= \frac{1}{2} \iint_S \Lambda_\mu(v, v) = \frac{1}{2} \iint_S \mu(v_{xx}^2 + v_{yy}^2) \\ &\quad + (1 - \mu)(v_{xx}^2 + v_{yy}^2 + 2v_{xy}^2). \end{aligned}$$

When $0 \leq \mu < 1$, condition $E(v) = 0$ leads to that $v_{xx} = v_{yy} = v_{xy} = 0$, then the linear functions are obtained, i.e., $v = a + bx + cy$ with constants a , b and c . To guarantee the unique solutions, the linear functions must be zero: $v = a + bx + cy \equiv 0$. For the mixed types of boundary conditions, there exist unique solutions for one edge, e.g., \overline{AB} in Figure 4.3, subjected to the clamped boundary condition. Since v_n (e.g., v_x) = $v = 0$ on \overline{AB} , then the constants $b = 0$ and $(a + cy)|_{x=1} = 0$. So $a = c = 0$ and then $v \equiv 0$. This confirms the unique solutions if one edge of a corner is subjected to the clamped boundary condition.

In summary, we have derived five typical boundary conditions for biharmonic equations on polygonal domains:

1. The symmetric condition: $u_n = 0, u_{nnn} = 0$.

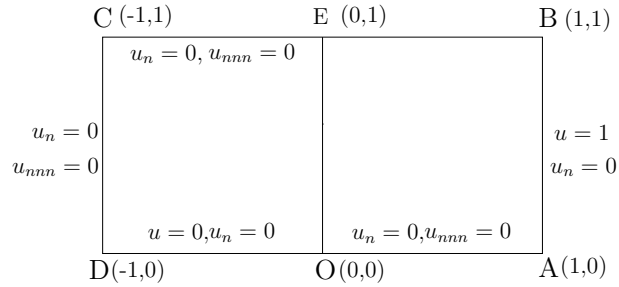


Figure 4.3: The boundary conditions of biharmonic equations for Model I.

2. **The clamped condition:** $u = c_0, u_n = c_1$.
3. **The simply supported condition:** $u = c_0, u_{nn} = c_2$.
4. **The natural condition:**

$$m(u) = -u_{nn} - \mu u_{ss} = c_3, \quad p(u) = u_{nnn} + (2 - \mu)u_{nss} = c_4.$$

5. **The natural corner condition:** $u_{xy} = c_5$.

Here c_i are the given constants, which are dependent of the problems to be solved. Note that for biharmonic equations, the interior and exterior boundary conditions and the corner conditions are important not only to the collocation TM in this chapter but also to the collocation methods using the radial basis functions, or the Sinc functions etc., see Chapter 7.

4.3 The Collocation Trefftz Methods

4.3.1 Three Crack Models

Consider the homogeneous biharmonic equation

$$\Delta^2 u = 0 \quad \text{in } S, \quad (4.3.1)$$

where the solution domain is the rectangle: $S = \{(x, y) \mid -1 < x < 1, 0 < y < 1\}$. In this chapter, we study three crack models of singularity problems, shown in Figures 4.3 – 4.5. The section \overline{OD} represents an interior crack under the clamped condition $u = u_n = 0$. From Section 4.2.3, the symmetric conditions, $u_n = u_{nnn} = 0$ on $\overline{OA} \cup \overline{BC} \cup \overline{CD}$, are required. Here n is the outward normal direction to the boundary ∂S . On \overline{AB} , when the

clamped conditions are provided, we propose the biharmonic boundary value problem with the following conditions, called Model I in this chapter, see Figure 4.3:

$$u|_{\overline{OD}} = 0, u_y|_{\overline{OD}} = 0, \tag{4.3.2}$$

$$u_y|_{\overline{OA}} = 0, u_{yyy}|_{\overline{OA}} = 0, \tag{4.3.3}$$

$$u|_{\overline{AB}} = 1, u_x|_{\overline{AB}} = 0, \tag{4.3.4}$$

$$u_y|_{\overline{BC}} = 0, u_{yyy}|_{\overline{BC}} = 0, \tag{4.3.5}$$

$$u_x|_{\overline{CD}} = 0, u_{xxx}|_{\overline{CD}} = 0. \tag{4.3.6}$$

We may replace the clamped condition on \overline{AB} by the simply supported condition,

$$u|_{\overline{AB}} = 1, u_{xx}|_{\overline{AB}} = 0,$$

but the other boundary conditions remain the same as those in Model I. Such a model is called Model II, see Figure 4.4. Note that Models I and II resemble the Motz's problem in Chapter 2.

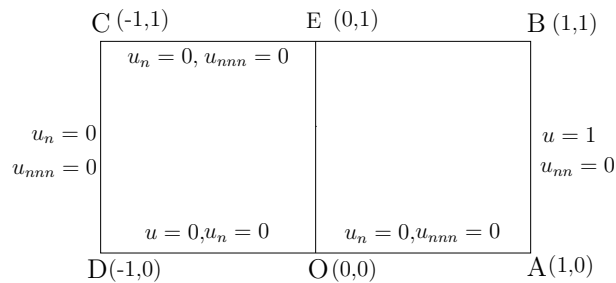


Figure 4.4: The boundary conditions of biharmonic equations for Model II.

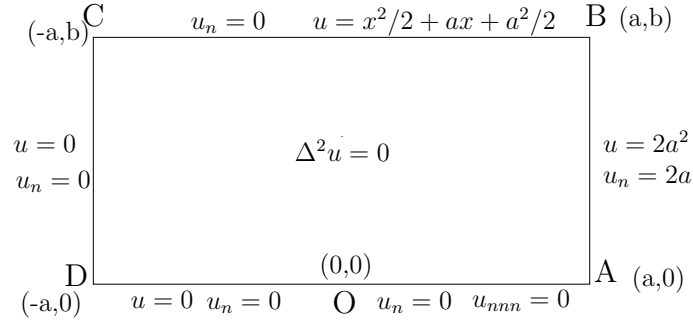


Figure 4.5: The boundary conditions of biharmonic equations for Model III.

Next, we choose the models in Schiff et al. [423] with all the clamped conditions on ∂S except \overline{OA} , see Figure 4.5,

$$\Delta^2 u = 0, \quad \text{on } S, \quad (4.3.7)$$

$$u|_{\overline{OD}} = 0, u_y|_{\overline{OD}} = 0, \quad (4.3.8)$$

$$u_y|_{\overline{OA}} = 0, u_{yyy}|_{\overline{OA}} = 0, \quad (4.3.9)$$

$$u|_{\overline{AB}} = 2a^2, u_x|_{\overline{AB}} = 2a, \quad (4.3.10)$$

$$u|_{\overline{BC}} = \frac{x^2}{2} + ax + \frac{a^2}{2}, u_y|_{\overline{BC}} = 0, \quad (4.3.11)$$

$$u|_{\overline{CD}} = 0, u_x|_{\overline{CD}} = 0, \quad (4.3.12)$$

where $S = \{(x, y) \mid -a < x < a, 0 < y < b\}$. When the parameters $a = b = 1$, the model (4.3.7) – (4.3.12) is called Model III in this chapter.

For the clamped crack on \overline{OD} , the particular solutions of these models are known, and given in Schiff et al. [423]:

$$u = \sum_{i=1}^{\infty} (d_i \phi_i(r, \theta) + c_i f_i(r, \theta)),$$

where d_i and c_i are expansion coefficients, and the singular particular solutions are

$$\phi_i(r, \theta) = r^{i+\frac{1}{2}} \left\{ \cos\left(i - \frac{3}{2}\right)\theta - \frac{i - \frac{3}{2}}{i + \frac{1}{2}} \cos\left(i + \frac{1}{2}\right)\theta \right\}, \quad (4.3.13)$$

and the analytic particular solutions

$$f_i(r, \theta) = r^{i+1} \{ \cos(i-1)\theta - \cos(i+1)\theta \}. \quad (4.3.14)$$

4.3.2 Description of the Method

We shall take Model I as an example to describe the collocation TM, since the algorithms of the collocation TM for other models may be similarly described. Choose finite terms of particular solutions

$$u_N = \sum_{i=1}^N (\tilde{d}_i \phi_i(r, \theta) + \tilde{c}_i f_i(r, \theta)), \quad (4.3.15)$$

where \tilde{d}_i and \tilde{c}_i are approximate coefficients to be sought. Since the particular solutions (4.3.13) and (4.3.14) satisfy the biharmonic equation (4.3.1) in S and the boundary conditions on \overline{OD} and \overline{OA} already, the unknown coefficients \tilde{c}_i and \tilde{d}_i can be obtained by satisfying the rest of boundary conditions as best as possible.

For Model I, there exists the crack tip at O . We split S into S^+ and S^- , where $S^+ = S \cap (x \geq 0)$ and $S^- = S \cap (x \leq 0)$. Then the Green formulas are applied to S^+ and S^- in Figure 4.3, to give

$$\begin{aligned} \iint_S \Lambda_\mu(u, v) &= \iint_{S^+} \Lambda_\mu(u, v) + \iint_{S^-} \Lambda_\mu(u, v) \\ &= \iint_S v \Delta^2 u - \int_{\partial S} \{m(u)v_n + p(u)v\} \\ &\quad + 2(1 - \mu)([u_{xy}v]_A^B - [u_{xy}v]_{O^+}^E + [u_{xy}v]_{O^-}^E - [u_{xy}v]_D^C), \end{aligned} \quad (4.3.16)$$

where point $E = (0, 1)$. From (4.3.2) – (4.3.6), we obtain

$$v(A) = v(B) = v(D) = v(O^-) = 0, \quad u_{xy}(C) = u_{xy}(E) = u_{xy}(O^+) = 0.$$

Hence, the last term on the right hand of (4.3.16) is zero automatically. In this case, the corner conditions at E and O may not be needed in the collocation TM, either. We confirm again the boundary conditions given in (4.3.2) – (4.3.6).

For Model I with the boundary conditions (4.3.2) – (4.3.6), define an energy on the boundary by

$$\begin{aligned} I(v) = I(d_i, c_i) &= \int_{\overline{AB}} \{(v-1)^2 + w_1^2 v_x^2\} \\ &\quad + \int_{\overline{BC}} (w_1^2 v_y^2 + w_3^2 v_{yyy}^2) + \int_{\overline{CD}} (w_1^2 v_x^2 + w_3^2 v_{xxx}^2), \end{aligned} \quad (4.3.17)$$

where the weights $w_i = \frac{1}{(N+1)^i}$, based on the analysis in Chapter 2. The approximate coefficients \tilde{d}_i and \tilde{c}_i can be found by

$$I(u_N) = I(\tilde{d}_i, \tilde{c}_i) = \min_{d_i, c_i} I(d_i, c_i).$$

To be more precise, we use the central rule to discretize the integrals in (4.3.17) with the uniform partitions are chosen for $\overline{AB} \cup \overline{BC} \cup \overline{CD}$, and the division number of \overline{AB} is

denoted by M . This is equivalent to the direct collocation method to establish the linear algebraic equations,

$$\mathbf{F}\mathbf{x} = \mathbf{b},$$

where \mathbf{x} consists of $2N$ coefficients \tilde{d}_i and \tilde{c}_i , and $\mathbf{F} \in R^{8M \times 2N}$ is the matrix, where $8M \gg 2N$. Its least squares solution is just the desired solution \mathbf{x} , e.g., the coefficients \tilde{d}_i and \tilde{c}_i .

In computation, we use the error norm for accuracy,

$$E_2 = \|\epsilon\|_B = \|u - v\|_B = \sqrt{I(v)}, \quad (4.3.18)$$

and the condition number for stability

$$\text{Cond.} = \left\{ \frac{\lambda_{max}(\mathbf{F}^T \mathbf{F})}{\lambda_{min}(\mathbf{F}^T \mathbf{F})} \right\}^{\frac{1}{2}}, \quad (4.3.19)$$

where $\lambda_{max}(\mathbf{A})$ and $\lambda_{min}(\mathbf{A})$ are the maximal and minimal eigenvalues of the matrix $\mathbf{A} = \mathbf{F}^T \mathbf{F}$.

4.3.3 The Collocation Trefftz Method with Natural Corners

Let the clamped and the natural conditions be given on \overline{AB} and $\overline{BC} \cup \overline{CD}$ in Figure 4.3, respectively:

$$u = 1, \quad u_n = 0, \quad \text{on } \overline{AB}; \quad m(u) = p(u) = 0 \quad \text{on } \overline{BC} \cup \overline{CD}.$$

Since point C is a natural corner, the corner condition is needed: $u_{xy}(C) = 0$. The collocation TM involving the natural corner C is given by

$$I^*(u_N) = I^*(\tilde{d}_i, \tilde{c}_i) = \min_{d_i, c_i} I^*(d_i, c_i),$$

where

$$\begin{aligned} I^*(v) = & \int_{\overline{AB}} ((v-1)^2 + w_1^2 v_n^2) \\ & + \int_{\overline{BC} \cup \overline{CD}} (w_2^2 m^2(v) + w_3^2 p^2(v)) + 2(1-\mu)w_2^2 v_{xy}^2(C), \end{aligned} \quad (4.3.20)$$

and the weights are $w_i = \frac{1}{(N+1)^i}$. Note that the corner term involving $v_{xy}^2(C)$ is *necessary* to the collocation TM for the biharmonic equations with natural corners. When the corner angles at $\angle DCB$ is not just $\pi/2$, the corner contribution in (4.3.20) is replaced by $(1-\mu)w_2^2(v_{ns}^+(C) - v_{ns}^-(C))^2$ based on the analysis in Section 4.2.2.

4.3.4 Formulas of Partial Derivatives

In this section, we provide useful formulas for partial derivatives $u_x, u_y, u_{xx}, u_{yy}, u_{xy}, u_{xxx}, u_{yyy}, u_{xxy}$ and u_{xyy} , which are required by the collocation TM. Since the particular solutions (4.3.13) and (4.3.14) in S are given in polar coordinates, we will find their explicit formulas of partial derivatives with respect to x and y . Let the origins of the Cartesian and polar coordinates be the same, we obtain

$$u_x = \cos \theta \frac{\partial u}{\partial r} - \sin \theta \frac{\partial u}{r \partial \theta}, \quad u_y = \sin \theta \frac{\partial u}{\partial r} + \cos \theta \frac{\partial u}{r \partial \theta}. \quad (4.3.21)$$

Based on (4.3.21), we have

$$\begin{aligned} u_{xx} &= (\cos \theta \frac{\partial}{\partial r} - \sin \theta \frac{\partial}{r \partial \theta})(\cos \theta \frac{\partial}{\partial r} - \sin \theta \frac{\partial}{r \partial \theta})u \\ &= \cos^2 \theta \frac{\partial^2 u}{\partial r^2} - \sin 2\theta (\frac{\partial}{r \partial r} \frac{\partial u}{\partial \theta} - \frac{\partial u}{r^2 \partial \theta}) + \frac{\sin^2 \theta}{r} \frac{\partial u}{\partial r} + \frac{\sin^2 \theta}{r^2} \frac{\partial^2 u}{\partial \theta^2}. \end{aligned} \quad (4.3.22)$$

Similarly, we have

$$u_{yy} = \sin^2 \theta \frac{\partial^2 u}{\partial r^2} + \sin 2\theta (\frac{\partial}{r \partial r} \frac{\partial u}{\partial \theta} - \frac{\partial u}{r^2 \partial \theta}) \quad (4.3.23)$$

$$+ \frac{\cos^2 \theta}{r} \frac{\partial u}{\partial r} + \frac{\cos^2 \theta}{r^2} \frac{\partial^2 u}{\partial \theta^2}, \quad (4.3.24)$$

and

$$\begin{aligned} u_{xy} &= \cos \theta \sin \theta \frac{\partial^2 u}{\partial r^2} + \frac{\cos^2 \theta}{r} \frac{\partial}{\partial r} \frac{\partial u}{\partial \theta} - \frac{\cos^2 \theta}{r^2} \frac{\partial u}{\partial \theta} - \frac{\sin^2 \theta}{r} \frac{\partial}{\partial r} \frac{\partial u}{\partial \theta} \\ &\quad - \frac{\cos \theta \sin \theta}{r} \frac{\partial u}{\partial r} - \frac{\cos \theta \sin \theta}{r^2} \frac{\partial^2 u}{\partial \theta^2} + \frac{\sin^2 \theta}{r^2} \frac{\partial u}{\partial \theta}. \end{aligned} \quad (4.3.25)$$

After some manipulation, we can also obtain

$$\begin{aligned} u_{xxx} &= (\cos \theta \frac{\partial}{\partial r} - \sin \theta \frac{\partial}{r \partial \theta}) \times \\ &[\cos^2 \theta \frac{\partial^2}{\partial r^2} - \sin 2\theta (\frac{\partial}{r \partial r} \frac{\partial}{\partial \theta} - \frac{\partial}{r^2 \partial \theta}) + \frac{\sin^2 \theta}{r} \frac{\partial}{\partial r} + \frac{\sin^2 \theta}{r^2} \frac{\partial^2}{\partial \theta^2}]u \\ &= \cos^3 \theta \frac{\partial^3 u}{\partial r^3} - \frac{3 \cos \theta \sin 2\theta}{2r} \frac{\partial^2}{\partial r^2} \frac{\partial u}{\partial \theta} + \frac{3 \sin \theta \sin 2\theta}{2r^2} \frac{\partial}{\partial r} \frac{\partial^2 u}{\partial \theta^2} \\ &\quad - \frac{\sin^3 \theta}{r^3} \frac{\partial^3 u}{\partial \theta^3} + \frac{3 \sin \theta \sin 2\theta}{2r} \frac{\partial^2 u}{\partial r^2} - \frac{3(\sin \theta - 3 \sin 3\theta)}{4r^2} \frac{\partial}{\partial r} \frac{\partial u}{\partial \theta} \\ &\quad - \frac{3 \sin \theta \sin 2\theta}{r^3} \frac{\partial^2 u}{\partial \theta^2} - \frac{3 \sin \theta \sin 2\theta}{2r^2} \frac{\partial u}{\partial r} - \frac{2 \sin 3\theta}{r^3} \frac{\partial u}{\partial \theta}. \end{aligned} \quad (4.3.26)$$

Other derivatives of third order are given by

$$\begin{aligned}
u_{yyy} &= \sin^3 \theta \frac{\partial^3 u}{\partial r^3} + \frac{3 \sin \theta \sin 2\theta}{2r} \frac{\partial^2}{\partial r^2} \frac{\partial u}{\partial \theta} + \frac{3 \cos \theta \sin 2\theta}{2r^2} \frac{\partial}{\partial r} \frac{\partial^2 u}{\partial \theta^2} \\
&+ \frac{\cos^3 \theta}{r^3} \frac{\partial^3 u}{\partial \theta^3} + \frac{3 \cos \theta \sin 2\theta}{2r} \frac{\partial^2 u}{\partial r^2} + \frac{3(\cos \theta + 3 \cos 3\theta)}{4r^2} \frac{\partial}{\partial r} \frac{\partial u}{\partial \theta} \\
&- \frac{3 \cos \theta \sin 2\theta}{r^3} \frac{\partial^2 u}{\partial \theta^2} - \frac{3 \cos \theta \sin 2\theta}{2r^2} \frac{\partial u}{\partial r} - \frac{2 \cos 3\theta}{r^3} \frac{\partial u}{\partial \theta}, \\
u_{xxy} &= \sin \theta \cos^2 \theta \frac{\partial^3 u}{\partial r^3} + \frac{\cos \theta + 3 \cos 3\theta}{4r} \frac{\partial^2}{\partial r^2} \frac{\partial u}{\partial \theta} + \frac{\sin \theta - 3 \sin 3\theta}{4r^2} \frac{\partial}{\partial r} \frac{\partial^2 u}{\partial \theta^2} \\
&+ \frac{\sin \theta \sin 2\theta}{2r^3} \frac{\partial^3 u}{\partial \theta^3} + \frac{\sin \theta - 3 \sin 3\theta}{4r} \frac{\partial^2 u}{\partial r^2} + \frac{\cos \theta - 9 \cos 3\theta}{4r^2} \frac{\partial}{\partial r} \frac{\partial u}{\partial \theta} \\
&- \frac{2 \sin \theta - 3 \sin 3\theta}{2r^3} \frac{\partial^2 u}{\partial \theta^2} - \frac{\sin \theta - 3 \sin 3\theta}{4r^2} \frac{\partial u}{\partial r} + \frac{2 \cos 3\theta}{r^3} \frac{\partial u}{\partial \theta}, \tag{4.3.27}
\end{aligned}$$

and

$$\begin{aligned}
u_{xyy} &= \cos \theta \sin^2 \theta \frac{\partial^3 u}{\partial r^3} + \frac{3 \sin 3\theta - \sin \theta}{4r} \frac{\partial^2}{\partial r^2} \frac{\partial u}{\partial \theta} + \frac{\cos \theta + 3 \cos 3\theta}{4r^2} \frac{\partial}{\partial r} \frac{\partial^2 u}{\partial \theta^2} \\
&- \frac{\sin \theta \cos^2 \theta}{r^3} \frac{\partial^3 u}{\partial \theta^3} + \frac{\cos \theta + 3 \cos 3\theta}{4r} \frac{\partial^2 u}{\partial r^2} - \frac{\sin \theta + 9 \sin 3\theta}{4r^2} \frac{\partial}{\partial r} \frac{\partial u}{\partial \theta} \\
&\frac{\cos \theta + 3 \cos 3\theta}{2r^3} \frac{\partial^2 u}{\partial \theta^2} - \frac{\cos \theta + 3 \cos 3\theta}{4r^2} \frac{\partial u}{\partial r} + \frac{2 \sin 3\theta}{r^3} \frac{\partial u}{\partial \theta}. \tag{4.3.28}
\end{aligned}$$

In the computation of (4.3.21) – (4.3.28), the derivatives of u with respect to r and θ can be easily obtained directly from (4.3.13) and (4.3.14). For the analytical particular solutions $f_i(r, \theta)$ in (4.3.14), the explicit derivatives, u_x, u_y, \dots, u_{xyy} , can be derived straightforward. However, for the singular particular solutions, $\phi_i(r, \theta)$ in (4.3.13), the above computational formulas are *essential* in computations.

4.4 Error Bounds

For simplicity, we consider the collocation TM for Model I in Figure 4.3. Let $S = S_1 \cup S_2$, where $S_1 = S \cap (x < 0)$ and $S_2 = S \cap (x > 0)$. We have the Green formulas (4.3.16) for $v = u_N$,

$$\begin{aligned}
\iint_S \Lambda_\mu(v, v) &= \iint_S v \Delta^2 v - \int_{\partial S} m(v) v_n - \int_{\partial S} p(v) v \\
&+ 2(1 - \mu) \{ [v_{xy} v]_A^B - [v_{xy} v]_{O^+}^E + [v_{xy} v]_{O^-}^E - [v_{xy} v]_D^C \},
\end{aligned}$$

where $E = (0, 1)$, $m(v) = -v_{nn}$ and $p(v) = v_{nnn}$ on $\overline{AB} \cup \overline{BC} \cup \overline{CD}$ for Model I. Hence for the particular solutions $v = v_N$ of biharmonic equations, since $v|_D = v|_{O^-} = 0$ and

$v_{xy}|_A = v_{xy}|_{O^+} = 0$, the Green formulas are simplified to

$$\iint_S \Lambda_\mu(v, v) = \int_{\overline{AB} \cup \overline{BC} \cup \overline{CD}} (v_{nn}v_n - v_{nnn}v) + 2(1 - \mu)[v_{xy}v]_C^B. \quad (4.4.1)$$

Moreover, the boundary norm (4.3.18) is expressed as

$$\begin{aligned} \|\epsilon\|_B = \|u - v\|_B = \sqrt{I(v)} = & \{ \|v - 1\|_{0, \overline{AB}}^2 + w_1^2 \|v_n\|_{0, \overline{AB}}^2 + w_1^2 \|v_n\|_{0, \overline{BC}}^2 \\ & + w_3^2 \|v_{nnn}\|_{0, \overline{BC}}^2 + w_1^2 \|v_n\|_{0, \overline{CD}}^2 + w_3^2 \|v_{nnn}\|_{0, \overline{CD}}^2 \}^{\frac{1}{2}}, \end{aligned} \quad (4.4.2)$$

where $w_i = 1/(N + 1)^i$. Then we have the following theorem.

Theorem 4.4.1 *Let $v = u_N$ in (4.3.15) be chosen for Model I. Suppose that the inverse inequalities hold:*

$$\|\epsilon_{nnn}\|_{0, \overline{AB}} \leq K_N \|\epsilon\|_{2, S}, \quad \|\epsilon_{nn}\|_{0, \overline{AB} \cup \overline{BC} \cup \overline{CD}} \leq K_N^* \|\epsilon\|_{2, S}, \quad (4.4.3)$$

$$|v_{xy}(B)| \leq K_N^{**} \|v_n\|_{0, \overline{BC}}, \quad |v_{xy}(C)| \leq K_N^{**} \|v_n\|_{0, \overline{BC}}, \quad (4.4.4)$$

where K_N , K_N^* and K_N^{**} may be unbounded as $N \rightarrow \infty$. Then there exist the error bounds,

$$\begin{aligned} \|\epsilon\|_{2, S} = \|u - v\|_{2, S} \\ \leq C \{ K_N + (K_N^{**} + K_N^*)/w_1 + 1/w_3 \} \|u - v\|_B, \end{aligned}$$

where C is a bounded constant independent of N .

Proof For $\mu \in [0, 1)$ and the clamped boundary conditions on $\overline{OD} \cup \overline{AB}$, from Marti [341] and (4.4.1) we have

$$\begin{aligned} \|\epsilon\|_{2, S}^2 & \leq C |\epsilon|_{2, S}^2 \leq C \iint_S \Lambda_\mu(\epsilon, \epsilon) \\ & \leq C \{ \|\epsilon_{nn}\|_{0, \overline{AB}} \|v_n\|_{0, \overline{AB}} + \|\epsilon_{nnn}\|_{0, \overline{AB}} \|v - 1\|_{0, \overline{AB}} + \|\epsilon_{nn}\|_{0, \overline{BC}} \|v_n\|_{0, \overline{BC}} \\ & + \|v_{nnn}\|_{0, \overline{BC}} \|\epsilon\|_{0, \overline{BC}} + \|\epsilon_{nn}\|_{0, \overline{CD}} \|v_n\|_{0, \overline{CD}} \\ & + \|v_{nnn}\|_{0, \overline{CD}} \|\epsilon\|_{0, \overline{CD}} + |v_{xy}(B)| |\epsilon(B)| + |v_{xy}(C)| |\epsilon(C)| \}. \end{aligned} \quad (4.4.5)$$

From the Sobolev imbedding theorem [438], there exist the bounds,

$$\|\epsilon\|_{0, \overline{BC} \cup \overline{CD}} \leq C \|\epsilon\|_{2, S}, \quad |\epsilon(B)| \leq C \|\epsilon\|_{2, S}, \quad |\epsilon(C)| \leq C \|\epsilon\|_{2, S}. \quad (4.4.6)$$

Hence from (4.4.3), (4.4.5) and (4.4.6) we have

$$\begin{aligned} \|\epsilon\|_{2, S}^2 & \leq C \{ K_N^* \|v_n\|_{0, \overline{AB}} + K_N \|v - 1\|_{0, \overline{AB}} + K_N^* \|v_n\|_{0, \overline{BC}} + \|v_{nnn}\|_{0, \overline{BC}} \\ & + K_N^* \|v_n\|_{0, \overline{CD}} + \|v_{nnn}\|_{0, \overline{CD}} + |v_{xy}(B)| + |v_{xy}(C)| \} \|\epsilon\|_{2, S}. \end{aligned} \quad (4.4.7)$$

Moreover, from (4.4.4)

$$|v_{xy}(B)| + |v_{xy}(C)| \leq 2K_N^{**} \|v_n\|_{0, \overline{BC}} \leq 2 \frac{K_N^{**}}{w_1} \|\epsilon\|_B. \quad (4.4.8)$$

Combining (4.4.7) and (4.4.8) leads to

$$\begin{aligned} \|\epsilon\|_{2,S} &\leq C\{K_N^* \|v_n\|_{0,\overline{AB}} + K_N \|v-1\|_{0,\overline{AB}} + K_N^* \|v_n\|_{0,\overline{BC}} + \|v_{nnn}\|_{0,\overline{BC}} \\ &\quad + K_N^* \|v_n\|_{0,\overline{CD}} + \|v_{nnn}\|_{0,\overline{CD}}\} + 2K_N^{**}/w_1 \|\epsilon\|_B \\ &\leq C\{K_N + (K_N^* + K_N^{**})/w_1 + 1/w_3\} \|\epsilon\|_B, \end{aligned}$$

where we have used (4.4.2). ■

Note that although the corner condition $v_{xy}(B) = v_{xy}(C)$ is not imposed explicitly on v , it is also satisfied approximately based on Theorem 4.4.1. The analysis for the collocation TM with interior boundary conditions can be made similarly by following Chapter 2 and this chapter. In fact, the assumption (4.4.4) can be obtained by

$$\begin{aligned} |v_{xy}(B)| &\leq |v_{xy}|_{\infty,\overline{BC}} \leq K_1 \|v_n\|_{\frac{3}{2},\overline{BC}} \\ &\leq K_1 K_2 \|v_n\|_{0,\overline{BC}} \leq K_N^{**} \|v_n\|_{0,\overline{BC}}, \end{aligned}$$

where $K_N^{**} = K_1 K_2$. When S is a sector, we can show that $K_N = O(N^2)$, $K_N^* = O(N)$ and $K_N^{**} = O(N^{\frac{3}{2}})$.

4.5 Numerical Experiments

We carry out the collocation TM using the central rule¹ in double precision for these crack models. For Model I, the computed results of errors, condition numbers, the effective condition numbers defined in Chapter 3, and coefficients are given in Tables 4.1 and 4.4 with the numerical asymptotic relations,

$$E_2 = O(0.83^N), \quad \text{Cond.} = O(N^3(\sqrt{2})^N), \quad \text{Cond.}_{\text{eff}} = O(N^3), \quad (4.5.1)$$

where E_2 and Cond. are defined in (4.3.18) and (4.3.19), respectively. For Model II, the results are listed in Tables 4.2 and 4.5, with

$$E_2 = O(0.58^N), \quad \text{Cond.} = O(N^3(\sqrt{2})^N), \quad \text{Cond.}_{\text{eff}} = O(N^3). \quad (4.5.2)$$

Obviously, Model II is better than Model I as a crack model due to higher accuracy. The important leading coefficient d_1 has eight significant digits for $N = M = 30$ in Tables 4.4 and 4.5. Note that the effective condition numbers $\text{Cond.}_{\text{eff}}$ and Cond._{EE} are significantly smaller than Cond. .

Note that for Models I and II, the particular solutions have $v_{xy}(B) \neq 0$ and $v_{xy}(C) \neq 0$. We may also add the corner contribution, $2(1-\mu)w_2^2\{v_{xy}^2(B) + v_{xy}^2(C)\}$, to the energy and carry out the corresponding collocation TM. The numerical solutions obtained are only slightly different from those in Tables 4.4 and 4.5. This fact verifies well the analysis in Section 4.4.

¹By following Chapter 2, we may use the Gaussian rule to raise the accuracy of the leading coefficients.

Next, we carry out the models of Schiff et al. In computation, take parameters $a = 0.4$ and $b = 0.7$ as in [423], and choose the uniform partition on ∂S . Denote by M_1 and M_2 the partitions number of \overline{AB} and \overline{BC} . Tables 4.6 – 4.9 list the computed results. It can be seen that the computed results coincide very well with other methods given in [423, 488].

When parameters $a = b = 1$, the model of Schiff et al. is our Model III with the clamped conditions in (4.3.10) – (4.3.12). The computed results are provided in Tables 4.3 and 4.10. It can be seen that the solutions have slower convergence than those of Models I and II. Interestingly, the leading coefficient of d_1 in Model III for $N = M = 30$ also have seven significant digits, see Table 4.3.

In summary, in this section we have provided the numerical solutions for Models I - III by the collocation TM. The advantage of Model II (as well as Model I) over Model III is that only one crack singularity exists at the origin. Note that in Model III, there may exist a mild singularity at the corners B and C from the clamped boundary condition, see Lefebvre [281], p. 55. We carry out the collocation TM by Mathematica using the decimal working digits ≤ 100 , for Models II and III, and the error curves given in Figures 4.6 and 4.7 display that Model II yields exponential convergent rates, but Model III does not. This fact indicates existence of a corner singularity in Model III. Since Model III provides much larger errors, Models I and II are better and Model II is the best crack model of singularity problems for biharmonic equations.

It is worth pointing out that the approximate solutions of those three models converge slower than those of the Motz's problem in Chapter 2. This result is reasonable because the biharmonic equations are more complicated than Laplace's equation.

4.6 Concluding Remarks

1. The terms $(u_{ns}^+ - u_{ns}^-)v$ at the corners and $u_{ns}v$ at those with the right angles, are developed for the Green formulas of biharmonic equations on polygons. The corner terms coincide with those in Chien [101], also see Remark 4.2.1. These terms are important to the natural corners, to yield the corner condition $u_{ns}^+ = u_{ns}^-$, which indicates in physics that the corner angles of thin plates remain invariant. Also based on the Green formulas, the interior continuity conditions, $u^+ = u^-$, $u_n^+ = u_n^-$, $u_{nn}^+ = u_{nn}^-$ and $u_{nnn}^+ = u_{nnn}^-$ on Γ_0 , can be derived, see [310].
2. Error bounds in Section 4.4 are derived for a brief analysis, which provides a justification for the collocation TM. The computational formulas of partial derivatives of the series solutions in Section 4.3.4 are provided for the collocation TM.
3. In addition, two new crack models I and II are proposed, which resemble Motz's problem in Chapter 2 with only one singularity point. Also Model III results from Schiff et al. [423].
4. The collocation TM (i.e., the BAM) are proposed to provide the most accurate solutions in double precision for these three models. The exponential convergence rates are obtained for Models I and II, but not for Model III. The slow convergence

of Model III indicates the existence of mild corner singularities in the model, which is explored in [213] in detail.

5. Model II with higher convergent rates is recommended for crack models, which leading coefficient d_1 is obtained with eight significant decimal digits. These crack models are important to test numerical methods, and the very accurate solutions given in this chapter may be used as the true solutions, to evaluate errors of other numerical methods, see [291]. For instant, the singular function boundary integral method is explored for fracture problems in Elliotis et al. [143], and numerical comparisons with the solutions in this chapter are made.

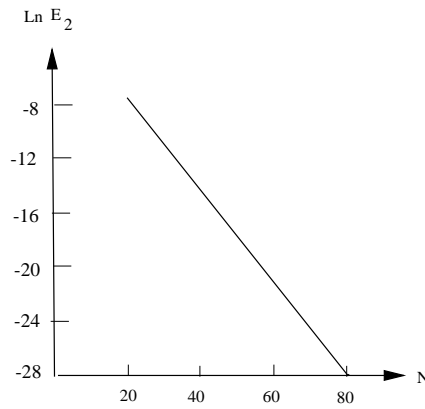


Figure 4.6: The error curves of E_2 from Model II.

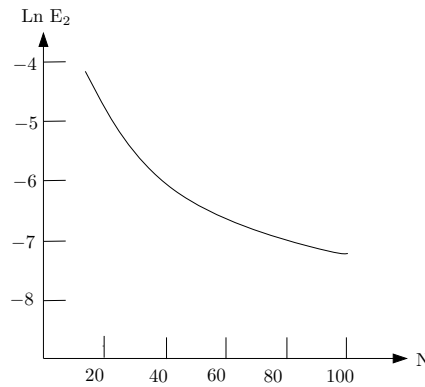


Figure 4.7: The error curves of E_2 from Model III.

N	M	E_2	Cond.	Cond_eff	Cond_EE	d_1	c_1
5	5	0.684(-2)	122	10.1	34.9	1.558314068	0.5439790(-1)
10	10	0.310(-3)	0.525(4)	91.5	279	1.579179739	0.8584309(-1)
15	15	0.172(-4)	0.897(5)	283	881	1.579103462	0.8433073(-1)
20	20	0.211(-5)	0.965(6)	641	0.199(4)	1.579146775	0.8451656(-1)
25	25	0.628(-6)	0.766(7)	0.122(4)	0.378(4)	1.579146331	0.8455956(-1)
30	30	0.292(-6)	0.737(8)	0.206(4)	0.641(4)	1.579144492	0.8455695(-1)
35	35	0.141(-6)	0.718(9)	0.324(4)	0.100(5)	1.579144356	0.8455997(-1)

Table 4.1: The computed results from Model I: the clamped condition on \overline{AB} and the symmetric condition on \overline{BC} .

N	M	E_2	Cond.	Cond_eff	Cond_EE	d_1	c_1
5	5	0.333(-2)	228	41.7	171	0.850292568	-0.1238970
10	10	0.568(-4)	0.678(4)	268	0.114(4)	0.843682925	-0.1339992
15	15	0.280(-5)	0.106(6)	820	0.372(4)	0.843237554	-0.1344272
20	20	0.138(-6)	0.111(7)	0.186(4)	0.876(4)	0.843266263	-0.1344504
25	25	0.330(-8)	0.961(7)	0.355(4)	0.176(5)	0.843265749	-0.1344259
30	30	0.234(-9)	0.958(8)	0.604(4)	0.309(5)	0.843265738	-0.1344254
35	35	0.151(-10)	0.860(9)	0.946(4)	0.481(5)	0.843265743	-0.1344254

Table 4.2: The computed results from Model II: the simply supported condition on \overline{AB} and the symmetric condition on \overline{BC} .

N	M	E_2	Cond.	Cond_eff	Cond_EE	d_1	c_1
5	5	0.382(-1)	75.3	7.67	12.6	2.0562025	0.12853961
10	10	0.112(-2)	0.908(3)	20.9	59.6	2.1270176	0.16689967
15	15	0.205(-3)	0.864(4)	45.6	0.189(4)	2.1275137	0.16675604
20	20	0.510(-4)	0.756(5)	83.4	0.141(4)	2.1275130	0.16676800
25	25	.142(-4)	0.675(6)	135	0.192(5)	2.1275131	0.16676291
30	30	0.622(-5)	0.530(7)	199	0.168(5)	2.1275135	0.16676210

Table 4.3: The computed results from Model III of Schiff et al. [423] with $a = b = 1$.

k	d_k	c_k
1	.157914449154(1)	.845569495127(-1)
2	-.101875081011(1)	.218682879130
3	-.388345996362	.147059328607
4	-.126596391437	.258957626846(-1)
5	-.901531703063(-2)	-.661047276514(-2)
6	-.410342771786(-2)	.692602886653(-2)
7	-.152219180639(-1)	.109004031831(-1)
8	-.105644615332(-1)	.533572185075(-2)
9	-.353330627848(-2)	.128477201276(-2)
10	-.108364832609(-2)	.799088937995(-3)
11	-.932961247848(-3)	.638532919383(-3)
12	-.560626543201(-3)	.321076862256(-3)
13	-.217242844519(-3)	.977392253721(-4)
14	-.883260517136(-4)	.702432472164(-4)
15	-.620368652529(-4)	.324466328939(-4)
16	-.285719771197(-4)	.252039158155(-4)
17	-.232213823882(-4)	.131914570651(-4)
18	-.102940821331(-4)	.666829468399(-5)
19	-.157042167188(-5)	-.394496927639(-5)
20	.320173251469(-5)	.183197951331(-5)
21	-.572645396667(-5)	.504462110589(-5)
22	-.311064327607(-5)	.563661160729(-6)
23	.131511891651(-5)	-.201658325294(-5)
24	.120638425971(-5)	.462845013470(-6)
25	-.155256612338(-5)	.131479847331(-5)
26	-.667684153216(-6)	.383815032080(-7)
27	.230910782803(-6)	-.222247821436(-6)
28	.866642073153(-7)	.784944120044(-7)
29	-.163894984647(-6)	.125626303448(-6)
30	-.631610177158(-7)	.148114879917(-7)

Table 4.4: The computed coefficients from Model I at $N = M = 30$.

k	d_k	c_k
1	.843265737636	-.134425410478
2	-.810315226397(-1)	.555684857969(-2)
3	-.760189138549(-1)	.389434470960(-1)
4	-.406409839309(-1)	.147075362850(-1)
5	-.107965037008(-2)	-.873849200785(-2)
6	.926519150105(-2)	-.352886098194(-2)
7	-.537688211088(-3)	.152504271457(-2)
8	-.159558209100(-2)	.619084537209(-3)
9	-.602403160151(-4)	-.295608460532(-3)
10	.312644128283(-3)	-.136655913609(-3)
11	-.171094471457(-4)	.703637646769(-4)
12	-.746810945381(-4)	.332124185817(-4)
13	-.202261881438(-5)	-.166584246932(-4)
14	.172358111626(-4)	-.770462588631(-5)
15	-.680975685900(-6)	.381985848508(-5)
16	-.393029468513(-5)	.177201776927(-5)
17	-.753002175322(-7)	-.889681257230(-6)
18	.908970763257(-6)	-.413094733348(-6)
19	-.347771312608(-7)	.210684813352(-6)
20	-.212002381035(-6)	.955540479240(-7)
21	-.117653124582(-8)	-.496876236952(-7)
22	.489076758087(-7)	-.212558167696(-7)
23	-.310394116929(-8)	.117984903867(-7)
24	-.106176086258(-7)	.417122852930(-8)
25	.436460058617(-9)	-.242925552763(-8)
26	.209830897613(-8)	-.795430112067(-9)
27	-.244865068337(-9)	.514646524550(-9)
28	-.366636428060(-9)	.883960453604(-10)
29	.436452408457(-10)	-.557222929732(-10)
30	.268911356390(-10)	-.756987886739(-11)

Table 4.5: The computed coefficients from Model II at $N = M = 30$.

N	M_1	M_2	E_2	Cond.	d_1	c_1
7	7	6	0.202(-2)	0.729(3)	-0.12545711	-0.84205789
14	14	16	0.161(-3)	0.724(5)	-0.12650102	-0.94471478
21	21	24	0.237(-4)	0.557(7)	-0.12650639	-0.94411067
28	28	32	0.585(-5)	0.357(9)	-0.12650611	-0.94427916

Table 4.6: The computed results from the model of Schiff et al. [423] with $a = 0.4$ and $b = 0.7$.

x	y	Refinement [423]	Whiteman [488]	collocation TM
-0.1	0.1	20.2	20.2	20.15
0	0.1	146.5	146.6	146.54
0.1	0.1	617.3	617.3	617.28
0.1	0	508.1	508.1	508.11
-0.2	0.2	23.8	23.8	23.82
0	0.3	503.5	503.7	503.59
0.2	0.2	1515.5	1515.5	1515.58
0.3	0.1	2321.8	2321.6	2321.83
-0.2	0.4	123.4	123.4	123.46
0	0.5	722.5	722.8	722.50
0.2	0.4	1703.2	1703.2	1703.21

Table 4.7: Comparison on some nodal solutions from the model of Schiff et al. [423] with $a = 0.4$ and $b = 0.7$.

d_i and c_i	Refinement [423]	Whiteman [488]	collocation TM
d_1	1.2649	1.2651	1.2650611
d_2	-0.9354	-0.9361	-0.9360218
d_3	-0.8013	-0.7985	-0.8010796
d_4	-1.0040	-0.9961	-0.9976181
c_1	-0.0945	-0.0944	-0.0944279
c_2	0.1007	0.1004	0.1011681
c_3	0.4684	0.4603	0.4641121

Table 4.8: Comparison of leading coefficients for the model of Schiff et al. [423] with $a = 0.4$ and $b = 0.7$.

k	d_k	c_k
1	.126506110061(1)	-.944279161457(-1)
2	-.936021839307	.101168072395
3	-.801079627221	.464112132938
4	-.997618091594	.396464688101
5	-.105301853401(1)	.123461423186(1)
6	-.229836599320(1)	.120497827195(1)
7	-.124156774129(1)	.155145289337(1)
8	-.381641467043(1)	.310537969427(1)
9	-.238720411821(1)	.173097719915(1)
10	-.591294036802(1)	.733160209882(1)
11	-.555017829366(1)	.572735184513
12	-.638776268248(1)	.151705915581(2)
13	-.151886092148(2)	-.501804399258
14	-.245308286590(1)	.263242128941(2)
15	-.369114292099(2)	.232732717009(1)
16	.105446614959(2)	.351213245198(2)
17	-.758820662861(2)	.223936816349(2)
18	.268975706382(2)	.324998364448(2)
19	-.125018972003(3)	.735139264579(2)
20	.245844631003(2)	.166808451244(2)
21	-.157558912596(3)	.143594590248(3)
22	-.156534339595(2)	.268733725020(1)
23	-.145629281481(3)	.184742907459(3)
24	-.750616959430(2)	.742968495770(1)
25	-.904763921775(2)	.149922923157(3)
26	-.938412699634(2)	.194247065221(2)
27	-.303834486338(2)	.646114763546(2)
28	-.535812083701(2)	.174429927114(2)

Table 4.9: The computed coefficients from the model of Schiff et al. [423] with $a = 0.4$ and $b = 0.7$.

k	d_k	c_k
1	.212751351189(1)	.166762096608
2	-.103669248813(1)	.624433242670(-1)
3	.371710686206(-1)	-.132473844421
4	.117748896104	-.102209420793(-1)
5	-.122728218338	.105845606844
6	-.109908664317	.311525254876(-1)
7	-.225523569851(-2)	-.714919699164(-2)
8	.686312696358(-2)	-.168432409440(-2)
9	-.593565985657(-2)	.948384227186(-2)
10	-.110320364140(-1)	.428077318143(-2)
11	-.372990401057(-3)	-.251437034002(-3)
12	-.434606261276(-3)	.300065928400(-3)
13	.395471328942(-3)	-.279833704674(-3)
14	-.363701441420(-3)	.415900781575(-3)
15	.849752152135(-4)	-.394160763591(-3)
16	.164814091626(-3)	.137207394892(-3)
17	-.134885562580(-3)	.114185322520(-4)
18	-.661256038945(-4)	.128433796144(-3)
19	-.442704344901(-4)	-.895164048915(-4)
20	.881231488859(-4)	.101254396117(-4)
21	-.513612091552(-4)	.237215483998(-4)
22	-.185089281333(-4)	.287229819371(-4)
23	-.110577269133(-4)	-.290039116621(-4)
24	.383799694523(-4)	-.783857638552(-5)
25	-.193733376681(-4)	.200879527653(-4)
26	-.123722918845(-4)	.597917917868(-5)
27	-.218094975397(-5)	-.273563392080(-5)
28	.496907945145(-5)	-.185227194727(-5)
29	-.211257805760(-5)	.303478369806(-5)
30	-.189383438010(-5)	.462805951252(-6)

Table 4.10: The computed coefficients for Model III of Schiff et al. [423] with $a = b = 1$ at $N = 30$ and $M = 30$.

*What is reasonable is real;
that which is real is reasonable.*
——— *Philosophy of Right (1821)* ———

*Georg Wilhelm Friedrich Hegel
(1770-1831)*

Part II

Collocation Methods

In fact, the collocation method (CM) can be classified into the category of the domain-type solution procedures. Compared with other domain-type methods such as FEM, FDM and FVM, CM is much easier to perform due to its simplicity in numerical algorithms. It is known that many methods have been developed to approximate the solutions of PDEs. Since the FEM has been developed in both wide applications and deep theoretical analysis, we employ the FEM theory in Ciarlet [105] and Oden and Reddy [365], to explore the theoretical framework of the CM and its combinations with other methods. Because the solution domains of problems will not be confined in polygons, domain decomposition approach can be taken into account. We may divide the domain into several small subdomains.

If the admissible functions are chosen to be analytical functions, e.g., trigonometric or other orthogonal functions, we may enforce them to satisfy exactly the PDEs at certain collocation nodes, by simply letting the residuals to be zero. This leads to the collocation method. The traditional CM has been described in a number of books: Bernardi and Maday [37], Canuto et al. [75], Gottlieb and Orszag [178], Li [291], Quarteroni and Valli [392] and Mercier [350]. We here also mention several important studies of CM. Bernardi et al. [36] provided a coupling finite element method and spectral method with two kinds of matching conditions on interface. Shen [429, 430, 431] gave a series of research study on spectral-Galerkin methods for elliptic equations. Haidvogel [191] applied double Chebyshev polynomials to Poisson's equation. Yin [499] used the Sinc-collocation method to singular Poisson-like problems. Other reports on CM are given by Arnold and Wendland [6], Canuto et al. [74], Pathria and Karniadakis [377], and Sneddon [437].

In this part, a new unified framework of combination of CM with other methods such as FEM, etc. will be analyzed. For the smooth solutions of problems, polynomials of different degree can be chosen to approximate the solutions properly. Besides, different kinds of admissible functions can be chosen such as orthogonal polynomials [37, 75], trigonometric functions [178], radial basis functions [247, 248], the Sinc functions [447] and particular solutions [291]. Using different admissible functions is more flexible for CM to apply the practical problems and to easily fit those on rather arbitrary domains.

This part consists of three chapters:

Chapter 5: Collocation Methods.

Chapter 6: Combinations of Collocation and Finite Element Methods.

Chapter 7: Radical Basis Collocation Methods.

The contents of this part are adopted mainly from [216, 217, 218, 219]. A brief description is given as follows.

Chapter 5 presents the generalized collocation methods, in which the piecewise admissible functions are used. Besides, the CM for the Robin boundary conditions is discussed. Three typical boundary conditions, Dirichlet, Neumann and Robin, can be handled well in the CM. Moreover, the collocation Trefftz methods in Part I is, in fact, the special

cases of the CM. Some numerical experiments for smooth and singularity problems are given to verify the analysis.

Chapter 6 provides a framework of combinations of collocation methods with the finite element method. The optimal convergence rates can be achieved, where the quadrature formulas play a role only in satisfying the uniformly V_h - elliptic inequality, because the higher order quadrature formulas do not improve much accuracy.

Chapter 7 is a sequential study for previous two chapters. We apply the radial basis functions (RBFs) to CM, simply denoted by RBCM. One important development is to apply RBFs for PDEs, while most of the existing literatures of RBFs deal with surface fitting and functional approximation. The optimal error bounds are derived; the important inverse inequalities are derived, although the entire approaches of proofs are similar to those in Chapters 4 and 5. Some numerical examples are given to display the effectiveness of the RBCM as well.

Chapter 5

Collocation Methods

In Chapters 1 - 4, the collocation method (CM) has been employed only on the boundary conditions. In Chapter 5 - 7, we employ the collocation method both in the solution domain and on its boundaries. Hence, orthogonal polynomials, trigonometric functions, radial basis functions, special functions, etc. can also be considered as the admissible functions that do not satisfy the partial differential equations. The collocation method in this part can be viewed as the collocation spectral method, or the collocation Ritz-Galerkin method, see [291]. In this chapter, we provide an analysis on the CM, which uses a broad range admissible functions such as orthogonal polynomials, trigonometric functions, radial basis functions and particular solutions, etc. The admissible functions can be chosen to be *piecewise*, i.e., different functions are used in different subdomains. The key idea is that the collocation method can be regarded as the least squares method involving integration approximation, and optimal convergence rates can be easily achieved from the traditional analysis of the finite element method. The key analysis is to prove the uniformly V_h - elliptic inequality and some inverse inequalities used. This chapter explores the interesting fact that for the collocation methods in this chapter, the integration rules only affect the uniformly V_h - elliptic inequality, but not on the solution accuracy. The advantage of the CM is to formulate easily the collocation equations as the associated algebraic equations, which can be solved directly by the least squares method, thus to greatly reduce the condition number of the stiffness matrix. Note that the boundary approximation method (BAM) in Li [291] and the CTM in Part I are a special case of the CM, where the admissible functions satisfy the governing equations exactly. Numerical experiments are also carried for Poisson's problem to support the analysis made.

5.1 Introduction

In this chapter, we present a new analysis of CM by following the ideas in Li [291] that every numerical method can be regarded as a special kind of the Ritz-Galerkin method. The CM is, indeed, the least squares method, which is treated as the Ritz-Galerkin method involving integration approximation. The advantages of the CM are twofold: (1) flexibility of application to different geometric shapes and different elliptic equations,

and (2) simplicity of computer programming. The optimal error bounds can be easily derived, based on the uniformly V_h - elliptic inequality, which is proved in detail in this chapter.

This chapter is organized as follows. In the next section, the collocation method with an interior interface is described, and in Section 5.3 an analysis is given. In Section 5.4 the CM for the Robin boundary conditions is discussed, and in Section 5.5, some inverse inequalities are provided. In the last section, the numerical experiments including singularity problems are carried out to support the analysis made.

5.2 Description of Collocation Methods

Consider Poisson's equation on domain S with the mixed type of the Dirichlet and Neumann conditions,

$$-\Delta u = -\left(\frac{\partial^2 u}{\partial x^2} + \frac{\partial^2 u}{\partial y^2}\right) = f(x, y) \quad \text{in } S, \quad (5.2.1)$$

$$u|_{\Gamma_D} = g_1 \quad \text{on } \Gamma_D, \quad (5.2.2)$$

$$u_\nu|_{\Gamma_N} = g_2 \quad \text{on } \Gamma_N, \quad (5.2.3)$$

where S is a polygon, $\partial S = \Gamma = \Gamma_D \cup \Gamma_N$ is its boundary, $u_\nu = \frac{\partial u}{\partial \nu}$, and ν is the unit outnormal to ∂S . Let S be divided by Γ_0 into two disjoint subregions, S_1 and S_2 (see Figure 5.1): $S = S_1 \cup S_2 \cup \Gamma_0$ and $S_1 \cap S_2 = \emptyset$. We give a few assumptions.

A1: The solutions in S_1 and S_2 can be expanded as

$$v = \begin{cases} v^- = \sum_{i,j=1}^{\infty} a_{ij} \Phi_i(x) \Phi_j(y) & \text{in } S_1, \\ v^+ = \sum_{i,j=1}^{\infty} b_{ij} \Psi_i(x) \Psi_j(y) & \text{in } S_2, \end{cases} \quad (5.2.4)$$

where $\{\Phi_i(x)\Phi_j(y)\}$ and $\{\Psi_i(x)\Psi_j(y)\}$ are complete and independent bases in S_1 and S_2 respectively, and a_{ij} and b_{ij} are the expansion coefficients.

A2: The basis functions

$$\Phi_i(x)\Phi_j(y) \in C^2(S_1) \cap C^1(\partial S_1), \quad \Psi_i(x)\Psi_j(y) \in C^2(S_2) \cap C^1(\partial S_2).$$

A3: The expansions in (5.2.4) converge exponentially to the true solutions u^\pm . Let

$$u^- = u_m^- + R_m^-, \quad u^+ = u_n^+ + R_n^+,$$

where $u^- = u|_{S_1}$ and $u^+ = u|_{S_2}$, and

$$u_m^- = \sum_{i,j=1}^m a_{ij} \Phi_i(x) \Phi_j(y), \quad u_n^+ = \sum_{i,j=1}^n b_{ij} \Psi_i(x) \Psi_j(y),$$

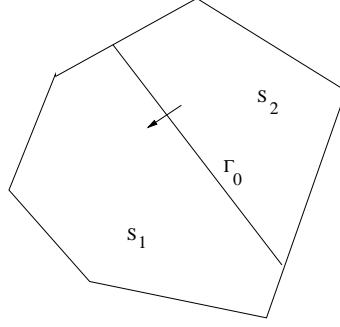


Figure 5.1: Partition of a convex polygon.

R_m^- and R_n^+ are the remainders, and a_{ij} and b_{ij} are the true expansion coefficients. Then

$$\max_{S_1} |R_m^-| = O(e^{-\bar{c}m}), \quad \max_{S_2} |R_n^+| = O(e^{-\bar{c}n}), \quad (5.2.5)$$

where $\bar{c} > 0$, $m > 1$ and $n > 1$.

Based on **A1-A3** we may choose the *piecewise* admissible functions,

$$v = \begin{cases} v^- = \sum_{i,j=1}^m \tilde{a}_{ij} \Phi_i(x) \Phi_j(y) & \text{in } \bar{S}_1, \\ v^+ = \sum_{i,j=1}^n \tilde{b}_{ij} \Psi_i(x) \Psi_j(y) & \text{in } \bar{S}_2, \end{cases} \quad (5.2.6)$$

where \tilde{a}_{ij} and \tilde{b}_{ij} are unknown coefficients to be sought, and $\bar{S}_i = S_i \cup \partial S_i$. Since v on Γ_0 are not continuous, v^\pm have to satisfy the interior continuity conditions

$$u^+ = u^-, \quad u_\nu^+ = u_\nu^-, \quad \text{on } \Gamma_0, \quad (5.2.7)$$

where $u_\nu = \frac{\partial u}{\partial \nu}$, and ν is the outward unit normal of ∂S_2 .

Based on **A2** we may seek the coefficients \tilde{a}_{ij} and \tilde{b}_{ij} by satisfying (5.2.1), (5.2.2), (5.2.3) and (5.2.7) directly at nodes Q_{ij} and Q_i ,

$$(\Delta v^\pm + f)(Q_{ij}^\pm) = 0, \quad Q_{ij}^\pm \in S^\pm, \quad (5.2.8)$$

$$(v - g_1)(Q_i) = 0, \quad Q_i \in \Gamma_D, \quad (5.2.9)$$

$$(v_\nu - g_2)(Q_i) = 0, \quad Q_i \in \Gamma_N, \quad (5.2.10)$$

$$(v^+ - v^-)(Q_i) = 0, \quad Q_i \in \Gamma_0, \quad (5.2.11)$$

$$(v_\nu^+ - v_\nu^-)(Q_i) = 0, \quad Q_i \in \Gamma_0, \quad (5.2.12)$$

where v^\pm also denotes $v^\pm|_{\Gamma_0}$, $S^- = S_1$ and $S^+ = S_2$. Eqs. (5.2.8) – (5.2.12) can be expressed by the linear algebraic equations,

$$\mathbf{F}\mathbf{x} = \mathbf{b}, \quad (5.2.13)$$

where \mathbf{x} is the unknown vector consisting of \tilde{a}_{ij} and \tilde{b}_{ij} , \mathbf{b} is the known vector, and $\mathbf{F} \in R^{M \times (m^2 + n^2)}$, where $M (\geq m^2 + n^2)$ is the total number of collocation nodes Q_{ij}^\pm in S^\pm , and Q_i on $\Gamma_D \cup \Gamma_N \cup \Gamma_0$. In this chapter, we always choose $M > (m^2 + n^2)$ and even $M \gg (m^2 + n^2)$. Then (5.2.13) is an over-determined system of linear algebraic equations. Hence we may use the least squares method (i.e. the QR method or the singular value decomposition (SVD) method) for solving (5.2.13), see Golub and Loan [176].

Below, let us view the CM as the least squares method involving integration approximation. Denote V_h the finite dimensional collection of the admissible functions (5.2.6). We give one more assumption.

A4: Suppose that there exists a positive constant $\mu (> 0)$ such that

$$\|v_\nu^\pm\|_{0, \Gamma_D \cap \bar{S}^\pm} \leq CL^\mu \|v^\pm\|_{1, S^\pm}, \quad v \in V_h, \quad (5.2.14)$$

$$\|v_\nu^+\|_{0, \Gamma_0 \cap \bar{S}^+} \leq CL^\mu \|v^+\|_{1, S^+}, \quad v \in V_h. \quad (5.2.15)$$

For polynomials of degree L , we will prove (5.2.14) and (5.2.15) with $\mu = 2$ in Section 5.5.

Then the approximate coefficients \tilde{a}_{ij} and \tilde{b}_{ij} can be obtained by the least squares methods: To seek the approximation solution $u_{m,n} \in V_h$ such that

$$E(u_{m,n}) = \min_{v \in V_h} E(v),$$

where

$$\begin{aligned} E(v) = & \frac{1}{2} \left\{ \iint_{S_1} (\Delta v^- + f)^2 + \iint_{S_2} (\Delta v^+ + f)^2 \right. \\ & + L^{2\mu} \int_{\Gamma_0} (v^+ - v^-)^2 + \int_{\Gamma_0} (v_\nu^+ - v_\nu^-)^2 \\ & \left. + L^{2\mu} \int_{\Gamma_D} (v - g_1)^2 + \int_{\Gamma_N} (v_\nu - g_2)^2 \right\}, \end{aligned} \quad (5.2.16)$$

where $L = \max\{m, n\}$, and ν is also the outward unit normal to ∂S_2 . Eq. (5.2.16) can be described equivalently

$$a(u_{m,n}, v) = f(v), \quad \forall v \in V_h, \quad (5.2.17)$$

where

$$\begin{aligned} a(u, v) = & \iint_{S_1} \Delta u \Delta v + \iint_{S_2} \Delta u \Delta v \\ & + L^{2\mu} \int_{\Gamma_0} (u^+ - u^-)(v^+ - v^-) + \int_{\Gamma_0} (u_\nu^+ - u_\nu^-)(v_\nu^+ - v_\nu^-) \\ & + L^{2\mu} \int_{\Gamma_D} uv + \int_{\Gamma_N} u_\nu v_\nu, \\ f(v) = & - \iint_{S_1} f \Delta v - \iint_{S_2} f \Delta v + L^{2\mu} \int_{\Gamma_D} g_1 v + \int_{\Gamma_N} g_2 v_\nu. \end{aligned} \quad (5.2.18)$$

The integrals in (5.2.18) can be approximated by some rules of integration:

$$\begin{aligned}
\widehat{\int\int}_{S^\pm} g &= \sum_{ij} \alpha_{ij}^\pm g(Q_{ij}^\pm), \quad Q_{ij}^\pm \in S^\pm, \\
\widehat{\int}_{\Gamma_0} g &= \sum_i \alpha_i g(Q_i), \quad Q_i \in \Gamma_0, \\
\widehat{\int}_{\Gamma_D} g &= \sum_i \alpha_i^D g(Q_i), \quad Q_i \in \Gamma_D, \\
\widehat{\int}_{\Gamma_N} g &= \sum_i \alpha_i^N g(Q_i), \quad Q_i \in \Gamma_N,
\end{aligned} \tag{5.2.19}$$

where $\alpha_{ij}^\pm, \alpha_i, \alpha_i^D$ and α_i^N are positive weights, and Q_{ij}^\pm and Q_i are integration nodes. The least squares method (5.2.17) is then reduced to

$$\hat{a}(\hat{u}_{m,n}, v) = \hat{f}(v), \quad \forall v \in V_h, \tag{5.2.20}$$

where

$$\begin{aligned}
\hat{a}(u, v) &= \widehat{\int\int}_{S_1} \Delta u \Delta v + \widehat{\int\int}_{S_2} \Delta u \Delta v \\
&+ L^{2\mu} \widehat{\int}_{\Gamma_0} (u^+ - u^-)(v^+ - v^-) + \widehat{\int}_{\Gamma_0} (u_\nu^+ - u_\nu^-)(v_\nu^+ - v_\nu^-) \\
&+ L^{2\mu} \widehat{\int}_{\Gamma_D} uv + \widehat{\int}_{\Gamma_N} u_\nu v_\nu, \\
\hat{f}(v) &= -\widehat{\int\int}_{S_1} f \Delta v - \widehat{\int\int}_{S_2} f \Delta v + L^{2\mu} \widehat{\int}_{\Gamma_D} g_1 v + \widehat{\int}_{\Gamma_N} g_2 v_\nu.
\end{aligned}$$

It is easy to see that by the rules (5.2.19), the following algebraic equations can be obtained from (5.2.20) directly,

$$\sqrt{\alpha_{ij}^\pm} (\Delta v^\pm + f)(Q_{ij}^\pm) = 0, \quad Q_{ij}^\pm \in S^\pm, \tag{5.2.21}$$

$$\sqrt{\alpha_i} L^\mu (v^+ - v^-)(Q_i) = 0, \quad Q_i \in \Gamma_0, \tag{5.2.22}$$

$$\sqrt{\alpha_i} (v_\nu^+ - v_\nu^-)(Q_i) = 0, \quad Q_i \in \Gamma_0, \tag{5.2.23}$$

$$\sqrt{\alpha_i^D} L^\mu (v - g_1)(Q_i) = 0, \quad Q_i \in \Gamma_D, \tag{5.2.24}$$

$$\sqrt{\alpha_i^N} (v_\nu - g_2)(Q_i) = 0, \quad Q_i \in \Gamma_N. \tag{5.2.25}$$

Compared with (5.2.8) – (5.2.12), Eqs. (5.2.21) – (5.2.25) can be denoted by

$$\mathbf{W}\mathbf{F}\mathbf{x} = \mathbf{W}\mathbf{b},$$

where \mathbf{F} is given in (5.2.13), and $\mathbf{W} \in R^{M \times M}$ is the diagonal weight matrix, consisting of the weights, $\sqrt{\alpha_{ij}^\pm}$, $L^\mu \sqrt{\alpha_i}$, $\sqrt{\alpha_i}$, $L^\mu \sqrt{\alpha_i^D}$ and $\sqrt{\alpha_i^N}$. We may also obtain the coefficients (i.e., \mathbf{x}) by solving the normal equations:

$$\mathbf{A}\mathbf{x} = \mathbf{b}^*,$$

where matrix $\mathbf{A} = \mathbf{F}^T \mathbf{W}^T \mathbf{W} \mathbf{F}$ is symmetric and positive definite, and the known vector $\mathbf{b}^* = \mathbf{F}^T \mathbf{W}^T \mathbf{W} \mathbf{b}$.

5.3 Error Analysis

We will provide the error bounds for the solutions from (5.2.17) and (5.2.20). Denote the space

$$H^* = \{v \mid v \in L^2(S), v^\pm \in H^1(S^\pm), \Delta v^\pm \in L^2(S^\pm)\},$$

accompanied with the norm

$$\begin{aligned} \|v\|_H = & \{ \|v\|_1^2 + \|\Delta v\|_{0,S_1}^2 + \|\Delta v\|_{0,S_2}^2 + L^{2\mu} \|v^+ - v^-\|_{0,\Gamma_0}^2 \\ & + \|v_\nu^+ - v_\nu^-\|_{0,\Gamma_0}^2 + L^{2\mu} \|v\|_{0,\Gamma_D}^2 + \|v_\nu\|_{0,\Gamma_N}^2 \}^{1/2}, \end{aligned}$$

where

$$\|v\|_1 = \{ \|v\|_{1,S_1}^2 + \|v\|_{1,S_2}^2 \}^{1/2}, \quad |v|_1 = \{ |v|_{1,S_1}^2 + |v|_{1,S_2}^2 \}^{1/2},$$

and $\|v\|_{1,S_1}$, $\|v\|_{0,\Gamma_0}$, etc. are the Sobolev norms [438]. Obviously, $V_h \subset H^*$. Then

$$\|v\|_H^2 = \|v\|_1^2 + a(v, v).$$

Now we have a theorem.

Theorem 5.3.1 *Suppose that there exist two inequalities,*

$$a(u, v) \leq C \|u\|_H \times \|v\|_H, \quad \forall v \in V_h, \quad (5.3.1)$$

$$a(v, v) \geq C_0 \|v\|_H^2, \quad \forall v \in V_h, \quad (5.3.2)$$

where $C_0 (> 0)$ and C are two constants independent of m and n . Then, the solution of the least squares method (5.2.17) has the error bound,

$$\|u - u_{m,n}\|_H = C \inf_{v \in V_h} \|u - v\|_H \quad (5.3.3)$$

$$\leq \varepsilon_1 = \|R_m^-\|_{2,S_1} + \|R_n^+\|_{2,S_2} + L^\mu \|R_L\|_{0,\Gamma_D \cup \Gamma_0} + \|(R_L)_\nu\|_{0,\Gamma_N \cup \Gamma_0},$$

where $|R_L| = |R_m^-| + |R_n^+|$.

Proof For the true solution, we have $a(u, v) = f(v)$, $\forall v \in V_h$. Then

$$a(u - u_{m,n}, v) = 0, \quad \forall v \in V_h. \quad (5.3.4)$$

Denote the projection solution on V_h

$$u_I = \begin{cases} u_I^- = \sum_{i,j=1}^m a_{ij} \Phi_i(x) \Phi_j(y) & \text{in } \bar{S}_1, \\ u_I^+ = \sum_{i,j=1}^n b_{ij} \Psi_i(x) \Psi_j(y) & \text{in } \bar{S}_2, \end{cases}$$

where a_{ij} and b_{ij} are the true expansion coefficients. Then $u_I \in V_h$. Let $v \in V_h$, and $w = u_{m,n} - v \in V_h$. We have from (5.3.2), (5.3.4) and (5.3.1)

$$\begin{aligned} C_0 \|w\|_H^2 &\leq a(u_{m,n} - v, w) = a(u - v, w) \\ &\leq C \|u - v\|_H \|w\|_H. \end{aligned}$$

This leads to

$$\|u_{m,n} - v\|_H = \|w\|_H \leq C \|u - v\|_H.$$

Then we obtain

$$\|u_{m,n} - u\|_H \leq \|u_{m,n} - v\|_H + \|u - v\|_H \leq C \|u - v\|_H,$$

and

$$\|u_{m,n} - u\|_H \leq C \inf_{v \in V_h} \|u - v\|_H.$$

Let $v = u_I$ we have

$$\begin{aligned} \|u_{m,n} - u\|_H &\leq C \inf_{v \in V_h} \|u - v\|_H \leq C \|u - u_I\|_H \\ &\leq C \{ \|R_m^-\|_{2,S_1} + \|R_n^+\|_{2,S_2} + L^\mu \|R_L\|_{0,\Gamma_D \cup \Gamma_0} + \|(R_L)_\nu\|_{0,\Gamma_N \cup \Gamma_0} \}. \blacksquare \end{aligned}$$

Since the solution u of (5.2.1) – (5.2.3) satisfies (5.2.21) – (5.2.25) exactly, then

$$\hat{a}(u, v) = \hat{f}(v), \quad \forall v \in V_n. \quad (5.3.5)$$

We can also prove the following theorem similarly, see Ciarlet [105] and Strang and Fix [446].

Theorem 5.3.2 *Suppose that there exist two inequalities*

$$\begin{aligned} \hat{a}(u, v) &\leq C \|u\|_H \times \|v\|_H, \quad \forall v \in V_h, \\ \hat{a}(v, v) &\geq C_0 \|v\|_H^2, \quad \forall v \in V_h, \end{aligned} \quad (5.3.6)$$

where $C_0 (> 0)$ and C are two constants independent of m and n . Then, the solution of the collocation method (5.2.20) has the error bound,

$$\|u - \hat{u}_{m,n}\|_H = C \inf_{v \in V_h} \|u - v\|_H \leq \varepsilon_1,$$

where ε_1 is given in (5.3.3).

Note that for the FEM, FDM, etc., the true solution does not satisfy (5.3.5), then Theorem 5.3.2 may not hold. Also, the analysis in this chapter is different from the traditional analysis in the collocation method in [37, 75, 178, 350, 392] where only the zeros of polynomials are used as the collocation nodes.

Below we prove the uniformly V_h - elliptic inequalities (5.3.2) and (5.3.6). We cite Lemma 1.1.1.

Lemma 5.3.1 *Let $\Gamma_D \cap S^- \neq \emptyset$. If $v \in H^*$, then there exists a positive constant C independent of v such that*

$$\|v\|_1 \leq C \{ |v|_1 + \|v\|_{0,\Gamma_D} + \|v^+ - v^-\|_{0,\Gamma_0} \}.$$

Lemma 5.3.2 *Let **A4** be given, and $\Gamma_D \cap S_1 \neq \emptyset$. There exists the bound for all $v \in V_h$,*

$$C_0 \|v\|_1^2 \leq a(v, v), \quad (5.3.7)$$

where $C_0(> 0)$ is a constant independent of m and n .

Proof We have

$$\begin{aligned} |v|_1^2 &= \iint_{S_1} |\nabla v|^2 + \iint_{S_2} |\nabla v|^2 & (5.3.8) \\ &= - \iint_{S_1} v \Delta v - \iint_{S_2} v \Delta v + \int_{\partial S_1} v_\nu^- v^- + \int_{\partial S_2} v_\nu^+ v^+ \\ &= - \iint_{S_1} v \Delta v - \iint_{S_2} v \Delta v + \int_{\Gamma_0} (v_\nu^+ v^+ - v_\nu^- v^-) + \int_{\Gamma_D} v_\nu v + \int_{\Gamma_N} v_\nu v, \end{aligned}$$

where ν is the unit outnormal to ∂S or ∂S_2 . Below, we give the bounds of all terms on the right hand side in the above equation.

First we have from (5.2.15)

$$\begin{aligned} \left| \int_{\Gamma_0} (v_\nu^+ v^+ - v_\nu^- v^-) \right| &\leq \left| \int_{\Gamma_0} (v^+ - v^-) v_\nu^+ \right| + \left| \int_{\Gamma_0} (v_\nu^+ - v_\nu^-) v^- \right| & (5.3.9) \\ &\leq \|v^+ - v^-\|_{0,\Gamma_0} \|v_\nu^+\|_{0,\Gamma_0} + \|v_\nu^+ - v_\nu^-\|_{0,\Gamma_0} \|v^-\|_{0,\Gamma_0} \\ &\leq C \{ L^\mu \|v^+ - v^-\|_{0,\Gamma_0} + \|v_\nu^+ - v_\nu^-\|_{0,\Gamma_0} \} \|v\|_1, \end{aligned}$$

where we have used the bounds,

$$\|v^-\|_{0,\Gamma_0} \leq \|v^-\|_{1,S^-}, \quad \|v^\pm\|_{1,S^\pm} \leq \|v\|_1.$$

Next, we obtain from (5.2.14)

$$\left| \int_{\Gamma_D} v_\nu v \right| \leq \|v\|_{0,\Gamma_D} \|v_\nu\|_{0,\Gamma_D} \leq CL^\mu \|v\|_{0,\Gamma_D} \|v\|_1, \quad (5.3.10)$$

$$\left| \int_{\Gamma_N} v_\nu v \right| \leq \|v_\nu\|_{0,\Gamma_N} \|v\|_{0,\Gamma_N} \leq C \|v_\nu\|_{0,\Gamma_N} \|v\|_1. \quad (5.3.11)$$

Moreover, there exist the bounds,

$$|\iint_{S_1} v \Delta v| \leq \|\Delta v\|_{0,S_1} \|v\|_{0,S_1} \leq \|\Delta v\|_{0,S_1} \|v\|_1, \quad (5.3.12)$$

$$|\iint_{S_2} v \Delta v| \leq \|\Delta v\|_{0,S_2} \|v\|_1. \quad (5.3.13)$$

From (5.3.8) – (5.3.13),

$$\begin{aligned} |v|_1^2 &\leq \{\|\Delta v\|_{0,S_1} + \|\Delta v\|_{0,S_2} \\ &+ CL^\mu(\|v^+ - v^-\|_{0,\Gamma_0} + \|v\|_{0,\Gamma_D}) + \|v_\nu^+ - v_\nu^-\|_{0,\Gamma_0} + \|v_\nu\|_{0,\Gamma_N}\} \|v\|_1. \end{aligned} \quad (5.3.14)$$

Hence we have from Lemma 5.3.1

$$\begin{aligned} \|v\|_1^2 &\leq C\{|v|_1^2 + \|v\|_{0,\Gamma_D}^2 + \|v^+ - v^-\|_{0,\Gamma_0}^2\} \\ &\leq C\{|v|_1^2 + (\|v\|_{0,\Gamma_D} + \|v^+ - v^-\|_{0,\Gamma_0})\|v\|_1\}. \end{aligned} \quad (5.3.15)$$

Combining (5.3.14) and (5.3.15) gives

$$\begin{aligned} \|v\|_1^2 &\leq C\{\|\Delta v\|_{0,S_1} + \|\Delta v\|_{0,S_2} \\ &+ L^\mu(\|v^+ - v^-\|_{0,\Gamma_0} + \|v\|_{0,\Gamma_D}) + \|v_\nu^+ - v_\nu^-\|_{0,\Gamma_0} + \|v_\nu\|_{0,\Gamma_N}\} \|v\|_1. \end{aligned}$$

This leads to

$$\begin{aligned} \|v\|_1 &\leq C\{\|\Delta v\|_{0,S_1} + \|\Delta v\|_{0,S_2} \\ &+ L^\mu(\|v^+ - v^-\|_{0,\Gamma_0} + \|v\|_{0,\Gamma_D}) + \|v_\nu^+ - v_\nu^-\|_{0,\Gamma_0} + \|v_\nu\|_{0,\Gamma_N}\}, \end{aligned}$$

and then

$$\begin{aligned} \|v\|_1^2 &\leq C\{\|\Delta v\|_{0,S_1}^2 + \|\Delta v\|_{0,S_2}^2 \\ &+ L^{2\mu}(\|v^+ - v^-\|_{0,\Gamma_0}^2 + \|v\|_{0,\Gamma_D}^2) + \|v_\nu^+ - v_\nu^-\|_{0,\Gamma_0}^2 + \|v_\nu\|_{0,\Gamma_N}^2\} = Ca(v, v). \end{aligned}$$

This is the desired result (5.3.7). ■

Theorem 5.3.3 *Let **A4** and $\Gamma_D \cap \partial S_1 \neq \emptyset$ hold. Then there exists the uniformly V_h -elliptic inequality (5.3.2).*

Proof From Lemma 5.3.2, we have the bound,

$$\begin{aligned} a(v, v) &= \frac{1}{2}a(v, v) + \frac{1}{2}a(v, v) \geq C_0\|v\|_1^2 + \frac{1}{2}\{\|\Delta v\|_{0,S_1}^2 + \|\Delta v\|_{0,S_2}^2 \\ &+ L^{2\mu}(\|v^+ - v^-\|_{0,\Gamma_0}^2 + \|v\|_{0,\Gamma_D}^2) + \|v_\nu^+ - v_\nu^-\|_{0,\Gamma_0}^2 + \|v_\nu\|_{0,\Gamma_N}^2\} \\ &\geq \bar{C}_0\|v\|_H^2, \end{aligned}$$

where $\bar{C}_0 = \min\{\frac{1}{2}, C_0\}$. ■

Next, we derive the uniformly V_h - elliptic inequality (5.3.6). We need a stronger assumption than **A4**.

A5: Suppose that there exists a positive constant $\mu(> 0)$ such that for $v \in V_h$

$$\begin{aligned} \|v^\pm\|_{k, \Gamma_D \cap \bar{S}^\pm} &\leq CL^{k\mu} \|v^\pm\|_{0, \Gamma_D \cap S^\pm}, \\ \|v^\pm\|_{k, \Gamma_0} &\leq CL^{k\mu} \|v^\pm\|_{0, \Gamma_0}, \\ \|v_\nu^\pm\|_{k, \Gamma_N \cap \bar{S}^\pm} &\leq CL^{(k+1)\mu} \|v^\pm\|_{1, S^\pm}, \\ \|v_\nu^\pm\|_{k, \Gamma_0 \cap \bar{S}^\pm} &\leq CL^{(k+1)\mu} \|v^\pm\|_{1, S^\pm}, \end{aligned} \quad (5.3.16)$$

where $k = 0, 1, \dots$. We will give an analysis for the integration approximation. Take $\widehat{\int}_{\Gamma_0} (v_\nu^+ - v_\nu^-)^2$ as example. Choose the integral rule of order r ,

$$\widehat{\int}_{\Gamma_0} g = \int_{\Gamma_0} \hat{g}, \quad (5.3.17)$$

where \hat{g} is the interpolant polynomial of g with order r on the partition of Γ_0 with the maximal meshspacing h . Denote

$$\overline{\|v\|_{0, \Gamma_0}^2} = \widehat{\int}_{\Gamma_0} v^2.$$

We have the following lemma.

Lemma 5.3.3 *Let (5.3.16) be given. For rule (5.3.17) with order r , there exists the bound for $v \in V_h$,*

$$| \overline{\|v_\nu^+ - v_\nu^-\|_{0, \Gamma_0}^2} - \|v_\nu^+ - v_\nu^-\|_{0, \Gamma_0}^2 | \leq Ch^{r+1} L^{(r+3)\mu} \|v\|_1^2. \quad (5.3.18)$$

Proof Let $g = (v_\nu^+ - v_\nu^-)^2$. We have

$$\begin{aligned} | \overline{\|v_\nu^+ - v_\nu^-\|_{0, \Gamma_0}^2} - \|v_\nu^+ - v_\nu^-\|_{0, \Gamma_0}^2 | &= | \int_{\Gamma_0} (\hat{g} - g) | \\ &\leq Ch^{r+1} |g|_{r+1, \Gamma_0}, \end{aligned} \quad (5.3.19)$$

where

$$\begin{aligned} |g|_{r+1, \Gamma_0} &= |(v_\nu^+ - v_\nu^-)^2|_{r+1, \Gamma_0} \\ &\leq 2|(v_\nu^+)^2|_{r+1, \Gamma_0} + 2|(v_\nu^-)^2|_{r+1, \Gamma_0}. \end{aligned} \quad (5.3.20)$$

From (5.3.16),

$$\begin{aligned}
|(v_\nu^+)^2|_{r+1, \Gamma_0} &\leq C \sum_{i=0}^{r+1} |v_\nu^+|_{r+1-i, \Gamma_0} |v_\nu^+|_{i, \Gamma_0} \\
&\leq C \sum_{i=0}^{r+1} (L^{(r-i+2)\mu} \|v\|_{1, S_2}) \times (L^{(i+1)\mu} \|v\|_{1, S_2}) \\
&\leq CL^{(r+3)\mu} \|v\|_{1, S_2}^2.
\end{aligned} \tag{5.3.21}$$

Similarly,

$$|(v_\nu^-)^2|_{r+1, \Gamma_0} \leq CL^{(r+3)\mu} \|v\|_{1, S_1}^2. \tag{5.3.22}$$

Combining (5.3.19), (5.3.20), (5.3.21) and (5.3.22) gives the desired result (5.3.18). ■

Similarly, we can prove the following lemma.

Lemma 5.3.4 *Let **A5** be given. For the rule (5.3.17) with order r , there exist the bounds for $v \in V_h$,*

$$\begin{aligned}
| \overline{\|v^+ - v^-\|_{0, \Gamma_0}^2} - \|v^+ - v^-\|_{0, \Gamma_0}^2 | &\leq Ch^{r+1} L^{(r+1)\mu} \|v\|_1^2, \\
| \overline{\|v\|_{0, \Gamma_D}^2} - \|v\|_{0, \Gamma_D}^2 | &\leq Ch^{r+1} L^{(r+1)\mu} \|v\|_1^2, \\
| \overline{\|v_\nu\|_{0, \Gamma_N}^2} - \|v_\nu\|_{0, \Gamma_N}^2 | &\leq Ch^{r+1} L^{(r+3)\mu} \|v\|_1^2.
\end{aligned}$$

Now we give an essential assumption.

A6: Suppose that

$$\|v^\pm\|_{k, S^\pm} \leq CL^{(k-1)\mu} \|v\|_{1, S^\pm}, \quad k \geq 1, \quad v \in V_h,$$

where μ is a constant independent of m and n . Choose the integral rule of order r in S ,

$$\widehat{\iint}_S g = \iint_S \hat{g}, \tag{5.3.23}$$

where \hat{g} is the interpolant of polynomials of order r . We can also prove the following lemma easily.

Lemma 5.3.5 *Let **A6** be given and the rule (5.3.23) be chosen with order r . There exists the bound,*

$$| (\widehat{\iint}_{S^\pm} - \iint_{S^\pm}) (\Delta v)^2 | \leq Ch^{r+1} L^{(r+3)\mu} \|v\|_{1, S^\pm}^2.$$

Theorem 5.3.4 Let **A5** – **A6** and $\Gamma_D \cap \partial S_1 \neq \emptyset$ hold. We choose h to satisfy

$$L^{(r+3)\mu} h^{r+1} = o(1). \quad (5.3.24)$$

Then there exists the uniformly V_h - elliptic inequality (5.3.6).

Proof We have from Theorem 5.3.3 and Lemmas 5.3.3 – 5.3.5,

$$\begin{aligned} \hat{a}(v, v) &\geq a(v, v) - CL^{(r+3)\mu} h^{r+1} \|v\|_1^2 \\ &\geq C_0 \|v\|_H^2 - CL^{(r+3)\mu} h^{r+1} \|v\|_1^2 \\ &\geq C_0 \left\{ \left(1 - \frac{C}{C_0} L^{(r+3)\mu} h^{r+1}\right) \|v\|_1^2 + \|\Delta v\|_{0,S_1}^2 + \|\Delta v\|_{0,S_2}^2 \right. \\ &\quad \left. + L^{2\mu} \|v^+ - v^-\|_{0,\Gamma_0}^2 + \|v_\nu^+ - v_\nu^-\|_{0,\Gamma_0}^2 + L^{2\mu} \|v\|_{0,\Gamma_D}^2 + \|v_\nu\|_{0,\Gamma_N}^2 \right\} \\ &\geq \frac{C_0}{2} \|v\|_H^2, \end{aligned}$$

provided that

$$\frac{C}{C_0} L^{(r+3)\mu} h^{r+1} \leq \frac{1}{2},$$

which is valid due to (5.3.24). ■

5.4 The Robin Boundary Conditions

In the above sections, only the Dirichlet and Neumann boundary conditions are discussed. In this section, we consider Poisson's equation involving the Robin boundary condition

$$-\Delta u = -\left(\frac{\partial^2 u}{\partial x^2} + \frac{\partial^2 u}{\partial y^2}\right) = f(x, y) \quad \text{in } S, \quad (5.4.1)$$

$$u_\nu|_{\Gamma_N} = g_1 \quad \text{on } \Gamma_N, \quad (5.4.2)$$

$$(u_\nu + \beta u)|_{\Gamma_R} = g_2 \quad \text{on } \Gamma_R, \quad (5.4.3)$$

where $\beta \geq \beta_0 > 0$, $\partial S = \Gamma = \Gamma_N \cup \Gamma_R$. Assume $\text{Meas}(\Gamma_R) > 0$ for the unique solution. For simplicity, let $\Gamma_0 = \emptyset$. (When $\Gamma_0 \neq \emptyset$, a similar analysis can be made easily by following Sections 5.2 and 5.3.) We also give two more assumptions.

A7: The solutions in S can be expanded as

$$v = \sum_{i=1}^{\infty} a_i \Phi_i \quad \text{in } S, \quad (5.4.4)$$

where $\Phi_i (\in C^2(S) \cap C^1(\partial S))$ are complete and independent bases in S , and a_i are the exact expansion coefficients.

A8: The expansions in (5.4.4) converge exponentially to the true solution u . Let

$$u = u_m + R_m,$$

where

$$u_m = \sum_{i=1}^m a_i \Phi_i, \quad R_m = \sum_{i=m+1}^{\infty} a_i \Phi_i,$$

and a_i are the true expansion coefficients. Then

$$\max_S |R_m| = O(e^{-\bar{c}m}),$$

where $\bar{c} > 0$ and $m > 1$.

Based on **A7-A8** we may choose the uniform admissible functions,

$$v = \sum_{i=1}^m \tilde{a}_i \Phi_i \quad \text{in } S, \quad (5.4.5)$$

where \tilde{a}_i are unknown coefficients to be sought. Denote by V_h the collection of the functions (5.4.5).

Choose the integral rules:

$$\widehat{\iint}_S g = \sum_{ij} \alpha_{ij} g(Q_{ij}), \quad Q_{ij} \in S, \quad (5.4.6)$$

$$\widehat{\int}_{\Gamma_N} g = \sum_i \alpha_i^N g(Q_i), \quad Q_i \in \Gamma_N, \quad (5.4.7)$$

$$\widehat{\int}_{\Gamma_R} g = \sum_i \alpha_i^R g(Q_i), \quad Q_i \in \Gamma_R. \quad (5.4.8)$$

We may seek the coefficients \tilde{a}_i by satisfying the equations (5.4.1), (5.4.2) and (5.4.3) directly at Q_{ij} and Q_i ,

$$\sqrt{\alpha_{ij}}(\Delta v + f)(Q_{ij}) = 0, \quad Q_{ij} \in S, \quad (5.4.9)$$

$$\sqrt{\alpha_i^N}(v_\nu - g_1)(Q_i) = 0, \quad Q_i \in \Gamma_N, \quad (5.4.10)$$

$$\sqrt{\alpha_i^R}(v_\nu + \beta v - g_2)(Q_i) = 0, \quad Q_i \in \Gamma_R. \quad (5.4.11)$$

The collocation method described in (5.4.9) – (5.4.11) can be written as

$$\hat{b}(\hat{u}_m, v) = \hat{f}(v), \quad \forall v \in V_h, \quad (5.4.12)$$

where

$$\begin{aligned}\hat{b}(u, v) &= \widehat{\iint}_S \Delta u \Delta v + \widehat{\int}_{\Gamma_N} u_\nu v_\nu + \widehat{\int}_{\Gamma_R} (u_\nu + \beta u)(v_\nu + \beta v), \\ \hat{f}(v) &= -\widehat{\iint}_S f \Delta v + \widehat{\int}_{\Gamma_N} g_1 v_\nu + \widehat{\int}_{\Gamma_R} g_2 (v_\nu + \beta v).\end{aligned}$$

The corresponding least squares methods are then denoted by

$$b(u_m, v) = f(v), \quad \forall v \in V_h,$$

where

$$\begin{aligned}b(u, v) &= \iint_S \Delta u \Delta v + \int_{\Gamma_N} u_\nu v_\nu + \int_{\Gamma_R} (u_\nu + \beta u)(v_\nu + \beta v), \\ f(v) &= -\iint_S f \Delta v + \int_{\Gamma_N} g_1 v_\nu + \int_{\Gamma_R} g_2 (v_\nu + \beta v).\end{aligned}$$

Denote the norm

$$\|v\|_h = \{\|v\|_{1,S}^2 + \|\Delta v\|_{0,S}^2 + \|v_\nu\|_{0,\Gamma_N}^2 + \|(v_\nu + \beta v)\|_{0,\Gamma_R}^2\}^{1/2},$$

Now we have a lemma.

Lemma 5.4.1 *Let $Meas(\Gamma_R) > 0$. There exists the uniformly V_h - elliptic inequality*

$$b(v, v) \geq C_0 \|v\|_{1,S}^2, \quad \forall v \in V_h. \quad (5.4.13)$$

Proof We have

$$\begin{aligned}|v|_{1,S}^2 &= \iint_S |\nabla v|^2 = -\iint_S v \Delta v + \int_{\partial S} v_\nu v \\ &\leq \|\Delta v\|_{0,S} \|v\|_{0,S} + \int_{\Gamma_N} v_\nu v + \int_{\Gamma_R} (v_\nu + \beta v)v - \int_{\Gamma_R} \beta v^2 \\ &\leq \|\Delta v\|_{0,S} \|v\|_{0,S} + \|v_\nu\|_{0,\Gamma_N} \|v\|_{0,\Gamma_N} + \|v_\nu + \beta v\|_{0,\Gamma_R} \|v\|_{0,\Gamma_R} - \int_{\Gamma_R} \beta v^2 \\ &\leq \{\|\Delta v\|_{0,S} + \|v_\nu\|_{0,\Gamma_N} + \|v_\nu + \beta v\|_{0,\Gamma_R}\} \|v\|_{1,S} - \int_{\Gamma_R} \beta v^2,\end{aligned}$$

where we have used the bounds

$$\|v\|_{0,\Gamma_N} \leq C \|v\|_{1,S}, \quad \|v\|_{0,\Gamma_R} \leq C \|v\|_{1,S}.$$

This leads to

$$\begin{aligned}|v|_{1,S}^2 + \int_{\Gamma_R} \beta v^2 \\ \leq \{\|\Delta v\|_{0,S} + \|v_\nu\|_{0,\Gamma_N} + \|v_\nu + \beta v\|_{0,\Gamma_R}\} \|v\|_{1,S}.\end{aligned} \quad (5.4.14)$$

On the other hand, for $\text{Meas}(\Gamma_R) > 0$,

$$\|v\|_{1,S}^2 \leq C(|v|_{1,S}^2 + \beta_0 \|v\|_{0,\Gamma_R}^2). \quad (5.4.15)$$

Combining (5.4.14) and (5.4.15) gives

$$\begin{aligned} \|v\|_{1,S}^2 &\leq C(|v|_{1,S}^2 + \int_{\Gamma_R} \beta v^2) \\ &\leq C\{\|\Delta v\|_{0,S} + \|v_\nu\|_{0,\Gamma_N} + \|v_\nu + \beta v\|_{0,\Gamma_R}\} \|v\|_{1,S}. \end{aligned}$$

This leads to

$$\|v\|_{1,S} \leq C\{\|\Delta v\|_{0,S} + \|v_\nu\|_{0,\Gamma_N} + \|v_\nu + \beta v\|_{0,\Gamma_R}\},$$

and then

$$\|v\|_{1,S}^2 \leq C\{\|\Delta v\|_{0,S}^2 + \|v_\nu\|_{0,\Gamma_N}^2 + \|v_\nu + \beta v\|_{0,\Gamma_R}^2\} = Cb(v, v).$$

This is (5.4.13). ■

Note that the true solution u also satisfies (5.4.12) exactly, $\hat{b}(\hat{u}_m, v) = \hat{f}(v), \forall v \in V_h$. A similar argument as in Theorem 5.3.4 can be given for (5.4.16): $\hat{b}(v, v) \geq C_0 \|v\|_h^2, \forall v \in V_h$. We can obtain the following theorem by following Sections 5.2 and 5.3.

Theorem 5.4.1 *Suppose that there exist two inequalities,*

$$\begin{aligned} \hat{b}(u, v) &\leq C \|u\|_h \times \|v\|_h, \quad \forall v \in V_h, \\ \hat{b}(v, v) &\geq C_0 \|v\|_h^2, \quad \forall v \in V_h, \end{aligned} \quad (5.4.16)$$

where $C_0 (> 0)$ and C are two constants independent of m . Then, the solution of the collocation method (5.4.12) has the error bound,

$$\begin{aligned} \|u - \hat{u}_m\|_h &= C \inf_{v \in V_h} \|u - v\|_h \\ &\leq C\{\|R_m\|_{2,S} + \|(R_m)_\nu\|_{0,\Gamma_N} + \|(R_m)_\nu\|_{0,\Gamma_R}\}. \end{aligned}$$

Note that when the admissible functions are chosen to satisfy Poisson's equation, the collocation TM, i.e., the BAM, is then obtained from the CM. Hence the collocation TM in Chapter 2 is a special case of the CM in this chapter. Moreover, in traditional CM, some difficulties are encountered for the Neumann boundary conditions, see [392]. In this chapter, the techniques given can handle very well for both the Neumann and the Robin boundary conditions.

5.5 Inverse Inequalities

In the above analysis, we need the inverse estimates in **A4**, **A5** and **A6**. In fact, the inverse estimates in **A6** is essential. Take the norms on Γ_0 as example. We have from assumption **A6**

$$\|v^+\|_{k,\Gamma_0} \leq C\|v^+\|_{k+1,S^+} \leq CL^{k\mu}\|v^+\|_{1,S^+}, \quad (5.5.1)$$

$$\|v_\nu^+\|_{k,\Gamma_0} \leq C\|v^+\|_{k+2,S^+} \leq CL^{(k+1)\mu}\|v^+\|_{1,S^+}. \quad (5.5.2)$$

Hence, **A5** can be replaced by (5.5.1), (5.5.2), etc., and the proof for Lemma 5.3.4 and Theorem 5.3.4 is similar.

To prove the inverse inequalities, in this chapter we confine ourselves to the smooth solution of (5.2.1) – (5.2.3), and choose admissible functions $\Phi_i(x)$ and $\Psi_i(x)$ in (5.2.4), and Φ_i in (5.4.4) as polynomials of order i . Theorem 5.5.1 yields the essential inverse inequality. As to other admissible functions, such as radial basis functions, the inverse inequality will be proven in Chapter 7. As long as the inverse inequalities hold, the uniformly V_h - elliptic inequality holds and then the optimal error estimates can be achieved easily.

First we cite the results in Li [291], pp. 161-163, as two lemmas.

Lemma 5.5.1 *Let $\rho_L = \rho_L(x)$ be an L -order polynomial on $[-1, 1]$. Then there exists a constant C independent of L such that*

$$\|\rho'_L\|_{0,[-1,1]} \leq CL^2\|\rho_L\|_{0,[-1,1]}.$$

Lemma 5.5.2 *Suppose that Γ_0 is made up of finite sections of straight lines, and that the admissible function w_h in S_2 is an L -order polynomial. Then there exists a constant C independent of L such that*

$$\sup_{w_h \in V_h} \frac{|w_h^+|_{k+1,\Gamma_0}}{\|w_h\|_1} \leq CL^{2(k+1)}.$$

Lemma 5.5.3 *Let $\square = \{(x, y) \mid -1 \leq x \leq 1, -1 \leq y \leq 1\}$, and choose*

$$w_L = \sum_{i,j=0}^L a_{ij} T_i(x) T_j(y), \quad (x, y) \in \square, \quad (5.5.3)$$

where a_{ij} are expansion coefficients, and $T_i(x)$ are the Chebyshev polynomials of order i . Then there exist the inverse inequalities,

$$\left\| \frac{\partial}{\partial x} w_L \right\|_{0,\square} \leq CL^2 \|w_L\|_{0,\square}, \quad (5.5.4)$$

$$\left\| \frac{\partial}{\partial y} w_L \right\|_{0,\square} \leq CL^2 \|w_L\|_{0,\square}, \quad (5.5.5)$$

where C is a constant independent of L .

Proof We prove (5.5.4) only, since the proof for (5.5.5) is similar. We may express w_L by the Legendre polynomials

$$w_L = \sum_{i,j=0}^L b_{ij} P_i(x) P_j(y), \quad (x, y) \in \square,$$

where the coefficients b_{ij} from (5.5.3) are uniquely determined. We have from the orthogonality of the Legendre polynomials,

$$\begin{aligned} \|w_L\|_{0,\square}^2 &= \int \int_{\square} \left(\sum_{i,j=0}^L b_{ij} P_i(x) P_j(y) \right)^2 \\ &= \sum_{i,j=0}^L \frac{4b_{ij}^2}{(2i+1)(2j+1)} = \sum_{j=0}^L \frac{2}{2j+1} \sum_{i=0}^L \frac{2b_{ij}^2}{2i+1} \\ &= \sum_{j=0}^L \frac{2}{2j+1} \|z_j\|_{0,[-1,1]}^2, \end{aligned} \quad (5.5.6)$$

where z_j are polynomials of order L ,

$$z_j = z_j(x) = \sum_{i=0}^L b_{ij} P_i(x), \quad x \in [-1, 1]. \quad (5.5.7)$$

On the other hand, we have

$$\begin{aligned} \left\| \frac{\partial}{\partial x} w_L \right\|_{0,\square}^2 &= \int \int_{\square} \left(\sum_{i,j=0}^L b_{ij} P_i'(x) P_j(y) \right)^2 \\ &= \sum_{j=0}^L \frac{2}{2j+1} \int_{-1}^1 \sum_{i,\bar{i}=0}^L b_{ij} b_{\bar{i}j} P_i'(x) P_{\bar{i}}'(x) dx \\ &= \sum_{j=0}^L \frac{2}{2j+1} \|z_j'(x)\|_{0,[-1,1]}^2, \end{aligned} \quad (5.5.8)$$

where the polynomials $z_j(x)$ are given in (5.5.7). Based on Lemma 5.5.1, we have from (5.5.6) and (5.5.8)

$$\begin{aligned} \left\| \frac{\partial}{\partial x} w_L \right\|_{0,\square}^2 &= \sum_{j=0}^L \frac{2}{2j+1} \|z_j'(x)\|_{0,[-1,1]}^2 \\ &\leq CL^4 \sum_{j=0}^L \frac{2}{2j+1} \|z_j(x)\|_{0,[-1,1]}^2 \\ &= CL^4 \sum_{i,j=0}^L \frac{4b_{ij}^2}{(2i+1)(2j+1)} = CL^4 \|w_L\|_{\square}^2. \end{aligned}$$

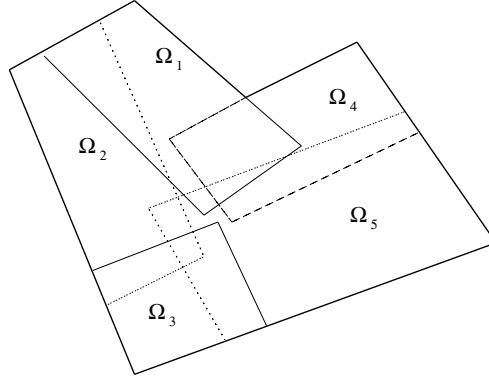


Figure 5.2: A polygon decomposed into finite number of parallelograms Ω_i .

This is the desired result (5.5.4). ■

A9: Let S be a polygon shown in Figure 5.2. Then S can be decomposed into finite number of quasiuniform parallelograms Ω_i : $S = \cup_i \Omega_i$, where overlap of Ω_i is allowed, see [17]. By the diagonal line, Ω_i is split into two triangles, Δ_i^+ and Δ_i^- . Suppose that all Δ_i^\pm are quasiuniform, e.g., $c_0 \leq \rho_i^\pm$, where ρ_i^\pm denotes the radius of the largest inscribed sphere of Δ_i^\pm , and c_0 is a positive constant. We have the following lemma.

Theorem 5.5.1 *Let A9 be given. Then for the polynomial w_L in (5.5.3). Then there exists a constant C independent of L such that*

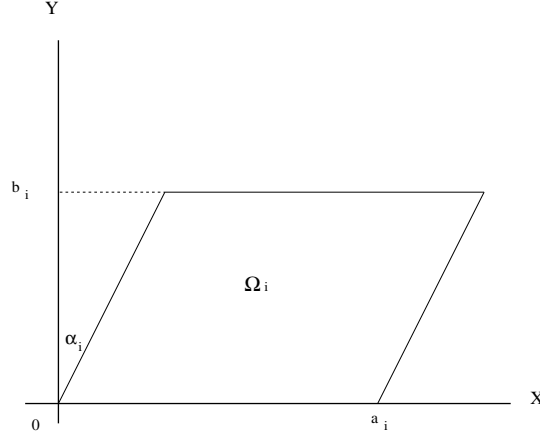
$$\|w_L\|_{k,S} \leq CL^{2k} \|w_L\|_{0,S}.$$

Proof Consider the parallelograms Ω_i in Figure 5.3, where a_i and b_i are the lengths of two edges, and α_i are the angles between Ω_i and the y axis. From the quasiuniform parallelograms, there exist the bounds,

$$0 < a_i, b_i < C, \frac{\max\{a_i, b_i\}}{\min\{a_i, b_i\}} \leq C, \quad 0 \leq \alpha_i \leq \alpha_M < \frac{\pi}{2}. \quad (5.5.9)$$

The parallelograms Ω_i can be transformed to \square by the linear transformation $T : (x, y) \rightarrow (\hat{x}, \hat{y})$, where

$$\begin{aligned} \hat{x} &= \frac{2}{a_i} [x - (\tan \alpha_i)y] - 1, \\ \hat{y} &= \frac{2}{b_i} y - 1. \end{aligned}$$

Figure 5.3: A parallelogram Ω_i .

Denote $\hat{w} = T(w)$. We have

$$\begin{aligned}\frac{\partial w}{\partial x} &= \frac{2}{a_i} \frac{\partial \hat{w}}{\partial \hat{x}}, \\ \frac{\partial w}{\partial y} &= -\frac{2}{a_i} (\tan \alpha_i) \frac{\partial \hat{w}}{\partial \hat{x}} + \frac{2}{b_i} \frac{\partial \hat{w}}{\partial \hat{y}}.\end{aligned}$$

Through the linear transformations T , we obtain

$$\begin{aligned}|w|_{1, \Omega_i}^2 &= \iint_{\Omega_i} (w_x^2 + w_y^2) dx dy \\ &= \frac{a_i b_i}{4} \iint_{\square} \left\{ \left(\frac{2}{a_i} \frac{\partial \hat{w}}{\partial \hat{x}} \right)^2 + \left(-\frac{2}{a_i} (\tan \alpha_i) \frac{\partial \hat{w}}{\partial \hat{x}} + \frac{2}{b_i} \frac{\partial \hat{w}}{\partial \hat{y}} \right)^2 \right\} d\hat{x} d\hat{y} \\ &\leq \frac{a_i b_i}{4} \iint_{\square} \left\{ \frac{4}{a_i^2} (1 + 2 \tan^2 \alpha_i) \left(\frac{\partial \hat{w}}{\partial \hat{x}} \right)^2 + 2 \frac{4}{b_i^2} \left(\frac{\partial \hat{w}}{\partial \hat{y}} \right)^2 \right\} d\hat{x} d\hat{y} \\ &\leq C \iint_{\square} \left\{ \left(\frac{\partial \hat{w}}{\partial \hat{x}} \right)^2 + \left(\frac{\partial \hat{w}}{\partial \hat{y}} \right)^2 \right\} d\hat{x} d\hat{y},\end{aligned}\tag{5.5.10}$$

where the constant

$$C = \max_i \left\{ \frac{b_i}{a_i} (1 + 2 \tan^2 \alpha_i) + \frac{2a_i}{b_i} \right\}.$$

The constant C is independent of i due to assumption (5.5.9). Under the linear transformation T , the polynomials of order L remain as well. Based on Lemma 5.5.3, we have

for $w = w_L$,

$$\iint_{\square} \left\{ \left(\frac{\partial \hat{w}}{\partial \hat{x}} \right)^2 + \left(\frac{\partial \hat{w}}{\partial \hat{y}} \right)^2 \right\} d\hat{x}d\hat{y} \leq CL^4 \iint_{\square} (\hat{w})^2 d\hat{x}d\hat{y}. \quad (5.5.11)$$

Moreover, through the inverse transformation \hat{T} , we obtain for $w = w_L$,

$$\iint_{\square} (\hat{w})^2 d\hat{x}d\hat{y} = \frac{4}{a_i b_i} \iint_{\Omega_i} w^2 dx dy \leq C \|w\|_{0, \Omega_i}^2. \quad (5.5.12)$$

Combining (5.5.10), (5.5.11) and (5.5.12) gives

$$|w|_{1, \Omega_i} \leq CL^2 \|w\|_{0, \Omega_i},$$

and

$$\|w\|_{1, \Omega_i} \leq CL^2 \|w\|_{0, \Omega_i}.$$

Consequently, for parallelograms Ω_i we have

$$\begin{aligned} \|w_L\|_{k, \Omega_i} &\leq C(L-k)^2 \|w_L\|_{k-1, \Omega_i} \\ &\leq CL^2 \|w_L\|_{k-1, \Omega_i} \leq CL^{2k} \|w_L\|_{0, \Omega_i}. \end{aligned}$$

From **A9** we obtain

$$\|w_L\|_{k, S}^2 \leq \sum_i \|w_L\|_{k, \Omega_i}^2 \leq CL^{4k} \sum_i \|w_L\|_{0, \Omega_i}^2 \leq CL^{4k} \|w_L\|_{0, S}^2,$$

by noting finite overlaps of Ω_i . ■

5.6 Numerical Experiments

In the section, we carry out two computational models to verify the analysis made, in which the radial basis functions and piecewise admissible functions have been applied into CM.

5.6.1 Radial Basis Functions for Different Boundary Conditions

When the radial basis functions are chosen as the admissible functions, the analysis (in particular the inverse inequalities) will be given in Section 7.4. Here, we only provide

numerical experiments, to show the effectiveness of the CM. First, we consider the Poisson's equation on domain S with the mixed type of boundary conditions,

$$\begin{aligned} -\Delta u &= 2\pi^2 \sin(\pi x) \cos(\pi y), \quad \text{in } S, \\ u &= 0 \quad \text{on } x = 1 \quad \wedge \quad 0 \leq y \leq 1, \\ u_x + 2u &= -\pi \cos(\pi y) \quad \text{on } x = -1 \quad \wedge \quad 0 \leq y \leq 1, \\ u_y &= 0 \quad \text{on } y = 1 \quad \wedge \quad -1 \leq x \leq 1, \\ u &= \sin(\pi x) \quad \text{on } y = 0 \quad \wedge \quad -1 \leq x \leq 1. \end{aligned}$$

where S is a rectangle, $S = \{(x, y) \mid -1 \leq x \leq 1, 0 \leq y \leq 1\}$, ∂S is its boundary, $u_n = \frac{\partial u}{\partial n}$, and n is the unit outnormal to ∂S . It has the exact solution

$$u(x, y) = \sin(\pi x) \cos(\pi y).$$

The purpose of the problem is to apply the collocation methods using the radial basis functions for different boundary conditions.

The admissible functions are chosen as:

$$v = \sum_{i=1}^{N_S} a_i g_i(x, y), \quad \text{in } S, \quad (5.6.1)$$

where a_i are unknown coefficients to be determined, and $g_i(x, y)$ are the radial basis functions. First, we choose the inverse multiquadric radial basis functions (IMQRB)

$$g_i(x, y) = \frac{1}{\sqrt{r_i^2 + c^2}},$$

where c is a constant parameter, $r_i = \sqrt{(x - x(P_i))^2 + (y - y(P_i))^2}$, and P_i are the source points which may not necessarily be chosen as the collocation nodes. Suitable additional functions may be added into (5.6.1), such as some polynomials and the singular functions if necessary. Next, we may choose the Gaussian radial basis functions (GRB)

$$g_i(x, y) = \exp\left(-\frac{r_i^2}{c^2}\right).$$

We use the collocation equations (5.4.9) – (5.4.11) on the uniform exterior collocation nodes, and choose the trapezoidal rules for (5.4.6) – (5.4.8). The error norms are listed in Tables 5.1 and 5.2 for IMQRB and GRB, respectively, where N_d denotes the number of partition along the y -direction in S . Let the source points of radial basis functions also

be the collocation nodes. And let $N_S = L^2$ in (5.6.1). From Table 5.1, we can see the following asymptotic relations for IMQRB,

$$\|u - v\|_{0,\infty,S} = O((0.16)^L), \quad (5.6.2)$$

$$\|u - v\|_{0,S} = O((0.17)^L), \quad (5.6.3)$$

$$\|u - v\|_{1,S} = O((0.19)^L). \quad (5.6.4)$$

And from Table 5.2 we can see for GRB,

$$\|u - v\|_{0,\infty,S} = O((0.15)^L), \quad (5.6.5)$$

$$\|u - v\|_{0,S} = O((0.14)^L), \quad (5.6.6)$$

$$\|u - v\|_{1,S} = O((0.16)^L). \quad (5.6.7)$$

Eqs. (5.6.2) – (5.6.7) indicate that the numerical solutions have the exponentially convergent rates. Note that the GRB collocation method converges slightly faster than the IMQRB collocation method.

5.6.2 Piecewise Admissible Functions

Next, consider the Poisson's equation,

$$\Delta u = \frac{\partial^2 u}{\partial x^2} + \frac{\partial^2 u}{\partial y^2} = 0, \quad \text{in } S,$$

where $S = \{(x, y) \mid -1 < x < 1, 0 < y < 1\}$, with the following boundary conditions:

$$\begin{aligned} u &= \cos(\pi y) \quad \text{on } \{x = -1\} \wedge \{0 \leq y \leq 1\}, \\ u &= \cosh(2\pi) \cos(\pi y) \quad \text{on } \{x = 1\} \wedge \{0 \leq y \leq 1\}, \\ u &= -\cosh((x+1)\pi) \quad \text{on } \{y = 1\} \wedge \{-1 \leq x \leq 1\}, \\ u_y &= 0 \quad \text{on } \{y = 0\} \wedge \{-1 \leq x \leq 1\}. \\ u^+ &= u^-, \quad u_\nu^+ = u_\nu^- \quad \text{on } \Gamma_0. \end{aligned}$$

The exact solution is $u(x, y) = \cosh(\pi(x+1)) \cos(\pi y)$. Divide S by Γ_0 into S_1 and S_2 , where $S_1 = \{(x, y) \mid -1 < x < 0, 0 < y < 1\}$ and $S_2 = \{(x, y) \mid 0 < x < 1, 0 < y < 1\}$. The admissible functions are chosen as:

$$v = \begin{cases} v^- = \sum_{i,j=0}^L a_{ij} T_i(2x+1) T_j(2y-1), & \text{in } S_1, \\ v^+ = \sum_{i,j=0}^M d_{ij} T_i(2x-1) T_j(2y-1), & \text{in } S_2, \end{cases}$$

where a_{ij} and d_{ij} are unknown coefficients to be determined, and $T_i(x)$ are the Chebyshev polynomials $T_k(x) = \cos(k \cos^{-1}(x))$.

Then, we use the collocation equations (5.2.21) – (5.2.25), and choose the trapezoidal rules for (5.2.19). Since v^\pm do not satisfy the boundary conditions, some additional collocation $v^\pm(P_i) = 0, P_i \in \partial S$, are also needed. The error norms are listed in Table 5.3, where different expansion terms L and M are used in S_1 and S_2 , respectively, and N is the number of collocation nodes along y-axis in a uniform distribution. The following asymptotic relations are observed:

$$\begin{aligned} \|u - v^-\|_{0,\infty,S_1} &= O((0.161)^L), \quad \|u - v^+\|_{0,\infty,S_2} = O((0.161)^M), \\ \|u - v^-\|_{0,S_1} &= O((0.166)^L), \quad \|u - v^+\|_{0,S_2} = O((0.166)^M), \\ \|u - v^-\|_{1,S_1} &= O((0.159)^L), \quad \|u - v^+\|_{1,S_2} = O((0.157)^M), \\ \|\varepsilon^+ - \varepsilon^-\|_{0,\Gamma_0} &= O((0.121)^{LM}), \quad \text{Cond.}(A) = O((1.78)^{LM}), \end{aligned}$$

where $L_M = \max \{L, M\}$. Above equations indicate that the numerical solutions have the exponential convergence rates as in (5.2.5), as demonstrated in the analysis in Section 5.3.

To close this section, let us comment on the assumptions A1 and A2.

Remark 5.6.1 *Usually, the solution of (5.2.1) – (5.2.3) is highly smooth inside S , but less smooth on ∂S . In particular, for concave corners of polygons or the intersection points of the Dirichlet and Neumann boundary conditions, the solution near the boundary nodes is singular with infinite derivatives. In this case, some special treatments should be solicited. For Motz's problem with the singular origin, the collocation equations may be established at the nodes Q_i far from the origin. Hence assumptions **A2** can be relaxed to*

$$v^\pm \in H^{1+\delta}(S) \cap C^2(D), \quad 0 < \delta < 1, \quad (5.6.8)$$

where the subdomain $D \subset S$ is far from the singularity. Moreover, when the singular functions or singular particular solution v^\pm are chosen, assumption **A3** may also hold. Hence, the collocation methods may also be applied to singularity problems if suitable treatments are used.

5.7 Final Remarks

1. In this chapter, the collocation method is treated as the least squares method, involving integration approximation. We employ the FEM theory to develop the theoretical analysis of CMs, in which the key analysis for the CMs is to prove the new V_h - elliptic inequality.
2. Three typical boundary conditions, Dirichlet, Neumann and Robin, can be handled well by the techniques of CMs in this chapter. The number of collocation nodes may be chosen to be much larger than the number of radial basis functions (i.e., source points). The collocation nodes are, indeed, the integration nodes of the rules used. Based on integration approximation, not only the collocation nodes can be easily located, but also the error analysis has been developed, see Sections 5.2 and 5.3.

3. Two computational examples in Section 5.6 show exponentially convergent rates: $\|u - v\|_{k,S} = O(\lambda^L)$, $k = 0, 1$, $0 < \lambda < 1$, which verify perfectly the analysis made. Section 5.6 displays that the CM can be applied to many kinds of admissible functions, such as radial basis functions. The detailed analysis is given in Chapter 7.
4. Piecewise admissible functions can be used in the CM, both the analysis and the computation are provided in this chapter, to enable the CM to be more flexible to complicated geometric domains for general PDEs, because different admissible functions can be chosen in different subdomains. Such an idea is also similar to the p -version FEM of Babuška and Guo [17], and the analysis of the CM may also be extended to singularity problems by following [17].

N_d, L	16, 4	16, 6	16, 8	16, 10
$\ u - v\ _{0,\infty,S}$	1.72	7.27(-2)	5.28(-4)	2.78(-5)
$\ u - v\ _{0,S}$	4.83(-1)	2.21(-2)	8.87(-5)	1.26(-5)
$\ u - v\ _{1,S}$	2.02	9.09(-2)	9.48(-4)	8.16(-5)
Cond.	2.00(3)	6.36(5)	3.81(8)	1.39(9)

Table 5.1: The error norms and condition number by the inverse multiquadric radial basis collocation method with parameter $c = 2.0$.

N_d, L	16, 4	16, 6	16, 8	16, 10
$\ u - v\ _{0,\infty,S}$	1.53	8.25(-2)	7.46(-4)	1.37(-5)
$\ u - v\ _{0,S}$	4.80(-1)	2.43(-2)	1.60(-4)	3.44(-6)
$\ u - v\ _{1,S}$	1.92	1.15(-1)	1.30(-3)	3.65(-5)
Cond.	1.08(4)	1.53(8)	1.05(9)	3.69(9)

Table 5.2: The error norms and condition number by the Gaussian radial basis collocation method with parameter $c = 2.0$.

L, M, N	3, 5, 6	4, 6, 8	5, 7, 10	6, 8, 12	7, 9, 14
$\ u - v^-\ _{0,\infty,S_1}$	3.41(-1)	1.39(-1)	9.23(-3)	1.86(-3)	2.29(-4)
$\ u - v^-\ _{0,S_1}$	6.92(-2)	3.75(-2)	2.12(-3)	4.54(-4)	5.31(-5)
$\ u - v^-\ _{1,S_1}$	5.23(-1)	1.85(-1)	1.69(-2)	3.82(-3)	3.33(-4)
$\ u - v^+\ _{0,\infty,S_2}$	3.09(-1)	1.46(-1)	8.15(-3)	1.83(-3)	2.06(-4)
$\ u - v^+\ _{0,S_2}$	6.26(-2)	3.59(-2)	1.91(-3)	3.59(-4)	4.72(-5)
$\ u - v^+\ _{1,S_2}$	4.74(-1)	1.74(-1)	1.43(-2)	3.30(-3)	2.86(-4)
$\ \varepsilon^+ - \varepsilon^-\ _{0,\Gamma_0}$	1.23(-3)	9.34(-4)	1.56(-5)	8.59(-6)	2.64(-7)
Cond.	7.96(2)	1.52(3)	2.82(3)	4.82(3)	7.80(3)

Table 5.3: The error norms and condition number by using piecewise Chebyshev polynomials with the different expansion terms L and M used in S_1 and S_2 , respectively, and the number N of collocation nodes along y -axis in a uniform distribution.

Chapter 6

Combinations of Collocation and Finite Element Methods

The collocation method (CM) in Chapter 5 can be combined with other numerical methods, such as the finite element method (FEM), the finite difference method (FDM) or the finite volume method (FVM) to solve complicated problems, e.g., those with singularities. Since the collocation method is, indeed, the Ritz-Galerkin method (i.e., the spectral method) involving integration approximation, the combined methods in this chapter can also be classified into those in [291]. However, new algorithms and error analysis are explored below. We only choose the FEM for exposition of the combinations of CM; other kinds of combinations of CM can be easily developed. In this chapter, we provide a framework of combinations of CM with the FEM. The key idea is to link the Galerkin method to the least squares method which is then approximated by integration rule, and led to the CM. The new important uniformly V_h^0 -elliptic inequality is proved. Interestingly, the integration approximation plays a role only in satisfying the uniformly V_h^0 -elliptic inequality. For the combinations of the finite element and collocation methods (FEM-CM), the optimal convergence rates can be achieved. The advantage of the CM is to formulate easily linear algebraic equations, where the stiffness matrices are positive definite but non-symmetric. We may also solve the algebraic equations of FEM and the collocation equations directly by the least squares method, thus to greatly improve numerical stability. Numerical experiments in Hu [216, 217] are also carried for Poisson's problem to support the analysis. Note that the analysis in this chapter is distinct from the existing literature, and it covers a large class of the CM using various admissible functions, such as the radial basis functions, the Sinc functions, etc.

6.1 Introduction

In this chapter, we follow the ideas of the combined methods in [291], and provide the combination of the finite element and collocation methods (FEM-CM). The advantages of this combination are threefold: (1) flexibility of applications to different geometric shapes and different elliptic equations, (2) simplicity of computer programming by straightfor-

ward mimicking the PDEs and the boundary conditions, (3) varieties of CMs using particular solutions, orthogonal polynomials, radial basis functions, the Sinc functions, etc. Moreover, optimal error bounds are derived, mainly based on the uniformly V_h^0 -elliptic inequalities, which are also proved in Sections 6.4 and 6.5. Note that the analysis of the CM in this chapter is distinct from the existing literature of CMs.

This chapter is organized as follows. In the next section, the combinations of FEM-CM are described, and in Section 6.3, linear algebraic equations are formulated, and the solution methods are provided. In Section 6.4, the important uniformly V_h^0 -elliptic inequality is derived, and in Section 6.5, the CM is expressed by approximation of integrals, and error bounds are derived. Numerical experiments to support the analysis made are provided in [216, 217].

6.2 Combinations of FEMs

Consider the Poisson's equation with the Dirichlet boundary condition,

$$-\Delta u = -\left(\frac{\partial^2 u}{\partial x^2} + \frac{\partial^2 u}{\partial y^2}\right) = f(x, y) \quad \text{in } S, \quad (6.2.1)$$

$$u|_{\Gamma} = 0 \quad \text{on } \Gamma,$$

where S is a polygon, and Γ is its boundary. Let S be divided by Γ_0 into two disjoint subregions, S_1 and S_2 (see Figure 6.1): $S = S_1 \cup S_2 \cup \Gamma_0$, $S_1 \cap S_2 = \emptyset$ and $\partial \bar{S}_1 \cap \partial \bar{S}_2 = \Gamma_0$.

On the interior boundary Γ_0 there exist the interior continuity conditions:

$$u^+ = u^-, \quad u_n^+ = u_n^-, \quad \text{on } \Gamma_0, \quad (6.2.2)$$

where $u_n = \frac{\partial u}{\partial n}$, $u^+ = u$ on $\Gamma_0 \cup S_2$ and $u^- = u$ on $\Gamma_0 \cup S_1$. Assume that the solution u in S_2 is smoother than u in S_1 . We choose the finite element method in S_1 and the least squares method in S_2 , whose discrete forms lead to the CM (see Section 6.3). Let S_1 be

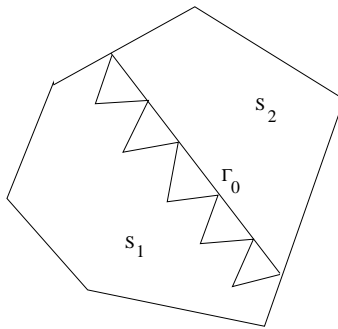


Figure 6.1: Partition of a polygon.

partitioned into small triangles: Δ_{ij} , i.e., $S_1 = \cup_{ij} \Delta_{ij}$. Denote h_{ij} the boundary length of Δ_{ij} . The Δ_{ij} are said to be quasiuniform if $\frac{h}{\min\{h_{ij}\}} \leq C$, where $h = \max\{h_{ij}\}$, and C is a constant independent of h . Then the admissible functions may be expressed by

$$v = \begin{cases} v^- = v_k & \text{in } S_1, \\ v^+ = \sum_{i=1}^L \tilde{a}_i \Psi_i & \text{in } S_2, \end{cases} \quad (6.2.3)$$

where \tilde{a}_i are unknown coefficients, and v_k are piecewise k -order Lagrange polynomials in S_1 . Assume that $\Psi_i \in C^2(S_2 \cup \partial S_2)$ so that $v^+ \in C^2(S_2 \cup \partial S_2)$. Therefore, we may evaluate (6.2.1) directly

$$(\Delta v^+ + f)(P_i) = 0, \quad \text{for } P_i \in S_2, \quad (6.2.4)$$

at certain collocation nodes $P_i \in S_2$. Note that v in (6.2.3) is not continuous on the interior interface Γ_0 . Hence, to satisfy (6.2.2) the interior collocation equations are needed:

$$v^+(P_i) = v^-(P_i), \quad \text{for } P_i \in \Gamma_0, \quad (6.2.5)$$

$$v_n^+(P_i) = v_n^-(P_i), \quad \text{for } P_i \in \Gamma_0, \quad (6.2.6)$$

Eqs. (6.2.4) – (6.2.6) are straightforward and easy to be formulated. In this chapter, we choose the total number of collocation nodes (e.g., P_i) to be larger (or much larger) than the number of unknown coefficients \tilde{a}_i . Hence we may seek the solutions of the entire CM by the least squares method (LSM) in Golub and Loan [176], see comments in Remark 6.2.1 below.

We assume that the solution expansion: $u = \sum_{i=1}^{\infty} a_i \Psi_i$ in S_2 where a_i are the true coefficients. Denote

$$u_L = \sum_{i=1}^L a_i \Psi_i, \quad \text{in } S_2. \quad (6.2.7)$$

Then $u = u_L + R_L$, and the remainder

$$R_L = \sum_{i=L+1}^{\infty} a_i \Psi_i.$$

Assume that (6.2.7) converges exponentially, to imply:

$$|R_L| = \left| \sum_{i=L+1}^{\infty} a_i \Psi_i \right| = O(e^{-\bar{c}L}), \quad \text{in } S_2,$$

where $\bar{c} > 0$ and $L > 1$.

Denote by V_h^0 the finite dimensional collections of (6.2.3) satisfying $v|_{\Gamma} = 0$, where we simply assume $\Psi_i|_{\partial S_2 \cap \Gamma} = 0$. If such a condition does not hold, the corresponding

collocation equations on $\partial S_2 \cap \Gamma$ are also needed, and the arguments of error analysis can be provided similarly. Then the combination of the FEM-CM is designed to seek the approximate solution $u_h \in V_h^0$ such that

$$a(u_h, v) = f(v), \quad \forall v \in V_h^0, \quad (6.2.8)$$

where

$$\begin{aligned} a(u, v) &= \iint_{S_1} \nabla u \cdot \nabla v + \int_{\Gamma_0} u_n^- v^- + P_c \iint_{S_2} \Delta u \Delta v \\ &+ \frac{P_c}{h} \int_{\Gamma_0} (u^+ - u^-)(v^+ - v^-) + P_c \int_{\Gamma_0} (u_n^+ - u_n^-)(v_n^+ - v_n^-), \\ f(v) &= \iint_{S_1} f v - P_c \iint_{S_2} f \Delta v, \end{aligned}$$

where $\nabla u = u_x \mathbf{i} + u_y \mathbf{j}$, $u_x = \frac{\partial u}{\partial x}$, $u_y = \frac{\partial u}{\partial y}$, $u_n = \frac{\partial u}{\partial n}$, and n is the unit outward normal to ∂S_2 . h is the maximal boundary length of \triangle_{ij} or \square_{ij} in S_1 , and constant $P_c > 0$ is chosen to be suitably large but still independent of h .

Denote the space

$$\begin{aligned} H^* &= \left\{ v \mid v \in L^2(S), v \in H^1(S_1), v \in H^1(S_2), \right. \\ &\left. \Delta v \in L^2(S_2), \text{ and } v|_{\Gamma} = 0 \right\}, \end{aligned}$$

accompanied with the norm

$$\begin{aligned} \|v\| &= \left(\|v\|_{1,S_1}^2 + P_c \|v\|_{1,S_2}^2 + P_c \|\Delta v\|_{0,S_2}^2 \right. \\ &\left. + \frac{P_c}{h} \|v^+ - v^-\|_{0,\Gamma_0}^2 + P_c \|v_n^+ - v_n^-\|_{0,\Gamma_0}^2 \right)^{1/2}, \end{aligned} \quad (6.2.9)$$

where $\|v\|_{1,S_1}$ and $\|v\|_{1,S_2}$ are the Sobolev norms. Obviously, $V_h^0 \subset H^*$. For the true solution u to (6.2.1), we have $a(u - u_h, v) = 0$, $\forall v \in V_h^0$. By means of a traditional argument in [105, 446], we have the following theorem.

Theorem 6.2.1 *Suppose that there exist two inequalities,*

$$a(u, v) \leq C \|u\| \times \|v\|, \quad \forall v \in V_h^0, \quad (6.2.10)$$

$$a(v, v) \geq C_0 \|v\|^2, \quad \forall v \in V_h^0, \quad (6.2.11)$$

where $C_0 (> 0)$ and C are two constants independent of h and L . Then, the solution of combination (6.2.8) has the error bound,

$$\|u - u_h\| = C \inf_{v \in V_h^0} \|u - v\|.$$

The proof for (6.2.11) is non-trivial and complicated, which is deferred to Section 6.4.

Choose an auxiliary function:

$$u_{I,L} = \begin{cases} u_I & \text{in } S_1, \\ \sum_{i=1}^L a_i \Psi_i, & \text{in } S_2, \end{cases} \quad (6.2.12)$$

where u_I is the piecewise k -order Lagrange interpolant of the true solution u , and a_i are the true coefficients. Then $u = \sum_{i=1}^L a_i \Psi_i + R_L$ in S_2 . By means of the auxiliary function (6.2.12), we obtain the following corollary.

Corollary 6.2.1 *Let all conditions in Theorem 6.2.1 hold. Suppose that*

$$u \in H^{k+1}(S_1) \quad \text{and} \quad u \in H^{k+1}(\Gamma_0). \quad (6.2.13)$$

Then there exists the error bound,

$$\begin{aligned} \|u - u_h\| &\leq C \{h^k |u|_{k+1, S_1} + \sqrt{P_c} \|R_L\|_{2, S_2} \\ &+ \sqrt{P_c} (h^{k+\frac{1}{2}} |u|_{k+1, \Gamma_0} + \frac{1}{\sqrt{h}} \|R_L\|_{0, \Gamma_0} + \|(R_L)_n\|_{0, \Gamma_0}) \}. \end{aligned}$$

Furthermore, suppose that the number L of v^+ in (6.2.3) is chosen such that

$$\|R_L\|_{2, S_2} = O(h^k), \quad \|R_L\|_{0, \Gamma_0} = O(h^{k+\frac{1}{2}}), \quad \|(R_L)_n\|_{0, \Gamma_0} = O(h^k). \quad (6.2.14)$$

Then, there exists the optimal convergence rate,

$$\|u - u_h\| = O(h^k). \quad (6.2.15)$$

Remark 6.2.1 *The combination (6.2.8) is nothing new (cf. [291]), although the proof of (6.2.11) is challenging. Particularly, the CM is used in S_2 , which can be obtained from (6.2.8) involving approximation of integration. Hence, the combination of Ritz-Galerkin-FEM is a backbone for the study, but more justification will be provided below.*

6.3 Linear Algebraic Equations of Combination of FEM and CM

Let $\widehat{\iint}_{S_2}$ and $\widehat{\int}_{\Gamma_0}$ denote the approximations of \iint_{S_2} and \int_{Γ_0} by some integration rules, respectively. The combination of FEM-CM of (6.2.8) involving integration approximation is given by: To seek the approximation solution $\hat{u}_h \in V_h^0$ such that

$$\hat{a}(\hat{u}_h, v) = \hat{f}(v), \quad \forall v \in V_h^0, \quad (6.3.1)$$

where

$$\begin{aligned}\hat{a}(u, v) &= \iint_{S_1} \nabla u \cdot \nabla v + \int_{\Gamma_0} u_n^- v^- + P_c \widehat{\iint}_{S_2} \Delta u \Delta v \\ &+ \frac{P_c}{h} \widehat{\int}_{\Gamma_0} (u^+ - u^-)(v^+ - v^-) + P_c \widehat{\int}_{\Gamma_0} (u_n^+ - u_n^-)(v_n^+ - v_n^-), \\ \hat{f}(v) &= \iint_{S_1} f v - P_c \widehat{\iint}_{S_2} f \Delta v.\end{aligned}$$

Eq. (6.3.1) can be described equivalently as:

$$\hat{a}^*(\hat{u}_h, v) = f_1(v), \quad \forall v \in V_h^0, \quad (6.3.2)$$

where

$$\begin{aligned}\hat{a}^*(u, v) &= \iint_{S_1} \nabla u \cdot \nabla v + \int_{\Gamma_0} u_n^- v^- + P_c \widehat{\iint}_{S_2} (\Delta u + f)(\Delta v + f) \\ &+ \frac{P_c}{h} \widehat{\int}_{\Gamma_0} (u^+ - u^-)(v^+ - v^-) + P_c \widehat{\int}_{\Gamma_0} (u_n^+ - u_n^-)(v_n^+ - v_n^-), \\ f_1(v) &= \iint_{S_1} f v.\end{aligned}$$

In S_2 , we choose the integration rules

$$\widehat{\iint}_{S_2} g^2 = \sum_{ij} \alpha_{ij} g^2(P_{ij}), \quad P_{ij} \in S_2, \quad (6.3.3)$$

$$\widehat{\int}_{\Gamma_0} g^2 = \sum_j \alpha_j g^2(P_j), \quad P_j \in \Gamma_0,$$

where α_{ij} and α_j are positive weights. In fact, we may formulate the collocation equations at $P_{ij} \in S_2$, and $P_j \in \Gamma_0$ directly. The collocation equations at P_{ij} , and P_j are given by:

$$(\Delta v^+ + f)(P_{ij}) = 0, \quad P_{ij} \in S_2, \quad (6.3.4)$$

$$(v^+ - v^-)(P_j) = 0, \quad P_j \in \Gamma_0, \quad (6.3.5)$$

$$(v_n^+ - v_n^-)(P_j) = 0, \quad P_j \in \Gamma_0, \quad (6.3.6)$$

where $v_n^-(P_j) = \frac{v_{1j} - v_{0j}}{h}$, $v_{0j} = v(P_j)$ and v_{1j} are the nodal variables in S_1 normal to Γ_0 . By introducing suitable weight functions, we rewrite the equations (6.3.4) – (6.3.6) as

$$\sqrt{P_c \alpha_{ij}} (\Delta v^+ + f)(P_{ij}) = 0, \quad P_{ij} \in S_2, \quad (6.3.7)$$

$$\sqrt{\frac{P_c \alpha_j}{2h}} (v^+ - v^-)(P_j) = 0, \quad P_j \in \Gamma_0, \quad (6.3.8)$$

$$\sqrt{\frac{P_c \alpha_j}{2}} (v_n^+ - v_n^-)(P_j) = 0, \quad P_j \in \Gamma_0, \quad (6.3.9)$$

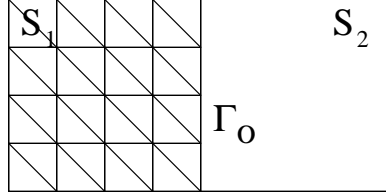


Figure 6.2: Uniform partition of a rectangular solution domain with $M = 4$, where M denotes the numbers of partitions along the y -direction in S_1 .

where P_{ij} are the interior element nodes of Γ_0 .

We give some rules of integration with explicit weights α_{ij} in (6.3.7). First, choose the trapezoidal rule,

$$\widehat{\int}_{P_1 P_2} g^2 = \frac{P_1 P_2}{2} (g^2(P_1) + g^2(P_2)) = \frac{H}{2} (g^2(P_1) + g^2(P_2)).$$

Let S_2 be a rectangle shown in Figure 6.2, and be divided into uniform difference grids with the meshspacing H , where P_{ij} denote the collocation nodes (i, j) . Hence, the weights α_{ij} in (6.3.7) have the following values,

$$\alpha_{ij} = \begin{cases} H^2, & (i, j) \in S_2, \\ \frac{1}{2}H^2, & (i, j) \in \partial S_2 \text{ excluding corners of } \partial S_2, \\ \frac{1}{4}H^2, & (i, j) \in \text{corners of } \partial S_2. \end{cases}$$

We may choose more efficient rules, such as the Legendre-Gauss rule with two boundary nodes fixed in [9, 392],

$$\widehat{\int}_{-1}^1 g^2(x) dx = \sum_{j=1}^n w_j g^2(x_j), \quad (6.3.10)$$

where x_j is the j th zero of $P_n(x)$, and $P_n(x)$ are the Legendre polynomials defined by

$$P_n(x) = \frac{(-1)^n}{2^n n!} \cdot \frac{d^n}{dx^n} [(1-x^2)^n], \quad n \geq 1. \quad (6.3.11)$$

The weights are given by

$$w_j = \frac{2}{(1-x_j)[P_n'(x_j)]^2}. \quad (6.3.12)$$

Then at the collocation nodes $P_{ij} = (x_i, y_j)$, the weights in (6.3.7) are obtained by

$$\alpha_{ij} = w_i w_j, \quad (i, j) \in S_2. \quad (6.3.13)$$

Let $f = g^2$ and $f \in C^{2n}[-1, 1]$, then the remainder of (6.3.10) is given by

$$E(f) = \frac{2^{2n+1}[n!]^4}{(2n+1)[(2n)!]^3} f^{(2n)}(\xi), \quad f = g^2, \quad -1 < \xi < 1.$$

Let g in $[-1, 1]$ be polynomials of order L . Then $f(= g^2)$ are polynomials of order $2L$. Choose $n = L + 1$, then the derivatives $f^{(2n)}(\xi) = f^{(2L+2)} \equiv 0$ and $E(f) \equiv 0$. Therefore, when S_2 is a rectangle, the functions v^+ in S_2 are chosen to be polynomials of order L . Since functions Δv^+ are polynomials of order $L - 2$, the Legendre-Gauss rule with $n = L - 1$ in (6.3.3) and (6.3.13) offers no error for $\widehat{\iint}_{S_2} (\Delta v^+)^2$, i.e.,

$$\widehat{\iint}_{S_2} (\Delta v^+)^2 = \iint_{S_2} (\Delta v^+)^2.$$

Now let us establish the linear algebraic equations of combination (6.3.2) of FEM-CM. First, consider the entire FEM in S_1 only,

$$a_1(\hat{u}_h, v) = f_1(v), \quad \forall v \in V_h,$$

where

$$a_1(u, v) = \iint_{S_1} \nabla u \nabla v + \int_{\Gamma_0} u_n^- v^-, \quad f_1(v) = \iint_{S_1} f v.$$

We obtain the linear algebraic equations,

$$\mathbf{A}_1 \mathbf{x}_1 = \mathbf{b}_1, \quad (6.3.14)$$

where \mathbf{x}_1 is a vector consisting of v_{ij} only, and matrix \mathbf{A}_1 is non-symmetric.

Next, Eqs. (6.3.7) – (6.3.9) in $S_2 \cup \Gamma_0$ are denoted by

$$\mathbf{A}_2 \mathbf{x}_2 = \mathbf{b}_2, \quad (6.3.15)$$

where \mathbf{x}_2 is a vector consisting of \tilde{a}_i , v_{1j} and v_{0j} , and v_{0j} and v_{1j} are the unknowns on the two boundary layer nodes in S_1 close to Γ_0 . Denote by M_1 the number of all

collocation nodes in S_2 and ∂S_2 , and by N_1 the number of v_{1j} and v_{0j} . Then matrix $\mathbf{A}_2 \in R^{M_1 \times (L+N_1)}$. Therefore, we can see

$$\begin{aligned} & \frac{1}{2} \mathbf{x}_2^T \mathbf{A}_2^T \mathbf{A}_2 \mathbf{x}_2 - \mathbf{A}_2^T \mathbf{b}_2 \mathbf{x}_2 + \mathbf{c} \\ &= \frac{P_c}{2} \iint_{S_2} (\Delta v + f)^2 + \frac{P_c}{2h} \int_{\Gamma_0} (v^+ - v^-)^2 + \frac{P_c}{2} \int_{\Gamma_0} (v_n^+ - v_n^-)^2. \end{aligned} \quad (6.3.16)$$

Combining (6.3.14) and (6.3.16) yields explicitly¹:

$$\mathbf{A} \mathbf{x} = \mathbf{b}, \quad (6.3.17)$$

$$\mathbf{A} = \mathbf{A}_1 + \mathbf{A}_2^T \mathbf{A}_2, \quad \mathbf{b} = \mathbf{b}_1 + \mathbf{A}_2^T \mathbf{b}_2, \quad (6.3.18)$$

where \mathbf{x} is a vector consisting of the coefficients \tilde{a}_i and v_{ij} in $S_1 \cup \Gamma_0$. Denote by N the number of nodes on $S_1 \cup \Gamma_0$, then the vector \mathbf{x} in (6.3.17) has $N + L$ dimensions. The matrix \mathbf{A} is non-symmetric, but positive definite, based on Theorem 6.5.1 given later. Note that the matrix and vector operations in (6.3.17) may be performed after extending the dimensions of \mathbf{A} and \mathbf{b} by filling up zero entries.

Let us briefly address the solution methods for (6.3.17). When P_c is chosen large enough, matrix $\mathbf{A} \in R^{(L+N) \times (L+N)}$ in (6.3.17) is positive definite and non-symmetric and sparse when $N \gg L$. When $L + N$ is not huge, to solve (6.3.17) we may choose the Gaussian elimination without pivoting, see Golub and Loan [176].

Again since the true solution u satisfies exactly $\hat{a}(u, v) = 0$, $\forall v \in V_h^0$, we have $\hat{a}(u - \hat{u}_h, v) = 0$, $\forall v \in V_h^0$. We obtain the following theorem.

Theorem 6.3.1 *Suppose that there exist two inequalities,*

$$\hat{a}(u, v) \leq C \|u\| \times \|v\|, \quad \forall v \in V_h^0, \quad (6.3.19)$$

$$\hat{a}(v, v) \geq C_0 \|v\|^2, \quad \forall v \in V_h^0, \quad (6.3.20)$$

where $C_0 (> 0)$ and C are two constants independent of h and L . Then, the solution of combination (6.3.1) has the error bound,

$$\|u - \hat{u}_h\| \leq C \inf_{v \in V_h} \|u - v\|.$$

Moreover, the optimal convergence rate (6.2.15) holds if the conditions (6.2.13) and (6.2.14) are satisfied.

The proof of inequality (6.3.20) is deferred to Section 6.5.

Remark 6.3.1 *Note that Eq. (6.3.17), called Method I, presents exactly the combination (6.3.2). There arises a question. Since Eq. (6.3.17) results from (6.3.14) and (6.3.15),*

¹Strictly speaking, the dimensions of matrices and vectors in (6.3.18) are inconsistent. Hence, the equalities in (6.3.18), (6.3.22) and (6.3.27) read as: the smaller dimensions are extended to the larger dimensions by filling out zero entries.

should we solve both (6.3.14) and (6.3.15) directly by the least squares method? The following arguments give a positive justification.

Method I. We rewrite (6.3.17) and (6.3.18) as

$$\mathbf{A}\mathbf{y} = \mathbf{b}, \quad (6.3.21)$$

$$\mathbf{A}_1\mathbf{y} + \mathbf{A}_2^T\mathbf{A}_2\mathbf{y} = \mathbf{b}_1 + \mathbf{A}_2^T\mathbf{b}_2. \quad (6.3.22)$$

Method II. The direct least squares method. Solve

$$\mathbf{A}_1\mathbf{x} = \mathbf{b}_1, \quad \mathbf{A}_2\mathbf{x} = \mathbf{b}_2, \quad (6.3.23)$$

by

$$I(\mathbf{x}) = \min_{\mathbf{z}} I(\mathbf{z}), \quad (6.3.24)$$

where

$$I(\mathbf{z}) = \|\mathbf{A}_1\mathbf{z} - \mathbf{b}_1\|^2 + \|\mathbf{A}_2\mathbf{z} - \mathbf{b}_2\|^2,$$

and $\|\cdot\|$ is the Euclidean norm.

Proposition 6.3.1 Let \mathbf{x} and \mathbf{y} be the solutions from (6.3.23) and (6.3.21) respectively, then $\mathbf{x} \approx \mathbf{y}$ with the relative error bound,

$$\frac{\|\mathbf{x} - \mathbf{y}\|}{\|\mathbf{y}\|} \leq \text{Cond.} \frac{\|\mathbf{r}\|}{\|\mathbf{b}\|} \leq \text{Cond.}(1 + \|\mathbf{A}_2\|) \frac{\varepsilon}{\|\mathbf{b}\|}, \quad (6.3.25)$$

where the error of Method II is

$$\varepsilon = (\|\mathbf{A}_1\mathbf{x} - \mathbf{b}_1\|^2 + \|\mathbf{A}_2\mathbf{x} - \mathbf{b}_2\|^2)^{1/2}.$$

Cond. denotes the condition number

$$\text{Cond.} = \sqrt{\frac{\lambda_{\max}(\mathbf{A}^T\mathbf{A})}{\lambda_{\min}(\mathbf{A}^T\mathbf{A})}},$$

and $\lambda_{\max}(\mathbf{A}^T\mathbf{A})$ and $\lambda_{\min}(\mathbf{A}^T\mathbf{A})$ are the maximal and minimal eigenvalues of $\mathbf{A}^T\mathbf{A}$, respectively.

Proof Let $I(\mathbf{x}) = \varepsilon^2$, we then obtain (6.3.24)

$$\|\mathbf{A}_1 \mathbf{x} - \mathbf{b}_1\| \leq \varepsilon, \quad \|\mathbf{A}_2 \mathbf{x} - \mathbf{b}_2\| \leq \varepsilon. \quad (6.3.26)$$

Consider the remainder of (6.3.22) when \mathbf{x} replaces \mathbf{y} :

$$\mathbf{r} = \mathbf{A} \mathbf{x} - \mathbf{b} = \mathbf{A}_1 \mathbf{x} - \mathbf{b}_1 + \mathbf{A}_2^T \mathbf{A}_2 \mathbf{x} - \mathbf{A}_2^T \mathbf{b}_2. \quad (6.3.27)$$

We have from (6.3.26)

$$\|\mathbf{r}\| \leq \|\mathbf{A}_1 \mathbf{x} - \mathbf{b}_1\| + \|\mathbf{A}_2\| \|\mathbf{A}_2 \mathbf{x} - \mathbf{b}_2\| \leq (1 + \|\mathbf{A}_2\|) \varepsilon.$$

Moreover, we have from Eqs. (6.3.21) and (6.3.27)

$$\mathbf{A}(\mathbf{x} - \mathbf{y}) = \mathbf{r}.$$

Since $\|\mathbf{y}\| \geq \|\mathbf{b}\|/\|\mathbf{A}\|$, the desired result (6.3.25) is obtained by following [9, 176]. Since ε is very small, the solution \mathbf{x} of Method II is almost the solution \mathbf{y} of Method I approximately. ■

6.4 Uniformly V_h^0 - Elliptic Inequality

The key analysis of combinations (6.2.8) and (6.3.1) is to prove the uniformly V_h^0 - elliptic inequalities (6.2.11) and (6.3.20), since the proof for (6.2.10) and (6.3.19) is much simpler. We shall prove (6.2.11) in this section and then (6.3.20) in the next section.

First, we consider $a(v, v)$ without the term $\int_{\Gamma_0} v_n^- v^-$. Define the norms

$$\|v\|_E = \left(|v|_{1,S_1}^2 + P_c \|\Delta v\|_{0,S_2}^2 + \frac{P_c}{h} \|v^+ - v^-\|_{0,\Gamma_0}^2 + P_c \|v_n^+ - v_n^-\|_{0,\Gamma_0}^2 \right)^{1/2}, \quad (6.4.1)$$

and

$$\overline{\|v^+ - v^-\|}_{\ell,\Gamma_0} = \|\hat{v}^+ - v^-\|_{\ell,\Gamma_0},$$

where $\ell = 0, \frac{1}{2}$, and \hat{v}^+ is the piecewise k -order polynomial interpolant of v^+ in S_2 . Then we have the following lemma.

Lemma 6.4.1 *Suppose that there exists a positive constant $\nu(> 0)$ such that*

$$\|v^+\|_{\ell, \Gamma_0} \leq CL^{\ell\nu} \|v^+\|_{0, \Gamma_0}, \quad \ell = 1, 2, \dots \quad (6.4.2)$$

Then, there exists the bound for $v \in V_h^0$,

$$\|v^+ - v^-\|_{\frac{1}{2}, \Gamma_0} \leq \frac{C}{\sqrt{h}} \|v^+ - v^-\|_{0, \Gamma_0} + Ch^{\frac{3}{2}} L^{2\nu} \|v^+\|_{1, S_2}, \quad (6.4.3)$$

where the norms

$$\|v\|_{\frac{1}{2}, \Gamma_0} = \left\{ \|v\|_{0, \Gamma_0}^2 + \int_{\Gamma_0} \int_{\Gamma_0} \frac{[v(P) - v(Q)]^2}{\|P - Q\|^2} dl(P) dl(Q) \right\}^{\frac{1}{2}},$$

$$\|u\|_{-\frac{1}{2}, \Gamma_0} = \frac{\text{Sup} \left| \int_{\Gamma_0} uv dl \right|}{\|v\|_{\frac{1}{2}, \Gamma_0}}.$$

Proof We have from triangle inequalities,

$$\|v^+ - v^-\|_{\frac{1}{2}, \Gamma_0} \leq \overline{\|v^+ - v^-\|}_{\frac{1}{2}, \Gamma_0} + \|\hat{v}^+ - v^+\|_{\frac{1}{2}, \Gamma_0},$$

$$\overline{\|v^+ - v^-\|}_{0, \Gamma_0} \leq \|v^+ - v^-\|_{0, \Gamma_0} + \|\hat{v}^+ - v^+\|_{0, \Gamma_0}.$$

Then from the inverse inequality for piecewise k -order polynomials, there exists the bound,

$$\begin{aligned} \|v^+ - v^-\|_{\frac{1}{2}, \Gamma_0} &\leq \overline{\|v^+ - v^-\|}_{\frac{1}{2}, \Gamma_0} + \|\hat{v}^+ - v^+\|_{\frac{1}{2}, \Gamma_0} \\ &\leq \frac{C}{\sqrt{h}} \overline{\|v^+ - v^-\|}_{0, \Gamma_0} + \|\hat{v}^+ - v^+\|_{\frac{1}{2}, \Gamma_0} \\ &\leq \frac{C}{\sqrt{h}} \|v^+ - v^-\|_{0, \Gamma_0} + \frac{C}{\sqrt{h}} \|\hat{v}^+ - v^+\|_{0, \Gamma_0} + \|\hat{v}^+ - v^+\|_{\frac{1}{2}, \Gamma_0}. \end{aligned} \quad (6.4.4)$$

Moreover, from (6.4.2) we have

$$\begin{aligned} h^{-\frac{1}{2}} \|\hat{v}^+ - v^+\|_{0, \Gamma_0} + \|\hat{v}^+ - v^+\|_{\frac{1}{2}, \Gamma_0} \\ \leq Ch^{\frac{3}{2}} \|v^+\|_{2, \Gamma_0} \leq Ch^{\frac{3}{2}} L^{2\nu} \|v^+\|_{0, \Gamma_0} \leq Ch^{\frac{3}{2}} L^{2\nu} \|v^+\|_{1, S_2}. \end{aligned} \quad (6.4.5)$$

Combining (6.4.4) and (6.4.5) yields the desired result (6.4.3). ■

Lemma 6.4.2 *There exist the bounds for $v \in V_h^0$,*

$$\|v^+\|_{1, S_2} \leq C \{ \|\Delta v^+\|_{-1, S_2} + \|v^+\|_{\frac{1}{2}, \partial S_2} \}, \quad (6.4.6)$$

$$\|v_n^+\|_{-\frac{1}{2}, \Gamma_0} \leq C \{ \|\Delta v^+\|_{-1, S_2} + \|v^+\|_{\frac{1}{2}, \partial S_2} \}, \quad (6.4.7)$$

where C is a constant independent of h and L , and the negative norm is defined by

$$\|u\|_{-1, S} = \sup_{v \in H_0^1(S)} \frac{|\iint_S uv ds|}{\|v\|_{1, S}}.$$

Proof We cite the bounds from Oden and Reddy [365], p. 189-192,

$$\|u\|_{\tilde{H}^{s,2m}(\Omega)}^2 \leq C\{\|Au\|_{H^{s-2m}(\Omega)}^2 + \sum_{k=0}^{m-1} \|B_k u\|_{H^{s-g_k-\frac{1}{2}}(\partial\Omega)}^2\}, \quad (6.4.8)$$

where $s < 2m$, and m is a positive integer. The notations are: $Au = \Delta u$, $B_0 u = u$, $B_1 u = u_n$, $g_0 = 0$ and $g_1 = 1$. The norm on the left hand side in (6.4.8) is defined in [365], p. 183,

$$\|u\|_{\tilde{H}^{s,r}(\Omega)}^2 = \|u\|_{H^s(\Omega)}^2 + \sum_{k=0}^{r-1} \|D_n^k u\|_{H^{s-k-\frac{1}{2}}(\partial\Omega)}^2, \quad (6.4.9)$$

where r is a positive integer, s is an integer, and $D_n^k = \frac{\partial^k}{\partial n^k}$ is the k th normal derivatives. In (6.4.8), choosing $s = 1$, $m = 1$ and $\Omega = S_2$, we obtain

$$\|u\|_{\tilde{H}^{1,2}(S_2)}^2 \leq C\{\|\Delta u\|_{H^{-1}(S_2)}^2 + \|u\|_{H^{\frac{1}{2}}(\partial S_2)}^2\}, \quad (6.4.10)$$

where the norm in the left hand side is given in (6.4.9) with $s = 1$, $r = 2$ and $\Omega = S_2$,

$$\|u\|_{\tilde{H}^{1,2}(S_2)}^2 = \|u\|_{H^1(S_2)}^2 + \|u\|_{H^{\frac{1}{2}}(\partial S_2)}^2 + \|u_n\|_{H^{-\frac{1}{2}}(\partial S_2)}^2. \quad (6.4.11)$$

Combining (6.4.10) and (6.4.11) gives the following bound,

$$\|u\|_{1,S_2}^2 + \|u\|_{\frac{1}{2},\partial S_2}^2 + \|u_n\|_{-\frac{1}{2},\partial S_2}^2 \leq C\{\|\Delta u\|_{-1,S_2}^2 + \|u\|_{\frac{1}{2},\partial S_2}^2\}. \quad (6.4.12)$$

The desired results (6.4.6) and (6.4.7) are obtained directly from (6.4.12). ■

Lemma 6.4.3 *Let (6.4.2) and the following bound hold,*

$$h^{\frac{3}{2}} L^{2\nu} = o(1). \quad (6.4.13)$$

Then, for $v \in V_h^0$ there exists the bound,

$$\|v^+\|_{1,S_2} \leq C\{\|v^-\|_{\frac{1}{2},\Gamma_0} + \frac{1}{\sqrt{h}}\|v^+ - v^-\|_{0,\Gamma_0} + \|\Delta v^+\|_{0,S_2}\}, \quad (6.4.14)$$

where C is a constant independent of h and L .

Proof From Lemma 6.4.1 we have

$$\begin{aligned} \|v^+\|_{\frac{1}{2},\Gamma_0} &\leq \|v^-\|_{\frac{1}{2},\Gamma_0} + \|v^+ - v^-\|_{\frac{1}{2},\Gamma_0} \\ &\leq \|v^-\|_{\frac{1}{2},\Gamma_0} + \frac{C}{\sqrt{h}} \|v^+ - v^-\|_{0,\Gamma_0} + Ch^{\frac{3}{2}} L^{2\nu} \|v^+\|_{1,S_2}. \end{aligned} \quad (6.4.15)$$

From Lemma 6.4.2 and (6.4.15)

$$\begin{aligned} \|v^+\|_{1,S_2} &\leq C\{\|v^+\|_{\frac{1}{2},\Gamma_0} + \|\Delta v^+\|_{-1,S_2}\} \\ &\leq C\{\|v^-\|_{\frac{1}{2},\Gamma_0} + \frac{1}{\sqrt{h}} \|v^+ - v^-\|_{0,\Gamma_0} + h^{\frac{3}{2}} L^{2\nu} \|v^+\|_{1,S_2} + \|\Delta v^+\|_{0,S_2}\}. \end{aligned}$$

This leads to

$$\begin{aligned} \|v^+\|_{1,S_2} &\leq \frac{C}{1 - Ch^{\frac{3}{2}} L^{2\nu}} \left\{ \|v^-\|_{\frac{1}{2},\Gamma_0} + \frac{1}{\sqrt{h}} \|v^+ - v^-\|_{0,\Gamma_0} + \|\Delta v^+\|_{0,S_2} \right\}. \end{aligned}$$

The desired result (6.4.14) follows from $Ch^{\frac{3}{2}} L^{2\nu} \leq \frac{1}{2}$ by assumption (6.4.13). ■

Lemma 6.4.4 *Let $\Gamma \cap \partial S_1 \neq \emptyset$, (6.4.2) and (6.4.13) hold, there exists an inequality*

$$C_0 \| |v| \| \leq \|v\|_E, \quad \forall v \in V_h^0, \quad (6.4.16)$$

where $\| |v| \|$ and $\|v\|_E$ are defined in (6.2.9) and (6.4.1) respectively, and $C_0 > 0$ has a lower bound independent of h and L .

Proof We prove by the contradiction. Suppose that can find a sequence $\{v_\ell\} \subseteq H^*$ such that

$$\| |v_\ell| \| = 1, \quad \|v_\ell\|_E \rightarrow 0, \quad \text{as } \ell \rightarrow \infty. \quad (6.4.17)$$

First, $\|v_\ell\|_E \rightarrow 0$ implies that for large ℓ , $|v_\ell^-|_{1,S_1} \leq 1$ and $v_\ell^-|_{\partial S_1 \cap \Gamma} = 0$, and then $\|v_\ell^-\|_{1,S_1}$ is bounded. Based on the Kandrosor or Rellich theorem [105], there exists a subsequence $\{v_\ell^-\}$ in $L^2(S_1)$ (also written as $\{\bar{v}_\ell^-\}$) such that $v_\ell^- \rightarrow \bar{v}^- \in L^2(S_1)$. Then, $\bar{v}^- \in H^1(S_1)$, since $|v_\ell^-|_{1,S_1}$ are bounded due to $|v_\ell^-|_{1,S_1} \leq 1$. Moreover, $\|v_\ell\|_E \rightarrow 0$ gives $|v_\ell^-|_{1,S_1} \rightarrow 0$ as $\ell \rightarrow \infty$. Since $H^1(S_1)$ is complete, we conclude that $|v_\ell^-|_{1,S_1} = \lim_{\ell \rightarrow \infty} |v_\ell^-|_{1,S_1} = 0$. Hence \bar{v}^- is a constant, and $\bar{v}^- \equiv 0$ in S_1 due to $v_\ell^-|_{\partial S_1 \cap \Gamma} = 0$.

From the trace theorem in [438]

$$\|v_\ell^-\|_{\frac{1}{2},\Gamma_0} \leq C \|v_\ell^-\|_{1,S_1},$$

$\|v_\ell^-\|_{\frac{1}{2},\Gamma_0}$ is also bounded, and

$$\lim_{\ell \rightarrow \infty} \|v_\ell^-\|_{\frac{1}{2},\Gamma_0} = \|\bar{v}^-\|_{\frac{1}{2},\Gamma_0} = 0. \quad (6.4.18)$$

Next, consider the sequence v_ℓ^+ in S_2 . We have from Lemma 6.4.3,

$$\begin{aligned} \|v_\ell^+\|_{\frac{1}{2},\Gamma_0} &\leq C\|v_\ell^+\|_{1,S_2} \\ &\leq C\{\|v_\ell^-\|_{\frac{1}{2},\Gamma_0} + \frac{1}{\sqrt{h}}\|v_\ell^+ - v_\ell^-\|_{0,\Gamma_0} + \|\Delta v_\ell^+\|_{0,S_2}\}. \end{aligned} \quad (6.4.19)$$

We conclude that $\|v_\ell^+\|_{\frac{1}{2},\Gamma_0}$ is bounded, and that $\lim_{\ell \rightarrow \infty} \|v_\ell^+\|_{\frac{1}{2},\Gamma_0} = 0$ from (6.4.19), (6.4.18) and $\|v_\ell\|_E \rightarrow 0$. Then, based on Lemma 6.4.2,

$$\begin{aligned} \|v_\ell^+\|_{1,S_2} &\leq C\{\|\Delta v_\ell^+\|_{-1,S_2} + \|v_\ell^+\|_{\frac{1}{2},\partial S_2}\} \\ &\leq C\{\|\Delta v_\ell^+\|_{0,S_2} + \|v_\ell^+\|_{\frac{1}{2},\Gamma_0}\}. \end{aligned}$$

Hence $\|v_\ell^+\|_{1,S_2}$ is also bounded from $\|v_\ell\|_E \rightarrow 0$, and then $\lim_{\ell \rightarrow \infty} \|v_\ell^+\|_{1,S_2} = 0$. By repeating the above arguments, there also exists a subsequence v_ℓ^+ to converge $\bar{v}^+ \in H^1(S_2)$. Moreover, we have $\|\bar{v}^+\|_{1,S_2} = \lim_{\ell \rightarrow \infty} \|v_\ell^+\|_{1,S_2} = 0$, and then $\bar{v}^+ \equiv 0$ in S_2 . Hence $\bar{v} \equiv 0$ in the entire S and $\|\bar{v}\| = 0$. This contradicts the assumption $\|\bar{v}\| = \lim_{\ell \rightarrow \infty} \|v_\ell\| = 1$ in (6.4.17). ■

Now, we give the main theorem.

Theorem 6.4.1 *Let $\Gamma \cap \partial S_1 \neq \emptyset$, (6.4.2) and (6.4.13) hold, and P_c be chosen to be suitably large but still independent of h . Then the uniformly V_h^0 - elliptic inequality holds,*

$$C_0\|v\|^2 \leq a(v, v), \quad \forall v \in V_h^0, \quad (6.4.20)$$

where $C_0 > 0$ is a constant independent of h and L .

Proof From Lemma 6.4.4, we obtain the bound,

$$\begin{aligned} a(v, v) &\geq \|v\|_E^2 - \int_{\Gamma_0} v_n^- v^- \geq C_1\|v\|^2 - \int_{\Gamma_0} v_n^- v^- \\ &= C_1 \left(\|v\|_{1,S_1}^2 + P_c\|v\|_{1,S_2}^2 + P_c\|\Delta v\|_{0,S_2}^2 + \frac{P_c}{h}\|v^+ - v^-\|_{0,\Gamma_0}^2 + P_c\|v_n^+ - v_n^-\|_{0,\Gamma_0}^2 \right) \\ &\quad - \int_{\Gamma_0} v_n^- v^-, \end{aligned} \quad (6.4.21)$$

where $C_1 > 0$ is a lower bound independent of h and L . Next we have

$$\left| \int_{\Gamma_0} v_n^- v^- \right| \leq \|v_n^-\|_{-\frac{1}{2},\Gamma_0} \|v^-\|_{\frac{1}{2},\Gamma_0}.$$

Moreover, there exist the bounds for $v \in V_h^0$,

$$\|v^-\|_{\frac{1}{2},\Gamma_0} \leq C\|v^-\|_{1,S_1}, \quad (6.4.22)$$

$$\begin{aligned} \|v_n^-\|_{-\frac{1}{2},\Gamma_0} &\leq \|v_n^+\|_{-\frac{1}{2},\Gamma_0} + \|v_n^+ - v_n^-\|_{-\frac{1}{2},\Gamma_0} \\ &\leq C\{\|v^+\|_{1,S_2} + \|\Delta v^+\|_{0,S_2} + \|v_n^+ - v_n^-\|_{0,\Gamma_0}\}, \end{aligned} \quad (6.4.23)$$

where we have used the bound from Lemma 6.4.2,

$$\begin{aligned} \|v_n^+\|_{-\frac{1}{2},\Gamma_0} &\leq C\{\|\Delta v^+\|_{-1,S_2} + \|v^+\|_{\frac{1}{2},\partial S_2}\} \\ &\leq C\{\|\Delta v^+\|_{0,S_2} + \|v^+\|_{1,S_2}\}. \end{aligned}$$

Since $Cab \leq \epsilon a^2 + \frac{C^2}{4\epsilon} b^2$ for any $\epsilon > 0$, we obtain from (6.4.22) and (6.4.23)

$$\begin{aligned} \left| \int_{\Gamma_0} v_n^- v^- \right| &\leq C \|v^-\|_{1,S_1} \{ \|v^+\|_{1,S_2} + \|\Delta v^+\|_{0,S_2} + \|v_n^+ - v_n^-\|_{0,\Gamma_0} \} \quad (6.4.24) \\ &\leq \frac{C_1}{2} \|v^-\|_{1,S_1}^2 + \frac{C^2}{2C_1} \{ \|v^+\|_{1,S_2} + \|\Delta v^+\|_{0,S_2} + \|v_n^+ - v_n^-\|_{0,\Gamma_0} \}^2 \\ &\leq \frac{C_1}{2} \|v^-\|_{1,S_1}^2 + \frac{3C^2}{2C_1} \{ \|v^+\|_{1,S_2}^2 + \|\Delta v^+\|_{0,S_2}^2 + \|v_n^+ - v_n^-\|_{0,\Gamma_0}^2 \}, \end{aligned}$$

where C_1 is given in (6.4.21). Combining (6.4.21) and (6.4.24) gives

$$\begin{aligned} a(v, v) &\geq \frac{C_1}{2} \|v\|_{1,S_1}^2 \\ &\quad + (C_1 P_c - \frac{3C^2}{2C_1}) (\|v\|_{1,S_2}^2 + \|\Delta v\|_{0,S_2}^2 + \|v_n^+ - v_n^-\|_{0,\Gamma_0}^2) + C_1 \frac{P_c}{h} \|v^+ - v^-\|_{0,\Gamma_0}^2 \\ &\geq \frac{C_1}{2} \|v\|^2, \end{aligned}$$

provided that $C_1 P_c - \frac{3C^2}{2C_1} \geq \frac{1}{2} C_1 P_c$. This leads to $P_c \geq 3\frac{C^2}{C_1^2}$, which is suitably large but still independent of h and L . Then the uniformly V_h^0 -elliptic inequality (6.4.20) holds with $C_0 = \frac{C_1}{2}$. ■

6.5 Uniformly V_h^0 -Elliptic Inequality Involving Integration Approximation

In this section, we prove the uniformly V_h^0 -elliptic inequality, (6.3.20). Choose the integration rule

$$\widehat{\int}_{\Gamma_0} v^2 = \int_{\Gamma_0} \hat{v}^2 = \overline{\|v\|_{0,\Gamma_0}^2},$$

where \hat{v} is the k -order polynomial interpolant of v . First, we give a few lemmas.

Lemma 6.5.1 *Let (6.4.2) and*

$$\|v_n^+\|_{1,\Gamma_0} \leq CL^{2\nu}\|v^+\|_{1,S_2}, \quad \forall v \in V_h^0 \quad (6.5.1)$$

hold, where $\nu(> 0)$ is a positive constant. There exist the bounds for $v \in V_h^0$,

$$\overline{\|v^+ - v^-\|_{0,\Gamma_0}} \geq \|v^+ - v^-\|_{0,\Gamma_0} - Ch^2L^{2\nu}\|v^+\|_{1,S_2}, \quad (6.5.2)$$

$$\overline{\|v_n^+ - v_n^-\|_{0,\Gamma_0}} \geq \|v_n^+ - v_n^-\|_{0,\Gamma_0} - ChL^{2\nu}\|v^+\|_{1,S_2}, \quad (6.5.3)$$

where C is a constant independent of h and L .

Proof We have

$$\|v^+ - v^-\|_{0,\Gamma_0} \leq \overline{\|v^+ - v^-\|_{0,\Gamma_0}} + \|\hat{v}^+ - v^+\|_{0,\Gamma_0}, \quad (6.5.4)$$

and from (6.4.2)

$$\|\hat{v}^+ - v^+\|_{0,\Gamma_0} \leq Ch^2|v^+|_{2,\Gamma_0} \leq Ch^2L^{2\nu}\|v\|_{0,\Gamma_0} \leq Ch^2L^{2\nu}\|v\|_{1,S_2}. \quad (6.5.5)$$

Then combining (6.5.4) and (6.5.5) gives the first desired bound (6.5.2),

$$\overline{\|v^+ - v^-\|_{0,\Gamma_0}} \geq \|v^+ - v^-\|_{0,\Gamma_0} - Ch^2L^{2\nu}\|v\|_{1,S_2}.$$

Similarly, we obtain from (6.5.1)

$$\begin{aligned} \overline{\|v_n^+ - v_n^-\|_{0,\Gamma_0}} &\geq \|v_n^+ - v_n^-\|_{0,\Gamma_0} - \|v_n^+ - \hat{v}_n^+\|_{0,\Gamma_0} \\ &\geq \|v_n^+ - v_n^-\|_{0,\Gamma_0} - Ch\|v_n\|_{1,\Gamma_0} \\ &\geq \|v_n^+ - v_n^-\|_{0,\Gamma_0} - ChL^{2\nu}\|v\|_{1,S_2}. \end{aligned}$$

This is the second desired bound (6.5.3). ■

Lemma 6.5.2 *Let all conditions in Lemma 6.5.1 hold. Then*

$$\overline{\|v^+ - v^-\|_{0,\Gamma_0}^2} \geq \frac{1}{2}\|v^+ - v^-\|_{0,\Gamma_0}^2 - Ch^4L^{4\nu}\|v^+\|_{1,S_2}^2, \quad (6.5.6)$$

$$\overline{\|v_n^+ - v_n^-\|_{0,\Gamma_0}^2} \geq \frac{1}{2}\|v_n^+ - v_n^-\|_{0,\Gamma_0}^2 - Ch^2L^{4\nu}\|v^+\|_{1,S_2}^2, \quad (6.5.7)$$

where C is a constant independent of h and L .

Proof Denote

$$\begin{aligned} x &= \overline{\|v^+ - v^-\|_{0,\Gamma_0}}, \quad y = \|v^+ - v^-\|_{0,\Gamma_0}, \\ z &= \|v^+\|_{1,S_2}, \quad w = Ch^2 L^{2\nu}. \end{aligned} \quad (6.5.8)$$

Eq. (6.5.2) is written simply as $x \geq y - wz \geq 0$ for small h . We have

$$x^2 \geq (y - wz)^2 = y^2 - 2wyz + w^2 z^2.$$

Since $2wyz \leq \frac{y^2}{2} + 2w^2 z^2$, we obtain

$$x^2 \geq y^2 - \left(\frac{y^2}{2} + 2w^2 z^2\right) + w^2 z^2 = \frac{y^2}{2} - w^2 z^2.$$

This is the desired result (6.5.6) by noting (6.5.8). The proof for (6.5.7) is similar. ■

Second, let us consider integration approximation for $\iint_{S_2} t$, where $t = t(x, y) = (\Delta u + f)(\Delta v + f)$. Let S_2 be divided into small triangles Δ_{ij} and small rectangles \square_{ij} ,

$$S_2 = (\cup_{ij} \Delta_{ij}) \cup (\cup_{ij} \square_{ij}). \quad (6.5.9)$$

Denote by \hat{t}_r the piecewise r -order interpolant of t on S_2 , i.e.,

$$\hat{t}_r = P_r(x, y) = \sum_{i+j=0}^r a_{ij} x^i y^j, \quad (x, y) \in \Delta_{ij},$$

or

$$\hat{t}_r = Q_r(x, y) = \sum_{i,j=0}^r a_{ij} x^i y^j, \quad (x, y) \in \square_{ij},$$

with the coefficients a_{ij} . Then, the integration rule in (6.3.3) can be viewed as

$$\begin{aligned} \sum_{ij} \alpha_{ij} g^2(P_{ij}) &= \widehat{\iint}_{S_2} g^2 = \widehat{\iint}_{S_2} t = \iint_{S_2} \hat{t}_r \\ &= \sum_{ij} \iint_{\Delta_{ij}} \hat{t}_r + \sum_{ij} \iint_{\square_{ij}} \hat{t}_r. \end{aligned} \quad (6.5.10)$$

The partition in (6.5.9) is regular if $\max_{ij} \frac{H_{ij}}{\rho_{ij}} \leq C$, where H_{ij} is the maximal boundary length of Δ_{ij} and \square_{ij} , ρ_{ij} is the diameter of the inscribed circle of Δ_{ij} and \square_{ij} , and C is constant independent of $H (= \max_{ij} H_{ij})$. The partition (6.5.9) is quasiuniform if $\frac{H}{\min_{ij} H_{ij}} \leq C$. Then we have the following lemma from the Bramble-Hilbert lemma [105].

Lemma 6.5.3 *Let the partition (6.5.9) be regular and quasiuniform. Then the integration rule (6.5.10) has the error bound,*

$$\left| \iint_{S_2} t - \widehat{\iint}_{S_2} t \right| = \left| \iint_{S_2} (t - \hat{t}_r) \right| \leq CH^{r+1} |t|_{r+1, S_2},$$

where C is a constant independent of H .

The integration rule on Δ_{ij} can be found in Strang and Fix [446], and the rule on \square_{ij} can be formulated by the tensor product of the rule in one dimension, such as the Newton-Cotes rule or the Gaussian rule. The Legendre-Gauss rule given in (6.3.10) – (6.3.13) is just one kind of Gaussian rules with two boundary nodes fixed. For the Newton-Cotes rule with order r , we may choose the uniform integration nodes. When $r = 1$ and 2, the popular trapezoidal and Simpson's rules are given. When v^+ in S_2 are polynomials of order L and choose $r = 2L$, the exact integration holds,

$$\widehat{\iint}_{S_2} (\Delta v^+)^2 = \iint_{S_2} (\Delta v^+)^2. \quad (6.5.11)$$

Below, we consider the approximate integration

$$\widehat{\iint}_{S_2} (\Delta v^+)^2 \approx \iint_{S_2} (\Delta v^+)^2,$$

by the rule with integration orders $r \leq 2L - 1$. We have the following lemma.

Lemma 6.5.4 *Let v^+ in S_2 be polynomials of order L , and the rule (6.5.10) with order $r \leq 2L - 1$ be used for $\iint_{S_2} (\Delta u + f)(\Delta v + f)$. Also assume*

$$\|v^+\|_{\ell, S_2} \leq CL^{(\ell-1)\nu} \|v^+\|_{1, S_2}, \quad \ell \geq 1, \quad \forall v \in V_h^0, \quad (6.5.12)$$

where $\nu > 0$ is a constant independent of L . Then there exists the bound,

$$\left| \left(\iint_{S_2} - \widehat{\iint}_{S_2} \right) (\Delta v)^2 \right| \leq CH^{r+1} L^{(r+3)\nu} \|v\|_{1, S_2}^2,$$

where H is the meshspacing of uniform integration nodes in S_2 , and C is a constant independent of H and L .

Proof For the rule of order $r \leq 2L - 1$, we have from Lemma 6.5.3 and (6.5.12),

$$\begin{aligned} & \left| \left(\iint_{S_2} - \widehat{\iint}_{S_2} \right) (\Delta v)^2 \right| \leq CH^{r+1} |(\Delta v)^2|_{r+1, S_2} \\ & \leq CH^{r+1} \sum_{i=0}^{r+1} |\Delta v|_{i, S_2} |\Delta v|_{r+1-i, S_2} \leq CH^{r+1} \sum_{i=0}^{r+1} \|v\|_{i+2, S_2} \|v\|_{r+3-i, S_2} \\ & \leq CH^{r+1} \sum_{i=0}^{r+1} (L^{(i+1)\nu} \|v\|_{1, S_2}) (L^{(r+2-i)\nu} \|v\|_{1, S_2}) \\ & \leq CH^{r+1} L^{(r+3)\nu} \|v\|_{1, S_2}^2. \quad \blacksquare \end{aligned}$$

Theorem 6.5.1 *Let (6.5.1) and all conditions of Theorem 6.4.1 and Lemma 6.5.4 hold. Suppose*

$$hL^{2\nu} = o(1), \quad (6.5.13)$$

$$HL^{(1+\frac{2}{r+1})\nu} = o(1). \quad (6.5.14)$$

Then the uniformly V_h^0 -elliptic inequality (6.3.20) holds.

Proof From Lemmas 6.5.2 and 6.5.4 and Theorem 6.4.1, we have

$$\begin{aligned} \hat{a}(v, v) &= \iint_{S_1} |\nabla v^-|^2 + \int_{\Gamma_0} v_n^- v^- + P_c \iint_{S_2} (\Delta v^+)^2 \\ &\quad + \frac{P_c}{h} \|v^+ - v^-\|_{0,\Gamma_0}^2 + P_c \|v_n^+ - v_n^-\|_{0,\Gamma_0}^2 \\ &\geq \iint_{S_1} |\nabla v^-|^2 + \int_{\Gamma_0} v_n^- v^- + P_c \iint_{S_2} (\Delta v^+)^2 \\ &\quad + \frac{P_c}{2h} \|v^+ - v^-\|_{0,\Gamma_0}^2 + \frac{P_c}{2} \|v_n^+ - v_n^-\|_{0,\Gamma_0}^2 \\ &\quad - CP_c(h^3 L^{4\nu} + h^2 L^{4\nu}) \|v\|_{1,S_2}^2 - CH^{r+1} L^{(r+3)\nu} \|v\|_{1,S_2}^2 \\ &\geq \frac{1}{2} a(v, v) - C\{P_c(h^3 L^{4\nu} + h^2 L^{4\nu}) + H^{r+1} L^{(r+3)\nu}\} \|v\|_{1,S_2}^2 \\ &\geq \frac{C_0}{2} \|v\|^2 - C\{P_c(h^3 L^{4\nu} + h^2 L^{4\nu}) + H^{r+1} L^{(r+3)\nu}\} \|v\|_{1,S_2}^2 \\ &\geq \frac{C_0}{2} \{\|v\|_{1,S_1}^2 + \{1 - 2\frac{C}{C_0}[P_c(h^3 L^{4\nu} + h^2 L^{4\nu}) + H^{r+1} L^{(r+3)\nu}]\}\|v\|_{1,S_2}^2 \\ &\quad + P_c \|\Delta v\|_{0,S_2}^2 + \frac{P_c}{h} \|v^+ - v^-\|_{0,\Gamma_0}^2 + P_c \|v_n^+ - v_n^-\|_{0,\Gamma_0}^2\} \\ &\geq \frac{C_0}{4} \|v\|^2, \end{aligned}$$

provided that

$$2\frac{C}{C_0}[P_c(h^3 L^{4\nu} + h^2 L^{4\nu}) + H^{r+1} L^{(r+3)\nu}] \leq \frac{1}{2},$$

which is satisfied by (6.5.13) and (6.5.14). ■

When there is no approximation for $\iint_{S_2} \Delta u^+ \Delta v^+$, we have the following corollary.

Corollary 6.5.1 *Let (6.5.1) and all conditions of Theorem 6.4.1 hold. Also let the numerical integration (6.5.11) in S_2 be exact. Suppose*

$$hL^{2\nu} = o(1).$$

Then the uniformly V_h^0 -elliptic inequality (6.3.20) holds.

Corollary 6.5.1 holds for the case that v^+ in S_2 are polynomials of order $L(> k)$, and that the Legendre-Gauss rule in (6.3.10) with $n = L - 1$ is used for $\widehat{\iint}_{S_2} \Delta^2 v^+$. Next, let us consider a special case: The functions v^+ in S_2 are chosen to be the particular solutions satisfying $-\Delta v^+ = f$ in S_2 exactly. The combination of FEM-CM in (6.3.2) is given by

$$\hat{a}^*(\hat{u}_h, v) = f_1(v), \quad \forall v \in V_h^0,$$

where

$$\begin{aligned} \hat{a}^*(u, v) &= \iint_{S_1} \nabla u \cdot \nabla v + \int_{\Gamma_0} u_n^- v^- \\ &+ \frac{P_c}{h} \widehat{\int}_{\Gamma_0} (u^+ - u^-)(v^+ - v^-) + P_c \widehat{\int}_{\Gamma_0} (u_n^+ - u_n^-)(v_n^+ - v_n^-), \\ f_1(v) &= \iint_{S_1} f v. \end{aligned}$$

In this case, we have

$$\begin{aligned} \hat{a}(v, v) &= \iint_{S_1} |\nabla v|^2 + \int_{\Gamma_0} v_n^- v^- + P_c \iint_{S_2} (\Delta v)^2 \\ &+ \frac{P_c}{h} \widehat{\int}_{\Gamma_0} (v^+ - v^-)^2 + P_c \widehat{\int}_{\Gamma_0} (v_n^+ - v_n^-)^2. \end{aligned}$$

Note that the term, $P_c \iint_{S_2} (\Delta v)^2$, disappears in computation.

Remark 6.5.1 Different integration rules for $\iint_{S_2} (\Delta u + f)(\Delta v + f)$ do not influence upon errors of the solutions by combinations of FEM-CM, but guarantee the uniformly V_h^0 -elliptic inequality (6.3.20), as long as H is chosen so small to satisfy (6.5.14), e.g., as long as the number of collocation nodes P_{ij} in quasiuniform distribution is large enough. This conclusion is a distinctive feature from that in the conventional analysis of FEMs.

Remark 6.5.2 For Theorems 6.4.1 and 6.5.1, three inverse inequalities, Eqs. (6.4.2), (6.5.1) and (6.5.12), are needed for a polygon S_2 . For polynomials v^+ of order L , Eq. (6.4.2) holds for $\nu = 2$ in [291]. The proof of (6.5.1) and (6.5.12) has been given in Section 5.5 of Chapter 5.

Remark 6.5.3 Eqs. (6.3.7) – (6.3.9) represent the generalized collocation equations using other admissible functions, such as radial basis functions, the Sinc functions, etc. The analysis of this chapter holds provided that the inverse inequalities (6.4.2), (6.5.1) and (6.5.12) are satisfied. In fact, these inequalities can be proved for radial basis functions, the Sinc functions, etc. Details of analysis and numerical examples will be given in Chapter 7.

6.6 Final Remarks

1. This chapter provides a theoretical framework of combinations of CM with other methods. The basic idea is to interpret CM as a special FEM, i.e., the LSM involving integration approximation. Eqs. (6.3.4) – (6.3.6) in CM are straightforward, and easily incorporated in the combined methods, see (6.3.14) and (6.3.15). The combination of CM in this chapter is also an important development from Li [291].
2. The key analysis for combinations of CMs is to prove the new uniformly V_h^0 -elliptic inequalities (6.2.11) and (6.3.20). The nontrivial proofs in Section 6.3 are new and intriguing, which consists of two steps: Step I for the simple one (6.4.16) without $\int_{\Gamma_0} v_n^- v^-$; Step II for Theorem 6.4.1. Note that both (6.2.5) and (6.2.6) are required in Combinations (6.2.8) because the integral $P_c \iint_{S_2} \Delta u \Delta v$ worked like the biharmonic equation in S_2 in the traditional FEMs, see Ciarlet [105], where the essential continuity conditions $u^+ = u^-$ and $u_n^+ = u_n^-$ should be imposed on the interior boundary Γ_0 .
3. In numerical algorithms, the integration approximation leads the LSM to the collocation method. In error analysis, the integration approximation plays a role only for satisfying the uniformly V_h^0 -elliptic inequality, but not for improving accuracy of the solutions. The algorithms and analysis in this chapter are distinctive from the existing literature in CMs.
4. In S_2 , Poisson's equation and the interior and exterior boundary conditions are copied straightforward into the collocation equations. This simple approach covers a large class of the CMs using various admissible functions, such as particular solutions, orthogonal polynomials, the radial basis functions (see Chapter 7), the Sinc functions, etc.

Chapter 7

Radial Basis Collocation Methods

In this chapter, we choose the radial basis functions (RBFs) as the admissible functions, and use the CM in Chapter 5 and the combination of CM and FEM in Chapter 6. The algorithms are called the radial basis collocation method (RBCM), and the error analysis will be made for other kinds of continuous admissible functions. This chapter also displays the importance of CMs given in previous two chapters. The RBFs are introduced into the collocation methods and the combined methods for elliptic boundary value problems. First, for Poisson's equation the Ritz-Galerkin method (RGM) is chosen using the RBFs, and the integration approximation leads to the collocation method of RBFs. The combinations of RBFs with the finite element method (FEM), the finite difference method (FDM), etc. can be easily formulated by following Li [291] and Chapters 5 and 6. More analysis of inverse estimates is explored in this chapter. Since the RBFs have the exponential convergence rates, and since the collocation nodes may be scattered in rather arbitrary fashions in various applications, the RBFs may be competitive to orthogonal polynomials for smooth solutions. Moreover, for singular solutions, we may use some singular functions and RBFs together. Numerical examples for smooth and singular problems are provided, to demonstrate the effectiveness of the methods and to support the analysis.

7.1 Introduction

In recent years, there have been many new developments for RBFs. The RBFs can be used for the interpolatory tool for smooth solutions, $u \in C^\infty(S)$. The convergence of their interpolants to a given continuous function has been discussed in the following work: Kansa [247] provided the surface approximations and partial derivative estimates, Madych [336] established several types of error bounds for multiquadric and related interpolators, and Wu and Schaback [494] focussed on local errors of scattered data interpolated by RBFs in suitable variational formulation, and Yoon [500] regarded the convergence of RBFs in an arbitrary Sobolev space. All of those reports show exponential convergence rates. Moreover, the applications of RBFs have been given as follows: Kansa [247, 248] presented a series of applications in computational fluid dynamics. Franke and

Schaback [158] gave some theoretical foundation for methods solving partial differential equations (PDEs). Wendland [484] derived error estimates for the solutions of smooth problems. Cheng et al. [97] introduced the $h - c$ meshless scheme for smooth problems, where numerical experiments were also provided. Hon and Schaback [212] used unsymmetrical collocation by radial basis functions, May-Duy and Tran-Cong [338, 339] used the radial basis function network methods for Poisson's equations, and Chen et al. [88] introduced systematically the method of RBFs.

We may classify the collocation method as a special kind of spectral methods, which numerical solutions have high accuracy, but with high instability due to the large condition numbers. In fact, the effective condition numbers given in Section 3.7 for the special applications may be much smaller. Fortunately, in practice, only a few terms of RBFs are needed so that the condition number and the effective condition number will not be huge, and useful numerical computation can be carried out even in double precision. Since by using Mathematica, unlimited number of significant digits are available, the CM and the spectral methods using RBFs are very promising.

In this chapter, we consider the collocation method using RBFs, simply called the radial basis collocation method (RBCM). We derive inverse estimates and new error analysis. The collocation method is treated as the Ritz-Galerkin method involving integration approximation. However, the integration quadrature is used in analysis only to satisfy the V_h -elliptic inequality, but not to reach the high exponentially convergence rates as shown in Chapters 2, 6 and 7. More explanations are given in Section 7.3. The advantages of the radial basis collocation method are twofold: (1) Source points of radial basis functions and collocation nodes may be scattered in rather arbitrary fashions in various applications, in which the solution domain is not confined to a rectangle. We need only a dense set of collocation nodes in any irregular domain. (2) Simplicity of the computing codes. A drawback of the radial basis collocation method is its high instability with large condition number.

This chapter is organized as follows. In the next section, the radial basis functions are described, and in Section 7.3, the collocation methods for different boundary conditions and combinations of FEM are discussed. In Section 7.4, the inverse estimates are derived. In Section 7.5, numerical experiments including smooth and singular problems are carried out to demonstrate the effectiveness of the methods proposed, and to support the analysis made.

7.2 Radial Basis Functions

For surface fitting on scattered points, using the RBFs shows remarkable advantages, see Hardy [196], Franke [157], Franke and Schaback [158], Schaback [422], Golberg [172], Kansa [247, 248], Madych and Nelson [337], Wu and Schaback [494], and Yoon [500]. Based on the theory of the FEM in Ciarlet [105], the errors of numerical solutions for elliptic equations are, basically, those of optimal approximations of admissible functions to the true solutions. Hence, the RBFs can be definitely applied to solve elliptic equations.

Let us describe the RBFs. The multiquadrics, the thin-plate splines and the Gaussian functions are defined by, see Cheng et al. [97],

$$\begin{aligned} g_i(\mathbf{x}) &= (r_i^2 + c^2)^{n-\frac{3}{2}}, \quad n = 1, 2, \dots, \\ g_i(\mathbf{x}) &= \begin{cases} r_i^{2n} \ln r_i, & n = 1, 2, \dots, \text{ in } R^2, \\ r_i^{2n-1}, & n = 1, 2, \dots, \text{ in } R^3, \end{cases} \\ g_i(\mathbf{x}) &= \exp\left(-\frac{r_i^2}{c^2}\right), \\ g_i(\mathbf{x}) &= (r_i^2 + c^2)^{n-\frac{3}{2}} \exp\left(-\frac{r_i^2}{a^2}\right), \quad n = 1, 2, \dots, \end{aligned}$$

where $\mathbf{x} = (x, y)$ in R^2 , and $\mathbf{x} = (x, y, z)$ in R^3 . The radius $r_i = \{(x - x_i)^2 + (y - y_i)^2\}^{\frac{1}{2}}$ in R^2 and $r_i = \{(x - x_i)^2 + (y - y_i)^2 + (z - z_i)^2\}^{\frac{1}{2}}$ in R^3 , where (x_i, y_i) and (x_i, y_i, z_i) are called source points of RBFs. The constants c and a are the shape parameters to be chosen later. When parameters c and a become larger, the RBFs become flatter.

Choose a linear combination of RBFs,

$$v = \sum_{i=1}^n a_i g_i(\mathbf{x}), \quad (7.2.1)$$

where the coefficients a_i are sought by the Ritz-Galerkin method or the collocation methods. For surface fitting, the coefficients are sought by satisfying

$$\begin{aligned} \sum_{i=1}^n a_i g_i(\mathbf{x}_j) + \sum_{i=1}^m b_i P_i(\mathbf{x}_j) &= f_j, \quad j = 1, 2, \dots, n, \\ \sum_{j=1}^n a_j P_i(\mathbf{x}_j) &= 0, \quad i = 1, 2, \dots, m. \end{aligned}$$

Based on the same ideas, we may add some singular functions $\psi_i(\mathbf{x})$ for fitting singular surfaces, or for solving singular problems of elliptic equations,

$$v = \sum_{i=1}^n a_i g_i(\mathbf{x}) + \sum_{i=0}^m b_i \psi_i(\mathbf{x}),$$

where

$$\sum_{i=1}^n a_i g_i(\mathbf{x}_j) + \sum_{i=0}^m b_i \psi_i(\mathbf{x}_j) = f_j, \quad j = 1, 2, \dots, n. \quad (7.2.2)$$

For Motz's problem given in Chapter 2, a benchmark of singularity problems, we may add a few leading singular functions as

$$\psi_i(\mathbf{x}) = r^{i+\frac{1}{2}} \cos\left(i + \frac{1}{2}\right)\theta, \quad i = 0, 1, \dots, L,$$

where (r, θ) are the polar coordinates with the origin $(0,0)$, $r = \sqrt{x^2 + y^2}$ and $\tan \theta = \frac{y}{x}$.

7.3 Description of Radial Basis Collocation Methods

By following the approaches in Chapters 5 and 6, the RBFs are chosen as the admissible functions in the Ritz-Galerkin methods. Since the RBFs do not satisfy the partial differential equation and the boundary conditions so that the residuals have to be enforced to zero at collocation points both in the solution domain and on its boundary. We obtain the collocation methods of RBFs, simply denoted by RBCM, and combined methods of RBCM with other numerical methods. The optimal error bounds are provided, and the proofs are given in the following subsection, or can be done by following the analysis in Chapters 5 and 6 straightforwardly. The crucial inverse estimates for radial basis functions will be proven in the next section.

7.3.1 Radial Basis Collocation Method (RBCM) for Different Boundary Conditions

Consider Poisson's equation with Robin boundary condition:

$$-\Delta u = -\left(\frac{\partial^2 u}{\partial x^2} + \frac{\partial^2 u}{\partial y^2}\right) = f(x, y) \quad \text{in } S, \quad (7.3.1)$$

$$u_\nu|_{\Gamma_N} = q_1 \quad \text{on } \Gamma_N, \quad (7.3.2)$$

$$(u_\nu + \beta u)|_{\Gamma_R} = q_2 \quad \text{on } \Gamma_R, \quad (7.3.3)$$

where $\beta \geq \beta_0 > 0$, β_0 is constant, S is a polygon, $\partial S = \Gamma = \Gamma_N \cup \Gamma_R$, and u_ν is the unit outer normal derivative to ∂S . Assume $\text{Meas}(\Gamma_R) > 0$ for guaranteeing the unique solution. We make two assumptions.

A1: The solutions in S can be expanded as

$$u = \sum_{i=1}^{\infty} a_i g_i(x, y) \quad \text{in } S, \quad (7.3.4)$$

where $g_i(x, y) \in C^2(S)$ and $g_i(x, y) \in C(\partial S)$. For the boundary singularity problems, since we may choose the particular solutions $g_i(x, y)$, the collocation nodes may be far from the singular points, so assumption (7.3.4) may be relaxed by $g_i(x, y) \in C^2(D) \cap C^1(\partial S^*)$, where $D \subset S$ and $\partial S^* \subset \partial S$, and a_i are the expansion coefficients.

A2: The expansions in (7.3.4) converge exponentially to the true solutions u ,

$$u = u_L + R_L,$$

where $u_L = \sum_{i=1}^L a_i g_i(x, y)$ and $R_L = \sum_{i=L+1}^{\infty} a_i g_i(x, y)$. Then

$$\max_S |R_L| = O(\lambda^{c/\delta}),$$

where $c > 0$, $L > 1$, $0 < \lambda < 1$, and δ is the radial distance defined as

$$\delta = \sup_{(x,y) \in S} \left\{ \inf_i [(x - x_i)^2 + (y - y_i)^2]^{\frac{1}{2}} \right\}, \quad (7.3.5)$$

where (x_i, y_i) are the source points of RBFs.

Based on **A1-A2** we may choose the admissible functions,

$$v = \sum_{i=1}^L \tilde{a}_i g_i(x, y) \quad \text{in } S, \quad (7.3.6)$$

where \tilde{a}_i are unknown coefficients to be sought. Denote by V_h the finite dimensional collection of the admissible functions (7.3.6). To solve (7.3.1) – (7.3.3), the Ritz-Galerkin method can be written as follows: To seek solution u_L such that

$$b(u_L, v) = f(v), \quad \forall v \in V_h,$$

where

$$\begin{aligned} b(u, v) &= \iint_S \Delta u \Delta v + \int_{\Gamma_N} u_\nu v_\nu + \int_{\Gamma_R} (u_\nu + \beta u)(v_\nu + \beta v), \\ f(v) &= - \iint_S f \Delta v + \int_{\Gamma_N} q_1 v_\nu + \int_{\Gamma_R} q_2 (v_\nu + \beta v). \end{aligned} \quad (7.3.7)$$

When we view the collocation method as a Ritz-Galerkin method involving approximate quadratures, the radial basis collocation method (RBCM) can be written as: To seek solution \hat{u}_L such that

$$\hat{b}(\hat{u}_L, v) = \hat{f}(v), \quad \forall v \in V_h, \quad (7.3.8)$$

where

$$\begin{aligned} \hat{b}(u, v) &= \widehat{\iint}_S \Delta u \Delta v + \widehat{\int}_{\Gamma_N} u_\nu v_\nu + \widehat{\int}_{\Gamma_R} (u_\nu + \beta u)(v_\nu + \beta v), \\ \hat{f}(v) &= - \widehat{\iint}_S f \Delta v + \widehat{\int}_{\Gamma_N} q_1 v_\nu + \widehat{\int}_{\Gamma_R} q_2 (v_\nu + \beta v), \end{aligned}$$

where $\widehat{\iint}_S$, $\widehat{\int}_{\Gamma_N}$, and $\widehat{\int}_{\Gamma_R}$ denote the approximations of \iint_S , \int_{Γ_N} , and \int_{Γ_R} by some integration rules, respectively. We may choose the Newton-Cotes rules or the Legendre-Gauss rules:

$$\widehat{\iint}_S F = \sum_{ij} \alpha_{ij} F(Q_{ij}), \quad Q_{ij} \in S, \quad (7.3.9)$$

$$\widehat{\int}_\Gamma F = \sum_i \alpha_i F(Q_i), \quad Q_i \in \Gamma, \quad (7.3.10)$$

where α_{ij} and α_i are positive weights. We can then formulate the collocation equations directly at Q_{ij} and Q_i :

$$\sqrt{\alpha_{ij}}(\Delta v + f)(Q_{ij}) = 0, \quad Q_{ij} \in S, \quad (7.3.11)$$

$$\sqrt{\alpha_i^N}(v_\nu - q_1)(Q_i) = 0, \quad Q_i \in \Gamma_N, \quad (7.3.12)$$

$$\sqrt{\alpha_i^R}(v_\nu + \beta v - q_2)(Q_i) = 0, \quad Q_i \in \Gamma_R. \quad (7.3.13)$$

Eqs. (7.3.11) – (7.3.13) in $S \cup \Gamma_N \cup \Gamma_R$ are written simply as

$$\mathbf{F}\mathbf{x} = \mathbf{b}, \quad (7.3.14)$$

where \mathbf{x} is a vector consisting of \tilde{a}_i , \mathbf{b} is a known vector, matrix $\mathbf{F} \in R^{N_c \times L}$, and N_c is the number of collocation nodes in $S \cup \Gamma_N \cup \Gamma_R$. In this chapter, let $N_c \geq L$, and we may seek the solutions of the entire RBCM by the least squares method (LSM) in Golub and Loan [176].

Now, we will provide the error estimates for solution \hat{u}_L in (7.3.8) by following the FEM theory, see [105] for more details. Denote the space

$$H^* = \{v, v \in L^2(S), v \in H^1(S), \Delta v \in L^2(S)\},$$

accompanied by the norm

$$\|v\|_h = \{\|v\|_{1,S}^2 + \|\Delta v\|_{0,S}^2 + \|v_\nu\|_{0,\Gamma_N}^2 + \|v_\nu + \beta v\|_{0,\Gamma_R}^2\}^{1/2},$$

where $\|v\|_{1,S}$ is the Sobolev norm. In order to derive our main theorem (Theorem 7.3.1) given later, the following lemmas are needed.

Lemma 7.3.1 *There exist two inequalities*

$$b(u, v) \leq C\|u\|_h \times \|v\|_h, \quad \forall v \in V_h, \quad (7.3.15)$$

$$b(v, v) \geq C_0\|v\|_h^2, \quad \forall v \in V_h, \quad (7.3.16)$$

where C_0 and C are two positive constants independent of L .

Proof From Eq. (7.3.7), we have

$$\begin{aligned}
b(u, v) &\leq C_1 \sqrt{\iint_S (\Delta u)^2} \sqrt{\iint_S (\Delta v)^2} + C_2 \sqrt{\int_{\Gamma_N} (u_\nu)^2} \sqrt{\int_{\Gamma_N} (v_\nu)^2} \\
&+ C_3 \sqrt{\int_{\Gamma_R} (u_\nu + \beta u)^2} \sqrt{\int_{\Gamma_R} (v_\nu + \beta v)^2} \\
&\leq C \{ \|\Delta u\|_{0,S} \|\Delta v\|_{0,S} + \|u_\nu\|_{0,\Gamma_N} \|v_\nu\|_{0,\Gamma_N} \\
&+ \|u_\nu + \beta u\|_{0,\Gamma_R} \|v_\nu + \beta v\|_{0,\Gamma_R} + \|u\|_{1,S} \|v\|_{1,S} \} \\
&\leq C \{ \|\Delta u\|_{0,S}^2 + \|u_\nu\|_{0,\Gamma_N}^2 + \|u_\nu + \beta u\|_{0,\Gamma_R}^2 + \|u\|_{1,S}^2 \}^{\frac{1}{2}} \\
&\times \{ \|\Delta v\|_{0,S}^2 + \|v_\nu\|_{0,\Gamma_N}^2 + \|v_\nu + \beta v\|_{0,\Gamma_R}^2 + \|v\|_{1,S}^2 \}^{\frac{1}{2}} \\
&\leq C \|u\|_h \times \|v\|_h,
\end{aligned}$$

where C_i and C are generic constants, and their values may be different in different contexts. The first desired result (7.3.15) is obtained.

Next, from the Green's formula, we have

$$\begin{aligned}
|v|_{1,S}^2 &= \iint_S \nabla v \cdot \nabla v = - \iint_S v \Delta v + \int_{\partial S} v_\nu v \\
&\leq \|\Delta v\|_{0,S} \|v\|_{0,S} + \int_{\Gamma_N} v_\nu v + \int_{\Gamma_R} (v_\nu + \beta v) v - \int_{\Gamma_R} \beta v^2 \\
&\leq \{ \|\Delta v\|_{0,S} + \|v_\nu\|_{0,\Gamma_N} + \|v_\nu + \beta v\|_{0,\Gamma_R} \} \|v\|_{1,S} - \int_{\Gamma_R} \beta v^2, \tag{7.3.17}
\end{aligned}$$

where $\partial S = \Gamma = \Gamma_N \cup \Gamma_R$, and two bounds are used:

$$\|v\|_{0,\Gamma_N} \leq C \|v\|_{1,S}, \quad \|v\|_{0,\Gamma_R} \leq C \|v\|_{1,S}.$$

Besides, from (7.3.17) we obtain

$$\begin{aligned}
\|v\|_{1,S}^2 &\leq C (|v|_{1,S}^2 + \int_{\Gamma_R} \beta v^2) \\
&\leq C \{ \|\Delta v\|_{0,S} + \|v_\nu\|_{0,\Gamma_N} + \|v_\nu + \beta v\|_{0,\Gamma_R} \} \|v\|_{1,S}.
\end{aligned}$$

This leads to

$$\|v\|_{1,S} \leq C \{ \|\Delta v\|_{0,S} + \|v_\nu\|_{0,\Gamma_N} + \|v_\nu + \beta v\|_{0,\Gamma_R} \},$$

and then

$$\|v\|_{1,S}^2 \leq C \{ \|\Delta v\|_{0,S}^2 + \|v_\nu\|_{0,\Gamma_N}^2 + \|v_\nu + \beta v\|_{0,\Gamma_R}^2 \} = Cb(v, v). \tag{7.3.18}$$

Moreover, from (7.3.18) and (7.3.7) we obtain

$$\begin{aligned} b(v, v) &= \frac{1}{2}b(v, v) + \frac{1}{2}b(v, v) \\ &\geq C_0 \|v\|_{1,S}^2 + \frac{1}{2} \{ \|\Delta v\|_{0,S}^2 + \|v_\nu\|_{0,\Gamma_N}^2 + \|v_\nu + \beta v\|_{0,\Gamma_R}^2 \} \geq \bar{C}_0 \|v\|_h^2, \end{aligned}$$

where $\bar{C}_0 = \min\{\frac{1}{2}, C_0\}$. The second desired result (7.3.16) is obtained. ■

We make one more assumption.

A3: Suppose that for v in (7.3.6) there exists positive constant C independent of L, k and v such that

$$\|v\|_{k,S} \leq CL^k \|v\|_{0,S}, \quad v \in V_h, \quad (7.3.19)$$

$$\|v\|_{k,\Gamma} \leq CL^k \|v\|_{0,\Gamma}, \quad v \in V_h, \quad (7.3.20)$$

$$\|v_\nu\|_{k,\Gamma} \leq CL^{k+1} \|v\|_{1,\Gamma}, \quad v \in V_h, \quad (7.3.21)$$

where ν is unit outward normal to Γ .

The inverse inequalities in (7.3.19) – (7.3.21) are crucial to following lemmas and theorem. Their proof is new to Chapters 5 and 6, and is deferred to Section 7.4.

Lemma 7.3.2 *For the rules (7.3.9) and (7.3.10) with order r , there exist the bounds for $v \in V_h$,*

$$\left| \left(\iint_S - \widehat{\iint}_S \right) (\Delta v)^2 \right| \leq CH^{r+1} L^{r+3} \|v\|_{1,S}^2, \quad (7.3.22)$$

$$\left| \left(\int_{\Gamma_N} - \widehat{\int}_{\Gamma_N} \right) (v_\nu)^2 \right| \leq CH^{r+1} L^{r+3} \|v\|_{1,S}^2, \quad (7.3.23)$$

$$\left| \left(\int_{\Gamma_R} - \widehat{\int}_{\Gamma_R} \right) (v_\nu + \beta v)^2 \right| \leq CH^{r+1} L^{r+3} \|v\|_{1,S}^2, \quad (7.3.24)$$

where H denotes the maximal spacing between the consecutive integration nodes, i.e. collocation points, and L denotes the number of RBFs.

Proof Choose the integration rules of order r

$$\widehat{\int}_\Gamma g = \int_\Gamma \hat{g},$$

where \hat{g} is the polynomial interpolant of order r on the partition of Γ with the maximal meshspacing H . Then we obtain

$$\left| \left(\int_\Gamma - \widehat{\int}_\Gamma \right) g \right| = \left| \int_\Gamma g - \int_\Gamma \hat{g} \right| = \left| \int_\Gamma (g - \hat{g}) \right| \leq CH^{r+1} |g|_{r+1,\Gamma}.$$

Based on **A3**, letting $g = (v_\nu)^2$ and $\Gamma = \Gamma_N$ we have

$$\begin{aligned} |g|_{r+1,\Gamma} &= |(v_\nu)^2|_{r+1,\Gamma_N} \leq C \sum_{i=0}^{r+1} |v_\nu|_{r+1-i,\Gamma_N} |v_\nu|_{i,\Gamma_N} \\ &\leq C \sum_{i=0}^{r+1} (L^{r+2-i} \|v\|_{1,S} \times L^{i+1} \|v\|_{1,S}) \leq CL^{r+3} \|v\|_{1,S}^2. \end{aligned}$$

Combining above two inequalities gives the desired result (7.3.23). Eqs. (7.3.22) and (7.3.24) can be similarly proven. ■

Lemma 7.3.3 *Let Lemmas 7.3.1 and 7.3.2 hold. We choose H to satisfy*

$$H^{r+1}L^{r+3} = o(1), \quad (7.3.25)$$

then there exists the uniformly V_h - elliptic inequality

$$\hat{b}(v, v) \geq C \|v\|_h^2, \quad \forall v \in V_h. \quad (7.3.26)$$

Proof From (7.3.16) and Lemma 7.3.2, we have

$$\begin{aligned} \hat{b}(v, v) &\geq b(v, v) - CH^{r+1}L^{r+3} \|v\|_{1,S}^2 \\ &\geq C_0 \|v\|_h^2 - CH^{r+1}L^{r+3} \|v\|_{1,S}^2 \\ &\geq C_0 \left\{ \left(1 - \frac{C}{C_0} H^{r+1}L^{r+3}\right) \|v\|_{1,S}^2 + \|\Delta v\|_{0,S}^2 + \|v_\nu\|_{0,\Gamma_N}^2 + \|v_\nu + \beta v\|_{0,\Gamma_R}^2 \right\} \\ &\geq \frac{C_0}{2} \|v\|_h^2. \end{aligned}$$

This is (7.3.26) with $C = C_0/2$. ■

We obtain an important theorem as follows.

Theorem 7.3.1 *Suppose that there exist two inequalities*

$$\begin{aligned} \hat{b}(u, v) &\leq C \|u\|_h \times \|v\|_h, \quad \forall v \in V_h, \\ \hat{b}(v, v) &\geq C_0 \|v\|_h^2, \quad \forall v \in V_h, \end{aligned} \quad (7.3.27)$$

where C_0 and C are two positive constants independent of L . Then, when choosing H and L as (7.3.25), the solution of the RBCM in (7.3.8) has the error bound,

$$\begin{aligned} \|u - \hat{u}_L\|_h &= C \inf_{v \in V_h} \|u - v\|_h \\ &\leq C \{ \|R_L\|_{2,S} + \|(R_L)_\nu\|_{0,\Gamma_N} + \|(R_L)_\nu\|_{0,\Gamma_R} \}, \end{aligned}$$

where C is a constant independent of L .

Proof Since the true solution u satisfies the collocation equations exactly, we have $\hat{b}(u, v) = \hat{f}(v)$. By using Lemma 7.3.2, we obtain

$$\hat{b}(u, v) \leq \hat{f}(v) + CH^{r+1}L^{r+3}\|v\|_{1,S}^2, \quad \forall v \in V_h.$$

Since \hat{u}_L is the solution of RBCM, we have

$$\hat{b}(\hat{u}_L, v) = \hat{f}(v), \quad \forall v \in V_h,$$

and then

$$\hat{b}(u - \hat{u}_L, v) \leq CH^{r+1}L^{r+3}\|v\|_{1,S}^2, \quad \forall v \in V_h.$$

Let $w = \hat{u}_L - v \in V_h$, from the above bound we obtain

$$\begin{aligned} C_0\|w\|_h^2 &\leq \hat{b}(\hat{u}_L - v, w) = \hat{b}(\hat{u}_L - u + u - v, w) \\ &\leq C(\|u - v\|_h\|w\|_h + H^{r+1}L^{r+3}\|w\|_{1,S}^2) \\ &\leq C(\|u - v\|_h\|w\|_h + H^{r+1}L^{r+3}\|w\|_h^2). \end{aligned}$$

This leads to

$$\{C_0 - CH^{r+1}L^{r+3}\}\|w\|_h^2 \leq \|u - v\|_h\|w\|_h.$$

Moreover, from (7.3.25) we have

$$\|\hat{u}_L - v\|_h = \|w\|_h \leq \frac{1}{(C_0 - C \times o(1))} \|u - v\|_h \leq C_1 \|u - v\|_h.$$

From the triangle inequality, we have

$$\|u - \hat{u}_L\|_h \leq \|u - v\|_h + \|\hat{u}_L - v\|_h \leq C\|u - v\|_h,$$

and then

$$\begin{aligned} \|u - \hat{u}_L\|_h &\leq C \inf_{v \in V_h} \|u - v\|_h \\ &\leq C \{ \|R_L\|_{1,S} + \|\Delta R_L\|_{0,S} + \|(R_L)_\nu\|_{0,\Gamma_N} + \|(R_L)_\nu\|_{0,\Gamma_R} \}. \blacksquare \end{aligned}$$

Remark 7.3.1 *Theorem 7.3.1 implies that the errors of the solutions for Poisson's equation using RBCM are bounded by the truncation errors of RBFs multiplied by a constant. From assumption A2, we assure that the errors of solution \hat{u}_L have exponential convergence. Moreover, Eq.(7.3.25) has the following relation*

$$HL^{(1+\frac{2}{r+1})} = o(1),$$

where H and L are given in Lemma 7.3.2. Then we take $L = N^2$, and assume that the radial distance δ defined in (7.3.5) satisfies the relation $\delta \approx O(\frac{1}{N})$. Furthermore, we obtain an important relation

$$H = o\left(\delta^{(2+\frac{4}{r+1})}\right). \quad (7.3.28)$$

From (7.3.28), we know how to balance the collocation nodes and the source points of RBFs.

Remark 7.3.2 *In this chapter, the Newton-Cotes rules of integration are chosen for simplicity in exposition. From (7.3.28), we need a dense set of integration nodes in order to satisfy the V_h -elliptic inequality, and then to obtain the exponential convergence rates. The solution domain may not be confined to rectangles (or boxes for three dimensions). When the collocation methods using the radial basis functions are applied to solving PDEs in three dimensions, the simplest central rule may also be used. An integral in a closed region of three dimensions is approximated by the value of the integrand at the center of gravity (or roughly at any point) of the region multiplied by the volume of the region. Hence, the integration quadrature is not a severe problem in the collocation methods described in this chapter.*

7.3.2 Combination of FEM and RBCM

Consider Poisson's equation with the Dirichlet boundary condition,

$$\begin{aligned} -\Delta u &= f(x, y) \quad \text{in } S, \\ u &= 0 \quad \text{on } \Gamma, \end{aligned} \quad (7.3.29)$$

where S is a polygon, and Γ is its boundary. Let S be divided by Γ_0 into two disjoint subregions, S_1 and S_2 : $S = S_1 \cup S_2 \cup \Gamma_0$ and $\partial S_1 \cap \partial S_2 = \Gamma_0$. On the interior boundary Γ_0 , there hold the interior continuity conditions:

$$u^+ = u^-, \quad u_\nu^+ = u_\nu^-, \quad \text{on } \Gamma_0, \quad (7.3.30)$$

where $u_\nu = \frac{\partial u}{\partial \nu}$, $u^+ = u$ on $\Gamma_0 \cup S_2$ and $u^- = u$ on $\Gamma_0 \cup S_1$. Assume that the solution u in S_2 is smoother than u in S_1 . We choose the finite element method (FEM) in S_1 and the Ritz-Galerkin method in S_2 , whose discrete forms lead to the CM. Let S_1 be partitioned into small triangles: Δ_{ij} , i.e., $S_1 = \cup_{ij} \Delta_{ij}$. Denote by h_{ij} the boundary length of Δ_{ij} . The Δ_{ij} are said to be quasiuniform if $\frac{h}{\min\{h_{ij}\}} \leq C$, $h = \max_{\Delta_{ij} \subset S_1} \{h_{ij}\}$, and C is a constant independent of h . Then, the admissible functions may be expressed by

$$v = \begin{cases} v^- = v_k & \text{in } S_1, \\ v^+ = \sum_{i=1}^L \tilde{a}_i g_i(x, y) & \text{in } S_2, \end{cases} \quad (7.3.31)$$

where \tilde{a}_i are unknown coefficients, and v_k are piecewise Lagrange polynomials of power k in S_1 in the FEM. Assume that **A1** and **A2** hold in S_2 , and $g_i(x, y) \in C^2(S_2 \cup \partial S_2)$ are the RBFs so that $v^+ \in C^2(S_2 \cup \partial S_2)$. Therefore, we may evaluate (7.3.29) directly from

$$(\Delta v^+ + f)(Q_{ij}) = 0, \quad \text{for } Q_{ij} \in S_2 \quad (7.3.32)$$

at certain collocation nodes $Q_{ij} \in S_2$. Note that v in (7.3.31) is not continuous on the interior boundary Γ_0 . Hence, to satisfy (7.3.30), the interior collocation equations are

obtained:

$$v^+(Q_i) = v^-(Q_i), \quad \text{for } Q_i \in \Gamma_0, \quad (7.3.33)$$

$$v_\nu^+(Q_i) = v_\nu^-(Q_i), \quad \text{for } Q_i \in \Gamma_0. \quad (7.3.34)$$

Note that Eqs. (7.3.32) – (7.3.34) are straightforward and easy to be formulated.

Denote by V_h^0 the finite dimensional collection of (7.3.31) satisfying $v|_\Gamma = 0$, where we simply assume $g_i(x, y)|_{\partial S_2 \cap \Gamma} = 0$. If such a condition does not hold, the corresponding collocation equations on $\partial S_2 \cap \Gamma$ are also needed, and the arguments can be provided similarly. The combination of the FEM-RBCM involving integration approximation is given by: To seek the approximation solution $\hat{u}_h \in V_h^0$ such that

$$\hat{a}^*(\hat{u}_h, v) = f_1(v), \quad \forall v \in V_h^0, \quad (7.3.35)$$

where

$$\begin{aligned} \hat{a}^*(u, v) &= \iint_{S_1} \nabla u \cdot \nabla v + \int_{\Gamma_0} u_\nu^- v^- + P_c \iint_{S_2} (\Delta u + f)(\Delta v + f) \\ &+ \frac{P_c}{h} \int_{\Gamma_0} (u^+ - u^-)(v^+ - v^-) + P_c \int_{\Gamma_0} (u_\nu^+ - u_\nu^-)(v_\nu^+ - v_\nu^-), \\ f_1(v) &= \iint_{S_1} f v, \end{aligned}$$

where $\nabla u = u_x \mathbf{i} + u_y \mathbf{j}$, $u_x = \frac{\partial u}{\partial x}$, $u_y = \frac{\partial u}{\partial y}$, $u_\nu = \frac{\partial u}{\partial \nu}$, and ν is the unit outward normal to ∂S_2 . Also h is the maximal boundary length of \triangle_{ij} or \square_{ij} in S_1 , and $P_c > 0$ is chosen to be suitably large but still independent of h .

Now, let us establish the linear algebraic equations of combinations (7.3.35) of FEM-RBCM. First, considering the FEM in S_1 only, we have

$$a_1(\hat{u}_h, v) = f_1(v), \quad \forall v \in V_h,$$

where

$$a_1(u, v) = \iint_{S_1} \nabla u \cdot \nabla v + \int_{\Gamma_0} u_\nu^- v^-, \quad f_1(v) = \iint_{S_1} f v.$$

By means of the traditional procedure of finite element method [105], we obtain the linear algebraic equations,

$$\mathbf{A}_1 \mathbf{x}_1 = \mathbf{b}_1, \quad (7.3.36)$$

where \mathbf{x}_1 is a vector consisting of v_{ij} only, and matrix \mathbf{A}_1 is non-symmetric.

Next, we choose the integration rules (Newton-Cotes rules or Legendre-Gauss rules) in S_2 . We may formulate collocation equations at $Q_{ij} \in S_2$, and $Q_i \in \Gamma_0$ directly. The collocation equations at Q_{ij} and Q_i are given by:

$$\sqrt{P_c \alpha_{ij}} (\Delta v^+ + f)(Q_{ij}) = 0, \quad Q_{ij} \in S_2, \quad (7.3.37)$$

$$\sqrt{\frac{P_c \alpha_i}{h}} (v^+ - v^-)(Q_i) = 0, \quad Q_i \in \Gamma_0, \quad (7.3.38)$$

$$\sqrt{\frac{P_c \alpha_i}{h}} (v_\nu^+ - v_\nu^-)(Q_i) = 0, \quad Q_i \in \Gamma_0, \quad (7.3.39)$$

where $v_\nu^-(Q_i) = \frac{v_{1i} - v_{0i}}{h}$, $v_{0i} = v(Q_i)$ and v_{1i} are the nodal variables in S_1 normal to Γ_0 .

Eqs. (7.3.37) – (7.3.39) in $S_2 \cup \Gamma_0$ are denoted by

$$\mathbf{A}_2 \mathbf{x}_2 = \mathbf{b}_2,$$

where \mathbf{x}_2 is a vector consisting of \tilde{a}_i , v_{1i} and v_{0i} , and v_{0i} and v_{1i} are the unknowns on the two boundary layer nodes in S_1 close to Γ_0 . Denote by M_C the number of all collocation nodes in S_2 and ∂S_2 , and by N_B the number of v_{1i} and v_{0i} . The matrix $\mathbf{A}_2 \in R^{M_C \times (L + N_B)}$. Therefore, we can see

$$\begin{aligned} & \frac{P_c}{2} \iint_{S_2} (\Delta v + f)^2 + \frac{P_c}{2h} \int_{\Gamma_0} (v^+ - v^-)^2 + \frac{P_c}{2} \int_{\Gamma_0} (v_\nu^+ - v_\nu^-)^2 \\ & = \frac{1}{2} \mathbf{x}_2^T \mathbf{A}_2^T \mathbf{A}_2 \mathbf{x}_2 - \mathbf{x}_2^T \mathbf{A}_2^T \mathbf{b}_2 + \mathbf{c}. \end{aligned} \quad (7.3.40)$$

Combining (7.3.36) and (7.3.40) yields explicitly:

$$\begin{aligned} \mathbf{A} \mathbf{x} &= \mathbf{b}, \\ \mathbf{A} &= \mathbf{A}_1 + \mathbf{A}_2^T \mathbf{A}_2, \quad \mathbf{b} = \mathbf{b}_1 + \mathbf{A}_2^T \mathbf{b}_2, \end{aligned} \quad (7.3.41)$$

where \mathbf{x} is a vector consisting of the coefficients \tilde{a}_i and v_{ij} in $S_1 \cup \Gamma_0$. Denote by N_E the number of nodes on $S_1 \cup \Gamma_0$. Then vector \mathbf{x} in (7.3.41) has $N_E + L$ dimensions. When P_c is chosen large enough, matrix $\mathbf{A} \in R^{(L + N_E) \times (L + N_E)}$ in (7.3.41) is positive definite but non-symmetric, and sparse when $N_E \gg L$. When $L + N_E$ is not huge, we may choose the Gaussian elimination without pivoting to obtain \mathbf{x} from (7.3.41), see Golub and Loan [176].

Now, we give error bounds for the solution \hat{u}_h from (7.3.35) which proofs have been reported in Chapter 6. The combination (7.3.35) can be described equivalently as follows: To seek $\hat{u}_h \in V_h^0$ such that

$$\hat{a}(\hat{u}_h, v) = \hat{f}(v), \quad \forall v \in V_h^0,$$

where

$$\begin{aligned}
\hat{a}(u, v) &= \iint_{S_1} \nabla u \cdot \nabla v + \int_{\Gamma_0} u_n^- v^- + P_c \iint_{S_2} \Delta u \Delta v \\
&+ \frac{P_c}{h} \int_{\Gamma_0} (u^+ - u^-)(v^+ - v^-) + P_c \int_{\Gamma_0} (u_\nu^+ - u_\nu^-)(v_\nu^+ - v_\nu^-), \\
\hat{f}(v) &= \iint_{S_1} f v - P_c \iint_{S_2} f \Delta v.
\end{aligned} \tag{7.3.42}$$

Denote the space

$$\begin{aligned}
H^{**} &= \{v, v \in L^2(S), v \in H^1(S_1), v \in H^1(S_2), \\
&\Delta v \in L^2(S_2), \text{ and } v|_{\Gamma} = 0\},
\end{aligned}$$

accompanied with the norm

$$\begin{aligned}
\|v\| &= \left\{ \|v\|_{1,S_1}^2 + P_c \|v\|_{1,S_2}^2 + P_c \|\Delta v\|_{0,S_2}^2 \right. \\
&\left. + \frac{P_c}{h} \|v^+ - v^-\|_{0,\Gamma_0}^2 + P_c \|v_\nu^+ - v_\nu^-\|_{0,\Gamma_0}^2 \right\}^{1/2},
\end{aligned}$$

where

$$\|v\|_1 = \{\|v\|_{1,S_1}^2 + \|v\|_{1,S_2}^2\}^{1/2}, \quad |v|_1 = \{|v|_{1,S_1}^2 + |v|_{1,S_2}^2\}^{1/2},$$

and $\|v\|_{1,S_1}$ and $\|v\|_{1,S_2}$ are the Sobolev norms. Obviously, $V_h^0 \subset H^{**}$. We obtain the following theorem.

Theorem 7.3.2 *Suppose that there exist two inequalities,*

$$\begin{aligned}
\hat{a}(u, v) &\leq C \|u\| \times \|v\|, \quad \forall v \in V_h^0, \\
\hat{a}(v, v) &\geq C_0 \|v\|^2, \quad \forall v \in V_h^0,
\end{aligned} \tag{7.3.43}$$

where $C_0(> 0)$ and C are two constants independent of h and L . Then, the solution of combination (7.3.35) has the error bound,

$$\|u - \hat{u}_h\| \leq C \inf_{v \in V_h} \|u - v\|.$$

We can obtain the following corollary easily from Theorem 7.3.2, also see Chapter 6.

Corollary 7.3.1 *Let all conditions in Theorem 7.3.2 hold. Suppose that*

$$u \in H^{k+1}(S_1) \quad \text{and} \quad u \in H^{k+1}(\Gamma_0).$$

Then, there exists the error bound,

$$\begin{aligned} \| |u - \hat{u}_h| \| &\leq C\{h^k |u|_{k+1, S_1} + \sqrt{P_c} \|R_L\|_{2, S_2} \\ &+ \sqrt{P_c} (h^{k+\frac{1}{2}} |u|_{k+1, \Gamma_0} + \frac{1}{\sqrt{h}} \|R_L\|_{0, \Gamma_0} + \|(R_L)_\nu\|_{0, \Gamma_0})\}. \end{aligned}$$

Furthermore, suppose that the number L in (7.3.31) is chosen such that

$$\begin{aligned} \|R_L\|_{2, S_2} &= O(h^k), \quad \|R_L\|_{0, \Gamma_0} = O(h^{k+\frac{1}{2}}), \\ \|(R_L)_\nu\|_{0, \Gamma_0} &= O(h^k). \end{aligned}$$

Then, the optimal convergence rate is given by

$$\| |u - \hat{u}_h| \| = O(h^k).$$

Remark 7.3.3 *The detailed proof for the V_h^0 -elliptic inequality (7.3.43) of Theorem 7.3.2 may follow Sections 6.4 and 6.5. Here we only give an outline of the proof, which consists of two steps: Step I for the original equation of (7.3.42) without integration approximation, we need to prove $a(v, v) \geq C_0 \|v\|^2$, $\forall v \in V_h^0$; Step II for the Newton-Cotes integration rules of order r , assume that the inverse inequalities in **A3** hold, then we obtain*

$$hL^2 = o(1), \quad HL^{(1+\frac{2}{r+1})} = o(1),$$

where $h = \max_{ij} \{h_{ij}\}$ in S_1 , and H denotes the maximal meshspacing between consecutive integration nodes, i.e. collocation nodes, and L denotes the number of RBFs in S_2 . When we take $L = N^2$, and assume that the radial distance δ defined in (7.3.5) satisfies that $\delta \approx O(\frac{1}{N})$, then, we have the relations

$$h = o(\delta^4), \quad H = o\left(\delta^{(2+\frac{4}{r+1})}\right). \quad (7.3.44)$$

From (7.3.44), we also know how to balance the mesh of FEM and the source points of RBFs.

Remark 7.3.4 *From those error analysis, we discover that the integration quadrature plays a role only for satisfying the uniformly V_h^0 -elliptic inequalities (7.3.27) and (7.3.43), but not for improving the accuracy of the solutions. As long as the maximal spacing H between consecutive collocation nodes is small enough, there always exist the optimal orders of solution errors from the radial basis collocation methods and their combinations.*

7.4 Inverse Estimates for Radial Basis Functions

Although there exist many papers on RBFs, only a few of them are related to solutions of partial differential equations, see Kansa [248], Franke and Schaback [158], and Golberg [172]. In the Ritz-Galerkin method (RGM) [291], orthogonal polynomials and particular solutions are chosen, which have been replaced by RBFs in Section 7.3.

Note that the theoretical framework for the collocation methods has been established in Chapters 5 and 6, which can be easily applied to RBCMs and their combinations, except that the crucial inverse estimates (7.3.19) – (7.3.21) of RBFs need to be proven. Note that our results in Chapter 5 and 6 and in this chapter are more comprehensive than those in [158, 172], because different boundary conditions are also involved, and because the combined methods are developed. Below, let us explore the inverse estimates (7.3.19) – (7.3.21) needed for the RBFs. Take the multiquadric functions for example,

$$Q_L(x, y) = a_0 + \sum_{i=1}^L a_i g_i(x, y),$$

where $g_i(x, y) = (r_i^2 + c^2)^{\frac{1}{2}}$. To approximate function $f(x, y)$, the collocation equations are given by

$$Q_L(x_i, y_i) = f(x_i, y_i), \quad i = 1, 2, \dots, L, \quad \sum_{i=1}^L a_i = 0. \quad (7.4.1)$$

Eq. (7.3.19) is essential, because Eqs. (7.3.20) and (7.3.21) can be easily derived from (or replaced by) (7.3.19), see Chapter 5. Hence, we focus on the proof of (7.3.19) for the multiquadratic functions. We have the following lemma.

Lemma 7.4.1 *Let $f(x, y)$ be defined on a rectangle and $c \geq 1$. There exists $\lambda \in (0, 1)$ independent of f, c, δ such that for sufficiently small δ ,*

$$\|f - Q_L\|_{0,S} \leq C \exp(\alpha c^2) \lambda^{c/\delta} \|f\|_{0,S}, \quad (7.4.2)$$

$$\|f - Q_L\|_{k,S} \leq C \delta^c \|f\|_{0,S}, \quad (7.4.3)$$

where $\alpha = \frac{\epsilon_h^2 \sigma}{2}$, ϵ_h and σ are two real constants in the Fourier transform, and C is a constant independent of δ and α .

Proof Based on Madych [336], Theorem 1 (cf. Eq. (10) on p. 124), there exists a bound,

$$\|f - Q_L\|_{0,\infty,S} \leq C \exp(\alpha c^2) \lambda^{c/\delta} \|f\|_{0,S}, \quad \alpha = \frac{\epsilon_h^2 \sigma}{2}.$$

Since S is a bounded domain, we have

$$\|f - Q_L\|_{0,S} \leq C \|f - Q_L\|_{0,\infty,S} \leq C \exp(\alpha c^2) \lambda^{c/\delta} \|f\|_{0,S}.$$

This is the first result (7.4.2).

Next, we also obtain from [336], Theorem 4, p. 127,

$$\|f - Q_L\|_{k,S} \leq C\delta^c \|f\|_{C_{h_c}}, \quad (7.4.4)$$

where the norm is defined by (cf. Eq. (6) in p. 124 on [336])

$$\|f\|_{C_{h_c}}^2 = \sum_{i=1}^2 \iint_S |\xi_i \hat{f}(\xi)|^2 (|\xi|^2 h_c(\xi))^{-1} d\xi,$$

where $h_c = \sqrt{r^2 + c^2}$, and the Fourier transform

$$\hat{f}(x) = \iint_S f(x) \exp(-i(x, \xi)) dx.$$

Since $h_c \geq h_1$ for $c \geq 1$, we have

$$\|f\|_{C_{h_c}} \leq \|f\|_{C_{h_1}}, \quad c \geq 1. \quad (7.4.5)$$

Moreover, there is an estimate in [336], p. 124, that for $g(x) = f(cx)$,

$$\|g\|_{C_{h_1}}^2 \leq C \exp(2\epsilon_h \sigma c) \|f\|_{0,S}^2, \quad (7.4.6)$$

where ϵ_h and σ are constants. Hence, if $c = 1$ and $g(x) = f(x)$, we have from (7.4.6)

$$\|f\|_{C_{h_1}}^2 \leq C \exp(2\epsilon_h \sigma) \|f\|_{0,S}^2. \quad (7.4.7)$$

Combining (7.4.4), (7.4.5) and (7.4.7) yields

$$\|f - Q_L\|_{k,S} \leq C\delta^c \|f\|_{C_{h_1}} \leq C \exp(\epsilon_h \sigma) \delta^c \|f\|_{0,S} \leq C_1 \delta^c \|f\|_{0,S},$$

where $C_1 = C \exp(\epsilon_h \sigma)$. This is the second result (7.4.3). ■

Lemma 7.4.1 and Madych [336] imply that the approximate solutions have the exponential convergence rate $O(\lambda^{c/\delta})$ with respect to δ , but the derivatives of low orders have only polynomially convergence rates $O(\delta^c)$. Although (7.4.3) is very conservative, the linear convergence rate $O(\delta)$, which is used as reasonable assumptions (7.4.9), leads to the inverse estimates shown below. Suppose that there exist the bounds,

$$\|f - Q_L\|_{0,S} \leq o(1) \|f\|_{0,S}, \quad (7.4.8)$$

$$\|f - Q_L\|_{k,S} \leq C \|f\|_{0,S}, \quad k = 1, 2, \dots, \quad (7.4.9)$$

where $0 < o(1) \ll 1$, and C is a bounded constant as $\delta \rightarrow 0$. Denote polynomials f by

$$f = f_N(x, y) = \sum_{i,j=0}^N b_{ij} x^i y^j. \quad (7.4.10)$$

We cite a Lemma from Chapter 5.

Lemma 7.4.2 *For the polynomials f of order N defined in S , there exists a constant independent of N such that*

$$\|f_N\|_{k,S} \leq CN^{2k}\|f_N\|_{0,S}. \quad (7.4.11)$$

Let (7.4.1) be given. For uniquely determining $Q_L(x, y)$, we choose

$$N^2 < L \leq (N + 1)^2, \quad (7.4.12)$$

and employ more collocation equations

$$Q_L(x_i, y_i) = f(x_i, y_i), \quad i = 1, 2, \dots, (N + 1)^2, \quad \sum_{i=1}^{(N+1)^2} a_i = 0, \quad (7.4.13)$$

where the first L collocation equations are the same as in (7.4.1). Hence the errors of the solutions and their derivatives would not decrease, and Lemma 7.4.1 also holds. Then we may still assume (7.4.8) and (7.4.9), and prove the following theorem:

Theorem 7.4.1 *Let (7.4.8) and (7.4.9) hold for f_N satisfying (7.4.10) and (7.4.13), where S is a rectangle. Then there exists the bound,*

$$\|Q_L\|_{k,S} \leq CL^k\|Q_L\|_{0,S}. \quad (7.4.14)$$

Proof From the triangle inequality, we have

$$\|Q_L\|_{k,S} \leq \|f_N\|_{k,S} + \|Q_L - f_N\|_{k,S}.$$

From Lemma 7.4.2 and (7.4.9),

$$\|Q_L\|_{k,S} \leq CN^{2k}\|f_N\|_{0,S} + C\|f_N\|_{0,S} \leq CN^{2k}\|f_N\|_{0,S}. \quad (7.4.15)$$

Similarly, from (7.4.8), we have

$$\|f_N\|_{0,S} \leq \|Q_L\|_{0,S} + \|Q_L - f_N\|_{0,S} \leq \|Q_L\|_{0,S} + o(1)\|f_N\|_{0,S}.$$

This leads to

$$\|f_N\|_{0,S} \leq \frac{1}{(1 - o(1))}\|Q_L\|_{0,S} \leq \frac{1}{2}\|Q_L\|_{0,S}. \quad (7.4.16)$$

Since $N \leq \sqrt{L}$ from (7.4.12), combining (7.4.15) and (7.4.16) yields

$$\|Q_L\|_{k,S} \leq CN^{2k}\|Q_L\|_{0,S} \leq CL^k\|Q_L\|_{0,S}.$$

This is the desired result (7.4.14). ■

For polynomials, the inverse estimates (7.4.11) are proven in Chapter 5, and the similar inverse estimates (7.4.14) hold for RBFs, based on the approximation properties.

Theorem 7.4.1 enables us to extend the combined methods and collocation methods in Chapters 5 and 6 to those using the RBFs. Similar arguments may be used for the collocation methods and their combinations using the Sinc functions [447], or the fundamental functions.

Remark 7.4.1 Eq. (7.4.8) implies the approximation $f \approx Q_L$, with small relative errors. Note that the bound of (7.4.9) can also be derived from Wendland [484]. In fact, we have, from [484], Theorem 5.3,

$$\|f - Q_L\|_{k,S} \leq Ch^{m-k} \|f\|_{m,S}, \quad m \geq k,$$

where $h = \delta$. Choosing $m = 2k$, we obtain from (7.4.11),

$$\begin{aligned} \|f_N - Q_L\|_{k,S} &\leq Ch^k \|f_N\|_{2k,S} \\ &\leq Ch^k N^{4k} \|f_N\|_{0,S} \leq C_1 \|f_N\|_{0,S}, \end{aligned}$$

provided that h can be chosen so small that $h^k N^{4k} \leq C_1$. This also leads to assumption (7.4.9). For $c \geq 1$, we may choose small h such that $(\frac{h}{c})^k N^{4k} \leq C$.

Remark 7.4.2 By following Chapter 5, the solution domain can be extended to a polygon. The reason is that a polygon can be decomposed into finite parallelograms with overlaps. A parallelogram may be transformed to a rectangle by linear transformations. Then, Eq. (7.4.14) also holds for the polygonal domain.

7.5 Numerical Experiments

In this section, first we carry out a computational procedure for smooth problems to support the theoretical analysis in Section 7.3. Then we carry out two methods for solving Motz's problem. Numerical experiments of combinations of FEM and RBCM are reported in Chapter 5.

7.5.1 Radial Basis Collocation Methods with Different Boundary Conditions

Consider Poisson's equation,

$$-\Delta u = -\left(\frac{\partial^2 u}{\partial x^2} + \frac{\partial^2 u}{\partial y^2}\right) = f(x, y) \quad \text{in } S, \quad (7.5.1)$$

where $S = \{(x, y) \mid 0 < x < 1, 0 < y < 1\}$, with the mixed type of different boundary conditions:

$$\begin{aligned} u|_{x=0} &= 0, \quad u|_{y=0} = 0, \\ u_\nu|_{x=1} &= g_N, \\ u_\nu + \alpha u|_{y=1} &= g_R, \end{aligned} \quad (7.5.2)$$

where $\alpha > 0$, (e.g., $\alpha = 2$). The exact solution is chosen to be exactly the same as in [97]

$$u = \sin\left(\frac{\pi x}{6}\right) \sin\left(\frac{7\pi x}{4}\right) \sin\left(\frac{3\pi y}{4}\right) \sin\left(\frac{5\pi y}{4}\right). \quad (7.5.3)$$

The functions f , g_N and g_R are then given explicitly.

The admissible functions are chosen as follows:

$$v = \sum_{i=1}^L \tilde{a}_i g_i(x, y), \text{ in } S, \quad (7.5.4)$$

where \tilde{a}_i are unknown coefficients to be determined, and $g_i(x, y)$ are the RBFs. First, we use the inverse multiquadric radial basis functions (IMQRB)

$$g_i(x, y) = \frac{1}{\sqrt{r_i^2 + c^2}}, \quad (7.5.5)$$

where c is a shape parameter constant, $r_i = \sqrt{(x - x_i)^2 + (y - y_i)^2}$, and (x_i, y_i) are the source points which should also be chosen as the collocation nodes. Suitable additional functions may be added into (7.5.4), such as some polynomials or singular functions if necessary. Next, we may use the Gaussian radial basis functions (GRB),

$$g_i(x, y) = \exp\left(-\frac{r_i^2}{c^2}\right). \quad (7.5.6)$$

In Section 7.4, we address that the number of collocation nodes may be larger than the number of terms of RBFs. Let L be the number of RBFs, and N be the number of source points in one direction. We use the collocation equations (7.3.11) – (7.3.13) on the uniform interior and boundary nodes with $L = N^2$. The distribution of source points in this chapter is chosen to be uniform for easy test, but it may, of course, be chosen rather arbitrarily. Then the radial distance $\delta = O(\frac{1}{N})$. The error norms by using IMQRB with shape parameter $c = 2.0$, are listed in Table 7.1, where the collocation nodes are also chosen to be uniform with the total number 196. From Table 7.1, we can see the following asymptotic relations:

$$\|u - v\|_{0,\infty,S} = O((0.22)^N), \quad (7.5.7)$$

$$\|u - v\|_{0,S} = O((0.24)^N), \quad (7.5.8)$$

$$\|u - v\|_{1,S} = O((0.20)^N). \quad (7.5.9)$$

Eqs. (7.5.7) – (7.5.9) indicate that the numerical solutions have the exponential convergence rates. In Table 7.1, the errors in the Sobolev norm and the infinite norm can be achieved in the order of 10^{-6} , when the number of RBFs is given by $L = 11^2 = 121$. Moreover, the shape parameter c of RBFs can also be chosen larger, e.g., $c = 2.5$ or 3.0 . It seems that these numerical results are better than these in Cheng et al. [97].

7.5.2 Adding Method of Singular Functions

Consider Motz's problem, its exact solution is given in [309], and the leading six coefficients for (7.2.3) are (also see Table 1.1)

$$\begin{aligned} d_0 &= 401.1624, & d_1 &= 87.6559, & d_2 &= 17.2379, \\ d_3 &= -8.0712, & d_4 &= 1.44027, & d_5 &= 0.33105. \end{aligned}$$

Because of singularity, some singular functions may be added into the RBFs. The admissible functions are chosen as

$$v = \sum_{i=1}^L \tilde{a}_i g_i(x, y) + \sum_{n=0}^M \tilde{d}_n \varphi_n(r, \theta) \quad \text{in } S, \quad (7.5.10)$$

where \tilde{a}_i and \tilde{d}_n are unknown coefficients to be determined, and $g_i(x, y)$ are the RBFs. In (7.5.10), $\varphi_n(r, \theta) = r^{n+\frac{1}{2}} \cos(n + \frac{1}{2})\theta$. We choose IMQRB and GRB. Let the distribution of source points be uniform in our computation, and use the collocation equations on uniform interior and boundary collocation nodes. The error norms are listed in Tables 7.2 and 7.3, for IMQRB($c=2.0$) and GRB($c=2.0$), respectively. The L denotes the number of RBFs, $L = N^2$, and M denotes the number of singular functions. The coupling techniques for L and M may refer to [291]. From Table 7.2, we can see the following asymptotic relations,

$$\|u - v\|_{0,\infty,S} = O((0.28)^N), \quad (7.5.11)$$

$$\|u - v\|_{0,S} = O((0.29)^N), \quad (7.5.12)$$

$$\|u - v\|_{1,S} = O((0.33)^N). \quad (7.5.13)$$

Also, from Table 7.3, we can see for GRB,

$$\|u - v\|_{0,\infty,S} = O((0.30)^N), \quad (7.5.14)$$

$$\|u - v\|_{0,S} = O((0.31)^N), \quad (7.5.15)$$

$$\|u - v\|_{1,S} = O((0.36)^N). \quad (7.5.16)$$

Eqs. (7.5.11) – (7.5.16) indicate that the numerical solutions obtained also have the exponential convergence rates, which verify the error bounds obtained.

7.5.3 Subtracting Method of Singular Functions

We also consider Motz's problem here, but which is solved by slightly different method. First, choose purely the radial basis functions (RBFs),

$$\bar{u} = \sum_{i=1}^L a_i g_i(x, y). \quad (7.5.17)$$

The Motz's solutions are known as

$$u(r, \theta) = \sum_{i=0}^{\infty} d_i r^{i+\frac{1}{2}} \cos(i + \frac{1}{2})\theta, \quad (7.5.18)$$

where the coefficients can also be obtained from

$$d_i = \frac{2}{\pi} r^{-(i+\frac{1}{2})} \int_0^\pi u(r, \theta) \cos(i + \frac{1}{2})\theta d\theta. \quad (7.5.19)$$

Usually, the solutions from the collocation method using (7.5.17) are poor only near the origin due to the singularity. Hence, choosing $r \geq \frac{1}{2}$, we may evaluate the approximate coefficients \tilde{d}_i from (7.5.19) very well, and obtain the singular solutions,

$$\bar{w} = \sum_{i=0}^M \tilde{d}_i r^{i+\frac{1}{2}} \cos(i + \frac{1}{2})\theta. \quad (7.5.20)$$

We may subtract the singular part (7.5.20) from u , and then obtain a rather smooth problem for $\bar{u} = u - \bar{w}$, with the following equations,

$$\Delta \bar{u} = 0 \quad \text{in } S, \quad (7.5.21)$$

$$\bar{u}_x = -\bar{w}_x \quad \text{on } x = -1 \quad \wedge \quad 0 \leq y \leq 1, \quad (7.5.22)$$

$$\bar{u} = 500 - \bar{w} \quad \text{on } x = 1 \quad \wedge \quad 0 \leq y \leq 1,$$

$$\bar{u}_y = -\bar{w}_y \quad \text{on } y = 1 \quad \wedge \quad -1 \leq x \leq 1,$$

$$\bar{u} = 0 \quad \text{on } y = 0 \quad \wedge \quad -1 \leq x < 0,$$

$$\bar{u}_y = 0 \quad \text{on } y = 0 \quad \wedge \quad 0 < x \leq 1.$$

Again, we choose (7.5.17) and use the radial basis collocation method in Section 7.3 to seek the rather smooth problem (7.5.21) – (7.5.22). We add singular part \bar{w} to the smooth part \bar{u} to obtain a better approximation to u . Repeat the evaluation (7.5.19) of coefficients d_i , and then subtract \bar{w} of (7.5.20) again. The above iteration repeats until a convergent solution is obtained.

The error norms are listed in Tables 7.4 and 7.5 for IMQRB(c=2.0) and GRB(c=2.0), respectively. We choose $r = 1$ to evaluate the approximate coefficients \tilde{d}_n , $n = 0, 1, \dots, 5$. The termination of iterations occurs when the absolute error becomes less than 10^{-6} , and the number of iteration needed is about 10. From Table 7.4, we can also observe the exponential convergence rates,

$$\|u - (\bar{u} + \bar{w})\|_{0,\infty,S} = O((0.34)^N), \quad (7.5.23)$$

$$\|u - (\bar{u} + \bar{w})\|_{0,S} = O((0.30)^N), \quad (7.5.24)$$

$$\|u - (\bar{u} + \bar{w})\|_{1,S} = O((0.33)^N). \quad (7.5.25)$$

And from Table 7.5,

$$\|u - (\bar{u} + \bar{w})\|_{0,\infty,S} = O((0.39)^N), \quad (7.5.26)$$

$$\|u - (\bar{u} + \bar{w})\|_{0,S} = O((0.34)^N), \quad (7.5.27)$$

$$\|u - (\bar{u} + \bar{w})\|_{1,S} = O((0.38)^N). \quad (7.5.28)$$

The exponential convergence rates, (7.5.23) – (7.5.28), also support the theoretical analysis made.

The adding method of singular solutions was reported in Fix, Gulati and Wakoff [154], and the subtracting method of singular solutions in Wigley [490], also see [291].

7.6 Comparisons and Conclusions

1. To solve Poisson's problem, this chapter provides the theoretical framework of RBCM and its combinations with other methods. This chapter is also an important extension of RBFs from the approximation theory of smooth functions to the solutions of partial differential equations. The RBCM is also an efficient tool for solving singular PDEs, in which a combination of RBFs and singular functions used.
2. From Table 7.1, we can observe the exponential convergence rates for smooth problems, which may be competitive to orthogonal polynomials. From Tables 7.2 – 7.5, we can find that the exponential convergence rates also exist for singularity problems, when some singular functions are applied as basis. From these tables, the following asymptotic relations are also observed:

$$\|u - v\|_{k,S} = O(\lambda^N) = O(\lambda^{\sqrt{L}}), \quad k = 0, 1,$$

where $0 < \lambda < 1$.

3. For Motz's problem, we find that the approximate solutions by RBCM adding method of singular solutions in Section 7.5.2 have much better convergence rates than those by RBCM subtracting method of singular solutions in Section 7.5.3. On the contrary, the leading coefficients of singular functions, \tilde{d}_n , $n = 0, 1, \dots, 5$, obtained by RBCM subtracting method are more accurate than those by RBCM adding method. We also observe that the IMQRB is superior to the GRB, in both accuracy and stability.
4. From the numerical results, we see that the RBFs have large condition numbers which imply high instability. This is the drawback of the radial basis collocation method. In practical computation, since only a few terms of RBFs are needed, such a drawback is not serious. Moreover, its effective condition number may be much smaller, see Section 3.7 of Chapter 3. In spite of this drawback, the RBCM is still a competitive method for PDEs due to high accuracy and a very low computational cost.

5. From Tables 7.6 – 7.7 and Figure 7.1 we can see that there exists convergence by increasing parameter c from 1.0 to 3.0. The following asymptotic relations are also observed:

$$\|u - v\|_{k,S} = O(\lambda^c), \quad k = 0, 1,$$

where $0 < \lambda < 1$.

6. All the numerical experiments indicate that the RBCM have exponential convergence rates

$$\|u - v\|_{k,S} = O(\lambda^{c/\delta}) \approx O(\lambda^{cN}) \approx O(\lambda^{c\sqrt{L}}), \quad k = 0, 1,$$

where $0 < \lambda < 1$. From the viewpoint of accuracy, the errors tend to zero as $c/\delta \rightarrow \infty$ (i.e. $L \rightarrow \infty$ and $c \rightarrow \infty$). However, from the viewpoint of stability, we can not increase L too much due to large condition number. Also, we can not increase c too much due to the flatness of RBFs, causing the ill-conditioned \mathbf{F} in (7.3.14). It seems that accuracy and instability are twins. Such a statement is also called the *Uncertainty Principle* in Schaback [422]. Either one goes for a small error and gets a bad sensitivity, or one wants a stable algorithm and has to take a comparably large error. In practical computation, we should keep some balance between them. In summary, Theorem 7.3.1 and the numerical examples display that the errors of the solutions of Poisson's equation by RBCM have the same exponential convergence rates as those of surface fitting by RBFs.

$L = N^2$	7^2	9^2	11^2	13^2
$\ u - v\ _{0,\infty,S}$	9.30(-3)	5.92(-5)	4.32(-6)	1.10(-6)
$\ u - v\ _{0,S}$	1.60(-3)	1.51(-5)	8.19(-7)	3.10(-7)
$\ u - v\ _{1,S}$	2.28(-2)	1.32(-4)	5.22(-6)	1.67(-6)
Cond.(\mathbf{A})	1.02(7)	2.28(8)	1.21(9)	2.01(9)

Table 7.1: The error norms and condition number by the IMQRB collocation method with parameter $c = 2.0$.

$L = N^2, M$	$4^2, 2$	$6^2, 3$	$8^2, 4$	$10^2, 5$
$\ u - v\ _{0,\infty,S}$	11.34	1.07	7.46(-2)	5.50(-3)
$\ u - v\ _{0,S}$	3.00	2.85(-1)	1.27(-2)	1.70(-3)
$\ u - v\ _{1,S}$	12.0	1.68	1.03(-1)	1.45(-2)
\tilde{d}_0	423.8219	403.9276	401.0821	401.1446
\tilde{d}_1	95.9485	111.1686	89.9612	87.7384
\tilde{d}_2	12.7307	26.5319	8.6550	16.5567
\tilde{d}_3	/	-12.2469	-10.7710	-3.4625
\tilde{d}_4	/	/	1.8867	-3.1864
\tilde{d}_5	/	/	/	-0.8645
Cond.(A)	2.58(3)	8.60(5)	5.38(8)	3.21(9)

Table 7.2: The error norms and condition number by the IMQRB collocation method adding singular functions with parameter $c = 2.0$.

$L = N^2, M$	$4^2, 2$	$6^2, 3$	$8^2, 4$	$10^2, 5$
$\ u - v\ _{0,\infty,S}$	8.07	7.32(-1)	9.40(-2)	5.90(-3)
$\ u - v\ _{0,S}$	1.86	1.95(-1)	1.39(-2)	1.60(-3)
$\ u - v\ _{1,S}$	8.13	1.07	1.45(-1)	1.78(-2)
\tilde{d}_0	416.4048	403.6369	401.0648	401.1865
\tilde{d}_1	72.9120	103.3334	88.9340	87.3105
\tilde{d}_2	16.4691	45.5082	24.7180	17.2233
\tilde{d}_3	/	-19.0671	-11.6812	-13.7762
\tilde{d}_4	/	/	-1.7538	7.8214
\tilde{d}_5	/	/	/	-0.4210
Cond.(A)	7.16(3)	2.73(8)	1.36(9)	5.79(9)

Table 7.3: The error norms and condition number by the GRB collocation method adding singular functions with parameter $c = 2.0$.

$L = N^2, M$	$4^2, 2$	$6^2, 3$	$8^2, 4$	$10^2, 5$
$\ u - (\bar{u} + \bar{w})\ _{0,\infty,S}$	6.99	6.10(-1)	7.40(-2)	7.00(-3)
$\ u - (\bar{u} + \bar{w})\ _{0,S}$	2.24	2.64(-1)	8.90(-3)	1.40(-3)
$\ u - (\bar{u} + \bar{w})\ _{1,S}$	7.82	1.45	1.11(-1)	1.63(-2)
\tilde{d}_0	399.8414	401.0809	401.1633	401.1627
\tilde{d}_1	86.0459	87.6951	87.6526	87.6556
\tilde{d}_2	18.0743	17.0752	17.2360	17.2378
\tilde{d}_3	/	7.8863	-8.0718	-8.0714
\tilde{d}_4	/	/	1.4386	1.4403
\tilde{d}_5	/	/	/	0.3310
Cond.(A)	1.14(3)	4.21(5)	6.16(8)	3.21(9)
Num. of iter.	10	10	9	9

Table 7.4: The error norms and condition number by the IMQRB collocation method subtracting singular functions with parameter $c = 2.0$.

$L = N^2, M$	$4^2, 2$	$6^2, 3$	$8^2, 4$	$10^2, 5$
$\ u - (\bar{u} + \bar{w})\ _{0,\infty,S}$	5.24	5.99(-1)	1.01(-1)	1.18(-2)
$\ u - (\bar{u} + \bar{w})\ _{0,S}$	1.62	2.69(-1)	2.10(-2)	2.10(-3)
$\ u - (\bar{u} + \bar{w})\ _{1,S}$	6.14	1.48	1.64(-1)	1.87(-2)
\tilde{d}_0	399.7470	401.0842	401.1625	401.1617
\tilde{d}_1	87.2125	87.7272	87.6501	87.6571
\tilde{d}_2	17.7888	17.1083	17.2329	17.2373
\tilde{d}_3	/	-7.8454	-8.0616	-8.0708
\tilde{d}_4	/	/	1.4393	1.4403
\tilde{d}_5	/	/	/	0.3310
Cond.(A)	6.06(3)	1.89(8)	1.01(9)	2.70(10)
Num. of iter.	11	10	10	9

Table 7.5: The error norms and condition number by the GRB collocation method subtracting singular functions with parameter $c = 2.0$.

c	$\ u - v\ _{0,\infty,S}$	$\ u - v\ _{0,S}$	$\ u - v\ _{1,S}$	Cond. (A)
1.0	6.71(-2)	1.96(-2)	1.17(-1)	2.34(6)
1.2	7.93(-2)	2.16(-2)	1.39(-1)	5.56(6)
1.4	9.36(-2)	2.12(-2)	1.44(-1)	1.66(7)
1.6	9.36(-2)	1.94(-2)	1.37(-1)	5.49(7)
1.8	8.59(-2)	1.63(-2)	1.21(-1)	1.94(8)
2.0	7.46(-2)	1.27(-2)	1.03(-1)	1.70(9)
2.2	6.29(-2)	9.70(-3)	8.74(-2)	8.27(8)
2.4	5.25(-2)	7.60(-3)	7.60(-2)	1.83(9)
2.6	4.38(-2)	6.10(-3)	6.81(-2)	1.92(9)
2.8	3.65(-2)	5.20(-3)	6.28(-2)	3.35(9)
3.0	3.30(-2)	4.80(-3)	5.96(-2)	2.01(9)

Table 7.6: The error norms and condition number by the IMQRB collocation method adding singular functions with $L = 8^2$ and $M = 4$.

c	$\ u - (\bar{u} + \bar{w})\ _{0,\infty,S}$	$\ u - (\bar{u} + \bar{w})\ _{0,S}$	$\ u - (\bar{u} + \bar{w})\ _{1,S}$	Cond. (A)
1.0	5.28(-2)	8.70(-3)	9.19(-2)	1.35(6)
1.2	8.02(-2)	9.80(-3)	1.14(-1)	2.97(6)
1.4	9.78(-2)	1.03(-2)	1.27(-1)	7.81(6)
1.6	9.63(-2)	1.01(-2)	1.27(-1)	2.32(7)
1.8	8.66(-2)	9.60(-3)	1.20(-1)	7.35(7)
2.0	7.40(-2)	8.90(-3)	1.11(-1)	1.95(8)
2.2	6.16(-2)	8.20(-3)	1.00(-1)	3.18(8)
2.4	5.06(-2)	7.50(-3)	9.06(-2)	4.75(8)
2.6	4.13(-2)	6.80(-3)	8.20(-2)	5.59(8)
2.8	3.36(-2)	6.20(-3)	7.48(-2)	9.11(8)
3.0	2.73(-2)	5.70(-3)	6.89(-2)	1.11(9)

Table 7.7: The error norms and condition number by the IMQRB collocation method subtracting singular functions with $L = 8^2$ and $M = 4$.

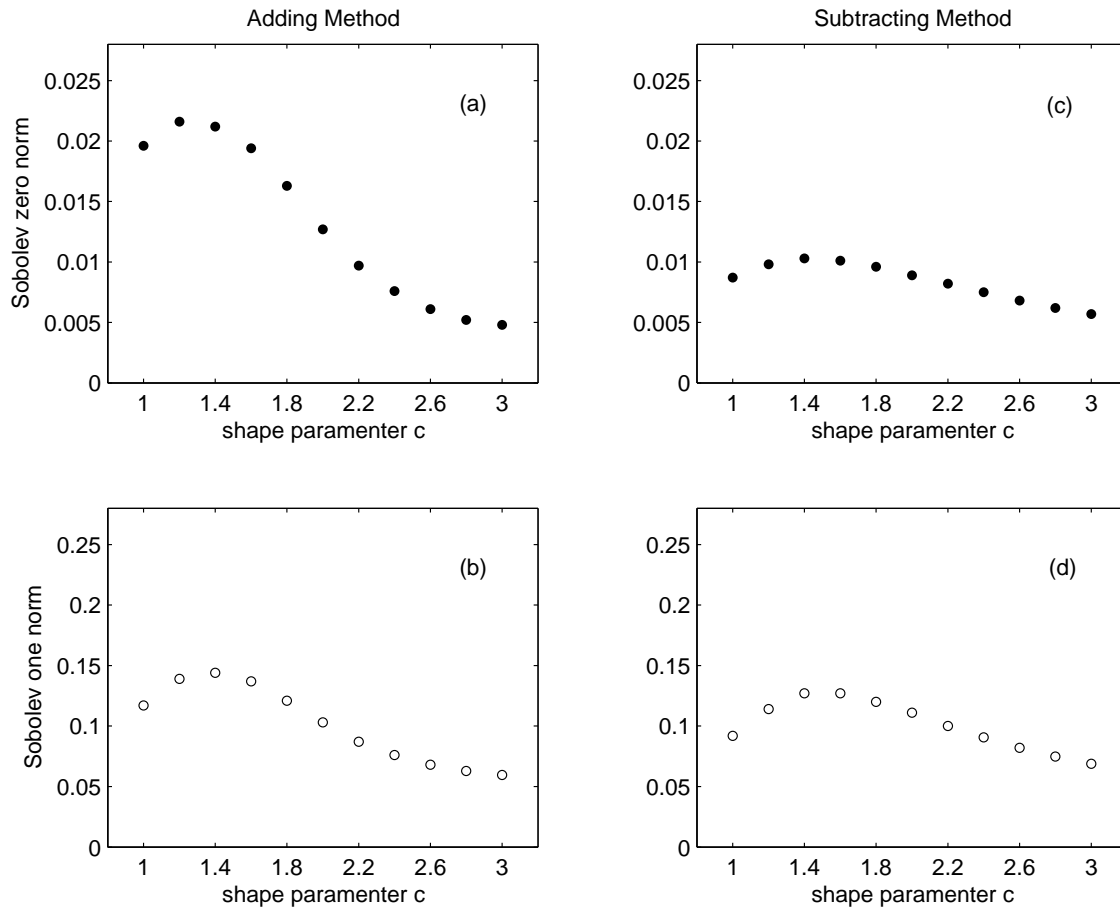


Figure 7.1: The solution errors versus parameter c , with $L = 8^2$ and $M = 4$.

*The firm, the enduring, the simple,
and the modest are near to virtue.*
—— *The Confucian Analects* ——

Confucius
(551-479 B.C.)

Part III

Advanced Topics

The remainder of this book is devoted to advanced topics, such as the hybrid TM, the interior boundary conditions of the Schwarz alternating method, the combinations with high order FEMs, the eigenvalue problems and the Helmholtz equation. In the last chapter of this part, particular solutions are provided for the Laplace equation on a polygon, and new models involving the discontinuity and mild singularity of the solutions are designed.

The advanced topics in this part are related more to the collocation Trefftz method (TM) in Part I. The first topic is to develop the hybrid TM, which is widely used in engineering computation. The simplified hybrid TM can be easily developed from the simplified hybrid combination of TM and FEM in Li and Liang [308], but the general hybrid TMs are new. These algorithms and analysis are given in Chapter 8.

Let the solution domain S be split into S_1 and S_2 . Suppose that the collocation TM is used in S_2 to deal with the solution singularity, and that the FEM in S_1 where the solution is smooth enough. Two methods can be incorporated with the Schwarz alternating method, or by the combined method using the coupling techniques. In the combined method, there is no overlap between S_1 and S_2 ; but there may or may not in the Schwarz alternating method. New interior boundary conditions are explored for the Schwarz alternating method. This is the second topic in Part III. The third topic is to combine the collocation TM with high order FEMs. The penalty plus hybrid techniques of Chapter 3 are used, and global superconvergence can be achieved. The fourth topic is to use the collocation TM for eigenvalue problems and the Helmholtz equation. By an iteration process, when there occurs a degeneracy of the Helmholtz equation, then an eigenvalue is obtained. High accuracy of the eigenvalues and eigenfunctions can also be achieved. This is just an example to extend the TM from elliptic equations in [291] to other problems. The TM can be applied to parabolic and hyperbolic equations, which results will be reported later.

When the particular functions satisfy the PDEs exactly, the Ritz-Galerkin method and the spectral methods are simplified into the TM. An efficient implementation of TM is developed in this book, called the collocation TM. The collocation TM becomes a very competitive method for solving PDEs, due to several merits: (1) simplicity of the algorithms, (2) high accuracy of the solutions, (3) explicit forms of the solutions, (4) the ease in dealing with singularity, (5) facile analysis, (6) savings in CPU time and computer storage. Evidently, the collocation TM is advantageous over the FEM, the FDM, and the FVM. Both the TM and the BEM may reduce the solved problems by one dimension. However, the collocation TM is more efficient and effective.

The particular solutions of PDEs are essential to the TM. Our efforts are focused on the explicit particular solutions of the Laplace equation on a polygon. Although those particular solutions can be found in Volkov [473], the formulas of the harmonic functions presented in Chapter 13 are easier to expose the mild singularity at the domain corners.

This part consists of six chapters for the advanced topics of Parts I and II.

Chapter 8: Hybrid and Other TMs Using Piecewise Particular Solution.

Chapter 9: Interior Boundary Conditions in the Schwarz Alternating Method.

Chapter 10: Combination with High Order FEMs.

Chapter 11: Eigenvalue Problems.

Chapter 12: Helmholtz Equation.

Chapter 13: Particular Solutions of Laplace's Equation.

A brief description of Part III is given as follows.

Chapter 8 discusses the hybrid TM using *piecewise* particular solutions with new error analysis. The simplified hybrid method for the TM and FEM was first analyzed in Li and Liang [308], which can be applied to the TMs. The new general hybrid TMs (in particular the symmetric hybrid TMs) are developed in this chapter. Moreover, the penalty plus hybrid TM and the direct TM (i.e., the Lagrange multiplier TM) using *piecewise* particular solutions are also studied, to derive the error bounds.

Chapter 9 explores new mixed types of the Schwarz alternating methods (SAMs) with or without overlapping, by using different interior boundary conditions, such as the Dirichlet, the Neumann and the Robin conditions. For a simple model: the Laplacian solutions on a sectorial domain, the mixed SAMs are explored, their convergence rates are analyzed, and effects of different interior boundary conditions are investigated.

Chapter 10 solves the Poisson equation on a polygonal domain wherein the bi-Lagrange p -order FEMs, $p \geq 2$, are chosen. We call these methods the p -rectangles. Let S be split into S_1 and S_2 , where only S_2 includes a singular point. Suppose that the solution in S_1 is highly smooth. Then the collocation TM and the p -rectangles may be used in S_2 and S_1 , respectively. In this chapter, we invoke the penalty plus hybrid techniques to couple the collocation TM and the p -rectangles, and derive *almost* the *best* global superconvergence $O(h^{p+2-\delta})$, where h denotes the meshspacing and $0 < \delta \ll 1$. When Adini's elements are used in S_1 instead of the p -rectangles, the *best* global superconvergence $O(h^{3.5})$ can be achieved. Some numerical experiments are carried out for the combination of the Ritz-Galerkin method and the Adini's elements, to verify the superconvergence $O(h^{3.5})$.

Chapter 11 deals with eigenvalue problems, by the new algorithms of the TM, based on the degeneracy of the Helmholtz solutions. The degeneracy is such that as the parameters k^2 used in the Helmholtz equation approaches to an eigenvalue of the Laplace operator, so the solution matrix becomes singular. Piecewise particular solutions are obtained for a sample of eigenvalue problems. Using piecewise particular solutions is advantageous for solving problems with complicated geometry, because uniform particular solutions may not always exist in the entire solution domain. Numerical experiments are carried out for the eigenvalue problems of two basic models, the L-shaped domain with the Dirichlet boundary condition, and the cracked beam. These two problems involve the singularity of eigenfunctions.

Chapter 12 employs the TM for finding the solution of the Helmholtz problem, where k^2 is very close to eigenvalues λ_ℓ of the Laplace operator, but not exactly equal. Denote the relative distance $\delta = \frac{k^2 - \lambda_\ell}{\lambda_\ell}$. Error analysis is made to derive the error bounds of the solutions with respect to δ , thus linking to the analysis of Part I and Chapter 11.

Chapter 13 derives the harmonic functions, i.e., the solutions of Laplace's equations, for the Dirichlet and Neumann boundary conditions on sectors. These harmonic functions clearly expose strong or mild singularity properties of the Laplace solutions at the domain corners. We also explore in detail the singularities of the sectors with the boundary angles, $\Theta = \frac{\pi}{2}, \frac{3\pi}{2}, \pi$ and 2π , which often occur in many testing models. Two new rectangular models with singularities are provided. One model involves the discontinuity of the solution, and the other the mild singularities. The collocation TM, the Schwarz alternating method, and their combinations may be chosen to seek the solutions with high accuracy.

Chapter 8

Hybrid and Other TMs Using Piecewise Particular Solutions

In Chapters 2 – 4, particular solutions that apply to the entire domain are chosen, and different TMs are studied in detail. In Chapter 1, piecewise particular solutions are considered for the original TM (i.e., the BAM), the error analysis for the CTM is investigated in Chapter 2. In this chapter, we will study other TMs, such as the hybrid TM, etc. by using piecewise particular solutions. Hence, this chapter is a continuing development of Chapter 3 by extending its application to include piecewise particular solutions. The Trefftz method may be described as follows. First, a set of particular solutions are chosen. A linear combination of those functions is then regarded as an approximate solution of PDEs, and their expansion coefficients are sought by satisfying the interior and exterior boundary conditions. When the solution domain is not rectangular or sectorial, the *piecewise* particular solutions may be chosen in different subdomains, and some coupling techniques must be employed along their common interior boundary. In Lu et al. [329], the collocation method is used for the Trefftz method, to lead to the collocation Trefftz method (i.e., the indirect Trefftz method). In this chapter, we will also discuss three other coupling techniques: (1) the hybrid techniques for the hybrid Trefftz method, (2) the penalty plus hybrid techniques, and (3) the Lagrange multiplier techniques for the direct Trefftz method. Error bounds are derived in detail for these three coupling methods, which show exponential convergence rates. Numerical experiments are carried out, and comparisons are made.

8.1 Introduction

For Laplace's equation or other second order partial differential equations (PDE), it is necessary to use piecewise particular solutions in the Trefftz method to solve complicated

problems. Let the solution domain S be divided by Γ_0 into two subdomains S^+ and S^- without overlaps¹, $S = S^+ \cup S^- \cup \Gamma_0$. We may choose different particular solutions in S^+ and S^- , denoted by

$$v = \begin{cases} v^+ = \sum_{i=1}^L a_i \Phi_i, & \text{in } S^+, \\ v^- = \sum_{i=1}^N b_i \Psi_i, & \text{in } S^-, \end{cases} \quad (8.1.1)$$

where v^\pm are the particular solutions satisfying the PDE in S^+ and S^- respectively, and a_i and b_i are the coefficients to be sought. Since the admissible functions v in (8.1.1) are not continuous along the interior boundary Γ_0 , some coupling techniques must be chosen to link v^+ and v^- to satisfy the interior continuity conditions,

$$v^+ = v^-, \quad p^+ \frac{\partial v^+}{\partial n} = p^- \frac{\partial v^-}{\partial n}, \quad \text{on } \Gamma_0, \quad (8.1.2)$$

where p^\pm are the positive coefficients, and n is the unit outward normal of ∂S^+ . The direct collocation for (8.1.2) is given by

$$v^+(Q_k) = v^-(Q_k), \quad p^+ \frac{\partial v^+}{\partial n}(Q_k) = p^- \frac{\partial v^-}{\partial n}(Q_k), \quad Q_k \in \Gamma_0. \quad (8.1.3)$$

This leads to the collocation Trefftz method (CTM); its error analysis has been provided in Chapter 2 and Lu et al. [329]. The CTM is called the indirect TM in [205, 246].

In this chapter, we pursue other efficient techniques to couple v^+ and v^- on Γ_0 . Consider the Laplace or the Debye-Huckel equation,

$$\mathcal{L}u = -\Delta u + cu = 0, \quad \text{in } S,$$

where $\Delta u = \frac{\partial^2 u}{\partial x^2} + \frac{\partial^2 u}{\partial y^2}$, and constant $c = 0$ or $c = 1$. For simplicity in exposition, we may assume that the particular solutions Φ_i and Ψ_i also satisfy the exterior boundary condition on ∂S .

Denote by $V_{L,N}$ the finite dimensional collection of v in (8.1.1). The following three coupling techniques on Γ_0 will be discussed in this chapter.

¹The Schwarz alternating methods can be employed for the TM, where S^+ and S^- may or may not have overlaps. Along the interior boundary, different interior boundary conditions are explored in Chapter 9 and Li et al. [302], such as the Dirichlet, the Neumann, the Robin conditions and their mixed types, to speed up the convergence of the iterative algorithms.

I. The hybrid techniques for the hybrid Trefftz method. To seek $u_{L,N} \in V_{L,N}$ such that

$$A_{Hyb}(u_{L,N}, v) = 0, \quad \forall v \in V_{L,N}, \quad (8.1.4)$$

where

$$A_{Hyb}(u, v) = \iint_{S^+} \nabla u \cdot \nabla v + \iint_{S^-} \nabla u \cdot \nabla v + I_{Hyb}^{(\alpha, \beta)}(u, v). \quad (8.1.5)$$

In (8.1.5), the hybrid coupling is

$$I_{Hyb}^{(\alpha, \beta)}(u, v) = \alpha \int_{\Gamma_0} \frac{\partial u^+}{\partial n} v^- - \beta \int_{\Gamma_0} \frac{\partial u^-}{\partial n} v^+ - \alpha \int_{\Gamma_0} \frac{\partial v^+}{\partial n} u^- + \beta \int_{\Gamma_0} \frac{\partial v^-}{\partial n} u^+, \quad (8.1.6)$$

where n is the unit outnormal of ∂S^+ , $u^\pm = u|_{\partial S^\pm \cap \Gamma_0}$, and α and β are real constants. For convergence of the solutions, we choose $\alpha + \beta = 1$, and for symmetry, $\alpha = \beta = \frac{1}{2}$.

In our previous study, we always choose $\alpha\beta = 0$, i.e., Case I: $\alpha = 1$ and $\beta = 0$ and Case II: $\alpha = 0$ and $\beta = 1$. Such couplings are called the simplified hybrid combinations of the Trefftz method and the FEM, and the error analysis was first reported in Li and Liang [308], and then in Li and Bui [296, 298], Li [293], and Li and Huang [303]. The bias derivatives $\frac{\partial u^+}{\partial n}$ and $\frac{\partial v^+}{\partial n}$ in $I_{Hyb}^{(1,0)}$ are easily formulated in the stiffness matrix, since the particular solutions used in S^+ are explicit. Hence, the simplified hybrid techniques are very efficient. However, when particular solutions are used in both S^+ and S^- , the symmetric hybrid techniques with $\alpha = \beta = \frac{1}{2}$ should also be studied. Since our previous analysis can not be applied directly to the case $\alpha\beta \neq 0$, new error analysis for the hybrid method (8.1.4) is needed.

Note that the original Trefftz method by Trefftz in 1926 [461] is a special case of (8.1.4) with $S^+ = S$, $S^- = \emptyset$, $\alpha = 1$ and $\beta = 0$, where Γ_0 is interpreted as ∂S . The Trefftz method using the hybrid techniques is also called the hybrid Trefftz method in engineering literature, see Qin [391].

II. The penalty plus hybrid techniques. To seek $u_{L,N}^* \in V_{L,N}$ such that

$$B_{H-P}(u_{L,N}^*, v) = 0, \quad \forall v \in V_{L,N}, \quad (8.1.7)$$

where

$$B_{H-P}(u, v) = \iint_{S^+} \nabla u \cdot \nabla v + \iint_{S^-} \nabla u \cdot \nabla v + I_{H-P}^{(\alpha, \beta, P_c)}(u, v). \quad (8.1.8)$$

In (8.1.8) the penalty plus hybrid coupling is

$$\begin{aligned} I_{H-P}^{(\alpha, \beta, P_c)}(u, v) &= - \int_{\Gamma_0} \left(\alpha \frac{\partial u^+}{\partial n} + \beta \frac{\partial u^-}{\partial n} \right) (v^+ - v^-) \\ &\quad - \int_{\Gamma_0} \left(\alpha \frac{\partial v^+}{\partial n} + \beta \frac{\partial v^-}{\partial n} \right) (u^+ - u^-) + P_c (L^\sigma + N^\tau) \int_{\Gamma_0} (u^+ - u^-) (v^+ - v^-), \end{aligned}$$

where the parameters $\alpha + \beta = 1$ for better convergence of the solutions, $\sigma \geq 1$ and $\tau \geq 1$ are two constants independent of L and N , and P_c is a large enough constant but also

independent of L and N . The hybrid plus penalty techniques have been used for the combinations of the Trefftz method and the FEM in [291, 297, 299], and in this chapter for the Trefftz method using piecewise particular solutions.

III. The Lagrange multiplier techniques for the direct TM. Consider the Debye-Huckel equation,

$$\mathcal{L}u = -\Delta u + u = 0, \quad \text{in } S. \quad (8.1.9)$$

Suppose that Φ_i and Ψ_i satisfy (8.1.9) in S^+ and S^- respectively. We also choose (8.1.1) as the admissible functions, and denote by $V_{L,N}$ their finite dimensional collection. Also denote V_h the piecewise k -order polynomials. The Lagrange multiplier technique is to seek $(u_{L,N}^\#, \lambda_h) \in V_{L,N} \times V_h$ such that

$$A_{Lag}(u_{L,N}^\#, \lambda_h; v, \mu) = 0, \quad \forall (v, \mu) \in V_{L,N} \times V_h, \quad (8.1.10)$$

where

$$A_{Lag}(u, \lambda; v, \mu) = \iint_{S^+} \nabla u \cdot \nabla v + \iint_{S^-} \nabla u \cdot \nabla v + D_{Lag}(u, \lambda; v, \mu). \quad (8.1.11)$$

In (8.1.11) the Lagrange multiplier coupling is given by

$$D_{Lag}(u, \lambda; v, \mu) = - \int_{\Gamma_0} \lambda(v^+ - v^-) - \int_{\Gamma_0} \mu(u^+ - u^-).$$

The error analysis for (8.1.10) can be obtained by following Li [291, 292]. Note that the direct Trefftz method is called the Lagrange multiplier Trefftz method in engineering literature, see [237, 262].

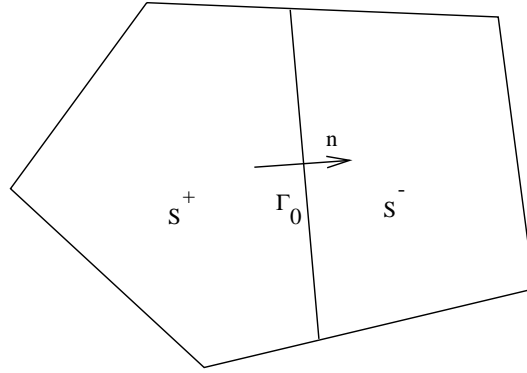
In summary, the error analysis of the Trefftz methods using the coupling techniques I, II, and III is important to the TMs. Error bounds are derived in this chapter, and numerical experiments are carried out.

This chapter is organized as follows. In Section 8.2, the hybrid techniques are described, and in Section 8.3, new error analysis is made. In Section 8.4, the penalty plus hybrid techniques are studied, and in Section 8.5, the Lagrange multiplier techniques are explored. In the last section, some numerical experiments are carried out for Motz's problem by the CTM and the hybrid TM.

8.2 The Hybrid Techniques

Consider the Laplace equation with the Dirichlet and Neumann boundary conditions, see Figure 8.1,

$$\begin{aligned} \Delta u &= \left(\frac{\partial^2 u}{\partial x^2} + \frac{\partial^2 u}{\partial y^2} \right) = 0 \quad \text{in } S, \\ u &= g_1 \quad \text{on } \Gamma_D, \\ \frac{\partial u}{\partial n} &= g_2 \quad \text{on } \Gamma_N, \end{aligned} \quad (8.2.1)$$

Figure 8.1: Partition of S into S^+ and S^- .

where S is a polygon, and ∂S is its boundary with $\partial S = \Gamma_D \cup \Gamma_N$. Let S be divided by the piecewise straight sections Γ_0 into two subdomains S^+ and S^- without overlaps (see Figure 8.1). Suppose that the admissible functions are given by

$$v = \begin{cases} v^+ = \sum_{i=1}^L a_i \Phi_i, & \text{in } S^+, \\ v^- = \sum_{i=1}^N b_i \Psi_i, & \text{in } S^-, \end{cases} \quad (8.2.2)$$

where a_i and b_i are the coefficients to be sought, and Φ_i and Ψ_i are the particular solutions

$$\Delta \Phi_i = 0 \quad \text{in } S^+, \quad \Delta \Psi_i = 0 \quad \text{in } S^-.$$

$\{\Phi_i\}$ and $\{\Psi_i\}$ are two complete and linearly independent bases in S^+ and S^- respectively. For simplicity in exposition, we let the partial solutions v^\pm satisfy the exterior boundary conditions

$$\begin{aligned} v^\pm \Big|_{\partial S^\pm \cap \Gamma_D} &= g_1, \\ \frac{\partial v^\pm}{\partial n} \Big|_{\partial S^\pm \cap \Gamma_N} &= g_2. \end{aligned} \quad (8.2.3)$$

Otherwise, the coupling techniques can be discussed as those for the interior boundary conditions. Denote by $V_{L,N}$ the finite dimensional collection of v in (8.2.2). Then we design the hybrid Trefftz method as follows. To seek $u_{L,N} \in V_{L,N}$ to satisfy (8.1.4). When $u = v$, the integral in (8.1.6) become

$$I_{Hyb}^{(\alpha,\beta)}(v, v) = 0.$$

Then for the nontrivial and non-constant $v \in V_{L,N}$ we have

$$A_{Hyb}(v, v) = \iint_{S^+} \nabla v \cdot \nabla v + \iint_{S^-} \nabla v \cdot \nabla v > 0.$$

This implies that the bilinear functional $A_{Hyb}(u, v)$ defined in (8.1.5) is positive definite. However, since $A_{Hyb}(u, v)$ is unsymmetric, more computational efforts and more computer storage are needed. In computation, we may seek $u_{L,N}$ differently. Since v^+ and v^- are independent to each other, we obtain from (8.1.4),

$$\iint_{S^+} \nabla u^+ \cdot \nabla v^+ - \alpha \int_{\Gamma_0} \frac{\partial v^+}{\partial n} u^- - \beta \int_{\Gamma_0} \frac{\partial u^-}{\partial n} v^+ = 0, \quad (8.2.4)$$

$$\iint_{S^-} \nabla u^- \cdot \nabla v^- + \alpha \int_{\Gamma_0} \frac{\partial u^+}{\partial n} v^- + \beta \int_{\Gamma_0} \frac{\partial v^-}{\partial n} u^+ = 0. \quad (8.2.5)$$

Subtracting (8.2.5) from (8.2.4) yields $B(u_{L,N}, v) = 0, \forall v \in V_{L,N}$, where

$$\begin{aligned} B(u, v) &= \iint_{S^+} \nabla u^+ \cdot \nabla v^+ - \iint_{S^-} \nabla u^- \cdot \nabla v^- \\ &\quad - \alpha \int_{\Gamma_0} \frac{\partial v^+}{\partial n} u^- - \beta \int_{\Gamma_0} \frac{\partial u^-}{\partial n} v^+ - \alpha \int_{\Gamma_0} \frac{\partial u^+}{\partial n} v^- - \beta \int_{\Gamma_0} \frac{\partial v^-}{\partial n} u^+. \end{aligned} \quad (8.2.6)$$

The new bilinear function $B(u, v)$ is symmetric but indefinite. Denote a function,

$$\begin{aligned} T(v) &= \frac{1}{2} \iint_{S^+} \nabla v^+ \cdot \nabla v^+ - \frac{1}{2} \iint_{S^-} \nabla v^- \cdot \nabla v^- \\ &\quad - \alpha \int_{\Gamma_0} \frac{\partial v^+}{\partial n} v^- - \beta \int_{\Gamma_0} \frac{\partial v^-}{\partial n} v^+. \end{aligned} \quad (8.2.7)$$

The variational equation of the function $T(v)$

$$\frac{\partial T(v)}{\partial v} = 0 \quad (8.2.8)$$

leads exactly to (8.2.6). Eq. (8.2.7) can be expressed in the matrix form

$$T(v) = \frac{1}{2} \mathbf{x}^T \mathbf{A} \mathbf{x} - \mathbf{x}^T \mathbf{b},$$

where $\mathbf{x} = \begin{pmatrix} \mathbf{y} \\ \mathbf{z} \end{pmatrix}$, $\mathbf{y} = (a_1, \dots, a_L)^T$ and $\mathbf{z} = (b_1, \dots, b_N)^T$. The stiffness matrix is

$$\mathbf{A} = \begin{pmatrix} \mathbf{A}_{11} & \mathbf{A}_{12} \\ \mathbf{A}_{12}^T & -\mathbf{A}_{22} \end{pmatrix},$$

where \mathbf{A}_{11} and \mathbf{A}_{22} resulting from $\iint_{S^+} \nabla v^+ \cdot \nabla v^+$ and $\iint_{S^-} \nabla v^- \cdot \nabla v^-$ are symmetric and positive definite. The variational equation (8.2.8) gives the linear algebraic equations

$$\mathbf{A} \mathbf{x} = \begin{pmatrix} \mathbf{A}_{11} & \mathbf{A}_{12} \\ \mathbf{A}_{12}^T & -\mathbf{A}_{22} \end{pmatrix} \begin{pmatrix} \mathbf{y} \\ \mathbf{z} \end{pmatrix} = \mathbf{b}. \quad (8.2.9)$$

Since the matrix \mathbf{A} is symmetric and nonsingular, we may use the symmetric Gaussian elimination without pivoting, to obtain the coefficients a_i and b_i easily. Note that the solution from (8.2.9) is easier than that directly solved from (8.1.4), and that the CPU time and computer storage are also much reduced.

Let us link the hybrid techniques to the interior continuity conditions (8.1.2). Assume that $\alpha + \beta = 1$. From the Green formulas and $\Delta u^\pm = \Delta v^\pm = 0$ in S^\pm , we have

$$\begin{aligned} \iint_{S^+} \nabla u^+ \cdot \nabla v^+ &= \int_{\Gamma_0} \frac{\partial u^+}{\partial n} v^+ = \int_{\Gamma_0} \frac{\partial v^+}{\partial n} u^+, \\ \iint_{S^-} \nabla u^- \cdot \nabla v^- &= - \int_{\Gamma_0} \frac{\partial u^-}{\partial n} v^- = - \int_{\Gamma_0} \frac{\partial v^-}{\partial n} u^-. \end{aligned}$$

Hence when $\alpha + \beta = 1$,

$$\iint_{S^+} \nabla u^+ \cdot \nabla v^+ = \alpha \int_{\Gamma_0} \frac{\partial v^+}{\partial n} u^+ + \beta \int_{\Gamma_0} \frac{\partial u^+}{\partial n} v^+, \quad (8.2.10)$$

$$\iint_{S^-} \nabla u^- \cdot \nabla v^- = -\alpha \int_{\Gamma_0} \frac{\partial u^-}{\partial n} v^- - \beta \int_{\Gamma_0} \frac{\partial v^-}{\partial n} u^-. \quad (8.2.11)$$

From (8.2.10), Eq. (8.2.4) leads to

$$\alpha \int_{\Gamma_0} \frac{\partial v^+}{\partial n} (u^+ - u^-) + \beta \int_{\Gamma_0} \left(\frac{\partial u^+}{\partial n} - \frac{\partial u^-}{\partial n} \right) v^+ = 0. \quad (8.2.12)$$

Also from (8.2.11), Eq. (8.2.5) leads to

$$\beta \int_{\Gamma_0} \frac{\partial v^-}{\partial n} (u^+ - u^-) + \alpha \int_{\Gamma_0} \left(\frac{\partial u^+}{\partial n} - \frac{\partial u^-}{\partial n} \right) v^- = 0. \quad (8.2.13)$$

Since v^+ and v^- are arbitrary, Eqs. (8.2.12) and (8.2.13) imply the condition (8.1.2) with $p^+ = p^- = 1$. Combining (8.2.12) and (8.2.13) gives

$$\int_{\Gamma_0} \left(\alpha \frac{\partial v^+}{\partial n} + \beta \frac{\partial v^-}{\partial n} \right) (u^+ - u^-) + \int_{\Gamma_0} (\beta v^+ + \alpha v^-) \left(\frac{\partial u^+}{\partial n} - \frac{\partial u^-}{\partial n} \right) = 0.$$

8.3 Error Analysis for the Hybrid Trefftz Method

Denote the norm

$$\|v\|_1 = \{ \|v\|_{1,S^+}^2 + \|v\|_{1,S^-}^2 \}^{\frac{1}{2}}, \quad |v|_1 = \{ |v|_{1,S^+}^2 + |v|_{1,S^-}^2 \}^{\frac{1}{2}},$$

where $\|v\|_{1,S^+}$ and $|v|_{1,S^+}$ are the Sobolev norms and seminorms, respectively.

8.3.1 Basic Error Analysis

In this section, we assume that there is no integration errors involved. We have the following lemma.

Lemma 8.3.1 *Let α and β be bounded. Then there exists a constant C_1 independent of u and v such that*

$$|A_{Hyb}(u, v)| \leq C_1 \|u\|_1 \|v\|_1, \quad v \in V_{L,N}.$$

Proof We have from (8.1.5)

$$\begin{aligned} |A_{Hyb}(u, v)| &\leq \left| \iint_{S^+} \nabla u \cdot \nabla v \right| + \left| \iint_{S^-} \nabla u \cdot \nabla v \right| \\ &+ \left| \alpha \int_{\Gamma_0} \frac{\partial u^+}{\partial n} v^- \right| + \left| \beta \int_{\Gamma_0} \frac{\partial u^-}{\partial n} v^+ \right| + \left| \alpha \int_{\Gamma_0} \frac{\partial v^+}{\partial n} u^- \right| + \left| \beta \int_{\Gamma_0} \frac{\partial v^-}{\partial n} u^+ \right|. \end{aligned} \quad (8.3.1)$$

From the Schwarz inequality,

$$\left| \iint_{S^+} \nabla u \cdot \nabla v \right| \leq |u|_{1,S^+} |v|_{1,S^+} \leq |u|_1 |v|_1 \leq \|u\|_1 \|v\|_1.$$

Similarly,

$$\left| \iint_{S^-} \nabla u \cdot \nabla v \right| \leq \|u\|_1 \|v\|_1.$$

Next, we have

$$\left| \int_{\Gamma_0} \frac{\partial u^+}{\partial n} v^- \right| \leq \left\| \frac{\partial u^+}{\partial n} \right\|_{-\frac{1}{2}, \Gamma_0} \|v^-\|_{\frac{1}{2}, \Gamma_0}, \quad (8.3.2)$$

where the non-integer and the negative norms are defined by

$$\|v\|_{\frac{1}{2}, \Gamma_0} = \left\{ \|v\|_{0, \Gamma_0}^2 + \int_{\Gamma_0} \int_{\Gamma_0} \frac{[v(P) - v(Q)]^2}{\|P - Q\|^2} d\ell(Q) d\ell(P) \right\}^{\frac{1}{2}},$$

$$\|u\|_{-\frac{1}{2}, \Gamma_0} = \sup_v \frac{|\int_{\Gamma_0} uv d\ell|}{\|v\|_{\frac{1}{2}, \Gamma_0}}.$$

From the imbedding theorem we have

$$\|v^-\|_{\frac{1}{2}, \Gamma_0} \leq C \|v\|_{1, S^-},$$

where C is a bounded constant independent of v . Also from the trace theorem and the solutions satisfying $\Delta u^+ = 0$, we obtain from Babuska and Aziz [15],

$$\left\| \frac{\partial u^+}{\partial n} \right\|_{-\frac{1}{2}, \Gamma_0} \leq C \|u\|_{1, S^+}. \quad (8.3.3)$$

Combining (8.3.2) – (8.3.3) gives

$$\left| \int_{\Gamma_0} \frac{\partial u^+}{\partial n} v^- \right| \leq C \|u\|_{1,S^+} \|v\|_{1,S^-}. \quad (8.3.4)$$

Similarly, there are the inequalities,

$$\begin{aligned} \left| \int_{\Gamma_0} \frac{\partial u^-}{\partial n} v^+ \right| &\leq C \|u\|_{1,S^-} \|v\|_{1,S^+}, \\ \left| \int_{\Gamma_0} \frac{\partial v^+}{\partial n} u^- \right| &\leq C \|v\|_{1,S^+} \|u\|_{1,S^-}, \\ \left| \int_{\Gamma_0} \frac{\partial v^-}{\partial n} u^+ \right| &\leq C \|v\|_{1,S^-} \|u\|_{1,S^+}. \end{aligned} \quad (8.3.5)$$

From (8.3.4) – (8.3.5), Eq. (8.3.1) leads to

$$\begin{aligned} |A_{Hyb}(u, v)| &\leq 2\|u\|_1 \|v\|_1 + C_0(\|u\|_{1,S^+} + \|u\|_{1,S^-})(\|v\|_{1,S^+} + \|v\|_{1,S^-}) \\ &\leq (2 + C_0)\|u\|_1 \|v\|_1, \end{aligned}$$

where we have used the boundedness of α and β . ■

Lemma 8.3.2 *Let the constant c be excluded in $V_{L,N}$. Then there exists a constant C_0 independent of v such that*

$$C_0 \|v\|_1^2 \leq A_{Hyb}(v, v), \quad \forall v \in V_{L,N}. \quad (8.3.6)$$

Proof When $u = v$, we have

$$A_{Hyb}(v, v) = |v|_{1,S^+}^2 + |v|_{1,S^-}^2.$$

Since the constant c is not in $V_{L,N}$, the norms $|v|_{1,S^+}$ and $\|v\|_{1,S^+}$ are equivalent to each other. Hence we obtain

$$C_2 \|v\|_{1,S^+} \leq |v|_{1,S^+}, \quad C_2 \|v\|_{1,S^-} \leq |v|_{1,S^-}, \quad (8.3.7)$$

where $C_2(> 0)$ is a constant independent of v . Combining (8.3.7) and (8.3.7) gives

$$A_{Hyb}(v, v) \geq C_2^2 (\|v\|_{1,S^+}^2 + \|v\|_{1,S^-}^2) \geq C_0 \|v\|_1^2.$$

This is just the desired uniformly $V_{L,N}$ -elliptic inequality (8.3.6) if letting $C_0 = C_2^2$. ■

Next, if both

$$S^+ \cap \Gamma_D \neq \emptyset, \quad S^- \cap \Gamma_D \neq \emptyset, \quad (8.3.8)$$

we obtain from the Poincaré inequality,

$$C_1 \|v\|_{1,S^+}^2 \leq |v|_{1,S^+}^2, \quad C_1 \|v\|_{1,S^-}^2 \leq |v|_{1,S^-}^2, \quad (8.3.9)$$

where C_1 is a constant independent of v . We also obtain from (8.3.9)

$$C_1 \|v\|_1^2 \leq A_{Hyb}(v, v).$$

We have the following lemma.

Lemma 8.3.3 *Let u and $u_{L,N}$ be the true solution and the solution from the hybrid Trefftz method (8.1.4), respectively. Suppose that $\alpha + \beta = 1$. Then there exists the equality*

$$A_{Hyb}(u - u_{L,N}, v) = 0, \quad \forall v \in V_{L,N}. \quad (8.3.10)$$

Proof For the true solution u , we have $u^+ = u^- = u$ on Γ_0 . Then we have from (8.1.6)

$$I_{Hyb}^{(\alpha,\beta)}(u, v) = \alpha \int_{\Gamma_0} \frac{\partial u}{\partial n} v^- - \beta \int_{\Gamma_0} \frac{\partial u}{\partial n} v^+ - \alpha \int_{\Gamma_0} \frac{\partial v^+}{\partial n} u + \beta \int_{\Gamma_0} \frac{\partial v^-}{\partial n} u. \quad (8.3.11)$$

Since u and v^+ satisfy $\Delta u = 0$ in S^+ , we have from the Green theory

$$\int_{\Gamma_0} \frac{\partial v^+}{\partial n} u = \iint_{S^+} \nabla u \cdot \nabla v = \int_{\Gamma_0} \frac{\partial u}{\partial n} v^+. \quad (8.3.12)$$

Similarly, since u and v^- satisfy $\Delta u = 0$ in S^- , we have

$$\int_{\Gamma_0} \frac{\partial v^-}{\partial n} u = \int_{\Gamma_0} \frac{\partial u}{\partial n} v^-. \quad (8.3.13)$$

Combining (8.3.11) – (8.3.13) gives

$$I_{Hyb}^{(\alpha,\beta)}(u, v) = -(\alpha + \beta) \int_{\Gamma_0} \frac{\partial u}{\partial n} (v^+ - v^-).$$

Hence for the true solution u , we obtain

$$\begin{aligned} A_{Hyb}(u, v) &= \int_{\partial S^+} \frac{\partial u}{\partial n} v^+ - \int_{\partial S^-} \frac{\partial u}{\partial n} v^- + I_{Hyb}^{(\alpha,\beta)}(u, v) \\ &= \int_{\Gamma_0} \frac{\partial u}{\partial n} (v^+ - v^-) + I_{Hyb}^{(\alpha,\beta)}(u, v) \\ &= [1 - (\alpha + \beta)] \int_{\Gamma_0} \frac{\partial u}{\partial n} (v^+ - v^-) = 0, \end{aligned} \quad (8.3.14)$$

where we have used the assumption $\alpha + \beta = 1$. The desired result (8.3.10) follows from (8.1.4) and (8.3.14). ■

Now we give a main theorem.

Theorem 8.3.1 *Let the constant be excluded in $V_{L,N}$ and $\alpha + \beta = 1$. Then the solutions $u_{L,N}$ from the hybrid Trefftz method have the optimal error bounds,*

$$\|u - u_{L,N}\|_1 \leq C \inf_{v \in V_{L,N}} \|u - v\|_1, \quad (8.3.15)$$

where C is a constant independent of L , N , u and v .

Proof Let $w = u_{L,N} - v$, where $v \in V_{L,N}$. Then $w \in V_{L,N}$. From Lemmas 8.3.1 – 8.3.3, we obtain

$$\begin{aligned} C_0 \|w\|_1^2 &\leq A_{Hyb}(u_{L,N} - v, w) \\ &= A_{Hyb}(u - v, w) \leq C_1 \|u - v\|_1 \|w\|_1. \end{aligned}$$

Hence we have

$$\|u_{L,N} - v\|_1 \leq \frac{C_1}{C_0} \|u - v\|_1.$$

Moreover,

$$\|u - u_{L,N}\|_1 \leq \|u - v\|_1 + \|v - u_{L,N}\|_1 \leq \left(1 + \frac{C_1}{C_0}\right) \|u - v\|_1,$$

the desired result (8.3.15) follows by letting $C = (1 + \frac{C_1}{C_0})$. ■

Suppose that the solutions can be expressed by

$$u = \sum_{i=1}^{\infty} \bar{a}_i \Phi_i = \bar{u}_L + R_L \quad \text{in } S^+,$$

where \bar{a}_i are the true expansion coefficients, and

$$\bar{u}_L = \sum_{i=1}^L \bar{a}_i \Phi_i, \quad R_L = \sum_{i=L+1}^{\infty} \bar{a}_i \Phi_i.$$

Moreover, suppose that the convergence rates of (8.3.16) are exponential, i.e., there exists a constant γ_1 with $0 < \gamma_1 < 1$ such that

$$|R_L| \leq \bar{C}_1 \gamma_1^L = \bar{C}_1 \exp(-\theta_1 L), \quad (8.3.16)$$

where $\gamma_1 = \exp(-\theta_1)$ with $\theta_1 > 0$, and \bar{C}_1 is a constant independent of L . Similarly, we also suppose that

$$u = \sum_{i=1}^{\infty} \bar{b}_i \Psi_i = \bar{u}_N + R_N \quad \text{in } S^-,$$

where \bar{b}_i are the true expansion coefficients,

$$\bar{u}_N = \sum_{i=1}^N \bar{b}_i \Psi_i, \quad R_N = \sum_{i=N+1}^{\infty} \bar{b}_i \Psi_i,$$

and

$$|R_N| \leq \bar{C}_2 \gamma_2^N = \bar{C}_2 \exp(-\theta_2 N), \quad (8.3.17)$$

where $\gamma_2 = \exp(-\theta_2) < 1$ with $\theta_2 > 0$, and \bar{C}_2 is a constant independent of N . We have the following corollary from Theorem 8.3.1.

Corollary 8.3.1 *Let all the conditions in Theorem 8.3.1, and (8.3.16) – (8.3.17) hold. Then there exist the exponential convergence rates.*

$$\|u - u_{L,N}\|_1 \leq C \left\{ \sqrt{L} \exp(-\theta_1 L) + \sqrt{N} \exp(-\theta_2 N) \right\}, \quad (8.3.18)$$

where $\theta_1 > 0$ and $\theta_2 > 0$, and C is a constant independent of L and N .

Proof Let $v = \bar{u}_{L,N}$, where

$$\bar{u}_{L,N} = \begin{cases} v_L = \sum_{i=1}^L \bar{a}_i \Phi_i, & \text{in } S^+, \\ v_N = \sum_{i=1}^N \bar{b}_i \Psi_i, & \text{in } S^-, \end{cases} \quad (8.3.19)$$

where \bar{a}_i and \bar{b}_i are the true coefficients. Hence from Theorem 8.3.1

$$\begin{aligned} \|u - u_{L,N}\|_1 &\leq C \|u - \bar{u}_{L,N}\|_1 \\ &= C \{ \|u - u_L\|_{1,S^+} + \|u - u_N\|_{1,S^-} \} = C \{ \|R_L\|_{1,S^+} + \|R_N\|_{1,S^-} \}. \end{aligned} \quad (8.3.20)$$

We have

$$\|R_L\|_{1,S^+}^2 \leq C |R_L|_{1,S^+}^2 = C \int_{\Gamma_0} \frac{\partial R_L}{\partial n} R_L \leq CL \exp(-2\theta_1 L), \quad (8.3.21)$$

to give

$$\|R_L\|_{1,S^+} \leq C |R_L|_{1,S^+} \leq C \sqrt{L} \exp(-\theta_1 L). \quad (8.3.22)$$

Similarly,

$$\|R_N\|_{1,S^-} \leq C |R_N|_{1,S^-} \leq C \sqrt{N} \exp(-\theta_2 N). \quad (8.3.23)$$

Combining (8.3.20) – (8.3.23) gives the desired result (8.3.18). ■

Remark 8.3.1 *There exist some limitations for applying the hybrid TM to Laplace's equation². Note that a constant solution may be included into the piecewise particular solutions. This fact violates the condition in Lemma 8.3.2. Let S be split into S_i , i.e., $S = \cup_i S_i$ and $S_i \cap S_j = \emptyset$, $i \neq j$. First the condition (8.3.7) leads to $\partial S_i \cap \Gamma_D \neq \emptyset$, where Γ_D is given in (8.2.1). This condition excludes any interior subdomains S_i with $\partial S_i \cap \partial S = \emptyset$. Next, let us consider the simplified hybrid TMs from (8.1.4) with $\alpha = 1$ and $\beta = 0$, to seek $u_{L,N} \in V_{L,N}$ such that*

$$A_{Simp-Hyb}(u_{L,N}, v) = 0, \quad \forall v \in V_{L,N}, \quad (8.3.24)$$

where

$$\begin{aligned} A_{Simp-Hyb}(u, v) = & \iint_{S^+} \nabla u \cdot \nabla v + \iint_{S^-} \nabla u \cdot \nabla v \\ & + \int_{\Gamma_0} \frac{\partial u^+}{\partial n} v^- - \int_{\Gamma_0} \frac{\partial v^+}{\partial n} u^-. \end{aligned} \quad (8.3.25)$$

Note that a constant in u^+ and v^+ does not make any difference in (8.3.25), so the constant must be excluded from the particular solution v^+ in V_L . Moreover, if a constant is involved in the particular solutions $v^- \in V_N$, the parameter $\beta = 0$ in (8.1.5) and then $\alpha = 1$ is also required to give (8.3.24). This is just the computational model for Motz's problem in Section 8.6. Therefore, the condition in Lemma 8.3.2 may be relaxed as that a constant solution may be included into the piecewise particular solutions $v^- \in V_L$, and only the simplified hybrid TM with $\alpha = 1$ and $\beta = 0$ is valid.

8.3.2 Integration Approximation for the Hybrid Trefftz Method

In this subsection, we will follow the traditional FEM analysis, to derive the error bounds of the hybrid Trefftz solution when the integration approximation is involved. The hybrid Trefftz method involving integration approximation is expressed as: To seek the solution $\tilde{u}_{L,N} \in V_{L,N}$ such that

$$\hat{A}_{Hyb}(\tilde{u}_{L,N}, v) = 0, \quad \forall v \in V_{L,N}, \quad (8.3.26)$$

where $V_{L,N}$ is the same collection of (8.2.2) satisfying (8.2.3), and

$$\hat{A}_{Hyb}(u, v) = \widehat{\iint}_{S^+} \nabla u \cdot \nabla v + \widehat{\iint}_{S^-} \nabla u \cdot \nabla v + \hat{I}_{Hyb}^{(\alpha, \beta)}(u, v).$$

In (8.1.5), the hybrid coupling with integration approximation is

$$\hat{I}_{Hyb}^{(\alpha, \beta)}(u, v) = \alpha \widehat{\int}_{\Gamma_0} \frac{\partial u^+}{\partial n} v^- - \beta \widehat{\int}_{\Gamma_0} \frac{\partial u^-}{\partial n} v^+ - \alpha \widehat{\int}_{\Gamma_0} \frac{\partial v^+}{\partial n} u^- + \beta \widehat{\int}_{\Gamma_0} \frac{\partial v^-}{\partial n} u^+.$$

²The hybrid TM can be applied similarly to the Debye-Huckel equation, $-\Delta u + u = 0$. The limitations described here are removed.

The notations $\widehat{\iint}_{S^+}$ and $\widehat{\int}_{\Gamma_0}$ denote the approximations of \iint_{S^+} and \int_{Γ_0} by some quadrature rules. Since

$$\begin{aligned}\iint_{S^+} \nabla u \cdot \nabla v &= \int_{\Gamma_0} \frac{\partial u^+}{\partial n} v^+, \\ \iint_{S^-} \nabla u \cdot \nabla v &= \int_{\Gamma_0} \frac{\partial u^-}{\partial n} v^-, \end{aligned}$$

the integration approximation of $\widehat{\iint}_{S^\pm}$ can be carried out as that of $\widehat{\int}_{\Gamma_0}$,

$$\begin{aligned}\widehat{\iint}_{S^+} \nabla u \cdot \nabla v &= \widehat{\int}_{\Gamma_0} \frac{\partial u^+}{\partial n} v^+, \\ \widehat{\iint}_{S^-} \nabla u \cdot \nabla v &= \widehat{\int}_{\Gamma_0} \frac{\partial u^-}{\partial n} v^-. \end{aligned}$$

Suppose the following inequalities hold,

$$\hat{A}_{Hyb}(u, v) \leq C_1 \|u\|_1 \|v\|_1, \quad v \in V_{L,N}, \quad (8.3.27)$$

$$C_0 \|v\|_1^2 \leq \hat{A}_{Hyb}(v, v), \quad \forall v \in V_{L,N}, \quad (8.3.28)$$

where C_0 and C_1 are two positive constants independent of L and N . We have the following theorem.

Theorem 8.3.2 *Let (8.3.27) and (8.3.28) hold. Suppose that $\alpha + \beta = 1$. Then the solutions $\tilde{u}_{L,N}$ from the hybrid Trefftz method involving integration approximation have the following error bounds,*

$$\begin{aligned} \|u - \tilde{u}_{L,N}\|_1 &\leq C \left\{ \inf_{v \in V_{L,N}} \|u - v\|_1 \right. \\ &+ \sup_{w \in V_{L,N}} \frac{1}{\|w\|_1} \left[\left| \left(\int_{\Gamma_0} - \widehat{\int}_{\Gamma_0} \right) \frac{\partial u}{\partial n} w^+ \right| + \left| \left(\int_{\Gamma_0} - \widehat{\int}_{\Gamma_0} \right) \frac{\partial u}{\partial n} w^- \right| \right. \\ &\left. \left. + \left| \left(\int_{\Gamma_0} - \widehat{\int}_{\Gamma_0} \right) \frac{\partial w^+}{\partial n} u \right| + \left| \left(\int_{\Gamma_0} - \widehat{\int}_{\Gamma_0} \right) \frac{\partial w^-}{\partial n} u \right| \right] \right\}. \end{aligned} \quad (8.3.29)$$

Proof Since $\alpha + \beta = 1$ we have from (8.3.14)

$$A_{Hyb}(u, v) = 0, \quad \forall v \in V_{L,N}.$$

Then

$$\hat{A}_{Hyb}(u, v) = A_{Hyb}(u, v) + (\hat{A}_{Hyb} - A_{Hyb})(u, v) = (\hat{A}_{Hyb} - A_{Hyb})(u, v). \quad (8.3.30)$$

From (8.3.26) and (8.3.30)

$$\hat{A}_{Hyb}(u - \tilde{u}_{L,N}, v) = (\hat{A}_{Hyb} - A_{Hyb})(u, v). \quad (8.3.31)$$

Let $w = \tilde{u}_{L,N} - v$, where $v \in V_{L,N}$. Then $w \in V_{L,N}$. We obtain from (8.3.27), (8.3.28) and (8.3.31)

$$\begin{aligned} C_0 \|w\|_1^2 &\leq \hat{A}_{Hyb}(\tilde{u}_{L,N} - v, w) \\ &= \hat{A}_{Hyb}(u - v, w) - (\hat{A}_{Hyb} - A_{Hyb})(u, w) \\ &\leq C_1 \|u - v\|_1 \|w\|_1 + |(\hat{A}_{Hyb} - A_{Hyb})(u, w)|. \end{aligned}$$

Hence we have

$$\|\tilde{u}_{L,N} - v\|_1 \leq \frac{C_1}{C_0} \|u - v\|_1 + \frac{1}{C_0 \|w\|_1} |(\hat{A}_{Hyb} - A_{Hyb})(u, w)|.$$

Moreover, there exists the bound

$$\begin{aligned} \|u - \tilde{u}_{L,N}\|_1 &\leq \|u - v\|_1 + \|v - \tilde{u}_{L,N}\|_1 \\ &\leq \left(1 + \frac{C_1}{C_0}\right) \|u - v\|_1 + \frac{1}{C_0 \|w\|_1} |(\hat{A}_{Hyb} - A_{Hyb})(u, w)|, \end{aligned} \quad (8.3.32)$$

where

$$\begin{aligned} |(\hat{A}_{Hyb} - A_{Hyb})(u, w)| &\leq \left| \left(\int_{\Gamma_0} - \widehat{\int}_{\Gamma_0} \right) \frac{\partial u}{\partial n} w^+ \right| + \left| \left(\int_{\Gamma_0} - \widehat{\int}_{\Gamma_0} \right) \frac{\partial u}{\partial n} w^- \right| \\ &+ \left| \left(\int_{\Gamma_0} - \widehat{\int}_{\Gamma_0} \right) \frac{\partial w^+}{\partial n} u \right| + \left| \left(\int_{\Gamma_0} - \widehat{\int}_{\Gamma_0} \right) \frac{\partial w^-}{\partial n} u \right|. \end{aligned} \quad (8.3.33)$$

Then the desired result (8.3.29) follows from (8.3.32) and (8.3.33). ■

Suppose that $v^+ \in V_{L,N}$ satisfies the following inequalities

$$|v^+|_{k,\Gamma_0} \leq C_1 L^{\sigma k} |v^+|_{0,\Gamma_0}, \quad (8.3.34)$$

$$\left| \frac{\partial v^+}{\partial n} \right|_{k,\Gamma_0} \leq C_1 L^{\sigma(k+1)} |v^+|_{0,\Gamma_0}, \quad (8.3.35)$$

where $\sigma \geq 1$ and C_1 are two constants independent of L and v^+ . Also suppose that $v^- \in V_{L,N}$ satisfies the following inequalities

$$\begin{aligned} |v^-|_{k,\Gamma_0} &\leq C_2 N^{\tau k} |v^-|_{0,\Gamma_0}, \\ \left| \frac{\partial v^-}{\partial n} \right|_{k,\Gamma_0} &\leq C_2 N^{\tau(k+1)} |v^-|_{0,\Gamma_0}, \end{aligned} \quad (8.3.36)$$

where $\tau \geq 1$ and C_2 are two constants independent of N and v^- . We have the following lemma.

Lemma 8.3.4 *Let v^+ satisfy (8.3.34) and (8.3.35). For the quadrature rules with the accuracy of order k , there exist the error bounds,*

$$\left| \left(\int_{\Gamma_0} - \widehat{\int}_{\Gamma_0} \right) \frac{\partial u}{\partial n} w^+ \right| \leq CL^{\sigma(k+1)} h^{k+1} \left| \frac{\partial u}{\partial n} \right|_{k+1, \Gamma_0} \|w^+\|_{1, S^+}, \quad w^+ \in V_{L, N}, \quad (8.3.37)$$

$$\left| \left(\int_{\Gamma_0} - \widehat{\int}_{\Gamma_0} \right) \frac{\partial w^+}{\partial n} u \right| \leq CL^{\sigma(k+2)} h^{k+1} |u|_{k+1, \Gamma_0} \|w^+\|_{1, S^+}, \quad w^+ \in V_{L, N}, \quad (8.3.38)$$

where h is the maximal length of consecutive integration nodes.

Proof We only prove (8.3.37), since the proof for (8.3.38) is similar. For the quadrature of k order, we have

$$\begin{aligned} \left| \left(\int_{\Gamma_0} - \widehat{\int}_{\Gamma_0} \right) \frac{\partial u}{\partial n} w^+ \right| &\leq Ch^{k+1} \left| \frac{\partial u}{\partial n} w^+ \right|_{k+1, \Gamma_0} \\ &\leq Ch^{k+1} \left| \frac{\partial u}{\partial n} \right|_{k+1, \Gamma_0} |w^+|_{k+1, \Gamma_0}, \quad w^+ \in V_{L, N}, \end{aligned} \quad (8.3.39)$$

where C is a constant independent of L and w . Next, since

$$|w^+|_{0, \Gamma_0} \leq C \|w^+\|_{1, S^+},$$

we have from (8.3.34)

$$|w^+|_{k+1, \Gamma_0} \leq C_1 L^{\sigma(k+1)} |w^+|_{0, \Gamma_0} \leq CL^{\sigma(k+1)} \|w^+\|_{1, S^+}. \quad (8.3.40)$$

Combining (8.3.39) and (8.3.40) gives the desired result (8.3.37). ■

We have the following corollary from Corollary 8.3.1, Theorem 8.3.2 and Lemma 8.3.4.

Corollary 8.3.2 *Assume (8.3.16), (8.3.17), (8.3.36) and all the conditions in Theorem 8.3.2 and Lemma 8.3.4 hold. Then there exist the error bounds,*

$$\begin{aligned} \|u - \tilde{u}_{L, N}\|_1 &\leq C \left\{ \sqrt{L} \exp(-\theta_1 L) + \sqrt{N} \exp(-\theta_2 N) \right. \\ &\quad \left. + (L^{\sigma(k+2)} + N^{\tau(k+2)}) h^{k+1} \left(\left| \frac{\partial u}{\partial n} \right|_{k+1, \Gamma_0} + |u|_{k+1, \Gamma_0} \right) \right\}, \end{aligned}$$

where C is a constant independent of L , N and h .

Below let us examine (8.3.27) and (8.3.28). Denote

$$\begin{aligned} \overline{|v|}_1 &= \left\{ \widehat{\iint}_{S^+} |\nabla v|^2 + \widehat{\iint}_{S^-} |\nabla v|^2 \right\}^{\frac{1}{2}}, \\ \overline{\|v\|}_1 &= \left\{ \overline{|v|}_1^2 + \|v\|_{0, S}^2 \right\}^{\frac{1}{2}}. \end{aligned}$$

Suppose that there exists the norm equivalence

$$|v|_1 \asymp \overline{|v|}_1, \quad \forall v \in V_{L,N},$$

i.e., there exist two positive constants C_0 and C_1 such that

$$C_0|v|_1 \leq \overline{|v|}_1 \leq C_1|v|_1, \quad \forall v \in V_{L,N}. \quad (8.3.41)$$

Then we have the following lemma.

Lemma 8.3.5 *If $\overline{|v|}_1 \asymp |v|_1$, then $\|\overline{v}\|_1 \asymp \|v\|_1$.*

Proof From (8.3.41), we have

$$C_0^2|v|_1^2 + \|v\|_{0,S}^2 \leq \|\overline{v}\|_1^2 = \overline{|v|}_1^2 + \|v\|_{0,S}^2 \leq C_1^2|v|_1^2 + \|v\|_{0,S}^2, \quad v \in V_{L,N}.$$

Then

$$\min\{1, C_0^2\}\|v\|_1^2 \leq \|\overline{v}\|_1^2 \leq \max\{1, C_1^2\}\|v\|_1^2, \quad v \in V_{L,N}.$$

This displays $\|\overline{v}\|_1 \asymp \|v\|_1$. ■

Lemma 8.3.6 *Let all the conditions in Lemma 8.3.2 and (8.3.34) – (8.3.36) hold. Suppose that the maximal length h in the quadrature rule of order k is chosen so small that³*

$$h^{k+1}L^{\sigma(k+2)} = o(1), \quad h^{k+1}N^{\tau(k+2)} = o(1). \quad (8.3.42)$$

Then the uniformly $V_{L,N}$ - elliptic inequality (8.3.28) holds.

Proof We have

$$\widehat{A}_{Hyb}(v, v) = \widehat{\iint}_{S^+} |\nabla v|^2 + \widehat{\iint}_{S^-} |\nabla v|^2 = \widehat{\int}_{\Gamma_0} \frac{\partial v^+}{\partial n} v^+ + \widehat{\int}_{\Gamma_0} \frac{\partial v^-}{\partial n} v^-. \quad (8.3.43)$$

For the quadrature rule of order k , we have

$$\left| \left(\widehat{\int}_{\Gamma_0} - \int_{\Gamma_0} \right) \frac{\partial v^+}{\partial n} v^+ \right| \leq Ch^{k+1} \left| \frac{\partial v^+}{\partial n} v^+ \right|_{k+1, \Gamma_0}. \quad (8.3.44)$$

From (8.3.34) – (8.3.35) we have

$$\begin{aligned} \left| \frac{\partial v^+}{\partial n} v^+ \right|_{k+1, \Gamma_0} &\leq C \sum_{i=0}^{k+1} \left| \frac{\partial v^+}{\partial n} \right|_{k+1-i, \Gamma_0} |v^+|_{i, \Gamma_0} \\ &\leq C \sum_{i=0}^{k+1} L^{\sigma(k+2-i)} \times L^{\sigma i} \|v^+\|_{0, \Gamma_0}^2 \leq CL^{\sigma(k+2)} \|v^+\|_{0, \Gamma_0}^2 \leq CL^{\sigma(k+2)} \|v\|_{1, S^+}^2, \end{aligned} \quad (8.3.45)$$

³Eq. (8.3.42) implies that $h = \min\{o(L^{-\sigma(1+\frac{1}{k+1})}), o(N^{-\tau(1+\frac{1}{k+1})})\}$.

where C is a constant independent of L and v . Combining (8.3.44) and (8.3.45) gives

$$\left| \left(\int_{\Gamma_0} - \widehat{\int}_{\Gamma_0} \right) \frac{\partial v^+}{\partial n} v^+ \right| \leq Ch^{k+1} L^{\sigma(k+2)} \|v\|_{1,S^+}^2, \quad \forall v \in V_{L,N}.$$

Similarly, we have

$$\left| \left(\int_{\Gamma_0} - \widehat{\int}_{\Gamma_0} \right) \frac{\partial v^-}{\partial n} v^- \right| \leq Ch^{k+1} N^{\tau(k+2)} \|v\|_{1,S^-}^2, \quad \forall v \in V_{L,N}.$$

Hence we have from (8.3.43)

$$\begin{aligned} \hat{A}_{Hyb}(v, v) &= \iint_{S^+} |\nabla v|^2 + \iint_{S^-} |\nabla v|^2 \\ &= \iint_{S^+} |\nabla v|^2 + \iint_{S^-} |\nabla v|^2 + \left(\int_{\Gamma_0} - \widehat{\int}_{\Gamma_0} \right) \frac{\partial v^+}{\partial n} v^+ + \left(\int_{\Gamma_0} - \widehat{\int}_{\Gamma_0} \right) \frac{\partial v^-}{\partial n} v^-. \end{aligned} \quad (8.3.46)$$

From Lemma 8.3.2, the uniformly $V_{L,N}$ - inequality holds,

$$\bar{C}_0 \|v\|_1^2 \leq A_{Hyb}(v, v), \quad \forall v \in V_{L,N}, \quad (8.3.47)$$

where \bar{C}_0 is a positive constant independent of L, N and h . Hence we obtain from (8.3.46) and (8.3.47)

$$\begin{aligned} \hat{A}_{Hyb}(v, v) &\geq \bar{C}_0 \|v\|_1^2 - \left| \left(\int_{\Gamma_0} - \widehat{\int}_{\Gamma_0} \right) \frac{\partial v^+}{\partial n} v^+ \right| - \left| \left(\int_{\Gamma_0} - \widehat{\int}_{\Gamma_0} \right) \frac{\partial v^-}{\partial n} v^- \right| \\ &\geq \left\{ \bar{C}_0 - Ch^{k+1} (L^{\sigma(k+2)} + N^{\tau(k+2)}) \right\} \|v\|_1^2. \end{aligned}$$

When the conditions (8.3.42) hold, we have

$$\hat{A}_{Hyb}(v, v) \geq \{\bar{C}_0 - o(1)\} \|v\|_1^2 \geq \frac{\bar{C}_0}{2} \|v\|_1^2.$$

This is the desired result (8.3.28) by letting $C_0 = \frac{\bar{C}_0}{2}$. ■

8.4 The Penalty plus Hybrid Techniques

In this section, we pursue the penalty plus hybrid techniques,

$$\begin{aligned} I_{H-P}^{(\alpha, \beta, P_c)}(u, v) &= - \int_{\Gamma_0} \left(\alpha \frac{\partial u^+}{\partial n} + \beta \frac{\partial u^-}{\partial n} \right) (v^+ - v^-) \\ &\quad - \int_{\Gamma_0} \left(\alpha \frac{\partial v^+}{\partial n} + \beta \frac{\partial v^-}{\partial n} \right) (u^+ - u^-) + P_c (L^\sigma + N^\tau) \int_{\Gamma_0} (u^+ - u^-) (v^+ - v^-), \end{aligned} \quad (8.4.1)$$

where $\alpha + \beta = 1$, P_c is a large enough constant that is independent of L, N , and $\sigma \geq 1$ and $\tau \geq 1$ are two constants given in (8.3.34) – (8.3.36).

Denote by $V_{L,N}$ the finite dimensional collection of v in (8.2.2). The penalty plus hybrid techniques is expressed by: To seek $u_{L,N}^* \in V_{L,N}$ such that

$$B_{H-P}(u_{L,N}^*, v) = 0, \quad \forall v \in V_{L,N}, \quad (8.4.2)$$

where

$$B_{H-P}(u, v) = \iint_{S^+} \nabla u \cdot \nabla v + \iint_{S^-} \nabla u \cdot \nabla v + I_{H-P}^{(\alpha, \beta, P_c)}(u, v).$$

Denote the norms

$$\|v\|_p = \left\{ \|v\|_{1,S^+}^2 + \|v\|_{1,S^-}^2 + P_c(L^\sigma + N^\tau) \|v^+ - v^-\|_{0,\Gamma_0}^2 \right\}^{\frac{1}{2}}.$$

Suppose that the following inequalities hold,

$$B_{H-P}(u, v) \leq C_1 \|u\|_p \|v\|_p, \quad \forall v \in V_{L,N}, \quad (8.4.3)$$

$$C_0 \|v\|_p^2 \leq B_{H-P}(v, v), \quad \forall v \in V_{L,N}, \quad (8.4.4)$$

where C_0 and C_1 are two positive constants independent of L and N . We have the following theorem.

Theorem 8.4.1 *Let (8.4.3) and (8.4.4) hold. Suppose that $\alpha + \beta = 1$. Then the solutions $u_{L,N}^*$ from the penalty plus hybrid Trefftz method have the following error bound,*

$$\|u - u_{L,N}^*\|_p \leq C \inf_{v \in V_{L,N}} \|u - v\|_p, \quad (8.4.5)$$

where C is a constant independent of L and N .

Proof For the true solution u , we have

$$B_{H-P}(u, v) = \left\{ 1 - (\alpha + \beta) \right\} \int_{\Gamma_0} \frac{\partial u^+}{\partial n} (v^+ - v^-) = 0. \quad (8.4.6)$$

Then from (8.4.2) and (8.4.6)

$$B_{H-P}(u - u_{L,N}^*, v) = 0, \quad \forall v \in V_{L,N}. \quad (8.4.7)$$

Let $w = u_{L,N}^* - v$, where $v \in V_{L,N}$. Then $w \in V_{L,N}$. From (8.4.3), (8.4.4) and (8.4.7)

$$\begin{aligned} C_0 \|w\|_p^2 &\leq B_{H-P}(u_{L,N}^* - v, w) \\ &= B_{H-P}(u - v, w) \leq C_1 \|u - v\|_p \|w\|_p. \end{aligned}$$

This gives

$$\|u_{L,N}^* - v\|_p \leq \frac{C_1}{C_0} \|u - v\|_p.$$

Moreover, since

$$\|u - u_{L,N}^*\|_p \leq \|u - v\|_p + \|v - u_{L,N}^*\|_p \leq \left(1 + \frac{C_1}{C_0} \right) \|u - v\|_p,$$

the desired result (8.4.5) follows by letting $C = (1 + \frac{C_1}{C_0})$. ■

We have the following corollary from Theorem 8.4.1.

Corollary 8.4.1 *Let all the conditions in Theorem 8.4.1, and (8.3.16) – (8.3.17) hold. Then there exist the exponential convergence rates,*

$$\begin{aligned} \|u - u_{L,N}^*\|_p &\leq C \left\{ \sqrt{L} \exp(-\theta_1 L) + \sqrt{N} \exp(-\theta_2 N) \right. \\ &\quad \left. + \sqrt{P_c} (L^{\frac{\sigma}{2}} + N^{\frac{\tau}{2}}) [\exp(-\theta_1 L) + \exp(-\theta_2 N)] \right\}, \end{aligned} \quad (8.4.8)$$

where $\theta_1 > 0$ and $\theta_2 > 0$, and C is a constant independent of L and N .

Proof Let $v = \bar{u}_{L,N}$, where $\bar{u}_{L,N}$ is given by (8.3.19). Then we have from Theorem 8.4.1

$$\begin{aligned} \|u - u_{L,N}^*\|_p &\leq C \|u - \bar{u}_{L,N}\|_p \\ &\leq C \{ \|u - \bar{u}_L\|_{1,S^+} + \|u - \bar{u}_N\|_{1,S^-} + \sqrt{P_c} (L^{\frac{\sigma}{2}} + N^{\frac{\tau}{2}}) \|\bar{u}_L - \bar{u}_N\|_{0,\Gamma_0} \} \\ &= C \{ \|R_L\|_{1,S^+} + \|R_N\|_{1,S^-} + \sqrt{P_c} (L^{\frac{\sigma}{2}} + N^{\frac{\tau}{2}}) (\|R_L\|_{0,\Gamma_0} + \|R_N\|_{0,\Gamma_0}) \} \\ &\leq C \left\{ \sqrt{L} \exp(-\theta_1 L) + \sqrt{N} \exp(-\theta_2 N) + \sqrt{P_c} (L^{\frac{\sigma}{2}} + N^{\frac{\tau}{2}}) [\exp(-\theta_1 L) + \exp(-\theta_2 N)] \right\}. \end{aligned} \quad (8.4.9)$$

This is the desired results (8.4.8). ■

Below, let us study (8.4.4), and give the following lemma.

Lemma 8.4.1 *Let the following bounds for $v \in V_{L,N}$ be given*

$$\left| \frac{\partial v^+}{\partial n} \right|_{0,\Gamma_0} \leq CL^{\frac{\sigma}{2}} \|v\|_{1,S^+}, \quad (8.4.10)$$

$$\left| \frac{\partial v^-}{\partial n} \right|_{0,\Gamma_0} \leq CN^{\frac{\tau}{2}} \|v\|_{1,S^-}, \quad (8.4.11)$$

where $\sigma \geq 1$ and $\tau \geq 1$ are two constants independent of L and N . Suppose that $\alpha, \beta \leq 1$. When P_c is chosen large enough but independent of L and N , then the uniformly $V_{L,N}$ -inequality (8.4.4) holds.

Proof We have

$$\begin{aligned} B_{H-P}(v, v) &= \iint_{S^+} |\nabla v|^2 + \iint_{S^-} |\nabla v|^2 \\ &\quad - 2 \int_{\Gamma_0} \left(\alpha \frac{\partial v^+}{\partial n} + \beta \frac{\partial v^-}{\partial n} \right) (v^+ - v^-) + P_c (L^\sigma + N^\tau) \int_{\Gamma_0} (v^+ - v^-)^2. \end{aligned} \quad (8.4.12)$$

There exists a positive constant C_0 independent of L and N such that

$$C_0^2 (\|v\|_{1,S^+}^2 + \|v\|_{1,S^-}^2) \leq |v|_{1,S^+}^2 + |v|_{1,S^-}^2.$$

Moreover, from (8.4.10) we have

$$\begin{aligned} \left| \int_{\Gamma_0} \frac{\partial v^+}{\partial n} (v^+ - v^-) \right| &\leq C \left\| \frac{\partial v^+}{\partial n} \right\|_{0,\Gamma_0} \|v^+ - v^-\|_{0,\Gamma_0} \\ &\leq CL^{\frac{\sigma}{2}} \|v^+\|_{1,S^+} \|v^+ - v^-\|_{0,\Gamma_0}. \end{aligned}$$

From $2xy \leq x^2 + y^2$ we obtain

$$\left| \int_{\Gamma_0} \frac{\partial v^+}{\partial n} (v^+ - v^-) \right| \leq \frac{C_0^2}{2} \|v\|_{1,S^+}^2 + \frac{C^2 L^\sigma}{2C_0^2} \|v^+ - v^-\|_{0,\Gamma_0}^2.$$

Similarly, from (8.4.11) we have

$$\left| \int_{\Gamma_0} \frac{\partial v^-}{\partial n} (v^+ - v^-) \right| \leq \frac{C_0^2}{2} \|v\|_{1,S^-}^2 + \frac{C^2 N^\tau}{2C_0^2} \|v^+ - v^-\|_{0,\Gamma_0}^2. \quad (8.4.13)$$

Hence we obtain from (8.4.12) – (8.4.13) and $0 \leq \alpha, \beta \leq 1$

$$\begin{aligned} B_{H-P}(v, v) &\geq C_0^2 (\|v\|_{1,S^+}^2 + \|v\|_{1,S^-}^2) \\ &\quad + P_c (L^\sigma + N^\tau) \|v^+ - v^-\|_{0,\Gamma_0}^2 - 2 \left| \int_{\Gamma_0} \left(\alpha \frac{\partial v^+}{\partial n} + \beta \frac{\partial v^-}{\partial n} \right) (v^+ - v^-) \right| \\ &\geq \frac{C_0^2}{2} (\|v\|_{1,S^+}^2 + \|v\|_{1,S^-}^2) + \left(P_c - \frac{C^2}{2C_0^2} \right) (L^\sigma + N^\tau) \|v^+ - v^-\|_{0,\Gamma_0}^2. \end{aligned}$$

If we choose P_c to be large enough such that

$$P_c - \frac{C^2}{2C_0^2} \geq \frac{P_c}{2},$$

i.e., $P_c \geq \frac{C^2}{C_0^2}$. Then we obtain

$$B_{H-P}(v, v) \geq \frac{C_0^2}{2} (\|v\|_{1,S^+}^2 + \|v\|_{1,S^-}^2) + \frac{P_c}{2} (L^\sigma + N^\tau) \|v^+ - v^-\|_{0,\Gamma_0}^2 \geq \bar{C}_0 \|v\|_p^2,$$

where $\bar{C}_0 = \min\{\frac{C_0^2}{2}, \frac{1}{2}\}$. ■

Next, consider the integration approximation. The penalty plus hybrid techniques involving integration approximation is expressed by: To seek $\tilde{u}_{L,N}^* \in V_{L,N}$ such that

$$\hat{B}_{H-P}(u_{L,N}^*, v) = 0, \quad \forall v \in V_{L,N}, \quad (8.4.14)$$

where

$$\hat{B}_{H-P}(u, v) = \widehat{\iint}_{S^+} \nabla u \cdot \nabla v + \widehat{\iint}_{S^-} \nabla u \cdot \nabla v + \hat{I}_{H-P}^{(\alpha, \beta, P_c)}(u, v)$$

where

$$\begin{aligned} \hat{I}_{H-P}^{(\alpha, \beta, P_c)}(u, v) &= - \widehat{\int}_{\Gamma_0} \left(\alpha \frac{\partial u^+}{\partial n} + \beta \frac{\partial u^-}{\partial n} \right) (v^+ - v^-) \\ &\quad - \widehat{\int}_{\Gamma_0} \left(\alpha \frac{\partial v^+}{\partial n} + \beta \frac{\partial v^-}{\partial n} \right) (u^+ - u^-) + P_c (L^\sigma + N^\tau) \widehat{\int}_{\Gamma_0} (u^+ - u^-) (v^+ - v^-), \end{aligned}$$

where $\widehat{\int}_{\Gamma_0}$ is the approximation of \int_{Γ_0} by some rules.

In computation, define the energy

$$\begin{aligned} T_{H-P}^{(\alpha,\beta,P_c)}(v,v) &= \frac{1}{2} \widehat{\int}_{\Gamma_0} \frac{\partial v^+}{\partial n} v^+ + \frac{1}{2} \widehat{\int}_{\Gamma_0} \frac{\partial v^-}{\partial n} v^- \\ &\quad - \widehat{\int}_{\Gamma_0} \left(\alpha \frac{\partial v^+}{\partial n} + \beta \frac{\partial v^-}{\partial n} \right) (v^+ - v^-) + \frac{P_c}{2} (L^\sigma + N^\tau) \widehat{\int}_{\Gamma_0} (v^+ - v^-)^2. \end{aligned}$$

The minimum of $T_{H-P}^{(\alpha,\beta,P_c)}(v,v)$, i.e.,

$$\frac{\partial T_{H-P}^{(\alpha,\beta,P_c)}(v,v)}{\partial v} = 0,$$

yields (8.4.14), which can be expressed in the matrix and vectors

$$\mathbf{Ax} = \mathbf{b},$$

where $\mathbf{x} = \{a_1, \dots, a_L, b_1, \dots, b_N\}^T$, \mathbf{b} is a known vector, and the matrix \mathbf{A} is positive definite and symmetric.

Suppose that the following inequalities hold,

$$\hat{B}_{H-P}(u,v) \leq C_1 \|u\|_p \|v\|_p, \quad \forall v \in V_{L,N}, \quad (8.4.15)$$

$$C_0 \|v\|_p^2 \leq \hat{B}_{H-P}(v,v), \quad \forall v \in V_{L,N}, \quad (8.4.16)$$

where C_0 and C_1 are two positive constants independent of L and N . We have the following theorem.

Theorem 8.4.2 *Let (8.4.15) and (8.4.16) hold. Suppose that $\alpha + \beta = 1$. Then the solutions $\tilde{u}_{L,N}^*$ from the penalty plus hybrid Trefftz method involving integration approximation have the following error bound,*

$$\begin{aligned} \|u - \tilde{u}_{L,N}^*\|_p &\leq C \left\{ \inf_{v \in V_{L,N}} \|u - v\|_p \right. \\ &\quad + \sup_{w \in V_{L,N}} \frac{1}{\|w\|_p} \left[\left| \left(\int_{\Gamma_0} - \widehat{\int}_{\Gamma_0} \right) \frac{\partial u}{\partial n} w^+ \right| + \left| \left(\int_{\Gamma_0} - \widehat{\int}_{\Gamma_0} \right) \frac{\partial u}{\partial n} w^- \right| \right. \\ &\quad \left. \left. + \left| \left(\int_{\Gamma_0} - \widehat{\int}_{\Gamma_0} \right) \frac{\partial u}{\partial n} (w^+ - w^-) \right| \right] \right\}. \end{aligned}$$

Proof For the true solution u , we have

$$\begin{aligned} \hat{B}_{H-P}(u,v) &= \left(\widehat{\iint}_{S^+} - \iint_{S^+} \right) \nabla u \cdot \nabla v + \left(\widehat{\iint}_{S^-} - \iint_{S^-} \right) \nabla u \cdot \nabla v \\ &\quad - \left(\widehat{\int}_{\Gamma_0} - \int_{\Gamma_0} \right) \frac{\partial u}{\partial n} (v^+ - v^-). \end{aligned}$$

Hence we have

$$\begin{aligned} \hat{B}_{H-P}(u - \tilde{u}_{L,N}^*, v) &= \left(\widehat{\iint}_{S^+} - \iint_{S^+} \right) \nabla u \cdot \nabla v + \left(\widehat{\iint}_{S^-} - \iint_{S^-} \right) \nabla u \cdot \nabla v \\ &\quad - \left(\widehat{\int}_{\Gamma_0} - \int_{\Gamma_0} \right) \frac{\partial u}{\partial n} (v^+ - v^-). \end{aligned}$$

The rest of proof is similar to that in Theorem 8.3.2. ■

To close this section, we explore the relation between the hybrid techniques in Section 8.3 and the penalty plus hybrid techniques in this section. We have the following lemma.

Lemma 8.4.2 *Let $\alpha = 1$ and $\beta = 0$. The simplified hybrid method in Section 8.3 is equivalent to the special case of $P_c = 0$ in (8.4.1).*

Proof For $\alpha = 1$ and $\beta = 0$, the simplified hybrid method in Section 8.3 is

$$A_{Simp-Hyb}(u_{L,N}, v) = 0, \quad \forall v \in V_{L,N}, \quad (8.4.17)$$

where

$$A_{Simp-Hyb}(u, v) = \iint_{S^+} \nabla u \cdot \nabla v + \iint_{S^-} \nabla u \cdot \nabla v + \int_{\Gamma_0} \frac{\partial u^+}{\partial n} v^- - \int_{\Gamma_0} \frac{\partial v^+}{\partial n} u^-.$$

On the other hand, when $P_c = 0$, $\alpha = 1$ and $\beta = 0$, Eq. (8.1.7) leads to

$$B_{H-P}(u_{L,N}^*, v) = 0, \quad \forall v \in V_{L,N}, \quad (8.4.18)$$

where

$$\begin{aligned} B_{H-P}(u, v) &= \iint_{S^+} \nabla u \cdot \nabla v + \iint_{S^-} \nabla u \cdot \nabla v \\ &\quad - \int_{\Gamma_0} \frac{\partial u^+}{\partial n} (v^+ - v^-) - \int_{\Gamma_0} \frac{\partial v^+}{\partial n} (u^+ - u^-). \end{aligned}$$

Since v^+ and v^- are independent to each other, we have from (8.4.17)

$$\iint_{S^+} \nabla u_L^+ \cdot \nabla v^+ - \int_{\Gamma_0} \frac{\partial v^+}{\partial n} u_N^- = 0, \quad (8.4.19)$$

$$\iint_{S^-} \nabla u_N^- \cdot \nabla v^- + \int_{\Gamma_0} \frac{\partial u_L^+}{\partial n} v^- = 0. \quad (8.4.20)$$

Note that the solution u_L^+ and v^+ satisfy the Laplace equation, and there exist the equalities

$$\iint_{S^+} \nabla u_L^+ \cdot \nabla v^+ = \int_{\Gamma_0} \frac{\partial u_L^+}{\partial n} v^+ = \int_{\Gamma_0} \frac{\partial v^+}{\partial n} u_L^+. \quad (8.4.21)$$

We obtain from (8.4.18) and (8.4.21)

$$\iint_{S^-} \nabla u \cdot \nabla v + \int_{\Gamma_0} \frac{\partial u_L^+}{\partial n} v^- - \left(\int_{\Gamma_0} \frac{\partial u_L^+}{\partial n} v^+ - \int_{\Gamma_0} \frac{\partial v^+}{\partial n} u_N^- \right) = 0. \quad (8.4.22)$$

Also since v^+ and v^- are independent to each other, we have from (8.4.22)

$$\int_{\Gamma_0} \frac{\partial u_L^+}{\partial n} v^+ - \int_{\Gamma_0} \frac{\partial v^+}{\partial n} u_N^- = 0, \quad (8.4.23)$$

$$\iint_{S^-} \nabla u_N^- \cdot \nabla v^- + \int_{\Gamma_0} \frac{\partial u_L^+}{\partial n} v^- = 0. \quad (8.4.24)$$

Eq. (8.4.23) is just (8.4.19) by noting (8.4.21), and Eq. (8.4.24) is exactly (8.4.20). This proves the equivalence of the two methods, (8.4.17) and (8.4.18). ■

Similarly, the equivalence for the two methods for $\beta = 1$ and $\alpha = 0$ can be shown. The two cases can be rewritten as $\alpha\beta = 0$. Note that Lemma 8.4.2 is also valid for the combinations of the Trefftz method in S^+ and the other methods such as FEM, FDM, FVM, etc. in S^- ,

$$v = \begin{cases} v^+ & \text{in } S^+, \\ v_k^- & \text{in } S^-, \end{cases}$$

where v_k^- are the piecewise k -order polynomials, because the key equalities (8.4.21) of particular solutions hold true for the Trefftz method in S^+ . It is worth noting that when $\alpha = \beta = \frac{1}{2}$, the hybrid Trefftz method is not equivalent to the special case of the penalty plus hybrid method with $P_c = 0$ and $\alpha = \beta = \frac{1}{2}$.

Remark 8.4.1 For the collocation TM and the penalty plus hybrid TM, there are no such limitations as in Remark 8.3.1, because the following lemma from Lemma 1.1.1 in Chapter 1.

Lemma 8.4.3 For the Laplace equation (8.2.1) with the mixed type of boundary conditions, let S be split by Γ_0 into S^+ and S^- . Suppose that $\Gamma_D \neq \emptyset$. Then there exists a constant C independent of u and v such that

$$\|v\|_1 \leq C\{|v|_1 + |v|_{0,\Gamma_D} + |v^+ - v^-|_{0,\Gamma_0}\}, \quad \forall v \in V_{L,N}.$$

By means of $P_c > 0$, Eq. (8.4.4) holds. When $S = \cup_i S_i$, an interior subdomain S_i may be allowed, and the constant solution is also permitted in piecewise particular solutions. Besides, for Laplace's equation, the Lagrange multiplier TM in the next section shares the same limitations as those in the hybrid TM.

8.5 Lagrange Multiplier Techniques

Let us consider the Debye-Huckel equation

$$\mathcal{L}u = -\Delta u + u = 0, \quad \text{in } S. \quad (8.5.1)$$

Suppose that Φ_i and Ψ_i satisfy (8.5.1) in S^+ and S^- , respectively. We also choose

$$v = \begin{cases} v^+ = \sum_{i=0}^M a_i \Phi_i & \text{in } S^+, \\ v^- = \sum_{i=0}^N b_i \Psi_i & \text{in } S^-, \end{cases} \quad (8.5.2)$$

where a_i and b_i are the coefficients to be sought. We have for the true solution u

$$\iint_{S^+} (\nabla u \cdot \nabla v + uv) + \iint_{S^-} (\nabla u \cdot \nabla v + uv) - \int_{\Gamma_0} \lambda(v^+ - v^-) = 0.$$

Denote $\lambda = \frac{\partial u}{\partial n}$ as a new variable. Let λ_L be the L -order polynomials on Γ_0 , for example,

$$\lambda_L = \sum_{i=0}^L d_i T_i, \quad (8.5.3)$$

where T_i are certain orthogonal polynomials of order i . Denote by $V_{M,N} \times V_L$ the collection of finite dimensions of (8.5.2) and (8.5.3). We may design the Lagrange multiplier TM: To seek $(u_{M,N}^\#, \lambda_L) \in V_{M,N} \times V_L$ such that

$$A_{Lag}(u_{M,N}^\#, v) + D_{Lag}(u_{M,N}^\#, \lambda_L; v, \mu) = 0, \quad \forall (v, \mu) \in V_{M,N} \times V_L,$$

where

$$\begin{aligned} A_{Lag}(u, v) &= \iint_{S^+} \nabla u \cdot \nabla v + \iint_{S^-} \nabla u \cdot \nabla v, \\ D_{Lag}(u, \lambda; v, \mu) &= - \int_{\Gamma_0} \lambda(v^+ - v^-) - \int_{\Gamma_0} \mu(u^+ - u^-). \end{aligned}$$

Define the error norms

$$\begin{aligned} \|(v, \mu)\|_H &= (\|v\|_1^2 + \|\mu\|_{-\frac{1}{2}, \Gamma_0}^2)^{1/2}, \quad \|v\|_1 = (\|v\|_{1, S_1}^2 + \|v\|_{1, S_2}^2)^{1/2}, \\ \|\mu\|_{-\frac{1}{2}, \Gamma_0} &= \sup_v \frac{\left| \int_{\Gamma_0} \mu(v^+ - v^-) d\ell \right|}{|v^+|_{\frac{1}{2}, \Gamma_0} + |v^-|_{\frac{1}{2}, \Gamma_0}}, \\ \|v\|_{\frac{1}{2}, \Gamma_0} &= \left\{ \int_{\Gamma_0} \int_{\Gamma_0} \frac{(v(P) - v(Q))^2}{\|P - Q\|^2} d\ell(Q) d\ell(P) + \frac{1}{2}(d_1^{-1} + d_2^{-1}) \|v\|_{0, \Gamma_0}^2 \right\}^{\frac{1}{2}}, \end{aligned}$$

where d_i is roughly the diameter of S^+ and S^- .

We need the following assumptions.

(A1) For $A_{Lag}(u, v)$ there exist the bounds,

$$C_0 \|v\|_1^2 \leq A_{Lag}(v, v), \quad |A_{Lag}(u, v)| \leq C_1 \|u\|_1 \|v\|_1, \quad \forall v \in V_{M,N}.$$

(A2) For $\int_{\Gamma_0} \mu(v^+ - v^-) d\ell$, the Ladyzhenskaya-Babuska-Brezzi (LBB) condition holds: $\forall \mu_L \in V_L, \exists v \in V_{M,N}, v \neq 0$, such that

$$\left| \int_{\Gamma_0} \mu_L(v^+ - v^-) d\ell \right| \geq \beta \|v\|_1 \|\mu_L\|_{-\frac{1}{2}, \Gamma_0}.$$

(A3) Also the following bounds hold,

$$\left| \int_{\Gamma_0} \lambda(v^+ - v^-) d\ell \right| \leq C \|\lambda\|_{-\frac{1}{2}, \Gamma_0} \|v\|_1, \quad \forall v \in V_{M,N}.$$

Now we cite a theorem and a Lemma from [291].

Theorem 8.5.1 *Let (A1) – (A3) hold. There exist the error bounds,*

$$\|\lambda - \lambda_L\|_{-\frac{1}{2}, \Gamma_0} \leq C \left\{ \inf_{v \in V_{M,N}} \|u - v\| + \inf_{\eta \in V_L} \|\lambda - \eta\|_{-\frac{1}{2}, \Gamma_0} \right\},$$

and

$$\|u - u_{M,N}\|_1 \leq C \left\{ \inf_{v \in V_{M,N}} \|u - v\|_1 + \inf_{\eta \in V_L} \|\lambda - \eta\|_{-\frac{1}{2}, \Gamma_0} \right\}.$$

Lemma 8.5.1 *There exists a constant $\beta(> 0)$ independent of u and v such that $\forall \mu \in H^{-\frac{1}{2}}(\Gamma_0), \exists v \in H^1(S), v \neq 0$ such that*

$$\int_{\Gamma_0} \mu(v^+ - v^-) d\ell \geq \beta \|\mu\|_{-\frac{1}{2}, \Gamma_0} \|v\|_1.$$

Below we prove a new lemma.

Lemma 8.5.2 *For all $\mu_L \in V_L, \exists v_{M,N} \in V_{M,N}$ such that $v = v_{M,N} + r_{M,N}$, i.e.,*

$$v^+ = v_M + r_M, \quad v^- = v_N + r_N. \quad (8.5.4)$$

Suppose that the following bound exists,

$$\frac{\|r_{M,N}\|_1}{\|v_{M,N}\|_1} = o(1). \quad (8.5.5)$$

Then the LBB condition holds: $\forall \mu_L \in V_L, \exists v \in V_{M,N}$ such that

$$\int_{\Gamma_0} \mu_L(v^+ - v^-) d\ell \geq \beta \|\mu_L\|_{-\frac{1}{2}, \Gamma_0} \|v\|_1.$$

where β is a positive constant independent of μ_L and v .

Proof We have from (8.5.4)

$$\begin{aligned} \int_{\Gamma_0} \mu_L(v_M^+ - v_N^-) d\ell &= \int_{\Gamma_0} \mu_L(v^+ - v^-) d\ell - \int_{\Gamma_0} \mu_L(r_M^+ - r_N^-) d\ell \\ &\geq \beta \|\mu_L\|_{-\frac{1}{2}, \Gamma_0} \|v\|_1 - C \|\mu_L\|_{-\frac{1}{2}, \Gamma_0} \|r_{M,N}\|_1 \\ &\geq \beta \|\mu_L\|_{-\frac{1}{2}, \Gamma_0} \|v_{M,N}\|_1 - (\beta + C) \|\mu_L\|_{-\frac{1}{2}, \Gamma_0} \|r_{M,N}\|_1. \end{aligned}$$

When (8.5.5) holds, we have

$$\begin{aligned} \int_{\Gamma_0} \mu_L(v_M^+ - v_N^-) d\ell &\geq \left[\beta - (\beta + C)o(1) \right] \|\mu_L\|_{-\frac{1}{2}, \Gamma_0} \|v_{M,N}\|_1 \\ &\geq \frac{\beta}{2} \|\mu_L\|_{-\frac{1}{2}, \Gamma_0} \|v_{M,N}\|_1. \blacksquare \end{aligned}$$

8.6 Numerical Experiments

In this section, we consider Motz's problem (see Figure 8.2)

$$\begin{aligned} \Delta u &= 0, \quad \text{in } S, \\ u &= 0, \quad \text{on } \overline{OD}, \\ u &= 500, \quad \text{on } \overline{AB}, \\ \frac{\partial u}{\partial n} &= 0, \quad \text{on } \overline{BC} \cup \overline{CD} \cup \overline{OA}, \end{aligned} \tag{8.6.1}$$

where $S = \{(x, y) \mid -1 < x < 1, 0 < y < 1\}$. The true solution has the form

$$u = \sum_{i=0}^{\infty} d_i r^{i+\frac{1}{2}} \cos\left(i + \frac{1}{2}\right)\theta, \quad \text{in } S, \tag{8.6.2}$$

where d_i are the true coefficients. Since the error analysis for the CTM using piecewise particular solutions can be established as in Chapters 1 and 2, we carry out only the numerical experiments for Motz's problem, which results are better than those in Chapter 2. Moreover, we also test the hybrid TM for Motz's problem, and a comparison is made.

In Chapter 3, for the entire domain S , the uniform particular solutions are chosen, and the numerical experiments have been carried out by four TMs: the collocation TM, the original TM, the penalty plus hybrid TM and the direct TM in [312]. Since the uniform particular solutions may not always be found, using the piecewise particular solutions is important for the TMs to solve general PDEs.

We consider the partition in Figure 8.3, where the solution domain S is divided into three subdomains, S_0 , S_1 and S_2 . For (8.6.1) the piecewise particular solutions are expressed as

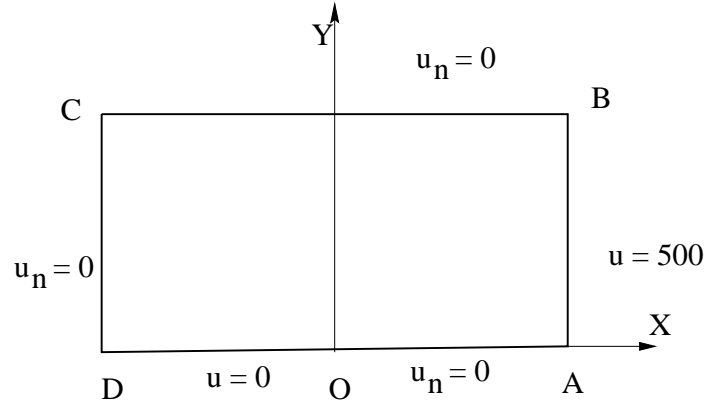


Figure 8.2: Motz's problem.

$$v_L = \sum_{i=0}^L \tilde{D}_i r^{i+\frac{1}{2}} \cos\left(i + \frac{1}{2}\right)\theta, \quad \text{in } S_0, \quad (8.6.3)$$

$$v_M = 500 + \sum_{i=0}^M \tilde{A}_i \rho^{2i+1} \cos(2i+1)\phi, \quad \text{in } S_1,$$

$$v_N = \tilde{B}_0 + \sum_{i=1}^N \tilde{B}_i \xi^{2i} \cos 2i\eta, \quad \text{in } S_2, \quad (8.6.4)$$

where \tilde{A}_i , \tilde{B}_i and \tilde{D}_i are the coefficients to be sought, (r, θ) , (ρ, ϕ) and (ξ, η) are the polar coordinates shown in Figure 8.3.

First we use the collocation TM from (8.1.3)

$$v^+(P_i) = v^-(P_i), \quad w \frac{\partial v^+}{\partial n}(P_i) = w \frac{\partial v^-}{\partial n}(P_i), \quad P_i \in \overline{AE}, \quad (8.6.5)$$

$$v^+(Q_i) = v^-(Q_i), \quad w \frac{\partial v^+}{\partial n}(Q_i) = w \frac{\partial v^-}{\partial n}(Q_i), \quad Q_i \in \overline{DE}, \quad (8.6.6)$$

where w is a suitable positive weight. The linear algebraic equations can be obtained from (8.6.5) and (8.6.6),

$$\mathbf{F}\mathbf{x} = \mathbf{b}, \quad (8.6.7)$$

where \mathbf{x} is the unknown vector consisting of the coefficients \tilde{A}_i , \tilde{B}_i and \tilde{D}_i , \mathbf{b} is the known vector, and \mathbf{F} is the stiffness matrix. Denote by M the number of the integration

nodes along \overline{AE} , then the dimensions of matrix \mathbf{F} are $m \times n$, where $m = 4\overline{M}$ and $n = L + M + N + 3$. In computation, we always choose $m > n$, then Eq. (8.6.7) is an over-determined system, and the least squares method is used to seek \mathbf{x} .

Denote by $V_{L,M,N} (= V_L \times V_M \times V_N)$ the finite dimensional collection of functions (8.6.3) – (8.6.4). Then the collocation TM is designed to seek the solution $u_{L,N,M} \in V_{L,N,M}$ such that

$$I(u_{L,M,N}) = \min_{v \in V_{L,N,M}} I(v),$$

where

$$I(v) = \widehat{\int}_{\Gamma_0} (v^+ - v^-)^2 + w^2 \widehat{\int}_{\Gamma_0} \left(\frac{\partial v^+}{\partial n} - \frac{\partial v^-}{\partial n} \right)^2. \quad (8.6.8)$$

In (8.6.8), $\Gamma_0 = \overline{AE} \cup \overline{ED}$, $v^+ = v_L$ in S_0 , $v^- = v_M$ in S_1 and $v^- = v_N$ in S_2 . The $\widehat{\int}_{\Gamma_0}$ is the approximation of \int_{Γ_0} by some rule of integration. The weight $w = \frac{1}{\max\{L, 2M, 2N\}}$ in (8.6.8) can be obtained based on the analysis in Chapter 1. After the solution $u_{L,N,M}$ has been obtained, we will compute the errors

$$\begin{aligned} |\varepsilon|_{\infty, \Gamma_0} &= |u_L^+ - u_{N,M}^-|_{0, \infty, \Gamma_0}, \\ |\varepsilon_n|_{\infty, \Gamma_0} &= \left| \frac{\partial u_L^+}{\partial n} - \frac{\partial u_{N,M}^-}{\partial n} \right|_{0, \infty, \Gamma_0}, \end{aligned}$$

where $u_{N,M}^- = u_M$ in S_1 and $u_{N,M}^- = u_N$ in S_2 , and u_L, u_M and u_N are the true solutions as in (8.6.3) – (8.6.4) with the true coefficients D_i, A_i and B_i , respectively. Moreover, the errors in the semi-norm of H^1 are defined by

$$|\varepsilon|_1 = \left\{ \int_{\overline{AE} \cup \overline{DE}} \frac{\partial \varepsilon^+}{\partial n} \varepsilon^+ + \int_{\overline{AE} \cup \overline{DE}} \frac{\partial \varepsilon^-}{\partial n} \varepsilon^- \right\}^{\frac{1}{2}},$$

where $\varepsilon = u - u_{L,N,M}$.

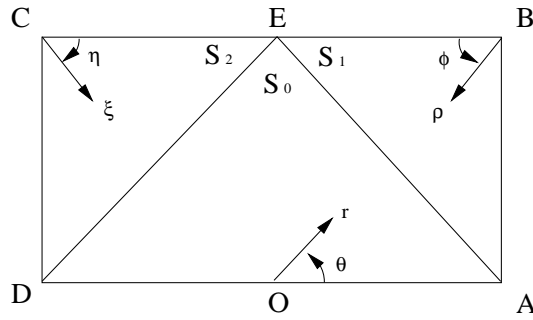


Figure 8.3: Partition of the rectangle.

Since the accuracy of the leading coefficients is important in applications, we also compute the relative errors

$$\left| \frac{\Delta D_i}{D_i} \right|, \quad i = 0, 1, 2, 3,$$

where $\Delta D_i = D_i - \tilde{D}_i$, and D_i are the true coefficients given in [309]. The condition number is defined by

$$\text{Cond.} = \left\{ \frac{\max_i \lambda_i(\mathbf{F}^T \mathbf{F})}{\min_i \lambda_i(\mathbf{F}^T \mathbf{F})} \right\}^{\frac{1}{2}},$$

where $\lambda_i(\mathbf{F}^T \mathbf{F})$ are the eigenvalues of the matrix $\mathbf{F}^T \mathbf{F}$.

In Chapter 2, the collocation TM is used for Motz's problem by using the uniform particular solutions (8.6.2), and the Gaussian rule of six nodes are used to raise the accuracy of the leading coefficients \tilde{D}_i . Hence, in this chapter, we always choose the Gaussian rule of six nodes. The solutions $u_{L,M,N}$ are obtained, and the errors and the condition numbers are listed in Tables 8.1 – 8.5. Note that when

$$L = 34, \quad M = N = 26, \quad \bar{M} = 36, \quad (8.6.9)$$

the leading coefficients are listed in Tables 8.4 and 8.5, where the coefficient \tilde{D}_0 has 17 significant digits, the same accuracy as that in Chapter 2. For the case of (8.6.9) the errors and condition numbers are given by

$$\begin{aligned} |\varepsilon|_1 &= 0.498(-10), \quad \text{Cond.} = 0.208(6), \\ |\varepsilon|_1 &= 0.175(-6), \quad \text{Cond.} = 0.679(6), \end{aligned}$$

from Table 8.1 and Table 3.1 respectively. Obviously, by using the piecewise particular solutions, the accuracy of the solutions from the collocation TM will be greatly improved, while the condition number is slightly smaller. This is also a new discovery, compared with [316, 291, 312, 329].

Next, consider the hybrid TM. First for the partition of Figure 8.3, condition (8.3.8) is satisfied by noting that $\partial S_2 \cap \Gamma_D \neq \emptyset$ due to

$$u \Big|_D = u(\xi, \eta) \Big|_{\xi=1, \eta=\frac{\pi}{2}} = 0, \quad \text{in } S_2. \quad (8.6.10)$$

Hence the particular solutions v_2 in (8.6.4) satisfying (8.6.10) lead to an additional condition

$$\tilde{B}_0 + \sum_{i=1}^N \tilde{B}_i \cos(i\pi) = \tilde{B}_0 + \sum_{i=1}^N (-1)^i \tilde{B}_i = 0.$$

This gives

$$\tilde{B}_0 = \sum_{i=1}^N (-1)^{i+1} \tilde{B}_i.$$

By removing the coefficient \tilde{B}_0 from (8.6.4), we modify the particular solutions in S_2 as

$$v_2^* = \sum_{i=1}^N \tilde{B}_i \Phi_i(\xi, \eta), \quad \text{in } S_2,$$

where the particular solutions are

$$\Phi_i(\xi, \eta) = (-1)^{i+1} + \xi^{2i} \cos(2i\eta), \quad i = 1, 2, \dots$$

For the hybrid TM, we choose the particular solutions

$$\begin{aligned} v_0 &= \sum_{i=0}^L \tilde{D}_i r^{i+\frac{1}{2}} \cos\left(i + \frac{1}{2}\right)\theta, \quad \text{in } S_0. \\ v_1 &= 500 + \sum_{i=0}^M \tilde{A}_i \rho^{2i+1} \cos(2i+1)\phi, \quad \text{in } S_1, \\ v_2^* &= \sum_{i=1}^N \tilde{B}_i \Phi_i(\xi, \eta), \quad \text{in } S_2. \end{aligned}$$

Since there exists a constant solution in v_1 and v_2^* , only the simplified hybrid TM in (8.3.24) can be applied for $S^+ = S_0$ and $S^- = S_1 \cup S_2$, based on Remark 8.3.1.

The computed solutions $u_{L,N,M}$ are obtained, and the errors and the condition numbers are listed in Tables 8.6 and 8.7. When

$$L = 34, \quad M = N = 15, \quad \bar{M} = 3840, \quad (8.6.11)$$

the leading coefficients are listed in Tables 8.8 and 8.9, where the coefficient \tilde{D}_0 also has 17 significant digits⁴. Note that the large \bar{M} should be used to balance the exponential convergence rates, based on Theorem 8.4.2. This is distinct from the collocation TM where $\bar{M} = 30$ is small.

Let us compare the errors from the collocation TM and the hybrid TM. The best results are given from Table 8.1 at (8.6.9) and from Table 8.8 at (8.6.11), respectively,

$$\begin{aligned} |\varepsilon|_{\infty, \Gamma_0} &= 0.401(-10), \quad |\varepsilon_n|_{\infty, \Gamma_0} = 0.454(-9), \quad |\varepsilon|_1 = 0.498(-10), \\ |\varepsilon|_{\infty, \Gamma_0} &= 0.767(-7), \quad |\varepsilon_n|_{\infty, \Gamma_0} = 0.119(-4), \quad |\varepsilon|_1 = 0.625(-6). \end{aligned}$$

Obviously, the global errors of the solutions by the collocation TM are more accurate than the hybrid TM. Moreover, less CPU is needed for the CTM because $\bar{M} = 30$ is much smaller than $\bar{M} = 3840$. Note that D_0 has 17 significant digits by both TMs. Since the accuracy of \tilde{D}_0 is just one criteria to evaluate the numerical methods for singularity problems, the collocation TM is superior to the hybrid TM and other TMs. Such a confirmation has been established with detailed comparisons in Chapter 3.

⁴For Motz's problem, when the uniform expansions of the particular solutions on S are used, the best \tilde{D}_0 obtained by the simplified (i.e., the original) TM has only 16 significant digits, see Chapter 3.

Second, we consider the Debye-Huckel equation $-\Delta u + u = 0$ with boundary conditions of the Motz type in (8.6.1). The piecewise particular solutions can be found as

$$v = \begin{cases} v_0 = \sum_{i=0}^L \tilde{d}_i \frac{I_{i+\frac{1}{2}}(r)}{I_{i+\frac{1}{2}}(\frac{1}{2})} \cos(i + \frac{1}{2})\theta, & \text{in } S_0, \\ v_1 = 500 \exp(-\rho \cos \phi) + \sum_{i=0}^M \tilde{a}_i \frac{I_{2i+1}(\rho)}{I_{2i+1}(\frac{1}{2})} \cos(2i + 1)\phi, & \text{in } S_1, \\ v_2 = \sum_{i=0}^N \tilde{b}_i \frac{I_{2i}(\xi)}{I_{2i}(\frac{1}{2})} \cos 2i\eta, & \text{in } S_2. \end{cases} \quad (8.6.12)$$

where \tilde{a}_i , \tilde{b}_i and \tilde{d}_i are the coefficients to be sought, and $I_\mu(r)$ are the Bessel function for a purely imaginary arguments. The hybrid TM with $\alpha = \beta = \frac{1}{2}$ and the direct TM can be used for the Debye-Huckel equation with the piecewise particular solutions (8.6.12). The numerical experiments will appear elsewhere.

To close this chapter, let us make a few final remarks.

1. New analysis is made for the hybrid TM, the penalty plus hybrid TM and the direct TM by using piecewise particular solutions, and the exponential convergence rates may be achieved. When the TMs involve integration approximation, only polynomial convergence rates can be obtained. By means of piecewise particular solutions, not only may the stability be improved significantly, but also the solution errors can be reduced, because the local particular solutions may better approximate the true solution. More importantly, the hybrid and other TMs can be applied to more complicated PDEs involving multiple singularities, see Chapter 13.
2. The symmetric hybrid TM is explored in this chapter. Some limitations as in Remark 8.3.1 exist for the Laplace equation. In order to remove such limitations, the penalty plus hybrid TM is suggested.
3. The numerical solutions by the CTM for Motz's problem given in this chapter are better than those given in Chapter 2. The reasons are twofold. (a) The partition by the straight line interior boundary as in Figure 8.3 is the best, based on the stability analysis in Section 1.5, while the partition in [316] is by the arc. (b) The Gaussian rule with high order is used to raise the accuracy of the leading coefficient D_0 , while only the central or the Simpson rules were chosen in [316, 291, 300].
4. From the numerical experiments for Motz's problem, the collocation TM is also superior to the hybrid TM, the detailed comparisons of the TMs in analysis and computation are explored in Chapter 3.

M	$\ \varepsilon\ _B$	$ \varepsilon _{\infty, \Gamma_0}$	$ \varepsilon_n _{\infty, \Gamma_0}$	$ \varepsilon _1$	$ \frac{\Delta D_0}{D_0} $	$ \frac{\Delta D_1}{D_1} $	$ \frac{\Delta D_2}{D_2} $	$ \frac{\Delta D_3}{D_3} $	Cond.
10	0.305(-4)	0.523(-4)	0.153(-2)	0.371(-3)	0.490(-11)	0.781(-10)	0.208(-8)	0.438(-7)	0.219(4)
12	0.298(-5)	0.525(-5)	0.155(-3)	0.285(-4)	0.334(-13)	0.489(-12)	0.252(-10)	0.617(-9)	0.220(4)
14	0.300(-6)	0.480(-6)	0.175(-4)	0.420(-5)	0.893(-14)	0.180(-13)	0.196(-12)	0.832(-11)	0.224(4)
16	0.306(-7)	0.399(-7)	0.178(-6)	0.427(-6)	0.112(-13)	0.613(-13)	0.118(-12)	0.220(-12)	0.236(4)
18	0.286(-8)	0.251(-8)	0.197(-6)	0.454(-7)	0.822(-14)	0.331(-13)	0.736(-13)	0.920(-13)	0.574(4)
20	0.228(-9)	0.315(-9)	0.302(-7)	0.572(-8)	0.439(-14)	0.144(-13)	0.196(-13)	0.623(-13)	0.152(5)
22	0.158(-10)	0.566(-10)	0.678(-8)	0.112(-8)	0.298(-14)	0.600(-14)	0.173(-13)	0.156(-13)	0.446(5)
24	0.122(-11)	0.158(-10)	0.187(-8)	0.256(-9)	0.425(-15)	0.162(-15)	0.948(-14)	0.176(-14)	0.146(6)
26	0.420(-12)	0.401(-11)	0.454(-9)	0.498(-10)	0*	0.648(-15)	0.412(-14)	0.462(-14)	0.208(6)
28	0.370(-11)	0.139(-10)	0.100(-8)	0.291(-9)	0.850(-15)	0.211(-14)	0.247(-14)	0.352(-14)	0.104(7)
30	0.281(-11)	0.728(-11)	0.111(-8)	0.275(-9)	0.850(-15)	0.373(-14)	0.227(-14)	0.169(-13)	0.354(7)

Table 8.1: The error norms, condition number and errors of leading coefficients from the collocation TM for Motz’s problem by the Gaussian rule of six nodes rule as $L = 34$, $M = N$ and $\bar{M} = 36$, where “0*” denotes the errors less then the rounding error of computer.

\bar{M}	$\ \varepsilon\ _B$	$ \varepsilon _{\infty, \Gamma_0}$	$ \varepsilon_n _{\infty, \Gamma_0}$	$ \varepsilon _1$	$ \frac{\Delta D_0}{D_0} $	$ \frac{\Delta D_1}{D_1} $	$ \frac{\Delta D_2}{D_2} $	$ \frac{\Delta D_3}{D_3} $	Cond.
24	0.137(-10)	0.523(-10)	0.335(-8)	0.143(-8)	0.171(-13)	0.708(-13)	0.148(-12)	0.314(-12)	0.760(6)
30	0.857(-12)	0.659(-11)	0.746(-9)	0.865(-10)	0.567(-15)	0.195(-14)	0.907(-14)	0.141(-13)	0.623(6)
36	0.420(-12)	0.401(-11)	0.454(-9)	0.498(-10)	0*	0.648(-15)	0.412(-14)	0.642(-14)	0.208(6)
42	0.455(-12)	0.131(-11)	0.149(-9)	0.209(-10)	0.850(-15)	0.130(-14)	0.115(-13)	0.242(-13)	0.344(6)
48	0.455(-12)	0.824(-12)	0.644(-10)	0.970(-11)	0.142(-15)	0.243(-14)	0.103(-13)	0.123(-13)	0.278(6)

Table 8.2: The error norms, condition number and errors of leading coefficients from the collocation TM for Motz’s problem by the Gaussian rule of six nodes rule as $L = 34$ and $M = N = 26$.

L	M	$\ \varepsilon\ _B$	$ \varepsilon _{\infty, \Gamma_0}$	$ \varepsilon_n _{\infty, \Gamma_0}$	$ \varepsilon _1$	$ \frac{\Delta D_0}{D_0} $	$ \frac{\Delta D_1}{D_1} $	$ \frac{\Delta D_2}{D_2} $	$ \frac{\Delta D_3}{D_3} $	Cond.
10	8	0.824(-3)	0.106(-2)	0.171(-1)	0.822(-2)	0.546(-8)	0.191(-7)	0.373(-8)	0.625(-4)	49.2
18	14	0.437(-6)	0.430(-6)	0.352(-4)	0.669(-5)	0.506(-13)	0.452(-12)	0.426(-11)	0.191(-8)	828
26	20	0.271(-9)	0.444(-9)	0.245(-7)	0.711(-8)	0.425(-14)	0.162(-13)	0.192(-13)	0.224(-13)	0.150(5)
34	26	0.420(-12)	0.401(-11)	0.454(-9)	0.498(-10)	0*	0.648(-15)	0.412(-14)	0.462(-14)	0.208(6)
40	30	0.281(-11)	0.171(-10)	0.860(-9)	0.182(-9)	0.128(-14)	0.308(-14)	0.453(-13)	0.143(-13)	0.424(7)

Table 8.3: The error norms, condition number and errors of leading coefficients from the collocation TM for Motz’s problem by the Gaussian rule of six nodes rule as $\bar{M} = 36$ and $M = N$.

i	\tilde{D}_i	i	\tilde{D}_i
0	.401162453745234416(3)	18	.115352471443778851(-4)
1	.876559201950879725(2)	19	-.529572415268499927(-5)
2	.172379150794468821(2)	20	.229123737707347517(-5)
3	-.807121525969817100(1)	21	.106323020872833201(-5)
4	.144027271702286663(1)	22	.531249576038153798(-6)
5	.331054885920768371	23	-.247431076339611956(-6)
6	.275437344509163740	24	.109928975890681925(-6)
7	-.869329945256786807(-1)	25	.516695735614091014(-7)
8	.336048784266203271(-1)	26	.257457708954766480(-7)
9	.153843744826868429(-1)	27	-.120317413747487121(-7)
10	.730230167385251521(-2)	28	.540803145614940174(-8)
11	-.318411391615677731(-2)	29	.260150547393998650(-8)
12	.122064610942808609(-2)	30	.131774021431445718(-8)
13	.530965480203339111(-3)	31	-.716717640212716954(-9)
14	.271512182358950110(-3)	32	.340026463417246646(-9)
15	-.120046375387525815(-3)	33	.145637472345680654(-9)
16	.505398334499953102(-4)	34	.646319941944504533(-10)
17	.231668222198537339(-4)		

Table 8.4: The leading coefficients \tilde{D}_i by the collocation TM for Motz's problem at $L = 34$ and $M = N = 26$ by the Gaussian rule of six nodes with $\tilde{M} = 36$ along AB .

i	\tilde{A}_i	\tilde{B}_i
0	-.324796539532479756(3)	.913597470506873464(2)
1	.232607975243312204(2)	.106454402511134788(3)
2	.749635805883399087(1)	.114358406001622779(2)
3	-.105838719294348760(1)	-.475017155047903383(1)
4	-.797801480899109294	-.712640969353020681
5	.133844127561235676	.522088231291717109
6	.115978763171984939	.889809563419886873(-1)
7	-.206752186506053218(-1)	-.773689919897273398(-1)
8	-.194544291456736733(-1)	-.139185098079888867(-1)
9	.358689091375572920(-2)	.131391643034147309(-1)
10	.354875859185069991(-2)	.243632356556054957(-2)
11	-.668408209585087893(-3)	-.241627546046592912(-2)
12	-.683773705768343765(-3)	-.456865396633695327(-3)
13	.130697557610920205(-3)	.468227837388299315(-3)
14	.136926484810349767(-3)	.897479231523365764(-4)
15	-.264552436403060604(-4)	-.941587491224513969(-4)
16	-.282148351496040590(-4)	-.182308972521741703(-4)
17	.549510252114114052(-5)	.194624182351141110(-4)
18	.594196246642652178(-5)	.379789786965780228(-5)
19	-.116159250071523603(-5)	-.410078867091007969(-5)
20	-.126951842989415352(-5)	-.805726533744082841(-6)
21	.244038929588239169(-6)	.861952521981058757(-6)
22	.268711101149843939(-6)	.170880067660462860(-6)
23	-.462051393846600188(-7)	-.164639262402756537(-6)
24	-.510670724598834558(-7)	-.331977632058908638(-7)
25	.564846976060578345(-8)	.205003005242903636(-7)
26	.624656884317372375(-8)	.424996984523008565(-8)

Table 8.5: The leading coefficients \tilde{A}_i and \tilde{B}_i by the collocation TM for Motz's problem at $L = 34$ and $M = N = 26$ by the Gaussian rule of six nodes with $\bar{M} = 36$ along \overline{AB} .

M	$ \varepsilon _{\infty, \Gamma_0}$	$ \varepsilon_n _{\infty, \Gamma_0}$	$ \varepsilon _1$	$ \frac{\Delta D_0}{D_0} $	$ \frac{\Delta D_1}{D_1} $	$ \frac{\Delta D_2}{D_2} $	$ \frac{\Delta D_3}{D_3} $	Cond.
21	13.9	0.155(4)	0.726(3)	0.627(-4)	0.114(-3)	0.815(-3)	0.192(-3)	0.502(9)
19	0.612	64.3	38.2	0.212(-5)	0.411(-5)	0.120(-4)	0.235(-4)	0.392(8)
17	0.516(-1)	5.37	4.34	0.985(-7)	0.202(-6)	0.237(-6)	0.191(-5)	0.353(7)
15	0.516(-1)	5.26	2.45	0.306(-7)	0.317(-6)	0.954(-6)	0.744(-7)	0.199(7)
13	0.444(-1)	4.66	2.48	0.386(-7)	0.333(-6)	0.984(-6)	0.111(-6)	0.200(7)
11	0.425(-1)	3.74	2.50	0.396(-7)	0.335(-6)	0.110(-5)	0.351(-6)	0.199(7)
9	0.418(-1)	3.64	2.51	0.400(-7)	0.345(-6)	0.637(-6)	0.485(-7)	0.195(7)
7	0.414(-1)	3.58	2.52	0.389(-7)	0.362(-6)	0.225(-5)	0.133(-4)	0.189(7)

Table 8.6: The condition number and errors of leading coefficients from the simplified hybrid TM for Motz's problem by the Gaussian rule of six nodes rule as $L = 34$, $M = N$ and $\bar{M} = 30$.

\bar{M}	$ \varepsilon _{\infty, \Gamma_0}$	$ \varepsilon_n _{\infty, \Gamma_0}$	$ \varepsilon _1$	$ \frac{\Delta D_0}{D_0} $	$ \frac{\Delta D_1}{D_1} $	$ \frac{\Delta D_2}{D_2} $	$ \frac{\Delta D_3}{D_3} $	Cond.
30	0.516(-1)	5.26	2.45	0.306(-7)	0.317(-6)	0.954(-6)	0.744(-7)	0.199(7)
60	0.180(-4)	0.212(-2)	0.643(-3)	0.162(-12)	0.194(-10)	0.218(-9)	0.593(-9)	0.192(7)
120	0.402(-5)	0.249(-3)	0.499(-4)	0.417(-13)	0.485(-11)	0.561(-10)	0.158(-9)	0.192(7)
240	0.119(-5)	0.822(-4)	0.112(-4)	0.106(-13)	0.121(-11)	0.140(-10)	0.402(-10)	0.191(7)
480	0.357(-6)	0.295(-4)	0.298(-5)	0.227(-14)	0.303(-12)	0.352(-11)	0.105(-10)	0.191(7)
960	0.147(-6)	0.161(-4)	0.140(-5)	0.425(-15)	0.757(-13)	0.911(-12)	0.314(-11)	0.191(7)
1920	0.899(-7)	0.128(-4)	0.902(-6)	0.113(-14)	0.199(-13)	0.220(-12)	0.129(-11)	0.191(7)
3840	0.767(-7)	0.119(-4)	0.625(-6)	0*	0.340(-14)	0.680(-13)	0.106(-11)	0.191(7)
7680	0.741(-7)	0.118(-4)	0.439(-5)	0.893(-14)	0.190(-14)	0.381(-13)	0.947(-12)	0.191(7)

Table 8.7: The condition number and errors of leading coefficients from the simplified hybrid TM for Motz's problem by the Gaussian rule of six nodes rule as $L = 34$ and $M = N = 15$.

i	\tilde{D}_i	i	\tilde{D}_i
0	.401162453745234416(3)	18	.119539425331155125(-4)
1	.876559201950882141(2)	19	-.997377878424553307(-5)
2	.172379150794479834(2)	20	-.218799988043284786(-5)
3	-.807121525970671527(1)	21	.123113699808094708(-4)
4	.144027271700217074(1)	22	-.861590585674063637(-7)
5	.331054886077918553	23	.112519712035018431(-4)
6	.275437344367627068	24	.101379541374730469(-4)
7	-.869329929651373179(-1)	25	-.213038668080027716(-4)
8	.336048812445294623(-1)	26	-.232568778053804656(-6)
9	.153843598338551015(-1)	27	-.128254949790181612(-4)
10	.730230881089648492(-2)	28	-.10480843332291741(-4)
11	-.318417994710996129(-2)	29	.192089636657504856(-4)
12	.122055808683248419(-2)	30	.122621067574900189(-5)
13	.531301275801784813(-3)	31	.522797705053408068(-5)
14	.271419809942469279(-3)	32	.411209726337550316(-5)
15	-.119177132893171268(-3)	33	-.653035080167190711(-5)
16	.514919906538434415(-4)	34	-.679587260047955378(-6)
17	.202800107498274560(-4)		

Table 8.8: The leading coefficients \tilde{D}_i by the simplified hybrid TM for Motz's problem at $L = 34$ and $M = N = 15$ by the Gaussian rule of six nodes with $\bar{M} = 3840$ along AE .

i	\tilde{A}_i	\tilde{B}_i
0	-.324796539532481859(3)	.913597470506882559(2)
1	.232607975243296679(2)	.106454402511139278(3)
2	.749635805872579919(1)	.114358406001376700(2)
3	-.105838719285406513(1)	-.475017155034118410(1)
4	-.797801467080026638	-.712640963620977508
5	.133844120961793767	.522088218619536693
6	.115978358085103983	.889807533637062276(-1)
7	-.206750825527241000(-1)	-.773686693148138288(-1)
8	-.194501444783602567(-1)	-.139161110779844714(-1)
9	.358572990720075610(-2)	.131359927538752877(-1)
10	.352852142710858522(-2)	.242420048076527270(-2)
11	-.663646884204361471(-3)	-.240186646894774295(-2)
12	-.636922005089684043(-3)	-.427600140136292529(-3)
13	.120671171672690993(-3)	.435524978752034240(-3)
14	.832019792254850188(-4)	.553634704333649501(-4)
15	-.156455892524474174(-4)	-.569941742981822615(-4)

Table 8.9: The leading coefficients \tilde{A}_i and \tilde{B}_i by the simplified hybrid TM for Motz's problem at $L = 34$ and $M = N = 15$ by the Gaussian rule of six nodes with $\bar{M} = 3840$ along \overline{AE} .

Chapter 9

Interior Boundary Conditions in the Schwarz Alternating Method

New types of the Schwarz alternating methods (SAMs) with and without overlapping are proposed, by using different interior boundary conditions, such as the Dirichlet, the Neumann and the Robin conditions. Those SAMs using different interior boundary conditions are called the *mixed* SAMs. For a simple continuous model, the Laplacian solutions on a sectorial domain, the convergence rates of the mixed SAMs are derived in detail for different interior boundary conditions. Compared with the classic overlapping SAM with the Dirichlet conditions, some of the mixed SAMs with the interior Neumann or Robin conditions will converge faster. Moreover, a number of new SAMs better than those in the existing literature are explored. Moreover, we also integrate the TM into SAMs, which numerical results for Motz's problem are given in Li et al. [302], to support the analysis made in this chapter for the simple model.

9.1 Introduction

There exist two types of the SAMs: the overlapping and the non-overlapping. For the overlapping SAM, only the interior Dirichlet boundary conditions are assigned; the maximum principle of the solutions of partial differential equations (PDEs) may guarantee the SAM convergence. This is the classic SAM proposed by Schwartz [424]. For the non-overlapping SAM, only the interior Robin conditions are studied in Lions [324] by the energy norms of solutions, to yield the SAM convergence. Besides, the substructuring iteration method may be viewed as the non-overlapping SAM with the Dirichlet-Neumann conditions (see Dryja and Widlund in [138, 137]). Here we may ask the following questions: How about the performance of other boundary conditions assigned on the interior boundary in the SAMs? For example, in the overlapping SAM, can we choose the Neumann condition or the Robin condition? Whether or not the mixed SAMs, as called in this chapter, are convergent? Below we consider a simple model: the Laplacian solutions on a sectorial domain, to investigate the convergence rates of the mixed SAMs. A number of interesting results are discovered. For instance, the convergence rates of the

interior Neumann condition may be faster than those of the interior Dirichlet condition, and the interior Robin condition may be suitably chosen to greatly speed up the SAM convergence.

Many studies are provided for the discrete overlapping SAMs, such as Miller [354], Lions [322, 323], Matsokin and Nepomnyaschikh [346], Chan et al. [84], Yanik [497], Badea [19], Mathew [343], Lu et al. [331], Smith et al. [436], Pavarino [372], Holst and Vandewalle [211], Guo and Cao [187], and Nataf and Nier [362]. But only a few, Douglas et al. [135, 136, 134], involve the discrete non-overlapping SAM. Also the interior Robin condition is used in Ganden et al. [162] for initial value problems, and the mixed SAM is adopted in Huang and Wang [220]. In Sections 9.3 - 9.4, we provide some interesting results on the mixed SAMs for the continuous problem. For the discrete mixed SAM, the convergence analysis is still an open question. In [302] we carry out the mixed SAM for the typical singularity problems, Motz's problem, by combining the Trefftz method (TM) for the singular solutions and the finite difference method (FDM). Interestingly, the numerical results in [302] are, basically, coincident with the analysis from the simple model in this chapter. For application, we may utilize the Robin condition to speed up the SAM convergence rates.

In this chapter, the mixed SAMs are discussed for the simple model on a sectorial domain. Consider a sector (see Figure 9.1)

$$S = \left\{ (r, \theta) \mid 0 \leq r \leq a, 0 \leq \theta \leq \Theta \right\}$$

with the mixed Dirichlet and Neumann conditions on the sectorial boundary:

$$\left. \frac{\partial u}{\partial n} \right|_{\theta=0} = 0, \quad u|_{\theta=\Theta} = 0, \quad (9.1.1)$$

$$u|_{r=a} = f(\theta). \quad (9.1.2)$$

Suppose that the function in (9.1.2) is given by

$$f(\theta) = \sum_{n=0}^{\infty} a_n \cos \sigma_n \theta, \quad (9.1.3)$$

where $\sigma_n = (n + 1/2)(\pi/\Theta)$. The true Laplacian solutions satisfying (9.1.1) - (9.1.3) are found:

$$u(r, \theta) = \sum_{n=0}^{\infty} a_n \left(\frac{r}{a} \right)^{\sigma_n} \cos \sigma_n \theta. \quad (9.1.4)$$

Now we adopt the classical Schwarz alternating method. Divide S into two subdomains S_1 and S_2 (see Figure 9.2),

$$S_1 = \left\{ (r, \theta) \mid c \leq r \leq a, 0 \leq \theta \leq \Theta \right\}, \quad S_2 = \left\{ (r, \theta) \mid 0 \leq r \leq b, 0 \leq \theta \leq \Theta \right\}.$$

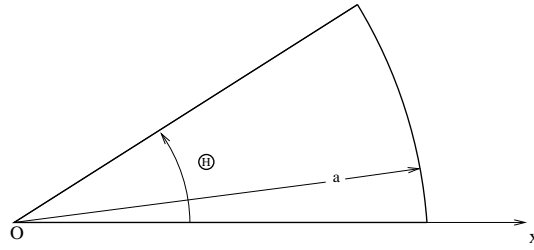


Figure 9.1: A sectorial domain.

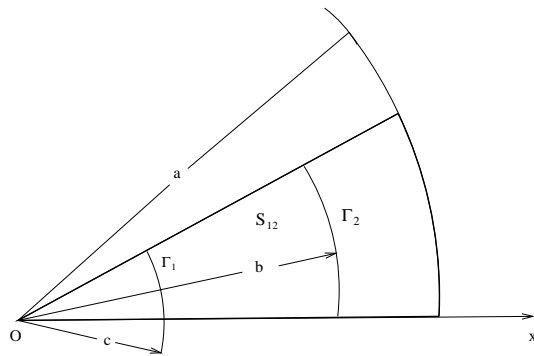


Figure 9.2: The partition of the sectorial domain in the SAM.

$\Gamma_1(r = c)$ and $\Gamma_2(r = b)$ are called the interior boundaries. To guarantee convergence of SAM, we assume

$$0 < c \leq b < a. \quad (9.1.5)$$

When $c < b$ and $c = b$, the SAMs are overlapping and non-overlapping, respectively.

This chapter is a continuing study of [288], and is organized as follows. In the next section, different boundary conditions are imposed on Γ_1 , and in Section 9.3, on both Γ_1 and Γ_2 . In Section 9.4, special cases of mixed SAMs are explored.

9.2 Different Boundary Conditions on Γ_1

In SAMs, we first fix the Dirichlet condition on the interior boundary Γ_2 of S_2 , and adopt different boundary conditions on the interior boundary Γ_1 of S_1 . Our attention will be focused on the convergence rates of the mixed SAMs, while the iterative methods for FEM, FDM, etc. are given in Varga [468] and Hageman and Young [189].

Define a Laplacian solution $\tilde{u}^{(1)}$ in S_1 and suppose that the initial values on Γ_2 are given by

$$\tilde{u}^{(1)}(b, \theta) = \sum_{n=0}^{\infty} a_n^* \cos \sigma_n \theta, \text{ on } \Gamma_2, \quad (9.2.1)$$

where a_n^* are real coefficients. By the Dirichlet condition (9.2.1) on Γ_2 , the Laplacian solutions on S_2 satisfying (9.1.1) are found:

$$\tilde{u}^{(2)}(r, \theta) = \sum_{n=0}^{\infty} a_n^* \left(\frac{r}{b}\right)^{\sigma_n} \cos \sigma_n \theta \text{ in } S_2. \quad (9.2.2)$$

On Γ_1 of S_1 , we choose the general boundary conditions

$$\alpha \frac{\partial u}{\partial n} + \beta u = g_2 \text{ on } \Gamma_1, \quad (9.2.3)$$

where n is the exterior unit normal to ∂S_1 , $\alpha \geq 0$ and $\beta \geq 0$. Hence, we have from (9.2.2)

$$g_2 = \alpha \frac{\partial \tilde{u}^{(2)}}{\partial n} + \beta \tilde{u}^{(2)} = -\alpha \frac{\partial \tilde{u}^{(2)}}{\partial r} + \beta \tilde{u}^{(2)} \text{ on } \Gamma_1, \quad (9.2.4)$$

where

$$g_2 = \sum_{n=0}^{\infty} a_n^* \left[-\frac{\alpha \sigma_n}{c} + \beta \right] \left(\frac{c}{b}\right)^{\sigma_n} \cos \sigma_n \theta.$$

Note that the general conditions (9.2.3) include three important boundary conditions on Γ_1 :

- I. The Dirichlet condition: $\alpha = 0$ and $\beta = 1$;
- II. The Neumann condition: $\alpha = 1$ and $\beta = 0$;
- III. The Robin condition: $\alpha > 0$ and $\beta > 0$.

Then the Laplacian solutions $\tilde{u}^{(3)}(r, \theta)$ in S_1 satisfying (9.1.1) – (9.1.3) and the interior boundary conditions (9.2.3) can be obtained.

Define the errors

$$\varepsilon^{(i)} = \tilde{u}^{(i)} - u, \quad i = 1, 2, 3,$$

where u is the true solution (9.1.4). Hence the errors from (9.2.1) and (9.2.2) are

$$\begin{aligned} \varepsilon^{(1)}(r, \theta) &= \sum_{n=0}^{\infty} b_n \cos \sigma_n \theta \text{ on } \Gamma_2, \\ \varepsilon^{(2)}(r, \theta) &= \sum_{n=0}^{\infty} b_n \left(\frac{r}{b}\right)^{\sigma_n} \cos \sigma_n \theta \text{ in } S_2, \end{aligned} \quad (9.2.5)$$

where $b_n = a_n^* - a_n$ and a_n are defined in (9.1.3). Since the errors $\varepsilon^{(3)}$ in S_1 satisfy (9.1.1) and

$$\varepsilon^{(3)}|_{r=a} = 0, \quad (9.2.6)$$

we obtain from (9.2.4)

$$\varepsilon^{(3)}(r, \theta) = \sum_{n=0}^{\infty} c_n (r^{\sigma_n} - a^{2\sigma_n} r^{-\sigma_n}) \cos \sigma_n \theta,$$

where

$$c_n = b_n \times \frac{\left(-\frac{\alpha\sigma_n}{c} + \beta\right) \left(\frac{c}{b}\right)^{\sigma_n}}{\left(-\frac{\alpha\sigma_n}{c} + \beta\right) c^{\sigma_n} - \left(\frac{\alpha\sigma_n}{c} + \beta\right) a^{2\sigma_n} \times c^{-\sigma_n}}.$$

Hence the errors $\varepsilon^{(3)}$ on Γ_2 are expressed by, through an iteration cycle in the mixed SAM,

$$\begin{aligned} \varepsilon^{(3)}(b, \theta) &= \sum_{n=0}^{\infty} c_n (b^{\sigma_n} - a^{2\sigma_n} b^{-\sigma_n}) \cos \sigma_n \theta \\ &= \sum_{n=0}^{\infty} b_n t(\alpha, \beta, \sigma_n) \cos \sigma_n \theta. \end{aligned}$$

The reduction factors, $t(\alpha, \beta, \sigma_n)$, to the coefficients b_n are simplified through some manipulations as:

$$t(\alpha, \beta, \sigma_n) = \frac{1 - \left(\frac{a}{b}\right)^{2\sigma_n}}{1 - S(\alpha, \beta, \sigma_n) \left(\frac{a}{c}\right)^{2\sigma_n}}, \quad (9.2.7)$$

and

$$S(\alpha, \beta, \sigma_n) = \frac{\alpha\sigma_n + \beta c}{-\alpha\sigma_n + \beta c}. \quad (9.2.8)$$

The absolute reduction factors $t(\alpha, \beta, \sigma_n)$ indicate the convergence rates of the SAM. We write these important results as a proposition:

Proposition 9.2.1 *Let the Dirichlet condition on Γ_2 and the general condition (9.2.3) on Γ_1 be given. There exist the reduction factors (9.2.7) to the coefficients b_n of the initial errors (9.2.5) after an iteration cycle of the mixed SAM.*

From Proposition 9.2.1, we reach the surprising result:

Corollary 9.2.1 *Let (9.1.5) and all conditions in Proposition 9.2.1 hold. Then the absolute reduction factors to b_n of the Neumann conditions on Γ_1 are smaller than those of the Dirichlet condition on Γ_1 .*

Proof For the Dirichlet condition ($\alpha = 0$ and $\beta = 1$), and the Neumann condition ($\alpha = 1$ and $\beta = 0$), the reduction factors are given from (9.2.7)

$$t^D(0, 1, \sigma_n) = \frac{\left(\frac{a}{b}\right)^{2\sigma_n} - 1}{\left(\frac{a}{c}\right)^{2\sigma_n} - 1}$$

and

$$t^N(1, 0, \sigma_n) = \frac{1 - \left(\frac{a}{b}\right)^{2\sigma_n}}{1 + \left(\frac{a}{c}\right)^{2\sigma_n}} = - \left| \frac{\left(\frac{a}{b}\right)^{2\sigma_n} - 1}{\left(\frac{a}{c}\right)^{2\sigma_n} + 1} \right|, \quad (9.2.9)$$

respectively. Obviously, we have from $c \leq b < a$

$$|t^N(1, 0, \sigma_n)| < |t^D(0, 1, \sigma_n)| \leq 1. \blacksquare$$

Here we use the superscripts D , N and R to denote the reduction factors or the functions corresponding to the Dirichlet, Neumann and Robin conditions on Γ_1 , respectively. The following corollary is even more surprising:

Corollary 9.2.2 *Let (9.1.5) and all conditions in Proposition 9.2.1 hold. Then the absolute reduction factors to b_n of the Robin condition on Γ_1 with $\alpha > 0$ and $\beta > 0$ are smaller than those of the Dirichlet condition on Γ_1 . Moreover, if the parameters in (9.2.3) satisfy*

$$\frac{\beta}{\alpha} \leq \frac{\sigma_0}{c}, \quad (9.2.10)$$

the absolute reduction factors to b_n of the Robin condition on Γ_1 are even smaller than those of the Neumann condition on Γ_1 .

Proof When $\alpha > 0$ and $\beta > 0$, the functions (9.2.8) satisfy either $S^R(\alpha, \beta, \sigma_n) > 1$ or $S^R(\alpha, \beta, \sigma_n) < 0$. In both cases, the factors $|t^R(\alpha, \beta, \sigma_n)| < |t^D(0, 1, \sigma_n)|$. This is the first conclusion of Corollary 9.2.2.

Next, it follows from the assumption (9.2.10) that $\frac{\beta}{\alpha} \leq \frac{\sigma_n}{c}$, $\forall n \geq 0$ due to $\sigma_0 \leq \sigma_n$. Then $-\alpha\sigma_n + \beta c \leq 0$. We obtain from (9.2.8) that $|S^R(\alpha, \beta, \sigma_n)| > 1$, which leads to the following inequality from (9.2.7) and (9.2.9)

$$|t^R(\alpha, \beta, \sigma_n)| = \frac{\left(\frac{a}{b}\right)^{2\sigma_n} - 1}{|S^R(\alpha, \beta, \sigma_n)| \left(\frac{a}{c}\right)^{2\sigma_n} + 1} < \frac{\left(\frac{a}{b}\right)^{2\sigma_n} - 1}{\left(\frac{a}{c}\right)^{2\sigma_n} + 1} = |t^N(1, 0, \sigma_n)|.$$

This is the second conclusion of Corollary 9.2.2. \blacksquare

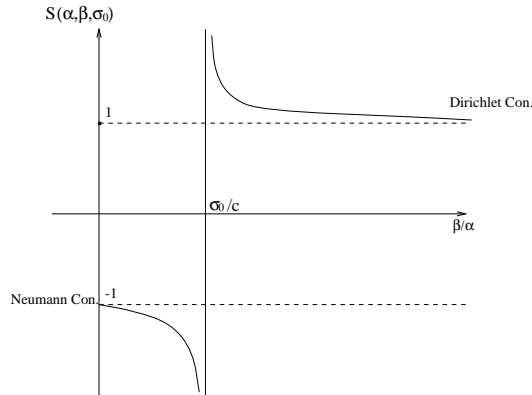


Figure 9.3: The curves of the function $S(\alpha, \beta, \sigma_0)$.

Corollaries 9.2.1 and 9.2.2 are extraordinary. We may explain the surprising results by the specific behavior of the functions $S(\alpha, \beta, \sigma_n)$ in (9.2.8). Consider the function

$$S(\alpha, \beta, \sigma_0) = \frac{\frac{\beta}{\alpha} + \frac{\sigma_0}{c}}{\frac{\beta}{\alpha} - \frac{\sigma_0}{c}}, \tag{9.2.11}$$

which is depicted in Figure 9.3. By noting the dominant reduction factor:

$$t(\alpha, \beta, \sigma_0) = \frac{\left(\frac{a}{b}\right)^{2\sigma_0} - 1}{S(\alpha, \beta, \sigma_0) \left(\frac{a}{c}\right)^{2\sigma_0} - 1},$$

the surprising conclusions in Corollaries 9.2.1 and 9.2.2 are reasonable.

Take Motz's problem as an example. When $\Theta = \pi$, $\sigma_n = n + 1/2$ and $\sigma_0 = 1/2$. Choose $c = 1/4$ (or $\sqrt{2}/4$) and $\alpha = 1$. Eq. (9.2.10) leads to

$$\beta \leq \frac{\sigma_0}{c} \alpha = 2 \text{ (or } \sqrt{2}\text{)}. \tag{9.2.12}$$

Note that when $c < b$ and n is large, the functions $S(\alpha, \beta, \sigma_n) \approx -1$, and $|t(\alpha, \beta, \sigma_n)| \approx \left| \left(\frac{c}{b}\right)^{2\sigma_n} \right| \ll 1$. The reduction factors to b_n with large n of all three boundary conditions are very small, and their differences are insignificant. This argument implies that the reduction factors of the leading coefficients b_i are dominant in the convergence rates of the mixed overlapping SAM. Therefore, we should focus on the reduction factor to the first leading coefficient b_0 in (9.2.5). From (9.2.11) and (9.2.12) it is better to choose

$$\beta = \frac{\sigma_0}{c} \alpha \in [\sqrt{2}, 2].$$

Usually, let $\alpha = 1$, a favorable Robin condition for this case is found as

$$\frac{\partial u}{\partial n} + \beta u = g_2 \text{ in } \Gamma_1, \quad \beta \in [\sqrt{2}, 2].$$

9.3 Different Boundary Conditions on Γ_1 and Γ_2

By the above encouraging results, we also consider the general conditions on the interior boundary Γ_2 of S_2 instead of (9.2.1), i.e.,

$$\alpha^* \frac{\partial u}{\partial n} + \beta^* u = g_2^* \text{ on } \Gamma_2, \quad (9.3.1)$$

where n is the exterior unit normal to ∂S_2 , $\alpha^* \geq 0$ and $\beta^* \geq 0$. Again, we define a Laplacian solution $\tilde{u}^{(1)}$ in S_1 , and suppose that the initial errors on Γ_2 are given by

$$\alpha^* \frac{\partial \varepsilon^{(1)}}{\partial n} + \beta^* \varepsilon^{(1)} = \alpha^* \frac{\partial \varepsilon^{(1)}(b, \theta)}{\partial r} + \beta^* \varepsilon^{(1)}(b, \theta) = \sum_{n=0}^{\infty} b_n \cos \sigma_n \theta. \quad (9.3.2)$$

Then we obtain the following Laplacian solutions in S_2 satisfying (9.1.1) and (9.3.2):

$$\varepsilon^{(2)}(r, \theta) = \sum_{n=0}^{\infty} \frac{b_n}{\left(\frac{\alpha^* \sigma_n}{b} + \beta^*\right)} \left(\frac{r}{b}\right)^{\sigma_n} \cos \sigma_n \theta.$$

Under the same general conditions (9.2.4) on Γ_1 , we can find the errors $\varepsilon^{(3)}$ in S_1 satisfying (9.1.1), (9.2.6) and (9.3.2). Through some manipulations, we obtain

$$\alpha^* \frac{\partial \varepsilon^{(3)}(b, \theta)}{\partial n} + \beta^* \varepsilon^{(3)}(b, \theta) = \sum_{n=0}^{\infty} b_n \tau(\alpha, \beta; \alpha^*, \beta^*, \sigma_n, b, c) \cos \sigma_n \theta,$$

where the coefficient reductions to b_n are given by

$$\tau(\alpha, \beta; \alpha^*, \beta^*; \sigma_n, b, c) = \frac{1 - P(\alpha^*, \beta^*, \sigma_n) \left(\frac{a}{b}\right)^{2\sigma_n}}{1 - S(\alpha, \beta, \sigma_n) \left(\frac{a}{c}\right)^{2\sigma_n}}. \quad (9.3.3)$$

The functions $S(\alpha, \beta, \sigma_n)$ are defined by (9.2.8), and the other functions in (9.3.3) are

$$P(\alpha^*, \beta^*, \sigma_n) = \frac{-\alpha^* \sigma_n + \beta^* b}{\alpha^* \sigma_n + \beta^* b}.$$

We also write this result as a proposition.

Proposition 9.3.1 *Let the conditions (9.3.1) on Γ_2 and (9.2.3) on Γ_1 be given. Then the reduction factors to coefficients b_n in the initial errors (9.3.2) are given by (9.3.3), after an iteration cycle of the mixed SAM.*

Corollary 9.3.1 *Let (9.1.5) and all conditions in Proposition 9.3.1 hold. Then the absolute reduction factors to b_n in (9.3.3) of the Dirichlet condition on Γ_2 are smaller than those of the Neumann condition on Γ_2 .*

Proof For the Dirichlet and Neumann conditions on Γ_2 , i.e., $\alpha^* = 0 \wedge \beta^* = 1$ and $\alpha^* = 1 \wedge \beta^* = 0$, the functions $P(0, 1, \sigma_n) = 1$ and $P(1, 0, \sigma_n) = -1$, respectively. We obtain the coefficient reductions

$$\tau^{R-D}(\alpha, \beta; 0, 1; \sigma_n, b, c) = \frac{1 - \left(\frac{a}{b}\right)^{2\sigma_n}}{1 - S(\alpha, \beta, \sigma_n) \left(\frac{a}{c}\right)^{2\sigma_n}},$$

and

$$\tau^{R-N}(\alpha, \beta; 1, 0; \sigma_n, b, c) = \frac{1 + \left(\frac{a}{b}\right)^{2\sigma_n}}{1 - S(\alpha, \beta, \sigma_n) \left(\frac{a}{c}\right)^{2\sigma_n}}.$$

The desired conclusion follows by

$$|\tau^{R-D}(\alpha, \beta; 0, 1; \sigma_n, b, c)| < |\tau^{R-N}(\alpha, \beta; 1, 0; \sigma_n, b, c)|. \quad \blacksquare$$

Below, we use the superscripts, $R-D$, to denote the different interior boundary conditions, where the Robin and Dirichlet conditions are assigned on Γ_1 and Γ_2 , respectively. The classic SAM is of the $D-D$ type of the interface boundary conditions.

Corollary 9.3.2 *Let (9.1.5) and all conditions in Proposition 9.3.1 hold. Then the absolute reduction factors to b_n in (9.3.3) of the Robin condition on Γ_2 with $\alpha^* > 0$ and $\beta^* > 0$ are smaller than those of the Neumann condition on Γ_2 . Moreover, if the parameters in (9.3.1) satisfy*

$$\frac{\alpha^*}{\beta^*} \leq q(\sigma_0) = \frac{b}{\sigma_0} \left\{ \left(\frac{a}{b}\right)^{2\sigma_0} - 1 \right\}, \quad (9.3.4)$$

the absolute reduction factors to all b_n of the Robin condition on Γ_2 are even smaller than those of the Dirichlet condition on Γ_2 .

Proof Since

$$|1 - P(\alpha^*, \beta^*, \sigma_n) \left(\frac{a}{b}\right)^{2\sigma_n}| < |1 + P(1, 0, \sigma_n) \left(\frac{a}{b}\right)^{2\sigma_n}|,$$

we have

$$|\tau^{R-R}(\alpha, \beta; \alpha^*, \beta^*; \sigma_n, b, c)| < |\tau^{R-N}(\alpha, \beta; 1, 0; \sigma_n, b, c)|.$$

This is the first desired conclusion of this corollary. To reach the second conclusion, it is sufficient to have the following bounds by noting (9.3.3),

$$\left| 1 - \frac{-\alpha^* \sigma_n + \beta^* b}{\alpha^* \sigma_n + \beta^* b} \left(\frac{a}{b}\right)^{2\sigma_n} \right| < \left| 1 - \left(\frac{a}{b}\right)^{2\sigma_n} \right|.$$

This is equivalent to

$$-\left[\left(\frac{a}{b}\right)^{2\sigma_n} - 1\right] < \left(\frac{a}{b}\right)^{2\sigma_n} \frac{b - \frac{\alpha^*}{\beta^*}\sigma_n}{b + \frac{\alpha^*}{\beta^*}\sigma_n} - 1 < \left(\frac{a}{b}\right)^{2\sigma_n} - 1. \quad (9.3.5)$$

Since $\frac{b - \frac{\alpha^*}{\beta^*}\sigma_n}{b + \frac{\alpha^*}{\beta^*}\sigma_n} < 1$, the right hand side of (9.3.5) obviously holds; the left hand side of (9.3.5) leads to

$$\frac{\alpha^*}{\beta^*} \leq q(\sigma_n) = \frac{b}{\sigma_n} \left\{ \left(\frac{a}{b}\right)^{2\sigma_n} - 1 \right\}.$$

The desired results (9.3.4) follow from $q(\sigma_0) \leq q(\sigma_n)$, because of the positive derivatives, $\frac{dq(\sigma_n)}{d\sigma_n} \geq 0$, shown below. In fact,

$$q'(\sigma_n) = \frac{dq(\sigma_n)}{d\sigma_n} = \frac{b}{\sigma_n^2} \left\{ \left(\frac{a}{b}\right)^{2\sigma_n} [2\sigma_n \ln\left(\frac{a}{b}\right) - 1] + 1 \right\} > 0, \quad \forall b < a.$$

The above inequality results from the fact that when $a = b$, $q'(\sigma_n) = 0$, and when $b < a$, $q'(\sigma_n) > 0$ since

$$\frac{dq'(\sigma_n)}{d\left(\frac{a}{b}\right)} = \frac{4b}{\sigma_n} \ln\left(\frac{a}{b}\right) \left(\frac{a}{b}\right)^{2\sigma_n - 1} > 0. \quad \blacksquare$$

Remark 9.3.1 Although Corollaries 9.2.1 and 9.2.2 are derived for the Dirichlet condition on Γ_2 , their conclusions are also valid for the general conditions on Γ_2 , because the arguments wherein also hold.

9.4 Special Cases of the Mixed SAMs

Now let us consider some special and important boundary conditions on Γ_1 and Γ_2 , to discuss the reduction factors to b_n and the overlapping effects.

Case I. The Dirichlet conditions on both Γ_1 and Γ_2 , i.e., $\alpha^* = \alpha = 0$ and $\beta^* = \beta = 1$. Then we have from (9.3.3)

$$|\tau_n^{D-D}| := |\tau^{D-D}(0, 1; 0, 1; \sigma_n, b, c)| = \frac{1 - \left(\frac{a}{b}\right)^{2\sigma_n}}{1 - \left(\frac{a}{c}\right)^{2\sigma_n}}.$$

Then $|\tau_n^{D-D}| < 1$ if and only if $c < b$. The overlapping is the necessary and sufficient condition for the convergent SAM. Moreover, the larger $(b - c)$ is, the smaller the factor $|\tau^{D-D}|$.

Case II. The Neumann condition on both Γ_1 and Γ_2 , i.e., $\alpha = \alpha^* = 1$ and $\beta = \beta^* = 0$. Then

$$|\tau_n^{N-N}| := |\tau^{N-N}(1, 0; 1, 0; \sigma_n, b, c)| = \frac{1 + \left(\frac{a}{b}\right)^{2\sigma_n}}{1 + \left(\frac{a}{c}\right)^{2\sigma_n}}.$$

The same conclusions as in Case I follow.

Case III. The Neumann condition on Γ_1 and Dirichlet condition on Γ_2 , i.e., $\alpha = 1 \wedge \beta = 0$ and $\alpha^* = 0 \wedge \beta^* = 1$. Then

$$|\tau_n^{N-D}| := |\tau^{N-D}(1, 0; 0, 1; \sigma_n, b, c)| = \frac{\left(\frac{a}{b}\right)^{2\sigma_n} - 1}{\left(\frac{a}{c}\right)^{2\sigma_n} + 1}.$$

The SAM converges if $b \leq c$. Note that even when $b = c$, the non-overlapping SAM is also convergent.

Case IV. The Dirichlet condition on Γ_1 and Neumann condition on Γ_2 , i.e., $\alpha = 0 \wedge \beta = 1$ and $\alpha^* = 1 \wedge \beta^* = 0$. Then

$$|\tau_n^{D-N}| := |\tau^{D-N}(0, 1; 1, 0; \sigma_n, b, c)| = \frac{\left(\frac{a}{b}\right)^{2\sigma_n} + 1}{\left(\frac{a}{c}\right)^{2\sigma_n} - 1}.$$

This is the worst situation in the SAM convergence. To guarantee the convergence, we need some minimal overlapping, i.e., $b - c \geq c_0 > 0$. Suppose $\Theta = \pi$ and $\sigma_n = n + 1/2$. Then to guarantee

$$|\tau^{D-N}(0, 1; 1, 0; \sigma_n, b, c)| < 1, \quad \forall n,$$

the relative overlap of S_1 and S_2 must satisfy the following condition

$$\frac{b - c}{b} > \frac{2c}{a}.$$

Otherwise, the SAM may be divergent.

Case V. The Neumann condition on Γ_1 but the Robin condition on Γ_2 , i.e., $\alpha = 1 \wedge \beta = 0$ and $\alpha^* > 0 \wedge \beta^* > 0$. Then we have from (9.3.3)

$$|\tau_n^{N-R}| := |\tau^{N-R}(1, 0; \alpha^*, \beta^*; \sigma_n, b, c)| = \frac{|1 - P(\alpha^*, \beta^*, \sigma_n)\left(\frac{a}{b}\right)^{2\sigma_n}|}{1 + \left(\frac{a}{c}\right)^{2\sigma_n}}.$$

Since $|P(\alpha^*, \beta^*, \sigma_n)| < 1$, then $|\tau_n^{N-R}| < 1$ even for $c = b$. Also it is easy to see $\frac{\partial |\tau_n^{N-R}|}{\partial c} > 0$. Therefore when c increases to b , i.e., the overlapping area decreases, $|\tau_n^{N-R}|$ increases, i.e., the convergence rates of the mixed SAM decline.

However, we should be cautious that if the mixed types, $D-R$ and $R-N$, are chosen, which resemble the type, $D-N$, in Case IV, because a minimal overlapping area is necessary for the SAM convergence.

Below let us consider the type, $R-R$, with equal parameters, $\alpha = \alpha^* = 1$ and $\beta = \beta^* > 0$. We have the following corollary.

Corollary 9.4.1 *Let (9.1.5) be given, $\alpha = \alpha^* = 1$ and $\beta = \beta^* > 0$. When $\Theta \leq \pi$, the SAM is always convergent.*

Proof We have from (9.3.3)

$$|\tau_n^{R-R}| = T \frac{|-\sigma_n + \beta c|}{|\sigma_n + \beta b|},$$

where

$$T = \left| \frac{\sigma_n [1 + (\frac{a}{b})^{2\sigma_n}] - \beta b [(\frac{a}{b})^{2\sigma_n} - 1]}{\sigma_n [1 + (\frac{a}{c})^{2\sigma_n}] + \beta c [(\frac{a}{c})^{2\sigma_n} - 1]} \right|.$$

Obviously, $|\frac{-\sigma_n + \beta c}{\sigma_n + \beta b}| < 1$. Then $T < 1$ if the following bounds hold:

$$\begin{aligned} -\{\sigma_n [1 + (\frac{a}{c})^{2\sigma_n}] + \beta c [(\frac{a}{c})^{2\sigma_n} - 1]\} &< \sigma_n [1 + (\frac{a}{b})^{2\sigma_n}] - \beta b [(\frac{a}{b})^{2\sigma_n} - 1] \\ &< \sigma_n \{ [1 + (\frac{a}{c})^{2\sigma_n}] + \beta c [(\frac{a}{c})^{2\sigma_n} - 1] \}. \end{aligned} \quad (9.4.1)$$

The left inequality of the above leads to

$$\begin{aligned} 0 &< 2\sigma_n + \sigma_n [(\frac{a}{c})^{2\sigma_n} + (\frac{a}{b})^{2\sigma_n}] \\ &+ \beta(b - c) + \beta a^{2\sigma_n} [(\frac{1}{c})^{2\sigma_n - 1} - (\frac{1}{b})^{2\sigma_n - 1}]. \end{aligned}$$

Since $\sigma_n = (n + \frac{1}{2}) \frac{\pi}{\Theta} \geq n + \frac{1}{2} \geq \frac{1}{2}$ by the assumption $\Theta \leq \pi$ and $c \leq b$, we have

$$\beta(b - c) + \beta a^{2\sigma_n} [(\frac{1}{c})^{2\sigma_n - 1} - (\frac{1}{b})^{2\sigma_n - 1}] \geq 0.$$

Then the left inequality of (9.4.2) holds because all the terms on the right hand side of the above are positive. Moreover, it is to see that the right hand side of (9.4.1) holds. Hence the reduction factors $|\tau_n^{R-R}| < 1$, this concludes the convergence of the SAM. ■

Again consider the different Robin conditions on Γ_1 and Γ_2 . Let $\alpha = \alpha^* = 1$ but $\beta > 0$ and $\beta^* > 0$. We may write from (9.3.3) the reduction factors to b_n as

$$\begin{aligned} |\tau_n^{R-R}| &= |\tau^{R-R}(1, \beta; 1, \beta^*; \sigma_n, b, c)| \\ &= \left| \frac{-\sigma_n + \beta c}{\sigma_n + \beta^* b} \right| \times \left| \frac{1 + (\frac{a}{b})^{2\sigma_n}}{1 + (\frac{a}{c})^{2\sigma_n}} \right| \times \left| \frac{1 - w_n(b)\beta^*}{1 + w_n(c)\beta} \right|, \end{aligned} \quad (9.4.2)$$

where the notation

$$w_n(b) = \frac{b (\frac{a}{b})^{2\sigma_n} - 1}{\sigma_n (\frac{a}{b})^{2\sigma_n} + 1}.$$

When $c < b$ and n is large, $|\tau_n^{R-R}| \approx O((\frac{c}{b})^{2\sigma_n}) \ll 1$. So the reduction factors of the leading coefficients b_n are dominant in the SAM convergence rates. To achieve a better

convergence, we may choose β and β^* to reduce, as small as possible, the errors for the first two leading coefficients, b_0 and b_1 respectively. From (9.4.2), we may choose

$$-\sigma_0 + \beta c = 0, \quad 1 - \beta^* w_1(b) = 0.$$

In the case of $b = c$ we may adopt the techniques in Douglas and Huang [134] by means of two cycles of parameters β_i and β_i^* .

Finally let us consider the non-overlapping SAM with $b = c$. Then the reduction factors are given from (9.4.2)

$$|\tau_n^{R-R}| = |\tau^{R-R}(1, \beta; 1, \beta^*; \sigma_n, b, b)| = \frac{[-1 + \beta \frac{b}{\sigma_n}][1 - w_n(b)\beta^*]}{[1 + \beta^* \frac{b}{\sigma_n}][1 + w_n(b)\beta]}. \quad (9.4.3)$$

Corollary 9.4.2 *Let $0 < c = b < a$ be given, and $\alpha = \alpha^* = 1$, $\beta > 0$ and $\beta^* > 0$. Then the absolute reductions factors to b_n are less than one, provided that*

$$\beta - \beta^* < [\sigma_n + \beta\beta^*bw_n(b)] \times [(\frac{a}{b})^{2\sigma_n} + 1]. \quad (9.4.4)$$

Proof To attain $|\tau_n^{R-R}| < 1$ in (9.4.3), it is sufficient to satisfy the following bounds,

$$-(1 + \beta^* \frac{b}{\sigma_n})(1 + \beta w_n(b)) < (1 - \beta \frac{b}{\sigma_n})[1 - \beta^* w_n(b)] < (1 + \beta^* \frac{b}{\sigma_n})[1 + \beta w_n(b)].$$

We only show the left inequality of the above inequalities, to give

$$(\beta - \beta^*)[\frac{b}{\sigma_n} - w_n(b)] < 2[1 + \frac{\beta\beta^*bw_n(b)}{\sigma_n}]. \quad (9.4.5)$$

Since

$$\frac{b}{\sigma_n} - w_n(b) = \frac{2b}{\sigma_n[(\frac{a}{b})^{2\sigma_n} + 1]},$$

the sufficient condition (9.4.4) is obtained from (9.4.5). ■

Corollary 9.4.2 implies that if $\beta^* \geq \beta$, Eq. (9.4.4) always holds. In other words, the Dirichlet portion in the Robin condition on Γ_2 is no less than that on Γ_1 , the non-overlapping SAM converges. For the same Robin conditions $\beta = \beta^*$, the convergence of Corollary 9.4.2 coincides with Corollary 9.4.1. This is just the case discussed in [134], with the reduction factors,

$$|\tau_n^{R-R}| = |\tau^{R-R}(1, \beta; 1, \beta; \sigma_n, b, b)| = \frac{(-\sigma_n + \beta b)[1 - w_n(b)\beta]}{(\sigma_n + \beta b)[1 + w_n(b)\beta]}.$$

Interesting numerical results are given in [302] for solving Motz's problems by combining the TM and the FDM, based on the interior boundary conditions in the SAM.

Chapter 10

Combinations with High Order FEMs

To solve Poisson's equation on a polygonal domain, the bi-Lagrange $p(\geq 2)$ -order FEMs (called the p -rectangles) are chosen. The global superconvergence $O(h^{p+2})$ in the H^1 norm was first derived in Lin and Yan [321] on the entire solution domain for smooth solutions, by means of an a posteriori polynomial interpolant of higher order. In this chapter, the *high* global superconvergence is applied to Poisson's equation with singularities. Let the solution domain S be split into S_1 and S_2 , where only S_2 includes a singular point. Suppose that the solution in S_1 is highly smooth. Then the Trefftz method (TM) using singular particular solutions and the $p(\geq 2)$ -rectangles may be used in S_2 and S_1 , respectively. In this chapter, we invoke the penalty plus hybrid techniques in Sections 3.5 and 8.4 to couple the TM and the $p(\geq 2)$ -rectangles, and derive almost the *best* global superconvergence $O(h^{p+2-\delta})$, $0 < \delta \ll 1$. When Adini's elements are used in S_1 instead of the p -rectangles, the *best* global superconvergence $O(h^{3.5})$ can be achieved. Some numerical experiments are carried out by the combination of the TM and Adini's elements, to verify the superconvergence $O(h^{3.5})$.

10.1 Introduction

In Li [291] only the linear and bilinear elements were discussed; in this chapter we intend to achieve *high* global superconvergence by using high order Lagrange FEMs and Adini's elements. There exist two kinds of superconvergence: *global* and *local interior pointwise*. The global superconvergence was reported in Krížek and Neittaanmäki [267] and Lin and Yan [321], and *local interior pointwise* superconvergence in Krížek and Neittaanmäki [266], MacKinnon and Carey [335], Nakao [361], Pehlivanov et al., [378], Wheeler and Whiteman [487], and Wahlbin [480, 481].

To solve singularity problems, let the solution domain S be split into two disjoint subdomains S_1 and S_2 . The $p(\geq 2)$ -order Lagrange rectangles (or simply $p(\geq 2)$ -rectangles) are used in S_1 where the solution is highly smooth, and the singular particular solutions are used in S_2 where the solution has a singularity. Coupling techniques play an important role in combining different numerical methods for solving elliptic equations. In a

recent study in [303, 225], the simplified hybrid techniques were chosen, to couple the $p(\geq 2)$ -order Lagrange rectangles in S_1 and the singular particular solutions in S_2 . The superclose $\|u_h - u_I\|_1 = O(h^{p+\frac{3}{2}})$ was obtained, where u_h is the approximate solution and u_I is the piecewise bi- p -order Lagrange polynomial interpolant of the true solution u . There is a loss of $O(h^{\frac{1}{2}})$ in superclose, compared with the best superclose $O(h^{p+2})$ given in [321]. Can we find better couple techniques to retain the best superclose $O(h^{p+2})$? To answer this question is an aim of this chapter. In this chapter, we employ the penalty plus hybrid techniques in Sections 3.5 and 8.4 to couple the different methods, and *almost* the *best* superclose estimate, $\|u_h - u_I\|_1 = O(h^{p+2-\delta})$, $0 < \delta \ll 1$, can be reached. Hence, by means of an a posteriori polynomial interpolant of order $p+2$ in S_1 , almost the *best* global superconvergence $O(h^{p+2-\delta})$ over the entire subdomains can also be achieved. The local superconvergence is also developed when the highly smooth solutions exist only in partial of S_1 . Moreover, when the Adini's elements are used in S_1 instead of p -rectangles, the superconvergence $O(h^{3.5})$ can be obtained, and verified by numerical experiments presented in this chapter. Here, we briefly mention the references of the penalty plus hybrid techniques, which are first proposed in Nitsche [363], and then developed in Arnold [5], Baker [21], Barrett and Elliott [26], Fairweather [150] and Li [291]. The materials in this chapter are adapted from Huang [223] and Huang and Li [224].

This chapter is organized as follows. The combined algorithm of the two methods is described in the next section. In Section 10.3, the $p(\geq 2)$ -rectangles are chosen in S_1 , to derive the global superconvergence $O(h^{p+2-\delta})$ of the solution derivatives, and local superconvergence is also discussed. In Section 10.4, the Adini's elements are chosen in S_1 , to yield the superconvergence $O(h^{3.5})$ of the solution derivatives. In Section 10.5, numerical experiments are provided for Motz's problem by the penalty plus hybrid combination of the TM and Adini's elements.

10.2 Combinations of TM and Lagrange FEMs

Consider Poisson's equation with the Dirichlet boundary condition:

$$\begin{aligned} -\Delta u &= -\left(\frac{\partial^2 u}{\partial x^2} + \frac{\partial^2 u}{\partial y^2}\right) = f(x, y) \quad \text{in } S, \\ u|_{\Gamma} &= 0, \quad \text{on } \Gamma, \end{aligned} \quad (10.2.1)$$

where S is a polygon and Γ is its boundary. Let S be divided by Γ_0 into two disjoint subregions, S_1 and S_2 , see Figure 10.1: $S = S_1 \cup S_2 \cup \Gamma_0$ and $S_1 \cap S_2 = \emptyset$. In this chapter we assume the following conditions.

- A1:** There exists a boundary singularity in S_2 , where $u \in H^{1+\alpha}(S_2)$ for $0 < \alpha < 1$.
A2: In S_2 , the true solution u can be spanned by particular solutions, $\{\Psi_i\}$, singular or analytical,

$$u = \Psi_0 + \sum_{i=1}^{\infty} a_i \Psi_i, \quad \text{in } \bar{S}_2, \quad (10.2.2)$$

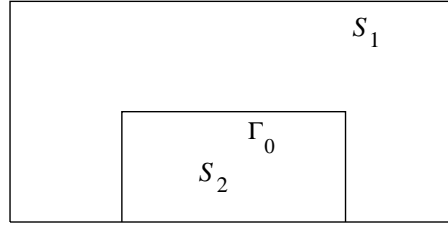


Figure 10.1: Partition of a rectangular domain.

where $\bar{S}_2 = S_2 \cup \partial S_2$, a_i are the expansion coefficients, and

$$-\Delta \Psi_0 = f, \quad \Delta \Psi_i = 0, \quad i \geq 1. \quad (10.2.3)$$

Also the particular solutions $\{\Psi_i\}$, $i = 1, 2, \dots$, are assumed completely and linearly independent.

A3: The expansion (10.2.2) converges exponentially. Denote

$$u_L = g_L(a_1, \dots, a_L) = \Psi_0 + \sum_{i=1}^L a_i \Psi_i,$$

then $u = u_L + R_L$, where the remainder

$$R_L = \sum_{i=L+1}^{\infty} a_i \Psi_i.$$

The exponential convergence rates imply

$$\max |R_L| = \max \left| \sum_{i=L+1}^{\infty} a_i \Psi_i \right| = O(e^{-\bar{c}L}), \quad \text{in } S_2,$$

where $\bar{c} > 0$ and $L \geq 1$.

A4: In S_1 , the solution u is highly smooth such that $u \in H^k(S_1)$, $k \geq 5$. Later, we may relax this assumption to $u \in H^k(D_1)$, $k \geq 5$, where D_1 is a subdomain of S_1 .

A5: S_1 is partitioned again into quasiuniform rectangular elements in 2×2 fashion shown in Figure 10.2¹, denoted by $S_1^h = \bigcup_{ij} \square_{ij}$, and h denotes the maximal boundary length of all \square_{ij} . The \square_{ij} are said to be *quasiuniform* if the following ratios are bounded,

$$\frac{h}{\min_{ij} \{h_i, k_j\}} \leq C,$$

where C is a constant independent of h .

¹When S_1 is not a rectangle, the triangulation is used, and the combinations with k -order FEMs are similar. However, only the superconvergence $O(h^{k+1})$ can be achieved.

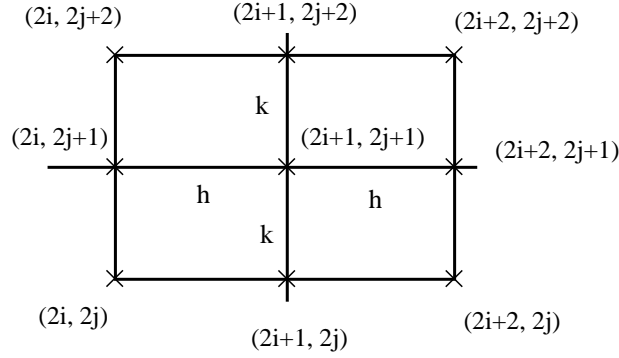


Figure 10.2: $\square_{2i+1, 2j+1}^{2 \times 2}$ in the 2×2 fashion of partition.

Based on **A1-A3**, we may choose the finite expansions

$$v^+ = f_L(\tilde{a}_1, \dots, \tilde{a}_L) = \Psi_0 + \sum_{i=0}^L \tilde{a}_i \Psi_i \quad (10.2.4)$$

as admissible functions, where Ψ_i are known and satisfy (10.2.3); but the coefficients \tilde{a}_i are unknown, to be sought by the combined algorithms given below.

Based on **A4-A5**, we will choose the piecewise Lagrange interpolation polynomial v_p on S_1 , and follow the superconvergence techniques of Lin and Yan [321] and Krížek and Neittaanmäki [267], to achieve the global superconvergence on the entire domain. The effort in this chapter is to combine the TM using the singular particular solutions and the high order FEMs, to solve effectively the singularity problems.

The admissible functions in S should be chosen as

$$v = \begin{cases} v^- = v_p & \text{in } \bar{S}_1, \\ v^+ = g_L(\tilde{a}_1, \dots, \tilde{a}_L) & \text{in } \bar{S}_2, \end{cases}$$

where $f_L(\tilde{a}_1, \dots, \tilde{a}_L)$ are given in (10.2.4), and v_p are the piecewise bi- p -order Lagrange polynomials.

In this chapter we consider the Lagrange elements with order $p(\geq 2)$ on rectangles. Based on [321, 227], the polynomial interpolant are designed sophisticatedly by means of the solution u at the vertices of \square_{ij} , the integrals of u along edges $\partial \square_{ij}$, and the integrals of u on the \square_{ij} . We call them the point-line-area elements (or variables). In the traditional $p(\geq 2)$ -rectangles in [105], only the nodal elements (or point variables) are used. We may obtain the point-line-area elements from the pure point variables through a matrix transformation.

The piecewise interpolation polynomials u_I^p are formulated as follows.

$$u_I^p(Z_i) = u(Z_i), \quad i = 1, 2, 3, 4.$$

When $p \geq 2$, more equations are satisfied:

$$\int_{\ell_r \cap \square_{ij}} (u_I^p - u)v \, d\ell = 0, \quad \forall v \in P_{p-2}(\ell_r), \quad r = 1, 2, 3, 4, \quad (10.2.5)$$

$$\int_{\square_{ij}} (u_I^p - u)v \, ds = 0, \quad \forall v \in Q_{p-2}(\square_{ij}), \quad (10.2.6)$$

where ℓ_r are the edges of \square_{ij} , and $P_p(x)$ and $Q_p(x, y)$ are the polynomials of order p defined by

$$P_p(x) = \sum_{i=0}^p a_i x^i, \quad Q_p(x, y) = \sum_{i,j=0}^p a_{ij} x^i y^j.$$

Construct the interpolant of u of (10.2.1):

$$u_{I,L} = \begin{cases} u_I^p, & \text{in } \bar{S}_1, \\ u_L = g_L(a_1, \dots, a_L), & \text{in } \bar{S}_2. \end{cases} \quad (10.2.7)$$

We choose the specific rules of integration,

$$\widehat{\int_0^1} uv = \int_0^1 uv, \quad \forall u, v \in P_p. \quad (10.2.8)$$

Also denote by V_h^* and V_h^0 the finite collections of the functions satisfying $v|_\Gamma = 0$ of

$$v_h = \begin{cases} v_p, & \text{in } \bar{S}_1, \\ v_L = \Psi_0 + \sum_{i=1}^L \tilde{a}_i \Psi_i, & \text{in } \bar{S}_2, \end{cases} \quad (10.2.9)$$

respectively.

In [303, 225], the simplified hybrid techniques are used to couple the TM and the $p(\geq 2)$ -rectangles. Unfortunately, there is a loss of $O(h^{\frac{1}{2}})$ in superclose [303, 225]. In this chapter we invoke the penalty plus hybrid techniques in Sections 3.5 and 8.4: To seek $u_h \in V_h^*$ such that

$$\widehat{A}_h(u_h, v) = \widehat{f}(v), \quad \forall v \in V_h^0, \quad (10.2.10)$$

where

$$\widehat{A}_h(u, v) = \iint_{S_1} \nabla u \cdot \nabla v + \iint_{S_2} \nabla u \cdot \nabla v + \widehat{D}_h(u, v) + \widehat{E}_h(u, v), \quad (10.2.11)$$

$$\widehat{f}(v) = \iint_{S_1} f v + \iint_{S_2} f v, \quad (10.2.12)$$

$$\widehat{D}_h(u, v) = \frac{P_c}{h^{2\sigma}} \int_{\Gamma_0} (u^+ - u^-)(v^+ - v^-), \quad (10.2.13)$$

$$\widehat{E}_h(u, v) = - \int_{\Gamma_0} \frac{\partial u^+}{\partial n} (v^+ - v^-) - \int_{\Gamma_0} \frac{\partial v^+}{\partial n} (u^+ - u^-). \quad (10.2.14)$$

$\widehat{D}_h(u, v)$ and $\widehat{E}_h(u, v)$ are the penalty and hybrid integrals respectively, and $P_c(> 0)$, $\sigma(> 0)$ are the parameters. In (10.2.12) – (10.2.14) we choose the rules of integration:

$$\int_{\Gamma_0} u v = \int_{\Gamma_0} \hat{u} \hat{v}, \quad \iint_{S_1} f v = \iint_{S_1} \hat{f} \hat{v},$$

where \hat{u} is the piecewise p -order Lagrange polynomial interpolant of u . We define the appropriate norm

$$\overline{\|v\|}_H = \{\|v\|_{1,S_1}^2 + \|v\|_{1,S_2}^2 + \frac{1}{h^{2\sigma}} \overline{\|v^+ - v^-\|}_{0,\Gamma_0}^2\}^{\frac{1}{2}}, \quad (10.2.15)$$

where

$$\overline{\|v\|}_{0,\Gamma_0}^2 = \int_{\Gamma_0} \hat{v}^2. \quad (10.2.16)$$

First let us give a basic theorem.

Theorem 10.2.1 (Basic Theorem) *Let \square_{ij} be quasiuniform. Assume that the uniformly V_h^0 -elliptic inequality holds,*

$$C_0 \overline{\|v\|}_H^2 \leq \widehat{A}_h(v, v), \quad \forall v \in V_h^0, \quad (10.2.17)$$

where $C_0(> 0)$ is a constant independent of h . Then there exists a constant C independent of h such that

$$\begin{aligned} \overline{\|u_h - u_{I,L}\|}_H &\leq C \sup_{w \in V_h^0} \frac{1}{\overline{\|w\|}_H} \left\{ \left| \iint_{S_1} \nabla(u - u_I) \cdot \nabla w \right| + \left| \iint_{S_2} \nabla(u - u_L) \cdot \nabla w \right| \right. \\ &\quad + \left| \left(\iint_{S_1} - \widehat{\iint}_{S_1} \right) f w \right| + \left| \left(\int_{\Gamma_0} - \widehat{\int}_{\Gamma_0} \right) \frac{\partial u}{\partial n} (w^+ - w^-) \right| \\ &\quad \left. + \left| \widehat{D}_h(u - u_{I,L}, w) \right| + \left| \widehat{E}_h(u - u_{I,L}, w) \right| \right\}, \end{aligned} \quad (10.2.18)$$

where u_h and u are the solutions of (10.2.10) and (10.2.1) respectively, and $u_{I,L}$ is the interpolant (10.2.7) of u .

Proof For the true solution, we have

$$\widehat{A}_h(u, v) = \left(\int_{\Gamma_0} - \widehat{\int}_{\Gamma_0} \right) \frac{\partial u^+}{\partial n} (v^+ - v^-) + \iint_{S_1} f v + \iint_{S_2} f v,$$

which leads to

$$\widehat{A}_h(u - u_h, v) = \left(\int_{\Gamma_0} - \widehat{\int}_{\Gamma_0} \right) \frac{\partial u^+}{\partial n} (v^+ - v^-) + \left(\iint_{S_1} - \widehat{\iint}_{S_1} \right) f v.$$

Let $w = u_h - u_{I,L} \in V_h^0$, then we obtain from the assumption (10.2.17)

$$\begin{aligned} C_0 \overline{\|w\|_H^2} &\leq \widehat{A}_h(u_h - u_{I,L}, w) \\ &= \widehat{A}_h(u - u_{I,L}, w) - \left(\int_{\Gamma_0} - \widehat{\int}_{\Gamma_0} \right) \frac{\partial u}{\partial n} (w^+ - w^-) - \left(\iint_{S_1} - \widehat{\iint}_{S_1} \right) f w \\ &\leq \left| \widehat{A}_h(u - u_{I,L}, w) \right| + \left| \left(\int_{\Gamma_0} - \widehat{\int}_{\Gamma_0} \right) \frac{\partial u}{\partial n} (w^+ - w^-) \right| + \left| \left(\iint_{S_1} - \widehat{\iint}_{S_1} \right) f w \right|. \end{aligned}$$

Hence, we have

$$\begin{aligned} \overline{\|u_h - u_{I,L}\|_H} &\leq C \frac{1}{\overline{\|w\|_H}} \left\{ \left| \widehat{A}_h(u - u_{I,L}, w) \right| + \left| \left(\int_{\Gamma_0} - \widehat{\int}_{\Gamma_0} \right) \frac{\partial u}{\partial n} (w^+ - w^-) \right| \right. \\ &\quad \left. + \left| \left(\iint_{S_1} - \widehat{\iint}_{S_1} \right) f w \right| \right\}. \end{aligned} \quad (10.2.19)$$

Also from (10.2.11),

$$\begin{aligned} \left| \widehat{A}_h(u - u_{I,L}, w) \right| &\leq \left| \iint_{S_1} \nabla(u - u_I) \cdot \nabla w \right| + \left| \iint_{S_2} \nabla(u - u_L) \cdot \nabla w \right| \\ &\quad + \left| \widehat{D}_h(u - u_{I,L}, w) \right| + \left| \widehat{E}_h(u - u_{I,L}, w) \right|. \end{aligned} \quad (10.2.20)$$

The desired result (10.2.18) follows from (10.2.19) and (10.2.20). ■

10.3 Global Superconvergence

We will derive the bounds of all terms on the right hand of (10.2.18) in Theorem 10.2.1. First define a semi-norm

$$\overline{|v^+ - v^-|}_{1, \Gamma_0} = |\hat{v}^+ - \hat{v}^-|_{1, \Gamma_0},$$

where \hat{v} is the piecewise p -order polynomial interpolant of v . We have the following lemma.

Lemma 10.3.1 *Suppose that there exists a constant $\nu(> 0)$ such that*

$$\|v^+\|_{k,\Gamma_0} \leq CL^{k\nu} \|v^+\|_{0,\Gamma_0}, \quad k = 1, 2, \quad v \in V_h^0. \quad (10.3.1)$$

Then there exists the bound,

$$\|v^-\|_{1,\Gamma_0} \leq C \{L^\nu + hL^{2\nu} + h^{\sigma-1}\} \overline{\|v\|}_H. \quad (10.3.2)$$

Proof We have from (10.2.16) and (10.3.1)

$$\begin{aligned} \|v^-\|_{1,\Gamma_0} &\leq \|v^+\|_{1,\Gamma_0} + \|v^+ - v^-\|_{1,\Gamma_0} \\ &\leq CL^\nu \|v^+\|_{0,\Gamma_0} + \overline{\|v^+ - v^-\|}_{1,\Gamma_0} + \|v^+ - \hat{v}^+\|_{1,\Gamma_0} + \|v^- - \hat{v}^-\|_{1,\Gamma_0}. \end{aligned} \quad (10.3.3)$$

Note that $v^- = \hat{v}^-$ in S_1 , we have $\|v^- - \hat{v}^-\|_{1,\Gamma_0} = 0$. Moreover, since \hat{v}^+ are piecewise p -order polynomials, there exists the inverse inequality:

$$\begin{aligned} \overline{\|v^+ - v^-\|}_{1,\Gamma_0} &= \|\hat{v}^+ - v^-\|_{1,\Gamma_0} \leq Ch^{-1} \|\hat{v}^+ - v^-\|_{0,\Gamma_0} \\ &= Ch^{-1} \overline{\|v^+ - v^-\|}_{0,\Gamma_0} \leq Ch^{\sigma-1} \overline{\|v\|}_H. \end{aligned} \quad (10.3.4)$$

Also we have from (10.3.1)

$$\begin{aligned} \|v^+ - \hat{v}^+\|_{1,\Gamma_0} &\leq Ch \|v^+\|_{2,\Gamma_0} \leq ChL^{2\nu} \|v^+\|_{0,\Gamma_0} \\ &\leq ChL^{2\nu} \|v^+\|_{1,S_2} \leq ChL^{2\nu} \overline{\|v\|}_H. \end{aligned} \quad (10.3.5)$$

Combining (10.3.3) – (10.3.5) yields the desired result (10.3.2). ■

Lemma 10.3.2 *Let (10.3.1) be given. Then there exists the bound,*

$$\begin{aligned} &\left| \iint_{S_1} \nabla(u - u_I) \nabla w \right| \\ &\leq Ch^{p+2} \|u\|_{p+3,S_1} (1 + L^\nu + hL^{2\nu} + h^{\sigma-1}) \overline{\|w\|}_H. \end{aligned} \quad (10.3.6)$$

Proof From [321, 227], we have

$$\left| \iint_{S_1} \nabla(u - u_I) \nabla w \right| \leq Ch^{p+2} \left\{ \|u\|_{p+3,S_1} \|w^-\|_{1,S_1} + \left| \frac{\partial u}{\partial n} \right|_{p+1,\Gamma_0} \|w^-\|_{1,\Gamma_0} \right\}.$$

The desired result (10.3.6) follows directly from Lemma 10.3.1 and $|\frac{\partial u}{\partial n}|_{p+1,\Gamma_0} \leq C \|u\|_{p+3,S_1}$. ■

Lemma 10.3.3 *Suppose there exists a constant $\nu(> 0)$ such that*

$$\left| \frac{\partial w^+}{\partial n} \right|_{k, \Gamma_0} \leq CL^{(k+1)\nu} \|w^+\|_{1, S_2}, \quad k = 0, 1, \quad w \in V_h^0. \quad (10.3.7)$$

Then there exist the bounds,

$$\left| \widehat{D}_h(u - u_{I,L}, w) \right| \leq Ch^{-\sigma} \overline{\|R_L\|_{0, \Gamma_0}} \overline{\|w\|_H}, \quad (10.3.8)$$

and

$$\begin{aligned} & \left| \widehat{E}_h(u - u_{I,L}, w) \right| \\ & \leq C \left\{ h^\sigma \left\| \frac{\partial R_L}{\partial n} \right\|_{0, \Gamma_0} + (L^\nu + hL^{2\nu}) \overline{\|R_L\|_{0, \Gamma_0}} \right\} \overline{\|w\|_H}, \end{aligned} \quad (10.3.9)$$

where the remainder $R_L = u - u_L$ in S_2 .

Proof Since $\widehat{\int}_{\Gamma_0} (u - u_I)(w^+ - w^-) = 0$ in view of (10.2.8), we have from (10.2.13) and (10.2.16),

$$\begin{aligned} |\widehat{D}_h(u - u_{I,L}, w)| &= \frac{P_c}{h^{2\sigma}} \left| \widehat{\int}_{\Gamma_0} ((u_L^+ - u) + (u - u_I^-))(w^+ - w^-) \right| \\ &= \frac{P_c}{h^{2\sigma}} \left| \widehat{\int}_{\Gamma_0} (u_L^+ - u)(w^+ - w^-) \right| \leq \frac{P_c}{h^{2\sigma}} \|\widehat{R}_L\|_{0, \Gamma_0} \overline{\|w^+ - w^-\|_{0, \Gamma_0}} \\ &\leq Ch^{-\sigma} \|\widehat{R}_L\|_{0, \Gamma_0} \overline{\|w\|_H} = Ch^{-\sigma} \overline{\|R_L\|_{0, \Gamma_0}} \overline{\|w\|_H}. \end{aligned}$$

This is the first estimate (10.3.8). Next we show (10.3.9). We have from (10.2.14)

$$\begin{aligned} \widehat{E}_h(u - u_{I,L}, w) &= - \widehat{\int}_{\Gamma_0} \left(\frac{\partial u^+}{\partial n} - \frac{\partial u_L^+}{\partial n} \right) (w^+ - w^-) \\ &\quad + \widehat{\int}_{\Gamma_0} \frac{\partial w^+}{\partial n} (u_L^+ - u + u - u_I^-). \end{aligned} \quad (10.3.10)$$

There exists the bound,

$$\begin{aligned} \left| \widehat{\int}_{\Gamma_0} \left(\frac{\partial u^+}{\partial n} - \frac{\partial u_L^+}{\partial n} \right) (w^+ - w^-) \right| &\leq \left\| \frac{\partial R_L}{\partial n} \right\|_{0, \Gamma_0} \overline{\|w^+ - w^-\|_{0, \Gamma_0}} \\ &\leq Ch^\sigma \left\| \frac{\partial R_L}{\partial n} \right\|_{0, \Gamma_0} \overline{\|w\|_H} = Ch^\sigma \overline{\left\| \frac{\partial R_L}{\partial n} \right\|_{0, \Gamma_0}} \overline{\|w\|_H}. \end{aligned} \quad (10.3.11)$$

Moreover, we obtain

$$\begin{aligned}
& \left| \widehat{\int}_{\Gamma_0} \frac{\partial w^+}{\partial n} ((u_L^+ - u) + (u - u_I^-)) \right| \\
&= \left| \widehat{\int}_{\Gamma_0} \frac{\partial w^+}{\partial n} (u_L^+ - u) \right| \leq \|\widehat{R}_L\|_{0,\Gamma_0} \left\| \frac{\partial w^+}{\partial n} \right\|_{0,\Gamma_0} \\
&= \overline{\|R_L\|_{0,\Gamma_0}} \overline{\left\| \frac{\partial w^+}{\partial n} \right\|_{0,\Gamma_0}}.
\end{aligned} \tag{10.3.12}$$

From assumption (10.3.7) we have

$$\begin{aligned}
\left\| \frac{\partial \widehat{w}^+}{\partial n} \right\|_{0,\Gamma_0} &\leq \left\| \frac{\partial w^+}{\partial n} \right\|_{0,\Gamma_0} + \left\| \frac{\partial w^+}{\partial n} - \frac{\partial \widehat{w}^+}{\partial n} \right\|_{0,\Gamma_0} \\
&\leq CL^\nu \|w^+\|_{1,S_2} + Ch \left| \frac{\partial w^+}{\partial n} \right|_{1,\Gamma_0} \\
&\leq C(L^\nu + hL^{2\nu}) \|w\|_{1,S_2} \leq C(L^\nu + hL^{2\nu}) \overline{\|w\|_H}.
\end{aligned} \tag{10.3.13}$$

Combining (10.3.10) – (10.3.13) yields

$$\begin{aligned}
& \left| \widehat{E}_h(u - u_{I,L}, w) \right| \\
&\leq C \left\{ h^\sigma \overline{\left\| \frac{\partial R_L}{\partial n} \right\|_{0,\Gamma_0}} + (L^\nu + hL^{2\nu}) \overline{\|R_L\|_{0,\Gamma_0}} \right\} \overline{\|w\|_H}.
\end{aligned}$$

This is (10.3.9). ■

Lemma 10.3.4 *Let (10.3.1) hold for $k \leq p + 1$. There exists the bound,*

$$\begin{aligned}
& \left| \left(\int_{\Gamma_0} - \widehat{\int}_{\Gamma_0} \right) \frac{\partial u}{\partial n} (w^+ - w^-) \right| \\
&\leq C \left\{ h^{p+2} L^{(p+1)\nu} \left| \frac{\partial u}{\partial n} \right|_{1,\Gamma_0} + h^{p+1+\sigma} \left| \frac{\partial u}{\partial n} \right|_{p+1,\Gamma_0} \right\} \overline{\|w\|_H}.
\end{aligned} \tag{10.3.14}$$

Proof Since $xy - \hat{x}\hat{y} = x(y - \hat{y}) + (x - \hat{x})\hat{y}$, we have

$$\begin{aligned}
& \left(\int_{\Gamma_0} - \widehat{\int}_{\Gamma_0} \right) \frac{\partial u}{\partial n} (w^+ - w^-) \\
&= \int_{\Gamma_0} \frac{\partial u}{\partial n} (w^+ - w^- - \hat{w}^+ + \hat{w}^-) + \int_{\Gamma_0} \left(\frac{\partial u}{\partial n} - \frac{\partial \hat{u}}{\partial n} \right) (\hat{w}^+ - \hat{w}^-).
\end{aligned} \tag{10.3.15}$$

Then we have

$$\begin{aligned} \left| \int_{\Gamma_0} \left(\frac{\partial u}{\partial n} - \widehat{\frac{\partial u}{\partial n}} \right) (\hat{w}^+ - \hat{w}^-) \right| &\leq C \left\| \frac{\partial u}{\partial n} - \widehat{\frac{\partial u}{\partial n}} \right\|_{0,\Gamma_0} \overline{\|w^+ - w^-\|}_{0,\Gamma_0} \\ &\leq Ch^{p+1} \left| \frac{\partial u}{\partial n} \right|_{p+1,\Gamma_0} \overline{\|w^+ - w^-\|}_{0,\Gamma_0} \leq Ch^{p+1+\sigma} \left| \frac{\partial u}{\partial n} \right|_{p+1,\Gamma_0} \overline{\|w\|}_H. \end{aligned} \quad (10.3.16)$$

For $p \geq 2$, there exists the equality from (10.2.5)

$$\int_{\Gamma_0} (u - u_I)v = \sum_{ij} \int_{\ell_{ij}} (u - u_I)v = 0, \quad \forall v \in P_{p-2}, \quad (10.3.17)$$

where P_{p-2} are the piecewise polynomials of order $p-2$ on edges $\ell_{ij} = \Gamma_0 \cap \square_{ij}$. Choose the piecewise constant with the mean $\frac{\partial u}{\partial n}|_{\ell_{ij}} = \int_{\ell_{ij}} \frac{\partial u}{\partial n} / |\ell_{ij}|$, then $\int_{\Gamma_0} \frac{\partial u}{\partial n} (w^+ - \hat{w}^+) = 0$. We have from (10.3.17) and (10.3.1) for $k \leq p+1$

$$\begin{aligned} \left| \int_{\Gamma_0} \frac{\partial u}{\partial n} (w^+ - w^- - \hat{w}^+ + \hat{w}^-) \right| &= \left| \int_{\Gamma_0} \frac{\partial u}{\partial n} (w^+ - \hat{w}^+) \right| \\ &\leq \left| \int_{\Gamma_0} \left(\frac{\partial u}{\partial n} - \overline{\frac{\partial u}{\partial n}} \right) (w^+ - \hat{w}^+) \right| + \left| \int_{\Gamma_0} \overline{\frac{\partial u}{\partial n}} (w^+ - \hat{w}^+) \right| \\ &= \left| \int_{\Gamma_0} \left(\frac{\partial u}{\partial n} - \overline{\frac{\partial u}{\partial n}} \right) (w^+ - \hat{w}^+) \right| \leq Ch \left| \frac{\partial u}{\partial n} \right|_{1,\Gamma_0} h^{p+1} |w^+|_{p+1,\Gamma_0} \\ &\leq Ch^{p+2} \left| \frac{\partial u}{\partial n} \right|_{1,\Gamma_0} L^{(p+1)\nu} \|w^+\|_{0,\Gamma_0} \leq Ch^{p+2} L^{(p+1)\nu} \left| \frac{\partial u}{\partial n} \right|_{1,\Gamma_0} \|w\|_{1,S_2} \\ &\leq Ch^{p+2} L^{(p+1)\nu} \left| \frac{\partial u}{\partial n} \right|_{1,\Gamma_0} \overline{\|w\|}_H. \end{aligned} \quad (10.3.18)$$

Combining (10.3.15), (10.3.16) and (10.3.18) yields the desired result (10.3.14). ■

Moreover, we have

$$\left| \iint_{S_2} \nabla(u - u_L) \nabla w \right| \leq C |R_L|_{1,S_2} \overline{\|w\|}_H. \quad (10.3.19)$$

Denote the piecewise constant interpolant \bar{w} in S_1 with the mean $\iint_{\square_{ij}} w / |\square_{ij}|$. We obtain from (10.2.6) that $\iint_{S_1} (f - f_I) \bar{w} = 0$ for $p \geq 2$. Hence we have

$$\begin{aligned} \left| \left(\iint_{S_1} - \widehat{\iint_{S_1}} \right) f w \right| &= \left| \iint_{S_1} (f - f_I) w \right| \\ &= \left| \iint_{S_1} (f - f_I) (w - \bar{w}) \right| \leq \|f - f_I\|_{0,S_1} \|w - \bar{w}\|_{0,S_1} \\ &\leq Ch^{p+1} |f|_{p+1,S_1} \times h |w|_{1,S_1} \leq Ch^{p+2} |f|_{p+1,S_1} \overline{\|w\|}_H. \end{aligned} \quad (10.3.20)$$

Based on Theorem 10.2.1, Lemmas 10.3.2 – 10.3.4, (10.3.19) and (10.3.20), we obtain the following theorem.

Theorem 10.3.1 *Let A1–A5, (10.2.17), (10.3.1) for $k \leq p + 1$ and (10.3.7) hold. There exists the error bound,*

$$\begin{aligned} \overline{\|u_h - u_{I,L}\|_H} \leq \varepsilon = C \{ & h^{p+2} \|u\|_{p+3, S_1} (1 + L^\nu + hL^{2\nu} + h^{\sigma-1}) \\ & + |R_L|_{1, S_2} + h^{p+2} |f|_{p+1, S_1} + (L^\nu + hL^{2\nu} + h^{-\sigma}) \overline{\|R_L\|_{0, \Gamma_0}} \\ & + h^\sigma \left\| \frac{\partial R_L}{\partial n} \right\|_{0, \Gamma_0} + h^{p+2} L^{(p+1)\nu} \left| \frac{\partial u}{\partial n} \right|_{1, \Gamma_0} + h^{p+1+\sigma} \left| \frac{\partial u}{\partial n} \right|_{p+1, \Gamma_0} \}. \end{aligned}$$

Corollary 10.3.1 *Let all conditions in Theorem 10.3.1 hold. Suppose $u \in H^{p+3}(S_1)$, $f \in H^{p+1}(S_1)$, $\sigma \geq 1$, and $L = O(|\ln h|)$ such that*

$$\begin{aligned} |R_L|_{1, S_2} &= O(h^{p+2}), \quad \overline{\|R_L\|_{0, \Gamma_0}} = O(h^{p+2+\sigma}), \\ \left\| \frac{\partial R_L}{\partial n} \right\|_{0, \Gamma_0} &= O(h^{p+2-\sigma}), \end{aligned}$$

there exists the superclose

$$\overline{\|u_h - u_{I,L}\|_H} = O(h^{p+2-\delta}),$$

where $0 < \delta \ll 1$.

In Theorem 10.3.1 and Corollary 10.3.1, the assumption $u \in H^{p+3}(S_1)$ is severe in application. In Huang [223], the local superconvergence of the combination is explored, by following the arguments in Xu and Zhou [495].

Remark 10.3.1 *For Theorem 10.3.1, two inverse inequalities, Eq. (10.3.1) for $k \leq p + 1$ and Eq. (10.3.7), hold for a polygon S_2 . Here we only give a brief argument of their validity. For polynomials v^+ of order L , Eq. (10.3.1) holds for $\nu = 2$. Let $\Gamma_0 = \cup_i \Gamma_0^i$, where Γ_0^i is a straight line segment, and let v^+ on Γ_0^i be expanded into the Legendre polynomials. Based on their orthogonality, Eq. (10.3.1) is proved for $\nu = 2$ in [291], p. 161. Next, suppose that S_2 is a polygon. The argument for (10.3.7) is given in Section 5.5 of Chapter 5 for polynomials, to prove $\nu = 2$. For a sectorial domain S_2 , when the particular solutions v^+ are chosen suitably, Eqs. (10.3.1) and (10.3.7) can be shown with $\nu = 1$. Therefore we may assume that in general, Eqs. (10.3.1) and (10.3.7) hold with $1 \leq \nu \leq 2$.*

10.4 Adini's Elements

In this section, we discuss again the penalty plus hybrid method, but choose the Adini's elements in S_1 instead of p -rectangles. We add two more assumptions.

A6: Let $S_1 = \bigcup_{ij} \square_{ij}$, where all \square_{ij} are *uniform* rectangles in 2×2 fashion. The rectangles \square_{ij} are said to be *uniform* if \square_{ij} are quasiuniform and $h_i = h$ and $k_j = k$, where we assume $h \geq k$.

A7: Choose the finite dimensional space

$$v_p \in V_A \equiv \left\{ v \in H^1(S), v|_{\square_{ij}} \in \widehat{P}_3, v_x, v_y \text{ are continuous at all vertices of } \square_{ij} \right. \\ \left. \text{and } v|_{\partial S_1 \cap \Gamma} = 0 \right\},$$

where

$$\widehat{P}_3 = \text{span}\{1, x, y, x^2, y^2, xy, x^3, y^3, x^3y, xy^2, x^2y, xy^3\}.$$

The spaces V_h^* and V_h^0 are similarly defined as (10.2.9), where v_A is given in **A7**. The polynomial interpolant u_I^A of u in S_1 can be formulated by u, u_x and u_y at four corners. Define the following interpolant of solution u ,

$$u_{I,L}^A = \begin{cases} u_I^- = u_I^A, & \text{in } \overline{S}_1, \\ u_L^+ = f_L(a_1, \dots, a_L), & \text{in } \overline{S}_2. \end{cases}$$

The penalty plus hybrid combined method is designed to seek $u_h^A \in V_h^*$ such that

$$\widehat{A}_h(u_h^A, v) = \widehat{f}(v), \quad \forall v \in V_h^0,$$

where $\widehat{A}_h(u, v)$ is given in (10.2.11). The rule of integration is given by

$$\widehat{\int}_{\Gamma_0} uv = \int_{\Gamma_0} \widehat{u} \widehat{v}, \quad (10.4.1)$$

where \widehat{u} is the piecewise cubic Hermite polynomial interpolant of u .

Theorem 10.4.1 *Let **A1–A7**, (10.2.17), (10.3.1) for $k \leq 4$ and (10.3.7) hold. Then there exists the bound,*

$$\overline{\|u_h^A - u_{I,L}\|_H} \leq C \{ (h^{3.5} + h^4 L^{4\nu} + h^{3+\sigma}) \|u\|_{5,S_1} + h^4 \|f\|_{4,S_1} \\ + |R_L|_{1,S_2} + (L^\nu + hL^{2\nu} + h^{-\sigma}) \overline{\|R_L\|_{0,\Gamma_0}} + h^\sigma \overline{\left\| \frac{\partial R_L}{\partial n} \right\|_{0,\Gamma_0}} \}. \quad (10.4.2)$$

Proof We obtain from Theorem 10.2.1,

$$\overline{\|u_h^A - u_{I,L}^A\|_H} \leq C \sup_{w \in V_h^0} \frac{1}{\|w\|_H} \left\{ \left| \iint_{S_1} \nabla(u - u_I^A) \cdot \nabla w \right| + \left| \iint_{S_2} \nabla(u - u_L) \cdot \nabla w \right| \right. \\ \left. + \left| \left(\iint_{S_1} - \widehat{\iint}_{S_1} \right) f w \right| + \left| \left(\widehat{\int}_{\Gamma_0} - \int_{\Gamma_0} \right) \frac{\partial u}{\partial n} (w^+ - w^-) \right| \right. \\ \left. + |\widehat{D}_h(u - u_{I,L}^A, w)| + |\widehat{E}_h(u - u_{I,L}^A, w)| \right\}. \quad (10.4.3)$$

We cite from [321, 226],

$$\begin{aligned} \left| \iint_{S_1} \nabla(u - u_I^A) \cdot \nabla w \right| &\leq Ch^4 \|u\|_{5,S_1} \left\{ \|w\|_{1,S_1} + \left\| \frac{\partial w^-}{\partial n} \right\|_{0,\partial S_1} \right\} \\ &\leq Ch^{3.5} \|u\|_{5,S_1} \|w\|_{1,S_1} \leq Ch^{3.5} \|u\|_{5,S_1} \overline{\|w\|}_H. \end{aligned} \quad (10.4.4)$$

Also there exist the bounds,

$$\begin{aligned} \left| \iint_{S_2} \nabla(u - u_L) \cdot \nabla w \right| &\leq |R_L|_{1,S_2} \overline{\|w\|}_H, \\ \left| \left(\iint_{S_1} - \widehat{\iint}_{S_1} \right) f w \right| &\leq Ch^4 |f|_{4,S_1} \overline{\|w\|}_H. \end{aligned} \quad (10.4.5)$$

Next, from (10.3.1) for $k \leq 4$ we have

$$\begin{aligned} &\left| \left(\widehat{\int}_{\Gamma_0} - \int_{\Gamma_0} \right) \frac{\partial u}{\partial n} (w^+ - w^-) \right| \\ &= \left| \int_{\Gamma_0} \left[\frac{\partial u}{\partial n} (w^+ - w^-) - \widehat{\frac{\partial u}{\partial n}} (\widehat{w}^+ - w^-) \right] \right| \\ &= \left| \int_{\Gamma_0} \frac{\partial u}{\partial n} (w^+ - \widehat{w}^+) + \int_{\Gamma_0} \left(\frac{\partial u}{\partial n} - \widehat{\frac{\partial u}{\partial n}} \right) (\widehat{w}^+ - w^-) \right| \\ &\leq \left\| \frac{\partial u}{\partial n} \right\|_{0,\Gamma_0} \|w^+ - \widehat{w}^+\|_{0,\Gamma_0} + \left\| \frac{\partial u}{\partial n} - \widehat{\frac{\partial u}{\partial n}} \right\|_{0,\Gamma_0} \overline{\|w^+ - w^-\|}_{0,\Gamma_0} \\ &\leq C \left\{ h^4 \left\| \frac{\partial u}{\partial n} \right\|_{0,\Gamma_0} |w^+|_{4,\Gamma_0} + h^3 \left| \frac{\partial u}{\partial n} \right|_{3,\Gamma_0} \cdot h^\sigma \overline{\|w\|}_H \right\} \\ &\leq C \left\{ h^4 L^{4\nu} \left\| \frac{\partial u}{\partial n} \right\|_{0,\Gamma_0} + h^{3+\sigma} \left| \frac{\partial u}{\partial n} \right|_{3,\Gamma_0} \right\} \overline{\|w\|}_H \\ &\leq C \{ h^4 L^{4\nu} + h^{3+\sigma} \} \|u\|_{5,S_1} \overline{\|w\|}_H. \end{aligned} \quad (10.4.6)$$

Therefore, the desired result (10.4.2) is obtained from (10.4.3) – (10.4.6) and Lemma 10.3.3. ■

Corollary 10.4.1 *Let the all conditions of Theorem 10.4.1 hold. Suppose $u \in H^5(S_1)$, $f \in H^4(S_1)$, $\sigma \geq 1$, and $L = O(|\ln h|)$ such that*

$$\begin{aligned} |R_L|_{1,S_2} &= O(h^{3.5}), \quad \overline{\|R_L\|}_{0,\Gamma_0} = O(h^{3.5+\sigma}), \\ \left\| \frac{\partial R_L}{\partial n} \right\|_{0,\Gamma_0} &= O(h^{3.5-\sigma}). \end{aligned}$$

Then there exists the superclose,

$$\overline{\|u_h^A - u_{I,L}^A\|_H} = O(h^{3.5}).$$

Construct the a posteriori interpolation

$$\Pi_p u_h^A = \begin{cases} \Pi_{2h}^5 u_h^A, & \text{in } \overline{S}_1, \\ u_h^A, & \text{in } \overline{S}_2, \end{cases}$$

where $\Pi_{2h}^5 u_h^A$ is the polynomial interpolant of order 5 based on the known u_h^A in $\square_{2i+1,2j+1}^{2 \times 2}$ in Figure 10.2. We obtain the following corollary.

Corollary 10.4.2 *Let all conditions in Corollary 10.4.1 hold. Then there exists the superconvergence:*

$$\overline{\|u - \Pi_p u_h^A\|_H} = O(h^{3.5}).$$

Proof For the operation Π_{2h}^5 , we have (see [321, 226])

$$\|\Pi_{2h}^5 v\|_{1,S_1} \leq C \|v\|_{1,S_1}.$$

Since $\Pi_{2h}^5 u_I$ is an interpolant from the nodal values of u_I , we have from the rule (10.4.1)

$$\begin{aligned} & \overline{\|u^+ - \Pi_{2h}^5 u_{I,L}^+ - (u^- - \Pi_{2h}^5 u_{I,L}^-)\|_{0,\Gamma_0}} \\ &= \overline{\|u - u_L\|_{0,\Gamma_0}} = \|\widehat{R}_L\|_{0,\Gamma_0}. \end{aligned}$$

Hence, from Corollary 10.4.1 we obtain

$$\begin{aligned} & \overline{\|u - \Pi_{2h}^5 u_h^A\|_H} \leq \overline{\|u - \Pi_{2h}^5 u_{I,L}\|_H} + \overline{\|\Pi_{2h}^5 (u_{I,L} - u_h^A)\|_H} \\ & \leq \|u - \Pi_{2h}^5 u_I\|_{1,S_1} + \|u - u_L\|_{1,S_2} \\ & + h^{-\sigma} \overline{\|u^+ - \Pi_{2h}^5 u_{I,L}^+ - (u^- - \Pi_{2h}^5 u_{I,L}^-)\|_{0,\Gamma_0}} + C \overline{\|u_{I,L} - u_h^A\|_H} \\ & \leq C h^4 |u|_{5,S_1} + |R_L|_{1,S_2} + h^{-\sigma} \overline{\|R_L\|_{0,\Gamma_0}} + C \overline{\|u_{I,L} - u_h^A\|_H} = O(h^{3.5}). \quad \blacksquare \end{aligned}$$

Note that $O(h^{3.5})$ is the best rate of superclose and superconvergence of Adini's elements for Poisson's equation with the Dirichlet boundary condition, see [321, 226].

10.5 Numerical Experiments

Since the number of unknowns in Adini's elements are only three quarters of that in 2-order rectangles, we only carry out the numerical experiments of the combinations of

TM and Adini's elements, and verify the global superclose and superconvergence made in Section 10.4. Consider the typical Motz problem

$$\begin{aligned} \Delta u &= \frac{\partial^2 u}{\partial x^2} + \frac{\partial^2 u}{\partial y^2} = 0 \quad \text{in } S, \\ u|_{\overline{DO}} &= 0, \quad u|_{\overline{AB}} = 500, \quad \frac{\partial u}{\partial n} \Big|_{\overline{BC \cup CD \cup AO}} = 0, \end{aligned}$$

where S is the rectangle, $S = \{(x, y) \mid -1 \leq x \leq 1, 0 \leq y \leq 1\}$. The origin $(0, 0)$ is a singular point due to the change from the Neumann to the Dirichlet boundary conditions.

First, we use only the Adini's elements in the entire solution domain for Motz's problem, to ignore the existence of the singularity. The errors of Adini's solutions u_h are listed in Table 10.1. From Table 10.1 we can see

$$\begin{aligned} \|u - u_h\|_{1,S} &= O(h^{\frac{1}{2}}), \quad \|u - u_h\|_{0,S} = O(h), \\ \|u_I - u_h\|_{1,S} &= O(h^{\frac{1}{2}}), \quad \|u_I - u_h\|_{0,S} = O(h). \end{aligned}$$

The poor convergence rate $O(h^{\frac{1}{2}})$ occurs for both $\|u - u_h\|_{1,S}$ and $\|u_I - u_h\|_{1,S}$. Table 10.1 displays that the pure Adini's elements fail to deal with the singularity problems.

We also compute the traditional condition number Cond. and the effective condition numbers Cond_E and Cond_EE. Denote the linear algebraic equations resulting from (10.2.10)

$$\mathbf{A}\mathbf{x} = \mathbf{b}, \tag{10.5.1}$$

where $\mathbf{A}(\in \mathbb{R}^{n \times n})$ is symmetric and positive definite, $\mathbf{x}(\in \mathbb{R}^n)$ and $\mathbf{b}(\in \mathbb{R}^n)$ are the unknown and known vectors, respectively. The traditional condition number is defined by

$$\text{Cond.} = \frac{\lambda_{\max}(\mathbf{A})}{\lambda_{\min}(\mathbf{A})}, \tag{10.5.2}$$

where $\lambda_{\max}(\mathbf{A})$ and $\lambda_{\min}(\mathbf{A})$ are the maximal and minimal eigenvalues, respectively. Denote the eigenvalue problem of (10.5.2)

$$\mathbf{A}\mathbf{y}_i = \lambda_i \mathbf{y}_i, \tag{10.5.3}$$

where λ_i and \mathbf{y}_i are the eigenvalues and orthogonal eigenvectors of \mathbf{A} , respectively, with $\lambda_{\max}(\mathbf{A}) = \lambda_1 \geq \lambda_2 \geq \dots \geq \lambda_n = \lambda_{\min}(\mathbf{A}) > 0$. The simplified effective condition numbers are defined in Section 3.7 of Chapter 3,

$$\text{Cond_E} = \frac{\|\mathbf{b}\|}{\sqrt{\frac{\|\mathbf{b}\|^2 - \beta_n^2}{\text{Cond.}^2} + \beta_n^2}},$$

and the simplest effective condition number

$$\text{Cond_EE} = \frac{\|\mathbf{b}\|}{|\beta_n|}, \quad \text{when } \beta_n \neq 0,$$

where $\beta_n = \mathbf{y}_n^T \mathbf{b}$ is the inner product of \mathbf{b} and \mathbf{y}_n .

To deal with the singularity, we invoke the combination of the TM and Adini's elements. Divide S by Γ_0 into S_2 and S_1 . The subdomain S_2 is chosen as the smaller rectangle: $S_2 = \{(x, y) \mid -\frac{1}{2} \leq x \leq \frac{1}{2}, 0 \leq y \leq \frac{1}{2}\}$. Also the subdomain S_1 is again split into uniform rectangular elements shown in Figure 10.3, where N is the division number along \overline{AB} . The admissible functions are chosen as:

$$v = \begin{cases} v^- = v_A & \text{in } S_1, \\ v^+ = \sum_{\ell=0}^L \tilde{d}_\ell r^{\ell+\frac{1}{2}} \cos(\ell + \frac{1}{2})\theta & \text{in } S_2, \end{cases}$$

where \tilde{d}_ℓ are unknown coefficients, and (r, θ) are the polar coordinates with origin $(0,0)$.

For the partition of Figure 10.3, by trial computation we find the good choices, $P_c = 50$ and $\sigma = 1.5$, and the following good matches between N and $L + 1$:

$$\begin{aligned} N = 2 \text{ and } L + 1 = 1, \quad N = 4 \text{ and } L + 1 = 2, \quad N = 8 \text{ and } L + 1 = 3, \quad (10.5.4) \\ N = 12 \text{ and } L + 1 = 4, \quad N = 16 \text{ and } L + 1 = 5. \end{aligned}$$

We have carried out numerical computation, and list the errors, condition number and the simplified effective condition number in Tables 10.2 – 10.3. From Tables 10.2 – 10.3,

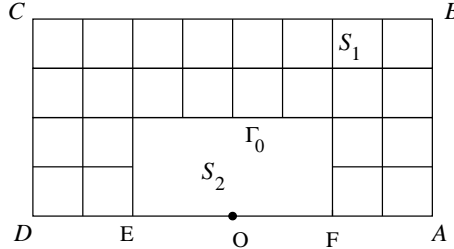


Figure 10.3: Partition for Motz's Problem.

we can find the following asymptotic rates for the combinations of the Trefftz method and Adini's elements,

$$\|u_h^A - u_I^A\|_{1,S_1} = O(h^4), \quad \|u - \Pi_{2h}^5 u_h^A\|_{1,S_1} = O(h^4), \quad (10.5.5)$$

$$\|u - u_h^A\|_{k,S_i} = O(h^4), \quad k = 0, 1, \quad i = 1, 2, \quad (10.5.6)$$

$$|\Delta \tilde{d}_0| = |d_0 - \tilde{d}_0| = O(h^4), \quad (10.5.7)$$

$$\text{Cond.} = O(h^{-5}), \quad \text{Cond.E} = O(h^{-3.2}). \quad (10.5.8)$$

The observed superclose and superconvergence, $O(h^4)$ in (10.5.5) – (10.5.7), are even higher than $O(h^{3.5})$ given in Corollaries 4.1 and 4.2. Note that Eq. (10.5.6) shows $\|u - u_h^A\|_{1,S_i} = O(h^4)$ already so that it is unnecessary to employ the a posteriori interpolation $\Pi_{2h}^5 u_h^A$ in (10.5.5) to reach the order $O(h^4)$ of the global superconvergence. Even so, we have also computed the errors of $u - \Pi_{2h}^5 u_h^A$, and listed in Table 10.2, by using the explicit formulas of $\Pi_{2h}^5 v$ given in [225]. Note that the values of Cond.E are smaller than those of Cond. to provide a better upper bounds of relative errors of the solution from rounding errors. The ratios of Cond. and Cond.E at $(N, L + 1) = (2, 1)$ and $(N, L + 1) = (16, 5)$ are found from Table 10.2,

$$\frac{\text{Cond.}|_{N=2}}{\text{Cond.E}|_{N=2}} = \frac{0.613(5)}{0.163(5)} = 3.76, \quad \frac{\text{Cond.}|_{N=16}}{\text{Cond.E}|_{N=16}} = \frac{0.127(10)}{0.155(8)} = 81.9, \quad (10.5.9)$$

respectively. Interestingly, when N is small, the Cond.E is close to Cond., and when N is large, the Cond.E is evidently smaller than Cond. A recent study shows that for Motz's problem by the penalty plus hybrid TM with Adini's elements in Section 10.4 and this section, there exist the bounds theoretically,

$$\frac{\text{Cond.}}{\text{Cond.E}} \leq Ch^{-2\sigma - \frac{1}{2}},$$

where C is a constant independent of h and N . Details appear elsewhere. When $\sigma = 1.5$,

$$\frac{\text{Cond.}}{\text{Cond.E}} \leq Ch^{-3.5}. \quad (10.5.10)$$

The numerical results in (10.5.8) are coincident with (10.5.10).

Besides the penalty plus hybrid combination (10.2.10) of the Trefftz method and Adini's elements, we also choose the hybrid combination. The hybrid combined method of the Trefftz method and Adini's elements was discussed in Li and Huang [303]: To seek $u_h^A \in V_h^*$ such that

$$E_h(u_h^A, v) = f(v), \quad \forall v \in V_h^0, \quad (10.5.11)$$

where $f(v) = \iint_S f v$ and

$$E_h(u, v) = \iint_{S_1} \nabla u \cdot \nabla v + \iint_{S_2} \nabla u \cdot \nabla v + \widehat{\int}_{\Gamma_0} \frac{\partial u^+}{\partial n} v^- - \widehat{\int}_{\Gamma_0} \frac{\partial v^+}{\partial n} u^-. \quad (10.5.12)$$

For the same partition (10.5.4), the computed errors and condition numbers are listed in Tables 10.4 and 10.5. From Tables 10.4 and 10.5, we can see the following asymptotic rates for the hybrid combination,

$$\|u_h^A - u_I^A\|_{1,S_1} = O(h^{3.5}), \quad (10.5.13)$$

$$\|u - u_h^A\|_{1,S_1} = O(h^{3.5}), \quad \|u - \Pi_{2h}^5 u_h^A\|_{1,S_1} = O(h^{3.5}), \quad (10.5.14)$$

$$\|u - u_h^A\|_{1,S_2} = O(h^4), \quad (10.5.15)$$

$$|\Delta \tilde{d}_0| = |d_0 - \tilde{d}_0| = O(h^{3.5}), \quad (10.5.16)$$

$$\text{Cond.} = O(h^{-2}), \quad \text{Cond.E} = O(h^{-2.2}). \quad (10.5.17)$$

For the hybrid TM combination, there is no improvement for Cond.E to measure the stability, compared to Cond.

Finally, the comparisons of numerical results of Tables 10.2 – 10.5 are listed in Table 10.6. It is clear that the accuracy of solutions by the penalty plus hybrid computation is higher, but the stability of the hybrid combination is better. Let us focus on the the condition number and the simplified effective condition number in Table 10.6 at $N = 16$,

$$\frac{\text{Cond.} \Big|_{Pen.\&Hyb.Com}}{\text{Cond.} \Big|_{Hyb.Com}} = \frac{0.127(10)}{0.451(5)} = 0.282(4), \quad (10.5.18)$$

$$\frac{\text{Cond.E} \Big|_{Pen.\&Hyb.Com}}{\text{Cond.E} \Big|_{Hyb.Com}} = \frac{0.155(8)}{0.399(5)} = 388.$$

From the viewpoint of Cond. the penalty plus hybrid combination has a serious drawback of instability; however from the viewpoint of Cond.E, it is only slightly worse in instability. Hence for both accuracy and stability, the the penalty plus hybrid combination is superior to the hybrid combination for Motz's problem. Such a comparable conclusion between the two methods is different from that in [303], p. 271-272, where the hybrid combination was considered to be better. The current analysis is also a useful demonstration of the application of the simplified effective condition number proposed in Section 3.7.

Note that when the values of Cond.EE are larger than Cond. (see the data in Table 10.5 marked by ‡), the Cond.EE is meaningless. On the other hand, the Cond.E has a wide range of applications, because the evaluation of β_n is so easy, such that we can always compute Cond.E. The worst case is that $\beta_n \approx 0$, then $\text{Cond.E} = \text{Cond.}$, with nothing lost. Sometimes, the computed Cond.E may be significant smaller than Cond., as reported in Li et al. [305, 306].

10.6 Concluding Remarks

1. This chapter is devoted to *high* global superconvergence of the penalty plus hybrid combinations for singularity problems. The particular solutions are chosen in the singular subdomain involving the singular points. The $p(\geq 2)$ -rectangles or Adini's elements are chosen in the rest of the solution domain, and the penalty plus hybrid techniques are employed to couple two different methods along their common boundary Γ_0 . The analysis is made in this chapter to derive almost the *best* global superconvergence $O(h^{p+2-\delta})$, $0 < \delta \ll 1$, for the combination using $p(\geq 2)$ -rectangles in S_1 , and the *best* global superconvergence $O(h^{3.5})$ for the combination using Adini's elements in S_1 . The numerical experiments are carried out for the combinations of the TM and Adini's elements, and the empirical superconvergence $O(h^4)$ observed in the numerical data is more promising. Moreover, the solutions from the combination given in this chapter are more accurate than those in [303, 225]. Take $N = 16$ and $L + 1 = 5$ as for example. The errors of the solutions from Table 10.6 are given by the penalty plus hybrid combination,

$$\|u_h - u_I\|_{1,S_1} = 0.0666, \quad \|u - u_L\|_{1,S_2} = 0.0779, \quad \frac{|\Delta \tilde{d}_0|}{|d_0|} = 0.505 \times 10^{-4},$$

which are smaller than those by the simplified hybrid TM:

$$\|u_h - u_I\|_{1,S_1} = 0.202, \quad \|u - u_L\|_{1,S_2} = 0.145, \quad \frac{|\Delta \tilde{d}_0|}{|d_0|} = 0.772 \times 10^{-4}.$$

In contrast, $\|u_h - u_I\|_{1,S} = 14.2$ obtained from the pure Adini's elements is much larger (see Table 10.1). This clearly shows the significance of the combinations given in this chapter.

2. The simplified effective condition numbers Cond_E are computed to show that the instability is not so severe as Cond indicates. Based on the high accuracy of the solution, and on the moderate large Cond_E , the penalty plus hybrid combination of Trefftz methods in this chapter is superior to the hybrid combination in [303] for Motz's problem. This is a new evaluation on the two TM combinations.
3. This chapter is also a further development of the book [291], where only linear or bilinear FEMs in the TM combinations are used. The high order FEMs, such as the bi-p-order FEM and Adini's elements, are chosen in this chapter, in order to achieve the highly accurate solutions.

N	2	4	8	16
$\ u_h^A - u\ _{1,S}$	164	114	80.5	56.9
$\ u_h^A - u\ _{0,S}$	31.8	11.9	4.38	1.61
$\ u_h^A - u_I\ _{1,S}$	43.3	29.2	20.2	14.2
$\ u_h^A - u_I\ _{0,S}$	14.3	6.36	2.59	1.02

Table 10.1: The solution errors of the Adini's elements used in the entire domain S for Motz's problem.

$N, L+1$	2,1	4,2	8,3	12,4	16,5
$\max_{S_1} \varepsilon_{ij} $	43.3	4.46	1.32	0.173	0.458(-1)
$\max_{S_1} (\varepsilon_x)_{ij} $	98.6	28.7	11.3	2.02	0.608
$\max_{S_1} (\varepsilon_y)_{ij} $	75.2	15.4	9.96	1.57	0.360
$ \varepsilon _{1,\infty,S_1}$	95.0	27.9	10.7	1.96	0.574
$ \varepsilon _{0,\infty,S_1}$	46.0	5.05	1.31	0.173	0.454(-1)
$\ \varepsilon\ _{1,S_1}$	63.4	9.74	3.05	0.370	0.669(-1)
$\ \varepsilon\ _{0,S_1}$	29.7	2.27	0.444	0.455(-1)	0.104(-1)
$ \tilde{u}_h^A - u_I _{1,\infty,S_1}$	93.8	27.9	10.7	1.96	0.576
$ \tilde{u}_h^A - u_I _{0,\infty,S_1}$	46.1	5.06	1.31	0.173	0.454(-1)
$\ \tilde{u}_h^A - u_I\ _{1,S_1}$	63.5	9.74	3.04	0.370	0.666(-1)
$\ \tilde{u}_h^A - u_I\ _{0,S_1}$	29.7	2.27	0.445	0.455(-1)	0.104(-1)
$ u - \Pi_p^5 \tilde{u}_h _{1,\infty,S_1}$	/	28.7	11.1	1.97	0.569
$ u - \Pi_p^5 \tilde{u}_h _{0,\infty,S_1}$	/	4.48	1.25	0.173	0.454(-1)
$\ u - \Pi_p^5 \tilde{u}_h\ _{1,S_1}$	/	6.97	2.67	0.341	0.636(-1)
$\ u - \Pi_p^5 \tilde{u}_h\ _{0,S_1}$	/	1.48	0.370	0.422(-1)	0.102(-1)
$ \varepsilon _{1,\infty,S_2}$	107	32.8	11.5	2.04	0.608
$ \varepsilon _{0,\infty,S_2}$	45.2	4.55	1.31	0.175	0.455(-1)
$\ \varepsilon\ _{1,S_2}$	60.5	9.57	2.94	0.368	0.779(-1)
$\ \varepsilon\ _{0,S_2}$	12.8	1.19	0.336	0.428(-1)	0.750(-2)
$\lambda_{max}(\mathbf{A})$	0.407(3)	0.259(4)	0.178(5)	0.570(5)	0.132(6)
$\lambda_{min}(\mathbf{A})$	0.663(-2)	0.165(-3)	0.413(-3)	0.184(-3)	0.103(-3)
Cond.	0.613(5)	0.157(7)	0.431(8)	0.311(9)	0.127(10)
$\ \mathbf{b}\ $	736.7	1123	1643	2035	2362
β_n	0.437(-1)	0.569(-2)	0.103(-2)	0.346(-3)	0.153(-3)
Cond.E	0.163(5)	0.169(6)	0.159(7)	0.589(7)	0.155(8)
Cond.EE	0.169(5)	0.197(6)	0.159(7)	0.589(7)	0.155(8)

Table 10.2: The error norms, condition numbers and simplified effective condition numbers for Motz's problem by the penalty plus hybrid combination of the Trefftz method and Adini's elements with $Pc=50$ and $\sigma = 1.5$, where $\varepsilon = u - \tilde{u}_h^A$.

N,L+1	2,1	4,2	8,3	12,4	16,5
\tilde{d}_0	418.1542	402.5432	402.0752	401.0326	401.1422
$\frac{ \Delta\tilde{d}_0 }{ \tilde{d}_0 }$	0.424(-1)	0.344(-2)	0.228(-2)	0.324(-3)	0.505(-4)
\tilde{d}_1	/	83.04471	87.70073	87.67332	87.65236
$\frac{ \Delta\tilde{d}_1 }{ \tilde{d}_1 }$	/	0.526(-1)	0.511(-3)	0.199(-3)	0.406(-4)
\tilde{d}_2	/	/	17.37581	17.30165	17.26693
$\frac{ \Delta\tilde{d}_2 }{ \tilde{d}_2 }$	/	/	0.800(-2)	0.370(-2)	0.168(-2)
\tilde{d}_3	/	/	/	-7.788614	-8.026155
$\frac{ \Delta\tilde{d}_3 }{ \tilde{d}_3 }$	/	/	/	0.350(-1)	0.558(-2)
\tilde{d}_4	/	/	/	/	1.291809
$\frac{ \Delta\tilde{d}_4 }{ \tilde{d}_4 }$	/	/	/	/	0.103

Table 10.3: The approximate leading coefficients for the penalty plus hybrid combination of the Trefftz method and Adini's elements with $Pc=50$ and $\sigma = 1.5$.

N,L+1	2,1	4,2	8,3	12,4	16,5	True Coeffs. [291]
\tilde{d}_0	379.8063	400.0124	400.2237	401.0602	401.1934	401.1624537
$\frac{ \Delta\tilde{d}_0 }{ \tilde{d}_0 }$	0.532(-1)	0.287(-2)	0.234(-2)	0.255(-3)	0.772(-4)	
\tilde{d}_1	/	91.73045	87.75318	87.65334	87.64282	87.65592020
$\frac{ \Delta\tilde{d}_1 }{ \tilde{d}_1 }$	/	0.465(-1)	0.111(-2)	0.295(-4)	0.149(-3)	
\tilde{d}_2	/	/	17.52948	17.29283	17.25341	17.23791508
$\frac{ \Delta\tilde{d}_2 }{ \tilde{d}_2 }$	/	/	0.169(-1)	0.319(-2)	0.899(-3)	
\tilde{d}_3	/	/	/	-7.977731	-7.832812	-8.071215260
$\frac{ \Delta\tilde{d}_3 }{ \tilde{d}_3 }$	/	/	/	0.116(-1)	0.295(-1)	
\tilde{d}_4	/	/	/	/	1.863284	1.440272717
$\frac{ \Delta\tilde{d}_4 }{ \tilde{d}_4 }$	/	/	/	/	0.294	

Table 10.4: The approximate leading coefficients by the hybrid combination of the Trefftz method and Adini's elements.

N,L+1	2,1	4,2	8,3	12,4	16,5
$\max_{S_1} \varepsilon_{ij} $	55.2	5.18	1.54	0.262	0.618(-1)
$\max_{S_1} (\varepsilon_x)_{ij} $	224	26.9	12.8	2.08	0.629
$\max_{S_1} (\varepsilon_y)_{ij} $	119	25.0	12.3	4.19	4.28
$ \varepsilon _{1,\infty,S_1}$	204	25.8	12.8	3.63	3.32
$ \varepsilon _{0,\infty,S_1}$	54.7	5.57	1.51	0.258	0.610(-1)
$\ \varepsilon\ _{1,S_1}$	80.5	9.88	2.96	0.526	0.203
$\ \varepsilon\ _{0,S_1}$	33.4	2.25	0.427	0.517(-1)	0.141(-1)
$ u_h^A - u_I _{1,\infty,S_1}$	204.	25.8	12.8	3.63	3.32
$ u_h^A - u_I _{0,\infty,S_1}$	54.7	5.58	1.51	0.258	0.610(-1)
$\ u_h^A - u_I\ _{1,S_1}$	80.2	9.87	2.96	0.526	0.202
$\ u_h^A - u_I\ _{0,S_1}$	33.3	2.25	0.426	0.517(-1)	0.141(-1)
$ u - \Pi_p^5 \tilde{u}_h _{1,\infty,S_1}$	/	23.4	14.5	5.25	3.96
$ u - \Pi_p^5 \tilde{u}_h _{0,\infty,S_1}$	/	4.38	1.51	2.51	0.763(-1)
$\ u - \Pi_p^5 \tilde{u}_h\ _{1,S_1}$	/	6.12	2.72	0.531	0.270
$\ u - \Pi_p^5 \tilde{u}_h\ _{0,S_1}$	/	1.50	0.377	0.436(-1)	0.138(-1)
$ \varepsilon _{1,\infty,S_2}$	125	36.4	11.1	2.13	0.874
$ \varepsilon _{0,\infty,S_2}$	47.5	9.93	2.65	0.174	0.116
$\ \varepsilon\ _{1,S_2}$	61.1	9.56	2.94	0.353	0.145
$\ \varepsilon\ _{0,S_2}$	13.5	1.64	0.478	0.356(-1)	0.145(-1)
$\lambda_{max}(\mathbf{A})$	3.12	4.32	4.58	4.65	4.66
$\lambda_{min}(\mathbf{A})$	0.598(-2)	0.299(-3)	0.413(-3)	0.163(-3)	0.103(-3)
Cond.	521	0.144(5)	0.111(5)	0.285(5)	0.451(5)
$\ \mathbf{b}\ $	736.7	1123	1643	2035	2362
β_n	1.13	0.477	0.110	0.479(-1)	0.271(-1)
Cond_E	392	0.178(4)	0.893(4)	0.217(5)	0.399(5)
Cond_EE	651‡	0.236(4)	0.149(4)	0.424(5)‡	0.870(5)‡

Table 10.5: The error norms, condition numbers and simplified effective condition numbers for Motz's problem by the hybrid combination of the Trefftz method and Adini's elements, where $\varepsilon = u - u_h^A$, where the Cond_EE denoted with ‡ is meaningless due to $\text{Cond_EE} > \text{Cond}$.

	Hyb.Com. in Tables 10.4 – 10.5	Pen.& Hyb.Com. in Tables 10.2 – 10.3	Ratios of two Results
$\max_{S_1} \varepsilon_{ij} $	0.618(-1)	0.458(-1)	0.741(=0.458(-1)/0.618(-1))
$\max_{S_1} (\varepsilon_x)_{ij} $	0.629	0.608	0.967
$\max_{S_1} (\varepsilon_y)_{ij} $	4.28	0.360	0.841(-1)
$ \varepsilon _{1,\infty,S_1}$	3.32	0.574	0.173
$ \varepsilon _{0,\infty,S_1}$	0.610(-1)	0.454(-1)	0.744
$\ \varepsilon\ _{1,S_1}$	0.203	0.669(-1)	0.330
$\ \varepsilon\ _{0,S_1}$	0.141(-1)	0.104(-1)	0.738
$ u_h - u_I _{1,\infty,S_1}$	3.32	0.576	0.173
$ u_h - u_I _{0,\infty,S_1}$	0.610(-1)	0.454(-1)	0.744
$\ u_h - u_I\ _{1,S_1}$	0.202	0.666(-1)	0.330
$\ u_h - u_I\ _{0,S_1}$	0.141(-1)	0.105(-1)	0.738
$ u - \Pi_p^5 \tilde{u}_h _{1,\infty,S_1}$	3.96	0.569	0.150
$ u - \Pi_p^5 \tilde{u}_h _{0,\infty,S_1}$	0.763(-1)	0.454(-1)	0.590
$\ u - \Pi_p^5 \tilde{u}_h\ _{1,S_1}$	0.270	0.636(-1)	0.236
$\ u - \Pi_p^5 \tilde{u}_h\ _{0,S_1}$	0.138(-1)	0.102(-1)	0.739
$ \varepsilon _{1,\infty,S_2}$	0.874	0.608	0.696
$ \varepsilon _{0,\infty,S_2}$	0.116	0.455(-1)	0.392
$\ \varepsilon\ _{1,S_2}$	0.145	0.779(-1)	0.537
$\ \varepsilon\ _{0,S_2}$	0.145(-1)	0.750(-2)	0.517
$\frac{ \Delta \tilde{d}_0 }{ d_0 }$	0.772(-4)	0.505(-4)	0.654
$\frac{ \Delta \tilde{d}_1 }{ d_1 }$	0.149(-3)	0.406(-4)	0.272
Cond.	0.451(5)	0.127(10)	0.281(4)
Cond_E	0.399(5)	0.155(8)	388

Table 10.6: Comparisons of the numerical solutions for Motz's problem by two combinations of the Trefftz method and Adini's elements at $N = 16$ and $L + 1 = 5$, where $u_h = u_h^A$ or $u_h = \tilde{u}_h^A$, and $\varepsilon = u - u_h^A$ or $\varepsilon = u - \tilde{u}_h^A$.

Chapter 11

Eigenvalue Problems

For the Laplace eigenvalue problems, this chapter presents new algorithms of the Trefftz method (TM), which solve the Helmholtz equation, and then use an iteration process to yield approximate eigenvalues and eigenfunctions. The new iterative method has super-linear convergence rates and gives a better performance in numerical testing, compared with the other popular methods of rootfinding. Piecewise particular solutions are used for a basic model of eigenvalue problems on the unit square with the Dirichlet condition. Moreover, error estimates are derived for the approximate eigenvalues and eigenfunctions. Numerical experiments are also conducted for the eigenvalue problems with singularities. Our new algorithms using piecewise particular solutions are well suited to seek very accurate solutions of eigenvalue problems, in particular those with multiple singularities, interfaces, and those on unbounded domains. Using piecewise particular solutions also has the advantage to solve complicated problems because uniform particular solutions may not always exist for the entire solution domain.

11.1 Introduction

There exist a number of numerical methods and their parallel implementation for solving eigenvalue problems, see Birkhoff and Lynch [47], Golub and van Loan [176], Kuttler and Sigilloto [272], Ortega [370], and Strang and Fix [446]. The use of the finite element method has been surveyed by Babuska and Osborn [18], and the important treatises on eigenvalue problems include Courant and Hilbert [109], Wilkinson [493], Parlett [373] and Golub and van Loan [176]. The approaches using particular solutions are given in Bergman [33], Eisenstat [142], Fox, Henrici and Moler [156], Mathon and Sermer [345] and Vekua [469]. We will follow Part I to employ the boundary approximation method (BAM) (i.e., the TM [461] called in this chapter). In the TM, the solution domain is divided into several subdomains, different particular solutions on subdomains (i.e., piecewise particular solutions) are used, and an approximation of the solutions is then obtained by satisfying only the interior and exterior boundary conditions. An important advantage of the TM is that high accuracy of solutions can be achieved with a modest effort in computation.

In this chapter, we seek the eigenvalues λ_l and the nonzero eigenfunction ϕ_l satisfying

$$\begin{cases} -\Delta\phi_l = \lambda_l\phi_l & \text{in } \Omega, \\ \phi_l|_{\Gamma} = 0, \end{cases} \quad (11.1.1)$$

where $\Delta = \frac{\partial^2}{\partial x^2} + \frac{\partial^2}{\partial y^2}$, and Ω is a polygonal domain with the external boundary Γ . For simplicity, only the Dirichlet boundary condition is investigated here; other boundary conditions are treated in Section 11.5 (also see [291, 316, 329]). Denote the eigenvalues in an ascending order:

$$0 < \lambda_1 \leq \lambda_2 \leq \dots \leq \lambda_l \leq \dots, \quad \lambda_1 = \lambda_{min}. \quad (11.1.2)$$

The normalized eigenfunctions will satisfy the orthogonality property:

$$(\phi_i, \phi_j) = \int \int_{\Omega} \phi_i \phi_j d\Omega = \delta_{ij} = \begin{cases} 1 & i = j, \\ 0 & i \neq j. \end{cases} \quad (11.1.3)$$

Let the solution domain Ω be divided into two subdomains, Ω^+ and Ω^- , by a piecewise straight line Γ_0 . Then the eigenfunction ϕ_l must satisfy the continuity conditions across the interface Γ_0

$$\begin{cases} -\Delta\phi_l = \lambda_l\phi_l & \text{in } \Omega^+ \text{ and } \Omega^-, \\ \phi_l^+ = \phi_l^-, & \frac{\partial\phi_l^+}{\partial\nu} = \frac{\partial\phi_l^-}{\partial\nu} & \text{on } \Gamma_0, \\ \phi_l|_{\Gamma} = 0, \end{cases} \quad (11.1.4)$$

where ν is the unit normal to Γ_0 , and ϕ_l^+ and ϕ_l^- are the values of ϕ_l on the two sides of Γ_0 .

Let us first recall from Ortega [370], p. 40, that the matrix eigenvalue problem $\mathbf{A}\mathbf{x} = \lambda\mathbf{x}$ can be solved by the linear algebraic equations,

$$(\mathbf{A} - k^2\mathbf{I})\mathbf{x} = \mathbf{b}, \quad (11.1.5)$$

where \mathbf{I} is the identity matrix, $k(> 0)$ is chosen, and \mathbf{b} is a nonzero vector. If (11.1.5) is ill-conditioned (called degeneracy in this chapter), then k^2 and \mathbf{x} can be regarded approximately as an eigenvalue and the corresponding eigenvector of matrix \mathbf{A} respectively. Note that the nonzero vector \mathbf{b} can be chosen rather arbitrarily, and not necessarily to be small.

Analogously, for solving (11.1.4), we may seek the following Helmholtz solutions instead

$$\begin{cases} -\Delta u = k^2 u, & \text{in } \Omega^+ \text{ and } \Omega^-, \\ u^+ = u^-, & \frac{\partial u^+}{\partial\nu} = \frac{\partial u^-}{\partial\nu} & \text{on } \Gamma_0, \\ u|_{\Gamma} = g, \end{cases} \quad (11.1.6)$$

where $k > 0$, $g \in H^{\frac{1}{2}}(\Gamma)$ is a given nonzero function, and $H^{\frac{1}{2}}(\Gamma)$ is the Sobolev space on Γ . Consequently, when k is suitably chosen so as to lead to a degeneracy (or ill-conditioning) of (11.1.6), k^2 and u can be regarded approximately as an eigenvalue and its corresponding eigenfunction of (11.1.4), respectively.

Define the smallest relative distance between k^2 and λ_i by

$$\delta = \min_i \left| \frac{k^2 - \lambda_i}{k^2} \right|.$$

When k^2 approaches one of λ_i , the solution u of (11.1.6) will approach an eigenfunction [156]. Besides, when $k^2 = \lambda_\ell$ (i.e., $\delta = 0$) and $u = \phi_\ell$, the nonhomogeneous term g must be zero. It seems to be a paradox due to the assumption $g \neq 0$ in (11.1.6). How can we clarify this paradox? In practical computation, we have either $\delta > 0$ or $u \neq \phi_\ell$ always happens due to rounding errors in computer or truncation errors in numerical algorithms. The equation (11.1.6) could be very ill-conditioned, but never be exactly singular. A further clarification is deferred to Section 11.2.2. Therefore, the Helmholtz solutions can be solved by some numerical methods, e.g., by the TM and the CTM in Part I. In fact, such a degeneracy of (11.1.6) can grant a very high accuracy of eigenvalues and eigenfunctions from the new algorithms developed below.

This chapter is organized as follows. In Section 11.2, we present new algorithms. In Sections 11.3 and 11.4, error bounds are derived for the eigenvalues and eigenfunctions by the TM. In Section 11.5, we test a simple eigenvalue problem to demonstrate the effectiveness of the algorithms proposed in this chapter. In Section 11.6, numerical experiments are carried for the eigenvalue problems with singularity. In the last section, summaries and discussions are given. The materials of this chapter are adapted from [294, 313].

11.2 New Numerical Algorithms for Eigenvalue Problems

To expose clearly our methods for eigenvalues and eigenfunctions, we first introduce the TM in Section 11.2.1 for (11.1.6), and then present some heuristic ideas in Section 11.2.2. The new algorithms are developed in Section 11.2.3. Since the degeneracy of (11.1.6) involves nonlinear solutions k to the minimal eigenvalue of the associated matrix, a specific iteration method is designed, and its superlinear convergence rates are also proven in [313].

11.2.1 The Trefftz Methods for (11.1.6)

First, the Trefftz method (TM) is applied to seek u of (11.1.6) under a fixed g and a given k . For simplicity, we split the solution domain into two subdomains Ω^+ and Ω^- . Some definitions of norms are needed to describe the TM. We define a space

$$H = \{v \in L_2(\Omega) | v \in H^1(\Omega^+), v \in H^1(\Omega^-) \text{ and } \Delta v + k^2 v = 0 \text{ in } \Omega^+ \text{ and } \Omega^-\},$$

and a functional

$$I(v) = \int_{\Gamma} (v - g)^2 ds + \int_{\Gamma_0} (v^+ - v^-)^2 ds + \sigma^2 \int_{\Gamma_0} (v_\nu^+ - v_\nu^-)^2 ds,$$

where $H^1(\Omega^+)$ and $H^1(\Omega^-)$ are the Sobolev spaces, and σ is a positive weight. Define a bilinear form $[u, v]$ on $H \times H$ by

$$[u, v] = \int_{\Gamma} uv \, ds + \int_{\Gamma_0} (u^+ - u^-)(v^+ - v^-) \, ds + \sigma^2 \int_{\Gamma_0} (u_{\nu}^+ - u_{\nu}^-)(v_{\nu}^+ - v_{\nu}^-) \, ds,$$

and the induced norm

$$|v|_B = \sqrt{[v, v]} = \{|v|_{0,\Gamma}^2 + |v^+ - v^-|_{0,\Gamma_0}^2 + \sigma^2 |v_{\nu}^+ - v_{\nu}^-|_{0,\Gamma_0}^2\}^{\frac{1}{2}}. \quad (11.2.1)$$

The norms $\|v\|_H$ and $|v|_H$ over H are defined by

$$\|v\|_H = \{\|v\|_{1,\Omega^+}^2 + \|v\|_{1,\Omega^-}^2\}^{1/2}, \quad |v|_H = \{|v|_{1,\Omega^+}^2 + |v|_{1,\Omega^-}^2\}^{1/2},$$

where $\|v\|_{1,\Omega^{\pm}}$ and $|v|_{1,\Omega^{\pm}}$ are the Sobolev norms.

Also define the finite-dimensional spaces $S_{m,n} \subseteq H$ such that

$$S_{m,n} = \left\{ v | v = v^+ = \sum_{i=1}^m c_i \Psi_i^+ \text{ in } \Omega^+, \text{ and } v = v^- = \sum_{i=1}^n d_i \Psi_i^- \text{ in } \Omega^- \right\}, \quad (11.2.2)$$

where $\{\Psi_i^{\pm}\}$ are the complete particular solutions of (11.1.6) in Ω^{\pm} , and c_i and d_i are the coefficients to be sought. A TM approximation $u_{m,n} \in S_{m,n}$ to the problem (11.1.6) can then be found by

$$I(u_{m,n}) = \min_{v \in S_{m,n}} I(v), \quad (11.2.3)$$

which can also be presented in a weak form

$$[u_{m,n}, v] = \int_{\Gamma} gv \, ds, \quad \forall v \in S_{m,n}. \quad (11.2.4)$$

Consequently, a system of linear algebraic equations

$$\mathbf{A}\mathbf{x} = \mathbf{A}(k)\mathbf{x} = \mathbf{b}, \quad (11.2.5)$$

can be obtained from (11.2.3) or (11.2.4), where \mathbf{x} is the unknown vector consisting of all the expansion coefficients c_i and d_i in (11.2.2), and the normal matrix $\mathbf{A}(k)$ is non-negative definite and symmetric, given by

$$[u_{m,n}, u_{m,n}] = \frac{1}{2} \mathbf{x}^T \mathbf{A}(k) \mathbf{x}. \quad (11.2.6)$$

From (11.2.3), we may also solve $u_{m,n}$ by the least squares solution using the QR method or the singular value decomposition (see Golub and van Loan [176], and Atkinson [9], p. 636), with smaller condition number

$$\text{Cond.} = \left[\frac{\lambda_{\max}(\mathbf{A}(k))}{\lambda_{\min}(\mathbf{A}(k))} \right]^{\frac{1}{2}}, \quad (11.2.7)$$

where $\lambda_{\max}(\mathbf{A}(k))$ and $\lambda_{\min}(\mathbf{A}(k))$ are the maximal and minimal eigenvalues of $\mathbf{A}(k)$, respectively.

11.2.2 Heuristic Ideas of Degeneracy of (11.1.6)

Below, we explain why the solutions of (11.1.6) in degeneracy will lead to solutions of eigenvalue problem (11.1.4). Let μ_ℓ be the eigenvalues of \mathbf{A} in (11.2.5),

$$\mathbf{A}(k)\bar{\mathbf{x}}_l = \mu_l\bar{\mathbf{x}}_l, \quad \bar{\mathbf{x}}_l^T \bar{\mathbf{x}}_j = \delta_{l,j} = \begin{cases} 1, & l = j, \\ 0, & l \neq j. \end{cases}$$

Then the non-negative eigenvalues μ_i can be arranged in an ascending order

$$0 \leq \mu_1 \leq \mu_2 \leq \mu_3 \leq \dots$$

The matrix \mathbf{A} is said to be degenerate if the minimal eigenvalue

$$\mu_1 = \lambda_{\min}(\mathbf{A}(k)) \rightarrow 0. \quad (11.2.8)$$

Such a degeneracy implies that

$$\exists \ell \text{ such that } k^2 \approx \lambda_\ell \text{ and } u \approx \phi_\ell. \quad (11.2.9)$$

Here we only give a preliminary argument to (11.2.9). If the coefficients of the Helmholtz solution $\bar{u}_{m,n}$ are approximated to $\bar{\mathbf{x}}_1$, where $\bar{u}_{m,n}$ is a normalization of $u_{m,n}$ in (11.2.2), we have from (11.2.6) and (11.2.8)

$$\begin{aligned} |\bar{u}_{m,n}|_B^2 &= \frac{1}{2} \mathbf{x}^T \mathbf{A}(k) \mathbf{x} \approx \frac{1}{2} \bar{\mathbf{x}}_1^T \mathbf{A}(k) \bar{\mathbf{x}}_1 \\ &= \frac{1}{2} \lambda_{\min}(\mathbf{A}(k)) \|\bar{\mathbf{x}}_1\|^2 = \frac{1}{2} \lambda_{\min}(\mathbf{A}(k)) \rightarrow 0, \end{aligned}$$

where $\|\cdot\|$ is the Euclidean norm. By noting the definition (11.2.1) of the B-norm, the following equations are approximately satisfied

$$\bar{u}|_\Gamma = 0, \quad \bar{u}^+ = \bar{u}^- \quad \text{and} \quad \bar{u}_\nu^+ = \bar{u}_\nu^- \quad \text{on } \Gamma_0.$$

Also since $\bar{u}_{m,n} (\in S_{m,n})$ satisfies

$$\Delta \bar{u} + k^2 \bar{u} = 0 \text{ in } \Omega^+ \text{ and } \Omega^-,$$

k^2 and $\bar{u}_{m,n}$ are an approximation of certain eigenvalue λ_l and eigenfunction ϕ_l . Hence Eq. (11.2.9) holds. Based on the above ideas, k^2 will be chosen to decrease $\lambda_{\min}(\mathbf{A}(k))$ as much as possible.

Given a nonzero function g on the exterior boundary Γ , and suppose

$$(g, \phi_l) \neq 0,$$

where $(g, v) = \iint_{\Omega} gv \, d\Omega$. The solutions $u_{m,n}$ can be obtained from (11.1.6) by the TM in Section 11.2.1. Since $\alpha\phi_l$ with any real $\alpha \neq 0$ also solves (11.1.4), a scaling condition is needed for the unique eigenfunction such as

$$\bar{u}_{m,n} = u_{m,n} / \|\mathbf{x}_{m,n}\|,$$

and $\mathbf{x}_{m,n}$ is the vector in (11.2.6). We may, however, use a simpler scale condition,

$$\bar{u}_{m,n} = u_{m,n}/c_1, \quad \bar{\mathbf{x}}_{m,n} = \mathbf{x}_{m,n}/c_1, \quad c_1 \neq 0, \quad (11.2.10)$$

where c_1 is the leading coefficient of $u_{m,n}^+$ on Ω^+ .

Based on Lemma 11.3.6 below, when $\lambda_{min}(\mathbf{A}) \rightarrow 0$ the leading coefficient $c_1 \rightarrow \infty$. For the scaled solution (11.2.10), the exterior boundary condition in (11.1.6) leads to

$$\bar{u}|_{\Gamma} = \frac{1}{c_1} u|_{\Gamma} = \frac{1}{c_1} g = O(g \sqrt{\lambda_{min}(\mathbf{A})}) \rightarrow 0,$$

where function g is bounded, but not necessarily small. Therefore, the solutions of (11.1.6) approach the eigenfunctions in (11.1.4), i.e., (11.1.1). This gives a clarification to the paradox raised in the Section 11.1.

The same conclusions can be made from the error bounds in the next two sections,

$$\frac{|k^2 - \lambda_l|}{k^2} \leq C(K_{m,n} + \sigma^{-1}) \frac{|u_{m,n}|_B}{|u_{m,n}|_{0,\Omega}},$$

and

$$\frac{\|u_{m,n} - a_l \phi_l\|_H}{|u_{m,n}|_{0,\Omega}} \leq C \lambda_l^{\frac{3}{2}} (K_{m,n} + \sigma^{-1}) \frac{|u_{m,n}|_B}{|u_{m,n}|_{0,\Omega}},$$

where C is a bounded constant independent of m and n , but $k_{m,n}$ may depend upon m and n , and the ratio

$$\rho = \frac{|u_{m,n}|_B}{|u_{m,n}|_{0,\Omega}} \leq C |\bar{u}_{m,n}|_B \leq C |g|_{0,\Gamma} \sqrt{\lambda_{min}(\mathbf{A})}.$$

Therefore, we conclude that if $\lambda_{min}(\mathbf{A}) \rightarrow 0$, then $k^2 \rightarrow \lambda_l$ and $u_{m,n} \rightarrow \alpha\phi_l$ in the H -norms even when $g = O(1)$. So we may simply let $g|_{\Gamma} = 1$ in the examples given below.

11.2.3 New Iteration Algorithms for Seeking Eigenvalues and Eigenfunctions

Based on the above ideas that a degeneracy of (11.1.6) implies the infinite small values of $\lambda_{min}(\mathbf{A}(k))$, we propose Algorithms (A) and (B) given below.

Suppose $k^2 = \lambda_l$, i.e., $\delta = 0$. Then $u_{m,n} \rightarrow \phi_l$ as $m \rightarrow \infty$ and $n \rightarrow \infty$, since the eigenfunctions ϕ_l can be spanned by the complete particular solutions $\{\Psi_i^\pm\}$. Therefore, we may choose k_i such that

$$\lambda_{min}(\mathbf{A}(k_i)) = \min_k \lambda_{min}(\mathbf{A}(k)), \quad (11.2.11)$$

as $m = m_i \rightarrow \infty$ and $n = n_i \rightarrow \infty$. We now present the following algorithm to find the sequence $\{k_i\}$.

Algorithm (A) for seeking eigenvalues and eigenfunctions:

- Step 1.** Choose suitable term numbers, m and n , and good initial values of k^2 near to the target eigenvalue λ_l .
- Step 2.** Based on the local particular solutions $\{\Psi_i^\pm\}$, form the admissible functions $u_{m,n}$ from (11.2.2).
- Step 3.** For solving problem (11.1.6), the solution $u_{m,n}$ is obtained from the TM by the least squares method using the singular value decomposition [9, 176]. Then the scaled solution $\bar{u}_{m,n}$ is computed by (11.2.10), and the minimal eigenvalue is given by

$$f(k) = \lambda_{min}(\mathbf{A}(k)) = d_{min}^2,$$

where λ_{min} is the smallest eigenvalue value of $\mathbf{A}(k)$.

- Step 4.** If $f(k)$ is satisfactorily small, the values k^2 can be regarded as a good approximation to λ_l ; so $\bar{u}_{m,n}$ in (11.2.10) is close to ϕ_l , in view of the analysis in Section 11.2.2. Otherwise, we obtain a new value of k to minimize $f(k)$ in (11.2.11), based on Algorithm (B) given in the next subsection, and then return back to Step 2. If $f(k)$ can not be reduced sufficiently after many iterations through Steps 2-3, we should reasonably increase the term numbers, m and n , and then go to Step 1 for a new trial computation.

11.2.4 Solution of Nonlinear Equations

From (11.2.11) a real value of k^* should be chosen such that

$$f(k^*) = \min_k f(k) = 0, \quad (11.2.12)$$

where

$$f(k) = \lambda_{min}(\mathbf{A}(k)) \geq 0. \quad (11.2.13)$$

The condition ≥ 0 in (11.2.13) may not really happen in computation due to rounding errors. For instance, the very small negative values of $\lambda_{min}(\mathbf{A}(\bar{k}))$ may even occur. Also when m and n are too small,

$$\min_k \lambda_{min}(\mathbf{A}(k)) \geq \varepsilon > 0.$$

Therefore, minimization of $f(k)$ should be taken into account in Algorithm (A) instead of (11.2.12).

Suppose that

$$f(k) \in C^3, \text{ when } k \in (0, \infty), \quad (11.2.14)$$

where C^n is the space of the functions having continuous n th-order derivatives. Consider $f(k^*) = \min_k f(k)$, thus having $f'(k^*) = 0$.

An interpolatory quadratic polynomial $P_2(k)$ to $f(k)$ can be formulated through three pairs of the values

$$(k_i, f(k_i)), i = 0, 1, 2,$$

where k_i are distinct. Hence, a new value, k_3 , is found by

$$P_2'(k_3) = 0, \quad (11.2.15)$$

in order to minimize $P_2(k)$. In fact, the quadratic function can be formed by the Newton divided differences (see [9]):

$$P_2(k) = f(k_2) + \bar{w}(k - k_2) + f[k_2, k_1, k_0](k - k_2)^2, \quad (11.2.16)$$

where

$$\bar{w} = f[k_2, k_1] + (k_2 - k_1)f[k_2, k_1, k_0], \quad (11.2.17)$$

and the divided differences are defined by

$$f[k_2, k_1] = (f(k_2) - f(k_1))/(k_2 - k_1),$$

$$f[k_2, k_1, k_0] = (f[k_2, k_1] - f[k_1, k_0])/(k_2 - k_0).$$

Consequently, we obtain from (11.2.16) and (11.2.17)

$$k_3 = k_2 - \bar{w} / (2f[k_2, k_1, k_0]) = \frac{k_2 + k_1}{2} - \frac{1}{2} \frac{f[k_2, k_1]}{f[k_2, k_1, k_0]}. \quad (11.2.18)$$

Let us summarize the above approaches as the following algorithm with three steps.

Algorithm (B) for minimizing $f(k)$:

Step 1. Give three good distinct initial values

$$k_i \approx \sqrt{\lambda_i}, \quad i = 0, 1, 2, \quad (11.2.19)$$

and evaluate $f(k_i)$, i.e., the target eigenvalue by some numerical methods, for instance, by the QR method or the singular value decomposition [9, 176].

Step 2. Compute

$$k_{n+1} = \frac{k_n + k_{n-1}}{2} - \frac{1}{2} \frac{f[k_n, k_{n-1}]}{f[k_n, k_{n-1}, k_{n-2}]}, \quad n \geq 2. \quad (11.2.20)$$

Step 3. Stop if k_{n+1} is satisfactory, otherwise return to Step 1.

To integrate Algorithm (B) with Algorithm (A), we may embed (11.2.20) into Step 4 of Algorithm (A), and should also supply three good guesses (11.2.19) in Step 1. We now prove superlinear convergence rates of Algorithm (B).

Definition 11.2.1 *The sequence $\{k_i\}$ has superlinear convergence rates if the errors $\varepsilon_i = |k_i - k^*|$ satisfy*

$$\varepsilon_{n+1} \leq \alpha_n \varepsilon_n + \beta_n \varepsilon_{n-1}, \quad n = 1, 2, \dots \tag{11.2.21}$$

where the constants $\alpha_n \geq 0$ and $\beta_n \geq 0$ such that

$$\alpha_n \rightarrow 0 \text{ and } \beta_n \rightarrow 0 \text{ as } n \rightarrow \infty. \tag{11.2.22}$$

We note that the definition of superlinear convergence given in [2] is a special case of (11.2.21) when $\beta_n = 0$. In fact, based on the recurrence solutions, we can easily show that when $n \rightarrow \infty$ the errors ε_n diminish faster than those of any linear convergence rates. We provide a proposition, whose proof is given in [313].

Proposition 11.2.1 *Let (11.2.11), $f(k) \in C^4$ and $|f''(k^*)| \geq \delta > 0$ hold, and suppose that the sequence $\{k_i\}$ from Algorithm (B) converges. Then $\{k_i\}$ has a superlinear convergence rate.*

Let us compare Algorithm (B) with other popular methods of nonlinear equations. In Muller’s method (see [9]), a closer root is sought from the same quadratic equation (11.2.16). Since $k > 0$, the real k_i are chosen, then Eq. (11.2.18) leads to a modification, called the modified Muller’s method. If the secant method is applied to (11.2.12), then

$$k_{n+1} = k_n - p \frac{f(k_n)}{f[k_n, k_{n-1}]}, \quad n \geq 1, \tag{11.2.23}$$

where p is multiplicity of the root k^* , and $p \geq 2$ always. The secant method (11.2.23) also has a superlinear convergence rate (see [2]). When p is unknown and let $p = 1$, the sequence $\{k_n\}$ from (11.2.23) has only a linear convergence rate. However, we may then employ the Aitkin extiapolation to speed up convergence rates. Algorithm (B) has been proven to be very effective by our many computational experiments.

11.3 Error Bounds of Eigenvalues

In the above algorithms, the magnitude as well as the accuracy of $\lambda_{min}(\mathbf{A})$ are an important criterion to measure accuracy of numerical eigenvalues and eigenfunctions. This fact will be justified by a posteriori error analysis below. The eigenvalue problem (11.1.1) can be presented in a weak form: Seek $\lambda \in R$ and $0 \neq u \in H_0^1(\Omega)$ such that

$$(\nabla u, \nabla v) = \lambda(u, v), \quad \forall v \in H_0^1(\Omega), \tag{11.3.1}$$

where $\nabla = (\frac{\partial}{\partial x}, \frac{\partial}{\partial y})^T$, $(\nabla u, \nabla v) = \frac{\partial u}{\partial x} \frac{\partial v}{\partial x} + \frac{\partial u}{\partial y} \frac{\partial v}{\partial y}$, and the Sobolev space $H_0^1(\Omega) = \{v|v \in H^1(\Omega), v|_{\Gamma} = 0\}$. Define another space H_0^* such that

$$H_0^* = \{v|v \in H^1(\Omega^+), v \in H^1(\Omega^-), v^+ = v^- \text{ in } \Gamma_0, v_\nu^+ = v_\nu^- \text{ in } \Gamma_0, v|_{\Gamma} = 0\}.$$

Problem (11.1.4) can also be written in a weak form: Seek $\lambda \in R, 0 \neq u \in H_0^*$ such that

$$\langle \nabla u, \nabla v \rangle = \lambda(u, v), \quad \forall v \in H_0^1(\Omega), \quad (11.3.2)$$

where

$$\langle u, v \rangle = \iint_{\Omega^+} uv \, d\Omega + \iint_{\Omega^-} uv \, d\Omega.$$

By following Hall and Porsching [192], we can prove the following lemma.

Lemma 11.3.1 *The weak forms (11.3.1) and (11.3.2) are equivalent to each other, and*

$$\langle \nabla \phi_i, \nabla \phi_j \rangle = (\nabla \phi_i, \nabla \phi_j) = \lambda \delta_{i,j}. \quad (11.3.3)$$

From Lemma 11.3.1, we conclude that any function $v(\in H_0^*)$ can be expressed by the eigenfunctions $\{\phi_i\}^1$, i.e.,

$$v = \sum_{i=1}^{\infty} \alpha_i \phi_i, \quad (11.3.4)$$

with the real expansion coefficients α_i . Suppose that there exist jumps ϵ_1 and ϵ_2 of v and v_ν across the interface Γ_0 , then the Helmholtz equation (11.1.6) is reduced to

$$\begin{cases} \Delta u + k^2 u = 0 & \text{in } \Omega^+ \text{ and } \Omega^-, \\ [u]_{\Gamma_0} = \epsilon_1, \quad [u_\nu]_{\Gamma_0} = \epsilon_2, \\ u|_{\Gamma} = g, \end{cases} \quad (11.3.5)$$

where the notation $[u]_{\Gamma_0} = (u^+ - u^-)|_{\Gamma_0}$. We use an auxiliary function w defined below:

$$\begin{cases} \Delta w = 0, & \text{in } \Omega^+ \text{ and } \Omega^-, \\ [w]_{\Gamma_0} = \epsilon_1, \quad [w_\nu]_{\Gamma_0} = \epsilon_2, \\ w|_{\Gamma} = g. \end{cases} \quad (11.3.6)$$

Note that the function w is only for analysis but not for real computation. Now we have the following lemma.

Lemma 11.3.2 *Let k^2 be close to a target eigenvalue λ , and let u and w be the solutions of (11.3.5) and (11.3.6) satisfying²*

$$|w|_{0,\Omega} \leq \frac{1}{2}|u|_{0,\Omega}. \quad (11.3.7)$$

¹In fact, when $v \in H_0^*$, we have $v^+ = v^-$ and $v^+ v_\nu^+ = v^- v_\nu^-$, to give $|v|_{1,\Omega^+}^2 + |v|_{1,\Omega^-}^2 = |v|_{1,\Omega}^2 + \int_{\Gamma_0} (v^+ v_\nu^+ - v^- v_\nu^-) = |v|_{1,\Omega}^2$. Hence $v \in H_0^*$ implies $v \in H_0^1(\Omega)$, and v can be expanded by the complete set of eigenfunctions $\phi_i(\in H_0^1(\Omega))$.

²When k^2 is close to a target eigenvalue, u is close to its eigenfunction. Hence $\epsilon = \max\{|g|, |\epsilon_1|, |\epsilon_2|\}$ is small, and $|u|_{0,\Omega} = O(1)$ for some kinds of normalization. On the other hand, the maximal value of Laplace's solution w occurs only on the boundary, and then $|w|_{0,\Omega} \leq \epsilon \text{Area}(\Omega)$. Hence the assumption (11.3.7) can be made.

Then there exists an eigenvalue λ_l such that

$$\frac{|k^2 - \lambda_l|}{k^2} \leq 2 \frac{|w|_{0,\Omega}}{|u|_{0,\Omega}}. \quad (11.3.8)$$

Proof Let $v = u - w$, then

$$\begin{cases} \Delta v + k^2 v = -k^2 w, & \text{in } \Omega^+ \text{ and } \Omega^-, \\ [v]_{\Gamma_0} = 0, & [v_\nu]_{\Gamma_0} = 0, \\ v|_\Gamma = 0. \end{cases} \quad (11.3.9)$$

So $v \in H_0^*$, and the function v can be expressed by (11.3.4). We obtain from (11.1.4), (11.3.9) and (11.3.4) that

$$|w|_{0,\Omega}^2 = \frac{1}{k^2} |\Delta v + k^2 v|_{0,\Omega}^2 = \sum_{i=1}^{\infty} \left(\frac{k^2 - \lambda_i}{k^2} \right)^2 \alpha_i^2. \quad (11.3.10)$$

Also from (11.1.3), (11.3.4) and assumption (11.3.7)

$$\sum_{i=1}^{\infty} \alpha_i^2 = |v|_{0,\Omega}^2 = |u - w|_{0,\Omega}^2 \geq (|u|_{0,\Omega} - |w|_{0,\Omega})^2 \geq \frac{1}{4} |u|_{0,\Omega}^2. \quad (11.3.11)$$

Therefore, combining (11.3.10) and (11.3.11) yields

$$\min_i \left| \frac{k^2 - \lambda_i}{k^2} \right|^2 \leq \frac{\sum_{i=1}^{\infty} \left(\frac{k^2 - \lambda_i}{k^2} \right)^2 \alpha_i^2}{\sum_{i=1}^{\infty} \alpha_i^2} \leq 4 \frac{|w|_{0,\Omega}^2}{|u|_{0,\Omega}^2}.$$

The desired bound (11.3.8) is obtained. ■

The bounds (11.3.8) can also be derived from Kuttler and Sigilloto [272] on the entire solution domain. We cite two lemmas from Chapter 1.

Lemma 11.3.3 *Suppose that the auxiliary function of (11.3.6) satisfies the following inverse properties*

$$|w_\nu|_{0,\Gamma} \leq K_w \|w\|_H, \quad |w_\nu^+|_{0,\Gamma_0} \leq K_w \|w\|_H, \quad \forall w \in H,$$

where the constant K_w may depend on w . Then for any $\sigma > 0$ there exists a constant C independent of w such that

$$\|w\|_H \leq C(K_w + \sigma^{-1})|w|_B.$$

Lemma 11.3.4 *Let u be the solution of (11.1.6). Then for $\sigma > 0$ there exists a unique function $u_{m,n} \in S_{m,n}$ by the TM such that*

$$|u_{m,n}|_B \leq |g|_{0,\Gamma}, \quad |u - u_{m,n}|_B \leq C \inf_{v \in S_{m,n}} |u - v|_B.$$

Now let us prove a new theorem.

Theorem 11.3.1 *Let u be the piecewise particular solution of the Helmholtz equation (11.3.5). Suppose that all conditions in Lemmas 11.3.2 and 11.3.3 hold. Then $\exists \lambda_l$ such that*

$$\frac{|k^2 - \lambda_l|}{k^2} \leq C(K_w + \sigma^{-1}) \frac{|u|_B}{|u|_{0,\Omega}}, \quad (11.3.12)$$

where C is a bounded constant independent of u . Moreover, let $u_{m,n} \in S_{m,n}$, then

$$\frac{|k^2 - \lambda_l|}{k^2} \leq C(K_w + \sigma^{-1}) \frac{|u_{m,n}|_B}{|u_{m,n}|_{0,\Omega}}. \quad (11.3.13)$$

Proof From Lemmas 11.3.2 and 11.3.3 we obtain that

$$\frac{|k^2 - \lambda_l|}{k^2} \leq 2 \frac{|w|_{0,\Omega}}{|u|_{0,\Omega}} \leq 2 \frac{\|w\|_H}{|u|_{0,\Omega}} \leq C(K_w + \sigma^{-1}) \frac{|w|_B}{|u|_{0,\Omega}}. \quad (11.3.14)$$

Recall that the functions u and w have the same values on Γ and Γ_0 , by comparing (11.3.5) with (11.3.6) the desired result (11.3.12) is obtained, and so is (11.3.13) by letting $u = u_{m,n}$. ■

It is worthy pointing out that the ratio in (11.3.13)

$$\rho = \frac{|u_{m,n}|_B}{|u_{m,n}|_{0,\Omega}} \quad (11.3.15)$$

plays an important role in error estimates for both eigenvalues and eigenfunctions. Note that $u_{m,n}$ satisfies the Helmholtz equation (11.1.6) approximately under a given g on Γ . From Lemma 11.3.4 we directly have the following lemma.

Lemma 11.3.5 *Let $u_{m,n} (\in S_{m,n})$ be the solution to (11.1.6) from the TM. Suppose that there exists a constant $\rho_{10} (> 0)$ independent of m and n such that*

$$|u_{m,n}|_{0,\Omega} \geq \rho_{10} |c_1|,$$

where ρ_{10} may depend on k . Then the ratio (11.3.15) has the bounds

$$\rho \leq \frac{1}{\rho_{10}} |\bar{u}_{m,n}|_B, \quad \rho \leq \frac{1}{\rho_{10}} \frac{1}{|c_1|} |g|_{0,\Gamma}, \quad (11.3.16)$$

where the scaled solution $\bar{u}_{m,n}$ is given by (11.2.10).

Let us consider the stiffness matrix \mathbf{A} in (11.2.6). Denote the eigenvalues μ_i and eigenvectors $\bar{\mathbf{x}}_i$, then $\mathbf{A}\bar{\mathbf{x}}_i = \mu_i \bar{\mathbf{x}}_i$, where $0 < \mu_1 \leq \mu_2 \leq \dots \leq \mu_N$, $N = m + n$, and $\bar{\mathbf{x}}_i^T \bar{\mathbf{x}}_j = \delta_{ij}$.

We can also prove the following lemma by following [9], p. 604.

Lemma 11.3.6 *Let $\bar{\mathbf{x}}_{m,n}$ be vector of the coefficients of the TM solution $\bar{u}_{m,n}$ for (11.1.6) using the least squares method. Suppose that $\mu_1 = \lambda_{\min}(\mathbf{A}) \ll 1$, the next minimal eigenvalue $\mu_2 = \lambda_{\text{next}}(\mathbf{A}) = O(1)$, and \mathbf{x}_1 is the leading eigenvector of $\mathbf{A}(k)$ corresponding to μ_1 such that*

$$(\bar{\mathbf{x}}_{m,n}, \mathbf{e}_1) = (\alpha \mathbf{x}_1, \mathbf{e}_1) = c_1 \neq 0,$$

where \mathbf{e}_1 is the N -dimensional unit vector, $\mathbf{e}_1 = (1, 0, \dots, 0)^T$. Then there exist the bounds

$$c_1 = O\left(\frac{1}{\sqrt{\lambda_{\min}(\mathbf{A})}}\right), \quad (11.3.17)$$

and

$$\|\bar{\mathbf{x}}_{m,n} - \alpha \mathbf{x}_1\| = O\left(\sqrt{\frac{\lambda_{\min}(\mathbf{A})}{\lambda_{\text{next}}(\mathbf{A})}}\right),$$

with a suitable constant $\alpha \neq 0$.

Applying (11.3.13), (11.3.16) and (11.3.17) leads to the following corollary.

Corollary 11.3.1 *Let all conditions in Theorem 11.3.1 and Lemmas 11.3.5 and 11.3.6 hold. Then $\exists \lambda_l$ such that*

$$\left|\frac{k^2 - \lambda_l}{k^2}\right| \leq C \frac{(K_w + \sigma^{-1})}{\rho_{10}} |g|_{0,\Gamma} \sqrt{\lambda_{\min}(\mathbf{A})}. \quad (11.3.18)$$

Note that the function $g|_{\Gamma}$ in (11.1.6) may not be necessarily small. In fact, let $g = O(1)$, we can still conclude that if $\lambda_{\min}(\mathbf{A}) \rightarrow 0$ then $k^2 \rightarrow \lambda_l$. Also bounds of K_w can be derived by following Chapter 1 to give $K_w \leq C\sqrt{\max\{m, n\}}$ for a circular domain Ω^+ .

11.4 Error Bounds of Eigenfunctions

In the algorithms in Section 2.2, the solution $\bar{u}_{m,n}$ in (11.2.10) from the TM can also be regarded as an approximation to the eigenfunctions ϕ_l . First, let us assume the distinct eigenvalues

$$0 < \lambda_1 < \lambda_2 < \dots < \lambda_l < \dots$$

Also the values k^2 should be chose to be close to a target eigenvalue λ_l . We provide the following lemma.

Lemma 11.4.1 *Let u and w be the solutions of (11.3.5) and (11.3.6) respectively, and suppose that*

$$|\lambda_i - \lambda_j| \geq \beta > 0, \quad i \neq j, \quad (11.4.1)$$

$$|w|_{0,\Omega} < \min\left\{\frac{1}{2}, \frac{\beta}{4k^2}\right\} |u|_{0,\Omega}. \quad (11.4.2)$$

Then there exists the bound,

$$|k^2 - \lambda_l| < \frac{1}{2}\beta. \quad (11.4.3)$$

Proof From (11.4.1), (11.4.2) and (11.3.14) we have

$$|k^2 - \lambda_l| = \min_i |k^2 - \lambda_i| = k^2 \min_i \frac{|k^2 - \lambda_i|}{k^2} \leq k^2 \frac{2|w|_{0,\Omega}}{|u|_{0,\Omega}} < \frac{\beta}{2},$$

where we have used (11.3.14) under assumption (11.3.7). ■

Theorem 11.4.1 *Let the conditions in Lemmas 11.3.3 and 11.4.1 hold. Then there exists a real constant $a_l \neq 0$ such that*

$$|u - a_l \phi_l|_{0,\Omega} \leq C \frac{\lambda_l}{\beta} (K_w + \sigma^{-1}) |u|_B.$$

Proof Let $v = u - w$, then v satisfies (11.3.9). The functions $v \in H_0^*$ can also be expressed by (11.3.4). Since the coefficients can be obtained explicitly from the orthogonality (11.3.3), we have

$$\alpha_i = -\frac{k^2}{k^2 - \lambda_i} (w, \phi_i). \quad (11.4.4)$$

Then the solution u of (11.3.5) is given by

$$\begin{aligned} u &= w + v = w - \sum_{i=1}^{\infty} \frac{k^2}{k^2 - \lambda_i} (w, \phi_i) \phi_i \\ &= w + a_l \phi_l - \sum_{i \neq l}^{\infty} \frac{k^2}{k^2 - \lambda_i} (w, \phi_i) \phi_i, \end{aligned} \quad (11.4.5)$$

where $a_l = -\alpha_l = \frac{k^2}{k^2 - \lambda_l} (w, \phi_l)$. Since $\min_{i \neq l} |k^2 - \lambda_i| \geq \frac{\beta}{2}$, we obtain from (11.4.5) and the Parseval's inequality in Courant and Hilbert [109]

$$\begin{aligned} |u - a_l \phi_l|_{0,\Omega} &\leq |w|_{0,\Omega} + \sqrt{\sum_{\substack{i=1 \\ i \neq l}}^{\infty} \left(\frac{k^2}{k^2 - \lambda_i}\right)^2 (w, \phi_i)^2} \\ &\leq |w|_{0,\Omega} + \frac{2k^2}{\beta} \sqrt{\sum_{i=1}^{\infty} (w, \phi_i)^2} \leq \left(1 + \frac{2k^2}{\beta}\right) |w|_{0,\Omega}. \end{aligned} \quad (11.4.6)$$

Also it follows from (11.4.3) that

$$k^2 \leq \lambda_l + |k^2 - \lambda_l| \leq \lambda_l + \frac{\beta}{2}. \quad (11.4.7)$$

Finally by applying (11.4.6), (11.4.7) and Lemma 11.3.3,

$$\begin{aligned} |u - a_l \phi_l|_{0,\Omega} &\leq C \frac{\lambda_l}{\beta} |w|_{0,\Omega} \leq C \frac{\lambda_l}{\beta} \|w\|_H \\ &\leq C \frac{\lambda_l}{\beta} (K_w + \sigma^{-1}) |w|_B = C \frac{\lambda_l}{\beta} (K_w + \sigma^{-1}) |u|_B. \quad \blacksquare \end{aligned}$$

Theorem 11.4.2 *Let all conditions in Theorem 11.4.1 hold. Then there exists a real constant a_l such that*

$$\|u - a_l \phi_l\|_H \leq C \frac{\lambda_l^{3/2}}{\beta} (K_w + \sigma^{-1}) |u|_B. \quad (11.4.8)$$

Proof Let $v = u - a_l \phi_l$, we have from (11.3.5), (11.1.4) and (11.1.6)

$$\begin{aligned} |v|_H^2 &\leq \langle -\Delta v, v \rangle + C(K_w + \sigma^{-1})^2 |v|_B^2 \\ &= (k^2 u - \lambda_l a_l \phi_l, v) + C(K_w + \sigma^{-1})^2 |v|_B^2 \\ &= (\lambda_l v + (k^2 - \lambda_l)u, v) + C(K_w + \sigma^{-1})^2 |v|_B^2, \end{aligned}$$

where we have used that $a_l \phi_l = u - v$. Hence we obtain

$$|v|_H^2 \leq \lambda_l |v|_{0,\Omega}^2 + |k^2 - \lambda_l| |u|_{0,\Omega} |v|_{0,\Omega} + C(K_w + \sigma^{-1})^2 |v|_B^2. \quad (11.4.9)$$

Moreover, from Theorem 11.3.1,

$$|k^2 - \lambda_l| |u|_{0,\Omega} \leq k^2 (K_w + \sigma^{-1}) |u|_B. \quad (11.4.10)$$

Consequently, we can conclude from Theorem 11.4.1, (11.4.7), (11.4.9) and (11.4.10) that

$$\begin{aligned} \|v\|_H^2 &= |v|_{0,\Omega}^2 + |v|_H^2 \\ &\leq (1 + \lambda_l) |v|_{0,\Omega}^2 + k^2 (K_w + \sigma^{-1}) |u|_B |v|_{0,\Omega} + C(K_w + \sigma^{-1})^2 |v|_B^2. \end{aligned} \quad (11.4.11)$$

From Theorem 11.4.1,

$$|v|_{0,\Omega} = |u - a_l \phi_l|_{0,\Omega} \leq C \frac{\lambda_l}{\beta} (K_w + \sigma^{-1}) |u|_B,$$

Eq. (11.4.11) is reduced to

$$\|v\|_H^2 \leq C \left\{ (1 + \lambda_l) \left(\frac{\lambda_l}{\beta} \right)^2 (K_w + \sigma^{-1})^2 + k^2 (K_w + \sigma^{-1})^2 \frac{\lambda_l}{\beta} \right\} |u|_B^2.$$

The desired results (11.4.8) are obtained immediately by noting $v = u - a_l \phi_l$. ■

Theorem 11.4.3 *Let all the conditions in Theorem 11.4.1 hold, and let $u (= u_{m,n} \in S_{m,n})$ be the solution of (11.1.6) by the TM. Then there exists real $a_l \neq 0$ such that*

$$\frac{|u_{m,n} - a_l \phi_l|_{0,\Omega}}{|u_{m,n}|_{0,\Omega}} \leq C \frac{\lambda_l}{\beta} (K_w + \sigma^{-1}) \frac{|u_{m,n}|_B}{|u_{m,n}|_{0,\Omega}}, \quad (11.4.12)$$

and

$$\frac{\|u_{m,n} - a_l \phi_l\|_H}{|u_{m,n}|_{0,\Omega}} \leq C \frac{\lambda_l^{3/2}}{\beta} (K_w + \sigma^{-1}) \frac{|u_{m,n}|_B}{|u_{m,n}|_{0,\Omega}}. \quad (11.4.13)$$

Compared with (11.3.13), the error bounds (11.4.12) and (11.4.13) for eigenfunctions contain the same ratios ρ of (11.3.15). Therefore, other results as (11.3.18) can be similarly provided from Theorem 11.4.3, Lemmas 11.3.5 and 11.3.6.

To close this section, we consider the eigenvalues with multiplicity $r \geq 1$:

$$\cdots < \lambda_{l-1} < \lambda_l = \lambda_{l+1} = \cdots = \lambda_{l+r-1} < \lambda_{l+r} < \cdots$$

By similar arguments as the above, we can conclude that when u_{min} is an approximation for an eigenvalue of λ_l , there exists a linear combination of the eigenfunctions, $\phi_l, \phi_{l+1}, \cdots, \phi_{l+r-1}$, such that $\phi_l^* = \sum_{j=0}^r a_{l+j} \phi_{l+j}$, with real coefficients a_{l+j} . There also exist the error bounds

$$\begin{aligned} \frac{|u_{m,n} - \phi_l^*|_{0,\Omega}}{|u_{m,n}|_{0,\Omega}} &\leq C \frac{\lambda_l}{\beta} (K_w + \sigma^{-1}) \frac{|u_{m,n}|_B}{|u_{m,n}|_{0,\Omega}}, \\ \frac{\|u_{m,n} - \phi_l^*\|_H}{|u_{m,n}|_{0,\Omega}} &\leq C \frac{\lambda_l^{\frac{3}{2}}}{\beta} (K_w + \sigma^{-1}) \frac{|u_{m,n}|_B}{|u_{m,n}|_{0,\Omega}}. \end{aligned}$$

11.5 Computational Models and Numerical Experiments

In order to show the effectiveness of the new algorithms proposed, we first introduce in Section 11.5.1 a basic sample of eigenvalue problems, and seek their particular solutions. We will describe the detailed algorithms in Section 11.5.2, and then investigate the behavior of the nonlinear function $f(k)$ in Section 11.5.3. Numerical experiments are carried out in Section 11.5.4.

11.5.1 A Sample of Eigenvalue Problems and Particular Solutions

Consider a sample of eigenvalue problems (see Figure 11.1) and their corresponding Helmholtz equation

$$\begin{cases} \Delta u + \lambda u = 0 & \text{in } \Omega^*, \\ u|_{\Gamma} = 0, \end{cases} \quad \begin{cases} \Delta u + k^2 u = 0 & \text{in } \Omega^*, \\ u|_{\Gamma} = 1, \end{cases} \quad (11.5.1)$$

where Ω^* is the square solution domain $\{(x, y) | -1 < x < 1, -1 < y < 1\}$. The minimal eigenvalue and its eigenfunction of (11.5.1) are our main task. For simplicity, we apply the symmetry and seek the solution only in Ω , one eighth, of Ω^* (see Figure 11.2)³

$$\begin{cases} \Delta u + k^2 u = 0 & \text{in } \Omega, \\ u_{\nu}|_{\overline{AC}} = 0, \quad u_{\nu}|_{\overline{AB}} = 0, \\ u|_{\overline{BC}} = 1. \end{cases} \quad (11.5.2)$$

³In (11.5.2), we only consider the symmetry on \overline{AC} , which covers the most important minimal eigenvalue of the eigenvalue problem in Ω^* .

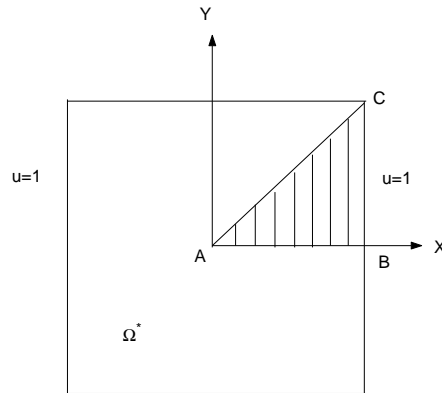


Figure 11.1: The entire solution domain.

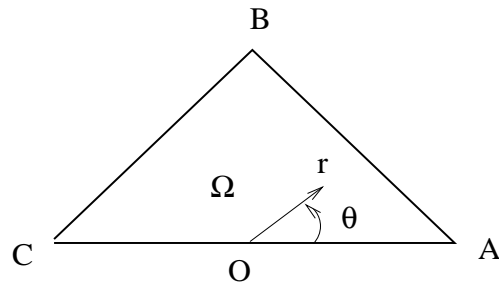


Figure 11.2: One-eighth of Figure 11.1 in Partition I.

Choose the admissible functions for the TM,

$$v_m = \sum_{i=0}^m \hat{c}_i J_i(kr) \cos i\theta, \tag{11.5.3}$$

where c_i are the coefficients to be sought, (r, θ) are the polar coordinates with the origin O, and $J_i(z)$ is the Bessel functions defined by [2, 181]

$$J_\mu(r) = \sum_{i=1}^{\infty} \frac{(-1)^i}{\Gamma(i+1)\Gamma(i+\mu+1)} \left(\frac{r}{2}\right)^{2i+\mu}. \tag{11.5.4}$$

Based on the study in Section 1.5 of Chapter 1, the following partition of Ω is beneficial to numerical stability:

$$\Omega = \Omega_0 \cup \Omega_1 \cup \Omega_2 \cup \Omega_3,$$

where the interface Γ_0 is composed of the piecewise straight lines as shown in Figures 11.3 and 11.4. The piecewise particular solutions can be found as follows:

$$\begin{aligned}
 v_m^{(0)} &= \sum_{i=0}^M \hat{c}_i J_i(kr) \cos i\theta \text{ in } \Omega_0, \\
 v_k^{(1)} &= 1 + \sum_{i=0}^K \hat{d}_i J_{2(2i+1)}(k\rho) \sin 2(2i+1)\phi \text{ in } \Omega_1, \\
 v_n^{(2)} &= 1 + \sum_{i=0}^N \hat{b}_i J_{2i+1}(k\xi) \sin(2i+1)w \text{ in } \Omega_2, \\
 v_l^{(3)} &= \sum_{i=0}^L \hat{a}_i J_{4i}(k\eta) \cos 4i\psi \text{ in } \Omega_3.
 \end{aligned} \tag{11.5.5}$$

In (11.5.6) $\hat{a}_i, \hat{b}_i, \hat{c}_i, \hat{d}_i$ are the unknown coefficients, and $(r, \theta), (\rho, \phi), (\xi, w)$ and (η, ψ) are the polar coordinates at the origins O, C, B, A, respectively. The division using the piecewise particular solutions in (11.5.6) is called Partition II; and the division in Figure 11.1 using (11.5.3) in the entire solution domain is called Partition I. Note that for the non-homogeneous boundary condition $u|_{\Gamma} = 1$, there exists a mild singularity $O(\rho^2 \ln \rho)$ at the corner C (i.e., the corners in Figure 11.2), and some singular solutions should be added for solving the Helmholtz equation exactly (see [314]). However for the homogeneous boundary condition $u|_{\Gamma} = 0$, such a mild singularity does not exist. Since for the eigenvalue problem, only the homogeneous Dirichlet conditions are involved, we ignore the singular functions given in [314], which have no effects on the stiffness matrix \mathbf{A} .

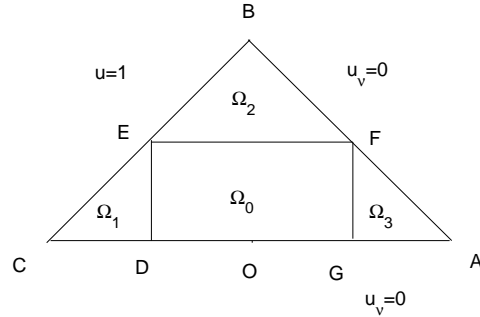


Figure 11.3: One-eighth of Figure 11.1 in Partition II.

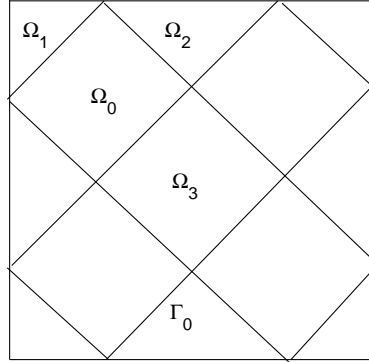


Figure 11.4: Partition II of the entire solution domain.

The eigenvalues and eigenfunctions of (11.5.1) are known as

$$\lambda_{i,j} = \frac{\pi^2}{4} [(2i-1)^2 + (2j-1)^2], \quad u_{i,j} = \cos \frac{(2i-1)\pi}{2} x \cos \frac{(2j-1)\pi}{2} y. \quad (11.5.6)$$

The following leading eigenvalue and eigenfunction are of most interest in physical problems:

$$\lambda_{min} = \lambda_{1,1} = \frac{\pi^2}{2}, \quad u_{1,1} = \cos \frac{\pi}{2} x \cos \frac{\pi}{2} y.$$

Below, let us provide the true expansions of $\hat{u}_{l,l}$ by means of the Bessel functions (11.5.4). Denote

$$\hat{k} = \sqrt{\lambda_{l,l}} = \frac{\pi}{\sqrt{2}}(2l-1), \quad l = 1, 2, \dots$$

and the eigenfunctions (11.5.6) with $i = j = l$ are reduced to

$$\hat{u}_{l,l} = 2 \cos \frac{\hat{k}}{\sqrt{2}} x \cos \frac{\hat{k}}{\sqrt{2}} y. \quad (11.5.7)$$

We have the following lemma.

Lemma 11.5.1 For the eigenfunctions (11.5.7), there exist the following expansions, spanned by the Bessel functions:

$$\begin{aligned} \hat{u}_{l,l} &= J_0(kr) + 2 \sum_{i=1}^{\infty} J_{2i}(\hat{k}r) \cos(2i)\theta \\ &+ 2(-1)^{l+1} \sum_{i=0}^{\infty} (-1)^i J_{2i+1}(\hat{k}r) \cos(2i+1)\theta \text{ in } \Omega_0, \end{aligned} \quad (11.5.8)$$

$$\hat{u}_{l,l} = 4 \sum_{i=0}^{\infty} (-1)^i J_{4i+2}(\hat{k}\rho) \sin(4i+2)\phi \text{ in } \Omega_1, \quad (11.5.9)$$

$$\hat{u}_{l,l} = 2\sqrt{2}(-1)^{l+1} \sum_{i=0}^{\infty} (-1)^{\lfloor \frac{i+1}{2} \rfloor} J_{2i+1}(\hat{k}\xi) \sin(2i+1)w \text{ in } \Omega_2, \quad (11.5.10)$$

$$\hat{u}_{l,l} = 2J_0(\hat{k}\eta) + 4 \sum_{i=1}^{\infty} (-1)^i J_{4i}(\hat{k}\eta) \cos 4i\psi \text{ in } \Omega_3, \quad (11.5.11)$$

where $\lfloor x \rfloor$ is the floor function of x .

Proof Firstly, to obtain (11.5.8), we have from (11.5.7)

$$\hat{u}_{l,l} = \cos \frac{\hat{k}}{\sqrt{2}}(x-y) + \cos \frac{\hat{k}}{\sqrt{2}}(x+y). \quad (11.5.12)$$

By using the coordinate transformation

$$x = \frac{1}{2} + r \cos\left(\theta - \frac{3}{4}\pi\right), \quad y = \frac{1}{2} + r \sin\left(\theta - \frac{3}{4}\pi\right),$$

we obtain after some manipulation

$$\hat{u}_{l,l} = \cos(\hat{k}r \sin \theta) + (-1)^{l+1} \sin(\hat{k}r \cos \theta).$$

Then the expansion (11.5.8) is obtained from the following formulas in [2], p. 361,

$$\begin{aligned} \cos(z \sin \theta) &= J_0(z) + 2 \sum_{i=1}^{\infty} J_{2i}(z) \cos 2i\theta, \\ \sin(z \cos \theta) &= 2 \sum_{i=0}^{\infty} (-1)^i J_{2i+1}(z) \cos(2i+1)\theta. \end{aligned}$$

Secondly, other formulas in [1] as such

$$\begin{aligned} \cos(z \cos \theta) &= J_0(z) + 2 \sum_{i=1}^{\infty} (-1)^i J_{2i}(z) \cos 2i\theta, \\ \sin(z \sin \theta) &= 2 \sum_{i=0}^{\infty} J_{2i+1}(z) \sin(2i+1)\theta, \end{aligned}$$

are also needed for proving (11.5.9) – (11.5.11). Based on the transformation

$$x = 1 - \xi \sin w, \quad y = \xi \cos w,$$

we obtain from (11.5.12) similarly

$$\begin{aligned} \hat{u}_{i,l} &= (-1)^{l+1} [\sin(\hat{k}\xi \sin(w + \frac{\pi}{4})) - \sin(\hat{k}\xi \cos(w + \frac{\pi}{4}))] \\ &= (-1)^{l+1} 2 \sum_{i=0}^{\infty} J_{2i+1}(\hat{k}\xi) [\sin(2i+1)(w + \frac{\pi}{4}) - (-1)^i \cos(2i+1)(w + \frac{\pi}{4})] \\ &= 2\sqrt{2}(-1)^{l+1} \sum_{i=0}^{\infty} (-1)^{\lfloor \frac{i+1}{2} \rfloor} J_{2i+1}(\hat{k}\xi) \sin(2i+1)w. \end{aligned} \quad (11.5.13)$$

This gives (11.5.10).

Thirdly, the expansions (11.5.9) and (11.5.11) can be obtained similarly by using the transformations $x = 1 - \rho \sin \phi, y = 1 - \rho \cos \phi$, and $x = \eta \cos \psi, y = \eta \sin \psi$, respectively. ■

Based on Lemma 11.5.1, we can find the true coefficients \hat{c}_i, \hat{a}_i , etc. in (11.5.3) and (11.5.6) of the eigenfunction $\hat{u}_{1,1}$:

$$\begin{aligned} \{\hat{c}_i\} &: 1, 2, 2, -2, 2, 2, 2, -2, \dots \\ \{\hat{a}_i\} &: 2, -4, 4, -4, 4, -4, 4, -4, \dots \\ \{\hat{b}_i\} &: 2\sqrt{2}, -2\sqrt{2}, -2\sqrt{2}, 2\sqrt{2}, 2\sqrt{2}, -2\sqrt{2}, -2\sqrt{2}, 2\sqrt{2}, \dots \\ \{\hat{d}_i\} &: 4, -4, 4, -4, 4, -4, 4, -4, \dots \end{aligned} \quad (11.5.14)$$

Since the leading coefficient $\hat{c}_0 = 1$ in (11.5.14), the errors of numerical eigenfunctions can be easily discovered. It is worth pointing out that this basic sample with particular solutions given in this subsection may serve for testing other numerical methods.

11.5.2 Description of the Detailed Algorithms for TM

In this subsection, we describe in detail the algorithms of the least squares methods to solve (11.2.4) (i.e., (11.2.5)).

In computation, it is better to choose the scaled forms of (11.5.3)

$$v_m = \sum_{i=0}^{4M-1} c_i \frac{J_i(kr)}{J_i(kr_0)} \cos i\theta, \quad \text{if } J_i(kr_0) \neq 0, \quad (11.5.15)$$

where $r_0 = \frac{1}{2}$ in computation. Hence $\hat{c}_i = \frac{c_i}{J_i(kr_0)}$, where \hat{c}_i are given in (11.5.3). Note that without such a scaling factor $\frac{1}{J_i(kr_0)}$, the convergence of Algorithm (A) will deteriorate. The admissible function (11.5.15) already satisfies the Helmholtz equation in Ω and the

boundary condition $u_\nu|_{\overline{AC}} = 0$. Hence the coefficients c_i should be chosen to satisfy the rest of the boundary conditions in (11.5.2). Define a quadratic functional

$$I(c_i) = \widehat{\int}_{\overline{BC}} (v-1)^2 dl + \sigma^2 \widehat{\int}_{\overline{AB}} v_\nu^2 dl, \quad (11.5.16)$$

where $\sigma = \frac{1}{4M}$. In (11.5.16), $\widehat{\int}_{\overline{BC}}$ is an approximation of $\int_{\overline{BC}}$, and the central and the Gaussian rules may be chosen for integration quadrature. The collocation TM in Partition I in [329] is designed for seeking the coefficients c_i such that

$$I(\tilde{c}_i) = \min_{c_i} I(c_i).$$

The boundary errors are defined by

$$|\varepsilon|_B = |\varepsilon|_I = \left(|\varepsilon|_{0,\overline{BC}}^2 + \sigma^2 |\varepsilon_\nu|_{0,\overline{AB}}^2 \right)^{\frac{1}{2}},$$

where the error $\varepsilon = u - u_m$.

For partition II, the continuity conditions across Γ_0 should be supplied to (11.5.2), thus leading to

$$\begin{cases} \Delta u + k^2 u = 0 \text{ in } \Omega_0, \Omega_1, \Omega_2, \Omega_3, \\ u^+ = u^-, \quad u_\nu^+ = u_\nu^- \text{ on } \Gamma_0, \\ u_\nu|_{\overline{AC}} = u_\nu|_{\overline{AB}} = 0, \\ u|_{\overline{BC}} = 1. \end{cases}$$

Similarly, the functions (11.5.6) should be scaled as

$$\begin{aligned} v_m^{(0)} &= \sum_{i=0}^{4M-1} c_i \frac{J_i(kr)}{J_i(kr_0)} \cos i\theta \text{ in } \Omega_0, \\ v_k^{(1)} &= 1 + \sum_{i=0}^K d_i \frac{J_{2(2i+1)}(k\rho)}{J_{2(2i+1)}(k\rho_0)} \sin(2i+1)\phi \text{ in } \Omega_1, \\ v_n^{(2)} &= 1 + \sum_{i=0}^N b_i \frac{J_{2i+1}(k\xi)}{J_{2i+1}(k\xi_0)} \sin(2i+1)w \text{ in } \Omega_2, \\ v_l^{(3)} &= \sum_{i=0}^L a_i \frac{J_{4i}(k\eta)}{J_{4i}(k\eta_0)} \cos 4i\psi \text{ in } \Omega_3, \end{aligned} \quad (11.5.17)$$

where $r_0 = \rho_0 = \psi_0 = \eta_0 = \frac{1}{2}$ in computation, and all the denominators in (11.5.18) are assumed to be nonzero. The admissible functions (11.5.18) satisfy the Helmholtz equations in Ω_i and the exterior boundary condition on $\partial\Omega$ already, i.e., $u_\nu|_{\overline{AC}} = u_\nu|_{\overline{AB}} =$

0, and $u|_{\overline{BC}} = 1$. Hence, the collocation TM in Partition II is designed for seeking the coefficients c_i, d_i, b_i, a_i so as to minimize the functional

$$II(\tilde{a}_i, \tilde{b}_i, \tilde{c}_i, \tilde{d}_i) = \min_{a_i, b_i, c_i, d_i} II(a_i, b_i, c_i, d_i),$$

where $II(\tilde{a}_i, \tilde{b}_i, \tilde{c}_i, \tilde{d}_i)$ involves only the interior boundary conditions,

$$II(\tilde{a}_i, \tilde{b}_i, \tilde{c}_i, \tilde{d}_i) = \int_{\Gamma_0} (v^+ - v^-)^2 dl + \sigma^2 \int_{\Gamma_0} (v_\nu^+ - v_\nu^-)^2 dl,$$

with $\sigma|_{DE} = \frac{1}{\max(4M, 4K+2, 2N+1, 4L)}$, etc. Also the error norm on the boundary is defined by

$$|\varepsilon|_{II} = (|v^+ - v^-|_{0, \Gamma_0}^2 + \sigma^2 |u_\nu^+ - u_\nu^-|_{0, \Gamma_0}^2)^{\frac{1}{2}}.$$

11.5.3 Investigation of Behavior for the Function $f(k)$ as $k^2 \rightarrow \lambda_1$.

To support Algorithm (B) we first study the function, $f(k) = \lambda_{min}(\mathbf{A}(k))$, as $k^2 = \lambda_{min}$ and $k^2 \rightarrow \lambda_{min}$, respectively, where $\lambda_{min} = \pi^2/2$.

Given $k^2 = \lambda_{min}$, the collocation TM in Partitions I and II are used to obtain the solutions, u_m and $u_{m,n,k,l}$. Studies on term distribution in Partition II may be referred refer to Chapter 1. When different terms are chosen, the calculated results are provided in Table 11.1, where $\lambda_{min}(\mathbf{A})$, $\lambda_{next}(\mathbf{A})$ and $\lambda_{max}(\mathbf{A})$ denote the minimal, next minimal and maximal eigenvalues of the associated matrix \mathbf{A} respectively. The condition numbers are computed from (11.2.7); the values $\sqrt{\frac{\lambda_{min}(\mathbf{A})}{\lambda_{next}(\mathbf{A})}}$ are also valuable to measure an approximate degree of eigenvectors (see Lemma 11.3.6). The errors $|\varepsilon^*|_I = |\varepsilon|_I/c_0$, and $|\varepsilon^*|_{II} = |\varepsilon|_{II}/c_0$, where c_0 is the leading coefficient of the eigenfunction of λ_{min} . From Table 11.1 we can see that $M = 1$ is inappropriate, but $M = 3 - 5$ will lead to a good approximation of λ_{min} .

To discover the behavior of $\lambda_{min}(\mathbf{A})$ as $k^2 \rightarrow \lambda_1$, we choose

$$k(\delta^*) = [\lambda_{min} + \delta^*(\lambda_{next} - \lambda_{min})]^{\frac{1}{2}}, \quad \lambda_{min} = \frac{\pi^2}{2}, \quad \lambda_{next} = 2.5\pi^2,$$

where $\delta^* = 0.5$ and $\delta^* = (0.1)^i, i = 1, 2, \dots, 9$. The results are listed in Table 11.2 for two partitions. When $\delta^* \rightarrow 0$, we can see

$$\lambda_{min}(\mathbf{A}) \rightarrow 10^{-11} \text{ in Partition I, } \lambda_{min}(\mathbf{A}) \rightarrow 10^{-14}, \text{ in Partition II.}$$

From Figure 11.5 we can see that the λ_{min} can be obtained by minimizing $\lambda_{min}(\mathbf{A}(k))$, which accuracy may reach to $O(10^{-8})$ and $O(10^{-9})$ in Partitions I and II, respectively. Obviously, the sensitivity of $\lambda_{min}(\mathbf{A})$ on δ^* in Partition II is higher than that in Partition I. We then expect that Partition II will have a better performance in seeking eigenvalues.

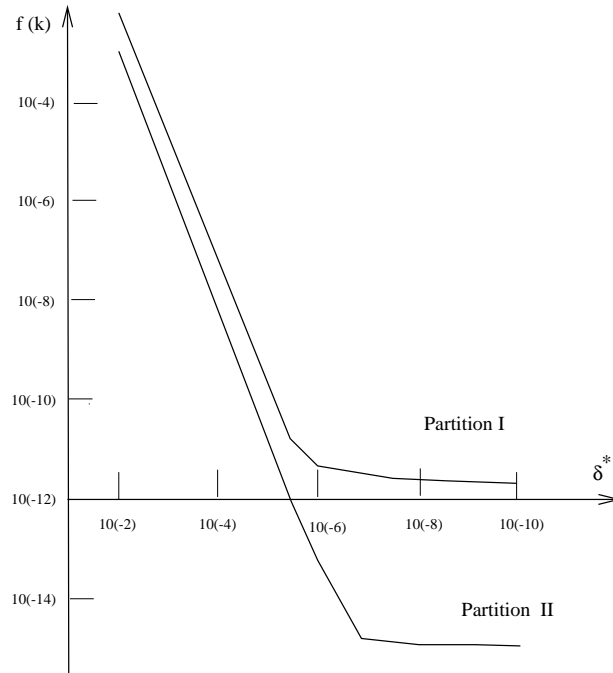


Figure 11.5: The curves of $f(k) = \lambda_{\min}(\mathbf{A}(k))$ versus δ^* from Table 11.2.

Moreover, straight lines with the slope -2 in Figure 11.5 demonstrates the asymptotic behavior

$$\delta = O(\delta^*) = O(\sqrt{\lambda_{\min}(\mathbf{A})}),$$

which also agrees with (11.3.16) – (11.3.17).

11.5.4 Computation for the Minimal Eigenvalue and Corresponding Eigenfunction

Let us apply Algorithms (A) and (B) to seek λ_{\min} and u_{11} . The initial values of k are chosen as

$$k_0 = 2, \quad k_1 = 2.001, \quad k_2 = 2.002 \quad (11.5.18)$$

and the iterative results are given in Tables 11.3, 11.4, 11.6 and 11.7. In Table 11.4(b), N_1 , N_2 , and N_3 denote the numbers of subintervals of the central rule on \overline{EF} , \overline{DE} and \overline{FG} in Figure 11.3, respectively. All data in the tables in this chapter are carried out by Fortran programs in double precision. Excellent eigenvalues and eigenfunctions have been obtained. Since the relative errors

$$\delta = \left| \frac{k^2 - \lambda_l}{k^2} \right| \approx \frac{2}{k} \Delta \tilde{\lambda}_l \text{ as } k \rightarrow \lambda_l,$$

we can see from Table 11.3

$$\delta \approx 1.7 \times 10^{-8}, \text{ and } 2.2 \times 10^{-9}$$

at the tenth iteration for Partition I and II, respectively. Compared the coefficients in Table 11.4 with the true values (11.5.14), the following coefficient errors of the eigenfunctions can be observed

$$\Delta \hat{c}_0 = 0, \quad \Delta \hat{c}_i \approx 2 \sim 7 \times 10^{-3}, \quad i = 1, 2, 3, 4$$

for Partition I, and

$$\Delta \hat{c}_0 = 0, \quad \Delta \hat{c}_i \approx 2 \times 10^{-4}, \quad i = 1, 2, 3, 4,$$

$$\Delta \hat{a}_0 \approx 1 \times 10^{-4}, \quad \Delta \hat{b}_0 \approx 2 \times 10^{-4}, \quad \Delta \hat{d}_0 \approx 3 \times 10^{-4}$$

for Partition II. Evidently, Partition II has a better performance, as expected.

To display the effectiveness of Algorithm (B), let us compare it with other popular nonlinear methods, such as Brent's method in [9], the Secant method, the Modified Muller's method, etc. described in Section 11.2.4. Numerical experiments under the same initial values in (11.5.18) are used and results are summarized in Table 11.5. Algorithm (B) exhibits the best performance by giving the most accurate solutions with the fewest iterations. Take Partition II as an example,

$$\Delta \sqrt{\tilde{\lambda}_{min}} = |\sqrt{\tilde{\lambda}_{min}} - \sqrt{\lambda_{min}}| \approx 2.5 \times 10^{-9}, \quad \lambda_{min}(A) \approx 4.7 \times 10^{-15}$$

by ten iterations including the three initial values. In contrast, the modified Muller's method and the Secant method can reach only the errors

$$\Delta \sqrt{\tilde{\lambda}_{min}} \approx 3 \times 10^{-7} \text{ and } 8 \times 10^{-6},$$

and they may, sometimes, have troubles in seeking other eigenvalues, based on trial computation. Furthermore, we have chosen other kinds of functions instead of (11.2.13), such as

$$f(k) = \sqrt{\lambda_{min}(\mathbf{A})}, \text{ or } \det|\mathbf{A}(k)| \text{ as in [156]}$$

to carry out Algorithms (A) and (B). Unfortunately, computation shows that the sequences obtained are either divergent or very slowly convergent.

From data of Partition I in Tables 11.6 and 11.7(a), we can discover that the following results at $M = 3$ are best:

$$\begin{aligned} \Delta \tilde{\lambda}_{min} &\approx 1.5 \times 10^{-8}, \quad i.e., \quad \delta \approx 1.3 \times 10^{-8}, \\ \lambda_{min}(\mathbf{A}) &\approx 9 \times 10^{-15}, \quad |\varepsilon^*|_I \approx 3.7 \times 10^{-11}, \\ \Delta \hat{c}_0 &= 0, \quad \Delta \hat{c}_1 \approx 3 \times 10^{-8}, \quad \Delta \hat{c}_2 \approx 2 \times 10^{-8}. \end{aligned}$$

From Tables 11.6 and 11.7(b), however, at $M = 3 \sim 5$ in Partition II the solutions are highly accurate. Take $L = M = K = 3$ and $L = 5$ as an example, we have

$$\begin{aligned}\Delta\tilde{\lambda}_{min} &\approx 2.5 \times 10^{-9}, \quad i.e., \quad \delta \approx 2 \times 10^{-9}, \\ \lambda_{min}(\mathbf{A}) &\approx 7 \times 10^{-18}, \quad |\varepsilon^*|_{II} \approx 2.5 \times 10^{-12}, \\ \Delta\hat{c}_0 &= 0, \quad \Delta\hat{c}_1 \approx 5 \times 10^{-9}, \quad \Delta\hat{c}_2 \approx 3 \times 10^{-9}, \\ \Delta\hat{a}_0 &\approx 8 \times 10^{-9}, \quad \Delta\hat{b}_0 \approx 4 \times 10^{-9}, \quad \Delta\hat{d}_0 \approx 5 \times 10^{-9}.\end{aligned}$$

Consequently, using piecewise particular solutions in Partition II is preferable. Note that the leading coefficients directly from the collocation TM may be extremely large due to degeneracy, i.e.,

$$\tilde{c}_0 \approx 4.2 \times 10^7 \text{ and } 2.5 \times 10^8 \text{ as } M = 3$$

for Partitions I and II, respectively (also see Lemma 11.3.6).

11.6 Eigenvalues for the Cracked Beam

Let us consider a new eigenvalue problem for the cracked beam (see Figure 11.6)

$$\begin{aligned}-\Delta u &= \lambda u, \quad \text{in } \Omega, \\ u &= 0, \quad \text{on } \overline{OD}, \\ u &= 1, \quad \text{on } \overline{BC}, \\ u_\nu &= 0, \quad \text{on } \overline{OA} \cup \overline{AB} \cup \overline{CD},\end{aligned}$$

where $\Omega = (-1, 1) \times (0, 1)$. We may solve the Helmholtz problem

$$\begin{aligned}-\Delta u &= k^2 u, \quad \text{in } \Omega, \\ u &= 0, \quad \text{on } \overline{OD}, \\ u &= 1, \quad \text{on } \overline{BC}, \\ u_\nu &= 0, \quad \text{on } \overline{OA} \cup \overline{AB} \cup \overline{CD}.\end{aligned}$$

The particular solutions are given by

$$v^+ = \sum_{i=1}^{\infty} \hat{c}_i J_{i-\frac{1}{2}}(kr) \cos\left(i - \frac{1}{2}\right)\theta, \quad (11.6.1)$$

where \hat{c}_i are expansion coefficients. In computation, we choose

$$v^+ = \sum_{i=1}^L c_i \frac{J_{i-\frac{1}{2}}(kr)}{J_{i-\frac{1}{2}}(kr_0)} \cos\left(i - \frac{1}{2}\right)\theta,$$

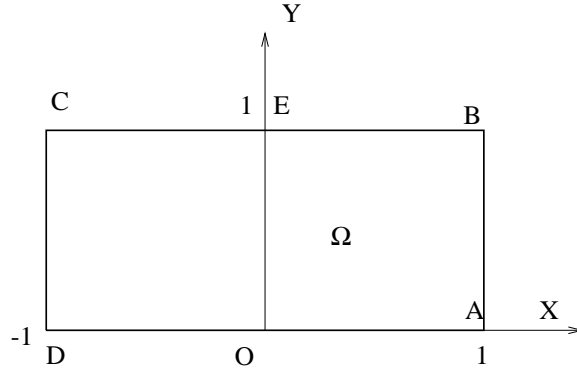


Figure 11.6: The crack beam problem.

where r_0 is a parameter chosen as $r_0 = 1$ in computation. There exist the relations between \hat{c}_i and c_i

$$\hat{c}_i = \frac{c_i}{J_{i-\frac{1}{2}}(kr_0)}.$$

In Algorithm (B), a good initial guess of $\sqrt{\lambda_{min}}$ (or $\sqrt{\lambda_{next}}$) is important to its convergence. Let us derive a bound of λ_{min} . First consider an auxiliary eigenvalue problem (Figure 11.7(a))

$$-\Delta u = \lambda u, \quad \text{in } \hat{S}, \quad (11.6.2)$$

$$u = 0, \quad \text{on } y = \pm 1, \quad (11.6.3)$$

where $\hat{S} = \{(x, y) \mid -\infty < x < \infty, -1 < y < 1\}$. The eigenfunctions of (11.6.2) and (11.6.3) are

$$u = \cos \left\{ \frac{(2i-1)\pi}{2} y \right\}.$$

Hence the minimal eigenvalue is found as

$$\hat{\lambda}_{min} = \frac{\pi^2}{4}. \quad (11.6.4)$$

In fact, the minimal eigenvalue of the crack beam is also that for the domain in the Figure 11.7(b), which has the additional Dirichlet condition on the middle broken sections. Hence

based on [109], there exists the bound

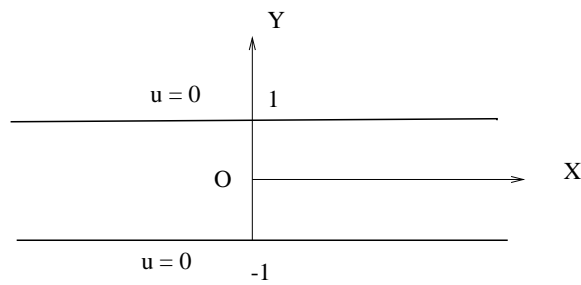
$$\frac{\pi^2}{4} = \hat{\lambda}_{min} \leq \lambda_{min}.$$

Next, consider another auxiliary eigenvalues on $S^+ = (-1, 1) \times (-\frac{1}{2}, \frac{1}{2})$ with the Dirichlet condition on the entire boundary ∂S . Since its eigenfunctions are

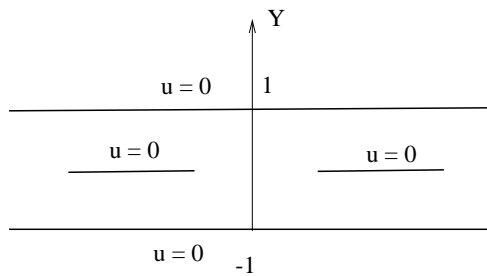
$$u = \cos \left\{ \frac{(2i-1)\pi}{2} x \right\} \cos(2j-1)\pi y,$$

the minimal eigenvalue is given by

$$\lambda_{min}^+ = \frac{\pi^2}{4} + \pi^2 = \frac{5}{4}\pi^2.$$



(a)



(b)

Figure 11.7: The auxiliary eigenvalue problem (a), and the expanded cracked beam eigenvalue problem (b).

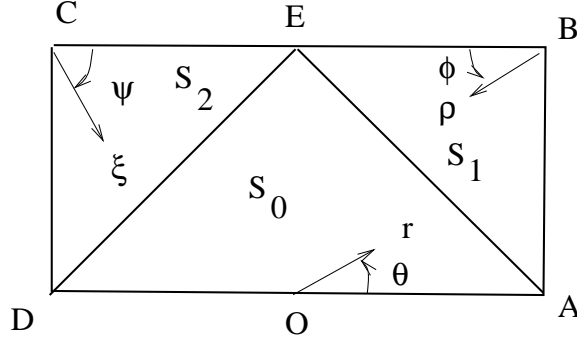


Figure 11.8: A partition for the crack beam eigenvalue problem

For the cracked beam eigenvalue problem in (11.6.1), there exists some Neumann condition on a part of ∂S^+ . Hence we have the bound from [109]

$$\lambda_{min} \leq \lambda_{min}^+ = \frac{5}{4}\pi^2. \quad (11.6.5)$$

Combining (11.6.4) and (11.6.5) gives

$$\frac{\pi^2}{4} \leq \lambda_{min} \leq \frac{5}{4}\pi^2, \quad \frac{\pi}{2} \leq \sqrt{\lambda_{min}} \leq \frac{\sqrt{5}}{2}\pi. \quad (11.6.6)$$

Based on the bound of (11.6.6), we may easily find a good initial value of k for λ_{min} . By increasing k , we can find a good initial value of k for λ_{next} of the cracked beam eigenvalue problem.

Let $\Omega = S_0 \cup S_1 \cup S_2$ in Figure 11.8. We choose the piecewise particular solutions,

$$\begin{aligned} v_L &= \sum_{i=1}^L c_i \frac{J_{i-\frac{1}{2}}(kr)}{J_{i-\frac{1}{2}}(kr_0)} \cos\left(i - \frac{1}{2}\right)\theta, \quad \text{in } S_0, \\ v_M &= 1 + \sum_{i=1}^M a_i \frac{J_{2i-1}(k\rho)}{J_{2i-1}(k\rho_0)} \sin(2i-1)\phi, \quad \text{in } S_1, \\ v_N &= 1 + \sum_{i=1}^N b_i \frac{J_{2i-1}(k\xi)}{J_{2i-1}(k\xi_0)} \sin(2i-1)\psi, \quad \text{in } S_2, \end{aligned}$$

where c_i, a_i and b_i are the unknown coefficients to be sought, and the parameters $r_0 = \rho_0 = \xi_0 = \frac{\sqrt{2}}{2}$. The polar coordinates (r, θ) , (ρ, ϕ) and (ξ, ψ) are shown in Figure 11.8.

The computed results are listed in Tables 11.8 and 11.9, and the coefficients of the eigenfunction of λ_{min} in Table 11.10. It can be seen from Tables 11.8 and 11.9 that

$$\sqrt{\lambda_{min}} = 2.01169, \quad \sqrt{\lambda_{next}} = 3.29315. \quad (11.6.7)$$

By Mathematica, the more accurate eigenvalues of λ_{min} and λ_{next} with 13 significant digits have been obtained as

$$\sqrt{\lambda_{min}} = 2.011697117212, \quad \sqrt{\lambda_{next}} = 3.293152635104. \quad (11.6.8)$$

Compared with (11.6.8), the values of $\sqrt{\lambda_{min}}$ and $\sqrt{\lambda_{next}}$ in (11.6.7) have six significant digits. Moreover, the more accurate values of ratios $(\frac{\hat{c}_i}{\hat{c}_1})$ of the leading eigenfunction $u_1(x, y)$ of λ_{min} have also been obtained by Mathematica,

$$\begin{aligned} \frac{\hat{c}_2}{\hat{c}_1} &= 0.6923013967, & \frac{\hat{c}_3}{\hat{c}_1} &= 0.9999999999, & \frac{\hat{c}_4}{\hat{c}_1} &= 0.6923013967, & (11.6.9) \\ \frac{\hat{c}_5}{\hat{c}_1} &= 0.1646930969, & \frac{\hat{c}_6}{\hat{c}_1} &= -2.5971209876, & \frac{\hat{c}_7}{\hat{c}_1} &= 0.1646930969. \end{aligned}$$

Compared with (11.6.9), although the values of $(\frac{\hat{c}_i}{\hat{c}_1}), i = 2, 3, \dots, 6$ in Table 11.10b are slightly more accurate than those in Table 11.10a, those in both Table 11.10a and 11.10b have five significant digits.

From Table 11.10, we observe the approximate relations

$$\hat{c}_{4i+1} \approx \hat{c}_{4i+3}, \quad \hat{c}_{4i+2} \approx \hat{c}_{4i+4}, \quad i = 0, 1, 2.$$

The above approximation also holds for the eigenfunctions of λ_{next} and other eigenvalues. Now we assume that there exist the equalities

$$\hat{c}_{4i+1} = \hat{c}_{4i+3}, \quad \hat{c}_{4i+2} = \hat{c}_{4i+4}, \quad i = 0, 1, \dots$$

To save the CPU time, we may join those duplicate coefficients to be unique coefficients, and employ the above algorithms to obtain the numerical solutions, which are very close to those in Table 11.10. Details are omitted.

11.7 Summaries and Discussions

To close this chapter, let us summarize the nature and novelties of the new methods for eigenvalue problems, and give a few concluding remarks.

1. The new algorithms for eigenvalue problems lie in solutions of the Helmholtz equation (11.1.6) by modifying k to lead to a degeneracy. The degeneracy is measured by the infinitesimal values of the minimal eigenvalue of the associate matrix $\mathbf{A}(k)$ in (11.2.5); and the modification to k is realized by Algorithm (B). Algorithms (A) and (B) are based on the fact that the eigenfunctions of (11.1.4) will dominate the solutions of (11.1.6) when a degeneracy occurs.

2. The degeneracy plays an important role in our algorithms. The leading coefficients such as c_1 are very large, and the scale solutions (11.2.10) are recommended due to the simplicity and high accuracy of c_1 . It is interesting to note that arbitrariness of the bounded function $g(\neq 0)$ in (11.1.6) does not influence much the final solutions of the algorithms. Hence we simply choose $g|_{\Gamma} = 1$ in the computational models.
3. Finding the minimum of an interpolatory quadratic polynomial, a specific iteration of Algorithm (B) is designed to find the eigenvalue and eigenfunctions effectively. Superlinear convergence rates are proven in [313], and comparison of numerical experiments is made in Table 11.5. Algorithm (B) may be regarded as a variation of Muller's method for real roots. Since matrix \mathbf{A} is symmetric, the eigenvalues of $\lambda_{\min}(\mathbf{A}(k))$ are all real. Of course, Algorithm (B) is expected to be better than Muller's method. Table 11.5 already reveals the best performance of Algorithm (B).
4. A basic sample of eigenvalue problems accompanied with piecewise particular solutions is given in Section 11.5.1; it can be adopted to test the effectiveness of numerical methods. Algorithms (A) and (B) are also applied to the eigenvalue problems with singularity. Since the eigenvalues and the expansion coefficients of eigenfunctions are very accurate, they can be treated as the true solution, to evaluate the true errors of solutions by other numerical methods, e.g., FEM, FDM, FVM, BEM, etc.
5. Only individual eigenvalues and eigenfunctions are sought by the methods given in this chapter. We may apply them to seek the leading eigenvalues in (11.1.2), which are of most interests in engineering problems.
6. However, the Trefftz method (TM) needs the explicit particular functions. This limitation confines these methods to linear eigenvalue problems, where local particular solutions can be found in textbooks or from some asymptotic analysis as done in Section 11.5.1 and in [314].
7. This chapter may be regarded as a further development of Fox, Henrici and Moler [156] by using piecewise particular solutions. The methods in [156] use *uniform* particular solutions to seek the eigenvalues of (11.1.1). The algorithms in this chapter adopt *piecewise* particular solutions, thus leading to a wide range of application of complicated eigenvalue problems, for instance those with multiple singularities. Hence we may partition the solution domain into finite subdomains, local particular solutions can be employed in the subdomains. This yields a frame work of the collocation TM for eigenvalue problems.

M		$ \epsilon _I$	Cond.	$\lambda_{min}(\mathbf{A})$	$\lambda_{next}(\mathbf{A})$	$\lambda_{max}(\mathbf{A})$	$\sqrt{\frac{\lambda_{min}(\mathbf{A})}{\lambda_{next}(\mathbf{A})}}$		
1		0.170	0.125(3)	0.207(-3)	1.02	3.23	0.0143		
2		0.304(-3)	0.298(7)	0.290(-11)	0.314	25.8	0.304(-5)		
3		0.209(-7)	0.190(9)	-0.746(-14)	0.146	26.9	0.226(-6)		
4		0.103(-13)	0.293(11)	-0.372(-17)	0.0838	0.314(4)	0.666(-8)		
5		0.122(-13)	0.1076(12)	-0.109(-18)	0.0541	0.403(5)	0.142(-8)		
L	M	N	K	$\ \epsilon\ _{II}$	Cond.	$\lambda_{min}(\mathbf{A})$	$\lambda_{next}(\mathbf{A})$	$\lambda_{max}(\mathbf{A})$	$\sqrt{\frac{\lambda_{min}(\mathbf{A})}{\lambda_{next}(\mathbf{A})}}$
1	1	2	1	0.337	706.	0.426(-5)	0.0667	0.212	0.799(-2)
2	2	3	2	0.827(-5)	0.216(8)	0.459(-14)	0.0148	2.14	0.557(-6)
3	3	5	3	0.166(-9)	0.212(9)	-0.480(-16)	0.245(-2)	2.15	0.140(-6)
4	4	7	4	0.121(-12)	0.197(9)	-0.555(-16)	0.387(-3)	2.16	0.379(-6)
5	5	9	5	0.789(-13)	0.140(9)	0.111(-15)	0.599(-4)	2.17	0.136(-5)

Table 11.1: The calculated results for Partitions I and II with $k = \sqrt{\lambda_1}$.

δ^*	Difference: $k(\delta^*) - \sqrt{\lambda_1}$	Partition I		Partition II	
		$ \epsilon _I$	$\lambda_{min}(\mathbf{A})$	$ \epsilon _{II}$	$\lambda_{min}(\mathbf{A})$
0.5	1.63	0.139(-2)	0.104	0.157	0.0150
0.1	0.407	0.184(-2)	0.548(-2)	0.772(-2)	0.0139
0.01	0.0440	0.111(-3)	0.497(-4)	0.333(-2)	0.121(-4)
0.1(-2)	0.444(-2)	0.931(-5)	0.493(-6)	0.304(-4)	0.119(-6)
0.1(-3)	0.444(-3)	0.154(-5)	0.492(-8)	0.309(-5)	0.119(-8)
0.1(-4)	0.444(-4)	0.206(-5)	0.521(-10)	0.405(-6)	0.119(-10)
0.1(-5)	0.444(-5)	0.534(-5)	0.338(-11)	0.182(-6)	0.124(-12)
0.1(-6)	0.444(-6)	0.432(-4)	0.290(-11)	0.374(-6)	0.586(-14)
0.1(-7)	0.444(-7)	0.190(-3)	0.289(-11)	0.518(-5)	0.457(-14)
0.1(-8)	0.444(-8)	0.302(-3)	0.289(-11)	0.112(-4)	0.463(-14)
0.1(-9)	0.444(-9)	0.287(-3)	0.289(-11)	0.849(-5)	0.471(-14)
0.0	0.0	0.304(-3)	0.290(-11)	0.827(-5)	0.459(-14)

Table 11.2: The calculated results for Partition I ($M = 2$) and Partition II ($L = M = K = 2, N = 3$) as $k(\delta^*) \rightarrow \sqrt{\lambda_1}$.

(a) for Partition I ($M = 2$)

n	$\sqrt{\tilde{\lambda}_1^{(n)}}$	$\Delta\sqrt{\tilde{\lambda}_1^{(n)}}$	$\lambda_{min}(\mathbf{A})$	$ \epsilon _I$	Cond.	$\sqrt{\frac{\lambda_{min}(\mathbf{A})}{\lambda_{next}(\mathbf{A})}}$
1	2.0		0.1054(-2)			
2	2.001		0.1045(-2)			
3	2.002		0.1036(-2)			
4	2.2852315962	0.0638	0.1059(-3)	0.166(-3)	0.493(3)	0.0186
5	2.2286927857	0.0725(-2)	0.1317(-5)	0.166(-5)	0.442(4)	0.205(-2)
6	2.2161309892	-0.531(-2)	0.7004(-6)	0.141(-5)	0.607(4)	0.149(-2)
7	2.2214700664	0.286(-4)	0.2325(-10)	0.216(-5)	0.105(7)	0.860(-5)
8	2.2214285150	-0.130(-4)	0.7088(-11)	0.227(-5)	0.191(7)	0.475(-5)
9	2.2214414601	-0.898(-8)	0.2894(-11)	0.352(-5)	0.299(7)	0.303(-5)
10	2.2214414879	0.185(-7)	0.2893(-11)	0.242(-4)	0.299(7)	0.303(-5)

(b) for Partition II ($L = M = K = 2, N = 3$)

n	$\sqrt{\tilde{\lambda}_1^{(n)}}$	$\Delta\sqrt{\tilde{\lambda}_1^{(n)}}$	$\lambda_{min}(\mathbf{A})$	$ \epsilon _{II}$	Cond.	$\sqrt{\frac{\lambda_{min}(\mathbf{A})}{\lambda_{next}(\mathbf{A})}}$
1	2.0		0.2490(-3)			
2	2.001		0.2469(-3)			
3	2.002		0.2449(-3)			
4	2.2994029817	0.0780	0.3900(-4)	0.644(-3)	237.	0.0513
5	2.2269757991	0.553(-2)	0.1856(-6)	0.380(-4)	0.339(4)	0.354(-2)
6	2.2141050490	-0.734(-2)	0.3229(-6)	0.486(-4)	0.257(4)	0.467(-2)
7	2.2213725668	-0.689(-4)	0.2865(-10)	0.412(-6)	0.273(6)	0.440(-4)
8	2.2214255292	-0.159(-4)	0.1538(-11)	0.144(-6)	0.118(7)	0.102(-4)
9	2.2214417167	-0.248(-6)	0.5031(-14)	0.641(-6)	0.206(8)	0.583(-6)
10	2.2214414716	0.252(-8)	0.4711(-14)	0.970(-6)	0.313(8)	0.564(-6)

Table 11.3: The iteration solution for Partition I and II to seek the minimal eigenvalue.

(a) Partition I with $M = 2$, $N_1 = 36$, $k = 2.2214414879$.

i	c_i	$\hat{c}_i = \frac{c_i/J_i(k/2)}{c_0/J_0(k/2)}$
0	-0.51189625231336(3)	1.000000000000
1	-0.68056228480074(3)	2.0041823521466
2	-0.19959301558621(3)	2.0050241968523
3	0.37819229035445(2)	-1.9986819732447
4	-0.53197729344948(1)	1.9933725915138
5	-0.60452403655422	2.0182850091578
6	-0.53549502477247(-1)	1.9172637624130
7	0.35021805606486(-2)	-1.5717345445127

(b) for Partition II with $L = K = M = 2$, $N = 3$, $N_1 = 36$, $N_2 = N_3 = 16$, $k = 2.2214414716$.

i	c_i	$\hat{c}_i = \frac{c_i/J_i(k/2)}{c_0/J_0(k/2)}$
0	0.12316821988238(5)	1.000000000000
1	0.16339609495803(5)	1.9998357077860
2	0.47900157048407(4)	1.9998365842009
3	-0.91051947498290(3)	-1.9998782636634
4	0.12841347393427(3)	1.9998125149512
5	0.14411011276208(2)	1.9996163638668
6	0.13356894789306(1)	1.9875370595556
7	-0.97611894579621(-1)	-1.8206510555810
i	a_i	$\hat{a}_i = \frac{a_i/J_{4i}(k/2)}{c_0/J_0(k/2)}$
0	0.24632611565408(5)	1.9999161787782
1	-0.25681467518868(3)	-3.9994339046411
2	0.15246233907367(-1)	4.0787852268429
i	b_i	$\hat{b}_i = \frac{b_i/J_{2i+1}(k/2)}{c_0/J_0(k/2)}$
0	0.23108363990284(5)	2.8282763714859
1	-0.12875804596318(4)	-2.8280605134600
2	-0.20375848721408(2)	-2.8272742106772
3	0.16014021904186	2.9869255186080
i	d_i	$\hat{d}_i = \frac{d_i/J_{4i+2}(k/2)}{c_0/J_0(k/2)}$
0	0.95801465838770(4)	3.9997212537494
1	-0.27769257940907(1)	-4.1321302701358
2	-0.26956118786962(-1)	-0.20912262144594(4)

Table 11.4: The calculated coefficients at the 10th iteration in seeking the minimal eigenvalue.

Partitions	Methods	iteration numbers	$\Delta\sqrt{\tilde{\lambda}_1}$	$\lambda_{min}(\mathbf{A})$
Partition I ($M = 2$)	Secant method with $p = 2$	11	0.856(-5)	0.473(-11)
	Secant method with $p = 1$ plus Aitkin method	26	0.375(-5)	0.324(-11)
	Brent method	32	0.603(-7)	0.289(-11)
	Modified Muller's method	11	0.303(-6)	0.289(-11)
	Method(B)	9	0.897(-8)	0.289(-11)
Partition II ($M = K = 2, N = 3$)	Method(B)	10	0.251(-8)	0.471(-14)

Table 11.5: Comparisons on different nonlinear methods to seek the minimal eigenvalue λ_1

M	$\sqrt{\tilde{\lambda}_1}$	$\Delta\sqrt{\tilde{\lambda}_1}$	$\lambda_{min}(\mathbf{A})$	$ \epsilon _I$	$\sqrt{\frac{\lambda_{min}(\mathbf{A})}{\lambda_{next}(\mathbf{A})}}$			
1	2.2170240851	-0.442(-2)	0.2053(-3)	1.74	0.0142			
2	2.2214414878	0.187(-7)	0.289(-11)	0.242(-3)	0.303(-5)			
3	2.2214414537	-0.154(-7)	0.933(-14)	0.375(-10)	0.253(-6)			
4	2.2214417873	0.318(-6)	0.886(-13)	0.446(-10)	0.103(-5)			
5	2.2214403561	-0.111(-5)	-0.289(-12)	0.590(-10)	0.231(-5)			
L	M	N	K	$\sqrt{\tilde{\lambda}_1}$	$\Delta\sqrt{\tilde{\lambda}_1}$	$\lambda_{min}(\mathbf{A})$	$ \epsilon _{II}$	$\sqrt{\frac{\lambda_{min}(\mathbf{A})}{\lambda_{next}(\mathbf{A})}}$
1	1	2	1	2.2218067548	0.365(-3)	0.426(-5)	0.627	0.799(-2)
2	2	3	2	2.2214414716	0.252(-8)	0.471(-14)	0.970(-5)	0.564(-6)
3	3	5	3	2.2214414665	-0.254(-8)	0.748(-17)	0.252(-11)	0.552(-7)
4	4	7	4	2.2214414676	-0.148(-8)	-0.111(-15)	0.653(-12)	0.535(-6)
5	5	9	5	2.2214414702	0.112(-8)	-0.111(-15)	0.219(-12)	0.136(-5)

Table 11.6: The minimal eigenvalues calculated for Partitions I and II.

(a) for Partition I

M	c_0	\hat{c}_0	\hat{c}_1	\hat{c}_2
1	-0.1370683964(1)	1.0	1.6633952166	1.830289310
2	-0.5118962523(3)	1.0	2.004182352	2.005024196
3	0.4190401959(8)	1.0	1.999999969	1.999999979
4	-0.2021863209(7)	1.0	2.000000642	2.000000439
5	0.5780419280(6)	1.0	1.999997753	1.999998465

(b) for Partition II

L	M	N	K	c_0	\hat{c}_0	\hat{c}_1	\hat{c}_2
1	1	2	1	-0.3109134477	1.0	8.295716631	8.278741850
2	2	3	2	0.3036872873(3)	1.0	1.993336522	1.999337114
3	3	5	3	0.2544534880(9)	1.0	1.999999995	1.999999997
4	4	7	4	0.4262991335(9)	1.0	1.999999997	1.999999998
5	5	9	5	-0.5606163341(9)	1.0	2.000000002	2.000000002
L	M	N	K	\hat{a}_0	\hat{b}_0	\hat{d}_0	
1	1	2	1	5.331766814	8.512259240	0.1475997688(2)	
2	2	3	2	1.996600014	2.822313087	3.988691347	
3	3	5	3	1.999999959	2.828427121	3.999999995	
4	4	7	4	1.999999998	2.828427123	3.999999997	
5	5	9	5	2.000000002	2.828427126	4.000000002	

Table 11.7: The leading coefficients calculated for λ_1

L	$\sqrt{\tilde{\lambda}_1}$	$\lambda_{min}(\mathbf{A})$	$\sqrt{\frac{\lambda_{min}(\mathbf{A})}{\lambda_{next}(\mathbf{A})}}$	$ \varepsilon _I$
8	2.0116 9644 24	0.218(-5)	0.314(-2)	0.277
12	2.0116 9636 12	0.401(-8)	0.201(-4)	0.187
16	2.0116 9633 84	0.194(-10)	0.185(-4)	0.141
20	2.0116 9473 95	0.705(-12)	0.439(-5)	0.765(-1)
L	$\sqrt{\tilde{\lambda}_{next}}$	$\lambda_{min}(\mathbf{A})$	$\sqrt{\frac{\lambda_{min}(\mathbf{A})}{\lambda_{next}(\mathbf{A})}}$	$ \varepsilon _I$
8	3.2928 0632 74	0.239(-4)	0.861(-2)	0.415
12	3.2931 5262 85	0.167(-7)	0.346(-3)	0.141
16	3.2931 4245 43	0.425(-10)	0.228(-4)	0.190
20	3.2931 4615 34	0.255(-11)	0.670(-5)	0.376(-1)

Table 11.8: The minimal and the next minimal eigenvalues for cracked beam problem.

L	M	N	$\sqrt{\tilde{\lambda}_1}$	$\lambda_{min}(\mathbf{A})$	$\sqrt{\frac{\lambda_{min}(\mathbf{A})}{\lambda_{next}(\mathbf{A})}}$	$ \varepsilon _{II}$
8	4	4	2.0116 8110 56	0.468(-6)	0.243(-2)	1.08
12	6	6	2.0116 8118 26	0.143(-8)	0.198(-3)	1.05
16	8	8	2.0116 9995 32	0.726(-11)	0.187(-4)	1.04
20	10	10	2.0116 9257 19	0.695(-12)	0.422(-5)	0.536
L	M	N	$\sqrt{\tilde{\lambda}_{next}}$	$\lambda_{min}(\mathbf{A})$	$\sqrt{\frac{\lambda_{min}(\mathbf{A})}{\lambda_{next}(\mathbf{A})}}$	$ \varepsilon _{II}$
8	4	4	3.2931 3146 34	0.126(-6)	0.116(-2)	0.140
12	6	6	3.2931 5351 97	0.362(-9)	0.924(-4)	0.114
16	6	8	3.2931 5394 44	0.234(-11)	0.986(-5)	0.112
20	10	10	3.2931 5358 63	0.116(-12)	0.274(-5)	0.973(-1)

Table 11.9: The minimal and the next minimal eigenvalues for cracked beam problem by subdomains.

(a) coefficients for $L = 20$ only

i	α_i	c_i	$\frac{c_i}{c_1}$	Ratios ($\frac{\hat{c}_i}{\hat{c}_1}$)
1	.5	.12987122205208(6)	.10000000000000(1)	.10000000000000(1)
2	1.5	.87119180587204(5)	.67081204912559	.69229261843941
3	2.5	.57793549918559(5)	.44500659195600	.99999626173678
4	3.5	.12324750564941(5)	.94899781261768(-1)	.69228829959188
5	4.5	.68412700421944(3)	.52677336318978(-2)	.16468289891991
6	5.5	-.20318539907228(4)	-.15645144156016(-1)	-.25971342642199(1)
7	6.5	.20366398087632(2)	.15681994645021(-3)	.16467932755367
8	7.5	-.43776966406169(2)	-.33707980655339(-3)	-.25969420279128(1)
9	8.5	.30057439721428(2)	.23144033948778(-3)	.14877253038594(2)
10	9.5	-.35472558770784(2)	-.27313640551221(-3)	-.16413059499893(3)
11	10.5	.31132495823320	.23971820185718(-5)	.14910350545718(2)
12	11.5	-.29726297918063	.22889056904494(-5)	-.16161974269382(3)
13	12.5	.26423714258412	.20346088872417(-5)	.17745984061500(4)
14	13.5	-.10613764221616(1)	-.81725297212953(-5)	-.95173630857246(5)
15	14.5	.24834780509944(-2)	.19122620175226(-7)	.31957750051437(4)
16	15.5	-.24143119319850(-2)	-.18590045537700(-7)	-.47684950314528(5)
17	16.5	.75059563670039(-2)	.57795377978299(-7)	.24233530245023(7)
18	17.5	-.32211047655409(-1)	-.24802298112272(-6)	-.18036751271349(9)
19	18.5	.36570580155663(-3)	.28159109907348(-8)	.37557973990831(8)
20	19.5	.24284981230395(-3)	.18699278290194(-8)	.48228917479237(9)

(b) coefficients for $L = 20$ and $N = M = 10$ in subdomains

c_i	α_i	c_i	$\frac{c_i}{c_1}$	Ratios ($\frac{c_i}{c_1}$)
c_1	.5	.11959800274219(7)	.1000(1)	.10000000000000(1)
c_2	1.5	.45835781616048(6)	.3832	.69230351162893
c_3	2.5	.20033295946321(6)	.1675	.10000004822442(1)
c_4	3.5	.29139127827595(5)	.2436(-1)	.69229753261298
c_5	4.5	.11188233333695(4)	.9355(-3)	.16469244837562
c_6	5.5	-.23146192586917(4)	-.1935(-2)	-.25970645016003(1)
c_7	6.5	.16241927226293(2)	.1358(-4)	.16480513237322
c_8	7.5	-.24475892724651(2)	-.2047(-4)	-.25979717534238(1)
c_9	8.5	.11801858282767(2)	.9868(-5)	.14876656974435(2)
c_{10}	9.5	-.97974538559522(1)	-.8192(-5)	-.16411858903386(3)
c_{11}	10.5	.64494435043749(-1)	.5393(-7)	.15882167357987(2)
c_{12}	11.5	-.54289594686471(-1)	-.4539(-7)	-.21540199608252(3)
c_{13}	12.5	.24609833731754(-1)	.2058(-7)	.17109131461698(4)
c_{14}	13.5	-.73474076227497(-1)	-.6143(-7)	-.96703959015733(5)
c_{15}	14.5	-.13428835379154(-4)	-.1123(-10)	-.35951689469272(3)
c_{16}	15.5	.46828464275265(-2)	.3915(-8)	.27267452664841(7)
c_{17}	16.5	.51175749224262(-3)	.4279(-9)	.69008642103446(7)
c_{18}	17.5	-.20797898883337(-3)	-.1739(-9)	-.68896964464141(8)
c_{19}	18.5	-.56691988809010(-3)	-.4740(-9)	-.48780610937869(10)
c_{20}	19.5	-.73924911914303(-3)	-.6181(-9)	-.17417418702430(12)
a_i	α_i	a_i	$\frac{a_i}{a_1}$	Ratios ($\frac{a_i}{a_1}$)
a_1	1	.17417469205398(7)	.1000(1)	.10000000000000(1)
a_2	3	-.71977936598662(5)	-.4133(-1)	-.42762032536556
a_3	5	.42831290006455(4)	.2459(-2)	.96342494238577
a_4	7	.13694877118753(4)	.7863(-3)	.25035176216706(2)
a_5	9	-.10391018786852(3)	-.5966(-4)	-.26693840926065(3)
a_6	11	-.37774783333337(2)	-.2169(-4)	-.20923378323255(5)
a_7	13	.33465391887796(1)	.1921(-5)	.56818642709975(6)
a_8	15	.13914068214727(1)	.7989(-6)	.97626431554463(8)
a_9	17	-.10291573115604	-.5909(-7)	-.38690230051291(10)
a_{10}	19	-.43555883159647(-1)	-.2501(-7)	-.11039166970715(13)
b_i	α_i	b_i	$\frac{b_i}{b_1}$	Ratios ($\frac{b_i}{b_1}$)
b_1	0	.19074274242055(6)	.1000(1)	.10000000000000(1)
b_2	2	.11796963314658(6)	.6185	.63997970945134(1)
b_3	4	.18045757779389(5)	.9461(-1)	.37065416407082(2)
b_4	6	-.32335618500723(3)	-.1695(-2)	-.53977244967773(2)
b_5	8	-.27668688592049(3)	-.1451(-2)	-.64905058012620(4)
b_6	10	.14191817944265(2)	.7440(-4)	.71780236674252(5)
b_7	12	.84243866909377(1)	.4417(-4)	.13060814527936(8)
b_8	14	-.57359529328306	-.3007(-5)	-.36749877433588(9)
b_9	16	-.25484228429272	-.1336(-5)	-.87483886082501(11)
b_{10}	18	.22963767388375(-1)	.1204(-6)	.53145885318436(13)

Table 11.10: The coefficients of the eigenfuctions for eigenvalues for the cracked beam problem using the central rule.

Chapter 12

The Helmholtz Equation

The Trefftz method (TM) [461] is developed to solve the Helmholtz equation, $\Delta u + k^2 u = 0$, where k^2 is not exactly equal (but may be very close) to an eigenvalue of the Laplace operator $-\Delta$. Piecewise particular solutions are chosen and then matched together in order to satisfy the exterior and interior boundary conditions. Error analysis is presented to estimate error bounds in the entire solution domain. Let δ be the smallest relative distance between k^2 and the eigenvalues of $-\Delta$. We prove that the error asymptote of the solutions by the TM is $O(\frac{1}{\delta})$ asymptotically as $\delta \rightarrow 0$, which is called degeneracy in this chapter. Such an asymptote $O(\frac{1}{\delta})$ has been verified by the numerical computations in Li [295]. We also explain why the exponential convergence rates of solutions can be obtained easily by splitting the solution domain into smaller subdomains.

12.1 Introduction

Studies on the Helmholtz solutions are of interest in both theory and application. Several important literatures on the Helmholtz equation should be mentioned here: particular solutions of Courant and Hilbert [109], the finite element method of Babuska and Osborn [18], the finite difference methods of Birkhoff and Lynch [47], the least squares method of Chang [85], the capacitance matrix method of Proskurwski and Widlund [390], the method converted to an integral equation of Lin [320], the coupling methods of the boundary integral and finite element methods of Johnson and Nedelec [244] and Jiang and Li [236], and the preconditioned conjugate gradient method of Bayliss, Goldstein and Turkel [28]. Moreover, studies have been done on the Helmholtz equation on the unbounded domains, see Aziz, Dorr and Kellogg [11], Goldstein [174, 175], and Harari and Hughes [195]. Recently, the Helmholtz eigenvalue problems in a multiply connected domain by the BEM are studied in Chen et al. [89, 90].

In this chapter we will follow Part I to use the Trefftz method (TM) [461] to solve the Helmholtz equation. In such methods the solution domain is divided into several subdomains, different particular solutions on subdomains (i.e., piecewise particular solutions) are used, and an approximation of the solution is then obtained by satisfying only

the interior and exterior boundary conditions. The methods using the entire particular solutions for solving the elliptic and eigenvalue problems can be found in Bergman [33], Eisenstat [142], Fox, Henrici and Moler [156], Mathon and Sermer [345], and Vekua [469]. The approaches in this chapter, however, use *piecewise* particular solutions for solving the Helmholtz equation. The Trefftz method is advantageous for solving elliptic problems with multiple singularities, multiple interfaces, or those on unbounded domains, which may cause some difficulty if using the standard, finite element method and finite difference method (see [47, 105, 446]). Furthermore, an important advantage of the TM is that high accuracy of solutions with exponential convergence rates can be achieved with a modest effort in computation.

Let us consider the Helmholtz equation in two dimensions

$$\begin{cases} \Delta u + k^2 u = 0 & \text{in } \Omega, \\ u = f & \text{on } \Gamma, \end{cases} \quad (12.1.1)$$

where $k > 0$, Δ is the Laplace operator: $\Delta = \frac{\partial^2}{\partial x^2} + \frac{\partial^2}{\partial y^2}$, and Ω is a polygonal domain with the exterior boundary Γ . This equation is also called the *reduced wave equation* by Birkhoff and Lynch [47]. We assume in this chapter that k^2 is not *exactly* equal (but may be very close) to any eigenvalue of the following eigenvalue problem [18, 109, 493]¹:

$$\begin{cases} -\Delta \phi_l = \lambda_l \phi_l & \text{in } \Omega, \\ \phi_l|_{\Gamma} = 0 & \text{on } \Gamma. \end{cases} \quad (12.1.2)$$

Let the eigenvalues $\{\lambda_l\}$ be arranged in an ascending order, i.e.,

$$0 < \lambda_1 \leq \lambda_2 \leq \dots \leq \lambda_n \leq \lambda_{n+1} \leq \dots$$

The complete eigenvalue functions $\{\phi_l\}$ are orthonormal,

$$(\phi_i, \phi_j) = \iint_{\Omega} \phi_i \phi_j \, d\Omega = \delta_{ij} = \begin{cases} 0 & \text{if } i \neq j, \\ 1 & \text{if } i = j. \end{cases} \quad (12.1.3)$$

Another Helmholtz equation is also given in [47]

$$\begin{cases} \Delta u + k^2 u = g & \text{in } \Omega, \\ u = f & \text{on } \Gamma. \end{cases} \quad (12.1.4)$$

Let the solution u^* be a particular solution to the equation $\Delta u^* + k^2 u^* = g$. Eq. (12.1.1) is then obtained from (12.1.4) by a transformation $v = u - u^*$ so that we only discuss (12.1.1).

We first provide an expansion of solution to (12.1.1). Let w denote the solution of the *Laplace equation*

$$\begin{cases} \Delta w = 0 & \text{in } \Omega, \\ w = f & \text{on } \Gamma. \end{cases}$$

By the transformation $v = u - w$, Eq. (12.1.1) is reduced to the following problem

¹When $k^2 \rightarrow \lambda_l$ in (12.1.2), the eigenvalue problem can be solved, see Chapter 11.

$$\begin{cases} \Delta v + k^2 v = -k^2 w & \text{in } \Omega, \\ v = 0 & \text{on } \Gamma. \end{cases} \quad (12.1.5)$$

Consequently, the solution v of the above problem can be found by $Span \{\phi_i\}$,

$$v = \sum_{i=1}^{\infty} a_i \phi_i, \quad (12.1.6)$$

where a_i are expansion coefficients. Substituting (12.1.6) into (12.1.5) yields the identity:

$$\sum_{i=1}^{\infty} a_i (k^2 - \lambda_i) \phi_i = -k^2 w.$$

Since k^2 is not an eigenvalue λ_l by the assumption, the coefficients a_i can be defined uniquely from the orthogonality of (12.1.3):

$$a_i = -\frac{k^2 (w, \phi_i)}{k^2 - \lambda_i},$$

thus giving a unique solution of (12.1.1)

$$u = w - \sum_{i=1}^{\infty} \frac{k^2}{k^2 - \lambda_i} (w, \phi_i) \phi_i. \quad (12.1.7)$$

Denote by δ the smallest relative distance between k^2 and λ_i , where $k > 0$

$$\delta = \min_i \left| \frac{k^2 - \lambda_i}{k^2} \right| > 0. \quad (12.1.8)$$

Based on Eq. (12.1.7) we can conclude the following.

1. When $\delta > 0$ the Helmholtz solution is unique.
2. When $\delta = 0$ the eigenvalue problem of (12.1.2) should be solved instead, see Chapter 11.
3. When $\delta \rightarrow 0$ the Helmholtz solution approaches to an eigenfunction of Eq. (12.1.2). This is called the case of degeneracy in this chapter.

Our questions for the last degenerate case, however, are:

1. When $0 < \delta \ll 1$, can we find an approximate solution to the Helmholtz equation?
2. If we can, how much error will it have as $\delta \rightarrow 0$?

Since the maximum principle can no longer be applied to the Helmholtz solution, a new analysis to Chapter 1 will be provided in this chapter to justify the TM. To our knowledge, there seems to be no literature yet to provide error analysis on the degenerate solutions (i.e., as $\delta \rightarrow 0$) of the Helmholtz equation.

The rest of the chapter is organized as follows. In the next two sections, we shall describe the TM, and then derive new error bounds. In the last section a few remarks are made. The materials in this chapter is adapted from Li [295].

12.2 The Trefftz Method

Let the solution domain Ω be divided by a piecewise straight line Γ_0 into two subdomains Ω^+ and Ω^- . Consider the piecewise Helmholtz equation:

$$\Delta u + k^2 u = 0, \text{ in } \Omega^+ \text{ and } \Omega^-, \quad (12.2.1)$$

with the interior and exterior boundary conditions:

$$u^+ = u^- \text{ on } \Gamma_0, \quad u_\nu^+ = u_\nu^- \text{ on } \Gamma_0, \quad u = f \text{ on } \Gamma, \quad (12.2.2)$$

where u_ν is the normal unit derivative of u on Γ_0 . Evidently, the solution u to (12.1.1) also satisfy (12.2.1) and (12.2.2). Define a space

$$H = \{v \in L_2(\Omega) | v \in H^1(\Omega^+), v \in H^1(\Omega^-) \text{ and } \Delta v + k^2 v = 0 \text{ in } \Omega^+ \text{ and } \Omega^-\},$$

and a functional

$$I(v) = \int_{\Gamma} (v - f)^2 ds + \int_{\Gamma_0} (v^+ - v^-)^2 ds + \sigma^2 \int_{\Gamma_0} (v_\nu^+ - v_\nu^-)^2 ds, \quad (12.2.3)$$

where σ is a positive weight. Define a finite-dimensional space $S_{m,n} \subseteq H$ such that

$$S_{m,n} = \left\{ v | v = v_m^+ = \sum_{i=1}^m c_i \psi_i^+ \text{ on } \Omega^+, \text{ and } v = v_n^- = \sum_{i=1}^n d_i \psi_i^- \text{ on } \Omega^- \right\},$$

where $\{\psi_i^+\}$ and $\{\psi_i^-\}$ are complete sets of local particular solutions of (12.2.1) in Ω^+ and Ω^- respectively, and c_i and d_i are the coefficients to be determined. A TM approximation $u_{m,n} \in S_{m,n}$ for the problem of (12.2.1) and (12.2.2) can then be found by

$$I(u_{m,n}) = \min_{v \in S_{m,n}} I(v). \quad (12.2.4)$$

Denote by \mathbf{x} the vector consisting of all unknown coefficients c_i and d_i , then it follows from (12.2.3) that

$$I(u_{m,n}) = \frac{1}{2} \mathbf{x}^T \mathbf{A} \mathbf{x} - \mathbf{b}^T \mathbf{x} + \int_{\Gamma} f^2 ds,$$

where

$$\frac{1}{2} \mathbf{x}^T \mathbf{A} \mathbf{x} = [u_{m,n}, u_{m,n}], \quad \mathbf{b}^T \mathbf{x} = 2 \int_{\Gamma} u_{m,n} f ds. \quad (12.2.5)$$

In (12.2.5) the bilinear form $[u, v]$ on $H \times H$ is defined by

$$[u, v] = \int_{\Gamma} uv ds + \int_{\Gamma_0} (u^+ - u^-)(v^+ - v^-) ds + \sigma^2 \int_{\Gamma_0} (u_\nu^+ - u_\nu^-)(v_\nu^+ - v_\nu^-) ds.$$

The stiffness matrix \mathbf{A} in (12.2.5) is symmetric and positive definite. Therefore, a system of linear algebraic equations can be reduced from (12.2.4):

$$\mathbf{A} \mathbf{x} = \mathbf{b}. \quad (12.2.6)$$

In computation, $u_{m,n}$ is solved from the least squares method (12.2.4) by using the QR method or the singular value decomposition instead of solving (12.2.6) directly, in order

to achieve the smaller condition number given by (see [9, 176])

$$\text{Cond.} = \text{Cond}(\mathbf{A}) = \left(\frac{\lambda_{max}(\mathbf{A})}{\lambda_{min}(\mathbf{A})} \right)^{\frac{1}{2}},$$

where $\lambda_{max}(\mathbf{A})$ and $\lambda_{min}(\mathbf{A})$ are the maximal and minimal eigenvalues of \mathbf{A} , respectively.

12.3 Error Analysis

The analysis in Chapter 1 can not apply directly to (12.1.1); but some error bounds for the Laplace solutions may be used to derive error bounds for the Helmholtz solutions. New analysis should display the error behavior of the Helmholtz solutions as $\delta \rightarrow 0$ and $k \rightarrow \infty$.

For error analysis, we define the induced norm on the interior and exterior boundary as

$$|v|_B = \sqrt{[v, v]} = \{ |v|_{\Gamma}^2 + |v^+ - v^-|_{0, \Gamma_0}^2 + \sigma^2 |v_{\nu}^+ - v_{\nu}^-|_{0, \Gamma_0}^2 \}^{\frac{1}{2}},$$

and the norms $\|v\|_H$ and $|v|_H$ over H by

$$\|v\|_H = \left\{ \|v\|_{1, \Omega^+}^2 + \|v\|_{1, \Omega^-}^2 \right\}^{\frac{1}{2}}, |v|_H = \left\{ |v|_{1, \Omega^+}^2 + |v|_{1, \Omega^-}^2 \right\}^{\frac{1}{2}},$$

where $\|v\|_{1, \Omega^+}$ and $|v|_{1, \Omega^+}$ are the Sobolev norms in [105, 365] defined by

$$\|v\|_{m, \Omega} = \left\{ \sum_{|\alpha| \leq m} \int_{\Omega} |D^{\alpha} v|^2 dx \right\}^{\frac{1}{2}}, |v|_{m, \Omega} = \left\{ \sum_{|\alpha|=m} \int_{\Omega} |D^{\alpha} v|^2 dx \right\}^{\frac{1}{2}}.$$

12.3.1 Preliminary Lemmas

Let us first prove several lemmas.

Lemma 12.3.1 *Let w satisfy the piecewise Laplace equation (see Dautray and Lions [122])*

$$\Delta w = 0 \text{ in } \Omega^+ \text{ and } \Omega^-, \quad (12.3.1)$$

$$\begin{cases} w^+ - w^- = \epsilon_1, & w_{\nu}^+ - w_{\nu}^- = \epsilon_2 & \text{on } \Gamma_0, \\ w = f & & \text{on } \Gamma. \end{cases} \quad (12.3.2)$$

Suppose that the following inverse properties hold,

$$\begin{cases} |w_{\nu}|_{0, \Gamma} \leq K_w \|w\|_H, \\ |w_{\nu}^+|_{0, \Gamma_0} \leq K_w \|w\|_H, \end{cases} \quad (12.3.3)$$

where K_w is a constant which may be unbounded (see [291, 316]). Then there exists a bounded constant C independent of w such that

$$\|w\|_H \leq K_w(|w|_{0,\Gamma} + |w^+ - w^-|_{0,\Gamma_0}) + C|w_\nu^+ - w_\nu^-|_{0,\Gamma_0}. \quad (12.3.4)$$

Proof By using the Green's theorem and (12.3.1), we obtain

$$\begin{aligned} |w|_H^2 &= \int_{\partial\Omega^+} w_\nu^+ w^+ ds + \int_{\partial\Omega^-} w_\nu^- w^- ds \\ &= \int_\Gamma w w_\nu ds + \int_{\Gamma_0} [(w_\nu^+ - w_\nu^-)w^- + w_\nu^+(w^+ - w^-)] ds. \end{aligned}$$

The following bounds can be found from the Schwarz inequality and the inverse properties (12.3.3).

$$\left| \int_\Gamma w w_\nu ds \right| \leq |w|_{0,\Gamma} |w_\nu|_{0,\Gamma} \leq K_w |w|_{0,\Gamma} \|w\|_H, \quad (12.3.5)$$

$$\left| \int_{\Gamma_0} w_\nu^+(w^+ - w^-) ds \right| \leq K_w |w^+ - w^-|_{0,\Gamma_0} \|w\|_H. \quad (12.3.6)$$

From the Sobolev imbedding theorem ([105]), we obtain

$$\left| \int_{\Gamma_0} (w_\nu^+ - w_\nu^-)w^+ ds \right| \leq |w_\nu^+ - w_\nu^-|_{0,\Gamma_0} |w^+|_{0,\Gamma_0} \leq C|w_\nu^+ - w_\nu^-|_{0,\Gamma_0} \|w\|_H. \quad (12.3.7)$$

Therefore, we have from (12.3.5) – (12.3.7) and the Poincare-Friedrichs inequality [105],

$$\|w\|_H^2 \leq C|w|_H^2 \leq \{K_w(|w|_{0,\Gamma} + |w^+ - w^-|_{0,\Gamma_0}) + C|w_\nu^+ - w_\nu^-|_{0,\Gamma_0}\} \|w\|_H. \quad (12.3.8)$$

The desired result (12.3.4) is obtained by dividing $\|w\|_H$ in both sides of inequality (12.3.8). ■

Lemma 12.3.2 λ_l and ϕ_l in (12.1.2) are also the eigenvalue and its eigenfunction of the following piecewise eigenvalue problem,

$$\Delta u + \lambda u = 0 \text{ in } \Omega^+ \text{ and } \Omega^-, \quad (12.3.9)$$

$$u^+ = u^- \text{ on } \Gamma_0, \quad u_\nu^+ = u_\nu^- \text{ on } \Gamma_0, \quad u = 0 \text{ on } \Gamma. \quad (12.3.10)$$

Also the inner product

$$\langle -\Delta\phi_i, \phi_j \rangle = \lambda_i \delta_{i,j}, \quad (12.3.11)$$

where

$$\langle u, v \rangle = \iint_{\Omega^+} uv d\Omega + \iint_{\Omega^-} uv d\Omega = (u, v). \quad (12.3.12)$$

Proof Eqs. (12.3.9) and (12.3.10) follow from (12.1.2) directly. From (12.3.9) and (12.3.10) we have

$$\begin{aligned} \langle -\Delta\phi_i, \phi_j \rangle &= \iint_{\Omega^+} (-\Delta\phi_i)\phi_j \, d\Omega + \iint_{\Omega^-} (-\Delta\phi_i)\phi_j \, d\Omega \\ &= \lambda_i \left[\iint_{\Omega^+} \phi_i\phi_j \, d\Omega + \iint_{\Omega^-} \phi_i\phi_j \, d\Omega \right] = \lambda_i(\phi_i, \phi_j) = \lambda_i\delta_{i,j}. \quad \blacksquare \end{aligned}$$

Lemma 12.3.3 *Let w and u satisfy the piecewise Laplace equation (12.3.1) – (12.3.2), and the following piecewise Helmholtz equation, respectively.*

$$\Delta u + k^2 u = 0 \text{ in } \Omega^+ \text{ and } \Omega^-, \quad (12.3.13)$$

$$u^+ - u^- = \epsilon_1 \text{ on } \Gamma_0, \quad u_\nu^+ - u_\nu^- = \epsilon_2 \text{ on } \Gamma_0, \quad u = f \text{ on } \Gamma. \quad (12.3.14)$$

Then there exists the bound,

$$|u|_{0,\Omega} \leq \left(1 + \frac{1}{\delta}\right) |w|_{0,\Omega}, \quad (12.3.15)$$

where δ is given in (12.1.8).

Proof Let $v = u - w$. Then the solution v satisfies

$$\Delta v + k^2 v = -k^2 w \text{ in } \Omega^+ \text{ and } \Omega^-,$$

and the homogeneous boundary conditions (12.3.10). We conclude that v can be expressed by *Span* $\{\phi_i\}$:

$$v = \sum_{i=1}^{\infty} a_i \phi_i \text{ in } \Omega.$$

In fact, based on Lemma 12.3.2 and an analogous argument in Section 12.1 we obtain (cf. (12.1.7)),

$$u = w - \sum_{i=1}^{\infty} \frac{k^2}{k^2 - \lambda_i} (w, \phi_i) \phi_i.$$

By using the Parseval's inequality in [109] and the definition of δ in (12.1.8), we have

$$\begin{aligned} |u|_{0,\Omega} &\leq |w|_{0,\Omega} + \frac{1}{\delta} \left| \sum_{i=1}^{\infty} (w, \phi_i) \phi_i \right|_{0,\Omega} \\ &\leq |w|_{0,\Omega} + \frac{1}{\delta} \left[\sum_{i=1}^{\infty} (w, \phi_i)^2 \right]^{\frac{1}{2}} \\ &\leq |w|_{0,\Omega} + \frac{1}{\delta} |w|_{0,\Omega} = \left(1 + \frac{1}{\delta}\right) |w|_{0,\Omega}. \quad \blacksquare \end{aligned} \quad (12.3.16)$$

Remark 12.3.1 *The bounds (12.3.15) have also been derived by Kuttler and Sigillito [272] in the entire solution domain.*

12.3.2 Error Bounds

Theorem 12.3.1 *Let (12.3.3) and $v \in S_{m,n}$ satisfy the following inverse properties:*

$$|v_\nu|_{0,\Gamma} \leq K_{m,n} \|v\|_H, \quad |v_\nu^\pm|_{0,\Gamma} \leq K_{m,n} \|v\|_H, \quad (12.3.17)$$

where the constant $K_{m,n}$ may be unbounded as $m, n \rightarrow \infty$. For any $\sigma > 0$, then there exists a bounded constant C independent of m, n and v such that

$$\|v\|_H \leq C \left(1 + \frac{k}{\delta}\right) (K_{u,w} + \sigma^{-1}) |v|_B, \quad (12.3.18)$$

where $K_{u,w} = \max(K_w, K_{m,n})$, and the constant K_w is given in (12.3.3).

Proof By using the Green's theorem and (12.3.13) and (12.3.14) we obtain

$$\|v\|_H^2 = \int_{\partial\Omega^+} v_\nu^+ v^+ ds + \int_{\partial\Omega^-} v_\nu^- v^- ds + (1 + k^2) |v|_{0,\Omega}^2.$$

By means of a similar argument in Eqs. (12.3.5) – (12.3.8), we have for $v \in S_{m,n}$

$$\begin{aligned} & \left| \int_{\partial\Omega^+} v_\nu^+ v^+ ds + \int_{\partial\Omega^-} v_\nu^- v^- ds \right| \\ &= \{K_{m,n} (|v|_{0,\Gamma} + |v^+ - v^-|_{0,\Gamma_0}) + C |v_\nu^+ - v_\nu^-|_{0,\Gamma_0}\} \|v\|_H \\ &\leq C \left(K_{m,n} + \frac{1}{\sigma}\right) |v|_B \|v\|_H. \end{aligned}$$

Hence, we obtain

$$\|v\|_H^2 \leq C \left(K_{m,n} + \frac{1}{\sigma}\right) |v|_B \|v\|_H + (1 + k^2) |v|_{0,\Omega}^2. \quad (12.3.19)$$

Let $x = \|v\|_H$, then (12.3.19) is an inequality of order 2 with respect to x ,

$$x^2 \leq px + q, \quad (12.3.20)$$

where $x, p, q > 0$, and

$$p = C \left(K_{m,n} + \frac{1}{\sigma}\right) |v|_B, \quad q = (1 + k^2) |v|_{0,\Omega}^2.$$

Then we have the following bounds by solving (12.3.20)

$$\|v\|_H = x \leq p + \sqrt{q} \leq C \left(K_{m,n} + \frac{1}{\sigma}\right) |v|_B + (1 + k) |v|_{0,\Omega}. \quad (12.3.21)$$

Next, let w be the piecewise Laplace solution in Eqs. (12.3.1) and (12.3.2) such that $w = v$ on Γ and Γ_0 . Then we obtain from Lemmas 12.3.3 and 12.3.1,

$$\begin{aligned}
|v|_{0,\Omega} &\leq (1 + \frac{1}{\delta})|w|_{0,\Omega} \leq (1 + \frac{1}{\delta})\|w\|_H \\
&\leq C(1 + \frac{1}{\delta}) \{K_w(|w|_{0,\Gamma} + |w^+ - w^-|_{0,\Gamma_0}) + |w_\nu^+ - w_\nu^-|_{0,\Gamma_0}\} \\
&= C(1 + \frac{1}{\delta}) \{K_w(|v|_{0,\Gamma} + |v^+ - v^-|_{0,\Gamma_0}) + |v_\nu^+ - v_\nu^-|_{0,\Gamma_0}\} \\
&\leq C(1 + \frac{1}{\delta})(K_w + \frac{1}{\sigma})|v|_B.
\end{aligned} \tag{12.3.22}$$

Combining (12.3.21) and (12.3.22) yields the desired results (12.3.18). ■

Theorem 12.3.2 *Let the inverse inequalities (12.3.3) and (12.3.17) be given, and $u \in H^1(\Omega)$ be the Helmholtz solution of (12.1.1). Then for any $\sigma > 0$, there exists a unique function, $u_{m,n} \in S_{m,n}$ by the TM, (12.2.4), such that*

$$[u_{m,n}, v] = \int_{\Gamma} f v ds \quad \forall v \in S_{m,n}, \tag{12.3.23}$$

$$[u - u_{m,n}, v] = 0 \quad \forall v \in S_{m,n}, \tag{12.3.24}$$

$$|u - u_{m,n}|_B \leq C \inf_{v \in S_{m,n}} |u - v|_B, \tag{12.3.25}$$

$$|u_{m,n}|_B \leq |f|_{0,\Gamma}, \tag{12.3.26}$$

$$\|u_{m,n}\|_H \leq C(1 + \frac{k}{\delta})(K_{u,w} + \sigma^{-1})|f|_{0,\Gamma}. \tag{12.3.27}$$

Also, $u_{m,n}$ minimizes $I(v)$ over $v \in S_{m,n}$, that is, Eq. (12.2.4) holds, if and only if Eq. (12.3.16) holds.

Proof Eq. (12.3.26) follows from (12.3.27) and Theorem 12.3.1. Other proofs are analogous to Chapter 1. ■

From (12.3.27) and (12.3.26) we can see that when f is bounded, the solutions $u_{m,n}$ are also bounded on the boundary Γ and Γ_0 , but not necessarily bounded in Ω as $\delta \rightarrow 0$ or $k \rightarrow \infty$. This is a key difference between the solutions in this chapter and those in Chapter 1. Now, we have a new theorem.

Theorem 12.3.3 *Let $u \in H^1(\Omega)$ be the solution to (12.1.1) and $u_{m,n}$ be the approximation from the TM (i.e. the BAM), see (12.3.23) or (12.2.4). Suppose that the inverse properties (12.3.3) and (12.3.17) hold for all functions in $S_{m,n}$. Then for any $\sigma > 0$ there exists a constant C independent of m, n and u such that*

$$\|u - u_{m,n}\|_H \leq \inf_{v \in S_{m,n}} \left\{ \|u - v\|_H + C(1 + \frac{k}{\delta})(K_{u,w} + \sigma^{-1})|u - v|_B \right\}.$$

Proof Let $\xi = v - u_{m,n}$ where $v \in S_{m,n}$. Applying the orthogonality property (12.3.24) gives

$$|\xi|_B^2 = [\xi, \xi] = [v - u, \xi] \leq |u - v|_B |\xi|_B.$$

Hence $|\xi|_B \leq |u - v|_B$. We have from Theorem 12.3.1

$$\begin{aligned} \|u - u_{m,n}\|_H &\leq \|u - v\|_H + \|\xi\|_H \\ &\leq \|u - v\|_H + C\left(1 + \frac{k}{\delta}\right)(K_{u,w} + \sigma^{-1})|\xi|_B. \\ &\leq \|u - v\|_H + C\left(1 + \frac{k}{\delta}\right)(K_{u,w} + \sigma^{-1})|u - v|_B. \blacksquare \end{aligned}$$

By following the proof of Theorem 12.3.1, and letting $v = u - u_{m,n}$, we give an a posteriori error estimate.

Theorem 12.3.4 *Let all the conditions in Theorem 12.3.3 hold. Suppose that if the inverse property of (12.3.17) also holds for the differences $u - u_{m,n}$, then for any $\sigma > 0$ there exist the error bounds*

$$\|u - u_{m,n}\|_H \leq C\left(1 + \frac{k}{\delta}\right)(K_{u,w} + \sigma^{-1})|u - u_{m,n}|_B. \quad (12.3.28)$$

Moreover, suppose that

$$K_{u,w} = CN^{\frac{1}{2}}, \quad N = \max\{m, n\}.$$

Then by choosing $\sigma^{-1} = O(N)$ there exist the bounds of the ratios of the solution errors,

$$\frac{\|u - u_{m,n}\|_H}{|u - u_{m,n}|_B} = O\left((N^{\frac{1}{2}} + N)\left(1 + \frac{k}{\delta}\right)\right). \quad (12.3.29)$$

The new estimates (12.3.28) and (12.3.29) are useful in practical application because the values $|u - u_{m,n}|_B$ can be obtained naturally from the TM algorithms in Section 12.2. In the above error bounds, the factor $1/\delta$ plays an important role. Hence the questions arising in Section 12.1 for the degenerate Helmholtz solutions have been answered by Theorems 12.3.1 – 12.3.4, thus to fill in the analysis gap between the cases $\delta = 0$ and $\delta > 0$.

12.3.3 Exponential Rates of Convergence

Let us give the series solutions of (12.1.1) and (12.2.1). The Helmholtz solution of (12.1.1) can be expanded by the following particular solutions:

$$u(r, \theta) = a_0 J_0(kr) + \sum_{i=1}^{\infty} J_i(kr)[a_i \cos i\theta + b_i \sin i\theta],$$

where (r, θ) are the polar coordinates, a_i and b_i are the expansion coefficients, and $J_i(z)$ is the Bessel functions defined by

$$J_\mu(r) = \sum_{i=0}^{\infty} \frac{(-1)^i}{\Gamma(i+1)\Gamma(i+\mu+1)} \left(\frac{r}{2}\right)^{2i+\mu}.$$

We may choose the following piecewise particular solutions:

$$u_{m,n} = \begin{cases} u_m^+ = a_0 J_0(kr) + \sum_{i=1}^m J_i(kr)[a_i \cos i\theta + b_i \sin i\theta], & \text{in } \Omega^+, \\ u_n^- = c_0 J_0(k\rho) + \sum_{i=1}^n J_i(k\rho)[c_i \cos i\phi + d_i \sin i\phi], & \text{in } \Omega^-, \end{cases} \quad (12.3.30)$$

where a_i, b_i, c_i and d_i are the coefficients. We then have the following theorem.

Theorem 12.3.5 *Suppose that all true expansion coefficients of the true solution are bounded:*

$$|\bar{a}_i|, |\bar{b}_i|, |\bar{c}_i|, |\bar{d}_i| < C, \quad (12.3.31)$$

and the term numbers m and n in (12.3.30) satisfy

$$\left(\frac{ekr_{max}^+}{2m}\right) \leq \alpha_+ < 1, \quad \left(\frac{ek\rho_{max}^-}{2n}\right) \leq \alpha_- < 1, \quad (12.3.32)$$

where $r_{max}^+ = \max_{\Omega^+} r$ and $\rho_{max}^- = \max_{\Omega^-} \rho$. Then there exist the exponential convergence rates

$$\|u - u_m\|_B \leq C[1 + \sigma \max(m, n)] \left\{ \frac{\alpha_+^{m+1}}{(m+1)^{\frac{1}{2}}} + \frac{\alpha_-^{n+1}}{(n+1)^{\frac{1}{2}}} \right\}. \quad (12.3.33)$$

Proof Let $\bar{u}_{m,n}$ be the piecewise particular solution (12.3.30), but with the true coefficients $\bar{a}_i, \bar{b}_i, \bar{c}_i, \bar{d}_i$. Then $u = \bar{u}_{m,n} + R_{m,n}$, where the remainder

$$R_{m,n} = \begin{cases} R_m^+ = \sum_{i=m+1}^{\infty} J_i(kr)[\bar{a}_i \cos i\theta + \bar{b}_i \sin i\theta], & \text{in } \Omega^+, \\ R_n^- = \sum_{i=n+1}^{\infty} J_i(k\rho)[\bar{c}_i \cos i\phi + \bar{d}_i \sin i\phi], & \text{in } \Omega^-. \end{cases} \quad (12.3.34)$$

We have from (12.3.25)

$$\begin{aligned} |u - u_{m,n}|_B &\leq C \inf_{v \in S_{m,n}} |u - v|_B \leq C|u - \bar{u}_{m,n}|_B \leq C|R_{m,n}|_B \\ &\leq C \left\{ |R_m^+|_{0, \partial\Omega^+} + |R_n^-|_{0, \partial\Omega^-} + \sigma \left[\left| \frac{\partial R_m^+}{\partial \nu} \right|_{0, \Gamma_0} + \left| \frac{\partial R_n^-}{\partial \nu} \right|_{0, \Gamma_0} \right] \right\}. \end{aligned}$$

Since there exist the asymptotic formulas in [2], p. 365:

$$J_n(z) \approx \frac{1}{(2n\pi)^{\frac{1}{2}}} \left(\frac{ez}{2n}\right)^n, \quad \text{when } n \text{ is large,} \quad (12.3.35)$$

we can obtain from (12.3.34) and the assumptions (12.3.31) and (12.3.32) that

$$\begin{aligned} |R_m^+|_{0,\partial\Omega^+} &\leq [\text{Length}(\partial\Omega^+)]^{\frac{1}{2}} |R_m^+|_{\infty,\partial\Omega^+} \leq C \max_{r \in \partial\Omega^+} \sum_{i=m+1}^{\infty} |J_i(kr)| \\ &\leq C \sum_{i=m+1}^{\infty} \frac{1}{(2\pi i)^{\frac{1}{2}}} \left(\frac{ekr_{max}^+}{2i} \right)^i \leq C \frac{1}{(m+1)^{\frac{1}{2}}} \alpha_+^{m+1}. \end{aligned}$$

Next, based on the derivative formulas along the direction ν in [2], p. 361:

$$\begin{aligned} \frac{\partial R_m^+}{\partial \nu}(r, \theta) &= \frac{\partial R_m^+}{\partial r} \cos(\nu, r) + \frac{1}{r} \frac{\partial R_m^+}{\partial \theta} \cos(\nu, \theta), \\ \frac{dJ_i(kr)}{dr} &= \frac{i}{r} J_i(kr) - kJ_{i+1}(kr), \end{aligned} \quad (12.3.36)$$

we can obtain from (12.3.35) and (12.3.36) similarly,

$$\left| \frac{\partial R_m^+}{\partial \nu} \right|_{0,\Omega} \leq C \max_{r \in \partial\Omega^+} \left\{ \sum_{i=m+1}^{\infty} \frac{i}{r} |J_i(kr)| + k \sum_{i=m+2}^{\infty} |J_i(kr)| \right\} \leq C(m+1)^{\frac{1}{2}} \alpha_+^{m+1}.$$

Bounds for the terms $|R_n^-|_{0,\Omega^-}$ and $\left| \frac{\partial R_n^-}{\partial \nu} \right|_{0,\Omega^-}$ can be found similarly, and the desired results (12.3.33) are derived. ■

Corollary 12.3.1 *Let all the conditions in Theorems 12.3.4 and 12.3.5 hold. Then*

$$\|u - u_{m,n}\|_H \leq C \frac{N^2}{\delta} \left[\frac{\alpha_+^{m+1}}{(m+1)^{\frac{1}{2}}} + \frac{\alpha_-^{n+1}}{(n+1)^{\frac{1}{2}}} \right].$$

The condition (12.3.32) is important for choosing the term numbers m, n for exponential convergence rates. Since

$$r_{max}^+, \rho_{max}^- \leq r_{max} = \max_{\Omega} r,$$

using piecewise particular solutions may give better accuracy of numerical solutions, or reduce numbers m and n . Fewer terms of expansions are desirable for reducing condition numbers in TM. Hence, better approximation of solutions may be obtained if the solution domain Ω is split into suitably smaller subdomains Ω_i .

12.3.4 Estimates on Bounds of Constant $K_{m,n}$

Since the bounds of constant $K_{u,w} = \max\{K_u, K_{m,n}\}$ are important to Theorems 12.3.1 – 12.3.4, we will focus on analyzing on the bounds of $K_{m,n}$; the analysis on those of K_u in (12.3.3) for harmonic functions can be easily found (also see Chapter 1). In this

subsection we estimate bounds of K_m for u_m and $u - u_m$ only on a disk domain Ω^+ , and proofs for sectorial domains are similar (see [291, 316]).

Lemma 12.3.4 *Let $u \in H_{2,\Omega^+}$ be the Helmholtz solution to (12.2.1) in Ω^+ and satisfy*

$$\|u\|_{\frac{3}{2},\Gamma_0} \leq C_0 \|u\|_{\frac{1}{2},\Gamma_0} \quad (12.3.37)$$

with a constant C_0 . Then there exists a bounded constant independent of k and u such that

$$\left\| \frac{\partial u}{\partial \nu} \right\|_{0,\Gamma_0} \leq C \sqrt{C_0} \|u\|_{1,\Omega^+}. \quad (12.3.38)$$

Proof Since $\Delta + k^2 I$ is an elliptic operator, based on the trace theorem and the interpolation theory in Babuska [15] (p. 25, p. 32), we have the bounds

$$\left\| \frac{\partial u}{\partial \nu} \right\|_{0,\Gamma_0} \leq C \|u\|_{\frac{1}{2},\Omega^+} \leq C \{ \|u\|_{1,\Omega^+} \|u\|_{2,\Omega^+} \}^{\frac{1}{2}}. \quad (12.3.39)$$

Next based on (12.3.37) and the regularity theorem in Oden [365], p. 176,

$$\|u\|_{2,\Omega^+} \leq C \{ \|\Delta u + k^2 u\|_{0,\Omega^+} + \|u\|_{\frac{3}{2},\Gamma_0} + \|u\|_{0,\Omega^+} \} \leq C \{ C_0 \|u\|_{\frac{1}{2},\Gamma_0} + \|u\|_{0,\Omega^+} \}. \quad (12.3.40)$$

Also from the trace theorem

$$\|u\|_{\frac{1}{2},\Gamma_0} \leq C \|u\|_{1,\Omega^+},$$

Eq. (12.3.40) leads to

$$\|u\|_{2,\Omega^+} \leq C C_0 (\|u\|_{\frac{1}{2},\Gamma_0} + \|u\|_{0,\Omega^+}) \leq C C_0 \|u\|_{1,\Omega^+}. \quad (12.3.41)$$

The desired results (12.3.38) follow from (12.3.39) and (12.3.41). ■

Lemma 12.3.5 *Let Ω^+ be a disk domain with the boundary $\Gamma_0 = \{(r, \theta), r \text{ is given}, \theta \in (0, 2\pi)\}$. Suppose that the admissible functions are chosen as*

$$u_m = a_0 J_0(kr) + \sum_{i=1}^m J_i(kr) [a_i \cos i\theta + b_i \sin i\theta] \text{ in } \Omega^+,$$

where a_i and b_i are arbitrary constants. Then there exists a constant C independent of m and k such that

$$\|u_m\|_{\frac{3}{2},\Gamma_0} \leq C m \|u_m\|_{\frac{1}{2},\Gamma_0} \quad (12.3.42)$$

Proof Based on the interpolation theory again (see Babuska [15], p. 25), for any integer $l \geq 2$ there exists the bound,

$$\|u\|_{\frac{3}{2}, \Gamma_0} \leq C \|u\|_{0, \Gamma_0}^{\frac{l-\frac{3}{2}}{l-\frac{1}{2}}} \|u\|_{l, \Gamma_0}^{\frac{1}{l-\frac{1}{2}}}, \quad (12.3.43)$$

where the norms

$$\|u\|_{l, \Gamma_0}^2 = \sum_{j=0}^l \left\| \frac{\partial^j u}{\partial s^j} \right\|_{0, \Gamma_0}^2. \quad (12.3.44)$$

By applying the orthogonality of trigonometric functions, we obtain

$$\begin{aligned} \left\| \frac{\partial^j u_m}{\partial s^j} \right\|_{0, \Gamma_0}^2 &= \left\| \frac{\partial^j u_m}{r^j \partial \theta^j} \right\|_{0, \Gamma_0}^2 = \pi r \sum_{i=1}^m \frac{i^{2j}}{r^{2j}} (a_i^2 + b_i^2) J_i^2(kr) \\ &\leq \left(\frac{m}{r}\right)^{2j} \{2\pi r a_0^2 J_0^2(kr) + \pi r \sum_{i=1}^m (a_i^2 + b_i^2) J_i^2(kr)\} \\ &\leq \left(\frac{m}{r}\right)^{2j} \|u_m\|_{0, \Gamma_0}^2. \end{aligned} \quad (12.3.45)$$

Since $\frac{m}{r} < 1$ due to large m and $\|u_m\|_{0, \Gamma_0} \leq C \|u_m\|_{\frac{1}{2}, \Gamma_0}$, we obtain from (12.3.44) and (12.3.45)

$$\begin{aligned} \|u_m\|_{l, \Gamma_0}^2 &= \sum_{j=0}^l \left\| \frac{\partial^j u_m}{\partial s^j} \right\|_{0, \Gamma_0}^2 = \left\{ \sum_{j=0}^l \left(\frac{m}{r}\right)^{2j} \right\} \|u_m\|_{0, \Gamma_0}^2 = \left| \frac{1 - \left(\frac{m}{r}\right)^{2(l+1)}}{1 - \frac{m}{r}} \right| \|u_m\|_{0, \Gamma_0}^2 \\ &\leq C \left(\frac{m}{r}\right)^{2(l+1)} \|u_m\|_{0, \Gamma_0}^2 \leq C \left(\frac{m}{r}\right)^{2(l+1)} \|u_m\|_{\frac{1}{2}, \Gamma_0}^2. \end{aligned}$$

Hence Eq. (12.3.43) leads to

$$\|u_m\|_{\frac{3}{2}, \Gamma_0} \leq C \left(\frac{m}{r}\right)^{\frac{l+1}{l-\frac{1}{2}}} \|u_m\|_{\frac{1}{2}, \Gamma_0}. \quad (12.3.46)$$

The desired result (12.3.42) follows from (12.3.46) as $l \rightarrow \infty$. ■

Let the true solution

$$u = \bar{u}_m + R_m \text{ in } \Omega^+,$$

where

$$\bar{u}_m = \bar{a}_0 J_0(kr) + \sum_{i=1}^m J_i(kr) [\bar{a}_i \cos i\theta + \bar{b}_i \sin i\theta] \text{ in } \Omega^+,$$

and the remainder term

$$R_m = R_m^+ = \sum_{i=m+1}^{\infty} J_i(kr) [\bar{a}_i \cos i\theta + \bar{b}_i \sin i\theta] \text{ in } \Omega^+,$$

with the true coefficients \bar{a}_i and \bar{b}_i . From Lemmas 12.3.4 and 12.3.5, we have the following proposition.

Proposition 12.3.1 *Let all the conditions in Lemmas 12.3.4 and 12.3.5 hold. There exists a constant C independent of k and m such that*

$$\left\| \frac{\partial u_m}{\partial \nu} \right\|_{0, \Gamma_0} = \left\| \frac{\partial u_m}{\partial r} \right\|_{0, \Gamma_0} \leq C\sqrt{m} \|u_m\|_{1, \Omega^+}.$$

From Proposition 12.3.1 we have $K_{m,n} = C(\max\{m, n\})^{\frac{1}{2}}$. Similarly we can show $K_w = C(\max\{m, n\})^{\frac{1}{2}}$, to lead to $K_{u,w} = C(\max\{m, n\})^{\frac{1}{2}}$. Note that these bounds are sharp, compared to those in Chapter 1.

12.4 Summaries and Discussions

To close this chapter, let us summarize the novelties of this chapter and give a few concluding remarks.

1. We have developed the Trefftz method using *piecewise* particular solutions for solving the Helmholtz equation $\Delta u + k^2 u = f$, and derived a new error analysis, which reveals the error bounds, particularly at the degeneracy case, i.e., $k^2 \rightarrow \lambda_l$. Theorems 12.3.3 – 12.3.5 with the asymptote

$$\|u - u_{m,n}\|_H = O\left(\frac{1}{\delta}\right) \text{ as } k^2 \rightarrow \lambda_l$$

indicate that the Helmholtz solutions quickly deteriorate as $O(\frac{1}{\delta})$ when $\delta \rightarrow 0$. The analysis given in this chapter fills up the analysis gap between the Helmholtz solutions at $\delta > 0$ and the eigenfunction solutions at $\delta = 0$.

2. In this chapter we choose $\sigma^{-1} = N = \max\{m, n\}$ and $N = O(k)$. Theorem 12.3.4 leads to

$$\frac{\|u - u_{m,n}\|_H}{|u - u_{m,n}|_B} = O\left(\frac{k^2 + k^{\frac{3}{2}}}{\delta}\right) \text{ as } k \rightarrow \infty. \quad (12.4.1)$$

The significance of error ratios in (12.4.1) to practical application is that the Sobolev norms over the entire domain may be evaluated from the errors on the boundary.

3. Let us recall the solutions of the following algebraic equations

$$(\mathbf{A} - k^2)\mathbf{x} = \mathbf{b}, \quad (\mathbf{A} - k^2)\tilde{\mathbf{x}} = \tilde{\mathbf{b}},$$

where \mathbf{A} is symmetric and positive definite, k is real, \mathbf{x} and \mathbf{b} are unknown and known vectors, and $\tilde{\mathbf{x}}$ and $\tilde{\mathbf{b}}$ their perturbation vectors. Denote the matrix eigenvalue problem $\mathbf{A}\mathbf{x}_l = \lambda_l\mathbf{x}_l$ with positive eigenvalues λ_l and the normalized eigenvectors \mathbf{x}_l . By following the arguments in Section 12.1, we can obtain easily

$$\|\mathbf{x} - \tilde{\mathbf{x}}\| \leq \frac{\|\mathbf{b} - \tilde{\mathbf{b}}\|}{\min_l |\lambda_l - k^2|} \leq \frac{k^2}{\delta} \|\mathbf{b} - \tilde{\mathbf{b}}\|,$$

where $\|\cdot\|$ is the Euclidean norm. The error asymptote $O(\frac{k^2}{\delta})$ is similar to $O(\frac{k^2 + k^{\frac{3}{2}}}{\delta})$. However, Eq. (12.4.1) includes not only the solution errors but also the derivative errors on the entire solution domain Ω .

4. The advantage of the Trefftz method is high accuracy of the Helmholtz solutions with exponential convergence rates, which are proven by the analysis in Section 12.3.3.
5. This chapter may be regarded as a development of Chapter 1, where the Trefftz method is used for the Laplace equation. On the other hand, when $k \rightarrow 0$, the piecewise Laplace equation (12.3.1) is reduced from (12.3.13). Since the factor $\frac{k}{\delta} = \max_i \left\{ \frac{k^3}{|k^2 - \lambda_i|} \right\} \rightarrow 0$ as $k \rightarrow 0$, all the error bounds in Chapter 1 can also be deduced from Theorems 12.3.2 – 12.3.5.

Chapter 13

Particular Solutions of Laplace's Equations

In this chapter, the harmonic functions of Laplace's equations on sectors are derived explicitly for the Dirichlet and the Neumann boundary conditions. These harmonic functions are more explicit than those of Volkov [473], and easier to expose the mild singularity of the Laplace solutions at the domain corners. Moreover, the particular solutions of Poisson's equation on the polygon are provided. We also explore in detail the singularities of the solutions on sectors with the boundary angles $\Theta = \frac{\pi}{2}, \frac{3\pi}{2}, \pi$ and 2π , which often occur in many testing models. In addition to the popular singularity models, Motz's and the cracked beam problems in Chapter 2, we design two new singularity models, one with discontinuous singularity, and the other with crack plus mild singularities. The collocation Trefftz method (CTM), the Schwarz alternating method, and their combinations may be chosen to seek their solutions with high accuracy, which may be used as the exact solution to test other numerical methods. The particular solutions of the Laplace's equations and their singularities are crucial to algorithms and error analysis.

13.1 Introduction

In this chapter, we derive explicitly the particular solutions of Laplace's equation in polygons with the Dirichlet, Neumann, and their mixed boundary conditions. We explore those in particular with the boundary angles of $\Theta = \frac{\pi}{2}, \frac{3\pi}{2}, \pi$ and 2π , which occur in Motz's problem, the L-shaped and the cracked beam problems. Although the particular solutions in this chapter may be found in Volkov [473], our formulas are more explicit than those of Volkov [473], and easier to expose the mild singularity of the Laplace solutions at the domain corners. Moreover, new models are designed for Laplace's equations including discontinuity, and the crack plus mild singularities, $r^k \ln r$. The TM using the piecewise particular solutions can provide their highly accurate solutions, which may be regarded as the exact solution to test other numerical methods.

When a solution domain can be split into several subdomains, the local particular solutions in each domain may be found in this chapter. Several methods for Laplace's equations with highly accurate solutions may then be chosen: (1) the collocation TM,

(2) the combinations of the collocation TM and the Schwarz alternating method, and (3) other methods such as the block method in Volkov [472, 473, 474] and Dosiyevev [133].

This chapter is organized as follows. In the next section, the particular solutions are derived for Laplace's equations in sectors with the Dirichlet boundary conditions, and their explicit formulas are provided for special angles Θ . In Section 13.3, the particular solutions of those involving the Neumann boundary conditions are discussed. In Section 13.4, the particular solutions of Poisson's equation are provided, and those are developed for the cases that the boundary functions of the Dirichlet and Neumann boundary conditions are not smooth. Especially, the singularities of the solutions on the boundary angles $\Theta = \frac{\pi}{2}, \frac{3\pi}{2}, \pi$ and 2π are analyzed especially. In Section 13.5, two new models with discontinuity, and with crack plus mild singularities are designed, and the collocation TM are used to provide the highly accurate solutions. The materials of this chapter are based on Li et al. [311].

13.2 The Harmonic Functions

Consider the Laplace equation with the Dirichlet boundary conditions, see Figure 13.1,

$$\begin{aligned}\Delta u &= \frac{\partial^2 u}{\partial x^2} + \frac{\partial^2 u}{\partial y^2} = 0 \text{ in } S^*, \\ u &= g \text{ on } \partial S^*,\end{aligned}$$

where S^* is a polygon.

For each angle, we seek the harmonic solutions in a sectorial domain, see Figure 13.2, $S = \{(r, \theta), 0 < r < R, 0 < \theta < \Theta\}$,

$$\Delta u = 0, \text{ in } S.$$

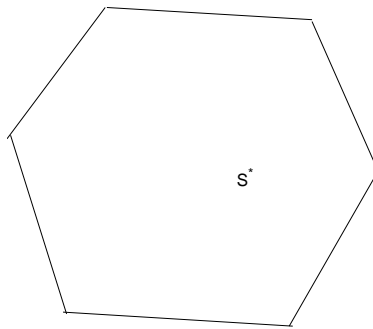


Figure 13.1: A polygonal domain.

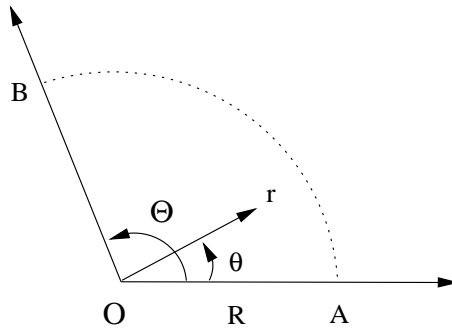


Figure 13.2: A sectorial domain

We suppose that the function g is highly smooth that it can be expressed by the power functions:

$$u|_{\overline{OA}} = g|_{\overline{OA}} = \sum_{i=0}^{\infty} \alpha_i r^i, \quad 0 \leq r \leq R, \quad \theta = 0, \quad (13.2.1)$$

$$u|_{\overline{OB}} = g|_{\overline{OB}} = \sum_{i=0}^{\infty} \beta_i r^i, \quad 0 \leq r \leq R, \quad \theta = \Theta, \quad (13.2.2)$$

where β_i and α_i are known coefficients. In fact, when the function $g|_{\overline{OB}} = g_1(r)$ is highly smooth, it can be expanded by Taylor's series:

$$g_1(r) = \sum_{i=0}^{\infty} \frac{g_1^{(i)}(0)r^i}{i!}.$$

Then $\beta_i = g_1^{(i)}(0)/i!$. Similarly, for $g|_{\overline{OA}} = g_0(r)$, we have

$$g_0(r) = \sum_{i=0}^{\infty} \frac{g_0^{(i)}(0)r^i}{i!}.$$

Hence, for any smooth Dirichlet boundary condition $u = g$ on ∂S , we may simply consider the following case in S , see Figure 13.3. In this chapter, we assume that the corresponding series are also convergent. Otherwise, we may consider only

$$u|_{\overline{OA}} = g|_{\overline{OA}} = \sum_{i=0}^M \alpha_i r^i, \quad 0 \leq r \leq R, \quad \theta = 0,$$

$$u|_{\overline{OB}} = g|_{\overline{OB}} = \sum_{i=0}^N \beta_i r^i, \quad 0 \leq r \leq R, \quad \theta = \Theta,$$

where β_i and α_i are known coefficients. This is the simple case of (13.2.1) and (13.2.2) because we may let $\beta_i = 0$ as $i > N$ and $\alpha_i = 0$ as $i > M$.

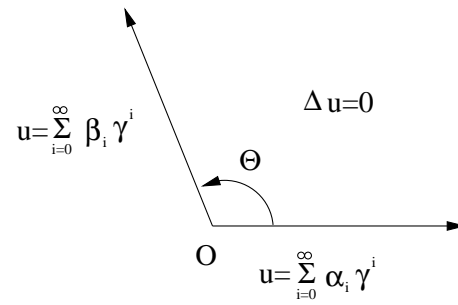


Figure 13.3: The Dirichlet boundary conditions

Let us consider the mixed Dirichlet-Neumann boundary conditions in Figure 13.4:

$$\begin{aligned} \Delta u &= 0, \quad \text{in } S, \\ u &= g_D \quad \text{on } \Gamma_D, \quad \frac{\partial u}{\partial n} = g_N \quad \text{on } \Gamma_N, \end{aligned}$$

where $\partial S = \Gamma_D \cup \Gamma_N$ and n is the unit outward normal of ∂S .

There are four types of mixed boundary conditions on two adjacent edges of a corner: (1) the D-D type, (2) the N-D type, (3) the D-N type, (4) the N-N type. The harmonic solutions of D-D type will be derived in this section, and those of the N-D, D-N and N-N types in the next section.

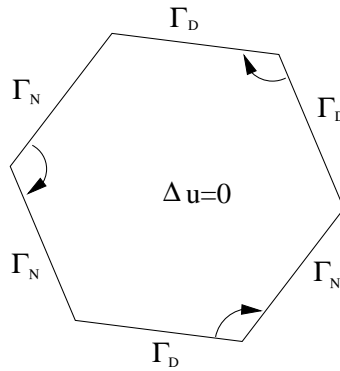


Figure 13.4: A polygon

13.2.1 General Cases

The general solutions of Laplace's equation satisfying (13.2.1) and (13.2.2) can be split into \bar{u} and u_g :

$$u = \bar{u} + u_g,$$

where the general solutions u_g satisfy

$$\begin{aligned} \Delta u_g &= 0 \quad \text{in } S, \\ u_g &= 0, \quad \theta = 0 \quad \text{and} \quad \theta = \Theta, \end{aligned} \quad (13.2.3)$$

where $0 < \Theta \leq 2\pi$, and the particular solution \bar{u} satisfies

$$\Delta \bar{u} = 0, \quad \text{in } S, \quad (13.2.4)$$

$$\bar{u} \Big|_{\theta=0} = \sum_{i=0}^{\infty} \alpha_i r^i, \quad \bar{u} \Big|_{\theta=\Theta} = \sum_{i=0}^{\infty} \beta_i r^i. \quad (13.2.5)$$

Note that in (13.2.3), the boundary condition on ℓ_k ($r = R, 0 \leq \theta \leq \Theta$) has not been given yet. Hence the general solutions u_g are not unique.

First for (13.2.3), the general solutions are $\phi_i = r^{\sigma_i} \sin \sigma_i \theta$, such that $\phi_i|_{\theta=0} = 0$ holds automatically, and $\phi_i|_{\theta=\Theta} = 0$ leads to $\sin \sigma_i \Theta = 0$. Hence, $\sigma_i \Theta = i\pi$, i.e., $\sigma_i = \frac{i\pi}{\Theta}$. We obtain the general solutions

$$u_g = \sum_{i=0}^{\infty} c_i r^{\frac{i\pi}{\Theta}} \sin\left(\frac{i\pi}{\Theta} \theta\right),$$

where c_i are the coefficients to be defined.

Second, we seek the particular solutions involving mild singularity $r^k \ln r$, $k = 1, 2, \dots$. These are called the *mild singularity* in this chapter, to compare with the rather strong singularity $O(r^\gamma)$, $0 < \gamma < 1$. Let $z = x + iy = r e^{i\theta}$. The real and imaginary parts of the complex functions, $z^p \ln z$, are harmonic, where p is real. We then have

$$\begin{aligned} z^p \ln z &= (r^p \cos p\theta + ir^p \sin p\theta) \times (\ln r + i\theta) \\ &= r^p \{\ln r \cos p\theta - \theta \sin p\theta\} + ir^p \{\ln r \sin p\theta + \theta \cos p\theta\}. \end{aligned}$$

Hence the following functions are also harmonic

$$\varphi_p = \varphi_p(r, \theta) = r^p \{\ln r \sin p\theta + \theta \cos p\theta\}, \quad (13.2.6)$$

$$\psi_p = \psi_p(r, \theta) = r^p \{\ln r \cos p\theta - \theta \sin p\theta\},$$

where p is real. When p is positive integer, $p = k$, $k = 1, 2, \dots$, we denote

$$\varphi_k = \varphi_k(r, \theta) = r^k \{\ln r \sin k\theta + \theta \cos k\theta\}, \quad (13.2.7)$$

$$\psi_k = \psi_k(r, \theta) = r^k \{\ln r \cos k\theta - \theta \sin k\theta\}. \quad (13.2.8)$$

Define the functions

$$\Phi_i = \Phi_i(r, \theta) = \begin{cases} \frac{r^i \sin i\theta}{\sin i\Theta}, & \text{if } i\Theta \neq k\pi, \quad k = 1, 2, \dots \\ \frac{(-1)^k}{\Theta} \varphi_i(r, \theta), & \text{if } i\Theta = k\pi \text{ for some } k, \end{cases} \quad (13.2.9)$$

where $i \geq 1$ and $\varphi_i(r, \theta)$ is given in (13.2.7). Hence,

$$\Phi_i \Big|_{\theta=0} = 0, \quad \Phi_i \Big|_{\theta=\Theta} = r^i, \quad \forall r > 0, \quad i = 1, 2, \dots$$

Choose the particular solutions for (13.2.4) and (13.2.5) as the following form

$$\bar{u} = \sum_{i=0}^{\infty} A_i r^i \cos i\theta + B_0 \theta + \sum_{i=1}^{\infty} B_i \Phi_i(r, \theta), \quad (13.2.10)$$

where A_i and B_i are the coefficients to be determined below. When $\theta = 0$ we have $A_i = \alpha_i$ from the boundary condition in (13.2.5), and when $\theta = \Theta$,

$$A_0 + B_0 \Theta = \beta_0, \quad A_i \cos i\Theta + B_i = \beta_i, \quad i = 1, 2, \dots$$

Hence we obtain

$$B_0 = \frac{\beta_0 - \alpha_0}{\Theta}, \quad B_i = \beta_i - \alpha_i \cos i\Theta, \quad i = 1, 2, \dots \quad (13.2.11)$$

Substituting (13.2.11) into (13.2.10) gives the particular solutions

$$\bar{u} = \frac{\beta_0 - \alpha_0}{\Theta} \theta + \sum_{i=0}^{\infty} \alpha_i r^i \cos i\theta + \sum_{i=1}^{\infty} (\beta_i - \alpha_i \cos i\Theta) \Phi_i(r, \theta). \quad (13.2.12)$$

In Volkov [473], the following forms of particular solutions for (13.2.4) and (13.2.5) are given

$$\bar{u} = \alpha_0 + \frac{\beta_0 - \alpha_0}{\Theta} \theta + \sum_{i=1}^{\infty} \alpha_i \bar{\Phi}_i(r, \theta) + \sum_{i=1}^{\infty} \beta_i \Phi_i(r, \theta), \quad (13.2.13)$$

where

$$\bar{\Phi}_i = \bar{\Phi}_i(r, \theta) = \Phi_i(r, \Theta - \theta), \quad (13.2.14)$$

to satisfy

$$\bar{\Phi}_i \Big|_{\theta=\Theta} = 0, \quad \bar{\Phi}_i \Big|_{\theta=0} = r^i, \quad \forall r > 0, \quad i = 1, 2, \dots$$

First, let us show the equivalence between (13.2.12) and (13.2.13). When $\Theta \neq \frac{k\pi}{i}$ for $i, k \geq 1$, we have from (13.2.13),

$$\bar{u} = \alpha_0 + \frac{\beta_0 - \alpha_0}{\Theta} \theta + \sum_{i=1}^{\infty} \alpha_i r^i \frac{\sin i(\Theta - \theta)}{\sin i\Theta} + \sum_{i=1}^{\infty} \beta_i \frac{r^i \sin i\theta}{\sin i\Theta}.$$

Since $\sin i(\Theta - \theta) = \sin i\Theta \cos i\theta - \sin i\theta \cos i\Theta$, we obtain from the above equation

$$\bar{u} = \frac{\beta_0 - \alpha_0}{\Theta} \theta + \sum_{i=0}^{\infty} \alpha_i r^i \cos i\theta + \sum_{i=1}^{\infty} (\beta_i - \alpha_i \cos i\Theta) r^i \frac{\sin i\theta}{\sin i\Theta}.$$

This is the very (13.2.12) for $\Theta \neq \frac{k\pi}{i}$.

When $i\Theta = k\pi$ for some i and k , to confirm the equivalence between (13.2.12) and (13.2.13), it suffices to show

$$\bar{\Phi} = r^i \cos i\theta - \cos i\Theta \Phi_i. \quad (13.2.15)$$

In fact, we have from (13.2.14) and (13.2.9)

$$\begin{aligned} \bar{\Phi}(r, \theta) &= \Phi(r, \Theta - \theta) \\ &= r^i \frac{(-1)^k}{\Theta} [\ln r \sin i(\Theta - \theta) + (\Theta - \theta) \cos i(\Theta - \theta)]. \end{aligned} \quad (13.2.16)$$

When $i\Theta = k\pi$, there exist the equalities

$$\sin i(\Theta - \theta) = \sin i\Theta \cos i\theta - \cos i\Theta \sin i\theta = (-1)^{k+1} \sin i\theta, \quad (13.2.17)$$

$$\cos i(\Theta - \theta) = \cos i\Theta \cos i\theta + \sin i\Theta \sin i\theta = (-1)^k \cos i\theta. \quad (13.2.18)$$

Substituting (13.2.17) and (13.2.18) into (13.2.16) gives the desired result (13.2.15).

Third, Volkov in [473] also considers the case of $i\Theta \neq k\pi$ but $i\Theta \approx k\pi$ so that the ratio $\frac{\sin i\theta}{\sin i\Theta}$ becomes very large. The basis functions are also introduced in [473] for the case that $0 < |\sin i\Theta| < \frac{1}{2}$. This is interesting for theory but not for application. In practical engineering problems, usually we may assume $\Theta = \frac{K}{L}\pi$, $0 < K \leq 2L$, and integer L and K are relative prime. Then we have

$$\min_i |\sin i\Theta| = \min_i \left| \sin \frac{iK}{L} \pi \right| = \left| \sin \frac{\pi}{L} \right| \approx \frac{\pi}{L}.$$

Hence, the ratio

$$\max_i \left| \frac{\sin i\theta}{\sin i\Theta} \right| \leq \frac{L}{\pi},$$

will not be very large. Consequently, we omit the case of $i\Theta \approx k\pi$ in this chapter.

Fourth, let us compare the formulas of the functions (13.2.12), and (13.2.13) of Volkov [473]. Eq. (13.2.13) has a symmetric form with respect to $\theta = \frac{\Theta}{2}$. In contrast, we may

rewrite (13.2.12) as

$$\begin{aligned} \bar{u} &= \alpha_0 + \frac{\beta_0 - \alpha_0}{\Theta} \theta \\ &+ \sum_{i=1}^{\infty} \alpha_i [r^i \cos i\theta - \cos i\Theta \Phi_i(r, \theta)] + \sum_{i=1}^{\infty} \beta_i \Phi_i(r, \theta), \end{aligned} \quad (13.2.19)$$

which is not exactly symmetric, indeed. From the viewpoint of computation, both (13.2.12) and (13.2.13) are effective. However, Eqs. (13.2.12) and (13.2.19) are more explicit. In particular, Eq. (13.2.12) displays explicitly the mild singularity. For instance, when $i\Theta = k\pi$ and $\beta_i \neq \alpha_i \cos i\Theta$, there does exist a mild singularity of $O(r^i \ln r)$. More exploration on the mild singularity is provided in Section 13.4.

Remark 13.2.1 *It is assumed that the series in (13.2.19) are convergent. Otherwise, we may consider the finite terms in (13.2.5),*

$$\bar{u} \Big|_{\theta=0} = \sum_{i=0}^M \alpha_i r^i, \quad \bar{u} \Big|_{\theta=\Theta} = \sum_{i=0}^N \beta_i r^i.$$

Hence, the solutions with finite terms

$$\bar{u} = \alpha_0 + \frac{\beta_0 - \alpha_0}{\Theta} \theta + \sum_{i=1}^M \alpha_i [r^i \cos i\theta - \cos i\Theta \Phi_i(r, \theta)] + \sum_{i=1}^N \beta_i \Phi_i(r, \theta)$$

are obtained to replace (13.2.19). For all infinite series given below, it is always assumed that they are convergent. Otherwise, a suitable modification should be made correspondingly.

13.2.2 Formulas for special Θ

Based on (13.2.12) and (13.2.9), we list the particular solutions which are often used in application.

(1) When $\Theta = \pi$,

$$\bar{u} = \frac{(\beta_0 - \alpha_0)}{\pi} \theta + \sum_{i=0}^{\infty} \alpha_i r^i \cos i\theta + \sum_{i=1}^{\infty} \frac{(-1)^i \beta_i - \alpha_i}{\pi} \varphi_i(r, \theta). \quad (13.2.20)$$

(2) When $\Theta = 2\pi$,

$$\bar{u} = \frac{\beta_0 - \alpha_0}{2\pi} \theta + \sum_{i=0}^{\infty} \alpha_i r^i \cos i\theta + \sum_{i=1}^{\infty} \frac{\beta_i - \alpha_i}{2\pi} \varphi_i(r, \theta). \quad (13.2.21)$$

(3) When $\Theta = \frac{\pi}{2}$,

$$\begin{aligned} \bar{u} &= \frac{2(\beta_0 - \alpha_0)}{\pi} \theta + \sum_{i=0}^{\infty} \alpha_i r^i \cos i\theta + \sum_{j=0}^{\infty} (-1)^j \beta_{2j+1} r^{2j+1} \sin(2j+1)\theta \\ &+ \sum_{j=1}^{\infty} \frac{2}{\pi} [(-1)^j \beta_{2j} - \alpha_{2j}] \varphi_{2j}(r, \theta). \end{aligned} \quad (13.2.22)$$

(4) When $\Theta = \frac{3\pi}{2}$,

$$\begin{aligned} \bar{u} &= \frac{2(\beta_0 - \alpha_0)}{3\pi} \theta + \sum_{i=0}^{\infty} \alpha_i r^i \cos i\theta + \sum_{j=0}^{\infty} (-1)^{j+1} \beta_{2j+1} r^{2j+1} \sin(2j+1)\theta \\ &+ \sum_{j=1}^{\infty} \frac{2}{3\pi} [(-1)^j \beta_{2j} - \alpha_{2j}] \varphi_{2j}(r, \theta). \end{aligned} \quad (13.2.23)$$

Note that the formulas of the particular solutions for $\Theta = \pi$ and $\Theta = 2\pi$ are very close, and so are those for $\Theta = \frac{\pi}{2}$ and $\Theta = \frac{3\pi}{2}$. Except the different angles Θ , the only difference is that the sign $(-1)^j$ may change in the series of β_j .

(5) When $\Theta = \frac{\pi}{3}, \frac{2\pi}{3}, \frac{4\pi}{3}, \frac{5\pi}{3}$,

$$\begin{aligned} \bar{u} &= \frac{\beta_0 - \alpha_0}{\Theta} \theta + \sum_{i=0}^{\infty} \alpha_i r^i \cos i\theta \\ &+ \sum_{j=0}^{\infty} \frac{\beta_{3j+1} - \alpha_{3j+1} \cos(3j+1)\Theta}{\sin(3j+1)\Theta} r^{3j+1} \sin(3j+1)\theta \\ &+ \sum_{j=0}^{\infty} \frac{\beta_{3j+2} - \alpha_{3j+2} \cos(3j+2)\Theta}{\sin(3j+2)\Theta} r^{3j+2} \sin(3j+2)\theta \\ &+ \sum_{j=1}^{\infty} \frac{1}{\Theta} (\beta_{3j} \cos 3j\Theta - \alpha_{3j}) \varphi_{3j}(r, \theta). \end{aligned}$$

(6) When $\Theta = \frac{\pi}{4}, \frac{3\pi}{4}, \frac{5\pi}{4}, \frac{7\pi}{4}$,

$$\begin{aligned} \bar{u} &= \frac{\beta_0 - \alpha_0}{\Theta} \theta + \sum_{i=0}^{\infty} \alpha_i r^i \cos i\theta \\ &+ \sum_{j=0}^{\infty} \sum_{k=1}^3 \frac{\beta_{4j+k} - \alpha_{4j+k} \cos(4j+k)\Theta}{\sin(4j+k)\Theta} r^{4j+k} \sin(4j+k)\theta \\ &+ \sum_{j=1}^{\infty} \frac{1}{\Theta} (\beta_{4j} \cos 4j\Theta - \alpha_{4j}) \varphi_{4j}(r, \theta). \end{aligned}$$

(7) When $\Theta = \frac{K}{L}\pi$, $0 < K < 2L$, and integers K and L are relatively prime,

$$\begin{aligned} \bar{u} &= \frac{\beta_0 - \alpha_0}{\Theta} \theta + \sum_{i=0}^{\infty} \alpha_i r^i \cos i\theta \\ &+ \sum_{j=0}^{\infty} \sum_{k=1}^{L-1} \frac{\beta_{Lj+k} - \alpha_{Lj+k} \cos(Lj+k)\Theta}{\sin(Lj+k)\Theta} r^{Lj+k} \sin(Lj+k)\theta \\ &+ \sum_{j=1}^{\infty} \frac{1}{\Theta} (\beta_{Lj} \cos Lj\Theta - \alpha_{Lj}) \varphi_{Lj}(r, \theta). \end{aligned}$$

13.3 Harmonic Solutions Involving Neumann Conditions

13.3.1 The case of the N-D type

Consider

$$\begin{aligned} \Delta u &= 0, \quad \text{in } S, \\ \frac{\partial u}{\partial n} \Big|_{\theta=0} &= \sum_{i=0}^{\infty} \alpha_i r^i, \quad u \Big|_{\theta=\Theta} = \sum_{i=0}^{\infty} \beta_i r^i. \end{aligned}$$

Let $u = \bar{u} + u_g$, where the general solutions are given by

$$u_g = \sum_{k=0}^{\infty} d_k r^{\sigma_k} \cos(\sigma_k \theta),$$

when $\sigma_k = (k + \frac{1}{2})\pi/\Theta$. The particular solution \bar{u} satisfies

$$\begin{aligned} \Delta \bar{u} &= 0, \quad \text{in } S, \\ \frac{\partial \bar{u}}{\partial n} \Big|_{\theta=0} &= \sum_{i=0}^{\infty} \alpha_i r^i, \quad \bar{u} \Big|_{\theta=\Theta} = \sum_{i=0}^{\infty} \beta_i r^i. \end{aligned} \tag{13.3.1}$$

Define the functions

$$\Psi_i = \Psi_i(r, \theta) = \begin{cases} \frac{r^i \cos i\theta}{\cos i\Theta}, & \text{if } i\Theta \neq (k + \frac{1}{2})\pi, \quad k = 0, 1, \dots \\ \frac{(-1)^{k+1}}{\Theta} \psi_i(r, \theta), & \text{if } i\Theta = (k + \frac{1}{2})\pi \text{ for some } k, \end{cases}$$

where $\psi_i(r, \theta)$ is given in (13.2.8). Hence,

$$\frac{\partial \Psi_i}{\partial n} \Big|_{\theta=0} = -\frac{\partial \Psi_i}{r \partial \theta} \Big|_{\theta=0} = 0, \quad \Psi_i \Big|_{\theta=\Theta} = r^i, \quad \forall r > 0, \quad i = 1, 2, \dots$$

Choose the particular solutions to (13.3.1)

$$\bar{u} = \sum_{i=1}^{\infty} A_i r^i \sin i\theta + B_0 + \sum_{i=1}^{\infty} B_i \Psi_i(r, \theta), \quad (13.3.2)$$

where A_i and B_i are the coefficients. When $\theta = 0$ we have

$$\sum_{i=0}^{\infty} \alpha_i r^i = \frac{\partial \bar{u}}{\partial n} \Big|_{\theta=0} = - \sum_{i=1}^{\infty} A_i i r^{i-1}.$$

Then

$$A_i = -\frac{\alpha_{i-1}}{i}, \quad i = 1, 2, \dots \quad (13.3.3)$$

Also when $\theta = \Theta$,

$$\sum_{i=1}^{\infty} \beta_i r^i = \bar{u} \Big|_{\theta=\Theta} = \sum_{i=1}^{\infty} A_i r^i \sin i\Theta + B_0 + \sum_{i=1}^{\infty} B_i r^i.$$

This gives

$$B_0 = \beta_0, \quad (13.3.4)$$

$$B_i = \beta_i - A_i \sin i\Theta = \beta_i + \frac{\alpha_{i-1}}{i} \sin i\Theta, \quad i = 1, 2, \dots$$

Hence from (13.3.2) – (13.3.4) we obtain the particular solutions

$$\bar{u} = - \sum_{i=1}^{\infty} \frac{\alpha_{i-1}}{i} r^i \sin i\theta + \beta_0 + \sum_{i=1}^{\infty} \left(\beta_i + \frac{\alpha_{i-1}}{i} \sin i\Theta \right) \Psi_i(r, \theta). \quad (13.3.5)$$

Eq. (13.3.5) is explicit for computation, in particular for directly displaying the existence of mild singularity when $i\Theta = (k + \frac{1}{2})\pi$ and $\beta_i + \frac{\alpha_{i-1}}{i} \sin i\Theta \neq 0$.

Below, we also list the useful formulas of the particular solutions for some special Θ from (13.3.5).

(1) When $\Theta = \frac{\pi}{2}$,

$$\begin{aligned} \bar{u} = & - \sum_{i=1}^{\infty} \frac{\alpha_{i-1}}{i} r^i \sin i\theta + \sum_{j=0}^{\infty} \frac{2}{\pi} \left[(-1)^{j+1} \beta_{2j+1} - \frac{\alpha_{2j}}{2j+1} \right] \psi_{2j+1}(r, \theta) \\ & + \sum_{j=0}^{\infty} (-1)^j \beta_{2j} r^{2j} \cos 2j\theta. \end{aligned} \quad (13.3.6)$$

(2) When $\Theta = \frac{3\pi}{2}$,

$$\begin{aligned} \bar{u} = & - \sum_{i=1}^{\infty} \frac{\alpha_{i-1}}{i} r^i \sin i\theta + \sum_{j=0}^{\infty} \frac{2}{3\pi} \left[(-1)^j \beta_{2j+1} - \frac{\alpha_{2j}}{2j+1} \right] \psi_{2j+1}(r, \theta) \\ & + \sum_{j=0}^{\infty} (-1)^j \beta_{2j} r^{2j} \cos 2j\theta. \end{aligned} \quad (13.3.7)$$

In Volkov [473], there are the different but equivalent formulas of (13.3.5). The discussions and comparisons between (13.3.5) and Volkov's are similar as the above.

13.3.2 The case of the D-N type

Now, we consider the mixed D-N type

$$\begin{aligned} \Delta u &= 0, \quad \text{in } S, \\ u|_{\theta=0} &= \sum_{i=0}^{\infty} \alpha_i r^i, \quad \frac{\partial u}{\partial n}|_{\theta=\Theta} = \sum_{i=0}^{\infty} \beta_i r^i. \end{aligned}$$

Let $u = \bar{u} + u_g$. We have the general solutions

$$u_g = \sum_{k=0}^{\infty} d_k r^{\sigma_k} \sin(\sigma_k \theta), \quad \sigma_k = \frac{(k + \frac{1}{2})}{\Theta} \pi.$$

The particular solution satisfies

$$\begin{aligned} \Delta \bar{u} &= 0, \quad \text{in } S, \\ \bar{u}|_{\theta=0} &= \sum_{i=0}^{\infty} \alpha_i r^i, \quad \frac{\partial \bar{u}}{\partial n}|_{\theta=\Theta} = \sum_{i=0}^{\infty} \beta_i r^i. \end{aligned} \tag{13.3.8}$$

Define the functions

$$\widehat{\Phi}_i = \widehat{\Phi}_i(r, \theta) = \begin{cases} \frac{r^i \sin i\theta}{i \cos i\Theta}, & \text{if } i\Theta \neq (k + \frac{1}{2})\pi, \quad k = 1, 2, \dots \\ \frac{(-1)^{k+1}}{i\Theta} \varphi_i(r, \theta), & \text{if } i\Theta = (k + \frac{1}{2})\pi \text{ for some } k. \end{cases}$$

Hence,

$$\widehat{\Phi}_i|_{\theta=0} = 0, \quad \frac{\partial \widehat{\Phi}_i}{\partial n}|_{\theta=\Theta} = \frac{\partial \widehat{\Phi}_i}{r \partial \theta}|_{\theta=\Theta} = r^{i-1}, \quad \forall r > 0, \quad i = 1, 2, \dots$$

Choose the particular solutions to (13.3.8) as

$$\bar{u} = \sum_{i=0}^{\infty} A_i r^i \cos i\theta + \sum_{i=1}^{\infty} B_i \widehat{\Phi}_i(r, \theta), \tag{13.3.9}$$

where A_i and B_i are the coefficients. When $\theta = 0$ we have $A_i = \alpha_i$, and when $\theta = \Theta$

$$\sum_{i=0}^{\infty} \beta_i r^i = \frac{\partial \bar{u}}{\partial n}|_{\theta=\Theta} = - \sum_{i=1}^{\infty} A_i r^{i-1} i \sin i\Theta + \sum_{i=1}^{\infty} B_i r^{i-1}.$$

This gives

$$B_i = \beta_{i-1} + i\alpha_i \sin i\Theta.$$

Hence we obtain from the particular solutions (13.3.9)

$$\bar{u} = \sum_{i=0}^{\infty} \alpha_i r^i \cos i\theta + \sum_{i=1}^{\infty} (\beta_{i-1} + i\alpha_i \sin i\Theta) \widehat{\Phi}_i(r, \theta). \quad (13.3.10)$$

Below, we also list the useful formulas from (13.3.10) for some special Θ .

(1) When $\Theta = \frac{\pi}{2}$,

$$\begin{aligned} \bar{u} &= \sum_{i=0}^{\infty} \alpha_i r^i \cos i\theta + \sum_{j=0}^{\infty} \frac{2}{\pi} \left[(-1)^{j+1} \frac{\beta_{2j}}{2j+1} - \alpha_{2j+1} \right] \varphi_{2j+1}(r, \theta) \\ &\quad + \sum_{j=1}^{\infty} (-1)^j \frac{\beta_{2j-1}}{2j} r^{2j} \sin 2j\theta. \end{aligned}$$

(2) When $\Theta = \frac{3\pi}{2}$,

$$\begin{aligned} \bar{u} &= \sum_{i=0}^{\infty} \alpha_i r^i \cos i\theta + \sum_{j=0}^{\infty} \frac{2}{3\pi} \left[(-1)^j \frac{\beta_{2j}}{2j+1} - \alpha_{2j+1} \right] \varphi_{2j+1}(r, \theta) \\ &\quad + \sum_{j=1}^{\infty} (-1)^j \frac{\beta_{2j-1}}{2j} r^{2j} \sin 2j\theta. \end{aligned}$$

13.3.3 The case of the N-N type

Consider

$$\begin{aligned} \Delta u &= 0, \quad \text{in } S, \\ \frac{\partial u}{\partial n} \Big|_{\theta=0} &= \sum_{i=0}^{\infty} \alpha_i r^i, \quad \frac{\partial u}{\partial n} \Big|_{\theta=\Theta} = \sum_{i=0}^{\infty} \beta_i r^i. \end{aligned}$$

Let $u = \bar{u} + u_g$, where $u_g = \sum_{i=0}^{\infty} r^{\sigma_i} \cos \sigma_i \theta$ with $\sigma_i = \frac{i\pi}{\Theta}$. The particular solution satisfies

$$\Delta \bar{u} = 0, \quad \text{in } S, \quad (13.3.11)$$

$$\frac{\partial \bar{u}}{\partial n} \Big|_{\theta=0} = \sum_{i=0}^{\infty} \alpha_i r^i, \quad \frac{\partial \bar{u}}{\partial n} \Big|_{\theta=\Theta} = \sum_{i=0}^{\infty} \beta_i r^i. \quad (13.3.12)$$

Define the functions

$$\widehat{\Psi}_i = \widehat{\Psi}_i(r, \theta) = \begin{cases} \frac{-r^i \cos i\theta}{i \sin i\Theta}, & \text{if } i\Theta \neq k\pi, \quad k = 1, 2, \dots \\ \frac{(-1)^{k+1}}{i\Theta} \psi_i(r, \theta), & \text{if } i\Theta = k\pi \text{ for some } k. \end{cases}$$

Hence,

$$\frac{\partial \widehat{\Psi}_i}{\partial n} \Big|_{\theta=0} = 0, \quad \frac{\partial \widehat{\Psi}_i}{\partial n} \Big|_{\theta=\Theta} = r^{i-1}, \quad \forall r > 0, \quad i = 1, 2, \dots$$

Choose the particular solutions

$$\bar{u} = \sum_{i=1}^{\infty} A_i r^i \sin i\theta + \sum_{i=1}^{\infty} B_i \widehat{\Psi}_i(r, \theta),$$

with the coefficients A_i and B_i . When $\theta = 0$ we have

$$\sum_{i=0}^{\infty} \alpha_i r^i = \frac{\partial \bar{u}}{\partial n} \Big|_{\theta=0} = -\frac{\partial \bar{u}}{r \partial \theta} \Big|_{\theta=0} = -\sum_{i=1}^{\infty} A_i i r^{i-1}.$$

Then $A_i = -\frac{\alpha_{i-1}}{i}$, $i = 1, 2, \dots$ Next, when $\theta = \Theta$,

$$\sum_{i=0}^{\infty} \beta_i r^i = \frac{\partial \bar{u}}{\partial n} \Big|_{\theta=\Theta} = \frac{\partial \bar{u}}{r \partial \theta} \Big|_{\theta=\Theta} = \sum_{i=0}^{\infty} A_i r^{i-1} i \cos i\Theta + \sum_{i=0}^{\infty} B_i r^{i-1}.$$

This gives

$$B_i = \beta_{i-1} + \alpha_{i-1} \cos i\Theta, \quad i = 1, 2, \dots$$

Hence we obtain from the particular solutions of (13.3.11) and (13.3.12)

$$\bar{u} = -\sum_{i=1}^{\infty} \frac{\alpha_{i-1}}{i} r^i \sin i\theta + \sum_{i=1}^{\infty} (\beta_{i-1} + \alpha_{i-1} \cos i\Theta) \widehat{\Psi}_i(r, \theta). \quad (13.3.13)$$

From (13.3.13), we also list the useful formulas.

(1) When $\Theta = \pi$,

$$\bar{u} = -\sum_{i=1}^{\infty} \frac{\alpha_{i-1}}{i} r^i \sin i\theta + \sum_{i=1}^{\infty} \frac{1}{i\pi} [(-1)^{i+1} \beta_{i-1} - \alpha_{i-1}] \psi_i(r, \theta). \quad (13.3.14)$$

(2) When $\Theta = 2\pi$,

$$\bar{u} = -\sum_{i=1}^{\infty} \frac{\alpha_{i-1}}{i} r^i \sin i\theta - \sum_{i=1}^{\infty} \frac{1}{2i\pi} (\beta_{i-1} + \alpha_{i-1}) \psi_i(r, \theta). \quad (13.3.15)$$

(3) When $\Theta = \frac{\pi}{2}$,

$$\begin{aligned} \bar{u} = & -\sum_{i=1}^{\infty} \frac{\alpha_{i-1}}{i} r^i \sin i\theta + \sum_{j=0}^{\infty} (-1)^{j+1} \frac{\beta_{2j}}{2j+1} r^{2j+1} \cos(2j+1)\theta \\ & + \sum_{j=1}^{\infty} \frac{1}{j\pi} [(-1)^{j+1} \beta_{2j-1} - \alpha_{2j-1}] \psi_{2j}(r, \theta). \end{aligned} \quad (13.3.16)$$

(4) When $\Theta = \frac{3\pi}{2}$,

$$\begin{aligned} \bar{u} = & - \sum_{i=1}^{\infty} \frac{\alpha_{i-1}}{i} r^i \sin i\theta + \sum_{j=0}^{\infty} (-1)^j \frac{\beta_{2j}}{2j+1} r^{2j+1} \cos(2j+1)\theta \\ & + \sum_{j=1}^{\infty} \frac{1}{3j\pi} [(-1)^{j+1} \beta_{2j-1} - \alpha_{2j-1}] \psi_{2j}(r, \theta). \end{aligned} \quad (13.3.17)$$

Interestingly, when $\Theta = \frac{i\pi}{2}$, $i = 1, 2, 3, 4$, for the N-D type, D-N type, and N-N type, the worst singularity of \bar{u} is $O(r \ln r)$. For the D-D type, the worst singularity of \bar{u} is $O(\frac{\theta}{\Theta})$.

13.4 Extensions and Analysis on Singularity

13.4.1 Particular Solutions for Poisson's Equations

In this section, we consider the simple case of Poisson's equation

$$-\Delta \bar{u} = f, \quad \text{in } S, \quad (13.4.1)$$

$$\bar{u} = g_D \Big|_{\Gamma_D}, \quad \frac{\partial \bar{u}}{\partial n} \Big|_{\Gamma_N} = g_N, \quad (13.4.2)$$

where $\partial S = \Gamma = \Gamma_D \cup \Gamma_N$, $f = ax^i y^j$, $i, j = 0, 1, \dots$, and a is a constant. Suppose that $i \geq j$ without loss of generality. We give a set of particular solutions of (13.4.1) in the following.

Case I. For $0 \leq j \leq 1$,

$$\bar{u} = -a \frac{x^{i+2} y^j}{(i+1)(i+2)}.$$

Case II. For $2 \leq j \leq 3$,

$$\bar{u} = -a \left\{ \frac{x^{i+2} y^j}{(i+1)(i+2)} - \frac{x^{i+4} y^{j-2} j(j-1)}{(i+4)(i+3)(i+2)(i+1)} \right\}.$$

Case III. For $2k \leq j \leq 2k+1$, $k = 0, 1, \dots$

$$\bar{u} = -a \frac{x^{i+2} y^j}{(i+1)(i+2)} + \frac{a}{(i+1)(i+2)} \sum_{\ell=1}^k (-1)^\ell b_{i,j,\ell} x^{i+2+2\ell} y^{j-2\ell},$$

where the coefficients

$$b_{i,j,\ell} = \prod_{m=1}^{\ell} \frac{(j-2m)(j-2m-1)}{(i+2+2m)(i+1+2m)}.$$

Besides, Cheng et al. [98] gave a different approach for deriving the particular solution for the same functions f . Their particular solutions are given as follow

$$\bar{u} = \begin{cases} \sum_{k=1}^{Int[\frac{i+2}{2}]} a(-1)^k \frac{i!j!x^{i+2k}y^{j-2k+2}}{(i+2k)!(j-2k+2)!}, & \text{for } i \geq j, \\ \sum_{k=1}^{Int[\frac{i+2}{2}]} a(-1)^k \frac{i!j!x^{i-2k+2}y^{j+2k}}{(i-2k+2)!(j+2k)!}, & \text{for } i < j, \end{cases}$$

where $Int[s]$ means the integer part of s . By the above arguments, we can obtain the particular solutions \bar{u} for

$$-\Delta\bar{u} = f, \quad f = \sum_{i=0}^M \sum_{j=0}^N a_{ij}x^i y^j.$$

Denote $\bar{v} = u - \bar{u}$, we obtain from (13.4.1) and (13.4.2)

$$\begin{aligned} \Delta\bar{v} &= 0, & \text{in } S, \\ \bar{v} &= g_D - \bar{u}, & \text{on } \Gamma_D, \\ \frac{\partial\bar{v}}{\partial n} &= g_N - \frac{\partial\bar{u}}{\partial n}, & \text{on } \Gamma_N. \end{aligned}$$

Hence, it is reduced to find the solutions for the Laplace equation with the Dirichlet-Neumann conditions, which have been provided in Sections 13.2 and 13.3.

13.4.2 Extensions to Not Smooth Functions of g_D and g_N

In this subsection, we consider functions g_D and g_N are not highly smooth. First, consider the D-D type

$$\begin{aligned} \Delta\bar{u} &= 0, & \text{in } S, \\ \bar{u}|_{\theta=0} &= ar^q, \quad \bar{u}|_{\theta=\Theta} = br^p, \end{aligned} \tag{13.4.3}$$

where p and q are real. For the solutions $u \in H^1(S)$ of the Laplace equation, the boundary functions of the Dirichlet and Neumann conditions have $g_D \in H^{\frac{1}{2}}(\Gamma_D)$ and $g_N \in H^{-\frac{1}{2}}(\Gamma_N)$ (see Babuska [15]). Hence we assume $p, q > -\frac{1}{2}$ in (13.4.3).

Hence p and q are not confined to be nonnegative integers (cf. Sections 13.2 and 13.3). When $p\Theta, q\Theta \neq \pm k\pi$, the particular solutions are given by

$$\bar{u} = br^p \frac{\sin p\theta}{\sin p\Theta} + ar^q \frac{\sin q(\Theta - \theta)}{\sin q\Theta}.$$

For simplicity, here we only give one term on the right hand in the Dirichlet condition (13.4.3). For more terms, the particular solutions can be obtained easily by linear superposition as in Sections 13.2 and 13.3. Since the solutions $O(r^p \ln r)$ for $p \in (-\frac{1}{2}, 1)$ have

strong singularity, we use the formulas in symmetry of the particular solutions as those in Volkov [473].

Suppose that $p\Theta = \pm m\pi$ and $q\Theta = \pm \ell\pi$, where m and ℓ are nonnegative integers. The particular solutions are given by

$$\begin{aligned} \bar{u} &= \frac{b}{\Theta} \frac{\varphi_p(r, \theta)}{\cos p\Theta} + \frac{a}{\Theta} \frac{\varphi_q(r, \Theta - \theta)}{\cos q\Theta} \\ &= \frac{(-1)^m}{\Theta} b\varphi_p(r, \theta) + \frac{(-1)^\ell}{\Theta} a\varphi_q(r, \Theta - \theta). \end{aligned}$$

When $p\Theta \neq \pm m\pi$ and $q\Theta \neq \pm \ell\pi$, the particular solutions can be easily obtained. Moreover, the function $\varphi_q(r, \Theta - \theta)$ is defined in (13.2.6), and may be further simplified, see Sections 13.2 and 13.3.

Next, consider the N-D type

$$\begin{aligned} \Delta \bar{u} &= 0, \quad \text{in } S, \\ \frac{\partial \bar{u}}{\partial n} \Big|_{\theta=0} &= ar^q, \quad \bar{u} \Big|_{\theta=\Theta} = br^p, \end{aligned}$$

where real $p > -\frac{1}{2}$ and $q > -\frac{3}{2}$. For $p\Theta, (q+1)\Theta \neq \pm(k + \frac{1}{2})\pi$, the particular solutions are

$$\bar{u} = br^p \frac{\cos p\theta}{\cos p\Theta} + \frac{a}{q+1} r^{q+1} \left\{ \frac{\sin(q+1)(\Theta - \theta)}{\cos(q+1)\Theta} \right\}.$$

For $p\Theta = \pm(m + \frac{1}{2})\pi$ and $(q+1)\Theta = \pm(\ell + \frac{1}{2})\pi$, where m and ℓ are positive integers, the particular solutions

$$\begin{aligned} \bar{u} &= -\frac{b}{\Theta} \frac{\psi_p(r, \theta)}{\sin p\Theta} - \frac{a}{(q+1)\Theta} \frac{\varphi_{q+1}(r, \Theta - \theta)}{\sin(q+1)\Theta} \\ &= -\frac{\pm(-1)^m}{\Theta} b\psi_p(r, \theta) - \frac{\pm(-1)^\ell}{(q+1)\Theta} a\varphi_q(r, \Theta - \theta). \end{aligned}$$

The particular solutions of D-N type can be obtained from those of the N-D type by $\varphi = \Theta - \theta$.

Finally, we consider the N-N type

$$\begin{aligned} \Delta \bar{u} &= 0, \quad \text{in } S, \\ \frac{\partial \bar{u}}{\partial n} \Big|_{\theta=0} &= ar^q, \quad \frac{\partial \bar{u}}{\partial n} \Big|_{\theta=\Theta} = br^p, \end{aligned}$$

where real $p, q > -\frac{3}{2}$. When $(p+1)\Theta, (q+1)\Theta \neq \pm k\pi, k = 0, 1, 2, \dots$, the particular solutions are

$$\bar{u} = -\frac{b}{p+1} r^{p+1} \frac{\cos(p+1)\theta}{\sin(p+1)\Theta} - \frac{a}{q+1} r^{q+1} \frac{\cos(q+1)(\Theta - \theta)}{\sin(q+1)\Theta}.$$

When $(p+1)\Theta = \pm m\pi$ and $(q+1)\Theta = \pm \ell\pi$, where $m, \ell = 0, 1, 2, \dots$, the particular solutions are

$$\begin{aligned}\bar{u} &= -\frac{b}{(p+1)\Theta} \frac{\psi_{p+1}(r, \theta)}{\cos(p+1)\Theta} - \frac{a}{(q+1)\Theta} \frac{\psi_{q+1}(r, \Theta - \theta)}{\cos(q+1)\Theta} \\ &= -\frac{(-1)^m}{(p+1)\Theta} b\psi_{p+1}(r, \theta) - \frac{(-1)^\ell}{(q+1)\Theta} a\psi_{q+1}(r, \Theta - \theta).\end{aligned}$$

Of course, we may derive the particular solutions for $\Theta = \frac{\pi}{2}, \frac{3\pi}{2}, 2\pi$ and π by following Sections 13.2 and 13.3

13.4.3 Regularity and Singularity of the Solutions of $\Theta = \frac{\pi}{2}, \frac{3\pi}{2}, \pi, 2\pi$

From the analysis in Sections 13.2 and 13.3, when g_D and g_N are highly smooth on ∂S , the solutions u inside S are also smooth for $\Theta = \frac{\pi}{2}, \frac{3\pi}{2}, \pi, 2\pi$. However, the solution u near the corners may have the mild singularities $O(r^k \ln r)$, $k = 1, 2, \dots$ Since the analysis of regularity and singularity on general solutions can be found in textbooks (cf. Li [291]), we focus on the analysis for the particular solution \bar{u} . In particular, we consider when $\Theta = \frac{i\pi}{2}$, $i = 1, 2, 3, 4$, which exist in Motz's and cracked beam problems, the L-shaped domain problems and the general cracked domains in Figure 13.5, see [329, 291].

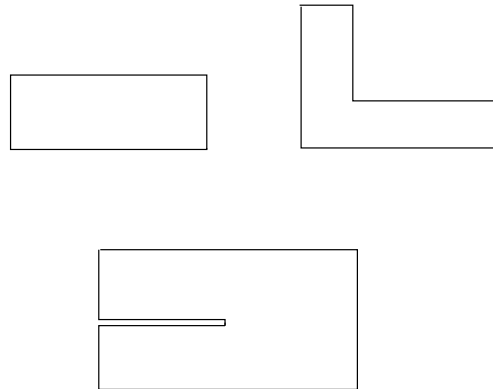


Figure 13.5: The popular domains in testing models with $\Theta = \frac{i\pi}{2}$, $i = 1, 2, 3, 4$

13.4.3.1 For the Case of $\Theta = \frac{\pi}{2}$

First, consider a simple case of the D-D type as $\Theta = \frac{\pi}{2}$

$$\begin{aligned}\Delta \bar{u} &= 0, \quad \text{in } S, \\ \bar{u} &= \alpha_0 + \alpha_1 r + \alpha_2 r^2, \quad \theta = 0, \\ \bar{u} &= \beta_0 + \beta_1 r + \beta_2 r^2, \quad \theta = \Theta,\end{aligned}\tag{13.4.4}$$

where β_i and α_i are constants. Only the quadratic polynomials in the Dirichlet conditions are chosen, because the resulted singularities are strongest among all kinds of mild singularities. We then obtain from (13.2.22)

$$\begin{aligned}\bar{u} &= \alpha_0 + \frac{(\beta_0 - \alpha_0)\theta}{\Theta} + \beta_1 r \sin \theta - \frac{\beta_2 + \alpha_2}{\Theta} \varphi_2(r, \theta) \\ &\quad + \alpha_1 r \cos \theta + \alpha_2 r^2 \cos 2\theta.\end{aligned}\tag{13.4.5}$$

In (13.4.5), when $\beta_0 \neq \alpha_0$, the function $\theta \notin H^1(S)$ is called the discontinuity singularity. Moreover, when $\beta_2 + \alpha_2 \neq 0$, the function $r^2 \ln r \notin H^3(S)$ is called the mild singularity, compared with the crack singularity

$$u = O(r^{\frac{1}{2}}) \notin H^2(S),$$

in the cracked beam problem. Interestingly, the case of $\beta_2 + \alpha_2 \neq 0$ implies $\bar{u}_{xx} + \bar{u}_{yy} = \beta_2 + \alpha_2 \neq 0$ against the Laplace equation. Note that the coefficients of β_1 or α_1 does not effect on singularities because that $r \sin \theta = y$ and $r \cos \theta = x$. In Section 13.5, Model II of crack plus mild singularities given later will be designed on the rectangles with $\Theta = \frac{\pi}{2}$.

Next, consider the N-D type

$$\begin{aligned}\Delta \bar{u} &= 0, \quad \text{in } S, \\ \frac{\partial \bar{u}}{\partial n} &= \alpha_0 + \alpha_1 r + \alpha_2 r^2, \quad \theta = 0, \\ \bar{u} &= \beta_0 + \beta_1 r + \beta_2 r^2, \quad \theta = \Theta.\end{aligned}\tag{13.4.6}$$

From (13.3.6) we obtain

$$\begin{aligned}\bar{u} &= \beta_0 - \frac{(\beta_1 + \alpha_0)}{\Theta} \psi_1(r, \theta) - \beta_2 r^2 \cos 2\theta - \alpha_0 r \sin \theta \\ &\quad - \frac{\alpha_1}{2} r^2 \sin 2\theta - \frac{\alpha_2}{3} \left\{ r^3 \sin 3\theta + \frac{1}{\Theta} \psi_3(r, \theta) \right\}.\end{aligned}\tag{13.4.7}$$

From (13.4.7), when $\beta_1 + \alpha_0 \neq 0$ which results from

$$\alpha_0 = \frac{\partial \bar{u}}{\partial n} \Big|_{\theta=0} = -\frac{\partial \bar{u}}{\partial y} \Big|_{\theta=0} \neq -\frac{\partial \bar{u}}{\partial r} \Big|_{\theta=\frac{\pi}{2}} = -\beta_1 \text{ at } r=0$$

there exists a mild singularity $O(r \ln r)$, and when $\alpha_2 \neq 0$, there exists $O(r^3 \ln r)$. Interestingly, β_0 , β_2 and α_1 do not cause any singularity in the N-D type since that $r^2 \cos 2\theta = (x^2 - y^2)$ and $r \sin 2\theta = 2xy$.

Similarly, we can draw the conclusion for the D-N type. Below we only consider the N-N type

$$\begin{aligned}\Delta \bar{u} &= 0, \quad \text{in } S, \\ \frac{\partial \bar{u}}{\partial n} &= \alpha_0 + \alpha_1 r + \alpha_2 r^2, \quad \theta = 0, \\ \frac{\partial \bar{u}}{\partial n} &= \beta_0 + \beta_1 r + \beta_2 r^2, \quad \theta = \Theta.\end{aligned}\tag{13.4.8}$$

From (13.3.16) we obtain

$$\begin{aligned}\bar{u} &= -\beta_0 r \cos \theta + \frac{(\beta_1 - \alpha_1)}{2\Theta} \psi_2(r, \theta) + \frac{\beta_2}{3} r^3 \cos 3\theta - \alpha_0 r \sin \theta \\ &\quad - \frac{\alpha_1}{2} r^2 \sin 2\theta - \frac{\alpha_2}{3} r^3 \sin 3\theta.\end{aligned}\tag{13.4.9}$$

Only that $\beta_1 - \alpha_1 \neq 0$ resulting from $\bar{u}_{xy} \neq \bar{u}_{yx}$ will cause the singularity $O(r^2 \ln r)$.

We summarize the singularities at corner O for $\Theta = \frac{\pi}{2}$ in Table 13.1. The discontinuity $\beta_0 \neq \alpha_0$ in the D-D type is the strongest. The next strongest singularity occurs in the N-D type of $\beta_1 + \alpha_0 \neq 0$, and then N-N type of $\beta_1 \neq \alpha_1$.

13.4.3.2 For the case of $\Theta = \pi$

Next, we consider the D-D type of (13.4.4) with $\Theta = \pi$. From (13.2.20) we obtain

$$\begin{aligned}\bar{u} &= \alpha_0 + \frac{(\beta_0 - \alpha_0)\theta}{\Theta} + \alpha_1 r \cos \theta + \alpha_2 r^2 \cos \theta \\ &\quad - \frac{(\beta_1 + \alpha_1)}{\Theta} \varphi_1(r, \theta) + \frac{(\beta_2 - \alpha_2)}{\Theta} \varphi_2(r, \theta).\end{aligned}$$

When $\beta_0 \neq \alpha_0$, the solution of $O(\frac{\theta}{\Theta})$ is discontinuous at origin O , and when $\beta_2 \neq \alpha_2$, the solutions of $O(r^2 \ln r)$ are obtained. Note that the case of $\beta_1 \neq -\alpha_1$ will also cause the singularity of $O(r \ln r)$. In fact, the case of $\beta_1 \neq -\alpha_1$ implies the existence of a piecewise boundary function on x -axis, because $r = x$ at $\theta = 0$ but $r = -x$ at $\theta = \pi$.

Consider the N-N type of (13.4.8) with $\Theta = \pi$. From (13.3.14) for $\Theta = \pi$

$$\begin{aligned}\bar{u} &= -\alpha_0 r \sin \theta - \frac{\alpha_1}{2} r^2 \sin 2\theta - \frac{\alpha_2}{3} r^3 \sin 3\theta \\ &\quad + \frac{(\beta_0 - \alpha_0)}{\Theta} \psi_1(r, \theta) - \frac{(\beta_1 + \alpha_1)}{2\Theta} \psi_2(r, \theta) + \frac{(\beta_2 - \alpha_2)}{3\Theta} \psi_3(r, \theta).\end{aligned}$$

When $\beta_0 \neq \alpha_0$, $\beta_1 \neq -\alpha_1$ and $\beta_2 \neq \alpha_2$, there exist the solutions with singularities, $u = O(r \ln r)$, $O(r^2 \ln r)$ and $O(r^3 \ln r)$ respectively.

Consider the N-D type of (13.4.6) with $\Theta = \pi$, which appears in Motz's and the cracked beam problems in [329]. The general solutions are $u_g = \sum_{i=0}^L d_i r^{i+\frac{1}{2}} \cos(i+\frac{1}{2})\theta$, and the particular solutions are obtained from (13.3.5)

$$\bar{u} = \sum_{k=0}^2 (-1)^k \beta_k r^k \cos k\theta - \sum_{k=1}^3 \frac{\alpha_{k-1}}{k} r^k \sin k\theta.$$

Interestingly, the singularity results only from the general solutions of $O(r^{\frac{1}{2}})$, but not from $\beta_i \neq 0$ and $\alpha_i \neq 0$.

13.4.3.3 For the case of $\Theta = \frac{3\pi}{2}$

The boundary angle $\Theta = \frac{3\pi}{2}$ exists in a typical concave polygon, such as the L-shaped domains. First, we consider the D-D type of (13.4.4) with $\Theta = \frac{3\pi}{2}$. The solution is $u = \bar{u} + u_g$, where $u_g = \sum_{i=1}^L d_i r^{\frac{2}{3}i} \sin(\frac{2i}{3}\theta)$, and the particular solutions from (13.2.23) are

$$\begin{aligned} \bar{u} = & \alpha_0 + \frac{(\beta_0 - \alpha_0)\theta}{\Theta} - \beta_1 r \sin \theta - \frac{\beta_2 + \alpha_2}{\Theta} \varphi_2(r, \theta) \\ & + \alpha_1 r \cos \theta + \alpha_2 r^2 \cos 2\theta. \end{aligned}$$

Compared the above function with that of $\Theta = \frac{\pi}{2}$ in (13.4.5), only the sign in front of the term $\beta_1 r \sin \theta$ is different. Note that when $d_1 \neq 0$, $u_g = O(r^{\frac{2}{3}}) \notin H^2(S)$ is the next strongest singularity to that of $O(\frac{\theta}{\Theta})$.

Consider the N-N type of (13.4.8) with $\Theta = \frac{3\pi}{2}$. The general solutions are $u_g = \sum_{i=0}^L d_i r^{\frac{2}{3}i} \cos(\frac{2i}{3}\theta)$, and the particular solutions (13.3.17) give

$$\begin{aligned} \bar{u} = & \beta_0 r \cos \theta + \frac{(\beta_1 - \alpha_1)}{2\Theta} \psi_2(r, \theta) - \frac{\beta_2}{3} r^3 \cos 3\theta - \alpha_0 r \sin \theta \\ & - \frac{\alpha_1}{2} r^2 \sin 2\theta - \frac{\alpha_2}{3} r^3 \sin 3\theta. \end{aligned} \quad (13.4.10)$$

Compared (13.4.10) with (13.4.9), only the sign in front of $\beta_0 r \cos \theta$ and $\frac{\beta_2}{3} r^3 \cos 3\theta$ is different.

Finally, consider the N-D type of (13.4.6) with $\Theta = \frac{3\pi}{2}$. The general solutions are $u_g = \sum_{i=0}^L d_i r^{\sigma_i} \cos(\sigma_i \theta)$, where $\sigma_i = \frac{2}{3}i + \frac{1}{3}$. The particular solutions of (13.3.7) give

$$\begin{aligned} \bar{u} = & \beta_0 + \frac{(\beta_1 - \alpha_0)}{\Theta} \psi_1(r, \theta) - \beta_2 r^2 \cos 2\theta - \alpha_0 r \sin \theta \\ & - \frac{\alpha_1}{2} r^2 \sin 2\theta - \frac{\alpha_2}{3} \{r^3 \sin 3\theta + \frac{1}{\Theta} \psi_3(r, \theta)\}. \end{aligned}$$

The strongest singularity of u is $O(r^{\frac{1}{3}})$.

13.4.3.4 For the case of $\Theta = 2\pi$

The boundary angle $\Theta = 2\pi$ occurs for the domains with an inside crack without symmetry. First, we consider the D-D type of (13.4.4) with $\Theta = 2\pi$. The general solutions are given by $u_g = \sum_{i=0}^L d_i r^{\frac{i}{2}} \sin(\frac{i}{2})\theta$, and the particular solutions from (13.2.21) are

$$\bar{u} = \alpha_0 + \frac{(\beta_0 - \alpha_0)\theta}{\Theta} + \sum_{k=1}^2 \alpha_k r^k \cos k\theta + \sum_{k=1}^2 \frac{(\beta_k - \alpha_k)}{\Theta} \varphi_k(r, \theta).$$

When $\beta_0 \neq \alpha_0$ the singularity $O(\frac{\theta}{\Theta})$ is the strongest. The next strongest singularity results from $u_g = O(r^{\frac{1}{2}})$. Also when $\beta_i \neq \alpha_i$, $i = 1, 2$, the mild singularities $O(r^i \ln r)$ occur.

Consider the N-N type of (13.4.8) with $\Theta = 2\pi$. The general solutions $u_g = d_0 + \sum_{i=1}^L d_i r^{\frac{i}{2}} \cos(\frac{i}{2})\theta$, where d_0 is an arbitrary constant. The particular solutions from (13.3.15) are

$$\bar{u} = - \sum_{k=1}^3 \frac{\alpha_{k-1} + \beta_{k-1}}{k\Theta} \psi_k(r, \theta) - \sum_{k=1}^3 \frac{\alpha_{k-1}}{k} r^k \sin k\theta.$$

Consider the N-D type of (13.4.6) with $\Theta = 2\pi$, $u_g = \sum_{i=0}^L d_i r^{\sigma_i} \cos \sigma_i \theta$, where $\sigma_i = \frac{i}{2} + \frac{1}{4}$. The particular solutions are from (13.3.5)

$$\bar{u} = \sum_{k=0}^2 \beta_k r^k \cos k\theta - \sum_{k=1}^3 \frac{\alpha_{k-1}}{k} r^k \sin k\theta.$$

Tables 13.2 – 13.4 list the overviews of the singularities of particular solutions for $\Theta = \frac{3\pi}{2}, \pi, 2\pi$.

Among all cases of $\Theta = \frac{\pi}{2}, \frac{3\pi}{2}, \pi, 2\pi$, the strongest singularity is still $O(\frac{\theta}{\Theta})$, and the next singularity is $O(r^{\frac{1}{4}})$, resulting from the N-D type of $\Theta = 2\pi$. Based on the analysis for the harmonic functions on the polygonal domains, we understand completely the regularity and singularity of Laplace's equations. Therefore, we may deliberately design the new models with different kinds of singularities. In this chapter, we consider the simplest rectangle in Figure 13.5 as the solution domain of testing models, and employ the particular solutions in Section 13.4. Of course, we may also design other testing models on the L-shaped and the inside cracked domains as shown in Figure 13.5, by means of Sections 4.3.2 – 4.3.4.

13.5 New Models of Singularities for Laplace's Equation

13.5.1 Two Models

The singularity models play an important role in the studying of numerical methods, because they can serve as benchmark problems to test the performance of different numerical methods. Two popular models, Motz's and the cracked beam problems, have been explored in Chapter 2. In this chapter, we propose a new discontinuity model, called **Model I**, see Figure 13.6.

$$\begin{aligned} \Delta u &= 0, \quad \text{in } S, \\ u &= 0, \quad \text{on } \overline{OD}, \\ u &= 500, \quad \text{on } \overline{OA} \cup \overline{AB}, \\ \frac{\partial u}{\partial n} &= 0, \quad \text{on } \overline{BC} \cup \overline{CD}. \end{aligned} \quad (13.5.1)$$

Note that Model I is different from the Motz's problem only on the boundary condition on \overline{OA} , where the Dirichlet condition $u = 500$ is used to replace the Neumann condition $\frac{\partial u}{\partial n} = 0$. The solution u at the origin is discontinuous, having much stronger singularity than that of Motz's problem. We have the solution expansion,

$$v = \frac{500(\pi - \theta)}{\pi} + \sum_{i=1}^L c_i r^i \sin i\theta, \quad (13.5.2)$$

where c_i are the unknown coefficients to be sought. Since the function (13.5.2) satisfies the boundary conditions on \overline{DO} and \overline{OA} already, c_i can be found to satisfy the rest of boundary conditions on ∂S as close as possible. We will solve it by the collocation TM described in Section 13.5.2 below, to solve the problem.

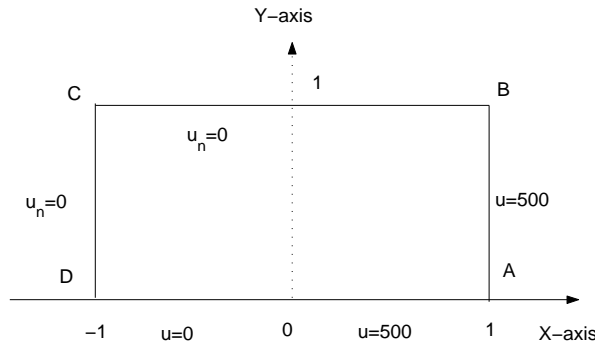


Figure 13.6: Model I.

Consider the following model of the crack plus mild singularities of $\rho^k \ln \rho$, $k = 1, 2$, which are developed from Motz's problem, called **Model II**, see Figure 13.7.

$$\begin{aligned} \Delta u &= 0, \quad \text{in } S, \\ u &= 0, \quad \text{on } \overline{OD}, \\ u &= 500, \quad \text{on } \overline{AB}, \\ \frac{\partial u}{\partial n} &= 0, \quad \text{on } \overline{OA} \cup \overline{CD}, \\ u &= 125(-x^2 + 2x + 3), \quad \text{on } \overline{BC}. \end{aligned}$$

Since the boundary function on \overline{BC} can be expressed by

$$u = 500(x + 1) - 125(x + 1)^2 = 500 - 125(x - 1)^2, \quad \text{on } \overline{BC},$$

we obtain the solutions near the corners B and C ,

$$\begin{aligned} v_1 &= \bar{v}_1 + \sum_{i=1}^M a_i \rho^{2i} \sin 2i\phi, \quad \text{in } S_1, \\ v_2 &= \bar{v}_2 + \sum_{i=1}^M b_i \xi^{2i+1} \sin(2i+1)\eta, \quad \text{in } S_2, \end{aligned}$$

where the coefficients a_i and b_i are unknowns, (ρ, ϕ) and (ξ, η) are the polar coordinates near corners B and C , respectively, and S_1 and S_2 are the subdomains (see Figure 13.8)

$$\begin{aligned} S_1 &= \{(\rho, \phi) | 0 \leq \rho \leq \rho_1, 0 \leq \phi \leq \frac{\pi}{4}\}, \\ S_2 &= \{(\xi, \eta) | 0 \leq \xi \leq \xi_1, 0 \leq \eta \leq \frac{\pi}{4}\}. \end{aligned}$$

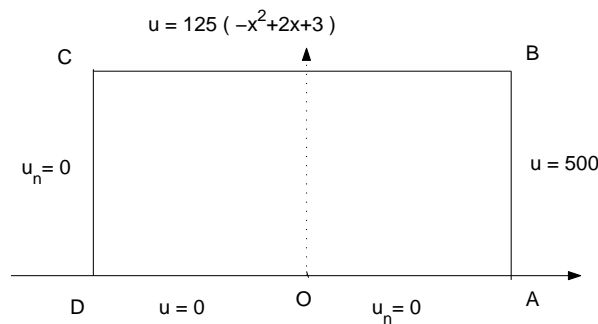


Figure 13.7: Model II.

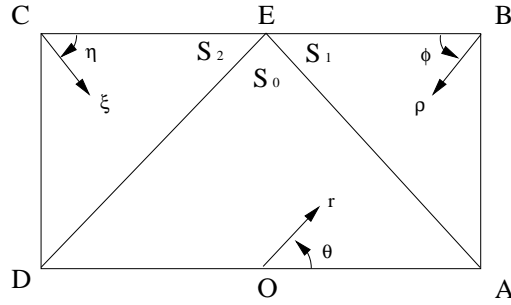


Figure 13.8: Partition of the rectangle.

The functions \bar{v}_1 and \bar{v}_2 can be found by following the particular solutions in Section 13.4

$$\begin{aligned}\bar{v}_1 &= 500 - 125\rho^2 \cos 2\phi + \frac{125}{\Theta} \varphi_2(\rho, \phi), \\ \bar{v}_2 &= -125\xi^2 \cos 2\eta + 500\xi \cos \eta - \frac{500}{\Theta} \varphi_1(\xi, \eta),\end{aligned}$$

where $\Theta = \frac{\pi}{2}$, and

$$\varphi_n(\rho, \varphi) = \rho^n \{\ln \rho \sin n\varphi + \varphi \cos n\varphi\}.$$

Let $S = S_0 \cup S_1 \cup S_2$ as shown in Figure 13.8. The piecewise admissible functions are given by

$$v = \begin{cases} v_0 = \sum_{i=0}^L d_i r^{i+\frac{1}{2}} \cos(i + \frac{1}{2})\theta & \text{in } S_0, \\ v_1 = \bar{v}_1 + \sum_{i=1}^M a_i \rho^{2i} \sin 2i\phi & \text{in } S_1, \\ v_2 = \bar{v}_2 + \sum_{i=0}^N b_i \xi^{2i+1} \sin(2i+1)\eta & \text{in } S_2, \end{cases} \quad (13.5.3)$$

where

$$\begin{aligned}\bar{v}_1 &= 500 - 125\rho^2 \cos 2\phi + \frac{125}{\Theta} \rho^2 (\ln \rho \sin 2\phi + \phi \cos 2\phi), \\ \bar{v}_2 &= -125\xi^2 \cos 2\eta + 500\xi \cos \eta - \frac{500}{\Theta} \xi (\ln \xi \sin \eta + \eta \cos \eta).\end{aligned}$$

Note that the solutions at corners B and C have the mild singularities, $O(\rho^2 \ln \rho)$ and $O(\xi \ln \xi)$, respectively.

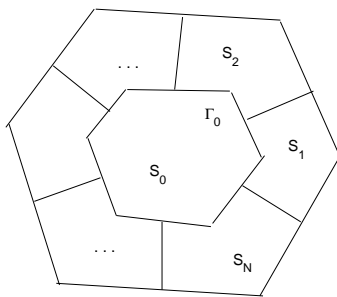


Figure 13.9: Partition for the collocation Trefftz method.

13.5.2 The Trefftz Methods

Based on the above analysis, we have found the local particular solutions near all the corners of S . If there exist the singularities, e.g., the discontinuity as $O(\frac{\theta}{\Theta})$, the angular singularity as $O(r^p)$, $0 < p < 1$, and the mild singularity as $O(r^k \ln r)$, $k = 1, 2, \dots$, we may split S by the interface Γ_0 into finite sub-polygons S_i , e.g., $S = \cup_{i=0}^N S_i$. In each S_i , there exists only one singularity point at one exterior corner, see Figure 13.9. We denote simply

$$v = v_i = \bar{v}_i + \sum_{k=0}^{N_i} c_k^{(i)} H_k^{(i)} \quad \text{in } S_i, \quad (13.5.4)$$

where \bar{v}_i are the particular solutions, $H_k^{(i)}$ are the known functions satisfying the Laplace's equation and certain boundary conditions, and $c_k^{(i)}$ are the unknown coefficients. In S_0 in Figure 13.9, the smooth solutions can be expressed by

$$u = \sum_{i=0}^{\infty} a_i r^i \cos i\theta + \sum_{i=1}^{\infty} b_i r^i \sin i\theta \quad \text{in } S_0,$$

where a_i and b_i are coefficients.

Suppose that the piecewise admissible functions (13.5.4) satisfy (13.5.1) in S_i and the exterior Dirichlet-Neumann conditions. Then the coefficients $c_k = c_k^{(i)}$ may be sought by satisfying the interior continuity conditions

$$u^+ = u^-, \quad \frac{\partial u^+}{\partial n} = \frac{\partial u^-}{\partial n} \quad \text{on } \Gamma_0.$$

Define the errors on Γ_0

$$\|v\|_B = \left\{ \int_{\Gamma_0} (v^+ - v^-)^2 d\ell + w^2 \int_{\Gamma_0} \left(\frac{\partial v^+}{\partial n} - \frac{\partial v^-}{\partial n} \right)^2 d\ell \right\}^{\frac{1}{2}},$$

where w is a suitable weight. For Model II, we choose $w = \max\{1/(L+1), 1/2M, 1/(2N+1)\}$ (see Chapters 1 and 3). Then the coefficients $\tilde{c}_k = \tilde{c}_k^{(i)}$ are found by

$$I(\tilde{c}_k) = \min_{c_k} I(c_k), \quad (13.5.5)$$

where

$$I(c_k) = \|v\|_B^2 = \int_{\Gamma_0} (v^+ - v^-)^2 dl + w^2 \int_{\Gamma_0} \left(\frac{\partial v^+}{\partial n} - \frac{\partial v^-}{\partial n} \right)^2 dl. \quad (13.5.6)$$

Eq (13.5.5) is called the TM. When the integrals in (13.5.6) involve numerical quadrature, we denote

$$\widehat{I}(c_k) = \widehat{\int}_{\Gamma_0} (v^+ - v^-)^2 dl + w^2 \widehat{\int}_{\Gamma_0} \left(\frac{\partial v^+}{\partial n} - \frac{\partial v^-}{\partial n} \right)^2 dl, \quad (13.5.7)$$

where $\widehat{\int}_{\Gamma_0}$ is evaluated by some rules. The collocation TM is to seek the coefficients $\hat{c}_k = \hat{c}_k^{(i)}$ by

$$\widehat{I}(\hat{c}_k) = \min_{c_k} \widehat{I}(c_k).$$

The detailed algorithms and error analysis are also provided in Chapter 2, and the exponential convergence rates can be achieved.

13.5.3 Numerical Experiments

First, consider Model I with discontinuous solutions. We divide \overline{AB} by NNP uniform sections, and use the central rule for integration computation. Based on our trial computation, we choose $NNP = L$, and carry out the collocation TM. The error norms, condition numbers (Cond.) of the associated matrix, and the leading coefficient \hat{c}_1 are listed in Table 13.5, and the computed coefficients in Table 13.6. From Table 13.5, we can see

$$\|\epsilon\|_B = O((0.56)^L), \quad \text{Cond.} = O((1.43)^L), \quad \text{Cond.eff} = O(L), \quad (13.5.8)$$

where Cond.eff is defined in (3.7.10) in Chapter 3. The coefficient \hat{c}_1 has 12 significant digits, if comparing the data in the last two rows in Table 13.5. From Table 13.6, the decreasing behavior of coefficients \hat{c}_i is like that in Motz's problem, and the errors $\|\epsilon\|_B$ in Table 13.5 is reduced by a factor about 10 if by increasing four terms of $\sin i\theta$, see Chapter 2.

The function $\hat{u} = \frac{500(\pi-\theta)}{\pi}$ in (13.5.2) satisfies $\hat{u} \notin H^1(S)$ but $\hat{u} \in H^{\frac{1}{2}}(S)$ only. This causes a dilemma for the error analysis of the TM for Model I. In fact, let $w = u - \hat{u}$. We obtain from (13.5.1)

$$\begin{aligned} \Delta w &= 0, \quad \text{in } S, \\ w &= 0, \quad \text{on } \overline{AD}, \\ w &= 500 - \hat{u}, \quad \text{on } \overline{AB}, \\ \frac{\partial w}{\partial n} &= -\frac{\partial \hat{u}}{\partial n}, \quad \text{on } \overline{BC} \cup \overline{CD}. \end{aligned}$$

The solution w is a smooth solution. Hence we may also have the exponential convergence rates by the collocation TM for Model I, see Chapter 2.

In computation, we also compute Cond_eff, Cond_EE and Cond_E defined in Section 3.7 of Chapter 3, and list them in the tables. In Table 13.5, Cond_eff is significantly smaller than Cond., and Cond_E and Cond_EE have the same three significant digits.

Next for Model II, we should choose the partition in Figure 13.8, and use the piecewise particular solutions in (13.5.3). Both the central rule and the Gaussian rule of six nodes are employed to compute the integrals in (13.5.7). Denote by NNP the partition number on each of \overline{AE} and \overline{ED} . In computation, we choose NNP as multiples of six. The errors, condition numbers, effective condition numbers and the leading coefficients \hat{c}_0 are listed in Tables 13.7 and 13.8. For these two integration rules, the errors and Cond. are slightly different, with the empirical rates

$$\|\epsilon\|_B = O((0.55)^L), \quad \text{Cond.} = \text{Cond_eff} = O((1.27)^L). \quad (13.5.9)$$

Compared with (13.5.8), the Cond. are significantly smaller, but Cond_eff \approx Cond. The solutions retain the same high accuracy. The better performance in accuracy is also an improvement from [291], based on the numerical data in [316].

Note that $\|\epsilon\|_B$ in (13.5.9) displays the exponential convergence rates. It is proved in Chapter 2 that when the uniformly V_h - elliptic inequality as well as the bilinear inequality is satisfied, the errors from the collocation TM are, basically (i.e., with a constant factor), the optimal truncation errors in (13.5.3), which have the exponential convergence rates for the harmonic functions on a sectorial domain, see Volkov [473], p. 41.

From Tables 13.7 and 13.8 the leading coefficient

$$\hat{d}_0 = 491.49398551255 \quad (13.5.10)$$

has 14 significant digits. When $L = 24$, coefficient \hat{d}_0 has 9 and 12 significant digits from Tables 13.7 and 13.8, respectively. This implies that the Gaussian rule with six nodes provides better leading coefficients, the same conclusion made in Chapter 2. Hence, we list in Tables 13.9 – 13.11 the computed coefficients from the Gaussian rule with six

nodes. Besides, the leading coefficients \hat{a}_1 and \hat{b}_0 have 15 and 16 significant digits, given by

$$\hat{a}_1 = -197.843688202747, \quad \hat{b}_0 = -108.3167742382339.$$

Moreover, we can see from $|\hat{d}_0 - \hat{d}_{48}|$ in Table 13.8 that the leading coefficient \hat{d}_0 also has the exponential convergence rates,

$$\Delta d_0 = |\hat{d}_0 - d_0| = O((0.56)^L).$$

Remark 13.5.1 *In Tang [453], a number of models for Laplace's equations with the Dirichlet-Neumann boundary conditions are computed on rectangle S . The uniform admissible functions,*

$$v = \sum_{i=0}^L d_i r^{i+\frac{1}{2}} \cos\left(i + \frac{1}{2}\right)\theta \quad \text{in } S, \tag{13.5.11}$$

are chosen. When there is only one crack singularity at the origin, the highly accurate solutions can be obtained by the collocation TM, and the exponential convergence rates are shown numerically. However, where there exists a mild singularity of $O(r^k \ln r)$, $k = 1, 2$ at some corners, the accuracy of the numerical solutions is declined significantly, and only the convergences rates of polynomials can be observed. From Tang [453] we conclude that the divisions of S into three subdomains and the use of piecewise admissible functions as (13.5.3) are absolutely necessary to achieve the highly accurate solutions by the collocation TM, and to retain the exponential convergence rates.

Now, we ignore the mild singularity at the corners B and C in Model II, choose the uniform functions (13.5.11) only, and carry out the collocation TM for Model II. The computed results are list in Table 13.11, and the leading coefficients in Table 13.12. From Table 13.11 we can see

$$\|\epsilon\|_B = O(L^{-2}), \quad \text{Cond.} = O((1.42)^L), \quad \text{Cond.eff} = O(L),$$

by noting the ratio from the data in Table 13.11

$$\frac{(\|\epsilon\|_B)_{L=24}}{(\|\epsilon\|_B)_{L=48}} = \frac{0.863}{0.177} = 4.88 = 2^{2.28}.$$

The convergence rate $O(L^{-2})$ is polynomial and slow. In Babuska and Guo [16], for the mild singularity $O(r^k \ln r)$, the polynomial convergence rates

$$\|\epsilon\|_{1,S} = O(L^{-2k}), \tag{13.5.12}$$

are proved for the p -version FEM. Since there is a mild singularity $O(\xi \ln \eta)$ at corner C , the convergence rate $O(L^{-2})$ coincides with (13.5.12) very well. Interestingly, although the slow convergence rates occur, the leading coefficients, \hat{d}_0^* and \hat{d}_1^* , still have five and four significant digits. This implies that the solutions near the origin may not be influenced

very much by the mild singularity at the far away corners. However, the convergence rates for d_0^* is also polynomial

$$\Delta d_0^* = O(L^{-2}),$$

by comparing \hat{d}_0^* in Table 13.11 with \hat{d}_0 in (13.5.10)

$$\frac{|\hat{d}_0 - \hat{d}_0^*|_{L=24}}{|\hat{d}_0 - \hat{d}_0^*|_{L=48}} = \frac{0.471(-2)}{0.112(-2)} = 4.21 = 2^{2.07}.$$

13.6 Concluding remarks

To close this chapter, let us give a few remarks.

1. The particular solutions of Poisson's and Laplace's equations on a polygon with the Dirichlet, the Neumann boundary conditions, and their mixed types are derived in detail. Although these solutions can be found in Volkov [472, 473], the solution formulas of harmonic functions given in this chapter are more explicit, and easier to expose the mild singularity at the domain corners than those in [473]. A number of useful particular solutions for the rectangular, the L-shaped and the cracked domains are derived. Obviously, the analysis in this chapter is also more comprehensive than that in Li [291] and Lu and Li [309]. Choosing the good basis functions, in particular those representing singularities, is essential for the collocation TM. Hence the analysis of the particular solutions in this chapter will allow the collocation TM to solve the Poisson and the Laplace equations on a polygon efficiently.
2. The particular solutions can display a clear view of regularity and singularity. In this chapter, we provide the particular solutions on special angles, $\Theta = \frac{i\pi}{2}$, $\Theta = \frac{(2i-1)\pi}{4}$, $i = 1, 2, 3, 4$. Those solution behavior is important to the choices of numerical methods because different numerical methods need different regularities of the true solution. Take linear finite element method and the finite difference method as examples. If $u \in H^2(S)$, the optimal convergence rate can be obtained, where $H^k(S)$ is the Sobolev space (cf. Ciarlet [105]). If $u \in H^3(S)$, the superconvergence of FDM may be achieved, see Li et al. [317]. Moreover, the existence of singularity may suggest that whether the refinement of elements is needed or not, and where this refinement should take place. When multiple singularities occur, the division of S should also be considered, and different numerical treatments must be used. In summary, the particular solutions in this chapter are imperative in numerical methods not only for the collocation TM, but also for other methods, such as the combined method in [291] and the Schwarz alternating method.
3. Two new models are designed, to include the discontinuity, and crack plus the mild singularities of $O(r^k \ln r)$, $k = 1, 2$. The high accuracy solutions with exponential convergence rates are also provided by the collocation TM, which can be regarded as the "true" solution for testing other numerical methods. By using piecewise particular solutions in subdomains, not only can the condition numbers be reduced

significantly, but also the high accuracy of the solutions may retain as well. This is a new discovery, compared with [291]. Moreover, the Gaussian rule with high order may raise the accuracy of the leading coefficients; this is also coincident with Chapter 2.

4. Highly accurate collocation TM in Chapter 2 can be extended to the complicated problems by using the piecewise particular solutions as shown in Model II, and by employing the Schwarz alternating method. For Model II, let S be divided into three overlapped subdomains S_0, S_1 and S_2 in Figure 13.10. We may carry out the collocation TM in each S_i including just one singularity, and use a few iterations to reach the solutions of Model II with the exponential convergence rates.

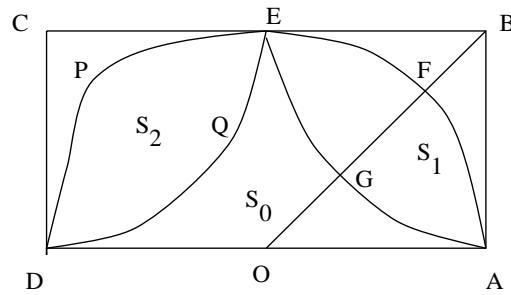


Figure 13.10: Overlapped subdomains of S .

Types	Conditions	Solutions	Not in $H^p(S)$
D-D	$\alpha_0 \neq \beta_0$	$O(\frac{\theta}{\Theta})$	$\notin H^1(S)$
	$\alpha_2 + \beta_2 \neq 0$	$O(r^2 \ln r)$	$\notin H^3(S)$
N-N	$\alpha_1 - \beta_1 \neq 0$	$O(r^2 \ln r)$	$\notin H^3(S)$
N-D	$\beta_1 + \alpha_0 \neq 0$	$O(r \ln r)$	$\notin H^2(S)$
	$\alpha_2 \neq 0$	$O(r^3 \ln r)$	$\notin H^4(S)$

Table 13.1: The singularities of $\Theta = \frac{\pi}{2}$ for the particular solutions for the Dirichlet-Neumann conditions assigned by quadratic polynomials.

Types	Conditions	Solutions	u_g
D-D	$\alpha_0 \neq \beta_0$	$O(\frac{\theta}{\Theta})$	/
	$\alpha_1 + \beta_1 \neq 0$	$O(r \ln r)$	/
	$\alpha_2 \neq \beta_2$	$O(r^2 \ln r)$	/
N-N	$\alpha_0 \neq \beta_0$	$O(r \ln r)$	/
	$\alpha_1 + \beta_1 \neq 0$	$O(r^2 \ln r)$	/
	$\alpha_2 \neq \beta_2$	$O(r^3 \ln r)$	/
N-D	/	/	$O(r^{\frac{1}{2}})$

Table 13.2: The singularities of $\Theta = \pi$ for the particular solutions for the Dirichlet-Neumann conditions assigned by quadratic polynomials.

Types	Conditions	Solutions	u_g
D-D	$\alpha_0 \neq \beta_0$	$O(\frac{\theta}{\Theta})$	$O(r^{\frac{2}{3}})$
	$\alpha_2 + \beta_2 \neq 0$	$O(r^2 \ln r)$	$O(r^{\frac{2}{3}})$
N-N	$\alpha_1 - \beta_1 \neq 0$	$O(r^2 \ln r)$	$O(r^{\frac{2}{3}})$
N-D	$\beta_1 \neq \alpha_0$	$O(r \ln r)$	$O(r^{\frac{1}{3}})$
	$\alpha_2 \neq 0$	$O(r^3 \ln r)$	$O(r^{\frac{1}{3}})$

Table 13.3: The singularities of $\Theta = \frac{3\pi}{2}$ for the particular solutions for the Dirichlet-Neumann conditions assigned by quadratic polynomials.

Types	Conditions	Solutions	u_g
D-D	$\alpha_0 \neq \beta_0$	$O(\frac{\theta}{\Theta})$	$O(r^{\frac{1}{2}})$
	$\alpha_1 \neq \beta_1$	$O(r \ln r)$	$O(r^{\frac{1}{2}})$
	$\beta_2 \neq \beta_2$	$O(r^2 \ln r)$	$O(r^{\frac{1}{2}})$
N-N	$\alpha_0 + \beta_0 \neq 0$	$O(r \ln r)$	$O(r^{\frac{1}{2}})$
	$\alpha_1 + \beta_1 \neq 0$	$O(r^2 \ln r)$	$O(r^{\frac{1}{2}})$
	$\alpha_2 + \beta_1 \neq 0$	$O(r^3 \ln r)$	$O(r^{\frac{1}{2}})$
N-D	/	/	$O(r^{\frac{1}{4}})$

Table 13.4: The singularities of $\Theta = 2\pi$ for the particular solutions for the Dirichlet-Neumann conditions assigned by quadratic polynomials.

L	NNP	$\ \varepsilon\ _B$	Cond.	Cond_eff	Cond_EE	\hat{c}_1
4	4	8.00	7.21	4.19	9.63	38.819237952022
8	8	0.374	39.4	7.67	16.8	43.170665114799
12	12	0.310(-1)	189	11.4	25.3	43.214376500110
16	16	0.262(-2)	865	15.2	33.7	43.214136607970
20	20	0.240(-3)	0.385(4)	19.0	42.1	43.214228064373
24	24	0.226(-4)	0.168(5)	22.7	50.5	43.214218726860
28	28	0.219(-5)	0.725(5)	26.5	58.9	43.214219772889
32	32	0.217(-6)	0.309(6)	30.3	67.3	43.214219655948
36	36	0.218(-7)	0.131(7)	34.1	75.7	43.214219669083
40	40	0.221(-8)	0.553(7)	37.9	84.1	43.214219667602
44	44	0.227(-9)	0.230(8)	41.6	92.5	43.214219667770
48	48	0.234(-10)	0.967(8)	45.4	101	43.214219667751

Table 13.5: The error norms, condition numbers and the leading coefficient from the collocation TM for Model I with discontinuity solutions.

i	\hat{c}_i	i	\hat{c}_i
1	.43214219667770(2)	23	.16489962791699(-5)
2	.31260955885527(2)	24	-.79051314384074(-6)
3	.18038119234387(2)	25	.37931215697053(-6)
4	-.50111963888576(1)	26	.18240663865146(-6)
5	.25247674269181(1)	27	.87840710016997(-7)
6	.79217647609612	28	-.42329123575021(-7)
7	.31101912715291	29	.20396909210300(-7)
8	-.15593842689060	30	.98583773313965(-8)
9	.64666484264955(-1)	31	.47728167326695(-8)
10	.31023130031003(-1)	32	-.23016373178046(-8)
11	.14574593153069(-1)	33	.10945497384787(-8)
12	-.64753673008044(-2)	34	.53140684243878(-9)
13	.30355950425750(-2)	35	.25906239084496(-9)
14	.13875866526055(-2)	36	-.12253369539977(-9)
15	.64253903347776(-3)	37	.52906242779061(-10)
16	-.30356334877807(-3)	38	.25805735672319(-10)
17	.14229592607503(-3)	39	.12740674743505(-10)
18	.67458107151949(-4)	40	-.56229016798380(-11)
19	.32016503381154(-4)	41	.16282561223942(-11)
20	-.15178192325529(-4)	42	.79889831908072(-12)
21	.72347424374442(-5)	43	.40231053525172(-12)
22	.34495750578571(-5)	44	-.15531526257412(-12)

Table 13.6: The coefficients from the collocation TM by the central rule for Model I with u_L as $L = 44$.

L	N	M	NNP	$\ \varepsilon\ _B$	Cond.	Cond_eff	Cond_E	\hat{d}_0
6	3	3	6	0.485	5.14	4.77	5.14	491.50375447935164
12	6	6	12	0.990(-2)	17.8	15.8	17.8	491.49403292439115
18	9	9	18	0.141(-3)	71.3	62.1	71.3	491.49398597288712
24	12	12	24	0.489(-5)	294	252	294	491.49398548887837
30	15	15	30	0.916(-7)	0.122(4)	0.104(4)	0.122(4)	491.49398551220833
36	18	18	36	0.371(-8)	0.514(4)	0.431(4)	0.514(4)	491.49398551257605
42	21	21	42	0.767(-10)	0.216(5)	0.181(5)	0.216(5)	491.49398551255416
48	24	24	48	0.354(-11)	0.916(5)	0.765(5)	0.916(5)	491.49398551255229

Table 13.7: The error norms, condition numbers and the leading coefficient from the collocation TM for Model II by the central rule.

L	N	M	NNP	$\ \varepsilon\ _B$	Cond.	Cond_eff	Cond_E	\hat{d}_0	$ \hat{d}_0 - \hat{d}_0 _{L=48}$
6	3	3	6	0.527	5.12	4.74	5.12	491.50984946552893	
12	6	6	12	0.959(-2)	17.0	15.0	17.0	491.49399162427318	.00001172067
18	9	9	18	0.152(-3)	67.5	58.5	67.5	491.49398552412674	.00000157423
24	12	12	24	0.454(-5)	278	236	278	491.49398551269798	.00000014547
30	15	15	30	0.995(-7)	1.15(4)	971	0.115(4)	491.49398551252898	.00000002353
36	18	18	36	0.361(-8)	0.481(4)	0.420(4)	0.481(4)	491.49398551255371	.00000000120
42	21	21	42	0.859(-10)	0.202(5)	0.168(5)	0.202(5)	491.49398551255291	.00000000040
48	24	24	48	0.392(-11)	0.861(5)	0.711(5)	0.861(5)	491.49398551255251	.00000000000

Table 13.8: The error norms, condition numbers and the leading coefficient from the collocation TM for Model II by the Gaussian rule of six nodes.

i	\hat{d}_i	i	\hat{d}_i
0	.49149398551255(3)	22	.28296876209014(-3)
1	.20065238223118(2)	23	.17445041211420(-3)
2	-.31336492129090(2)	24	-.30575467669084(-3)
3	.84502739982599(1)	25	.19077594908752(-3)
4	.15443903862693(2)	26	-.50780058124318(-4)
5	-.52203007093797(1)	27	-.31978418070731(-4)
6	.10853377508385(1)	28	.55851059563915(-4)
7	.45247368697120	29	-.35445135492159(-4)
8	-.71447060802058	30	.95349846596053(-5)
9	.34620015754709	31	.60578683131418(-5)
10	-.75107200195077(-1)	32	-.10476743650533(-4)
11	-.39753375330083(-1)	33	.66984928968357(-5)
12	.82736452629329(-1)	34	-.17784188813767(-5)
13	-.45334765014809(-1)	35	-.10897146397864(-5)
14	.11220412185256(-1)	36	.18351999362232(-5)
15	.63615937532872(-2)	37	-.11574049991123(-5)
16	-.11139219730940(-1)	38	.27828600655526(-6)
17	.65343214462257(-2)	39	.13463498937738(-6)
18	-.16594741652122(-2)	40	-.21339700669832(-6)
19	-.99468983459638(-3)	41	.12852559004887(-6)
20	.17769148561836(-2)	42	-.22265448089398(-7)
21	-.10807339151966(-2)		

Table 13.9: The coefficients d_i from the collocation TM by the Gaussian rule with six nodes for Model II with $L = 42$, $M = 21$ and $N = 21$.

i	\hat{a}_i	i	\hat{b}_i
1	-.19784368820275(3)	0	-.10831677423823(3)
2	-.31926930057149(1)	1	.29780407286597(2)
3	.64293346822787(1)	2	.12655253431819(2)
4	.75030546466542	3	-.14499389726714(1)
5	-.60862066562632	4	-.10047797333552(1)
6	-.92423658976556(-1)	5	.15330929917106
7	.93708777642456(-1)	6	.14978794259931
8	.15521001580253(-1)	7	-.24773993470475(-1)
9	-.15878893208957(-1)	8	-.24629343903207(-1)
10	-.27632100592619(-2)	9	.42813849810836(-2)
11	.29306574648338(-2)	10	.44706691928972(-2)
12	.52625553145008(-3)	11	-.80216072455720(-3)
13	-.56856704278497(-3)	12	-.85704781612190(-3)
14	-.10419605918837(-3)	13	.15720069031688(-3)
15	.11420949850474(-3)	14	.17078652690669(-3)
16	.20936766448185(-4)	15	-.31858002906200(-4)
17	-.23074560887560(-4)	16	-.34434427308903(-4)
18	-.38768970065648(-5)	17	.65258826319999(-5)
19	.42150857308363(-5)	18	.63676400596069(-5)
20	.47049774548533(-6)	19	-.12273737750039(-5)
21	-.49013499517408(-6)	20	-.76595590808321(-6)
		21	.14902151022334(-6)

Table 13.10: The coefficients a_i and b_i from the collocation TM by the Gaussian rule with six nodes for Model II with $L = 42$, $M = 21$ and $N = 21$.

L	NNP	$\ \varepsilon\ _B$	Cond.	Cond_eff	Cond_EE	\hat{d}_0^*	$\hat{d}_0^* - \hat{d}_0$
6	6	13.7	5.99	1.81	4.90	492.34847235119	
12	12	3.58	82.8	3.56	24.8	491.51252765213	0.185(-1)
18	18	1.71	636	5.20	40.2	491.50221240460	
24	24	0.863	0.720(4)	6.81	53.8	491.49869961824	0.471(-2)
30	30	0.583	0.513(5)	8.46	67.2	491.49694490581	
36	36	0.350	0.556(6)	10.1	8.05	491.49602070057	
42	42	0.262	0.385(7)	11.7	93.8	491.49546168905	
48	48	0.177	0.429(8)	13.4	107	491.49510320203	0.112(-2)

Table 13.11: The error norms, condition numbers and the leading coefficient from the collocation TM by the central rule for Model II by ignoring the mild singularities at the corners B and C.

i	\hat{d}_i^*	i	\hat{d}_i^*
0	.49149546168905(3)	22	-.38732308021276(-2)
1	.20061741631796(2)	23	.15222922823156(-1)
2	-.31332682690943(2)	24	-.18537659186308(-1)
3	.84476705355138(1)	25	.13164570233705(-1)
4	.15444654497322(2)	26	-.36127640611058(-2)
5	-.52197549909606(1)	27	.13507935540894(-1)
6	.10843997742414(1)	28	-.15269033237590(-1)
7	.45314965063084	29	.97379816592412(-2)
8	-.71469113400049	30	-.14839402178926(-2)
9	.34610701298805	31	.64905517111838(-2)
10	-.74935909769621(-1)	32	-.70035779273999(-2)
11	-.39632984998754(-1)	33	.41042351379424(-2)
12	.82256535112322(-1)	34	-.25528371216394(-3)
13	-.44645267648607(-1)	35	.15575280684639(-2)
14	.10533093384599(-1)	36	-.16258709839073(-2)
15	.88658956518358(-2)	37	.89428271787672(-3)
16	-.14897241354148(-1)	38	.24127768058350(-5)
17	.10194437974102(-1)	39	.14814295972461(-3)
18	-.40342227174215(-2)	40	-.15230483989584(-3)
19	.77421337052198(-2)	41	.80339732143722(-4)
20	-.98722765968634(-2)	42	.31972123443789(-5)
21	.84599449662161(-2)		

Table 13.12: The coefficients \hat{d}_i^* from the collocation TM by the central rule for Model II with $L = 42$ by ignoring the mild singularities at corners B and C.

Appendix

Historic Review of Boundary Methods

This appendix explores the rich heritage of boundary methods, which are not limited to the Trefftz method treated in this book. By “boundary methods” we refer to numerical methods for solving boundary value problems of partial differential equations that discretizes only the boundary of the solution domain. This is in contrast to the “domain methods” such as the Finite Element Method (FEM) and the Finite Difference Method (FDM) that requires the discretization of the entire domain into discrete unknowns.

This reduction of dimension in discretization leads to a smaller size solution system, which not only reduces the computer storage requirement, but also results in more efficient computer solution. This effect is most pronounced when the domain is unbounded. In domain methods, unbounded domain must be truncated and approximated. Boundary methods, on the other hand, often automatically satisfy the condition at infinity and no additional effort is needed.

In the industrial setting, mesh generation is generally the most labor intensive part of numerical modeling, particularly in terms of the preparation of connectivity data for the FEM [32]. Without the need of interior mesh, boundary methods are more cost effective in mesh preparation. For problems involving moving boundaries, the frequent re-meshing is also much easier with boundary methods. Hence boundary methods, whenever applicable, should be the numerical methods of the first choice.

In this appendix, we shall examine the mathematical foundation of boundary methods from the historic perspective, including the potential theory, boundary value problems, Green’s functions, Green’s identities, Fredholm integral equations, and Ritz and Trefftz methods. For the interest the beginners of the field, biographical sketches of the pioneers of the field are provided.

This appendix is adopted from the article by Cheng and Cheng [96].

A.1 Potential Theory

The Laplace equation is one of the most widely used partial differential equations for modeling science and engineering problems. It typically comes from the physical consequence of combining a phenomenological gradient law (such as the Fourier law in heat conduction and the Darcy law in groundwater flow) with a conservation law (such as the heat energy conservation and the mass conservation of an incompressible substance). For example, Fourier law was presented by *Jean Baptiste Joseph Fourier* (1768–1830) in 1822 [155]. It states that the heat flux in a thermal conducting medium is proportional to the spatial gradient of temperature distribution:

$$\mathbf{q} = -k \nabla T, \quad (\text{A.1.1})$$

where \mathbf{q} is the heat flux vector, k is the thermal conductivity, and T is the temperature. The steady state heat energy conservation requires that at any point in space

$$\nabla \cdot \mathbf{q} = 0. \quad (\text{A.1.2})$$

Combining (A.1.1) and (A.1.2) and assuming that k is a constant, we obtain the Laplace equation

$$\nabla^2 T = 0. \quad (\text{A.1.3})$$

For groundwater flow, similar procedure leads to

$$\nabla^2 h = 0, \quad (\text{A.1.4})$$

where h is the piezometric head. It is of interest to mention that the notation ∇ used in the above came from *William Rowan Hamilton* (1805–1865). The symbol ∇ , known as “nabla”, is a Hebrew stringed instrument that has a triangular shape [167].

The above theories are based on physical quantities. The second way that the Laplace equation arises is through the mathematical concept of finding a “potential” that has no direct physical meaning. In fluid mechanics, the velocity of an incompressible fluid flow satisfies the divergence equation

$$\nabla \cdot \mathbf{v} = 0, \quad (\text{A.1.5})$$

which is again based on the mass conservation principle. For an inviscid fluid flow that is irrotational, it satisfies the equation of curl

$$\nabla \times \mathbf{v} = 0. \quad (\text{A.1.6})$$

It can be shown mathematically that the identity (A.1.6) guarantees the existence of a scalar potential ϕ such that

$$\mathbf{v} = \nabla \phi, \quad (\text{A.1.7})$$

Combining (A.1.5) and (A.1.7) we again obtain the Laplace equation. We notice that ϕ , called the velocity potential, is a mathematical creation; it is not associated with

any measurable physical quantity. In fact, the phrase “potential function” was coined by *George Green* (1793–1841) in his 1828 study [183] of electrostatics and magnetics: electric and magnetic potentials were used as convenient tools for manipulating the solution of electric and magnetic forces.

The original derivation of Laplace equation, however, was based on the study of gravitational attraction, based on the third law of motion of *Isaac Newton* (1643–1727):

$$\mathbf{F} = -\frac{G m_1 m_2 \mathbf{r}}{|\mathbf{r}|^3}, \quad (\text{A.1.8})$$

where \mathbf{F} is the force field, G is the gravitational constant, m_1 and m_2 are two concentrated masses, and \mathbf{r} is the distance vector between the two masses. *Joseph-Louis Lagrange* (1736–1813) in 1773 was the first to recognize the existence of a potential function that satisfied the above equation [275]

$$\phi = \frac{1}{r}, \quad (\text{A.1.9})$$

whose spatial gradient gave the gravity force field

$$\mathbf{F} = G m_1 m_2 \nabla \phi. \quad (\text{A.1.10})$$

Subsequently, *Pierre-Simon Laplace* (1749–1827) in his study of celestial mechanics demonstrated that the gravity potential satisfies the Laplace equation. The equation was first presented in polar coordinates in 1782, and then in the Cartesian form in 1787 [276] as:

$$\frac{\partial^2 \phi}{\partial x^2} + \frac{\partial^2 \phi}{\partial y^2} + \frac{\partial^2 \phi}{\partial z^2} = 0. \quad (\text{A.1.11})$$

The Laplace equation, however, had been used earlier in the context of hydrodynamics by *Leonhard Euler* (1707–1783) in 1755 [148], and by Lagrange in 1760 [274]. But Laplace was credited for making it a standard part of mathematical physics [53, 253]. We note that the gravity potential (A.1.9) satisfying (A.1.11) represents a concentrated mass. It is a “fundamental solution” of the Laplace equation.

Simeon-Denis Poisson (1781–1840) derived in 1813 [385] the equation of force potential for points interior to a body with density ρ as

$$\nabla^2 \phi = -4\pi\rho. \quad (\text{A.1.12})$$

This is known as the Poisson equation.

A.1.1 Euler

Leonhard Euler (1707–1783) was the son of a Lutheran pastor who lived near Basel, Switzerland. While studying theology at the University of Basel, Euler was attracted

to mathematics by the leading mathematician at the time, *Johann Bernoulli* (1667–1748), and his two mathematician sons, *Nicolaus* (1695–1726) and *Daniel* (1700–1782). With no opportunity in finding a position in Switzerland due to his young age, Euler followed Nicolaus and Daniel to Russia. Later, at the age of 26, he succeeded Daniel as the chief mathematician of the Academy of St. Petersburg. Euler surprised the Russian mathematicians by computing in three days some astronomical tables whose construction was expected to take several months.

In 1741 Euler accepted the invitation of Frederick the Great to direct the mathematical division of the Berlin Academy, where he stayed for 25 years. The relation with the King, however, deteriorated toward the end of his stay; hence Euler returned to St. Petersburg in 1766. Euler soon became totally blind after returning to Russia. By dictation, he published nearly half of all his papers in the last seventeen years of his life. In his words, “Now I will have less distraction.” Without doubt, Euler was the most prolific and versatile scientific writer of all times. During his lifetime, he published more than 700 books and papers, and it took St. Petersburg’s Academy next 47 years to publish the manuscripts he left behind [71]. The modern effort of publishing Euler’s collected works, the *Opera Omnia* [149], begun in 1911. However, after 73 volumes and 25,000 pages, the work is unfinished to the present day.

Euler contributed to many branches of mathematics, mechanics, and physics, including algebra, trigonometry, analytical geometry, calculus, complex variables, number theory, combinatorics, hydrodynamics, and elasticity. He was the one who set mathematics into the modern notations. We owe Euler the notations of “ e ” for the base of natural logs, “ π ” for pi, “ i ” for $\sqrt{-1}$, “ Σ ” for summation, and the concept of functions.

Carl Friedrich Gauss (1777–1855) has been called the greatest mathematician in modern mathematics for his setting up the rigorous foundation for mathematics. Euler, on the other hand, was more intuitive and has been criticized by pure mathematicians as being lacking modern day rigor. However, by the abundance of deep and indelible marks that Euler made in science and engineering, he can certainly earn the title of the greatest *applied* mathematician ever lived [139].

A.1.2 Lagrange

Joseph-Louis Lagrange (1736–1813), Italian by birth, German by adoption, and French by choice, was next to Euler the foremost mathematician of the eighteenth century. At age eighteen he was appointed professor of geometry at the Royal Artillery School in Turin. Euler was impressed by his work, and arranged a prestigious position for him in Prussia. Despite the inferior condition in Turin, Lagrange only wanted to be able to devote his time to mathematics; hence declined the offer. However, in 1766, when Euler left Berlin for St. Petersburg, Frederick the Great arranged for Lagrange to fill the vacated post. Accompanying the invitation was a modest message saying, “It is necessary that the greatest geometer of Europe should live near the greatest of Kings.” To D’Alembert, who recommended Lagrange, the king wrote, “To your care and recommendation am

I indebted for having replaced a half-blind mathematician with a mathematician with both eyes, which will especially please the anatomical members of my academy.”

After the death of Frederick, the situation in Prussia became unpleasant for Lagrange. He left Berlin in 1787 to become a member of the Académie des Sciences in Paris, where he remained for the rest of his career. Lagrange’s contributions were mostly in the theoretical branch of mathematics. In 1788 he published the monumental work *Mécanique Analytique* that unified the knowledge of mechanics up to that time. He banished the geometric idea and introduced differential equations. In the preface, he proudly announced: “One will not find figures in this work. The methods that I expound require neither constructions, nor geometrical or mechanical arguments, but only algebraic operations, subject to a regular and uniform course” [71, 364].

A.1.3 Laplace

Pierre-Simon Laplace (1749–1827), born in Normandy, France, came from relatively humble origins. But with the help of *Jean le Rond D’Alembert* (1717–1783), he was appointed professor of mathematics at the Paris Ecole Militaire when he was only twenty-year old. Some years later, as examiner of the scholars of the royal artillery corps, Laplace happened to examine a sixteen-year old sub-lieutenant named Napoleon Bonaparte. Fortunately for both their careers, the examinee passed. When Napoleon came to power, Laplace was rewarded: he was appointed the minister of interior for a short period of time, and later the president of the senate. Upon presenting the monumental work to Napoleon, the emperor teasingly chided Laplace for an apparent oversight: “They told me that you have written this huge book on the system of the universe without once mentioning its Creator.” Whereupon Laplace drew himself up and bluntly replied, “I have no need for that hypothesis” [71].

Among Laplace’s greatest achievement was the five-volume *Traité du Mécanique Céleste* that incorporated all the important discoveries of planetary system of the previous century, deduced from Newton’s law of gravitation. He was eulogized by his disciple Poisson as “the Newton of France” [190]. Other important contributions of Laplace in mathematics and physics included probability, Laplace transform, celestial mechanics, the velocity of sound, and capillary action. He was considered more than anyone else to have set the foundation of the probability theory [171].

A.1.4 Fourier

Jean Baptiste Joseph Fourier (1768–1830), born in Auxerre, France, was the ninth of the twelve children of his father’s second marriage. One of his letters showed that he really wanted to make a major impact in mathematics: “Yesterday was my 21st birthday; at that age Newton and Pascal had already acquired many claims to immortality.” In 1790 Fourier became a teacher at the Benedictine College, where he had studied earlier. Soon after, he was entangled in the French Revolution and joined the local revolutionary committee.

He was arrested in 1794, and almost went to the guillotine. Only the political changes resulted in his being released. In 1794 Fourier was admitted to the newly established Ecole Normale in Paris, where he was taught by Lagrange, Laplace, and *Gaspard Monge* (1746–1818). In 1797 he succeeded Lagrange in being appointed to the chair of analysis and mechanics.

In 1787, Fourier joined Napoleon's army in its invasion of Egypt as a scientific advisor. It was there that he recorded many observations that later led to his work in heat diffusion. Fourier returned to Paris in 1801. Soon Napoleon appointed him as the Prefect of Isère, headquartered at Grenoble. Among his achievements in this administrative position included the draining of swamps of Bourgoin and the construction of a new highway between Grenoble and Turin. Some of his most important scientific contributions came during this period (1802–1814). In 1807 he completed his memoir *On the Propagation of Heat in Solid Bodies* in which he not only expounded his idea about heat diffusion, but also outlined his new method of mathematical analysis, which we now call Fourier analysis. This memoir however was never published, because one of its examiner, Lagrange, objected to his use of trigonometric series to express initial temperature. Fourier was elected to the Académie des Sciences in 1817. In 1822 he published *The Analytical Theory of Heat* [155], ten years after its winning the Institut de France competition of the Grand Prize in Mathematics in 1812. The judges however criticized that he had not proven the completeness of the trigonometric (Fourier) series. The proof will come many years later by others [182].

A.1.5 Poisson

Simeon-Denis Poisson (1781–1840) was born in Pithiviers, France. In 1796 Poisson was sent to Fontainebleau to enroll in the Ecole Centrale there. He soon showed great talents for learning, especially mathematics. His teachers at the Ecole Centrale were extremely impressed and encouraged him to sit in the entrance examinations for the Ecole Polytechnique in Paris, the premiere institution at the time. Although he had far less formal education than most of the young men taking the examinations, he achieved the top place. His teachers Laplace and Lagrange quickly saw his mathematical talents. They were to become friends for life with their extremely able young student and they gave him strong support in a variety of ways. In his final year of study he wrote a paper on the theory of equations and Bezout's theorem, and this was of such quality that he was allowed to graduate in 1800 without taking the final examination. He proceeded immediately to the position equivalent to the present-day assistant professor in the Ecole Polytechnique at the age of nineteen, mainly on the strong recommendation of Laplace. It was quite unusual for anyone to gain their first appointment in Paris, as most of the top mathematicians had to serve in the provinces before returning to Paris. Poisson was named associate professor in 1802, a position he held until 1806 when he was appointed to the professorship at the Ecole Polytechnique, which Fourier vacated when he was sent by Napoleon to Grenoble. In 1813 in his effort to answer the challenge question for the election to the Académie des Sciences, he developed the Poisson's equation (A.1.12) to solve the electrical field caused by distributed electrical charges in a body.

Poisson made great contributions in both mathematics and physics. His name is attached to a wide variety of ideas, for example, Poisson's integral, Poisson equation, Poisson brackets in differential equations, Poisson's ratio in elasticity, and Poisson's constant in electricity [364].

A.1.6 Hamilton

William Rowan Hamilton (1805–1865) was an extremely precocious child. At the age of five, he read Greek, Hebrew, and Latin; at ten, he was acquainted with half a dozen oriental languages. He entered Trinity College, Dublin at the age of 18. His performance was so outstanding that he was appointed Professor of Astronomy and the Royal Astronomer of Ireland when he was still an undergraduate at Trinity. Hamilton was knighted at the age of thirty for the scientific work he had already achieved.

Among Hamilton's most important contributions is the establishment of an analogy between the optical theory of systems of rays and the dynamics of moving bodies. With the further development by *Carl Gustav Jacobi* (1804–1851), this theory is generally known as the Hamilton-Jacobi Principle. By this construction, for example, it was possible to determine the ten planetary orbits around the sun, a feat normally required the solution of thirty ordinary differential equations, by merely two equations involving Hamilton's characteristic functions. However, this method was more elegant than practical; hence for almost a century, Hamilton's great method was more praised than used [366].

This situation, however, changed when *Irwin Schrödinger* (1887–1961) introduced the revolutionary wave-function model for quantum mechanics in 1926. Schrödinger had expressed Hamilton's significance quite unequivocally: "*The modern development of physics is constantly enhancing Hamilton's name. His famous analogy between optics and mechanics virtually anticipated wave mechanics, which did not have much to add to his ideas and only had to take them more seriously ... If you wish to apply modern theory to any particular problem, you must start with putting the problem in Hamiltonian form*" [53].

A.2 Existence and Uniqueness

The potential problems we solve are normally posed as boundary value problems. For example, given a closed region Ω with the boundary Γ and the boundary condition

$$\phi = f(\mathbf{x}), \quad \mathbf{x} \in \Gamma, \quad (\text{A.2.1})$$

where $f(\mathbf{x})$ is a continuous function, we are asked to find a harmonic function (meaning a function satisfying the Laplace equation) $\phi(\mathbf{x})$ that fulfills the boundary condition (A.2.1). This is known as the Dirichlet problem, named after *Johann Peter Gustav Lejeune Dirichlet* (1805–1859). The corresponding problem of finding a harmonic function

with the normal derivative boundary condition,

$$\frac{\partial \phi}{\partial n} = g(\mathbf{x}), \quad \mathbf{x} \in \Gamma, \quad (\text{A.2.2})$$

where n is the outward normal, is called the Neumann problem, after *Carl Gottfried Neumann* (1832–1925).

The question of whether a solution of a Dirichlet or a Neumann problem exists, and when it exists, whether it is unique or not, is of great importance in mathematics. Obviously, if we cannot guarantee the existence of a solution, the effort of finding it can be in vain. If a solution exists, but may not be unique, then we cannot tie the solution to the associated physical problem, because we believe the physical state is unique.

The question of uniqueness is easier to answer: if a solution exists, it is unique for the Dirichlet problem, and it is unique to within an arbitrary constant for the Neumann problem. (See, for example, the proof in the classical monograph *Foundations of Potential Theory* [253] by *Oliver Dimon Kellogg* (1878–1932).) The existence theorem, however, is more difficult to prove.

To a physicist, the existence question seems to be moot. We may argue that if the mathematical problem correctly describes a physical problem, then a mathematical solution must exist, because the physical state exists. For example, Green in his 1828 seminal work [183], in which he developed Green's identities and Green's functions, presented a similar argument. He reasoned that if for a given closed region Ω , there *exists* a harmonic function U (an assumption that will be justified later) that satisfies the boundary condition

$$U = -\frac{1}{r} \quad \text{on } \Gamma, \quad (\text{A.2.3})$$

then one can define the function

$$G = \frac{1}{r} + U. \quad (\text{A.2.4})$$

It is clear that G satisfy the the Laplace equation everywhere except at the pole, where it is singular. Furthermore, G takes the null value at the boundary Γ . G is known as the Green's function. Green went on to prove that for a harmonic function ϕ , whose boundary value is given by a continuous function $\phi(\mathbf{x})$, $\mathbf{x} \in \Gamma$, its solution is represented by the boundary integral equation [253, 454]

$$\phi(\mathbf{x}) = -\frac{1}{4\pi} \int \int_{\Gamma} \phi \frac{\partial G}{\partial n} dS, \quad \mathbf{x} \in \Omega, \quad (\text{A.2.5})$$

where dS denotes surface integral. Since (A.2.5) gives the solution of the Dirichlet boundary value problem, hence the solution exists!

The above proof hinges on the existence of U , which is taken for granted at this point. How can we be sure that U exists for an arbitrary closed region Ω ? Green argued that U is nothing but the electrical potential created by the charge on a grounded sheet

conductor, whose shape takes the form of Γ , induced by a single charge located inside Ω . This physical state obviously exists; hence U must exist! It seems that the Dirichlet problem is proven. But is it?

In fact, mathematicians can construct counter examples for which a solution does not exist. An example was presented by *Henri Léon Lebesgue* (1875–1941) [279], which can be described as follows. Consider a deformable body whose surface is pushed inward by a sharp spine. If the tip of the deformed surface is sharp enough, for example, given by the revolution of the curve $y = \exp(-1/x)$, then the tip is an exceptional point and the Dirichlet problem is not always solvable. (See Kellogg [253] for more discussion.) Furthermore, if the deformed surface closes onto itself to become a single line protruding into the body, then a Dirichlet condition cannot be arbitrarily prescribed on this degenerated boundary, as it is equivalent to prescribing a value inside the domain!

Generally speaking, the existence and uniqueness theorem for potential problems has been proven for interior and exterior boundary value problems of the Dirichlet, Neumann, Robin, and mixed type, if the bounding surface and the boundary condition satisfy certain smoothness condition [253, 234]. (For interior Neumann problem, the uniqueness is only up to an arbitrarily additive constant.) For the existing proofs, the bounding surface Γ needs to be a “Liapunov surface,” which is a surface of the $C^{1,\alpha}$ continuity class, where $0 \leq \alpha < 1$. Put it simply, the smoothness of the surface is such that on every point there exists a tangent plane and a normal, but not necessarily a curvature. Corners and edges, on which a tangent plane does not exist, are not allowed in this class. This puts great restrictions on the type of problems that one can solve. On the other hand, in numerical solutions such as the finite element method and the boundary element method, the solution is often sought in the weak sense by minimizing an energy norm in some sense, such as the well-known Galerkin scheme. In this case, the existence theorem has been proven for surface Γ in the $C^{0,1}$ class [107], known as the Lipschitz surface, which is a more general class than the Liapunov surface, such that edges and corners are allowed.

A.2.1 Dirichlet

Johann Peter Gustav Lejeune Dirichlet (1805–1859) was born in Düren (present day Germany), French Empire. He attended the Jesuit College in Cologne at the age of 14. There he had the good fortune to be taught by *Georg Simon Ohm* (1789–1854). At the age of 16 Dirichlet entered the Collège de France in Paris, where he had some of the leading mathematicians as teachers. In 1825, he published his first paper proving a case in Fermat’s Last Theorem, which gained him instant fame. Encouraged by *Alexander von Humboldt* (1769–1859), who made recommendations on his behalf, Dirichlet returned to Germany the same year. From 1827 Dirichlet taught at the University of Breslau. Again with von Humboldt’s help, he moved to Berlin in 1828 where he was appointed at the Military College. Soon after this he was appointed a professor at the University of Berlin where he remained from 1828 to 1855. Dirichlet was appointed to the Berlin Academy of Sciences in 1831. An improved salary from the university put him in a position to marry, and he married Rebecca Mendelssohn, one of the composer Felix Mendelssohn’s

two sisters. Dirichlet had a lifelong friendship with Jacobi, who taught at Königsberg, and the two exerted considerable influence on each other in their researches in number theory. Dirichlet had a high teaching load and in 1853 he complained in a letter to his pupil *Leopold Kronecker* (1823–1891) that he had thirteen lectures a week to give, in addition to many other duties. It was therefore something of a relief when, on Gauss's death in 1855, he was offered his chair at Göttingen. Sadly he was not to enjoy the new life for long. He died in 1859 after a heart attack.

Dirichlet made great contributions to the number theory, and the analytic number theory may be said to begin with him. In mechanics he investigated Laplace's problem on the stability of the solar system, which led him to the Dirichlet problem concerning harmonic functions with given boundary conditions. Dirichlet is also well known for his papers on conditions for the convergence of trigonometric series. Because of this work Dirichlet is considered the founder of the theory of Fourier series [364].

A.2.2 Neumann

Carl Gottfried Neumann (1832–1925) was the son of *Franz Neumann* (1798–1895), a famous physicist who made contributions in thermodynamics. His mother was a sister-in-law of *Friedrich Wilhelm Bessel* (1784–1846). Neumann was born in Königsberg where his father was the Professor of Physics at the university. Neumann entered the University of Königsberg and received his doctorate in 1855. He worked on his habilitation at the University of Halle in 1858. He taught several universities, including Halle, Basel, and Tübingen. Finally, he moved to a chair at the University of Leipzig in 1868, and would stay there until his retirement in 1911.

He worked on a wide range of topics in applied mathematics such as mathematical physics, potential theory, and electrodynamics. He also made important pure mathematical contributions. He studied the order of connectivity of Riemann surfaces. During the 1860s Neumann wrote papers on the Dirichlet principle and the "logarithmic potential" was a term he coined [364].

A.2.3 Kellogg

Oliver Dimon Kellogg (1878–1932) was born at Linnwood, Pennsylvania. His interest in mathematics was aroused as an undergraduate at Princeton University, where he received his B.A. in 1899. He was awarded a fellowship for graduate studies and obtained a Master degree in 1900 at Princeton. The same fellowship allowed him to spend the next year at the University of Berlin. He then moved to Göttingen to pursue his doctorate. He attended lectures by *David Hilbert* (1862–1943). At that time, *Erik Ivar Fredholm* (1866–1927) had just made progress in proving the existence of Dirichlet problem using integral equations. Hilbert was excited about the development and suggested Kellogg to undertake research on the Dirichlet problem for boundary containing corners, where Fredholm's solution did not apply. Kellogg, however, failed to answer the question satisfactorily in his thesis and

several subsequent papers. With the realization of his errors, he never referred to these papers in his later work. Kellogg was hard to blame because similar errors were later made by both Hilbert and *Jules Henri Poincaré* (1854–1912), and to this date the proof of Dirichlet problem for boundary containing corners has not been accomplished.

Kellogg received his Ph.D. in 1903 and returned to the United States to take up a post of instructor in mathematics at Princeton. Two years later he joined the University of Missouri as an assistant professor. He spent the next 14 fruitful years at Missouri until he was called by Harvard University in 1919. Kellogg continued to work at Harvard until his death from a heart attack suffered while climbing [46, 141]. His book “*Foundations of Potential Theory*” [253], first published in 1929, remains among the most authoritative work to this date.

A.3 Reduction in Dimensions and Green's Formula

A key to the success of boundary element method is the reduction of spatial dimension in its integral equation representation, leading to a more efficient numerical discretization. One of the most celebrated technique of this type is the divergence theorem, which transforms a volume integral into a surface integral,

$$\iiint_{\Omega} \nabla \cdot \mathbf{A} \, dV = \iint_{\Gamma} \mathbf{A} \cdot \mathbf{n} \, dS, \quad (\text{A.3.1})$$

where \mathbf{A} is a vector, \mathbf{n} is the unit outward normal of Γ , and dV stands for volume integral. Early development of this type was found in the work of Lagrange [274] and Laplace. Equation (A.3.1), also called Gauss' theorem, is generally attributed to Gauss [164]. However, Gauss in 1813 only presented a few special cases in the form [252]

$$\iint_{\Gamma} n_x \, dS = 0, \quad (\text{A.3.2})$$

where n_x is the x -component of outward normal, and

$$\iint_{\Gamma} \mathbf{A} \cdot \mathbf{n} \, dS = 0, \quad (\text{A.3.3})$$

where the components of \mathbf{A} are given by $A_x = A_x(y, z)$, $A_y = A_y(x, z)$ and $A_z = A_z(x, y)$. The general theorem should be credited to *Mikhail Vasilevich Ostrogradski* (1801–1862), who in 1826 presented the following result to the Paris Académie des Sciences [252]

$$\iiint_{\Omega} \mathbf{a} \cdot \nabla \phi \, dV = \iint_{\Gamma} \phi \mathbf{a} \cdot \mathbf{n} \, dS, \quad (\text{A.3.4})$$

where \mathbf{a} is a constant vector.

Another useful formula is the Stokes' theorem, presented by *George Gabriel Stokes* (1819–1903), which transforms a surface integral into a contour integral [445]:

$$\int \int_S (\nabla \times \mathbf{A}) \cdot \mathbf{n} \, dS = \int_C \mathbf{A} \cdot d\mathbf{s}, \quad (\text{A.3.5})$$

where S is an open, two sided curve surface, C is the closed contour bounding S , and $d\mathbf{s}$ denotes line integral.

The most important work related to the boundary integral equation solving potential problems came from George Green, whose groundbreaking work remained obscure during his lifetime. Green in 1828 [183] presented the three Green's identities. The first identity is

$$\int \int \int_{\Omega} (\phi \nabla^2 \psi + \nabla \phi \cdot \nabla \psi) \, dV = \int \int_{\Gamma} \phi \frac{\partial \psi}{\partial n} \, dS. \quad (\text{A.3.6})$$

The above equation easily leads to the second identity

$$\int \int \int_{\Omega} (\phi \nabla^2 \psi - \psi \nabla^2 \phi) \, dV = \int \int_{\Gamma} \left(\phi \frac{\partial \psi}{\partial n} - \psi \frac{\partial \phi}{\partial n} \right) \, dS. \quad (\text{A.3.7})$$

Using the fundamental solution of Laplace equation $1/r$ in (A.3.7), the third identity is obtained:

$$\phi = \frac{1}{4\pi} \int \int_{\Gamma} \left[\frac{1}{r} \frac{\partial \phi}{\partial n} - \phi \frac{\partial (1/r)}{\partial n} \right] \, dS, \quad (\text{A.3.8})$$

which is exactly the formulation of the present-day boundary element method.

A.3.1 Gauss

Carl Friedrich Gauss (1777–1855) was born an infant prodigy into a poor and unlettered family. According to a well-authenticated story, he corrected an error in his father's payroll calculations as a child of three. However, his early career was not very successful and had to continue to rely on the support from his benefactor Duke Ferdinand of Braunschweig. At the age of 22, he published as his doctoral thesis the most celebrated work, the *Fundamental Theorem of Algebra*. In 1807 Gauss was finally able to secure a position as the director of the newly founded observatory at the Göttingen University, a job he held for the rest of his lifetime.

Gauss devoted more of his time in theoretical astronomy than in mathematics. This is considered a great loss for mathematics—just imagine how much more mathematics can be accomplished. He devised a procedure for calculating the orbits planetoids that included the use of least square that he developed. Using his superior method, Gauss redid in an hour's time the calculation on which Euler had spent three days, and which sometimes was said to have led to Euler's loss of sight. Gauss remarked unkindly, “*I should also have gone blind if I had calculated in that fashion for three days.*”

Gauss not only adorned every branches of pure mathematics and was called the Prince of Mathematicians, he also pursued work in several related scientific fields, notably physics, mechanics, and astronomy. Together with *Wilhelm Eduard Weber* (1804–1891), he explored electromagnetism. They were the first to have successfully transmitted telegraph [70, 71].

A.3.2 Green

George Green (1793–1841) was virtually unknown as a mathematician during his lifetime. His most important piece of work was discovered posthumously. As the son of a semi-literate, but well-to-do Nottingham baker and miller, Green was sent to a private academy at the age of eight, and left school at nine. This was the only formal education that he received until adulthood. For the next twenty years after leaving primary school, no one knew how, and from whom Green could have acquainted himself to the advanced mathematics of his day in a backwater place like Nottingham. Even the whole country of England in those days was scientifically depressed as compared to the continental Europe. Hence it was a mystery how Green could have produced as his first publication such a masterpiece.

The next time there existed a record about Green was in 1823. At the age of thirty, he joined the Nottingham Subscription Library as a subscriber. In the library he had access to books and journals. Also he had the opportunity to meet with people from the higher society. The next five years was not easy for Green; he had to work full time in the mill, had two daughters born (he had seven children with Jane Smith, but never married her), and his mother died in 1825. Despite these difficulties in life and his flimsy mathematical background, in 1828 he self-published one of the most important mathematical works of all times—*An Essay on the Application of Mathematical Analysis to the Theories of Electricity and Magnetism* [183]. The essay had 51 subscribers, each paid 7 shillings 6 pence, a sum equal to a poor man's weekly wage, for a work which they could hardly understand a word. One subscriber, Sir Edward Bromhead, however, was impressed by Green's prowess in mathematics. He encouraged and recommended Green to attend Cambridge University.

Several years later, Green finally enrolled at Cambridge University at the age of 40. From 1833 to 1836, Green wrote three more papers, two on electricity published by the Cambridge Philosophical Society, and one on hydrodynamics published by the Royal Society of Edinburgh. After graduating in 1837, he stayed at Cambridge for a few years to work on his own mathematics and to wait for an appointment. In 1838 to 1839 he had two papers in hydrodynamics, two papers on reflection and refraction of light, and two papers on sound [184]. In 1839, he was elected to a Parse Fellowship in Cambridge, a junior position. Due to poor health, he had to return to Nottingham in 1840. He died in 1841 at the age of 47. At his death, his work was virtually unknown.

A few weeks before Green's death, *William Thomson (Lord Kelvin)* (1824–1907) was admitted to Cambridge. While studying the subject of electricity as a part of preparation

for his Senior Wrangler exam, he first noticed the existence of Green's paper in a footnote of a paper by Robert Murphy. He started to look for a copy, but no one knew about it. After his graduation in 1845, and before his departure to France to enrich his education, he mentioned it to his teacher *William Hopkins* (1793–1866). It happened that Hopkins had three copies. Thomson was immediately excited about what he had read in the paper. He brought the article to Paris and showed it *Jacques Charles François Sturm* (1803–1855) and *Joseph Liouville* (1809–1882). Later Thomson republished Green's essay, rescuing it from sinking into permanent obscurity [73].

Green's 1828 essay has profoundly influenced Thomson and *James Clerk Maxwell* (1831–1879) in their study of electrodynamics and magnetism. The methodology has also been applied to many classical fields of physics such as acoustics, elasticity, and hydrodynamics. During the bicentennial celebration of Green's birth in 1993, physicists *Julian Seymour Schwinger* (1918–1994) and *Freeman J. Dyson* (1923–) delivered speeches on the role of Green's functions in the development of 20th century quantum electrodynamics [73].

A.3.3 Ostrogradski

Mikhail Vasilevich Ostrogradski (1801–1862) was born in Pashennaya, Ukraine. He entered the University of Kharkov in 1816 and studied physics and mathematics. In 1822 he left Russia to study in Paris. Between 1822 and 1827 he attended lectures by Laplace, Fourier, *Adrien-Marie Legendre* (1752–1833), Poisson, and *Augustin-Louis Cauchy* (1789–1857). He made rapid progress in Paris and soon began to publish papers in the Paris Academy. His papers at this time showed the influence of the mathematicians in Paris and he wrote on physics and the integral calculus. These papers were later incorporated in a major work on hydrodynamics, which he published in Paris in 1832.

Ostrogradski went to St. Petersburg in 1828. He presented three important papers on the theory of heat, double integrals and potential theory to the Academy of Sciences. Largely on the strength of these papers he was elected an academician in the applied mathematics section. In 1840 he wrote on ballistics introducing the topic to Russia. He should also be considered as the founder of the Russian school of theoretical mechanics [364].

A.3.4 Stokes

George Gabriel Stokes (1819–1903) was born in Skreen, County Sligo, Ireland. In 1837 he entered Pembroke College of Cambridge University. He was coached by William Hopkins, who had among his students Thomson, Maxwell, and *Peter Guthrie Tait* (1831–1901), and had the reputation as the “senior wrangler maker.” In 1841 Stokes graduated as Senior Wrangler (the top First Class degree) and was also the first Smith's prizeman. Pembroke College immediately gave him a fellowship.

Inspired by the recent work of Green, Stokes started to undertake research in hydrodynamics and published papers on the motion of incompressible fluids in 1842. After completing the research Stokes discovered that *Jean Marie Constant Duhamel* (1797–1872) had already obtained similar results for the study of heat in solids. Stokes continued his investigations, looking into the internal friction in fluids in motion. After he had deduced the correct equations of motion, Stokes discovered that again he was not the first to obtain the equations, since *Claude Louis Marie Henri Navier* (1785–1836), Poisson and *Adhémar Jean Claude Barré de Saint-Venant* (1797–1886) had already considered the problem. Stokes decided that his results were sufficiently different and published the work in 1845. Today the fundamental equation of hydrodynamics is called the Navier-Stokes equations. The viscous flow in slow motion is called Stokes flow. The mathematical theorem that carries his name, Stokes theorem, first appeared in print in 1854 as an examination question for the Smith's Prize. It is not known whether any of the students answered the question at that time.

In 1849 Stokes was appointed the Lucasian Professor of Mathematics at Cambridge, the chair Newton once held. In 1851 Stokes was elected to the Royal Society, awarded the Rumford Medal in 1852, and he was appointed Secretary of the Society in 1854. He held the secretary position until 1885, and was President of the Society from 1885–1890. Stokes received the Copley Medal from the Royal Society in 1893, and served as the Master of Pembroke College in 1902–1903 [364].

A.4 Integral Equations

Inspired by the use of influence functions as a method for solving beam deflection problems subject to distributed load, Fredholm investigated integral equations [167]. He proved in 1903 [159] the existence and uniqueness of solution of the linear integral equation known as the Fredholm integral equation of the second kind:

$$\mu(x) - \lambda \int_a^b K(x, \xi) \mu(\xi) d\xi = f(x), \quad a \leq x \leq b, \quad (\text{A.4.1})$$

where λ is a constant, $f(x)$ and $K(x, \xi)$ are given continuous functions, and $\mu(x)$ is the solution sought for.

By the virtue of the Fredholm theorem, we can solve a Dirichlet problem by the following formula [444]

$$\phi(\mathbf{x}) = \mp 2\pi\mu(\mathbf{x}) + \iint_{\Gamma} K(\mathbf{x}, \xi) \mu(\xi) dS(\xi), \quad \mathbf{x} \in \Gamma. \quad (\text{A.4.2})$$

In the above the upper sign corresponds to the interior problem, the lower sign the exterior problem, μ is the distribution density, Γ is a closed Liapunov surface, $\phi(\mathbf{x})$ is the Dirichlet boundary condition, and the kernel K is given by

$$K(\mathbf{x}, \xi) = \frac{\partial}{\partial n(\xi)} \left[\frac{1}{r(\mathbf{x}, \xi)} \right]. \quad (\text{A.4.3})$$

The kernel is known as a dipole, or a “double-layer potential”. The Fredholm theorem guarantees the existence and uniqueness of μ . Once the distribution density μ is solved from (A.4.2) by some technique, the full solution of the boundary value problem is given by

$$\phi(\mathbf{x}) = \iint_{\Gamma} \frac{\partial [1/r(\mathbf{x}, \xi)]}{\partial n(\xi)} \mu(\xi) dS(\xi), \quad \mathbf{x} \in \Omega, \quad (\text{A.4.4})$$

which is a continuous distribution of the double-layer potential on the boundary.

For the Neumann problem, we can utilize the following boundary equation:

$$\frac{\partial \phi(\mathbf{x})}{\partial n(\mathbf{x})} = \pm 2\pi \sigma(\mathbf{x}) + \iint_{\Gamma} K(\xi, \mathbf{x}) \sigma(\xi) dS(\xi), \quad \mathbf{x} \in \Gamma. \quad (\text{A.4.5})$$

Here again the upper and lower sign respectively correspond to the interior and exterior problems respectively, σ is the distribution density, Γ is the bounding Liapunov surface, $\partial\phi/\partial n$ is the Neumann boundary condition, and the kernel is given by

$$K(\xi, \mathbf{x}) = \frac{\partial}{\partial n(\mathbf{x})} \left[\frac{1}{r(\mathbf{x}, \xi)} \right]. \quad (\text{A.4.6})$$

After solving for σ , the potential for the whole domain is given by

$$\phi(\mathbf{x}) = \iint_{\Gamma} \frac{1}{r(\mathbf{x}, \xi)} \sigma(\xi) dS(\xi), \quad \mathbf{x} \in \Omega. \quad (\text{A.4.7})$$

This is equivalent to a distribution of the source, or the “single-layer potential”. Fredholm suggested a discretization procedure to solve the above equations. Without a fast computer, however, the idea was impractical; hence further development of utilizing these equations was limited to analytical work.

For mixed boundary value problems, a pair of integral equations is needed. For the single-layer method applied to interior problems, the following pair

$$\phi(\mathbf{x}) = \iint_{\Gamma} \frac{1}{r(\mathbf{x}, \xi)} \sigma(\xi) dS(\xi), \quad \mathbf{x} \in \Gamma_{\phi}, \quad (\text{A.4.8})$$

$$\frac{\partial \phi(\mathbf{x})}{\partial n(\mathbf{x})} = \iint_{\text{CPV}} \frac{\partial [1/r(\mathbf{x}, \xi)]}{\partial n(\mathbf{x})} \sigma(\xi) dS(\xi), \quad \mathbf{x} \in \Gamma_q, \quad (\text{A.4.9})$$

can be selectively imposed at the Dirichlet part Γ_{ϕ} and the Neumann part Γ_q of the boundary. We note that (A.4.8) is a Fredholm integral equation of the first kind and is weakly singular. For solving Dirichlet problems, numerical modelers often prefer this formulation [234] to the theoretically more stable second kind integral (A.4.2). We also notice that (A.4.9) contains a strong singularity as $\xi \rightarrow \mathbf{x}$. It cannot be integrated in the ordinary sense and needs to be interpreted in the “Cauchy principal values” sense, as denoted by CPV under the integral sign. On a smooth part of the boundary, the result of the limit is just (A.4.5). This idea of interpreting the non-integrable singularity was introduced by Cauchy in 1814 [82].

A double-layer method can also be formulated to solve mixed boundary value problems, using the following pair of equations

$$\phi(\mathbf{x}) = \iint_{\text{CPV}} \frac{\partial [1/r(\mathbf{x}, \xi)]}{\partial n(\xi)} \mu(\xi) dS(\xi), \quad \mathbf{x} \in \Gamma, \quad (\text{A.4.10})$$

$$\frac{\partial \phi(\mathbf{x})}{\partial n(\mathbf{x})} = \iint_{\text{HFP}} \frac{\partial}{\partial n(\mathbf{x})} \left[\frac{\partial 1/r(\mathbf{x}, \xi)}{\partial n(\xi)} \right] \mu(\xi) dS(\xi), \quad \mathbf{x} \in \Gamma. \quad (\text{A.4.11})$$

The integral in (A.4.11) contains a “hypersingularity” and is marked with HFP under the integral sign, standing for “Hadamard finite part.” This concept was introduced by *Jacques Salomon Hadamard* (1865–1963) in 1908 [188].

In boundary element terminology, the single- and double-layer methods are referred to as the “indirect methods”, because the distribution density, not the potential itself, is solved. The numerical method based on Green’s third identity (A.3.8) is called the “direct method”.

Similar formula exists in the complex variable domain. Cauchy in 1825 [81] presented one of the most important theorems in complex variable—the Cauchy integral theorem, from which came the Cauchy integral formula expressed as:

$$f(z) = \frac{1}{2\pi i} \int_C \frac{f(\zeta)}{\zeta - z} d\zeta, \quad (\text{A.4.12})$$

where z and ζ are complex variables, f is an analytic function, and C is a smooth, closed contour in the complex plane. When z is located on the contour, $z \in C$, equation (A.4.12) can be exploited for the numerical solution of boundary value problems, a procedure known as the complex variable boundary element method.

A.4.1 Cauchy

Augustin-Louis Cauchy (1789–1857) was born in Paris during the difficult time of French Revolution. Cauchy’s father was active in the education of young Augustin-Louis. Laplace and Lagrange were frequent visitors at the Cauchy family home, and Lagrange particularly took interest in young Cauchy’s mathematical ability. In 1805 Cauchy took the entrance examination for the Ecole Polytechnique and was placed second. In 1807 he entered Ecole des Ponts et Chaussées to study engineering, specializing in highways and bridges, and finished school in two years. At the age of 20, he was appointed as a junior engineer to work on the construction of Port Napoléon in Cherbourg. He worked there for three years and performed excellently. In 1812, he became ill and decided to returned to Paris to seek a teaching position.

Although Cauchy continued to publish important pieces of mathematical work, his initial attempts in seeking academic appointment were unsuccessful. He lost in competition for academic position to Legendre, to *Louis Poinsot* (1777–1859), and to *André Marie Ampère* (1775–1836). But his mathematical output remained strong and in 1814

he published the memoir on definite integrals that later became the basis of his theory of complex functions. In 1815 Cauchy lost out to *Jacques Philippe Marie Binet* (1786–1856) for a mechanics chair at the Ecole Polytechnique, but then he was finally appointed assistant professor of analysis there. In 1816 he won the Grand Prix of the Académie des Sciences for a work on waves, and was later admitted to the Académie. In 1817, he was able to substitute for *Jean-Baptiste Biot* (1774–1862), chair of mathematical physics at the Collège de France, and later for Poisson. It was not until 1821 that he was able to obtain a full position replacing Ampère.

Cauchy was staunchly Catholic and was politically a royalist. By 1830 the political events in Paris forced him to leave Paris and he visited Switzerland. He soon lost all his positions in Paris. In 1831 Cauchy went to Turin and later accepted an offer to become a chair of theoretical physics. In 1833 Cauchy went from Turin to Prague, and returned to Paris in 1838. He regained his position at the Académie but not his teaching positions because he had refused to take an oath of allegiance to the new regime. Due to his political and religious views, he continued to have difficulty in winning important appointment.

Cauchy was probably next to Euler the most published author in mathematics, having produced five textbooks and over 800 articles. Cauchy and his contemporary Gauss were credited for introducing rigor into modern mathematics. It was said that when Cauchy read to the Académie des Sciences in Paris his first paper on the convergence of series, Laplace hurried home to verify that he had not made mistake of using any divergence series in his *Mécanique Céleste*. The formulation of elementary calculus in modern textbooks is essentially what Cauchy expounded in his three great treatises: *Cours d'Analyse de l'École Royale Polytechnique* (1821), *Résumé des Leçons sur le Calcul Infinitésimal* (1823), and *Leçons sur le Calcul Différentiel* (1829). Cauchy was also credited for setting the mathematical foundation for complex variable and elasticity. The basic equation of elasticity is called the Navier-Cauchy equation [31, 180].

A.4.2 Hadamard

Jacques Salomon Hadamard (1865–1963) began his schooling at the Lycée Charlemagne in Paris, where his father taught. In his first few years at school he was not good at mathematics; he wrote in 1936: “. . . in arithmetic, until the fifth grade, I was last or nearly last.” It was a good mathematics teacher turned him around. In 1884 Hadamard was placed first in the entrance examination for École Normale Supérieure, where he obtained his doctorate in 1892. His thesis on functions of a complex variable was one of the first to examine the general theory of analytic functions, in particular it contained the first general work on singularities. In the same year Hadamard received the Grand Prix des Sciences Mathématique for his paper “*Determination of the number of primes less than a given number.*” The topic proposed for the prize, concerning filling gaps in work of *Bernhard Riemann* (1826–1866) on zeta functions, had been put forward by *Charles Hermite* (1822–1901) with his friend *Thomas Jan Stieltjes* (1856–1894) in mind. However, Stieltjes discovered a gap in his proof and never submitted an entry. The next four years Hadamard was first a lecturer at Bordeaux, and then promoted to Professor of Astronomy

and Rational Mechanics in 1896. During this time he published his famous determinant inequality. Matrices satisfying this relation are today called Hadamard matrices, which are important in the theory of integral equations, coding theory and other areas.

In 1897 he resigned his chair in Bordeaux and moved to Paris to take up posts in Sorbonne and Collège de France. His research turned more toward mathematical physics from the time he took up the posts in Paris, yet he always argued strongly that he was a mathematician, not a physicist. His famous 1898 work on geodesics on surfaces of negative curvature laid the foundations of symbolic dynamics. Among the other topics he considered were elasticity, geometrical optics, hydrodynamics and boundary value problems. He introduced the concept of a well-posed initial value and boundary value problem. Hadamard continued to receive prizes for his research and he was further honoured in 1906 with the election as the President of the French Mathematical Society. In 1909 he was appointed to the chair of mechanics at the Collège de France. In the following year he published *Leçons sur le calcul des variations*, which helped lay the foundations of functional analysis (the word “functional” was introduced by him). Then in 1912 he was appointed as professor of analysis at the École Polytechnique. Near the end of 1912 Hadamard was elected to the Academy of Sciences to succeed Poincaré. After the start of World War II, when France fell to Germany in 1940, Hadamard, being a Jew, escaped to the United States where he was appointed to a visiting position at Columbia University. He left America in 1944 and spent a year in England before returning to Paris after the end of the war. He was lauded as one of the last universal mathematicians whose contributions broadly span the fields of mathematics. He lived to 98 year old [348, 364].

A.4.3 Fredholm

Erik Ivar Fredholm (1866–1927) was born in Stockholm, Sweden. After his baccalaureate, Fredholm enrolled in 1886 at the University of Uppsala, which was the only doctorate granting university in Sweden at that time. Through an arrangement he studied under *Magnus Gösta Mittag-Leffler* (1846–1927) at the newly founded University of Stockholm, and acquired his Ph.D. from the University of Uppsala in 1893. Fredholm’s first publication “*On a special class of functions*” came in 1890. It’s impressed Mittag-Leffler that he sent a copy of the paper to Poincaré. In 1898 he received the degree of Doctor of Science from the same university.

Fredholm is best remembered for his work on integral equations and spectral theory. Although *Vito Volterra* (1860–1940) before him had studied the integral equation theory, it was Fredholm who provided a more thorough treatment. This work was accomplished during the months of 1899 which Fredholm spent in Paris studying the Dirichlet problem with Poincaré, *Charles Emile Picard* (1856–1941), and Hadamard. In 1900 a preliminary report was published and the work was completed in 1903 [159]. Fredholm’s contributions quickly became well known. Hilbert immediately saw the importance and extended Fredholm’s work to include a complete eigenvalue theory for the Fredholm integral equation. This work led directly to the theory of Hilbert spaces.

After receiving his Doctor of Science degree, Fredholm was appointed as a lecturer in mathematical physics at the University of Stockholm. He spent his whole career at the University of Stockholm being appointed to a chair in mechanics and mathematical physics in 1906. In 1909-1910 he was Pro-Dean and then Dean in Stockholm University.

Fredholm wrote papers with great care and attention so he produced work of high quality that quickly gained him a high reputation throughout Europe. However his papers required so much effort that he wrote only a few. In fact, his *Complete Works* in mathematics comprises of only 160 pages. After 1910 he wrote little beyond revisiting his earlier work [364].

A.5 Extended Green's Formula

Green's formula (A.3.8), originally designed to solve electrostatic problems, was such a success that the idea was followed to solve many other physical problems [454]. For example, *Hermann Ludwig Ferdinand von Helmholtz* (1821–1894) in his study of acoustic problems presented the following equation in 1860 [197], known as the Helmholtz equation:

$$\nabla^2\phi + k^2\phi = 0, \quad (\text{A.5.1})$$

where k is a constant known as the wave number. He also derived the fundamental solution of (A.5.1) as

$$\phi = \frac{\cos kr}{r}. \quad (\text{A.5.2})$$

In the same paper he established the equivalent Green's formula:

$$\phi = \frac{1}{4\pi} \iint_{\Gamma} \left[\frac{\cos kr}{r} \frac{\partial\phi}{\partial n} - \phi \frac{\partial}{\partial n} \left(\frac{\cos kr}{r} \right) \right] dS, \quad (\text{A.5.3})$$

which can be compared to (A.3.8).

For elasticity, an important step toward deriving Green's formula was made by *Enrico Betti* (1823–1892) in 1872, when he introduced the reciprocity theorem, one of the most celebrated relation in mechanics [38]. The theory can be stated as follows: given two independent elastic states in a static equilibrium, $(\mathbf{u}, \mathbf{t}, \mathbf{F})$ and $(\mathbf{u}', \mathbf{t}', \mathbf{F}')$, where \mathbf{u} and \mathbf{u}' are displacement vectors, \mathbf{t} and \mathbf{t}' are tractions on a closed surface Γ , and \mathbf{F} and \mathbf{F}' are body forces in the enclosed region Ω , they satisfy the following reciprocal relation

$$\iint_{\Gamma} (\mathbf{t}' \cdot \mathbf{u} - \mathbf{t} \cdot \mathbf{u}') dS = \iiint_{\Omega} (\mathbf{F} \cdot \mathbf{u}' - \mathbf{F}' \cdot \mathbf{u}) dV. \quad (\text{A.5.4})$$

The above theorem, known as the Betti-Maxwell reciprocity theorem, was a generalization of the reciprocal principle derived earlier by Maxwell [347] using trusses. *John William Strutt (Lord Rayleigh)* (1842–1919) further generalized the above theorem to elastodynamics in the frequency domain, and also extended the forces and displacements concept to generalized forces and generalized displacements [396, 397].

In the same sequence of papers [38, 39], Betti presented the fundamental solution known as the center of dilatation [327]

$$\mathbf{u}^* = \frac{1-2\nu}{8\pi G(1-\nu)} \nabla \left(\frac{1}{r} \right), \quad (\text{A.5.5})$$

where G is the shear modulus, and ν is the Poisson ratio. The use of (A.5.5) in (A.5.4) produced the integral representation for dilatation

$$e = \nabla \cdot \mathbf{u} = \int \int_{\Gamma} (\mathbf{t} \cdot \mathbf{u}^* - \mathbf{t}^* \cdot \mathbf{u}) dS + \int \int \int_{\Omega} \mathbf{F} \cdot \mathbf{u}^* dV, \quad (\text{A.5.6})$$

where \mathbf{t}^* is the boundary traction vector of the fundamental solution (A.5.5).

The more useful formula that gives the integral equation representation of displacements, rather than dilatation, requires the fundamental solution of a point force in infinite space, which was provided by Kelvin in 1848 [257],

$$u_{ij}^* = \frac{1}{16\pi G(1-\nu)} \frac{1}{r} \left[\frac{x_i x_j}{r^2} + (3-4\nu)\delta_{ij} \right], \quad (\text{A.5.7})$$

where δ_{ij} is the Kronecker delta. In the above we have switched to the tensor notation, and the second index in u_{ij}^* indicates the direction of the applied point force. Utilizing (A.5.7), *Carlo Somigliana* (1860–1955) in 1885 [439] developed the following integral representation for displacements:

$$u_j = \int \int_{\Gamma} (t_i u_{ij}^* - t_{ij}^* u_i) dS + \int \int \int_{\Omega} F_i u_{ij}^* dV. \quad (\text{A.5.8})$$

Equation (A.5.8), called the Somigliana identity, is the elasticity counterpart of Green's formula (A.3.8).

Volterra in 1907 [476] presented the dislocation solution of elasticity, as well as other singular solutions such as the force double and the disclination, generally known as the nuclei of strain [327]. Further dislocation solutions were given by Somigliana in 1914 [440] and 1915 [441]. For a point dislocation in unbounded three-dimensional space, the resultant displacement field is

$$u_{ijk}^* = \frac{1}{4\pi(1-\nu)} \frac{1}{r^2} \left[(1-2\nu)(\delta_{kj}x_i - \delta_{ij}x_k - \delta_{ik}x_j) - \frac{2}{r^2}x_i x_j x_k \right]. \quad (\text{A.5.9})$$

This singular solution can be distributed over the boundary Γ to give the Volterra integral equation of the first kind [475]:

$$u_k = \int \int_{\Gamma} u_{kji}^* n_j \mu_i dS + \int \int \int_{\Omega} u_{ki}^* F_i dV, \quad (\text{A.5.10})$$

where μ_i is the component of the distribution density vector μ , also known as the displacement discontinuity. Equation (A.5.10) is equivalent to (A.4.10) of the potential problem,

and can be called the double layer method. The counterpart of the single layer method (A.4.8) is given by the Somigliana integral equation

$$u_j = \int \int_{\Gamma} u_{ji}^* \sigma_i dS + \int \int \int_{\Omega} u_{ji}^* F_i dV, \quad (\text{A.5.11})$$

where σ_i is the component of the distribution density vector σ , known as the stress discontinuity.

Similar to Cauchy integral (A.4.12) for potential problems, the complex variable potentials and integral equation representation for elasticity exist, which was formulated by *Gury Vasilievich Kolosov* (1867–1936) in 1909 [264]. These were further developed by *Nikolai Ivanovich Muskhelishvili* (1891–1976) [359, 360].

We can derive the above extended Green's formulae in a unified fashion. Consider the generalized Green's theorem [356]

$$\int_{\Omega} (\mathbf{v} \mathcal{L} \{\mathbf{u}\} - \mathbf{u} \mathcal{L}^* \{\mathbf{v}\}) d\mathbf{x} = \int_{\Gamma} (\mathbf{v} \mathcal{B} \{\mathbf{u}\} - \mathbf{u} \mathcal{B}^* \{\mathbf{v}\}) d\mathbf{x}. \quad (\text{A.5.12})$$

In the above \mathbf{u} and \mathbf{v} are two independent vector functions, \mathcal{L} is a linear partial differential operator, \mathcal{L}^* is its adjoint operator, \mathcal{B} is the generalized boundary normal derivative, and \mathcal{B}^* is its adjoint operator. The right hand side of (A.5.12) is the consequence of integration by parts of the left hand side operators. Equation (A.5.12) may be compared with the Green's second identify (A.3.7). If we assume that \mathbf{u} is the solution \mathbf{G} of the homogeneous equations

$$\mathcal{L} \{\mathbf{u}\} = 0 \quad \text{in } \Omega, \quad (\text{A.5.13})$$

subject to certain boundary conditions, and \mathbf{v} is replaced by the fundamental solution \mathbf{G} of the adjoint operator satisfying

$$\mathcal{L}^* \{\mathbf{G}\} = \delta, \quad (\text{A.5.14})$$

equation (A.5.12) becomes the boundary integral equation

$$\mathbf{u} = \int_{\Gamma} (\mathbf{u} \mathcal{B}^* \{\mathbf{G}\} - \mathbf{G} \mathcal{B} \{\mathbf{u}\}) d\mathbf{x}. \quad (\text{A.5.15})$$

As an example, we consider that the general second order linear partial differential equation is two dimensions

$$\mathcal{L} \{u\} = A \frac{\partial^2 u}{\partial x^2} + 2B \frac{\partial^2 u}{\partial x \partial y} + C \frac{\partial^2 u}{\partial y^2} + D \frac{\partial u}{\partial x} + E \frac{\partial u}{\partial y} + Fu, \quad (\text{A.5.16})$$

where the coefficients A , B , \dots , and F are functions of x and y . The generalized Green's second identity in the form of (A.5.12) exists with the definition of the operators [185]

$$\mathcal{L}^* \{v\} = \frac{\partial^2 Av}{\partial x^2} + 2 \frac{\partial^2 Bv}{\partial x \partial y} + \frac{\partial^2 Cv}{\partial y^2} - \frac{\partial Dv}{\partial x} - \frac{\partial Ev}{\partial y} + Fv, \quad (\text{A.5.17})$$

$$\mathcal{B} \{u\} = \left(A \frac{\partial u}{\partial x} + 2B \frac{\partial u}{\partial y} \right) n_x + \left(C \frac{\partial u}{\partial y} + Eu \right) n_y, \quad (\text{A.5.18})$$

$$\mathcal{B}^* \{v\} = \left(\frac{\partial Av}{\partial x} - Dv \right) n_x + \left(2 \frac{\partial Bv}{\partial x} + \frac{\partial Cv}{\partial y} \right) n_y. \quad (\text{A.5.19})$$

If we require u and v to satisfy (A.5.13) and (A.5.14) respectively, we then obtain the boundary integral equation formulation (A.5.15).

A.5.1 Helmholtz

Hermann Ludwig Ferdinand von Helmholtz (1821–1894) was born in Potsdam, Germany. He attended Potsdam Gymnasium where his father was a teacher. His interests at school were mainly in physics. However, due to the financial situation of his family, he accepted a government grant to study medicine at the Royal Friedrich-Wilhelm Institute of Medicine and Surgery in Berlin. His research career began in 1841 when he worked on the connection between nerve fibers and nerve cells in his dissertation. He rejected the dominant physiology theory at that time based on vital forces, and strongly argued for founding physiology on the principles of physics and chemistry. He graduated from the Medical Institute in 1843 and had to serve as a military doctor for ten years. He spent all his spare time doing research. In 1847 he published the important paper “*Über die Erhaltung der Kraft*” that established the law of conservation of energy. In the following year, Helmholtz was released from his obligation as an army doctor and became an assistant professor and director of the Physiological Institute at Königsberg. In 1855, he was appointed to the chair of anatomy and physiology in Bonn. Although at this time Helmholtz had gained a world reputation, complaints were made to the Ministry of Education from traditionalist that his lectures on anatomy were incompetent. Helmholtz reacted strongly to these criticisms and moved to Heidelberg in 1857 to set up a new Physiology Institute. Some of his most important work was carried out during this time. In 1858 Helmholtz published his important paper on the motion of a perfect fluid by decomposing it into translation, rotation and deformation. The study of vortex tube bore important consequences in the later study of turbulence in hydrodynamics, and knot theory in topology. Helmholtz also studied mathematical physics and acoustics, producing in 1863 “*On the Sensation of Tone as a Physiological Basis for the Theory of Music*” [198]. From around 1866 Helmholtz began to move away from physiology and towards physics. When the chair of physics in Berlin became vacant in 1871, he was able to negotiate a new Physics Institute under his control. In 1883, he was ennobled by William I. In 1888, he was appointed as the first President of the Physikalisch-Technische Reichsanstalt at Berlin, a post that he held for the rest of his life [72, 364, 492].

A.5.2 Betti

Enrico Betti (1823–1892) studied mathematics and physics at the University of Pisa. He graduated in 1846 and was appointed as an assistant at the university. He worked at the university at a time when political and military events in Italy were intensifying as the country came nearer to unification. In 1849 Betti returned to his home town of Pistoia where he became a teacher of mathematics at a secondary school. In 1854 he moved to Florence where again he taught in a secondary school. He was appointed as professor of higher algebra at the University of Pisa in 1857. In the following year Betti visited the mathematical centres of Europe, including Göttingen, Berlin, and Paris, making many important mathematical contacts. In particular, in Göttingen Betti met and became friendly with Riemann. Back in Pisa he moved in 1859 to the chair of analysis and higher geometry. In 1859 there was a war with Austria and by 1861 the Kingdom of Italy was formally created. Betti served in the government of the new country when he became a member of Parliament in 1862.

In 1863 Riemann left his post as professor in mathematics at Göttingen and move to Pisa, hoping that warmer weather would cure his tuberculosis. Influenced by his friend Riemann, Betti started to work on potential theory and elasticity. His famous theory of reciprocity in elasticity was published in 1872.

Over quite a number of years Betti mixed political service with service for his university. He served a term as Rector of the University of Pisa and in 1846 became the Director of its teacher's college, the Scuola Normale Superiore, a position he held until his death. Under his leadership the Scuola Normale Superiore in Pisa became the leading Italian centre for mathematical research and mathematical education. He served as an Undersecretary of State for education for a few months, and a Senator in the Italian Parliament in 1884 [364].

A.5.3 Kelvin

William Thomson (Lord Kelvin) (1824–1907) was well prepared by his father, James Thomson, professor of mathematics at the University of Glasgow, for his career. He attended Glasgow University at the age of ten, and later entered Cambridge University at seventeen. It was expected that he would win the senior wrangler position at graduation, but to his and his father's disappointment, he finished the second wrangler in 1845. The fierce competition of the "tripos", an honors examination instituted at Cambridge in 1824, attracted many best young minds to Cambridge in those days. Among Thomson's contemporaries were Stokes, a senior wrangler in 1841, and Maxwell, a second wrangler in 1854. In 1846 the chair of natural philosophy in Glasgow became vacant. Thomson's father ran a successful campaign to get his son elected to the chair at the age of 22.

Thomson was foremost among the small group of British scientists who helped to lay the foundations of modern physics. His contributions to science included a major role in the development of the second law of thermodynamics, the absolute temperature

scale (measured in “kelvins”), the dynamical theory of heat; the mathematical analysis of electricity and magnetism, including the basic ideas for the electromagnetic theory of light, the geophysical determination of the age of the Earth, and fundamental work in hydrodynamics. His theoretical work on submarine telegraphy and his inventions of mirror-galvanometer for use on submarine cables aided Britain in laying the transatlantic cable, thus gaining the lead in world communication. His participation in the telegraph cable project earned him the knighthood in 1866, and a large personal fortune [425, 457].

A.5.4 Rayleigh

John William Strutt (Lord Rayleigh) (1842–1919) was the eldest son of the second Baron Rayleigh. After studying in a private school without showing extraordinary signs of scientific capability, he entered Trinity College, Cambridge, in 1861. As an undergraduate, he was coached by *Edward John Routh* (1831–1907), who had the reputation of being an outstanding teacher in mathematics and mechanics. Rayleigh (a title he did not inherit until he was 30 years old) was greatly influenced by Routh, as well as by Stokes. He graduated in 1865 with top honors garnering not only the Senior Wrangler title, but also the first Smith's prizeman. Rayleigh was faced with a difficult decision: knowing that he would succeed to the title of the third Baron Rayleigh, taking up a scientific career was not really acceptable to the members of his family. By this time, however, Rayleigh was determined to devote his life to science so that his social obligations would not stand in his way.

In 1866, Rayleigh was elected to a fellowship of Trinity College. Around that time he read Helmholtz' book *On the Sensations of Tone* [198], and became interested in acoustics. Rayleigh was married in 1871, and had to give up his fellowship at Trinity. In 1872, Rayleigh had an attack of rheumatic fever and was advised to travel to Egypt for his health. He took his wife and several relatives sailed down the Nile during the last months of 1872, returning to England in the spring of 1873. It was during that trip that he started his work on the famous two volume treatise *The Theory of Sound* [397], eventually published in 1877. Rayleigh's father died in 1873. He became the third Baron Rayleigh and had to devote part of his time supervising the estate. In 1879, Maxwell died, and Rayleigh was elected to the vacated post of Cavendish Professor of experimental physics at Cambridge. At the end of 1884, Rayleigh resigned his Cambridge professorship and settled in his estate. There in his “book-room” and self-funded laboratory, he continued his intensive scientific work to the end of his life. Rayleigh made many important scientific contributions including the first correct light scattering theory that explained why the sky is blue, the theory of soliton, the surface wave known as Rayleigh wave, the hydrodynamic similarity theory, and the Rayleigh-Ritz method in elasticity. In 1904 Rayleigh won a Nobel Prize for his 1895 discovery of argon gas. He also served many public functions including being the President of the London Mathematical Society (1876–78), President of the Royal Society of London (1905–08), and Chancellor of Cambridge University (1908 until his death) [459, 398].

A.5.5 Volterra

Vito Volterra (1860–1940) was born in Ancona, Italy, a city on the Adriatic Sea. When Volterra was two-year old, his father died and he was raised by his uncle. Volterra was able to begin his studies at the Faculty of Natural Sciences of the University of Florence in 1878. In the following year he won a competition to become a student at the Scuola Normale Superiore di Pisa, and it was at the University of Pisa where he completed his studies in mathematics and physics, graduating in 1882 with a doctorate in physics. Among his teachers were Betti, who held the chair of rational mechanics. Betti was so impressed by his student that upon graduation he appointed Volterra his assistant. In 1883 Volterra was given a professorship in rational mechanics at Pisa; following Betti's death in 1892 he was also in charge of mathematical physics. From 1893 until 1900 he held the chair of rational mechanics at the University of Torino. In 1900 he moved to the University of Rome, succeeding *Eugenio Beltrami* (1835–1900) as professor of mathematical physics. Volterra's work encompassed integral equations, the theory of functions of a line (called functionals since *Jacques Salomon Hadamard* (1865–1963)), the theory of elasticity, integro-differential equations, the description of hereditary phenomena in physics, and mathematical biology. Beginning in 1912, Volterra regularly lectured at the Sorbonne in Paris which became like a second home to him.

In 1922, when the Fascists seized power in Italy, Volterra—a Senator of the Kingdom of Italy since 1905—was one of the few who spoke out against fascism, especially the proposed changes to the educational system. At that time (1923–1926) he was President of the Accademia Nazionale dei Lincei, and he was regarded as the most eminent man of science in Italy. As a direct result of his unwavering stand, especially his signing of the “Intellectual's Declaration” against fascism in 1926 and, five years later, his refusal to swear the oath of allegiance to the fascist government imposed on all university professors, Volterra was dismissed from his chair at the University of Rome in 1931. In the following year he was deprived of all his memberships in the scientific academies and cultural institutes in Italy. From that time on he lectured and lived mostly abroad, in Paris, in Spain, and in other European countries. Volterra died in isolation on October 11, 1940 [67].

A.5.6 Somigliana

Carlo Somigliana (1860–1955) began his university study at Pavia, where he was a student of Beltrami. Later he transferred to Pisa and had Betti among his teachers, and Volterra among his contemporaries. He graduated from Scuola Normale Superiore di Pisa in 1881. In 1887 Somigliana began teaching as an assistant at the University of Pavia. In 1892, as the result of a competition, he was appointed as university professor of mathematical physics. Somigliana was called to Turin in 1903 to become the chair of mathematical physics. He held the post until his retirement in 1935, and moved to live in Milan. During the World War II, his apartment was destroyed. After the war he retreated to his family villa in Casanova Lanza and stayed active in research until near

his death in 1955.

Somigliana was a classical physicist-mathematician faithful to the school of Betti and Beltrami. He made important contributions in elasticity. The Somigliana integral equation for elasticity is the equivalent of Green's formula for harmonic functions. He is also known for the Somigliana dislocations. His other contributions included seismic wave propagation and gravimetry [463].

A.5.7 Kolosov

Gury Vasilievich Kolosov (1867–1936) was educated at the University of St. Petersburg. After working at Yurev University from 1902 to 1913, he returned to St. Petersburg where he spent the rest of his career. He studied the mechanics of solid bodies and the theory of elasticity, particularly the complex variable theory. In 1907 Kolosov derived the solution for stresses around an elliptical hole. It showed that the concentration of stress became far greater as the radius of curvature at an end of the hole becomes small compared with the overall length of the hole. Engineers have to understand Kolosov's results so that stresses can be kept to safe levels [364].

A.6 Pre-Electronic Computer Era

Numerical efforts solving boundary value problems predate the emergence of digital computers. One important effort is the Ritz method, proposed by *Walter Ritz* (1878–1909) in 1908 [401]. When applied to subdomains, the Ritz method is considered as the forerunner of the Finite Element Method [509]. Ritz' idea involves the use of variational method and trial functions to find approximate solutions of boundary value problems. For example, for the following functional

$$\Pi = \int \int \int_{\Omega} \frac{1}{2} (\nabla \phi)^2 dV - \int \int_{\Gamma} \frac{\partial \phi}{\partial n} (\phi - f) dS, \quad (\text{A.6.1})$$

finding its stationary value by variational method leads to

$$\delta \Pi = - \int \int \int_{\Omega} \delta \phi \nabla^2 \phi dV - \int \int_{\Gamma} \delta \left(\frac{\partial \phi}{\partial n} \right) (\phi - f) dS = 0. \quad (\text{A.6.2})$$

Since the variation is arbitrary, the above equation is equivalent to the statement of Dirichlet problem

$$\nabla^2 \phi = 0 \quad \text{in } \Omega,$$

and

$$\phi = f(\mathbf{x}) \quad \text{on } \Gamma.$$

Ritz proposed to approximate ϕ using a set of trial functions ψ_i by the finite series

$$\phi \approx \sum_{i=1}^n \alpha_i \psi_i, \quad (\text{A.6.3})$$

where a_i are constant coefficients to be determined. Equation (A.6.3) is substituted into the functional (A.6.1) and the variation is taken with respect to the n unknown coefficients a_i . The domain and boundary integration were performed, often in the subdomains, to produce numerical values. This leads to a linear system that can be solved for α_i . The approximate solution is then evaluated as (A.6.3). The above procedure involves the integration over the solution domain; hence it is considered as a domain method, not a boundary method.

Based on the same idea, *Erich Trefftz* (1888–1937) in his 1926 article “*A counterpart to Ritz method*” [461] devised the boundary method, known as the Trefftz method. Utilizing Green’s first identity (A.3.6), we can write (A.6.1) in an alternate form

$$\Pi = - \int \int \int_{\Omega} \frac{1}{2} \phi \nabla^2 \phi \, dV - \int \int_{\Gamma} \frac{\partial \phi}{\partial n} \left(\frac{1}{2} \phi - f \right) \, dS. \quad (\text{A.6.4})$$

In making the approximation (A.6.3), Trefftz proposed to use trial functions ψ_i that satisfy the governing differential equation

$$\nabla^2 \psi_i = 0, \quad (\text{A.6.5})$$

but not necessarily the boundary condition. For Laplace equation, these could be the harmonic polynomials

$$\psi_i = \{1, x, y, z, x^2 - y^2, y^2 - z^2, z^2 - x^2, xy, yz, \dots\}. \quad (\text{A.6.6})$$

With the substitution of (A.6.3) into (A.6.4), the domain integral vanishes, and the functional is approximated as

$$\Pi \approx - \int \int_{\Gamma} \sum_{i=1}^n \alpha_i \frac{\partial \psi_i}{\partial n} \left(\frac{1}{2} \sum_{i=1}^n \alpha_i \psi_i - f \right) \, dS. \quad (\text{A.6.7})$$

Taking variation of (A.6.7) with respect to the undetermined coefficients α_j , and setting each part associated with the variations $\delta \alpha_j$ to zero, we obtain the linear system

$$\sum_{i=1}^n a_{ij} \alpha_i = b_j; \quad j = 1, \dots, n, \quad (\text{A.6.8})$$

where

$$\begin{aligned} a_{ij} &= \frac{1}{2} \int \int_{\Gamma} \frac{\partial \psi_i \psi_j}{\partial n} \, dS, \\ b_j &= \int \int_{\Gamma} f \frac{\partial \psi_j}{\partial n} \, dS. \end{aligned} \quad (\text{A.6.9})$$

Equation (A.6.8) can be solved for α_i .

The above procedure requires the integration of functions over the solution boundary. Even though this is only a boundary integral, it can still be a tedious job. In the present

day Trefftz method, a simpler procedure is often taken. Rather than minimizing the functional over the whole boundary, the boundary condition is enforced point-wise on a finite set of boundary points \mathbf{x}_j as:

$$\phi(\mathbf{x}_j) \approx \sum_{i=1}^n \alpha_i \psi_i(\mathbf{x}_j) = f(\mathbf{x}_j), \quad j = 1, \dots, n \quad \text{and} \quad \mathbf{x}_j \in \Gamma. \quad (\text{A.6.10})$$

This is a point collocation method and there is no integration involved. Equation (A.6.10) can also be derived in a weighted residual formulation using Dirac delta function as the test function.

Following the same spirit of the Trefftz method, one can use the fundamental solution as the trial function. Since fundamental solution satisfies the governing equation as

$$\mathcal{L}\{G(\mathbf{x}, \mathbf{x}')\} = \delta(\mathbf{x}, \mathbf{x}'), \quad (\text{A.6.11})$$

where \mathcal{L} is a linear partial differential operator, G is the fundamental solution of that operator, and δ is the Dirac delta function. It is obvious that the approximate solution

$$\phi(\mathbf{x}) \approx \sum_{i=1}^n \alpha_i G(\mathbf{x}, \mathbf{x}_i), \quad \mathbf{x} \in \Omega, \quad \mathbf{x}_i \notin \Omega, \quad (\text{A.6.12})$$

satisfies the governing equation as long as the source points \mathbf{x}_i are placed outside of the domain. To ensure that the boundary condition is satisfied, again the point collocation is applied:

$$\phi(\mathbf{x}_j) \approx \sum_{i=1}^n \alpha_i G(\mathbf{x}_j, \mathbf{x}_i) = f(\mathbf{x}_j), \quad j = 1, \dots, n \quad \text{and} \quad \mathbf{x}_j \in \Gamma. \quad (\text{A.6.13})$$

This is called the method of fundamental solutions.

For exterior domain problems, this technique is well known in fluid mechanics. *William John Macquorn Rankine* (1820–1872) in 1864 [394] showed that the superposition of sources and sinks along an axis, together with a rectilinear flow, creates the flow field of a uniform flow around closed bodies, known as the Rankine bodies. Various combinations were experimented to create different bodies. However, there was no control over the shape of the body. *Theodore von Kármán* (1881–1963) in 1927 [477] proposed a collocation procedure to create the desirable body shapes. He distributed $n + 1$ sources and sinks of unknown strengths along the axis inside an axisymmetric body, together with a rectilinear flow

$$\phi(\mathbf{x}) \approx Ux + \sum_{i=1}^{n+1} \frac{\sigma_i}{4\pi r(\mathbf{x}, \mathbf{x}_i)}, \quad (\text{A.6.14})$$

where U is the uniform flow velocity, \mathbf{x}_i are located on x -axis, and σ_i are source/sink strengths. The strengths can be determined by forcing the normal flux to vanish at n

specified points on the meridional trace of the axisymmetric body. An auxiliary condition

$$\sum_{i=1}^{n+1} \sigma_i = 0, \quad (\text{A.6.15})$$

is needed to ensure that the closure of the body. In fact, other singularities, such as doublets (dipoles) and vortices, can be distributed inside a body to create flow around arbitrarily shaped two- and three-dimensional bodies [464].

In 1930 von Kármán [478] further proposed the distribution of singularity along a line inside a two-dimensional streamlined body to generate the potential

$$\phi(\mathbf{x}) = - \int_L \ln r(\mathbf{x}, \xi) \sigma(\xi) ds(\xi), \quad \mathbf{x} \in \Omega_e, \quad (\text{A.6.16})$$

where ϕ is the perturbed potential from the uniform flow field, σ is the distribution density, L is a line inside the body, and Ω_e is the external domain (Figure A.1a). For vanishing potential at infinity, the following auxiliary condition is needed

$$\int_L \sigma(\xi) ds(\xi) = 0. \quad (\text{A.6.17})$$

To find the distribution density, Neumann boundary condition is enforced on a set of discrete points \mathbf{x}_i , $i = 1, \dots, n$, on the surface of the body

$$\frac{\partial \phi(\mathbf{x}_i)}{\partial n(\mathbf{x}_i)} = - \int_L \frac{\partial \ln r(\mathbf{x}_i, \xi)}{\partial n(\mathbf{x}_i)} \sigma(\xi) ds(\xi), \quad \mathbf{x}_i \in C, \quad (\text{A.6.18})$$

where C is the boundary contour (Figure A.1a).

Prager [388] in 1928 proposed a different idea: vortices are distributed on the surface of a streamlined body (Figure A.1b) to generate the desirable potential. When this is written in terms of stream function ψ , the integral equation becomes

$$\psi(\mathbf{x}) = - \int_C \ln r(\mathbf{x}, \xi) \sigma(\xi) ds(\xi), \quad \mathbf{x} \in \Omega_e. \quad (\text{A.6.19})$$

In this case, Dirichlet condition is enforced on the surface of the body.

Lotz in 1932 [326] proposed the discretization of Fredholm integral equation of the second kind on the surface of an axisymmetric body for solving external flow problems. The method was further developed by Vandrey in 1951 and 1960 [466, 467]. Other early efforts in solving potential flows around obstacles, prior to the invention of electronic computers, can be found in a review [209].

In 1937 Muskhelishvili derived the complex variable equations for elasticity and suggested to solve them numerically [358]. The actual numerical implementation was accomplished by Gorgidze and Rukhadze [177] in a procedure that resembled the present-day

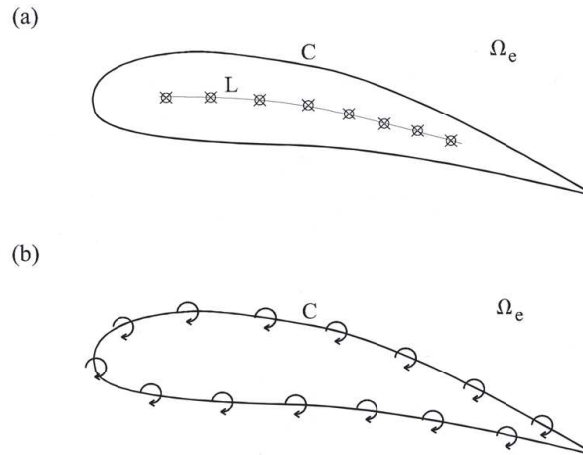


Figure A.1: Two methods of distributing singularities: (a) sources, sinks and doublets on a line L inside the airfoil; (b) vortices on the surface C of the airfoil.

BEM: it divided the contour into elements, approximated the function within the elements, and formed a linear algebraic system consisting the unknown coefficients.

The above review demonstrates that finding approximate solutions of boundary value problems using boundary or boundary-like discretization is not a new idea. These early attempts of Trefftz, von Kármán, and Muskhelishvili existed before the electronic computers. However, despite these heroic attempts, without the aid of modern computing tools these calculations had to be performed by human or mechanical computers. The drudgery of computation was a hindrance for their further development; hence these methods remained dormant for a while and had to wait for a later date to flourish.

A.6.1 Ritz

Walter Ritz (1878–1909) was born in Sion in the southern Swiss canton of Valais. As a specially gifted student, the young Ritz excelled academically at the Lycée communal of Sion. In 1897 he entered the Polytechnic school of Zurich where he began studies in engineering. He soon found that he couldn't live with the approximations and compromises involved with engineering so he switched to the more mathematically exacting studies in physics, where *Albert Einstein* (1879–1955) was one of his classmates. In 1901 he transferred to Göttingen, where his forming aspirations were strongly influenced by *Woldemar*

Voigt (1850–1919) and Hilbert. Ritz’s dissertation on spectroscopic theory led to what is known as the Ritz combination principle. In the next few years he continued his work on radiation, magnetism, electrodynamics, and variational method. But in 1904 his health failed and he returned to Zurich. During the following three years, Ritz unsuccessfully tried to regain his health and was outside the scientific centers. In 1908 he relocated to Göttingen where he qualified as a Privat Dozent. There he produced his opus magnum *Recherches critiques sur l’Électrodynamique Générale*. In 1908–1909 Ritz and Einstein held a war in *Physikalische Zeitschrift* over the proper way to mathematically represent black-body radiation and over the theoretical origin of the second law of thermodynamics; it was judged in his favor. Six weeks after the publication of this series, Ritz died at age 31, leaving behind a short but brilliant career in physics [161].

A.6.2 von Kármán

Theodore von Kármán (1881–1963) was born in Budapest, Hungary. He was trained as a mechanical engineer in Budapest and graduated in 1902. He did further graduate studies at Göttingen and earned his Ph.D. in 1908 under *Ludwig Prandtl* (1875–1953). In 1911 he made an analysis of the alternating double row of vortices behind a bluff in a fluid stream, known as Kármán’s vortex street. In 1912, at the age of 31, he became Professor and Director of Aeronautical Institute at Aachen, where he built the world’s first wind tunnel. In World War I, he was called into military service for the Austro-Hungarian Empire and became head of research in the air force, where he led the effort to build the first helicopter. After the war, he was instrumental in calling an international congress on aerodynamics and hydrodynamics at Innsbruck, Austria, in 1922. This meeting became the forerunner of the International Union of Theoretical and Applied Mechanics (IUTAM) with von Kármán as its honorary president. He first visited the United States in 1926. In 1930 he headed the Guggenheim Aeronautical Lab at the Caltech. In 1944, he cofounded of the present NASA Jet Propulsion Laboratory and undertook America’s first governmental long-range missile and space-exploration research program. His personal scientific work included contributions to fluid mechanics, turbulence theory, supersonic flight, mathematics in engineering, and aircraft structures. He is widely recognized as the father of modern aerospace science.

A.6.3 Trefftz

Erich Trefftz (1888–1937) was born on February 21, 1888 in Leipzig, Germany. In 1890, the family moved to Aachen. In 1906 he began his studies in mechanical engineering at the Technical University of Aachen, but soon changed to mathematics. In 1908 Trefftz transferred to Göttingen, at that time the Mecca of mathematics and physics. Here after Gauss, Dirichlet, and Riemann, now Hilbert, *Felix Christian Klein* (1849–1925), *Carle David Tolmé Runge* (1856–1927) and Prandtl created a continuous progress of first class mathematical progress. Trefftz’ most important teachers were Runge, Hilbert and also Prandtl, the genius mechanician in modern fluid- and aero-dynamics. Trefftz spent one

year at the Columbia University, New York, and then left Göttingen for Strassburg to study under the guidance of the famous Austrian applied mathematician *Richard von Mises* (1883–1953), who founded the GAMM (Gesellschaft für Angewandte Mathematik und Mechanik) in 1922 together with Prandtl. Mises was also the first editor of ZAMM (Zeitschrift für Angewandte Mathematik und Mechanik).

Trefftz' academic career began with his doctoral thesis in Strassburg in 1913, where he solved a mathematical problem of hydrodynamics. He was a soldier in the first world war, but already in 1919 he got his habilitation and became a full professor of mathematics in Aachen. In the year 1922 he got a call as a full professor with a chair in the faculty of mechanical engineering at the Technical University of Dresden. There he became responsible for teaching and research in strength of materials, theory of elasticity, hydrodynamics, aerodynamics and aeronautics. In 1927 he moved from the engineering to the mathematical and natural science faculty, being appointed there as a chair holder in Technical (Applied) Mechanics.

Trefftz had a lifelong friendship with von Mises who, being a Jew, had to leave Germany in 1933. Trefftz felt and showed outgoing solidarity and friendship to von Mises, and he clearly was in expressed distance to the Hitler regime until his early death in 1937. Feeling the responsibility for science, he took over the presidentship of GAMM, and became the editor of ZAMM in 1933 in full accordance with von Mises [442].

A.6.4 Muskhelishvili

Nikolai Ivanovich Muskhelishvili (1891–1976) was a student at the University of St. Petersburg. He was naturally influenced by the glorious tradition of the St. Petersburg mathematical school, which began with Euler and continued by the prominent mathematicians such as Ostrogradsky, *Pafnuty Lvovich Chebyshev* (1821–1894), and *Aleksandr Mikhailovich Lyapunov* (1857–1918). As a undergraduate student, Muskhelishvili was greatly impressed by the lectures of Kolosov on the complex variable theory of elasticity. Muskhelishvili took this topic as his graduation thesis and performed brilliantly that Kolosov decided to publish these results as a coauthor with his student in 1915. In 1922 Muskhelishvili became a professor at the Tbilisi State University, where he remained until his death. In 1935 he published the masterpiece *Some Basic Problems of the Mathematical Theory of Elasticity*, which won him the Stalin Prize of the first degree. He held many positions such as Chair, Director, President, at Tbilisi and the Georgian Branch of USSR Academy of Sciences, and received many honors [511, 510].

A.7 Electronic Computer Era

Although electronic computers were invented in the 1940s, they did not become widely available to common researchers until the early 1960s. It is not surprising that the development of finite element method started around that time [106]. A number of independent efforts of creating boundary methods also emerged in the early 1960s. Some of the more

significant ones are reviewed below.

Friedman and Shaw [160] in 1962 solved the scalar wave equation

$$\nabla^2 \phi - \frac{1}{c^2} \frac{\partial^2 \phi}{\partial t^2} = 0, \quad (\text{A.7.1})$$

where ϕ is the velocity potential and c is the wave speed, for the scattered wave field resulting from a shock wave impinging on a cylindrical obstacle. The use of the fundamental solution

$$G = -\frac{1}{r} \delta \left[\frac{r}{c} - (t - t_0) \right], \quad (\text{A.7.2})$$

where δ is the Dirac delta function, in Green's second identity (A.3.7) produces the boundary integral equation

$$\phi_s(\mathbf{x}, t) = \frac{1}{4\pi} \int_0^{t^+} \iint_{\Gamma} \left[G \frac{\partial \phi_s}{\partial n} - \phi_s \frac{\partial G}{\partial n} \right] dS dt_0, \quad (\text{A.7.3})$$

where ϕ_s is the scattered wave field. Equation (A.7.3) was further differentiated with respect to time to create the equation for acoustic pressure. For a two-dimensional problem, the equation was discretized in space (boundary contour) and in time that resulted into a double summation. Variables were assumed to be constant over space and time subintervals, so the integration could be performed exactly. Finite difference explicit time-stepping scheme was used and the resultant algebraic system required only successive, not simultaneous solution. The computation was performed by hand. The scattering due to a box-shaped rigid obstacle was solved. The work was extended in 1967 by Shaw [426] to handle different boundary conditions on the obstacle surface, and by Mitzner [355] using the retarded potential integral representation.

Banaugh and Goldsmith [22] in 1963 tackled the two-dimensional wave equation in the frequency domain, governed by the Helmholtz equation (A.5.1). The 2-D boundary integral equation counterpart to the 3-D version (A.5.3) is

$$\phi = \frac{i}{4} \int_C \left[H_0^{(1)}(kr) \frac{\partial \phi}{\partial n} - \phi \frac{\partial H_0^{(1)}(kr)}{\partial n} \right] ds, \quad (\text{A.7.4})$$

where $H_0^{(1)}$ is the Hankel function of the first kind of order zero, k is the wave number, and $i = \sqrt{-1}$. Equation (A.7.4) is solved in the complex variable domain. Similar to Friedman and Shaw [160], the integration over a subinterval was made easy by assuming constant variation of the potential on the subinterval. The problem of a steady state wave scattered from the surface of a circular cylinder was solved as a demonstration. An IBM 7090 mainframe computer was used for the numerical solution. It is of interest to observe that the discretization was restricted to 36 points, corresponding to 72 unknowns (real and imaginary parts), due to the memory restriction of the computer. A larger linear system would have required the read/write operation on the tape storage and special linear system solution algorithm.

In the same year (1963) Chen and Schweikert [93] solved the three-dimensional sound radiation problem in the frequency domain using the Fredholm integral equation of the second kind

$$\frac{\partial \phi(\mathbf{x})}{\partial n(\mathbf{x})} = -2\pi\sigma(\mathbf{x}) + \iint_{\Gamma} \sigma(\xi) \frac{\partial}{\partial n(\mathbf{x})} \left(\frac{e^{ikr}}{r} \right) dS(\xi), \quad \mathbf{x} \in \Gamma. \quad (\text{A.7.5})$$

Problems of vibrating spherical and cylindrical shells in infinite fluid domain were solved. The surface of the body was divided into triangular elements. An IBM 704 mainframe was used, which allowed up to 1,000 degrees of freedom to be modeled.

Maurice Aaron Jaswon (1922–) and Ponter [232] in 1963 employed Green's third identity (A.3.8), but in two-dimensional form,

$$\phi(\mathbf{x}) = \frac{1}{\pi} \int_C \left[\phi(\xi) \frac{\partial \ln r(\mathbf{x}, \xi)}{\partial n(\xi)} - \ln r(\mathbf{x}, \xi) \frac{\partial \phi(\xi)}{\partial n(\xi)} \right] ds(\xi), \quad \mathbf{x} \in C, \quad (\text{A.7.6})$$

for the numerical solution of prismatic bars subjected to torsion. The boundary conditions were Dirichlet type. Ponter [386] in 1966 extended it to multiple domain problems.

Jaswon [234] and Symm [451] in 1963 used the single-layer method, namely the Fredholm equation of the first kind as shown in (A.4.8), but in two dimensions,

$$\phi(\mathbf{x}) = - \int_C \ln r(\mathbf{x}, \xi) \sigma(\xi) ds(\xi), \quad \mathbf{x} \in C, \quad (\text{A.7.7})$$

for the solution of Dirichlet problems. The above equation was typically avoided by mathematicians as it was considered unsolvable. However, apparently good solutions were obtained. For Neumann problems, the Fredholm integral equation of the second kind

$$\frac{\partial \phi(\mathbf{x})}{\partial n(\mathbf{x})} = \pi\sigma(\mathbf{x}) - \int_C \frac{\partial \ln r(\mathbf{x}, \xi)}{\partial n(\mathbf{x})} \sigma(\xi) ds(\xi), \quad \mathbf{x} \in C, \quad (\text{A.7.8})$$

was used. In the same paper [451], a mixed boundary value problem was solved using Green's formula (A.7.6), rather than the Fredholm integral equations.

Hess and Smith [210] in 1964 utilized the single-layer method (A.4.5) to solve problems of external potential flow about arbitrary three-dimensional bodies:

$$\frac{\partial \phi(\mathbf{x})}{\partial n(\mathbf{x})} = -2\pi\sigma(\mathbf{x}) + \iint_{\Gamma} \frac{\partial (1/r(\mathbf{x}, \xi))}{\partial n(\mathbf{x})} \sigma(\xi) dS(\xi), \quad \mathbf{x} \in \Gamma. \quad (\text{A.7.9})$$

The formulation is the same as that of Lotz [326] and Vandrey [466, 467]. The surface of the body is discretized into quadrilateral elements and the source density is assumed to be constant on the element. This technique, called the surface source method, has developed into a powerful numerical tool for the aircraft industry [209].

Massonet [342] in 1965 discussed a number of ideas of using boundary integral equations solving elasticity problems. However, only in two cases that numerical solutions were

carried out. In the first case, Fredholm integral equation of the second kind was used to solve torsion problems:

$$\phi(\mathbf{x}) = -\pi\mu(\mathbf{x}) - \int_C \frac{\partial \ln r(\mathbf{x}, \xi)}{\partial n(\xi)} \mu(\xi) ds(\xi), \quad \mathbf{x} \in C. \quad (\text{A.7.10})$$

In the second case, plane elasticity problems were solved using the distribution of the radial stress field resulting from a half-plane point force on the boundary. The following Fredholm equation of the second kind was used:

$$\mathbf{t}(\mathbf{x}) = \mu(\mathbf{x}) - \frac{2}{\pi} \int_C \mu(\xi) \frac{\cos \varphi \cos \alpha}{r} \mathbf{e}_r ds(\xi), \quad \mathbf{x} \in C, \quad (\text{A.7.11})$$

where \mathbf{t} is the boundary traction vector, μ is the intensity of the fictitious stress and μ is its magnitude, \mathbf{e}_r is the unit vector in the r direction, φ is the angle between the two vectors μ and \mathbf{e}_r , and α is the angle between \mathbf{e}_r and the boundary normal. Solutions were found using the iterative procedure of successively approximating the function μ . Due to the half-plane kernel function used, this technique applies only to simply-connected domains.

During the first decade of the 20th century, the introduction of the Fredholm integral equation theorems puts the potential theory on a solid foundation. For elasticity problems, however, similar level rigorousness was not accomplished for another forty years. Started in the 1940s, a Georgian school of elasticians led by Muskhelishvili [511, 510] and followed by *Ilia Nestorovich Vekua* (1907–1977) [469], *Nikolai Petrovich Vekua* (1913–1993) [470], and *Viktor Dmitrievich Kupradze* (1903–1985) [269, 271], all associated with the Tbilisi State University, together with *Solomon Grigorevich Mikhlin* (1908–1991) [351] of St. Petersburg, made important progresses in the theory of vector potentials (elasticity) through the study of singular integral equations. The initial development, however, was limited to one-dimensional singular integral equations, which solve only two-dimensional problems. The development of multi-dimensional integral equations started in the 1960s [166].

Kupradze in 1964 [270] and 1965 [269] discussed a method for finding approximate solutions of potential and elasticity (static and dynamic) problems. He called the approach “method of functional equations.” Numerical examples were given in two dimensions. For potential problems with the Dirichlet boundary condition

$$\phi = f(\mathbf{x}), \quad \mathbf{x} \in C,$$

where C is the boundary contour, the solution is represented by the pair of integral equations

$$\phi(\mathbf{x}) = \frac{1}{2\pi} \int_C f(\xi) \frac{\partial \ln r(\mathbf{x}, \xi)}{\partial n(\xi)} ds(\xi) + \frac{1}{\pi} \int_C \sigma(\xi) \ln r(\mathbf{x}, \xi) ds(\xi), \quad \mathbf{x} \in \Omega, \quad (\text{A.7.12})$$

$$0 = \frac{1}{2\pi} \int_C f(\xi) \frac{\partial \ln r(\mathbf{x}, \xi)}{\partial n(\xi)} ds(\xi) + \frac{1}{\pi} \int_C \sigma(\xi) \ln r(\mathbf{x}, \xi) ds(\xi), \quad \mathbf{x} \in C'. \quad (\text{A.7.13})$$

In the above C' is an arbitrary auxiliary boundary that encloses C , and σ is the distribution density, which needs to be solved from (A.7.13). We notice that the above equations involve the distribution of both the single-layer and the double-layer potential. Another observation is that in (A.7.13) the center of singularity \mathbf{x} is located on C' , which is *outside* of the solution domain Ω . Since C and C' are distinct contours, equation (A.7.13) is not an integral equation in the classical sense, in which the singularities are located on the boundary. This is why the term “functional equation” was used instead. In the numerical implementation, C' was chosen as a circles, upon which n nodes were selected to place the singularity. Since the singularities are not located on the boundary C , the integrals in (A.7.12) are regular and can be numerically evaluated using a simple quadrature rule. Gaussian quadrature with n nodes was used for the integration. The resultant linear system was solved for the n discrete σ values located at the quadrature nodes. Equation (A.7.12) was then used to find solution at any point in the domain.

For elasticity problem, the same technique was employed. For static, two-dimensional problems with prescribed boundary displacement,

$$u_i = f_i(\mathbf{x}), \quad \mathbf{x} \in C,$$

the following pair of vector integral equations solve the boundary value problem:

$$u_j(\mathbf{x}) = \frac{1}{\pi} \int_C \sigma_i(\xi) u_{ij}^f(\mathbf{x}, \xi) ds(\xi) - \frac{1}{2\pi} \int_C f_i(\xi) u_{ij}^d(\mathbf{x}, \xi) ds(\xi), \quad \mathbf{x} \in \Omega, \quad (\text{A.7.14})$$

$$0 = \frac{1}{\pi} \int_C \sigma_i(\xi) u_{ij}^f(\mathbf{x}, \xi) ds(\xi) - \frac{1}{2\pi} \int_C f_i(\xi) u_{ij}^d(\mathbf{x}, \xi) ds(\xi), \quad \mathbf{x} \in C', \quad (\text{A.7.15})$$

where σ_i is the distribution density (vector), and the kernel

$$u_{ij}^f = \frac{1}{4G(1-\nu)} \left[(3-4\nu)\delta_{ij} \ln r - \frac{x_i x_j}{r^2} \right], \quad (\text{A.7.16})$$

is the fundamental solution due to a point force (single-layer potential) in the x_j direction, and

$$u_{ij}^d = \frac{1}{2(1-\nu)} \frac{1}{r} \left[(1-2\nu) \left(\frac{n_i x_j}{r} - \frac{n_j x_i}{r} + \delta_{ij} \frac{\partial r}{\partial n} \right) + 2 \frac{x_i x_j}{r^2} \frac{\partial r}{\partial n} \right], \quad (\text{A.7.17})$$

is the fundamental solution due to a dislocation (double-layer potential) oriented in the x_j direction. Kupradze's method was closely followed in Russia under the name “potential method”, particularly in the solution of shells [465, 165] and plates [268, 471].

Kupradze's technique of distributing fundamental solutions on an exterior, auxiliary boundary has also been considered as the origin of the “method of fundamental solutions” [50]. However, in a narrower definition, the method of fundamental solutions [151] often bypasses the integral equation formulation. It considers the distribution of admissible solutions of discrete and unknown density on an external auxiliary boundary, for example, in the form of (A.6.12). The boundary conditions are satisfied by collocating at a set of

boundary nodes. Hence the method of fundamental solutions can be viewed as a special case of the method of functional equations and in fact was independently developed. Oliveira in 1968 [367] proposed the use of fundamental solutions of point forces linearly distributed over linear segments to solve plan elasticity problems. For potential problems, its origin can be traced to Mathon and Johnston in 1977 [344].

Another type of problems that has traditionally used boundary methods involves problems with discontinuities such as fractures, dislocations resulting from imperfections of crystalline structures, interface between dissimilar materials, and other discontinuities. In these cases, certain physical quantities, such as displacements or stresses, suffer a jump. These discontinuities can be simulated by the distribution of singular solutions such as the Volterra [476] and Somigliana dislocations [440, 441] over the physical surface, which often results in integral equations [147, 45]. For example, integral equation of this type

$$A(x)\psi(x) + \frac{1}{\pi} \int_a^b \frac{B(x')\psi(x')}{x' - x} dx' + \int_a^b K(x, x')\psi(x') dx' = f(x), \quad a < x < b, \quad (\text{A.7.18})$$

and other types were numerically investigated by Erdogan and Gupta in 1972 [145, 146] using Chebyshev and Jacobi polynomials for the approximation. These type of one-dimensional singular integral equations has also been solved using piece-wise, low degree polynomials [170].

The review presented so far has focused on the solution of physical and engineering problems, and omitted the development of numerical solution of integral equations in the applied mathematics community. We seek the integral equation representations that allow the numerical schemes with reduction in mesh dimensions. The formulations often borrow the physical idea of distributing concentrated loads; hence the integral equations are typically singular. Due to the multiple spatial and time dimensions present in physical problems, the integral equations are also multi-dimensional.

For the mathematical community, the effort of finding approximate solutions of integral equations existed since the presentation of fundamental existence theorems of Fredholm in the 1900s. Early efforts involved the finding of successive approximations of linear, one-dimensional, and non-singular integral equations. Different kinds of integral equations that may or may not have physical origin were investigated. One of the first monographs on numerical solution of integral equations is by Bückner in 1952 [69]. Another early monograph is by Mikhlin and Smolitsky [352] in 1967. The field flourished in the 1970s with the publication of several monographs—Kagiwada and Kalaba [245] in 1974, Atkinson [8] in 1976, Ivanov [230] in 1976, and Baker [20] in 1977. As mentioned above, mostly one-dimensional integral equations were investigated. Some integral equations have physical origin such as flow around hydrofoil, population competition, and quantum scattering [127], while others do not. The methods used include projection method, polynomial collocation, Galerkin method, least squares, quadrature method, among others [173]. It is of interest to observe that the developments in the two communities, the applied mathematics and the engineering, seems to run parallel to each other, almost devoid of any cross citations, although it is clear that many of the techniques have much

in common and cross-fertilization is needed¹.

As seen from the review above, the “origin” of boundary numerical methods, as well as other numerical methods, can be traced to this period, during which many ideas sprouted. However, even though methods like those by Jaswon and Kupradze started to receive attention, these efforts did not immediately coalesce into a single “movement” and grow rapidly. In the following sections we shall review those significant events that led to the development of the boundary integral equation method and the boundary element method, and the ensuing movement that establishes these methods as one of the leading numerical methods.

A.7.1 Kupradze

Viktor Dmitrievich Kupradze (1903–1985) was born in the village of Kela, Russian Georgia. He was enrolled in the Tbilisi State University in 1922 and was awarded the diploma in mathematics in 1927. He stayed on as a lecturer in mathematical analysis and mechanics until 1930. In that year he entered the Steklov Mathematical Institute in Leningrad for postgraduate study and obtained his doctor of mathematics degree in 1935. In 1933 Muskhelishvili founded a research institute of mathematics, physics and mechanics in Tbilisi. In 1935, Muskhelishvili and his closest associates Kupradze and I. Vekua transformed the institute to become affiliated with the Georgian Academy of Sciences, with Kupradze serving as its first director from 1935 to 1941. The Institute was later known as A. Razmadze. From 1937 until his death, Kupradze served as the Head of Differential and Integral Equations Department at Tbilisi. Kupradze’s research interest covers theory of partial differential equations and integral equations, and mathematical theory of elasticity and thermoelasticity. He received many honors, including political ones. He was elected as an Academician of the Georgian Academy in 1946. From 1954-1958 he served as the Rector of Tbilisi University, and from 1954-1963 the Chairman of Supreme Soviet of the Georgian SSR.

A.7.2 Jaswon

Maurice Aaron Jaswon (1922–) was born in Dublin, Ireland. He was enrolled in the Trinity College, Dublin, and obtained his B.Sc. degree in 1944. He entered the University of Birmingham, U.K. and was awarded his Ph.D. degree in 1949. In the same year he started his academic career as a Lecturer in Mathematics at the Imperial College, London. His early research was focused on the mathematical theory of crystallography and dislocation, which cumulated into a book published in 1965 [231], with a updated version in 1983 [233]. In 1957 Jaswon was promoted to the Reader position and stayed at the Imperial College until 1967. It was during this period that he started his seminal work on numerical solution of integral equations with his students George Thomas

¹It is our hope that this book could stimulate a merge of research on the TM and boundary methods in both applied mathematics and engineering.

Symm [452] and Alan R.S. Ponter. In 1963-1964 Jaswon visited Brown University. In 1965-1966 he was a visiting professor at the University of Kentucky. His presence there was what initially made Rizzo aware of an opening position at Kentucky [404]. Upon Rizzo's arrival in 1966, they had a few months of overlapping before Jaswon's returning to England. In 1967 Jaswon left the Imperial College to take a position as Professor and Head of Mathematics at the City University of London, where he stayed for the next twenty years until his retirement at 1987. He remains active as an Emeritus Professor at City University. Jaswon was considered by some as the founder of the boundary integral equation method based on his 1963 work [232] implementing Green's formula.

A.8 Boundary Integral Equation and Boundary Element Method

A turning point marking the rapid growth of numerical solutions of boundary integral equations, known as the *boundary integral equation method*, happened in 1967, when *Frank Joseph Rizzo* (1938-) published the article "*An integral equation approach to boundary value problems of classical elastostatics*" [403]. In this paper, a numerical procedure was applied for solving the Somigliana identity (A.5.8) for elastostatics problems. The work was an extension of Rizzo's doctoral dissertation [402] at the University of Illinois, Urbana-Champaign, which described the numerical algorithm, yet without actual implementation. The work was heavily influenced by the earlier work of Jaswon [234] on potential problems.

In collaboration with David J. Shippy, Rizzo continued the work on boundary integral equation method by extending its application to elasticity problems with inclusions [407], plane anisotropic bodies [408], and by utilizing Laplace transform and the numerical Laplace inversion, to transient heat conduction [409] and quasi-static viscoelasticity problems [410].

Thomas Allen Cruse (1941-), suggested by Rizzo, completed a doctoral dissertation on boundary integral solution of elastodynamics [111], which was published in 1968 in two papers [119, 112]. In 1970 and 1971, Cruse published boundary integral solutions of three-dimensional fracture problems [114, 121]; these were among the first numerical solutions of three-dimensional fracture problems [117]. In 1971 Cruse in his work on elastoplastic flow [450] referred the methods that distributed single- and double-layer potential at fictitious densities, such as those based on the Fredholm integrals and Kupradze's method, as the "indirect potential methods", and the methods that utilized Green's formality, such as Green's third identity and the Somigliana integral, as the "direct potential methods".

In 1975, Cruse and Rizzo organized the first dedicated boundary integral equation method meeting under the auspices of the Applied Mechanics Division of the American Society of Mechanical Engineers (ASME) in Troy, New York. The proceedings of the meeting [120] reflected the rapid growth of the boundary integral equation method to cover a broad range of applications that included water waves [427], transient phenomena in solids (heat conduction, viscoelasticity, and wave propagation) [432], fracture mechanics [115], elastoplastic problems [349], and rock mechanics [3]. The next international

meeting on boundary integral equation method was held in 1977 as the First International Symposium on Innovative Numerical Analysis in Applied Engineering Sciences, at Versailles, France, organized by Cruse and Lachat [118]. In the same year, Jaswon and Symm published the first book on numerical solution of boundary integral equations [234].

In the late 1960s, Hugh Tottenham and his students at the University of Southampton in U.K. started the investigation of integral equation method using Kupradze's [269] approach (indirect method). Doctoral dissertations based on indirect methods produced around this time included that by P.K. Banerjee [23] in 1970, and by J.O. Watson [483] and G.R. Tomlin [460] in 1973.

Up to 1977 the numerical method for solving integral equations had been called the "boundary integral equation method", following Cruse's naming. However, with the growing popularity of the finite element method, it became clear that many of the finite element ideas can be applied to the numerical technique solving boundary integral equations. This is particularly demonstrated in the work of Lachat and Watson [273]. Furthermore, parallel to the theoretical development of finite element method, it was shown that the weighted residual technique can be used to derive the boundary integral equations [63, 60]. The term "boundary element method", mirroring "finite element method", finally emerged in 1977.

Carlos Alberto Brebbia (1938–) presented the boundary element method using the weighted residuals formulation [63, 60, 59]. The development of solving boundary value problems using functions defined on local domains with low degree of continuity was strongly influenced by the development of extended variational principles and weighted residuals in the mid 1960s. Key players included Eric Reissner [399] and Kyuichiro Washizu [482], who pioneered the use of mixed variational statements that allowed the flexibility in choosing localized functions. To deal with non-conservative and time-dependent problems, the strategy shifted from the variational approach to the method of weighted residuals combined with the concept of weak forms. Brebbia [60] showed that one could generate a spectrum of methods ranging from finite elements to boundary elements.

Consider a function ϕ satisfying the linear partial differential operator \mathcal{L} in the following fashion

$$\mathcal{L}\{\phi\} = b(\mathbf{x}), \quad \mathbf{x} \in \Omega, \quad (\text{A.8.1})$$

and subject to the essential and natural boundary conditions

$$\begin{aligned} S\{\phi\} &= f(\mathbf{x}), & \mathbf{x} \in \Gamma_1, \\ N\{\phi\} &= g(\mathbf{x}), & \mathbf{x} \in \Gamma_2, \end{aligned} \quad (\text{A.8.2})$$

where S and N are the corresponding differential operators. Our goal is to find the approximate solution that minimizes the error with respect to a weighing function w in the following fashion:

$$\langle \mathcal{L}\{\phi\} - b, w \rangle_{\Omega} = \langle N\{\phi\} - g, S^*\{w\} \rangle_{\Gamma_2} - \langle S\{\phi\} - f, N^*\{w\} \rangle_{\Gamma_1}, \quad (\text{A.8.3})$$

where S^* and N^* are the adjoint operators of S , and N , and the angle brackets denote the inner product,

$$\langle \alpha, \beta \rangle_\gamma = \int_\gamma \alpha(\mathbf{x})\beta(\mathbf{x}) d\mathbf{x}. \quad (\text{A.8.4})$$

Equation (A.8.3) can be considered as the theoretical basis for a number of numerical methods [60]. For example, finite difference can be interpreted as a method using Dirac delta function as the weighing function and enforcing the boundary conditions exactly. The well-known Galerkin formulation in finite element method uses of the basis function for w the same as that used for the approximation of ϕ .

For the boundary element formulation, we perform integration by parts on (A.8.3) for as many times as needed to obtain

$$\begin{aligned} \langle \phi, \mathcal{L}^* \{w\} \rangle_\Omega &= \langle S \{ \phi \}, N^* \{w\} \rangle_{\Gamma_2} - \langle N \{ \phi \}, S^* \{w\} \rangle_{\Gamma_1} \\ &+ \langle f, N^* \{w\} \rangle_{\Gamma_1} - \langle g, S^* \{w\} \rangle_{\Gamma_2} + \langle b, w \rangle_\Omega, \end{aligned} \quad (\text{A.8.5})$$

where \mathcal{L}^* is the adjoint operators of \mathcal{L} . The idea for the boundary method is to replace w by the fundamental solution G^* , which satisfies

$$\mathcal{L}^* \{G^*\} = \delta, \quad (\text{A.8.6})$$

such that (A.8.5) reduces to

$$\begin{aligned} \phi &= \langle S \{ \phi \}, N^* \{G^*\} \rangle_{\Gamma_2} - \langle N \{ \phi \}, S^* \{G^*\} \rangle_{\Gamma_1} \\ &+ \langle f, N^* \{G^*\} \rangle_{\Gamma_1} - \langle g, S^* \{G^*\} \rangle_{\Gamma_2} + \langle b, G^* \rangle_\Omega. \end{aligned} \quad (\text{A.8.7})$$

This is the weighted residual formulation for boundary element method. For the case of Laplace equation, which is self-adjoint, with the boundary conditions

$$\begin{aligned} \phi &= f(\mathbf{x}), & \mathbf{x} \in \Gamma_1, \\ \frac{\partial \phi}{\partial n} &= g(\mathbf{x}), & \mathbf{x} \in \Gamma_2, \end{aligned} \quad (\text{A.8.8})$$

equation (A.8.7) becomes

$$\begin{aligned} \phi &= -\frac{1}{4\pi} \iint_{\Gamma_1} \frac{1}{r} \frac{\partial \phi}{\partial n} dS + \frac{1}{4\pi} \iint_{\Gamma_1} f \frac{\partial(1/r)}{\partial n} dS \\ &- \frac{1}{4\pi} \iint_{\Gamma_2} \frac{1}{r} g dS + \frac{1}{4\pi} \iint_{\Gamma_2} \phi \frac{\partial(1/r)}{\partial n} dS. \end{aligned} \quad (\text{A.8.9})$$

which is just (A.3.8) with boundary conditions substituted in.

In 1978, Brebbia published the first textbook on BEM “*The Boundary Element Method for Engineers*” [60]. In the same year, Brebbia organized the first conference dedicated to the BEM: the First International Conference on Boundary Element Methods, at the University of Southampton [61]. This conference series has become an annual event.

A.8.1 Rizzo

Frank Joseph Rizzo (1938–) was born in Chicago, Illinois. After graduating from St. Rita High School in 1955, he attended the University of Illinois at Chicago. Two years later he transferred to the Urbana campus and received his B.S. degree in 1960, M.S. degree in 1961, and Ph.D. in 1964. While pursuing the graduate degrees, he was employed as a half-time teaching staff in the Department of Theoretical and Applied Mechanics. In 1964, he began his career as an assistant professor at the University of Washington. Two years later, he left for the University of Kentucky, where he stayed for the next twenty years. In 1987, Rizzo moved to Iowa State University and served as the Head of the Department of Engineering Sciences and Mechanics, which later became a part of the Aerospace Engineering and Engineering Mechanics Department. In late 1989, he returned to his alma mater, the University of Illinois at Urbana-Champaign, to become the Head of the Department of Theoretical and Applied Mechanics. Near the end of 1991, he returned to the Iowa State University and remained there until his retirement in 2000. Rizzo's 1967 article "*An integral equation approach to boundary value problems of classical elastostatics*," which was cited more than 300 times as of 2003 based on the *Web of Science* search [512], is generally considered as the turning point that sets off the modern day development of boundary element (boundary integral equation) method.

A.8.2 Cruse

Thomas Allen Cruse (1941–) was born in Anderson, Indiana. After graduation from Riverside Polytechnic High School, Cruse entered Stanford University, where he obtained a B.S. degree in Mechanical Engineering in 1963, and a M.S. in Engineering Mechanics in 1964. After a year working with the Boeing Company, he enrolled in 1965 at the University of Washington to pursue a Ph.D. degree, which he was awarded in 1967. In the same year, Cruse joined Carnegie-Mellon University as an assistant professor. In 1973 Cruse resigned from Carnegie Mellon and joined Pratt & Whitney Aircraft Group, where he spent the next 10 years. In 1983, he moved to the Southwest Research Institute at San Antonio, Texas, where he stayed until 1990. In that year Cruse returned to the academia by joining the Vanderbilt University as the holder of the H. Fort Flower Professor of Mechanical Engineering. He retired in 1999 as the Associate Dean for Research and Graduate Affairs of the College of Engineering at Vanderbilt University.

A.8.3 Brebbia

Carlos Alberto Brebbia (1938–) was born in Rosario, Argentina. He received a B.S. degree in civil engineering from the University of Litoral, Rosario in 1962. He did early research on the application of Volterra equations to creep buckling and other problems. His mentor there was José Nestor Distefano, latterly of the University of California, Berkeley. Brebbia went to the University of Southampton, UK to carry out his Ph.D. study under Hugh

Tottenham. During the whole 1966 and first 6 months in 1967, he visited MIT and conducted research under Eric Reissner and Jerry Connor. He attributed his success with FEM as well as BEM to these great teachers. Brebbia was granted his Ph.D. at Southampton in 1967. After a year's research at the UK Electricity Board Laboratories, in 1970 Brebbia started working as a Lecturer at Southampton. In 1975, he accepted a position as Associate Professor at Princeton University, where he stayed for over a year. He then returned to Southampton where he eventually became a Reader. In 1979, Brebbia was again in the US holding a full professor position at the University of California, Irvine. In 1981, he moved back to the UK and founded the Wessex Institute of Technology as an international focus for BEM research. He has been serving as its director since.

References

- [1] Abou-Dina, M.S, Implementation of Trefftz method for the solution of some elliptic boundary value problems, *Appl. Math. and Comp.*, **127**, pp. 125-147, 2002.
- [2] Abramowitz, M. & Stegun, I.A., *Handbook of Mathematical Functions with Formulas, Graphs and Mathematical Tables*, Devor Publications, Inc, New York, 1970.
- [3] Altiero, N.J. & Sikarskie, D.L., An integral equation method applied to penetration problems in rock mechanics, *Boundary-Integral Equation Method: Computational Applications in Applied Mechanics*, AMD**11**, eds. T.A. Cruse & F.J. Rizzo, pp. 119-141, 1975.
- [4] Arad, A., Yakhot, A. & Ben-Dor, G., A highly accurate numerical solution of a biharmonic equation, *Numer. Meth. PDE*, **13**, pp. 375-397, 1997.
- [5] Arnold, D., An interior penalty finite element method with discontinuous elements, *SIAM J. Numer. Anal.*, **19**, pp. 742-760, 1982.
- [6] Arnold, D.N. & Wendland, W.L., On the asymptotic convergence of collocation method, *Math. Comp.*, **41(164)**, pp. 349-381, 1983.
- [7] Ascher, U.M., Mattheij, R.M. & Russell, R.D., *Numerical Solution of Boundary Value Problems for Ordinary Differential Equations*, Prentice Hall, Englewood Cliffs, NJ, 1988.
- [8] Atkinson, K.E., *A Survey of Numerical Methods for the Solution of Fredholm Integral Equations of the Second Kind*, SIAM, 1976.
- [9] Atkinson K.E., *An Introduction to Numerical Analysis*, John Wiley & Sons, 1989.
- [10] Atkinson K.E., *The Numerical Solution of Integral Equations of The second kind*, Cambridge University Press, 1997.
- [11] Aziz, A.K., Dorr, M.R. & Kellogg, R.B., An new approximation method for the Helmholtz equation method in an exterior domain, *SIAM J. Numer. Anal.*, **19**, pp. 899-908, 1982.
- [12] Aziz, A.K., Kellogg, R.B. & Stephen, A.B., Least squares methods for elliptic systems, *Math. Comp.*, **44**, pp. 53-70, 1985.
- [13] Aziz, A.K. & Liu, J.L., A weighted least-squares method for the backward-forward heat-equation, *SIAM J. Numer. Anal.*, **28**, pp. 156-167, 1991.
- [14] Babuška, I., The finite element method with Lagrangian multipliers *Numer. Math.*, **20**, pp. 179-192. 1973.
- [15] Babuška, I. & Aziz, A.K., Survey lectures on the mathematical foundations of the finite element method, *The Mathematical foundations of the Finite Element with Applications to Partial Differential Equations*, ed. A.K. Aziz, Academic Press, Inc., pp. 3-358, 1971.
- [16] Babuška, I. & Guo, B., *Direct and inverse approximation theorems for the p-version of the finite element method in the framework of weighted Besov spaces, Part I: Approximability of functions on the weighted Besov space*, Technical Report, Department of Mathematics, University of Manitoba, 2001.
- [17] Babuška, I. & Guo, B., *Direct and inverse approximation theorems for the p-version of the finite element method in the framework of weighted Besov spaces, Part III: Inverse approximation theorems*, Technical Report, Department of Mathematics, University of Manitoba, 2002.
- [18] Babuška, I. & Osborn, J., Eigenvalue problems, *Handbook of Numerical Analysis, II., Finite Element Methods (Part I)*, eds. P.G. Ciarlet & J.L. Lions, pp. 641-787, North Holland, Amsterdam, 1991.
- [19] Badea, L., A generalization of the Schwarz alternating method to an arbitrary number of subdomain, *Numer. Math.*, **55**, pp. 61-81, 1989.
- [20] Baker, C.T.H., *The Numerical Treatment of Integral Equations*, Oxford Univ. Press, 1977.
- [21] Baker, G.A., Finite element methods for elliptic equations using nonconforming elements, *Math. Comp.*, **31**, pp. 45-59, 1977.

- [22] Banaugh, R.P. & Goldsmith, W., Diffraction of steady acoustic waves by surfaces of arbitrary shape, *J. Acoust. Soc. Am.*, **35**, pp. 1590-1601, 1963.
- [23] Banerjee, P.K., *A contribution to the study of axially loaded pile foundations*, Doctoral dissertation, University of Southampton, 1970.
- [24] Banoczi, J.M., Chiu, N. C., Cho, G. E. & Ipsen, I. C. P., The lack of influence of the right-hand side on the accuracy of linear system solution, *SIAM J. Stat. Comput.*, **20**, pp. 203-227, 1998.
- [25] Barbosa, H.J.C. & Hughes, T.J.R., Boundary Lagrange multipliers in finite element methods: error analysis in natural norms, *Numer. Math.*, **62**, pp. 1-15, 1992.
- [26] Barrett, J.W. & Elliott, C.M., Finite element approximation of the Dirichlet problem using the boundary penalty method, *Numer. Math.*, **49**, pp. 343-366, 1986.
- [27] Bartlett, J. & Kaplan, J., *Familiar Quotations*, 6th ed., Little, Brown and Company, Boston, 1992.
- [28] Bayliss, A., Goldstein, C.I. & Turkel, E., Preconditioned conjugate gradient methods for the Helmholtz equation, *Elliptic Problems Solvers II*, eds. G. Birkhoff & A. Schoenstadt, pp. 734-754. Academic Press, 1984.
- [29] Bayliss, A., Gunzburger, M. & Turkel, E., Boundary conditions for the numerical solution of elliptic equations in exterior regions, *SIAM J. Appl. Math.*, **42(2)**, pp. 430-451, 1982.
- [30] Begehr, H., & Gilbert, R.P., Transformations, transmutation, and kernel functions, *Longman Scientific & Technical*, **1**, pp. 108-127, 1992.
- [31] Belhoste, B., *Augustin-Louis Cauchy. A Biography*, Springer-Verlag, 1991.
- [32] Belytschko, T., Lu, Y.Y. & Gu, L., Element-free Galerkin methods, *Int. J. Numer. Meth. Engrg.*, **37**, pp. 229-256, 1994.
- [33] Bergman, S., *Integral Operations in the Theory of Partial Differential Equations*, Springer-Verlag, New York, 1969.
- [34] Bergman, S. & John, G.H., Application of the method of the kernel function for solving boundary value problems, *Numer. Math.*, **3**, pp. 209-225, 1961.
- [35] Bergman, S. & John, G.H., Numerical solution of boundary value problems by the method of integral operator, *Numer. Math.*, **7**, pp. 42-65, 1965.
- [36] Bernardi, C., Debit, N. & Maday, Y., Coupling finite element and spectral methods: First result, *Math. Comp.*, **54**, pp. 21-39, 1990.
- [37] Bernardi, C. & Maday, Y., Spectral methods, *Handbook of Numerical Analysis*, **V**, *Techniques of Scientific Computing (Part 2)*, eds. P.G. Ciarlet & J.L. Lions, pp. 209-485, Elsevier Science, 1997.
- [38] Betti, E., Teoria della elasticità, *Nuovo Cimento*, **2**, pp. 6-10, 1872.
- [39] Betti, E., Sopra l'equazioni di equilibrio dei corpi solidi elastici, *Annali delle Università Toscane*, **10**, pp. 143-158, 1874.
- [40] Bialecki, B., Convergence analysis of orthogonal spline collocation for elliptic boundary value problems, *SIAM J. Numer. Anal.*, **35**, pp. 617-631, 1998.
- [41] Bialecki, B. & Cai, X.C., H^1 - norm error bounds for piecewise Hermite bicubic orthogonal spline collocation schemes for elliptic boundary value problems, *SIAM J. Numer. Anal.*, **31**, pp. 1128-1146, 1994.
- [42] Bialecki, B. & Dryja, M., Multilevel additive and multiplicative methods for orthogonal spline collocation problems, *Numer. Math.*, **77**, pp. 35-58, 1997.
- [43] Bialecki, B., Fairweather, G. & Kargeorghis, A., Matrix decomposition algorithms for modified spline collocation for Helmholtz problems, *SIAM J. Sci. Comput.*, **24**, pp. 1733-1753, 2003.
- [44] Bialecki, B. & Fernandes, R.I., An orthogonal spline collocation alternating direction implicit Crank-Nicolson method for linear parabolic problems on rectangles, *SIAM J.*

- Numer. Anal.*, **36**, pp. 1414-1434, 1999.
- [45] Bilby, B.A., Continuous distributions of dislocations, *Progress in Solid Mechanics*, eds. I.N. Sneddon & R. Hill, North-Holland, pp. 329-398, 1960.
- [46] Birkhoff, G.D., Oliver Dimon Kellogg—in memoriam, *Bull. Amer. Math. Soc.*, **39**, pp. 171-177, 1933.
- [47] Birkhoff, G. & Lynch, R.E., *Numerical Solution of Elliptic Equations*, SIAM, Philadelphia, 1984.
- [48] Bjorck, A., Least squares methods, *Handbook of Numerical Analysis*, **1**, eds. Ciarlet, P.G. & Lions, J.L., pp. 465-652, North-Holland, 1990.
- [49] Bochev, P.B. & Gunzburger, M.D., Analysis of least squares finite element methods for the Stokes equations, *Math. Comp.*, **63(208)**, pp. 479-506, 1994.
- [50] Bogomolny, A., Fundamental solutions method for elliptic boundary value problems, *SIAM J. Numer. Anal.*, **22**, pp. 644-669, 1985.
- [51] Bohmer, K. & Locker, J., Asymptotic expansions for the discretization error of least squares solutions of linear boundary value problems, *Math. Comp.*, **51(183)**, pp. 75-91, 1988.
- [52] Boyd, J.P., Chebyshev and Fourier Spectral Methods, *Lectures Notes in Engineering*, **49**, Springer, Berlin, 1989.
- [53] Boyer, C.B., *A History of Mathematics*, 2nd ed., Wiley, 1991.
- [54] Bramble, J.H., The Lagrange multiplier methods for Dirichlet's problem, *Math. Comp.*, **37(155)**, pp. 1-12, 1981.
- [55] Bramble, J.H. & Nitsche, J.A., A generalized Ritz-least-squares method for Dirichlet problems, *SIAM J. Numer. Anal.*, **10**, pp. 81-93, 1973.
- [56] Bramble, J.H. & Schatz, A.H., Rayleigh-Ritz-Galerkin methods for Dirichlet's problem using subspaces without boundary conditions, *Comm. Pure Appl. Math.*, **23**, pp. 653-675, 1970.
- [57] Bramble, J.H. & Schatz, A.H., Least squares methods for 2^mth order elliptic boundary-value problems, *Math. Comp.*, **25(113)**, pp. 1-32, 1971.
- [58] Bramble, J.H. & Schatz, A.H., Higher order local accuracy by averaging in the finite element method, *Math. Comp.*, **31**, pp. 94-111, 1977.
- [59] Brebbia, C.A., Introduction to boundary element methods, in *Recent Advances in Boundary Element Methods*, *Proc. of the 1st Int. Conf. Boundary Element Methods*, ed. C.A. Brebbia, Univ. Southampton, Pentech, pp. 1-42, 1978.
- [60] Brebbia, C.A., *The Boundary Element Method for Engineering*, Pentech Press, London, 1978.
- [61] Brebbia, C.A., (ed). *Recent Advances in Boundary Element Methods*, *Proc. of the 1st Int. Conf. Boundary Element Methods*, Univ. Southampton, Pentech, 1978.
- [62] Brebbia, C.A., Tribute to Tom Cruse, *Tom Cruse Commemorative Issue*, eds. C.A. Brebbia & A.H.-D. Cheng, *Eng. Anal. Bound. Elem.*, **24**, pp. 701, 2000.
- [63] Brebbia, C.A. & Dominguez, J., Boundary element methods for potential problems, *Appl. Math. Modelling*, **1**, pp. 372-378, 1977.
- [64] Brebbia, C.A. & Dominguez, J., *The Boundary Elements*, In *Introductory Course*, McGraw-Hill Book Company, New York, 1989.
- [65] Brezzi, F. & Fortin, M., *Mixed and Hybrid Finite Element Methods*, Springer-Verlag, New York, 1991.
- [66] Browder, F.E., Approximation by solutions of partial differential equations, *Amer. J. Math.*, **84**, pp. 134-160, 1962.
- [67] Brunner, H., 1896-1996: One hundred years of Volterra integral equations of the first kind, *Appl. Numer. Math.*, **24**, pp. 83-93, 1997.
- [68] Brunner, H., Pedas, A. & Vainikko, G., Piecewise polynomial collocation methods for linear

- Volterra integro-differential equations with weakly singular kernels, *SIAM J. Numer. Anal.*, **39**, pp. 957-982, 2001.
- [69] Bückner, H.F., *Die praktische Behandlung von Integralgleichungen*, Springer-Verlag, 1952.
- [70] Bühler, W.K., *Gauss, A Biographical Study*, Springer-Verlag, 1981.
- [71] Burton, D.M., *The History of Mathematics—An Introduction*, Allyn & Bacon, 1985.
- [72] Cahan, D., (ed). *Hermann von Helmholtz and the Foundation of Nineteenth Century Science*, U. California Press, 1993.
- [73] Cannell, D.M., *George Green, Mathematician and Physicist 1793-1841, The Background to His Life and Work*, 2nd ed., SIAM, 2001.
- [74] Canuto, C., Hariharan, S.I. & Lustman, L., Spectral methods for exterior elliptic problems, *Numer Math.* **46**, pp. 505-520, 1985.
- [75] Canuto, C., Hussaini, M.Y., Quarteroni, A. & Zhang, T.A., *Spectral Methods in Fluid Dynamics*, Springer-Verlag, New York, 1987.
- [76] Canuto, C. & Quarteroni, A., Approximation results for orthogonal polynomials in Sobolev spaces, *Math. Comp.*, **52**, pp. 67-86, 1982.
- [77] Cao, Y., Herdman, T. & Xu, Y., A hybrid collocation method for Volterra integral equations with weakly singular kernels, *SIAM J. Numer. Anal.*, **41**, pp. 364-381, 2003.
- [78] Carey, G.F. & Oden, J.T., *Finite Elements, A Second Course, II*, Prentice Hall, Inc., Englewood Cliffs, N.J., 1983.
- [79] Carey, G.F. & Shen, Y., Convergence studies of least-squares finite elements for first order systems, *Comm. Appl. Numer. M.*, **5**, pp. 427-434, 1989.
- [80] Carstensen, C. & Praetorius, D., A posteriori error control in adaptive quadrature boundary element analysis for a logarithmic kernel integral equation of the first kind, *SIAM J. Sci. Comput.*, **25**, pp. 259-283, 2003.
- [81] Cauchy, A.-L., *Leçons sur les applications de calcul infinitésimal à la géométries*, 1826-28.
- [82] Cauchy, A.-L., Mémoire sur les intégrales définies, *Mémoires des divers savants*, ser. 2, **1**, pp. 601-799 (written in 1814), 1827.
- [83] Chan, T.F. & Foulser, D., Effectively well-conditioned linear systems, *SIAM J. Sci. Comput.*, **9**, pp. 963-969, 1988.
- [84] Chan, T.F., Hou, T.Y. & Lions, P.L., Geometry related convergence results for domain decomposition algorithm problems, *SIAM J. Numer. Anal.*, **28**, pp. 378-391, 1991.
- [85] Chang, C.L., A least-squares finite element method for the Helmholtz equation, *Comput. Method. Appl. M.*, **83**, pp. 1-7, 1990.
- [86] Chang, J.R., Liu, R.F., Kuo, S.R., et al., Application of symmetric indirect Trefftz method to free vibration problems in 2D, *Inter. J. Numer. Meth. Engrg.*, **56(8)**, pp. 1175-1192, 2003.
- [87] Chen, C.H., *Further study on Motz's problem*, Master thesis, Department of Applied Mathematics, National Sun Yat-sen University, Kaohsiung, 1998.
- [88] Chen, C.S., Hon, Y.C. & Schaback R.A., *Scientific Computing with Radius Basis Functions*, Book manuscript, Göttingen, 2005.
- [89] Chen, J.T., Lin, L.W. & Hong, H.K., Spurious and true eigensolutions of Helmholtz BIEs and BEMs for a multiply-connected problem, *Proc. Royal Society of London Ser. A.*, **459**, pp. 1891-1925, 2003.
- [90] Chen, J.T., Lin, J.T., Kuo, S.R., & Chyuan, S.W., Boundary element analysis for the Helmholtz eigenvalue problems with a multiply connected domain, *Proc. Royal Society of London Ser. A.*, **457**, pp. 2521-2546, 2001.
- [91] Chen, J.T., Wu, C.S., Chen, I.L., & Chen, K.H., *On the equivalence of the Trefftz method and method of fundamental solutions for Laplace and biharmonic equations*, to appear in *Computer Math. Applic.*

- [92] Chen, G. & Zhou, J., *Boundary Element Methods*, Academic Press, New York, 1992.
- [93] Chen, L.H. & Schweikert, D.G., Sound radiation from an arbitrary body, *J. Acoust. Soc. Am.*, **35**, pp. 1626-1632, 1963.
- [94] Chen, Z., Micchelli, C.A. & Xu, Y., Fast collocation methods for second kind integral equations, *SIAM J. Numer. Anal.*, **40**, pp. 344-375, 2002.
- [95] Cheney, E.W., *Introduction to Approximation Theory*, McGraw-Hill, New York, 1966.
- [96] Cheng, A.H.-D. & Cheng, D.T., Heritage and early development of boundary element, *Eng. Anal. Bound. Elem.*, **29**, pp. 268-302, 2005.
- [97] Cheng, A.H.-D., Golberg, M.A., Kansa, E.J. & Zammito G., Exponential convergence and H-c multiquadrics collocation method for partial differential equations, *Numer. Meth. PDE*, **19(5)**, pp. 571-594, 2003.
- [98] Cheng, A.H.-D., Lafe, O. & Grilli, S., Dual-reciprocity BEM based on global interpolation functions, *Eng. Anal. Bound. Elem.*, **13**, pp. 303-311, 1994.
- [99] Cheung, Y.K., Jin, W.G. & Zienkiewicz, O.C., Direct solution procedure for solution of Harmonic problems using complete, non-singular, Trefftz functions, *Commun. Appl. Numer. M.*, **5**, pp. 159-169, 1989.
- [100] Cheung, Y.K., Jin, W.G. & Zienkiewicz, O.C., Solution of Helmholtz equation by Trefftz method, *Inter. J. for Numer. Meth. Engrg.*, **32**, pp. 63-78, 1991.
- [101] Chien, W.Z., *Variational and Finite Element Methods* (in Chinese), East Asia Publishing, Taipei, 1989.
- [102] Christiansen, S., Condition number of matrices derived from two classes of integral equations, *Math. Meth. Applis. Sci.*, **3**, pp. 364-392, 1981.
- [103] Christiansen, S. & Hansen, P.C., The effective condition number applied to error analysis of certain boundary collocation methods, *J. Comput. Appl. Math.*, **54(1)**, pp. 15-36, 1994.
- [104] Christiansen, S. & Saranen, J., The conditioning of some numerical methods for first kind boundary integral equations, *J. Comput. Appl. Math.*, **67(1)**, pp. 43-58, 1996.
- [105] Ciarlet, P.G., Basic error estimates for elliptic problems, *Finite Element Methods (Part I)*, eds. P.G. Ciarlet & J.L. Lions, pp. 17-352, North-Holland, 1991.
- [106] Clough, R.W., The finite element method in plane stress analysis, *Proc. 2nd ASCE Conf. Electronic Computation*, 1960.
- [107] Costabel, M., Boundary integral operators on Lipschitz domains: Elementary results, *SIAM J. Math. Anal.*, **19**, pp. 613-626, 1988.
- [108] Costabel, M., Ervin V. J. & Stephan E. P., On the convergence of collocation methods for Symm's integral equation on open curves, *Math. Comp.*, **51**, pp. 167-179, 1988.
- [109] Courant, R. & Hilbert, D., *Methods of Mathematical Physics, I*, Wiley Intersciences Publishers, New York, 1953.
- [110] Courant, R. & Hilbert, D., *Methods of Mathematical Physics, II, Partial Differential Equations*, Interscience Publishers, New York, 1962.
- [111] Cruse, T.A., *The transient problem in classical elastodynamics solved by integral equations*, Doctoral dissertation, University of Washington, pp. 117, 1967.
- [112] Cruse, T.A., A direct formulation and numerical solution of the general transient elastodynamic problem—II, *J. Math. Anal. Appl.*, **22**, pp. 341-355, 1968.
- [113] Cruse, T.A., Numerical solutions in three dimensional elastostatics, *Int. J. Solids Structures*, **5**, pp. 1259-1274, 1969.
- [114] Cruse, T.A., Lateral constraint in a cracked, three-dimensional elastic body, *Int. J. Fracture Mech.*, **6**, pp. 326-328, 1970.
- [115] Cruse, T.A., Boundary-integral equation fracture mechanics analysis, *Boundary-Integral Equation Method: Computational Applications in Applied Mechanics*, AMD **11**, eds. T.A. Cruse & F.J. Rizzo, pp. 31-46, 1975.

- [116] Cruse, T.A., *Boundary Element Analysis in Computational Fracture Mechanics*, Kluwer Academic Publishers, Dordrecht, 1988.
- [117] Cruse, T.A., BIE fracture mechanics: 25 years of developments, *Comp. Mech.*, **18**, pp. 1-11, 1996.
- [118] Cruse, T.A. & Lachat, J.-C., *Proceedings of the International Symposium on Innovative Numerical Analysis in Applied Engineering Sciences*, Versailles, France, 1977.
- [119] Cruse, T.A. & Rizzo, F.J., A direct formulation and numerical solution of the general transient elastodynamic problem—I, *J. Math. Anal. Appl.*, **22**, pp. 244-259, 1968.
- [120] Cruse, T.A. & Rizzo, F.J., *Boundary-Integral Equation Method: Computational Applications in Applied Mechanics*, AMD **11**, Applied Mechanics Conference, ASME, Rensselaer Polytechnic Institute, June 23-25, 1975.
- [121] Cruse, T.A. & VanBuren, W., Three-dimensional elastic stress analysis of a fracture specimen with an edge crack, *Int. J. Fracture Mech.*, **7**, pp. 1-15, 1971.
- [122] Dautray, R. & Lions, J.L., *Mathematical Analysis and Numerical Methods for Science and Technology, II. Functional and Variational Methods*, Springer-Verlag, Berlin Heidelberg, New York, 1988.
- [123] de Freitas, J.A.T. & Leitao, V.M.A., A boundary integral Trefftz formulation with symmetric collocation, *Comp. Mech.*, **25(6)**, pp. 515-523, 2003.
- [124] Delves, L.M., Global and regional methods, *A Survey of Numerical Methods for Partial Differential Equations*, eds. L. Gladwell & R. Wait, Clarendon Press, Oxford, pp. 106-127, 1979.
- [125] Delves, L.M. & Freeman, T.L., *Analysis of Global Expansion Methods: Weakly Asymptotically Diagonal Systems*, Academic Press, London, New York, 1981.
- [126] Delves, L.M. & Hall, C.A., An implicit matching principle for global element calculations, *J. Inst. Math. Appl.*, **23(2)**, pp. 223-234, 1979.
- [127] Delves, L.M. & Mohamed, J.L., *Computational Methods for Integral Equations*, Cambridge Univ. Press, 1985.
- [128] Demmel, J.W., *Applied Numerical Linear Algebra*, SIAM, Philadelphia, pp. 132, 1997.
- [129] Dennis, J.E.Jr. & Schnabel, R.B., *Numerical Methods for Unconstrained Optimization in Nonlinear Equations*, Prentice-Hall, Inc. Englewood, Cliffs, New Jersey, 1983.
- [130] Diaz, J.C., A collocation-Galerkin method for the two point boundary value problem using continuous piecewise polynomial spaces, *SIAM J. Numer. Anal.*, **14**, pp. 844-858, 1977.
- [131] Domingues, J.S., Portela, A., & de Castro, P.M.S.T., Trefftz boundary element method applied to fracture mechanics, *Engrg. Fract. Mech.*, **64**, pp. 67-85, 1999.
- [132] Dong, C.Y., Lo, S.H., Cheung, Y.K. & Lee, K.Y., Anisotropic thin plate bending problem by Trefftz boundary collocation method, *Eng. Anal. Bound. Elem.*, **28**, pp. 1017-1024, 2004.
- [133] Dosiyevev, The high accurate block-grid method for solving Laplace's boundary problem with singularities, *SIAM J. Numer. Anal.*, **42**, pp. 153-178, 2004.
- [134] Douglas, J.Jr. & Huang, C.S., An accelerated domain decomposition procedure based on Robin transmission conditions, *BIT*, **37**, pp. 678-686, 1997.
- [135] Douglas, J.Jr., Leme, P.J.P., Roberts, J.E. & Wang, J., A parallel iterative procedure applicable to the approximate solution of second order partial differential equations by mixed element methods, *Numer. Math.*, **65**, pp. 95-108, 1993.
- [136] Douglas, J.Jr., Santos, J.E., Sheen, D. & Ye, X., *Nonconforming Galerkin methods based on quadrilateral elements for second order elliptic problems*, Reprint.
- [137] Dryja, M., Smith, B.F. & Widlund, O.B., Schwarz analysis of iterating substructuring alternating algorithms for elliptic problems in three dimensions, *SIAM J. Numer. Anal.*, **31**, pp. 1662-1694, 1994.
- [138] Dryja, M. & Widlund, O.B., Domain decomposition algorithms with small overlap, *SIAM*

- J. Sci. Comput.*, **15**, pp. 604-620, 1994.
- [139] Dunham, W., *Euler, The Master of Us All*, Math. Assoc. Am., 1999.
- [140] Dunn, R.J. & Wheeler, M.F., Some collocation-Galerkin methods for two-point boundary value problems, *SIAM J. Numer. Anal.*, **13**, pp. 720-733, 1977.
- [141] Ehrlich, P., Kellogg, Bliss, Hedrick—Mizzou math pioneers, *Critical Points*, **4**, Dept. Mathematics, Univ. Missouri, 1999, <http://www.math.missouri.edu/~news/issue4/pioneers.html>.
- [142] Eisenstat, S.C., On the note of convergence of the Bergman-Vekua methods for the numerical solution of elliptic boundary-value problems, *SIAM J. Numer. Anal.*, **11**, pp. 654-680, 1974.
- [143] Elliotis, M., Georgiou, G. & Xenophontos, C., *The singular function boundary integral method for a two-dimensional fracture problem*, accepted by Eng. Anal. Bound. Elem.
- [144] Elschner, J. & Graham, I., An optimal order collocation method for first kind boundary integral equations on polygons, *Numer. Math.*, **70**, pp. 1-31, 1995.
- [145] Erdogan, F. & Gupta, G.D., Numerical solution of singular integral-equations, *Quart. Appl. Math.*, **29**, pp. 525-534, 1972.
- [146] Erdogan, F., Gupta, G.D. & Cook, T.S., Numerical solution of singular integral equations, *Mechanics of Fracture 1, Methods of Analysis and Solutions of Crack Problems*, ed. G.C. Sih, Noordhoff, pp. 368-425, 1973.
- [147] Eshelby, J.D., The continuum theory of lattice defects, *Solid State Phys.*, **3**, pp. 79-114, 1956.
- [148] Euler, L., Principes généraux du mouvement des fluides, *Mém. Acad. Sci. Berlin*, **11**, pp. 274-315, 1755.
- [149] Euler, L., *Opera Omnia*, Series prima: Opera mathematica (29 volumes), Series secunda: Opera mechanica et astronomica (31 volumes), Series tertia: Opera physica, Miscellanea (12 volumes), Series quarta: A. Commercium epistolicum (10 volumes), edited by the Euler Committee of the Swiss Academy of Science, Birkhäuser, Basel, 2003.
- [150] Fairweather, G., *Finite Element Galerkin Methods for Partial Differential Equations*, Marcel Dekker, Inc., New York, 1978.
- [151] Fairweather, G. & Karageorghis, A., The method of fundamental solutions for elliptic boundary value problems, *Adv. Comput. Math.*, **9**, pp. 69-95, 1998.
- [152] Feng, K. & Yu, D.H., A theorem for the natural integral operator of harmonic equation (in Chinese), *Math. Num. Sinica*, **16**, pp. 221-226, 1994.
- [153] Fix, G.M., Hybrid finite element methods, *SIAM Review*, **18(3)**, pp. 460-485, 1976.
- [154] Fix, G.J., Gulati, S. & Wakoff, G.I., On the use of singular functions with finite element approximations, *J. Comp. Phys.*, **13**, pp. 209-238, 1973.
- [155] Fourier, J.B.J., *Théorie Analytique de la Chaleur (The Analytical Theory of Heat)*, 1822.
- [156] Fox, L., Henrici, P. & Moler, C., Approximations and bounds for eigenvalues of elliptic operators, *SIMA J. Numer. Anal.*, **4**, pp. 89-102, 1967.
- [157] Franke, R., Scattered data interpolation tests of some methods, *Math. Comp.*, **38**, pp. 181-200, 1982.
- [158] Franke, R. & Schaback, R., Solving partial differential equations by collocation using radial functions, *Appl. Math. and Comp.*, **93**, pp. 73-82, 1998.
- [159] Fredholm, I., Sur une classe d'équations fonctionnelles, *Acta. Math.*, **27**, pp. 365-390, 1903.
- [160] Friedman, M.B. & Shaw, R., Diffraction of pulse by cylindrical obstacles of arbitrary cross section, *J. Appl. Mech.*, *Trans. ASME*, **29**, pp.40-46, 1962.
- [161] Fritzius, R.S., Abbreviated biographical sketch of Walter Ritz, Appendix, *Lorentz and Poincaré Invariance—100 Years of Relativity*, eds. J.-P. Hsu & Y.-Z. Zhang, World Scientific Publ., 2003.

- [162] Ganden, M.J., Halpern, L. & Nataf, F., *Optimal convergence for overlapping and non-overlapping Schwarz waveform relaxation*, Reprint.
- [163] Gatica, G.N., Harbrecht, H. & Schneider, R., Least squares methods for the coupling of FEM and BEM, *SIAM J. Numer. Anal.*, **41**, pp. 1974-1995, 2003.
- [164] Gauss, C.F., Theoria attractionis corporum sphaeroidicorum ellipticorum homogeneorum methodo novo tractata, *Commentationes societatis regiae scientiarum Gottingensis recentiores*, **II**, pp. 2-5, 1813.
- [165] Gavelya, S.P., Periodical problems for shallow shells of arbitrary curvature with apertures, *Reports of Ukrainian Academy of Sciences*, **8**, pp. 703-708, 1969.
- [166] Gegelia, T. & Jentsch, L., Potential methods in continuum mechanics, *Georgian Mathematical Journal*, **1(6)**, pp. 599-640, 1994.
- [167] Gellert, W., Gottwald, S., Hellwich, M., Kästner, H. & Küstner, H. (eds.), *The VNR Concise Encyclopedia of Mathematics*, 2nd ed., Van Nostrand Reinhold, 1989.
- [168] Georgiou, G.C., Boudouvis, A. & Poulikkas, A., Comparison of two methods for the computation of singular solution in elliptic problem, *J. Comput. Appl. Math.*, **79**, pp. 277-289, 1997.
- [169] Georgiou, G.C., Olson, L.G. & Smyrlis, Y.S., A singular function boundary integral method for the Laplace equation, *Commun. Numer. Meth. En.*, **12**, pp. 127-134, 1996.
- [170] Gerasoulis, A., The use of piecewise quadratic polynomials for the solution of singular integral equations of the Cauchy type, *Comp. Math. Appls.*, **8**, pp. 15-22, 1982.
- [171] Gillispie, C.C., *Pierre-Simon Laplace, 1749-1827, A Life in Exact Science*, Princeton Univ. Press, 1997.
- [172] Golberg, M., Recent developments in the numerical evaluation of partial solutions in the boundary element methods, *Appl. Math. and Comp.*, **75**, pp. 91-101, 1996.
- [173] Golberg, M.A., A survey of numerical methods for integral equations, Chap. 1, *Solution Methods for Integral Equations*, ed. M.A. Golberg, Plenum, pp. 1-58, 1978.
- [174] Goldstein, C.I., The infinite element method with nonuniform mesh sizes applied to the exterior Helmholtz problem, *Numer. Math.*, **38**, pp. 61-82, 1982.
- [175] Goldstein, C.I., A finite element method for solving Helmholtz type equations in waveguides and other unbounded domains, *Math. Comp.*, **39**, pp. 309-324, 1982.
- [176] Golub, G.H. & van Loan, C.F., *Matrix Computations*, 2nd ed., The Johns Hopkins University Press, Baltimore and London, 1989.
- [177] Gorgidze, A.Y. & Rukhadze, A.K., On the numerical solution of the integral equations of the plane theory of elasticity, (in Russian), *Soobshchenia Gruz. Filiala A.N.S.S.S.R.*, **1**, pp. 255-258, 1940.
- [178] Gottlieb, D. & Orszag, S.A., *Numerical Analysis of Spectral Methods: Theory and Applications*, SIAM, Philadelphia, 1977.
- [179] Gourgeon, H. & Herrera, I., Boundary methods C-complete systems for the biharmonic equations, in *Boundary Element Methods* (Irvine, Calif., 1981), pp. 431-441, CML Publ., Springer, Berlin, 1981.
- [180] Grabiner, J.V., *The Origin of Cauchy's Rigorous Calculus*, MIT Press, 1981.
- [181] Gradshteyn, S. & Ryzhik, I. M., *Table of Integrals, Series, and Products, Corrected and Enlarged Edition*, Academic Press, New York, 1980.
- [182] Grattan-Guinness, I., *Joseph Fourier, 1768-1830*, MIT Press, 1972.
- [183] Green, G., *An Essay on the Application of Mathematical Analysis to the Theories of Electricity and Magnetism*, Printed for the Author by T. Wheelhouse, Nottigham, pp. 72, 1828. Also in, *Mathematical Papers of George Green*, Chelsea Publ. Co., pp. 1-115, 1970.
- [184] Green, G., *Mathematical Papers of George Green*, ed. N.M. Ferrers, 1871, reprinted by Chelsea Publ. Co., New York, 1970.

- [185] Greenberg, M.D., *Application of Green's Functions in Science and Engineering*, Prentice-Hall, 1971.
- [186] Grisvard, P., *Elliptic Problems in Non-smooth Domains*, Pitman Advanced Publishing Program, Boston, 1985.
- [187] Guo, B. & Cao, W., Additive Schwarz methods for the h-p version of the finite element method in two dimensions, *SIAM J. Sci. Comput.*, **18**, pp. 1267-1288, 1997.
- [188] Hadamard, J., Theorie des équations aux dérivées partielles linéaires hyperboliques et du problème de Cauchy, *Acta Math.*, **31**, pp. 333-380, 1908.
- [189] Hageman, L.A. & Young, D.M., *Applied Iterative Methods*, Academic Press Inc., 1981
- [190] Hahn, R., *Laplace as a Newtonian Scientist*, a paper delivered at a Seminar on the Newtonian Influence, Clark Library, UCLA, 1967.
- [191] Haidvogel, D.B., The accurate solution of Poisson's equation by expansion in Chebyshev polynomials, *J. Comp. Phys.*, **30**, pp. 167-180, 1979.
- [192] Hall, C.A. & Porsching, T.A., *Numerical Analysis of Partial Differential Equations*, Prentice-Hall Inc. Englewood Cliffs, New Jersey, 1990.
- [193] Han, H.D., The numerical solutions of interface problems by infinite element method, *Numer. Math.*, **39**, pp. 39-50, 1982.
- [194] Han, H.D. & Wu, X.N., Approximation of infinite boundary condition and its application to finite element methods, *J. Comp. Appl. Math.*, **3(2)**, pp. 179-192, 1985.
- [195] Harari, I. & Hughes, T.J.R., Finite element methods for the Helmholtz equation in an exterior domain: Model problems, *Comput. Method. Appl. M.*, **87**, pp. 59-96, 1991.
- [196] Hardy, R.L., Multiquadric equations of topography and other irregular surfaces, *J. of Geophysical Research*, **76**, pp. 1905-1915, 1971.
- [197] Helmholtz, H., Theorie der Luftschwingungen in Röhren mit offenen Enden, *Journal für die reine und angewandte Mathematik*, **57**, pp. 1-72, 1860.
- [198] Helmholtz, H., *Die Lehre von den Tonempfindungen*, (On the Sensations of Tone), 1863.
- [199] Herrera, I., Boundary methods, A criterion for completeness, *Proc. National Academy of Sciences, USA*, **77(8)**, pp. 4395-4398. 1980.
- [200] Herrera, I., Boundary methods: Development of complete systems of solutions, *Finite Element in Flow Analysis*, eds. T. Kawai, University of Tokyo Press, pp. 897-906. 1982.
- [201] Herrera, I., *Boundary Methods: An Algebraic Theory*, Pitman, Boston, 1984.
- [202] Herrera, I., Unified formulation of numerical methods. Part I. Green's formulas for operators in discontinuous fields, *Numer. Meth. PDE*, **1**, pp. 25-44, 1985.
- [203] Herrera, I., Trefftz-Herrera domain decomposition, *Adv. Eng. Softw.*, **24**, pp. 43-56, 1995.
- [204] Herrera, I., Trefftz method: A general theory, *Numer. Meth. PDE*, **16(6)**, pp. 561-580, 2000.
- [205] Herrera, I. & Diaz, M., Indirect methods of collocation: Trefftz-Herrera collocation, *Numer. Meth. PDE*, **15**, pp. 709-738, 1999.
- [206] Herrera, I. & Diaz, M., General theory of domain decomposition: Indirect methods, *Numer. Meth. PDE*, **18**, pp. 296-322, 2002.
- [207] Herrera, I. & Gourgeon H., Boundary methods: T-complete system for Stokes problems, *Comput. Method. Appl. M.*, **30**, pp. 225-241, 1982.
- [208] Herrera, I. & Solano, J., A non-overlapping TH-domain decomposition, *Adv. Eng. Softw.*, **28(4)**, pp. 223-229, 1997.
- [209] Hess, J.L., Review of integral-equation techniques for solving potential-flow problems with emphasis on the surface source method, *Comput. Method. Appl. M.*, **5**, pp. 145-196, 1975.
- [210] Hess, J.L. & Smith, A.M.O., Calculations of nonlifting potential flow about arbitrary three-dimensional bodies, *J. Ship Res.*, **8**, pp. 22-44, 1964.
- [211] Holst, M. & Vandewalle, S., Schwarz methods to symmetrize or not to symmetrize, *SIAM*

- J. Numer. Anal.*, **34**, pp. 699-722, 1997.
- [212] Hon, Y.C. & Schaback, R., *On unsymmetric collocation by radial basis functions*, Preprint Göttingen, 1999.
- [213] Hsu, C.H., *Biharmonic boundary value problem with singularity*, Master thesis, Department of Applied Mathematics, National Sun Yat-sen University, Kaohsiung, 2002.
- [214] Hsiao, G.C., Boundary element methods for a class of exterior singular perturbation problems, in *BAIL IV*, pp. 89-97, Boole, Dun Laoghaire, 1986.
- [215] Hsiao, G.C., Boundary element methods for exterior problems in elasticity and fluid mechanics, *The Mathematics of Finite Elements and Applications VI*, ed. Whiteman, J.R., Academic Press, London, pp. 323-341, 1988.
- [216] Hu, H.Y., *The Trefftz and collocation methods for elliptic equations*, Doctoral dissertation, Department of Applied Mathematics, National Sun Yat-sen University, Kaohsiung, June, 2003.
- [217] Hu, H.Y. & Li, Z.C., *Combinations of collocation methods for Poisson's equations*, accepted by *Comp. Math. Appls.*
- [218] Hu, H.Y. & Li, Z.C., *Collocation methods for Poisson's equation*, accepted by *Comput. Method. Appl. M.*
- [219] Hu, H.Y., Li, Z.C. & Cheng, A.H.-D., Radial basis collocation method for elliptic boundary value problem, *Comp. Math. Appls.*, **50**, pp. 289-320, 2005.
- [220] Huang, C.S. & Wang, N.C., *An accelerated domain decomposition procedure for mixed Schwarz alternating method*, Technical Report, National Sun Yat-sen University, Kaohsiung, 2003.
- [221] Huang, J., *The mechanical quadrature methods with the high accuracy and splitting extrapolations for solving boundary integral equations for the first kind of scientific and engineering problems on nonsmooth domains*, Doctoral dissertation, Mathematical College, Sichuan University, ChengDo, China, 2004.
- [222] Huang, J. & Lü, T., The mechanical quadrature methods and their extrapolation for solving BIE of Steklov eigenvalue problems, *J. Comput. Appl. Math.*, **22(5)**, pp. 719-726, 2004.
- [223] Huang, H.T., *Global superconvergence of finite element methods for elliptic equations*, Doctoral dissertation, Department of Applied Mathematics, National Sun Yat-sen University, Kaohsiung, June, 2002.
- [224] Huang, H.T. & Li, Z.C., Effective condition number and superconvergence of the Trefftz method coupled with high order FEM for singularity problems, *Eng. Anal. Bound. Elem.*, **30**, pp. 270-283, 2006.
- [225] Huang, H.T. & Li, Z.C., Global superconvergence of Adini's elements coupled with the Trefftz method for singular problems, *Eng. Anal. Bound. Elem.*, **27(3)**, pp. 227-240, 2003.
- [226] Huang, H.T., Li, Z.C. & Yan, N., New error estimates for Adini's elements, *Appl. Numer. Math.*, **50**, pp. 49-74, 2004.
- [227] Huang, H.T., Li, Z.C. & Zhou, A., New error estimates of Lagrange bi-quadratic elements, *Appl. Numer. Math.*, **56**, pp. 712-744, 2006.
- [228] Huang, S.C. & Shaw, R.P., The Trefftz method as an integral equation, *Adv. Eng. Softw.*, **24**, pp. 57-63, 1995.
- [229] Huffel, S.V. & Vandewalle, J., *The Total Least Squares Problem: Computational Aspects and Analysis*, SIAM, Philadelphia, 1991.
- [230] Ivanov, V.V., *The Theory of Approximate Methods and Their Application to the Numerical Solution of Singular Integral Equations*, Noordhoff, (Russian edition 1968), 1976.
- [231] Jaswon, M.A., *An Introduction to Mathematical Crystallography*, American Elsevier, New York, 1965.

- [232] Jaswon, M.A. & Ponter, A.R., An integral equation solution of the torsion problem, *Proc. Roy. Soc., A*, **273**, pp. 237-246, 1963.
- [233] Jaswon, M.A. & Rose, M.A., *Crystal Symmetry: Theory of Colour Crystallography*, Halsted Press, New York, 1983.
- [234] Jaswon, M.A. & Symm, G.T., *Integral Equation Methods in Potential Theory and Elastostatics*, Academic Press, 1977.
- [235] Jiang, B.N., On the least squares method, *Comput. Method. Appl. M.*, **152(1-2)**, pp. 239-257, 1998.
- [236] Jiang, S. & Li, K.T., The coupling of finite element method and boundary method for two-dimensional Helmholtz equation in an exterior domain, *J. Comput. Appl. Math.*, **5**, pp. 21-37, 1987.
- [237] Jin, W.G. & Cheung, Y.K., Trefftz direct method, *Adv. Eng. Softw.*, **24(1-3)**, pp. 65-69, 1995.
- [238] Jin, W.G., Cheung, Y.K. & Zienkiewicz, O.C., Trefftz method for Kirchoff plate bending problems, *Int. J. Numer. Meth. Engrg.*, **36(5)**, pp. 765-781, 1993.
- [239] Jirousek, J. & Guex, L., The hybrid-Trefftz finite element model and its application to plate bending, *Int. J. Numer. Meth. Engrg.*, **23**, pp. 651-693, 1986.
- [240] Jirousek, J. & Leon, N., A powerful finite element element for plate blending, *Comput. Method. Appl. M.*, **12**, pp. 77-96, 1977.
- [241] Jirousek, J. & Wróblewski, A., T-elements: A finite element approach with advantages of boundary solution methods, *Adv. Eng. Softw.*, **24**, pp. 71-88, 1995.
- [242] Jirousek, J. & Wróblewski, A., T-elements - state of the art and further trends, *Archiv. Comput. Method. Eng.*, **3**, pp. 323-424, 1995.
- [243] Jirousek, J. & Zielinski, A.P., Survey of Trefftz-type element formulations, *Computers & Structures*, **64**, pp. 225-242, 1997.
- [244] Johnson, C. & Nedelec, C., On the coupling of boundary integral and finite element methods, *Math. Comp.*, **35**, pp. 1063-1079, 1980.
- [245] Kagiwada, H. & Kalaba, R.E., *Integral Equations via Imbedding Methods*, Addison-Wesley, 1974.
- [246] Kamiya, N. & Kita, E., Trefftz method 70 years, *Adv. Eng. Softw.*, **24 (1-3)**, pp. 1, 1995.
- [247] Kansa, E.J., Multiquadrics - A scattered data approximation scheme with applications to computational fluid-dynamics - I Surface approximations and partial derivatives, *Comp. Math. Appls.*, **19(8-9)**, pp. 127-145, 1992.
- [248] Kansa, E.J., Multiquadrics - A scattered data approximation scheme with applications to computational fluid-dynamics - II Solutions to parabolic, hyperbolic and elliptic partial differential equations, *Comp. Math. Appls.*, **19(8-9)**, pp. 147-161, 1992.
- [249] Kantorovich, L.V. & Krylov, V.I., *Approximate Methods of Higher Analysis*, Wiley-Interscience Publication, New York, 1958.
- [250] Karageorghis, A., Modified methods of fundamental solutions for harmonic and biharmonic problems with boundary singularities, *Numer. Meth. PDE*, **8**, pp. 1-18, 1992.
- [251] Katsurda, M. & Okamoto, H., The collocation points of the fundamental solution method for the potential problem, *Comp. Math. Appls.*, **31**, pp. 123-137, 1996.
- [252] Katz, V.J., The history of Stokes' theorem, *Math. Mag.*, **52**, pp. 146-156, 1979.
- [253] Kellogg, O.D., *Foundations of Potential Theory*, Dover, 1953.
- [254] Kellogg, R.B., Singularities in interface problems, *Numer. Solution of PDE, II (SYNSPADE 1970)*, pp. 351-400, Academic Press, New York, 1971.
- [255] Kellogg, R.B., Higher order singularities for interface problems, *The Mathematical Foundations of the Finite Element Method with Applications to Partial Differential Equations*, ed. A.K. Aziz, pp. 589-602, Academic Press, New York, 1972.

- [256] Kellogg, R.B., On the Poisson equations with intersecting interfaces, *Appl. Anal.*, **4**, pp. 101-129, 1975.
- [257] Kelvin, W.T., Note on the integrations of the equations of equilibrium of an elastic solid, *Cambridge Dublin Math. J.*, **3**, 1848.
- [258] Kim, S.D., Lee, H.C. & Shin, B.C., Pseudospectral least-squares methods for the second-order elliptic boundary value problem, *SIAM J. Numer. Anal.*, **41**, pp. 1370-1380, 2003.
- [259] Kita, E., Kamiya, N. & Ikeda, Y., Boundary-type sensitivity analysis scheme based on indirect Trefftz formulation, *Adv. Eng. Softw.*, **24**, pp. 89-96, 1995.
- [260] Kita, E., Ikeda, Y. & Kamiya, N., Indirect Trefftz method for boundary value problem of Poisson equation, *Eng. Anal. Bound. Elem.*, **27(8)**, pp. 825-833, 2003.
- [261] Kita, E. & Kamiya, N., Trefftz method, An overview, *Adv. Eng. Softw.*, **24 (1-3)**, pp. 3-12, 1995.
- [262] Kita, E., Kamiya, N. & Iio, T., Application of a direct Trefftz method with domain decomposition to 2D potential problems, *Eng. Anal. Bound. Elem.*, **23(7)**, pp. 539-548, 1999.
- [263] Kolodziej, J., Review of application of boundary collocation methods in mechanics of continuous media, *SM Archives*, **12(4)**, pp. 187-231, 1987.
- [264] Kolosov, G.V., *On an Application of Complex Function Theory to a Plane Problem of the Mathematical Theory of Elasticity*, (in Russian), Yuriev, 1909.
- [265] Kreiss, H.O. & Olinger, J., Stability of Foirurier method, *SIAM J. Numer. Anal.*, **16**, pp. 421-433, 1979.
- [266] Krížek, M. & Neittaanmäki, P., Superconvergence phenomenon in the finite element method arising from averaging gradients, *Numer. Math.*, **45**, pp. 105-116, 1984.
- [267] Krížek, M. & Neittaanmäki, P., On a global-superconvergence of the gradient of linear triangular elements, *J. Comput. Appl. Math.*, **18**, pp. 221-233, 1987.
- [268] Kulakov, V.M. & Tolkachev, V.M., Bending of plates of an arbitrary shape, *Reports of Russian Academy of Sciences*, **230**, 1976.
- [269] Kupradze, V.D., *Potential Methods in the Theory of Elasticity*, Israeli Program for Scientific Translation, 1965. (Earlier edition: Kupradze, V.D., *Dynamical Problems in Elasticity*, **III** in *Progress in Solid Mechanics*, eds I.N. Sneddon and R. Hills, North-Holland, 1963.)
- [270] Kupradze, V.D. & Aleksidze, M.A., The method of functional equations for the approximate solution of some boundary value problems, (in Russian), *Zh. vichisl. mat. i. mat. fiz.*, **4**, pp. 683-715, 1964.
- [271] Kupradze, V.D., Gegelia, T.G., Basheleishvili, M.O. & Burchuladze, T.V., *Three-Dimensional Problems of the Mathematical Theory of Elasticity and Thermoelasticity*, (Russian edition 1976), North-Holland, 1979.
- [272] Kuttler, J.R. & Sigilloto, V.G., Eigenvalues of the Laplacian in two dimensions, *SIAM Review*, **26**, pp. 163-193, 1984.
- [273] Lachat, J.C. & Watson, J.O., Effective numerical treatment of boundary integral equations: A formulation for three-dimensional elastostatics, *Int. J. Numer. Meth. Engng.*, **10**, pp. 991-1005, 1976.
- [274] Lagrange, J.-L., *Miscellanea Taurinasia*, **2**, pp. 273, 1760-61.
- [275] Lagrange, J.-L., *Mémoires de l'Académie Royale des Sciences de Paris, Savants étrangers*, **VII**, 1773.
- [276] Laplace, P.-S., *Histoire de l'Académie des Sciences de Paris*, pp. 135, 1782/85, and pp. 252, 1787/89.
- [277] Laubin, P. & Baiwir, M., Spline collocation for a boundary integral equation on polygons with cuts, *SIAM J. Numer. Anal.*, **35**, pp. 1452-1472, 1998.
- [278] Layton, A.T., A semi-Lagrangian collocation method for the shallow water equations on the sphere, *SIAM J. Sci. Comput.*, **24**, pp. 1433-1449, 2003.

- [279] Lebesgue, H., Sur des cas d'impossibilité du problème de Dirichlet, *Comptes Rendus de la Société Mathématique de France*, **41**, pp. 17, 1913.
- [280] Lee, P., A Lagrange multiplier method for the interface equations from electromagnetic applications, *SIAM J. Numer. Anal.*, **30(2)**, pp. 478-506, 1993.
- [281] Lefebvre, D., *Solving Problems with Singularities Using Boundary Elements*, Computational Mechanics Publications, Southampton, 1989.
- [282] Leitao, V.M.A., Application of multi-region Trefftz-collocation to fracture mechanics, *Eng. Anal. Bound. Elem.*, **22(3)**, pp. 251-256, 1998.
- [283] Li, B., Fairweather, G. & Bialecki, B., Discrete-time orthogonal spline collocation methods for vibration problems, *SIAM J. Numer. Anal.*, **39**, pp. 2045-2065, 2002.
- [284] Li, Z.C., A nonconforming combined method for solving Laplace's boundary value problems with singularities, *Numer. Math.*, **49**, pp. 475-497, 1986.
- [285] Li, Z.C., *Numerical methods for elliptic boundary value problems with singularities*, Doctoral dissertation, Department of Mathematics, University of Toronto, May 1986, the 1987 Annual CAM/CAM Doctoral Dissertation Award, 1987.
- [286] Li, Z.C., A note on Kellogg's eigenfunctions of periodic Sturm-Liouville system, *Appl. Math. Letters*, **1**, pp. 123-126, 1988.
- [287] Li, Z.C., *Numerical Methods for Elliptic Equations with Singularities, Boundary Methods and Nonconforming Combinations*, World Scientific, Singapore, 1990.
- [288] Li, Z.C., The Schwarz alternating method for the singularity problems, *SIAM J. Sci. Comput.*, **15(5)**, pp. 1064-1082, 1994.
- [289] Li, Z.C., Parallel penalty combinations for singularity problems, *Eng. Anal. Bound. Elem.*, **18**, pp. 119-130, 1996.
- [290] Li, Z.C., Penalty combinations of Ritz-Galerkin and finite difference method for singularity problems, *J. Comput. Appl. Math.*, **81**, pp. 1-17, 1997.
- [291] Li, Z.C., *Combined Methods for Elliptic Equations with Singularities, Interfaces and Infinities*, Kluwer Academic Publishers, Boston, London, 1998.
- [292] Li, Z.C., Lagrange multipliers and other coupling techniques for combined methods and other coupling techniques for combined methods for elliptic equations, *Inter. J. Information*, **1(2)**, pp. 5-21, 1998.
- [293] Li, Z.C., Global superconvergence of simplified hybrid combinations for elliptic equations with singularities, I. Basic theory, *Computing*, **65**, pp. 27-44, 2000.
- [294] Li, Z.C., *Error analysis for boundary approximation methods solving eigenvalue problems*, accepted by J. Comput. Appl. Math.
- [295] Li, Z.C., *The Trefftz method for the Helmholtz equation with degeneracy*, Technical report, Department of Applied Mathematics, National Sun Yet-sen University, Kaohsiung, 2005.
- [296] Li, Z.C. & Bui, T.D., Generalized hybrid-combined methods for singularity problems of homogeneous equations, *Int. J. Numer. Meth. Engrg.*, **26**, pp. 785-803, 1988.
- [297] Li, Z.C. & Bui, T.D., Six combinations of the Ritz-Galerkin and finite element methods for elliptic boundary value problems, *Numer. Meth. PDE*, **4**, pp. 197-218, 1988.
- [298] Li, Z.C. & Bui, T.D., The simplified hybrid-combined methods for Laplace equation with singularities, *J. Comput. Appl. Math.*, **29**, pp. 171-193, 1990.
- [299] Li, Z.C. & Bui, T.D., Coupling techniques in boundary-combined methods, *Eng. Anal. Bound. Elem.*, **10**, pp. 75-85, 1992.
- [300] Li, Z.C., Chan, Y.L., Georgiou, G.C. & Xenophontos, C., Special boundary approximation methods for Laplace equation problems with boundary singularities-Applications to the Motz problem, *Computer Math. Applic*, **51**, pp. 115-142, 2006.
- [301] Li, Z.C., Chien, C.S., & Huang, H. T., *Effective condition number for finite difference method*, accepted by J. Comput. Appl. Math.

- [302] Li, Z.C., Huang, C.S. & Chen, R.C., Interior boundary conditions in the Schwarz alternating method for the Trefftz method, *Eng. Anal. Bound. Elem.*, **29**, pp. 477-493, 2005.
- [303] Li, Z.C. & Huang, H.T., Global superconvergence of simplified hybrid combinations of the Ritz-Galerkin and FEMs of elliptic equations with singularities, II. Lagrange elements and Adini's elements, *Appl. Numer. Math.*, **43**, pp. 253-273, 2002.
- [304] Li, Z.C. & Huang, H.T., Hybrid and other Trefftz methods using piecewise particular solutions, Technical report, 2005.
- [305] Li, Z.C., Huang, H.T. & Chen, J.T., Effective condition number for collocation Trefftz methods, Technical report, Department of Applied Mathematics, National Sun Yat-sen University, Kaohsiung, Taiwan, 2005.
- [306] Li, Z.C., Huang, H.T., Huang, C.S. & Lu, T.T., Effective condition number of finite difference method for Poisson's equation involving singularities, Technical report, National Sun Yat-sen University, Kaohsiung, Taiwan, 2005.
- [307] Li, Z.C., Huang, H.T., Huang, J. & Ling, L., New stability analysis for the penalty plus hybrid and the direct Trefftz methods for singularity problems, Technical report, Department of Mathematics, National Sun Yat-sen University, Kaohsiung, Taiwan, 2005.
- [308] Li, Z.C. & Liang, G.P., On the simplified hybrid-combined method, *Math. Comp.*, **41**, pp. 13-25, 1983.
- [309] Li, Z.C. & Lu, T.T., Singularities and treatments of elliptic boundary value problems, *Mathematical and Computer Modeling*, **31**, pp. 79-145, 2000.
- [310] Li, Z.C., Lu, T.T. & Hu, H.Y., Collocation Trefftz methods for biharmonic equations with crack singularities, *Eng. Anal. Bound. Elem.*, **28(1)**, pp. 79-96, 2004.
- [311] Li, Z.C., Lu, T.T., Hu, H.Y. & Cheng, A.H.-D., Particular solutions of Laplace's equations on polygons and new models involving mild singularities, *Eng. Anal. Bound. Elem.*, **29**, pp. 59-75, 2005.
- [312] Li, Z.C., Lu, T.T., Huang, H.T. & Cheng, A.H.-D., *Trefftz, collocation and other boundary methods - A comparison*, accepted by Numer. Meth. PDE.
- [313] Li, Z.C., Lu, T.T., Tsai, H.S. & Cheng, A.H.-D., The Trefftz method for solving Laplace eigenvalue problems, *Eng. Anal. Bound. Elem.*, **30**, pp. 292-308, 2006.
- [314] Li, Z.C. & Mathon, R., Boundary methods for elliptic problems on unbounded domains, *J. Comp. Phys.*, **89**, pp. 414-431, 1990.
- [315] Li, Z.C. & Mathon, R., Error and stability analysis of boundary methods for elliptic problems with interfaces, *Math. Comp.*, **54**, pp. 41-61, 1990.
- [316] Li, Z.C., Mathon, R. & Sermer, P., Boundary methods for solving elliptic problem with singularities and interfaces, *SIAM J. Numer. Anal.*, **24**, pp. 487-498, 1987.
- [317] Li, Z.C., Yamamoto, T. & Fang, Q., Superconvergence of solution derivatives for the Shortly-Weller difference approximation of Poisson's equation, Part I, smoothness problems, *J. Comput. Appl. Math.*, **151**, pp. 307-333, 2003.
- [318] Liang, G.P. & He, J.H., The non-conforming domain decomposition method for elliptic problems with Lagrangian multipliers (in Chinese), *Math. Numer. Sinica*, **14(2)**, pp. 207-215, 1992.
- [319] Liang, G.P. & Liang, P., Non-conforming domain decomposition with hybrid method, *J. Comp. Math.*, **8(4)**, pp. 363-370, 1990.
- [320] Lin, T.C., *The numerical solution of the Helmholtz's equation for the exterior Dirichlet problems in three dimensions*, *SIAM J. Numer. Anal.*, **22**, pp. 670-686, 1985.
- [321] Lin, Q. & Yan, N., *The Construction and Analysis of High Efficient FEMs* (in Chinese), Hobei University Publishing, 1996.
- [322] Lions, P.L., On the Schwarz alternating method I, *The First Inter. Symposium on Domain Decomposition Method for Partial Differential Equations*, eds. R. Glowinski et al., SIAM,

- Philadelphia, PA, pp. 1-61, 1988.
- [323] Lions, P.L., On the Schwarz alternating method II, Stochastic interpretation and order properties, *Domain Decomposition Methods*, eds. T.F. Chan et al., SIAM, Philadelphia, PA, pp. 47-70, 1989.
- [324] Lions, P.L., On the Schwarz alternating method III, A variant for non-overlapping subdomains, *Domain Decomposition Methods for Partial Differential Equations*, eds. T.F. Chan et al., SIAM, Philadelphia, PA, pp. 202-223, 1990.
- [325] Liu, J.L., Exact a posteriori error analysis of the least squares finite element method, *Appl. Math. and Comp.*, **116(3)**, pp. 297-305, 2000.
- [326] Lotz, I., *Calculation of potential flow past airship body in a yaw*, NACA TM 675, 1932.
- [327] Love, A.E.H., *A Treatise on the Mathematical Theory of Elasticity*, 4th ed., Dover, 1944.
- [328] Lu, T.T., & Li, Z.C., The cracked-beam problem by boundary approximation method, *Applied Mathematics Letters*, **28**, pp. 11-16, 2005.
- [329] Lu, T.T., Hu, H.Y. & Li, Z.C., Highly accurate solutions of Motz's and the cracked beam problems, *Eng. Anal. Bound. Elem.*, **28**, pp. 1387-1403, 2004.
- [330] Lu, T.T., Wei, Y. & Li, Z.C., Effective condition number for weighted least squares problem and Applications to the collocation Trefftz method, Technical report, Department of Mathematics, National Sun Yat-sen University, Kaohsiung, Taiwan, 2006.
- [331] Lü, T., Shin, T.M. & Liem, C., *Domain Decomposition Methods: Techniques of Numerical solution for PDE* (in Chinese), Scientific publishing, Beijing, 1992.
- [332] Lucas, T.R. & Oh, H.S., The method of auxiliary mapping for the finite element solutions of elliptic problems containing singularities, *J. Comp. Phys.*, **1108**, pp. 327 - 352, 1993.
- [333] Lucas, T.R. & Reddien, G.W., Some collocation methods for nonlinear boundary value problems, *SIAM J. Numer. Anal.*, **9**, pp. 341-356, 1972.
- [334] Ma, H. & Sun, W., A Legendre-Petrov-Galerkin and Chebyshev collocation method and the third-order Differential equations, *SIAM J. Numer. Anal.*, **38**, pp. 1425-1438, 2000.
- [335] MacKinnon, R.J. & Carey, G.F., Nodal superconvergence and solution enhancement for a class of finite-element and finite difference methods, *SIAM. J. Sci. Stat. Comput.*, **11**, pp. 343-353, 1990.
- [336] Madych, W.R., Miscellaneous error bounds for multiquadric and related interpolatory, *Comp. Math. Applic.*, **24(12)**, pp. 121-138, 1992.
- [337] Madych, W.R. & Nelson, S.A., Multivariate interpolation and conditionally positive definite functions, I, *Math. Comp.* **54**, pp. 211-230, 1990.
- [338] Mai-Duy, N. & Tran-Cong, T., Numerical solution of differential equations using multiquadric radial basis function networks, *Neural Networks*, **14**, pp. 185-199, 2001.
- [339] Mai-Duy, N. & Tran-Cong, T., Mesh-free radial basis function network methods with domain decomposition for approximation of functions and numerical solution of Poisson's equations, *Eng. Anal. Bound. Elem.*, **26**, pp. 133-156, 2002.
- [340] Mandel, J. & Tezaur, R., Convergence of a substructuring method with Lagrange multipliers, *Numer. Math.*, **73**, pp. 473-487, 1996.
- [341] Marti, J.T., *Introduction to Sobolev Spaces and Finite Element Solutions of Elliptic Boundary Value Problems*, Academic Press, London, 1986.
- [342] Massonet, C.E., Numerical use of integral procedures (Chapter 10). in *Stress Analysis*, eds. O.C. Zienkiewicz & G.S. Hollister, Wiley, pp. 198-235, 1965.
- [343] Mathew, T.P., Schwarz alternating and iterative refinement methods for mixed formulations of elliptic problems, Part I, Algorithms and numerical results, *Numer. Math.*, **65**, pp. 445-468, 1993. Part II. Theory, *Numer. Math.*, **65**, pp. 469-492, 1993.
- [344] Mathon, R. & Johnston, R.L., The approximate solutions of elliptic boundary-value problems by fundamental solutions, *SIAM J. Numer. Anal.*, **14**, pp. 638-650, 1977.

- [345] Mathon, R. & Sermer, P., Numerical solution of the Helmholtz equation, *Congressus Numerantium*, **34**, pp. 313-330, 1982.
- [346] Matsokin, A.M. & Nepomnyaschikh, S.V., A Schwarz alternating method in a subspace, *Soviet Math.*, **29**, pp. 78-84, 1985.
- [347] Maxwell, J.C., On the calculation of the equilibrium and stiffness of frames, *Phil. Mag.*, **27**, pp. 294-299, 1864.
- [348] Maz'ya, V. & Shaposhnikova, T., *Jacques Hadamard, A Universal Mathematician*, Am. Math. Soc., 1998.
- [349] Mendelson, A. & Albers, L.U., Application of boundary integral equation to elastoplastic problems, *Boundary-Integral Equation Method: Computational Applications in Applied Mechanics*, AMD **11**, eds. T.A. Cruse & F.J. Rizzo, pp. 47-84, 1975.
- [350] Mercier, B., *Numerical Analysis of Spectral Method*, Springer-Verlag, Berlin, 1989.
- [351] Mikhlin, S.G., *Integral Equations and Their Applications to Certain Problems in Mechanics, Mathematical Physics and Technology*, (1st Russian edition 1949), 2nd rev. ed., Pergamon, 1964.
- [352] Mikhlin, S.G. & Smolitsky, J.L., *Approximation Methods for the Solution of Differential and Integral Equations*, Elsevier, 1967.
- [353] Miller, J.J.H., O'Roordan, E. & Shiskin, G.I., *Fitted Numerical Methods for Singular Perturbation Problems*, World Scientific, Singapore, 1996.
- [354] Miller, K., Numerical analogy to the Schwarz alternating procedure, *Numer. Math.*, **7**, pp. 91-103, 1965.
- [355] Mitzner, K.M., Numerical solution for transient scattering from a hard surface of arbitrary shape—Retarded potential technique, *J. Acoust. Soc. Am.*, **42**, pp. 391-397, 1967.
- [356] Morse, P.M. & Feshbach, H., *Methods of Theoretical Physics*, McGraw-Hill, 1953.
- [357] Motz, M., The treatment of singularities of partial differential equations by relaxation methods, *Quart Appl. Math.*, **4**, pp. 371-377, 1947.
- [358] Muskhelishvili, N.I., On the numerical solution of the plane problems of the theory of elasticity, (in Georgian), *Trudy Tbilisskogo Matematicheskogo Instituta*, **1**, pp. 83-87, 1937.
- [359] Muskhelishvili, N.I., *Singular Integral Equations*, (Russian edition 1946), Noordhoff, 1953.
- [360] Muskhelishvili, N.I., *Some Basic Problems of the Mathematical Theory of Elasticity*, (First Russian edition 1933), Noordhoff, 1959.
- [361] Nakao, M.T., Superconvergence of the gradient of Galerkin approximations for elliptic problems, *J. Comput. Appl. Math.*, **20**, pp. 341-348, 1987.
- [362] Nataf, F. & Nier, F., *Convergence rate of some domain decomposition methods for overlapping and non-overlapping subdomains*, **75**, pp. 357-377, 1997.
- [363] Nitsche, J.A., Über ein variationsprinzip zur losung von Dirichlet problemem bei verwendung von teilraumen, die keinen randbekingungen unterworfen sind, *Adhes. Math. Sem. Univ.*, **36**, pp. 9-15, Hamburg, 1971.
- [364] O'Connor, J.J. & Robertson, E.F., *MacTutor History of Mathematics Archive*, <http://www-groups.dcs.st-and.ac.uk/history/>, 2003.
- [365] Oden, J.T. & Reddy, J.N., *An Introduction to the Mathematical Theory of Finite Elements*, John Wiley & Sons, New York, 1976.
- [366] O'Donnell, S., *William Rowan Hamilton—Portrait of a Prodigy*, Boole Press, Dublin, 1983.
- [367] Oliveira, E.R.A., Plane stress analysis by a general integral method, *J. Eng. Mech. Div., ASCE*, **94**, pp. 79-101, 1968.
- [368] Oliveira, F.A., Collocation and residual correction, *Numer. Math.*, **36**, pp. 27-31, 1980.
- [369] Olson, L.G., Georgiou, G.C. & Schultz, W.W., An efficient finite element method for treating singularities in Laplace's equations, *J. Comp. Phys.*, **96**, pp. 319-410, 1991.
- [370] Ortega, M., *Numerical Analysis, A Second Course*, SIAM, Philadelphia, 1990.

- [371] Papamichael, N. & Whiteman, J.R., A numerical conformal transformation method for harmonic mixed boundary value problems in polygonal domain, *J. Appl. Math. and Phys. (ZAMP)*, **124**, pp. 304-316, 1973.
- [372] Pavarino, L.F., Additive Schwarz methods for the p-version finite element method, *Numer. Math.*, **66**, pp. 493-515, 1994.
- [373] Parlett, B.N., *The Symmetric Eigenvalue Problems*, Prentice Hall, Inc., 1980.
- [374] Parter, S.V., Preconditioning Legendre spectral collocation methods for elliptic problems I: Finite difference operators, *SIAM J. Numer. Anal.*, **39**, pp. 330-347, 2001.
- [375] Parter, S.V., Preconditioning Legendre spectral collocation methods for elliptic problems II: Finite element operators, *SIAM J. Numer. Anal.*, **39**, pp. 348-362, 2001.
- [376] Parter, S.V. & Sun W., Spline collocation differentiation matrices, *SIAM J. Numer. Anal.*, **34**, pp. 2274-2287, 1997.
- [377] Pathria, D. & Karniadakis, G.E., Spectral element methods for Elliptic problems in non-smooth domains, *J. Comp. Phys.*, **122**, pp. 83-95, 1995.
- [378] Pehlivanov, A.I., Lazarov, R.D., Carey, C.F. & Chow, S.S., Superconvergence analysis of approximate boundary-flux calculations, *Numer. Math.*, **63**, pp. 483-501, 1992.
- [379] Percell, P. & Wheeler, M.F., A local residual finite element procedure for elliptic equations, *SIAM J. Numer. Anal.*, **15**, pp. 705-714, 1978.
- [380] Percell, P. & Wheeler, M.F., A C^1 finite element collocation method for elliptic equations, *SIAM J. Numer. Anal.*, **17**, pp. 605-622, 1980.
- [381] Piltner, R., Recent developments in the Trefftz method for finite element and boundary element applications, *Adv. Eng. Softw.*, **24**, pp. 107-115, 1995.
- [382] Piltner, R. & Taylor, R. L., The solution of plate blending problems with the aid of a boundary element algorithm based on singular complex function, in *Boundary Elements XII, Proc. 12nd World Conf. on BEM, Sapporo, Japan*, pp. 437-445 1990.
- [383] Pitkaranta, J., Boundary subspaces for the finite element method with Lagrange multipliers, *Numer. Math.*, **33**, pp. 273-289, 1979.
- [384] Pitkaranta, J., The finite element method with Lagrange multipliers for domains with corners, *Math. Comp.*, **37(155)**, pp. 13-30, 1981.
- [385] Poisson, P.-S., *Bulletin de in société philomatique*, **3**, pp. 388, 1813.
- [386] Ponter, A.R.S., An integral equation solution of the inhomogeneous torsion problem, *SIAM J. Appl. Math.*, **14**, pp. 819-830, 1966.
- [387] Portela, A. & Charafi, A., Trefftz boundary element-multi-region formulation, *Inter. J. Numer. Meth. Engrg.*, **45**, pp. 821-840, 1999.
- [388] Prager, W., Die Druckverteilung an Körpern in ebener Potentialströmung, *Physik Zeitschr.*, **29**, pp. 865, 1928.
- [389] Prenter, P.M. & Russell, R.D., Orthogonal collocation for elliptic partial differential equations, *SIAM J. Numer. Anal.*, **13**, pp. 923-939, 1976.
- [390] Proskurwsky, W. & Widlund, O., On the numerical solution of Helmholtz equation by the capacitance matrix method, *Math. Comp.*, **30**, pp. 433-468, 1976.
- [391] Qin, Q.H., *The Trefftz Finite and Boundary Element Methods*, WIT Press, Southamtopn, Boston, 2000.
- [392] Quarteroni, A. & Valli, A., *Numerical Approximation of Partial Differential Equations*, Springer-Verlag, Berlin, 1994.
- [393] Quarteroni, A. & Zampieri, E., Finite element preconditioning for Legendre spectral collocation approximations to elliptic equations and systems, *SIAM J. Numer. Anal.*, **29**, pp. 917-936, 1992.
- [394] Rankine, W.J.M., On plane water-lines in two dimensions, *Phil. Trans.*, 1864.
- [395] Raviart, P.A. & Thomas, J.M., Primal hybrid finite element methods for 2nd order elliptic

- equations, *Math. Comp.*, **31(138)**, pp. 391-413, 1977.
- [396] Rayleigh, J.W.S., *Proc. London Math. Soc.*, **4**, pp. 357-368, 1873.
- [397] Rayleigh, J.W.S., *The Theory of Sound*, (originally published in 1877), 2nd ed., **1 & 2**, Dover, 1945.
- [398] Rayleigh, R.J.S., *Life of John William Strutt, Third Baron Rayleigh*, London, 1924.
- [399] Reissner, E., On a variational theorem in elasticity, *J. Math. Phys.*, **29**, pp. 90-95, 1950.
- [400] Reutskiy, S., A boundary method of Trefftz type with approximate trial functions, *Eng. Anal. Bound. Elem.*, **26(4)**, pp. 341-353, 2002.
- [401] Ritz, W., Über eine neue methode zur Lösung gewissen variations—Problems der mathematischen physik, *J. Reine Angew. Math.*, **135**, pp. 1-61, 1908.
- [402] Rizzo, F.J., *Some integral equation methods for plane problems of classical elastostatics*, Doctoral dissertation, University of Illinois, Urbana-Champaign, pp. 34, 1964.
- [403] Rizzo, F.J., An integral equation approach to boundary value problems of classical elastostatics, *Quart. Appl. Math.*, **25**, pp. 83-95, 1967.
- [404] Rizzo, F.J., The boundary element method, some early history—a personal view, *Boundary Element Methods in Structural Analysis*, ed. D.E. Beskos, ASCE, pp. 1-16, 1989.
- [405] Rizzo, F.J., In honor of T.A. Cruse, *Tom Cruse Commemorative Issue*, eds. C.A. Brebbia & A.H.-D. Cheng, *Eng. Anal. Bound. Elem.*, **24**, pp. 703-705, 2000.
- [406] Rizzo, F.J., Springs, formulas and flatland: A path to boundary integral methods in elasticity, *Electronic J. Boundary Elements*, **1**, pp. 1-7, 2003.
- [407] Rizzo, F.J. & Shippy, D.J., Formulation and solution procedure for the general non-homogeneous elastic inclusion problem, *Int. J. Solids Structures*, **4**, pp. 1161-1179, 1968.
- [408] Rizzo, F.J. & Shippy, D.J., A method for stress determination in plane anisotropic bodies, *J. Composite Materials*, **4**, pp. 36-61, 1970.
- [409] Rizzo, F.J. & Shippy, D.J., A method of solution for certain problems of transient heat conduction, *AIAA J.*, **8**, pp. 2004-2009, 1970.
- [410] Rizzo, F.J. & Shippy, D.J., An application of the correspondence principle of linear viscoelasticity theory, *SIAM J. Appl. Math.*, **21**, pp. 321-330, 1971.
- [411] Roos, H.G., Stynes, M., & Tobiska, L., *Numerical Methods for Singularly Perturbed Differential Equations, Convection-Diffusion and Flow Problems*, Springer, 1996.
- [412] Rosser, J.B. & Papamichael, N., *A power series solution of a harmonic mixed boundary value problem*, MRC, Technical report, University of Wisconsin, 1975.
- [413] Ruge, P., *The complete Trefftz method*, ACTA Mechanica, **78(3-4)**, pp. 234-242, 1989.
- [414] Russell, R.D., Collocation for systems of boundary value problems, *Numer. Math.*, **23**, pp. 119-133, 1974.
- [415] Russell, R.D., A comparison of collocation and finite difference methods for two-point boundary value problems, *Numer. Math.*, **14**, pp. 19-39, 1977.
- [416] Russell, R.D. & Shampine, L.F., A collocation method for boundary value problems, *Numer. Math.*, **19**, pp. 1-28, 1972.
- [417] Russell, R.D. & Sun, W., Spline collocation differentiation matrices, *SIAM J. Numer. Anal.*, **34**, pp. 2274-2287, 1997.
- [418] Russo, R., A Green formulas for plane crack problems, *Boll. Un. Mat. Ital.* A(7), No. 1, pp. 59-67, 1987.
- [419] Sanchez-Sesma, F.J., Herrera, I. & Aviles, J., A boundary method for elastic wave diffraction, Application to scattering of AH-waves by surface irregularities, *Bull. Seismological Society of America*, **72**, pp. 473-490, 1982.
- [420] Saranen, J., The modified quadrature method for logarithmic-kernel integral equations on closed curves, *J. Inter. Equation Appl.*, **3**, pp. 575-600, 1991.
- [421] Saranen, J. & Sloan, I., Quadrature methods for logarithmic-kernel integral equations on

- closed curves, *IMA J. Numer. Anal.*, **12**, pp. 167-187, 1992.
- [422] Schaback, R., Error estimates and condition numbers for radial basis function interpolation, *Advances in Computational Mathematics*, **3**, pp. 251-264, 1995.
- [423] Schiff, B.D., Fishelov, D. & Whitman, J.R., Determination of a stress intensity factor using local mesh refinement, in *The Mathematics of Finite Elements and Applications III*, pp. 55-64, Eds. by J. R. Whiteman, Academic Press, London, 1979.
- [424] Schwarz, H.A., Uber einige Abbildungsaufgaben, *Ges. Math. Abh.*, **1**, pp. 65-83, 1869.
- [425] Sharlin, H.I., Kelvin, William Thomson, Baron, *Encyclopædia Britannica*, 2003.
- [426] Shaw, R.P., Diffraction of acoustic pulses by obstacles of arbitrary shape with a Robin boundary condition, *J. Acoust. Soc. Am.*, **41**, pp. 855-859, 1967.
- [427] Shaw, R.P., Boundary integral equation methods applied to water waves, *Boundary-Integral Equation Method: Computational Applications in Applied Mechanics*, AMD **11**, eds. T.A. Cruse & F.J. Rizzo, pp. 7-14, 1975.
- [428] Shaw, R.P., Huang, S.C. & Zhao, C.X., The embedding integral and the Trefftz method for potential problems with partitioning, *Eng. Anal. Bound. Elem.*, **9(1)**, pp. 83-90, 1992.
- [429] Shen, J., Efficient Spectral-Galerkin method I. Direct solvers of second- and fourth- order equations using Legendre polynomials, *SIAM. J. Sci. Comput.*, **14**, pp. 1489-1505, 1994.
- [430] Shen, J., Efficient Spectral-Galerkin method II. Direct solvers of second- and fourth- order equations using Chebyshev polynomials, *SIAM. J. Sci. Comput.*, **15**, pp. 74-87, 1995.
- [431] Shen, J., Efficient Spectral-Galerkin method III. polar and cylindrical geometries, *SIAM. J. Sci. Comput.*, **18**, pp. 1583-1604, 1997.
- [432] Shippy, D.J., Application of the boundary-integral equation method to transient phenomena in solids, In: *Boundary-Integral Equation Method: Computational Applications in Applied Mechanics*, AMD **11**, eds. T.A. Cruse & F.J. Rizzo, pp. 15-30, 1975.
- [433] Sidi, A. & Israrli, M., Quadrature methods for periodic singular Fredholm integral equation, *J. Sci. Comp.*, **3**, pp. 201-231, 1988.
- [434] Sladek, J., Sladek, V. & van Keer, R., Global and local Trefftz boundary integral formulation for sound vibration, *Adv. Eng. Softw.*, **33**, pp. 469-476, 2002.
- [435] Sloan, I. H., & Spence, A., The Galerkin method for integral equations of first-kind with logarithmic kernel: applications, *IMA J. Numer.*, **8**, pp. 123-140, 1988.
- [436] Smith, B., Bjorstad, P. & Gropp, W., *Domain Decomposition, Parallel Multilevel Methods for Elliptic Partial Differential Equations*, Cambridge University Press, 1996.
- [437] Sneddon, G.E., Second-order spectral differentiation matrices, *SIAM J. Numer. Anal.*, **33**, pp. 2468-2487, 1996.
- [438] Sobolev, S.L., *Application of Fundamental Analysis in Mathematical Physics*, AMS, Providence, RI, 1963.
- [439] Somigliana, C., Sopra l'equilibrio di un corpo elastico isotropo, *Nuovo Cimento*, **3**, pp. 17-20, 1885.
- [440] Somigliana, C., Sulla teoria delle distorsioni elastiche, *Note I e II. Atti Accad. Naz. Lincei. Classe Sci. Fis. Mat. e Nat.*, **23**, pp. 463-472, 1914.
- [441] Somigliana, C., Sulla teoria delle distorsioni elastiche, *Note I e II. Atti Accad. Naz. Lincei. Classe Sci. Fis. Mat. e Nat.*, **24**, pp. 655-666, 1915.
- [442] Stein, E., An appreciation of Erich Trefftz, *Computer Assisted Mechanics & Engineering Sciences*, **4**, pp. 301-304, 1997.
- [443] Stephan, E. P. & Wendland, W. L., An augmented Galerkin procedure for the boundary integral method applied to two-dimensional screen and crack problems, *Appl. Anal.*, **18**, pp. 183-219, 1984.
- [444] Sternberg, W.J. & Smith, T.L., *The Theory of Potential and Spherical Harmonics*, Univ. Toronto Press, 1944.

- [445] Stokes, G.G., *A Smith's Prize Paper*, Cambridge University Calendar, 1854.
- [446] Strang, G. & Fix, G.J., *An Analysis of the Finite Element Method*, Prentice-Hall, 1973.
- [447] Strenger, F., *Numerical Methods based on Sinc and Analytic Functions*, Springer-Verlag, Berlin, 1993.
- [448] Sun, W., Block iterative algorithms for solving Hermite bicubic collocation equations, *SIAM J. Numer. Anal.*, **33**, pp. 589-601, 1996.
- [449] Swartz, B. & Wendroff, B., The relation between the Galerkin and collocation methods using smooth splines, *SIAM J. Numer. Anal.*, **11**, pp. 994-996, 1974.
- [450] Swedlow, J.L. & Cruse, T.A., Formulation of boundary integral equations for three-dimensional elasto-plastic flow, *Int. J. Solids Structures*, **7**, pp. 1673-1683, 1971.
- [451] Symm, G.T., Integral equation methods in potential theory, II, *Proc. Roy. Soc., A*, **275**, pp. 33-46, 1963.
- [452] Symm, G.T., *Integral equation methods in elasticity and potential theory*, Doctoral dissertation, Imperial College, 1964.
- [453] Tang, L.D., *The Cracked-beam and Related Singularity Problems*, Master thesis, Department of Applied Mathematics, National Sun Yat-sen University, Kaohsiang, 2001.
- [454] Tazzioli, R., Green's function in some contributions of 19th century mathematicians, *Historia Mathematica*, **28**, pp. 232-252, 2001.
- [455] Thatcher, R.W., The use of infinite grid refinement at singularities in the solution of Laplace's equation, *Numer. Math.*, **25**, pp. 163-178, 1976.
- [456] Thatcher, R.W., On the finite element method for unbounded regions, *SIAM J. Numer. Anal.*, **15(3)**, pp. 466-477, 1978.
- [457] Thompson, S.P., *The Life of William Thomson, Baron Kelvin of Largs*, **1 & 2**, Macmillan, 1910.
- [458] Tikhonov, A.N. & Samarskii, A.A., *Equations of Mathematical Physics*, The MacMillan Company, New York, 1973.
- [459] Timoshenko, S.P., *History of Strength of Materials*, Dover, 1983.
- [460] Tomlin, G.R., *Numerical analysis of continuum problems in zoned anisotropic media*, Doctoral dissertation, University of Southampton, 1973.
- [461] Trefftz, E., Ein Gegenstück zum Ritz'schen Verfahren, proc, *2nd Int. Cong. Appl. Mech.*, Zurich, pp. 131-137, 1926.
- [462] Trefftz, E., Konvergenz und fehlerabschätzung beim Ritz'schen verfahren, *Math. Ann.*, **100**, pp. 503-521, 1928.
- [463] Tricomi, G.F., Matematici italiani del primo secolo dello stato unitario, *Memorie dell'Accademia delle Scienze di Torino, Classe di Scienze fisiche matematiche e naturali*, **IV,I**, 1962.
- [464] Twaites, B., (ed). *Incompressible Aerodynamics*, Oxford University Press, 1960.
- [465] Vainberg, D.V. & Sinyavskii, A.L., Application of the potential method for numerical analysis of deformation in cylindrical shells, *Reports of the Ukrainian Academy of Sciences*, **7**, pp. 907-912, 1960.
- [466] Vandrey, F., *On the calculation of the transverse potential flow past a body of revolution with the aid of the method of Mrs. Flügge-Lotz*, Astia AD40 089, 1951.
- [467] Vandrey, F., *A method for calculating the pressure distribution of a body of revolution moving in a circular path through a perfect incompressible fluid*, Aeronautical Research Council R & M, No. 3139, 1960.
- [468] Varga, R.S., *Matrix Iterative Analysis*, Prentice-Hall Inc., Englewood Cliffs, New York, 1962.
- [469] Vekua, I.N., *New Method for Solving elliptic equations*, North-Holland, Amsterdam, New York, 1967.

- [470] Vekua, N.P., *Systems of Singular Integral Equations and Some Boundary Value Problems*, Noordhoff, 1967.
- [471] Veriuzhskii, Y.V., *Numerical Potential Methods in Some Problems of Applied Mechanics*, Kiev State University Publ., 1978.
- [472] Volkov, E.A., An exponentially convergent method for the solution of Laplace's equation on polygons, *Math. USSR Sbornik*, **37(3)**, 1980.
- [473] Volkov, E.A., *Block Method for Solving the Laplace Equation and for Constructing Conformal Mappings*, CRC Press, Boca Raton, Ann Arbor, London, Tokyo, 1994.
- [474] Volkov, E.A., & Kornoukhov, A.K., On solving the Motz's problem by a block meth, *Comp. Meths. Math. Phys*, **43**, pp. 138-1391, 2003.
- [475] Volterra, V., Sulla inversione degli integrali multipli , *Atti Accad. Naz. Lincei Rend. Cl. Sci. Fis. Mat. Natur.*, **5**, pp. 289-300, 1896.
- [476] Volterra, V., Sur l'équilibre des carps élastiques multiplement connexes, *Anna. Sci. de l'École Norm. Super., Paris*, **24**, pp. 401-517, 1907.
- [477] von Kármán, T., Berechnung der druckverteilung an luftschiffkörpern *Abhandl. Aerodynamischen Inst. Tech. Hoch. Aachen*, **6**, pp. 3-13, 1927.
- [478] von Kármán, T., *Calculation of pressure distribution on airship hulls*, NACA TM 574, 1930.
- [479] von Kármán, T. (with Edson, L.), *The Wind and Beyond*, Little Brown and Co., 1967.
- [480] Wahlbin, L.L., Local behaviour in finite element method, Chap. VII., Superconvergence, *Finite Element Methods (Part I)*, eds. P.G. Ciarlet & J.L. Lions, pp. 501-522, North-Holland, 1991.
- [481] Wahlbin, L.L., *Superconvergence in Galerkin Finite Element Methods*, Lecture Notes in Mathematics, Springer, Berlin, 1995.
- [482] Washizu, K., *Variational Methods in Elasticity and Plasticity*, Pergamon, 1968.
- [483] Watson, J.O., *The analysis of stress in thick shells with holes, by integral representation with displacement*, Doctoral dissertation, University of Southampton, 1973.
- [484] Wendland, H., Meshless Galerkin methods using radial basis functions, *Math. Comp.*, **68(228)**, pp. 1521-1531, 1999.
- [485] Wendland, W.L., *Boundary element methods and their asymptotic convergence*, in *Theoretical Acoustics and Numerical Techniques*, Springer, Vienna, pp. 135-216, 1983.
- [486] Wheeler, M.F., A C^0 - collocation-finite element method for two-point boundary value problems and one space dimensional parabolic problems, *SIAM J. Numer. Anal.*, **14**, pp. 71-90, 1977.
- [487] Wheeler, M.F. & Whiteman, J.R., Superconvergent recovery of gradients on subdomains from piecewise linear finite-element approximation, *Numer. Meth. PDE*, **3**, pp. 65-82 & pp. 357-374, 1987.
- [488] Whiteman, J.R., Numerical treatment of a problem from linear fracture mechanics, *in Numerical Methods in Fracture Mechanics*, eds. D.R.J. Owen & A.R. Luxmoore, University of Wales, Swansea, pp. 128-136, 1978.
- [489] Whiteman, J.R. & Papamichael, N., Treatment of harmonic mixed boundary by conformal transformation method, *ZAMP*, **23**, pp. 655-664, 1972.
- [490] Wigley, N.M., On a method to subtract off a singularity at a corner for the Dirichlet or Neumann problem, *Math. Comp.*, **23**, pp. 395-401, 1968.
- [491] Wigley, N.M., An efficient method for subtracting off singularities at corners for Laplace's equation, *J. Comp. Phys*, **78**, pp. 368-376, 1988.
- [492] Williams, L.P., *Helmholtz, Hermann von*, Encyclopædia Britannica, 2003.
- [493] Wilkinson, J.H., *The Algebraic Eigenvalue Problems*, Oxford University Press, 1965.
- [494] Wu, Z. & Schaback, R., Local error estimates for radial basis function interpolation of

- scattered data, *IMA J. Numer. Anal.*, **13**, pp. 13-27, 1993.
- [495] Xu, J. & Zhou, A., local and parallel finite element algorithms based on the two-grid discretization, *Math. Comp.*, **69**, pp. 881-909, 2000.
- [496] Yan, Y., The collocation method for first-kind boundary integral equations on polygonal regions, *Math. Comp.*, **54**, pp. 139-154, 1990.
- [497] Yanik, E.G., A Schwarz alternating procedure using spline collection methods, *Int. J. Numer. Meth. Engrg.*, **28**, pp. 621-627, 1989.
- [498] Yi, D.H., *Natural Boundary Integral Method and its Application*, Science Press/Kluwer Academic Publishers, Beijing, Dordrecht, 2002.
- [499] Yin, G., Sinc-Collocation method with orthogonalization for singular Poisson-like problems, *Math. Comp.*, **62(205)**, pp. 21-40, 1994.
- [500] Yoon, J., Local error estimates for radial basis function interpolation of scattered data, *J. Approx. Theory*, **112(1)**, pp. 1-15, 2001.
- [501] Zheng, X.P. & Yao, Z.H., Some applications of the Trefftz method in linear elliptic boundary-value problem, *Adv. Eng. Softw.*, **24**, pp. 133-145, 1995.
- [502] Zhou, T.X. & Feng, M.F., A least squares Petrov-Galerkin finite element method for stationary Navier-Stokes equations, *Math. Comp.*, **60**, pp. 331-543, 1993.
- [503] Zieliński, A.P., Trefftz method: elastic and elastoplastic problems, *Comput. Method. Appl. M.*, **69(2)**, pp. 185-204, 1988.
- [504] Zieliński, A.P., On trial functions applied in the generalized Trefftz method, *Adv. Eng. Softw.*, **24(1-3)**, pp. 147-155, 1995.
- [505] Zieliński, A.P., Special Trefftz elements and improvements of their conditioning, *Commun. Numer. Meth. En.*, **13(10)**, pp. 765-775, 1997.
- [506] Zieliński, A.P. & Herrera, I., Trefftz method-fitting boundary conditions, *Int. J. Numer. Meth. Engrg.*, **24(5)**, pp. 871-891, 1987.
- [507] Zieliński, A.P. & Zienkiewicz, O.C., Generalized finite element analysis with T-complete boundary solution functions, *Int. J. Numer. Meth. Engrg.*, **21**, pp. 509-528, 1985.
- [508] Zienkiewicz, O.C., Kelley, D.W. & Bettess, P., The coupling of the finite element method and boundary solution procedures, *Int. J. Numer. Meth. Engrg.*, **11**, pp. 355-375, 1977.
- [509] Zienkiewicz, O.C. & Taylor, R.L., *Finite Element Method*, 5th ed., Butterworth-Heinemann, 2000.
- [510] *A survey of Muskhelishvili's scientific heritage*, <http://kr.cs.ait.ac.th/~radok/mus/mus10.htm>, 2003.
- [511] *Niko Muskhelishvili, Curriculum Vitae*, <http://www.rmi.acnet.ge/person/muskhel/>, 2003.
- [512] *Science Citation Index Expanded, the Web of Science*, Institute for Scientific Information, <http://www.isinet.com/isi/products/citation/scie/index.html>, 2003.

Glossary of Symbols

- BAM* : the boundary approximation method.
- BEM* : the boundary element method.
- BIE* : the boundary integral equation.
- BIEM* : the boundary integral equation method.
- CM* : the collocation method.
- CTM* : the collocation Trefftz method.
- D-D, N-N, D-N* : the Dirichlet and Neumann conditions are assigned to two edges of a sector.
- DDM* : the domain decomposition method.
- FDM* : the finite difference method.
- FEM* : the finite element method.
- FEM-CM* : the combinations of the finite element and the collocation methods.
- FEM-RBCM* : the combination of the FEM and the RBCM.
- FVM* : the finite volume method.
- GRB* : the Gaussian radial basis functions.
- GTM* : the generalized Trefftz method.
- I.B.C.* : the interior boundary condition.
- IMQRB* : the inverse multiquadratic radial basis functions.
- LSM* : the least squares method.
- Models I, II* : the models of the biharmonic equations with the crack singularities.
- Model III* : the model of Schiff et al. [423] in the rectangle
 $S = \{ (x, y) \mid -1 < x < 1, 0 < y < 1 \}$ with the Dirichlet boundary condition.
- PDE* : the partial differential equation.
- RBCM* : the collocation method using the radial basis functions, or the radial basis collocation method.
- RBF* : the radial basis functions.
- RGM* : the Ritz-Galerkin method.
- SAM* : the Schwarz alternating method.
- TM* : the Trefftz method.
- C* : a positive bounded constant.
- D_l : the expansion coefficients.
- \widetilde{D}_l : the approximate coefficient of D_l .
- P_c : the penalty constant.

S : the solution domain.

S^+ : the subdomain of S possibly involving solution singularities.

S^- : another subdomain of S with smooth solutions.

$S_h = (\cup_{ij} \square_{ij}) \cup (\cup_{ij} \triangle_{ij})$: the partition of S .

u : the true solution.

u_I : the interpolant of u .

u_h, \widetilde{u}_h : the approximate solutions.

V_h : a finite dimensional subspace, $V_h \subset H^1(S)$.

V_h^0 : a finite dimensional subspace, $V_h^0 \subset H_1^0(S)$.

ω : the weight constant.

Γ : the exterior boundary of the solution domain.

Γ_D : the exterior boundary with the Dirichlet boundary condition.

Γ_N : the exterior boundary with the Neumann boundary condition.

Γ_0 : the interface boundary, artificial or material.

α, β : coupling parameters.

σ : penalty power.

λ : Lagrange multiplier.

λ_{\max} : the maximal eigenvalue.

λ_{\min} : the minimal eigenvalue.

$\widehat{\int}, \widehat{\iint}$: approximation of the integrals \int, \iint .

$u = f_L + R_L$: the solution expansion.

$f_L = \sum_{i=1}^L a_i \phi_i$: the leading terms.

$R_L = \sum_{i=L+1}^{\infty} a_i \phi_i$: the remainder.

$Cond.(\mathbf{A}) = \left\{ \frac{\lambda_{Max}(\mathbf{A})}{\lambda_{Min}(\mathbf{A})} \right\}$: the traditional condition number of the symmetric and positive definite matrix \mathbf{A} .

$I_\mu(r) = \sum_{k=0}^{\infty} \frac{1}{\Gamma(k+1)\Gamma(k+\mu+1)} \left(\frac{r}{2}\right)^{2k+\mu}$: the Bessel functions for a purely imaginary argument.

$K_n(\rho) = \frac{1}{2} \int_{-\infty}^{\infty} e^{-\rho \cosh \eta - n\eta} d\eta$: the Hankel functions for a purely imaginary argument.

$J_\mu(r) = \sum_{k=1}^{\infty} \frac{(-1)^k}{\Gamma(k+1)\Gamma(k+\mu+1)} \left(\frac{r}{2}\right)^{2k+\mu}$: the Bessel functions of the first kind.

$H_\mu^{(1)}(r) = \frac{i}{\sin(\mu\pi)} \{ \exp(-\mu\pi i) J_\mu(r) - J_{-\mu}(r) \}$: the Hankel functions of the first kind.

$\omega = \frac{1}{2\pi} \ln \frac{1}{r}$, $r = \sqrt{(x-x_0)^2 + (y-y_0)^2}$, $M_0 = (x_0, y_0) \in S$: the fundamental solution of the

Laplace equation.

$K(r, \theta, \xi) = \frac{1-r^2}{2\pi} \frac{1}{1-2r \cos(\theta-\xi)+r^2}$: Poisson's kernel.

$T_i(x) = \cos(i \arccos(x))$, $-1 \leq x \leq 1$: the Chebyshev polynomial.

$\mathbf{Ax} = \mathbf{b}$: the linear algebraic equation, where $\mathbf{A} \in R^{n \times n}$ is symmetric and positive definite,

$\mathbf{x} \in R^n$ and $\mathbf{b} \in R^n$ are the unknown and known vectors, respectively.

$\mathbf{Fx} = \mathbf{b}$: the over-determined system : $\mathbf{F} \in R^{m \times n}$ ($m \geq n$) is the stiffness matrix, $\mathbf{x} \in R^n$ and

$\mathbf{b} \in R^m$ are the unknown and known vectors, respectively.

$\mathbf{F} = \mathbf{U}\mathbf{\Sigma}\mathbf{V}^T$: the singular value decomposition for matrix $\mathbf{F} \in R^{m \times n}$, where $\mathbf{\Sigma} \in R^{m \times n}$ is a

diagonal matrix with the singular values $\sigma_i \geq 0$, $i = 1, 2, \dots, n$, $\mathbf{U} \in R^{m \times m}$ and

$\mathbf{V} \in R^{n \times n}$ are two orthogonal matrices.

$\text{Cond.} = \frac{\sigma_1}{\sigma_n}$: the traditional condition number in the 2-norm.

$\text{Cond. eff} = \frac{\|\mathbf{b}\|}{\sigma_n \|\mathbf{x}\|} = \frac{\|\mathbf{b}\|}{\sigma_n \sqrt{\sum_{i=1}^n (\frac{\beta_i}{\sigma_i})^2}}$: the effective condition number, where $\beta_i = \mathbf{u}_i^T \mathbf{b}$, \mathbf{u}_i

are

given in $\mathbf{U} = \{\mathbf{u}_1, \mathbf{u}_2, \dots, \mathbf{u}_n\}$ of the singular value decomposition for matrix

\mathbf{A}

(or \mathbf{F}), σ_n is the minimal singular value, \mathbf{x} and \mathbf{b} are unknown and known

vectors

respectively in $\mathbf{Ax} = \mathbf{b}$ (or $\mathbf{Fx} = \mathbf{b}$).

$\text{Cond. eff} = \frac{\|\mathbf{b}\|}{\sigma_n \|\tilde{\mathbf{x}}\|}$: the a posteriori effective condition number, where $\tilde{\mathbf{x}}$ is the approximate

solution from $\mathbf{Ax} = \mathbf{b}$ (or $\mathbf{Fx} = \mathbf{b}$).

$\text{Cond. E} = \frac{\|\mathbf{b}\|}{\sqrt{\frac{\|\mathbf{b}\| - \beta_n^2}{\text{Cond.}^2} + \beta_n^2}}$: the simplified effective condition for $\mathbf{Ax} = \mathbf{b}$, where $\beta_n = \mathbf{u}_n^T \mathbf{b}$.

$\text{Cond. E} = \frac{\|\mathbf{b}\|}{\sqrt{\frac{\|\mathbf{F}\mathbf{x}\|^2 - \beta_n^2}{\text{Cond.}^2} + \beta_n^2}}$: the simplified effective condition number for $\mathbf{Fx} = \mathbf{b}$, where $\beta_n = \mathbf{u}_n^T \mathbf{b}$.

$\text{Cond. EE} = \frac{\|\mathbf{b}\|}{|\beta_n|}$: the simplest effective condition number, where $\beta_n = \mathbf{u}_n^T \mathbf{b}$.

$L + 1 = O(|\ln h|)$: the coupling relation in combinations.

$\text{span} \{\psi_i\}$: to be spanned by the basis functions ψ_i .

$u_\nu = \frac{\partial u}{\partial \nu}$: the normal derivative of u .

$\Delta = \frac{\partial^2}{\partial x^2} + \frac{\partial^2}{\partial y^2}$: the Laplace operator.

$\Delta \sqrt{\lambda_{min}} = \sqrt{\lambda_{min}} - \sqrt{\tilde{\lambda}_{min}}$.

$\Delta D_i = D_i - \tilde{D}_i$.

$\varepsilon = u - u_n$.

$u^+ = u|_{S^+}$ or $u^+ = u|_{S_2}$.

$$u^- = u|_{S^-} \text{ or } u^- = u|_{S_1}.$$

$$H^1(S) = \{v, v_x, v_y \in L^2(S)\}.$$

$$H_0^1(S) = \{v, v_x, v_y \in L^2(S), \text{ and } v|_{\Gamma_D} = 0\}.$$

$$H_*^1(S) = \{v, v_x, v_y \in L^2(S), \text{ and } v|_{\Gamma_D} = g\}.$$

$$\max_S |\epsilon| = \|\epsilon\|_{\infty, S}.$$

$$\delta = \min_i \left| \frac{k^2 - \lambda_i}{k^2} \right|.$$

$$\|v\|_{l, \partial S} = \left[\sum_{|\alpha| \leq l} \int_{\partial S} \left(\frac{\partial^\alpha v}{\partial s^\alpha} \right)^2 dl \right]^{\frac{1}{2}}.$$

$$|v|_{l, \partial S} = \left[\sum_{|\alpha|=l} \int_{\partial S} \left(\frac{\partial^\alpha v}{\partial s^\alpha} \right)^2 dl \right]^{\frac{1}{2}}.$$

$$\|v\|_{m, S} = \left\{ \sum_{|\alpha| \leq m} \int_S |D^\alpha v|^2 dx \right\}^{\frac{1}{2}}.$$

$$|v|_{m, S} = \left\{ \sum_{|\alpha|=m} \int_S |D^\alpha v|^2 dx \right\}^{\frac{1}{2}}.$$

$$\|v\|_1 = \left\{ \|v\|_{1, S^+}^2 + \|v\|_{1, S^-}^2 \right\}^{\frac{1}{2}}.$$

$$|v|_1 = \left\{ |v|_{1, S^+}^2 + |v|_{1, S^-}^2 \right\}^{\frac{1}{2}}.$$

$$|v|_H = \{ |v|_{1, \Omega^+}^2 + |v|_{1, \Omega^-}^2 \}^{\frac{1}{2}}.$$

$$\|v\|_H = \{ \|v\|_{1, \Omega^+}^2 + \|v\|_{1, \Omega^-}^2 \}^{\frac{1}{2}} \text{ or } \|v\|_H = \left(\|u\|_{1, S_1}^2 + \|u\|_{1, S_2}^2 + \frac{1}{h^\sigma} \|u^+ - u^-\|_{0, \Gamma_0}^2 \right)^{\frac{1}{2}}.$$

$$\|v\|_B = \{ \int_{\Gamma_D} v^2 dl + \int_{\Gamma_N} v_\nu^2 dl \}^{\frac{1}{2}}.$$

$$\|v\|_{\tilde{B}} = \{ \tilde{\int}_{\Gamma_D} v^2 dl + \tilde{\int}_{\Gamma_N} v_\nu^2 dl \}^{\frac{1}{2}}.$$

$$|\epsilon|_2 = \{ |\epsilon|_{0, \overline{BC}}^2 + \sigma^2 |\epsilon|_{0, \overline{AB}}^2 \}^{\frac{1}{2}}.$$

$$|\epsilon|_{II} = \{ |v^+ - v^-|_{0, \Gamma_0}^2 + \sigma^2 |u_\nu^+ - u_\nu^-|_{0, \Gamma_0}^2 \}^{\frac{1}{2}}.$$

$$\overline{\|v^+ - v^-\|_{0, \Gamma_0}} = \left(\widehat{\int}_{\Gamma_0} (v^+ - v^-)^2 dl \right)^{\frac{1}{2}}.$$

$$\|v\|_{\frac{1}{2}, \Gamma_0} = \left(\|v\|_{0, \Gamma_0}^2 + \int_{\Gamma_0} \int_{\Gamma_0} \frac{(v(P) - v(Q))^2}{(P - Q)^2} dl(Q) dl(P) \right)^{\frac{1}{2}}.$$

$$\|u\|_{-\frac{1}{2}, \Gamma_0} = \sup_v \frac{\left| \int_{\Gamma_0} uv dl \right|}{\|v\|_{\frac{1}{2}, \Gamma_0}}.$$

Index

- p*-order Lagrange polynomial interpolant, 302
- p*-order polynomial, 304
- p*-order polynomial interpolant, 303
- p*-rectangle, 297, 308
- p*-version, 186
- p*(≥ 2)-rectangle, 297, 300, 301, 316
- 2-order rectangle, 311

- Académie des Sciences, 434
- acoustics, 430
- Adhémar Jean Claude Barré de Saint-Venant, 431
- Adini's element, 297, 298, 311–314, 316–318
- Adrien-Marie Legendre, 430
- affine transformation, 67, 78
- aircraft structure, 448
- Albert Einstein, 447
- Aleksandr Mikhailovich Lyapunov, 449
- Alexander von Humboldt, 425
- algebraic approach, 18
- André Marie Ampère, 433
- approximability property, 40, 47
- associated least squares matrix, 37
- astronomy, 429
- Augustin-Louis Cauchy, 430, 433

- bending moment, 141
- Bergman-Vekua space, 47
- Berlin Academy, 420
- Bernhard Riemann, 434
- bi-*p*-order Lagrange polynomial, 300
- bi-*p*-order Lagrange polynomial interpolant, 298
- bi-Lagrange, 297
- bi-Lagrange *p*-order, 242

- biharmonic solution, 140
- bilinear element, 297
- boundary blending moment, 140
- boundary contour, 450
- boundary layer singularity, 20
- boundary solution procedure, 3
- boundary-type solution procedure, 33
- Bramble-Hilbert lemma, 206

- Carl Friedrich Gauss, 420, 428
- Carl Gottfried Neumann, 424, 426
- Carl Gustav Jacobi, 423
- Carle David Tolmé Runge, 448
- Carlo Somigliana, 437, 442
- Carlos Alberto Brebbia, 459
- Cartesian coordinate, 147
- Cartesian coordinate system, 78
- Cartesian form, 419
- Cauchy principal values, 432
- celestial mechanics, 421
- central rule, 28, 61, 64, 65, 67, 97, 145, 150, 359
- Charles Emile Picard, 435
- Charles Hermite, 434
- Chebyshev polynomial, 111, 161, 178, 184, 187
- clamped crack, 144
- Claude Louis Marie Henri Navier, 431
- collocation node, 183
- combined algorithm, 300
- complex variable potential, 438
- computer complexity, 68
- concave polygon, 397
- condition
 - clamped boundary condition, 13, 133, 141, 149, 151

- clamped condition, 140–144, 151, 153
- corner condition, 141, 145, 150, 151
- Dirichlet boundary condition, 161, 164, 174, 190, 221, 242, 283–288, 311, 312, 377, 378, 406, 431, 452
- Dirichlet condition, 64, 246, 425
- Dirichlet-Neumann boundary condition, 283, 377, 380, 392, 405, 407, 408
- Dirichlet-Neumann mixed boundary condition, 406
- exterior boundary condition, 28, 33, 37, 46, 47, 133, 140, 321
- exterior Dirichlet-Neumann boundary condition, 402
- interior boundary condition, 28, 34, 46, 133, 150, 242, 321
- interior continuity condition, 37
- interior Dirichlet boundary condition, 284
- interior jump condition, 20
- interior Neumann boundary condition, 283
- interior Robin boundary condition, 283
- Ladyzhenskaya-Babuska-Brezzi condition, 28, 112, 113, 270
- mixed Dirichlet-Neumann condition, 57
- natural boundary condition, 17, 139, 141
- natural condition, 142
- natural corner condition, 142
- Neumann boundary condition, 161, 164, 174, 177, 242, 283, 284, 286–288, 312, 377, 406, 432, 446
- Neumann condition, 246, 425
- Neumann-Dirichlet boundary condition, 61, 62
- Robin boundary condition, 4, 161, 164, 174, 177, 185, 214, 242, 283, 284, 286, 288, 290
- Robin condition, 4, 246, 425
- Robin-Dirichlet boundary condition, 291
- simply supported condition, 140–143, 153
- Sommerfeld radiation condition, 11
- symmetric condition, 140, 141, 153
- condition number, 51, 116
- convection-dominant flow, 20
- corner effect, 136
- corner singularity, 151
- corner term, 133, 136, 140, 141
- CPU, 28, 241
- crack model, 133, 134, 142, 150, 152
- crack plus mild singularity, 378, 395, 406
- crack singularity, 33, 34, 133, 395
- cracked beam, 38, 76, 82, 242, 346
- cracked domain, 406
- Creator, 421
- crystalline structure, 454
- cubic spline, 2
- D'Alembert, 420
- D-D type, 380, 396
- D-N type, 380, 388, 391, 393, 396
- Daniel, 420
- Darcy law, 418
- David Hilbert, 426
- degeneracy, 241, 242, 323, 325, 350, 361
- dipole, 446
- Dirichlet, 12, 15–17, 24–26
- Dirichlet principle, 426
- Dirichlet type, 451
- disclination, 437
- discontinuity, 402
- discontinuity model, 399
- discontinuity singularity, 395
- discontinuous, 396
- disk, 82
- dislocation solution of elasticity, 437
- displacement discontinuity, 437
- dissimilar material, 454
- distribution density, 433, 446
- distribution density vector, 437, 438
- divergence series, 434
- domain decomposition, 28, 51
- double integrals, 430

- double layer of density, 25
- double-layer potential, 432, 453
- doublet, 446

- Edward John Routh, 441
- effective condition number, 116, 212
- elastic plate, 133
- elasticity, 420, 430
- electrodynamics, 426, 430
- electromagnetic theory of light, 441
- electromagnetism, 429
- elliptic operator, 373
- empirical asymptotes, 80
- empirical exponential convergent, 77
- energy conservation, 418
- Enrico Betti, 436, 440
- equation
 - algebraic normal equation, 6
 - biharmonic equation, 11, 13, 33, 34, 133, 134, 140, 141, 151
 - boundary integral equation, 26, 424, 450, 456, 457, 459
 - Debye–Huckel equation, 11, 46, 47
 - elliptic equation, 27, 37
 - Fredholm equation, 26
 - Fredholm integral equation, 417, 451
 - Helmholtz equation, 11, 12, 241, 242, 330, 332, 336, 341, 342, 361, 364, 367, 375, 436, 450
 - hyperbolic equation, 9, 241
 - integral equation, 431, 454
 - Laplace equation, 10, 16, 21, 24–26, 61, 63, 75, 78, 365, 378, 406, 418
 - Laplace solution, 83
 - Navier–Stokes equation, 431
 - nonlinear equation, 327
 - normal equation, 7, 68
 - parabolic equation, 241
 - piecewise Laplace equation, 376
 - Poisson’s equation, 21, 98, 177, 184, 221, 311, 406, 422
 - reduced wave equation, 362
 - scalar wave equation, 450
 - self-adjoint elliptic equation, 37
 - Somigliana integral equation, 438
 - variational equation, 17
 - vector integral equation, 453
- Erich Trefftz, 444, 448
- Erik Ivar Fredholm, 426, 435
- Euclidean norm, 25, 325, 375
- Eugenio Beltrami, 442
- Euler, 420
- existence, 41
- explicit kernel, 24
- exponentially convergent rate, 186
- exterior boundary, 26
- external potential flow, 451

- Felix Christian Klein, 448
- first-order system, 9
- floating point number, 69
- flop, 68
- formula
 - Cauchy integral formula, 433
 - Green’s formula, 21, 99, 133, 134, 138–140, 145, 148, 149, 151, 217, 251, 427, 436, 437
- Fortran program, 69
- Fourier analysis, 422
- Fourier law, 418
- Fourier series, 426
- Fourier transform, 226, 227
- fourth order PDE, 133
- Frank Joseph Rizzo, 456, 459
- Franz Neumann, 426
- Frederick the Great, 420
- Fredholm integral equation of the second kind, 26, 431, 451, 452
- French Empire, 425
- Friedrich Wilhelm Bessel, 426
- function
 - Bessel function, 11, 54, 337, 371
 - delta function, 3
 - density function, 26
 - Dirac delta function, 445, 450
 - Fourier function, 2
 - fundamental function, 24, 84
 - Gaussian function, 213
 - Gaussian radial basis function, 183
 - Green’s function, 417
 - Hankel function, 11, 450

- harmonic function, 24, 241, 426
- inverse multiquadric radial basis function, 183, 184
- Kellogg's function, 47
- Kellogg's singular function, 47
- kernel function, 452
- multiquadric function, 226
- potential function, 419
- radial basis function, 142, 182, 183, 185, 211, 212, 214
- Sinc function, 142, 161, 229
- singular function, 84
- stream function, 446
- trial function, 47
- trigonometric function, 45, 81, 374
- unique function, 41
- fundamental solution, 21, 95, 419, 437, 445, 453
- Fundamental Theorem of Algebra, 428
- Galerkin scheme, 425
- Gaspard Monge, 422
- Gauss-Lobatto node, 4, 10
- Gaussian elimination, 64, 68, 197, 223
- Gaussian rule, 28, 34, 61, 63, 64, 67, 69, 74, 77, 82, 83, 89, 97, 122, 124, 126–128, 130, 131, 134, 207, 342, 404, 411, 412
- geodesic, 435
- geophysical determination, 441
- Georg Simon Ohm, 425
- George Gabriel Stokes, 428, 430
- George Green, 419, 428, 429
- Gesellschaft für Angewandte Mathematik und Mechanik, 449
- global, 297
- global interior pointwise, 297
- global superconvergence, 297, 303
- global target, 66
- Grand Prix, 434
- Grand Prize, 422
- Green theory, 254
- Green's formality, 456
- Green's identity, 417, 424, 428
- Green's second identity, 439, 450
- Green's third identity, 451
- Grenoble, 422
- Gury Vasilievich Kolosov, 438, 443
- Hadamard finite part, 433
- half-disk, 82
- half-disk domain, 80
- Hamilton, 423
- Hamilton-Jacobi Principle, 423
- Helmholtz solution, 242, 361, 365, 369, 373
- Henri Léon Lebesgue, 425
- Hermann Ludwig Ferdinand von Helmholtz, 436, 439
- Hermite element, 28
- Householder orthogonalization, 68
- hybrid integral, 302
- hydrodynamic similarity theory, 441
- hydrodynamics, 420, 430, 431
- hypersingularity, 433
- Ilia Nestorovich Vekua, 452
- ill-conditioning, 37
- IMSL subroutine
 - DEVESF, 120
 - IMSL subroutines, 120
- incompressible fluids, 431
- incompressible substance, 418
- inequality
 - V_h - elliptic inequality, 185, 212, 221
 - V_h^0 - elliptic inequality, 225
 - Hölder's inequality, 41
 - bilinear inequality, 404
 - inverse inequality, 162, 182, 200, 209, 304, 308, 369
 - Minkowski inequality, 43
 - Parseval's inequality, 334, 367
 - Poincare-Friedrichs inequality, 112, 366
 - Schwarz inequality, 42, 109, 252, 366
 - uniformly V_h - elliptic inequality, 10, 162–164, 170–172, 176, 178, 219, 404
 - uniformly V_h^0 - elliptic inequality, 189, 199, 204, 208–210, 225
 - uniformly $V_{L,N}$ - inequality, 262
- infinite element, 47

- integral approximation, 70
- integral equation representation, 438
- interface on unbounded domain, 321
- interface singularity, 46
- interior boundary, 26, 283, 285
- interior crack, 133
- interpolation theory, 373
- inverse estimate, 226, 228
- inverse property, 40–43, 47–51, 70, 365, 366, 368, 369
- inverse transformation, 182
- Irwin Schrödinger, 423
- Isaac Newton, 419

- Jacques Charles François Sturm, 430
- Jacques Philippe Marie Binet, 434
- Jacques Salomon Hadamard, 433, 434, 442
- James Clerk Maxwell, 430
- James Thomson, 440
- Jean Baptiste Joseph Fourier, 418, 421
- Jean le Rond D’Alembert, 421
- Jean Marie Constant Duhamel, 431
- Jean-Baptiste Biot, 434
- Jesuit College in Cologne, 425
- Johann Bernoulli, 420
- Johann Peter Gustav Lejeune Dirichlet, 423, 425
- John William Strutt, 436, 441
- Joseph Liouville, 430
- Joseph-Louis Lagrange, 419, 420
- Jules Henri Poincaré, 427
- Julian Seymour Schwinger, 430

- L-shaped, 377, 398
- L-shaped domain, 394
- Lagrange, 27, 422
- Lagrange interpolant, 193
- Lagrange interpolation polynomial, 14
- Lagrange multiplier, 16, 17, 111, 129
- Lagrange multiplier coupling, 17, 248
- Lagrange polynomial, 191, 221
- Lagrange rectangle, 297
- Laplace, 422, 427
- Laplace solution, 24, 78, 84, 330
- Laplace transform, 421

- Laplace’s operator, 11
- Laplacian solution, 57, 109, 283, 284, 286, 290
- least squares procedure, 50
- least squares solution, 68
- Legendre polynomial, 179, 195, 308
- Legendre-Gauss rule, 195, 207, 209, 215, 223
- Leonhard Euler, 419
- Leopold Kronecker, 426
- Liapunov surface, 425, 431, 432
- linear element, 297
- linear transformation, 180, 181
- Lipschitz surface, 425
- local interior pointwise, 297
- logarithmic potential, 426
- Lord Kelvin, 429, 440
- Lord Rayleigh, 436
- Louis Poincot, 433
- Ludwig Prandtl, 448

- magnetism, 430
- Magnus Gösta Mittag-Leffler, 435
- mass conservation, 418
- material interface, 37
- Mathematica, 69, 76, 79, 121, 151, 212, 350
- matrix eigenvalue, 322
- Maurice Aaron Jaswon, 451, 455
- maximum principle, 37, 283
- mechanics, 429
- method
 - h - p version of FEM, 47
 - p - version FEM, 405
 - block method, 24, 378
 - boundary approximation method, 5, 33, 62
 - boundary element method, 16, 33, 95, 115, 116, 133, 458
 - boundary integral equation method, 457
 - boundary method, 444
 - Brent’s method, 345
 - classic overlapping Schwarz alternating method, 283

- classical Schwarz alternating method, 284
- collocation method, 189, 190, 192, 193, 209
- collocation Trefftz method, 121–125, 245, 246, 268, 271, 274, 406, 411
- combined method, 47
- conformal transformation method, 38, 58, 63
- direct method, 84, 433
- direct Trefftz method, 1, 17, 28, 114, 116, 122, 124, 128, 245, 248
- domain method, 444
- double-layer method, 433
- FEM-RBCM, 222
- finite difference method, 46, 417
- finite element method, 46, 189, 190, 192, 193, 209
- Galerkin-FEM, 1, 4, 10
- Gaussian radial basis collocation method, 187
- generalized Trefftz method, 124
- high order finite element method, 241
- Householder QR method, 68
- hybrid Trefftz method, 97, 104, 111, 122–126, 245, 247, 254, 255, 258, 268, 271, 275, 276
- indirect method, 84, 433
- indirect TM, 33
- indirect Trefftz method, 1, 3, 7, 114, 245
- inverse multiquadric radial basis collocation method, 187
- inverse power method, 120
- Kupradze's method, 456
- Lagrange finite element method, 14, 298
- Lagrange multiplier method, 17, 97, 111
- Lagrange multiplier Trefftz method, 97, 116, 124, 248, 268, 269
- least squares method, 3, 7, 8, 10, 61, 185, 189, 198, 216, 327
- mixed and hybrid method, 17
- mixed overlapping Schwarz alternating method, 289
- mixed Schwarz alternating method, 283, 284, 287, 290
- modified Muller's method, 329
- Muller's method, 329, 345, 351
- multiplier method, 112
- natural boundary element method, 23
- non-overlapping Schwarz alternating method, 283
- normal method, 65
- original Trefftz method, 1, 16, 126, 247
- penalty plus hybrid combined method, 309
- penalty plus hybrid Trefftz method, 97, 100, 110, 111, 114, 122–125, 127, 263, 266, 268, 271, 276
- penalty Trefftz method, 97, 100, 102, 111
- potential method, 453
- power method, 120
- QR method, 8, 68, 328, 364
- radial basis collocation method, 162, 212, 214–216, 219, 220, 226
- relaxation method, 61
- residual method, 3
- Ritz method, 443, 444
- Ritz-Galerkin method, 98, 189, 212, 214, 215, 226
- Ritz-Galerkin-FEM, 193
- Schwarz alternating method, 24, 241, 242, 246, 283, 377, 378, 406, 407
- secant method, 329, 345
- simplified hybrid Combined method, 15
- simplified hybrid method, 16, 28, 267
- simplified hybrid Trefftz method, 100, 104, 241
- Sinc-collocation method, 161
- single-layer method, 433, 438, 451
- singular value decomposition method, 8
- spectral method, 117, 189, 212

- substructuring iteration method, 283
- symmetric hybrid Trefftz method, 242, 276
- Trefftz method, 117, 298, 312, 313, 351, 362, 375, 445
- Trefftz-Herrera method, 28
- weighted least squares method, 46
- Mikhail Vasilevich Ostrogradski, 427, 430
- mild corner singularity, 152
- mild singularity, 151, 241, 377, 381, 395, 398, 405
- minimal energy, 141
- mirror-galvanometer, 441
- mixed type, 98
- Model I, 142, 143, 145
- Model II, 143, 150
- Model III, 144, 151
- modern aerospace science, 448
- multiple singularity, 321
- multiquadrics, 213

- N-D type, 380, 386, 391, 393, 396
- N-N type, 380, 389, 391, 396
- Napoleon, 422
- Napoleon Bonaparte, 421
- Natural Corner, 146
- Navier-Stokes, 9
- Neumann, 12, 26
- Newton, 421
- Newton of France, 421
- Newton-Cotes, 225
- Newton-Cotes rule, 64, 207, 215, 221, 223
- Nicolaus, 420
- Nikolai Ivanovich Muskhelishvili, 438, 449
- Nikolai Petrovich Vekua, 452
- non-overlapping, 283, 285, 293
- nonconforming combination, 15
- Nottingham Subscription Library, 429
- nuclei of strain, 437

- Oliver Dimon Kellogg, 424, 426
- optimal truncation error, 404
- orthogonal polynomial, 2, 4, 226
- orthogonal system, 45
- orthogonality, 45, 55, 81, 308, 334, 363, 374
- orthogonality property, 322
- Ostrogradsky, 449
- over-determined system, 3, 7, 8, 65–67, 75, 82, 117
- overlapping, 242, 283, 285, 292

- Pafnuty Lvovich Chebyshev, 449
- paradox, 326
- parallel implementation, 321
- parallelogram, 180, 182, 229
- particular solution, 46
- Pascal, 421
- penalty combination, 15, 97
- penalty integral, 302
- penalty plus hybrid combination, 316–318
- perturbation, 42
- pesudoinverse matrix, 118
- Peter Guthrie Tait, 430
- physics, 429
- piecewise cubic Hermite polynomial interpolant, 309
- piecewise Lagrange interpolation polynomial v_p , 300
- Pierre-Simon Laplace, 419, 421
- Poisson bracket, 423
- Poisson integral, 24, 423
- Poisson ratio, 423, 437
- Poisson's constant, 423
- Poisson's kernel, 25
- polar coordinate, 147
- posteriori analysis, 77, 82
- posteriori estimate, 82
- potential theory, 417, 418, 424, 426, 427, 430
- Price of Mathematicians, 429
- probability theory, 421
- problem
 - 3D elliptic problem, 23
 - beam deflection problems, 431
 - biharmonic boundary value problem, 143
 - coupling problem, 18
 - crack problem, 12
 - cracked beam eigenvalue problem, 348, 349

- cracked beam problem, 34, 57, 61, 63, 74, 75, 77, 79, 82, 83, 89, 357, 359, 377, 394, 395, 397
- Dirichlet problem, 423, 431, 443
- domain problem, 33
- eigenvalue problem, 241, 242, 321
- exterior domain problem, 445
- exterior problem, 26
- Helmholtz problem, 346
- interface problem, 33, 47
- Laplace boundary value problem, 74
- Laplace's problem, 426
- Motz's problem, 12, 58, 82, 102, 105, 110, 114, 126, 127, 130, 131, 143, 271, 289, 397, 399
- Neumann problem, 424, 425, 432, 451
- Neumann-Laplace problem, 23
- potential problem, 438, 454
- scaled cracked beam problem, 78, 83, 91
- second order elliptic boundary problem, 1
- singularity problem, 34, 61, 117, 142, 300
- sound radiation problem, 451
- traditional cracked beam problem, 79, 92
- projection solution, 169
- quasiuniform, 180, 299
- quasiuniform parallelogram, 180
- quasiuniform rectangular element, 299
- radial distance, 225
- rank, 68
- recurrence solution, 329
- reduction factor, 287
- retarded potential integral representation, 450
- rhomboid, 56
- Richard von Mises, 449
- Ritz combination principle, 448
- Robert Murphy, 430
- rounding error, 327
- Royal Artillery School, 420
- Rumford Medal, 431
- second identity, 428
- second inverse property, 48–51
- second law of thermodynamics, 440
- sectorial domain, 404
- sectors of disk, 82
- seminorm, 38
- senior wrangler, 430
- Simeon-Denis Poisson, 419, 422
- simplified effective condition number, 119
- simplified hybrid combination, 241, 247
- Simpson's rule, 207
- single layer of density, 26
- single-layer potential, 432, 453
- singular boundary layer, 33
- singular particular solution, 144
- singular value decomposition, 68, 117, 327, 328, 364
- singularity, 37, 45, 242
- Smith's Prize, 431
- Sobolev norm, 38, 40, 121, 168, 192, 224, 251, 365
- Sobolev space, 9, 17, 38, 39, 98, 101, 211, 324
- Solomon Grigorevich Mikhlin, 452
- Somigliana dislocation, 454
- Somigliana identity, 437, 456
- spectroscopic theory, 448
- stiffness matrix, 15, 28, 82
- Stokes flow, 431
- stress intensity factor, 133
- submarine cable, 441
- submarine telegraphy, 441
- superclose, 311
- superconvergence, 311, 314
- superlinear convergence, 329
- superlinear convergence rate, 321, 323, 329
- supersonic flight, 448
- symbolic dynamics, 435
- symmetric combination, 15
- symmetric Gaussian elimination, 251
- Taylor's series, 379
- technique

- coupling technique, 28, 33, 246, 297
- hybrid technique, 245, 247
- Lagrange multiplier technique, 245, 248
- penalty plus hybrid technique, 13, 241, 242, 245, 247, 262, 265, 267, 298, 301, 316
- penalty technique, 6
- simplified hybrid technique, 247, 298, 301
- weighted residual technique, 457
- techniques of separation of variable, 10
- Theodore von Kármán, 445, 448
- theorem
 - basic theorem, 302
 - Betti-Maxwell reciprocity theorem, 436
 - Cauchy integral theorem, 433
 - divergence theorem, 427
 - Fredholm integral equation theorem, 452
 - Fredholm theorem, 432
 - Gauss' theorem, 427
 - Green's theorem, 5, 21, 41, 48, 366, 368
 - imbedding theorem, 41, 252
 - Kandrosov theorem, 202
 - regularity theorem, 373
 - Rellich theorem, 202
 - Sobolev imbedding theorem, 39, 41, 45, 48, 53, 149, 366
 - trace theorem, 252, 373
- theory of elasticity, 443
- theory of reciprocity, 440
- thin plate, 151
- thin-plate spline, 213
- third identity, 428
- Thomas Allen Cruse, 459
- Thomas Jan Stieltjes, 434
- traditional scaled cracked beam, 82
- Traité du Mécanique Céleste, 421
- translation, 98
- trapezoidal rule, 64, 195
- Trefftz-Herrera approach, 18
- Trefftz-Herrera domain decomposition, 20
- turbulence theory, 448
- unbounded domain, 10, 11, 26, 37, 46, 417
- uncertainty principle, 234
- uniform difference grid, 195
- uniqueness, 41
- Viktor Dmitrievich Kupradze, 452, 455
- Vito Volterra, 435, 442
- Volterra integral equation of the first kind, 437
- Walter Ritz, 443, 447
- wave number, 436
- weakly singular, 432
- weighted residuals formulation, 445, 457
- Wilhelm Eduard Weber, 429
- William Hopkins, 430
- William John Macquorn Rankine, 445
- William Rowan Hamilton, 418, 423
- William Thomson, 429, 440
- Woldemar Voigt, 448
- World War II, 435
- Zeitschrift für Angewandte Mathematik und Mechanik, 449